Herbert Fromm
Mark Hargrove

Essentials of Biochemistry

Springer

Essentials of Biochemistry

Herbert J. Fromm • Mark S. Hargrove

Essentials of Biochemistry

Springer

Dr. Herbert J. Fromm
Iowa State University
Dept. Biochemistry, Biophysics &
Molecular Biology
Ames Iowa
USA

Dr. Mark S. Hargrove
Iowa State University
Dept. Biochemistry, Biophysics &
Molecular Biology
Ames Iowa
USA

ISBN 978-3-642-19623-2 e-ISBN 978-3-642-19624-9
DOI 10.1007/978-3-642-19624-9
Springer Heidelberg Dordrecht London New York

Library of Congress Control Number: 2011940318

Printed on acid-free paper

Springer is part of Springer Science+Business Media (www.springer.com)

This book is dedicated to the memory of
Fred Rudolph (1945–2003), superb scientist,
student (HJF), mentor (MSH), and friend.

Preface

Based on exceptional intellectual and experimental achievements of biochemists and structural biologists, biochemical information continues to accumulate at a nearly exponential rate well into the twenty-first century. What becomes obvious is that neither the student nor the instructor can be expected to comprehend this enormous volume of material in a classroom setting, and certainly not in any first course. We have therefore chosen to present those topics and details that we believe are central to contemporary biochemistry and that will remain relevant to the science of biochemistry well into the foreseeable future.

This textbook is aimed at undergraduate chemistry and biochemistry students as well as first-year biochemistry graduate students. Based on lectures given to students with strong chemistry backgrounds at Iowa State University, this book emphasizes metabolism and enzyme reaction mechanisms. By omitting regulatory pathways and such structural details as residue numbers provided in more comprehensive textbooks, "Essentials of Biochemistry" helps students to focus on how enzymes function and how their reactions are studied. Moreover, while contemporary biochemistry includes what is often termed cell biology, many universities (including ours) teach such topics within their biology curriculum, thus eliminating any need to cover them herein in detail.

As the title of the book implies, the text lays the basis for an understanding of the "Essentials of Biochemistry" and is not intended to be an encyclopedia of biochemistry nor a substitute for any of the excellent comprehensive texts currently available. We believe that such an approach benefits those seeking to master biochemistry by relying on what we trust is a well-explained account of its underlying principles.

Ames, June 2011

Herbert J. Fromm
Mark S. Hargrove

Acknowledgements

The authors wish to acknowledge and thank the following individuals: Donald Beitz, Thomas Bobik, George Kraus, Gustavo MacIntosh, Scott Nelson, Daniel Purich, Martin Spalding, and John Robyt, for their reading of a draft of the text and for their constructive criticisms.

Contents

Chapter 1
The Cell and Its Components

Cells which are the basic organized units of life can be divided into two different types: prokaryotic and eukaryotic. The fundamental distinction between the two cell types involves the existence of cell membranes. The prokaryotic cell does not have a membrane enclosing its genetic material, deoxyribonucleic acid (DNA). On the other hand, in eukaryotic cells the DNA is contained within a membrane, and the structure referred to as the nucleus. The typical eukaryotic cell has a number of membrane-enclosed organelles, whereas prokaryotic cells lack membrane-bound organelles.

1.1 Typical Prokaryotic Cell: *Escherichia coli*

The rod-like prokaryotic *E. coli* cell, which is the most frequently used cellular research tool in biochemistry, is illustrated in Fig. 1.1. The *E. coli* cell itself is extremely small (1.5 × 0.5 μm); roughly 10% the size of a typical animal cell.

The cell is surrounded by an *outer membrane*, a *cell wall*, and an *inner membrane*. The inner membrane is the primary permeability barrier of the cell. The cell wall provides strength and shape while the outer membrane is a secondary permeability barrier that also contributes to structural integrity.

Components within the *E. coli* cell are:

1. The *cytosol* or *cytoplasm* is the milieu of the cell. It contains aqueous soluble enzymes and other water soluble material.
2. *Cellular or nucleoid deoxyribonucleic acid (DNA)*, which contains the cell's genetic material, is found in the cytosol.
3. The *plasma membrane*, which consists of a lipid bilayer surrounds the cytoplasm.
4. The *periplasmic space* (not shown) is the space between the plasma membrane and the outer membrane.

H.J. Fromm and M.S. Hargrove, *Essentials of Biochemistry*,
DOI 10.1007/978-3-642-19624-9_1,

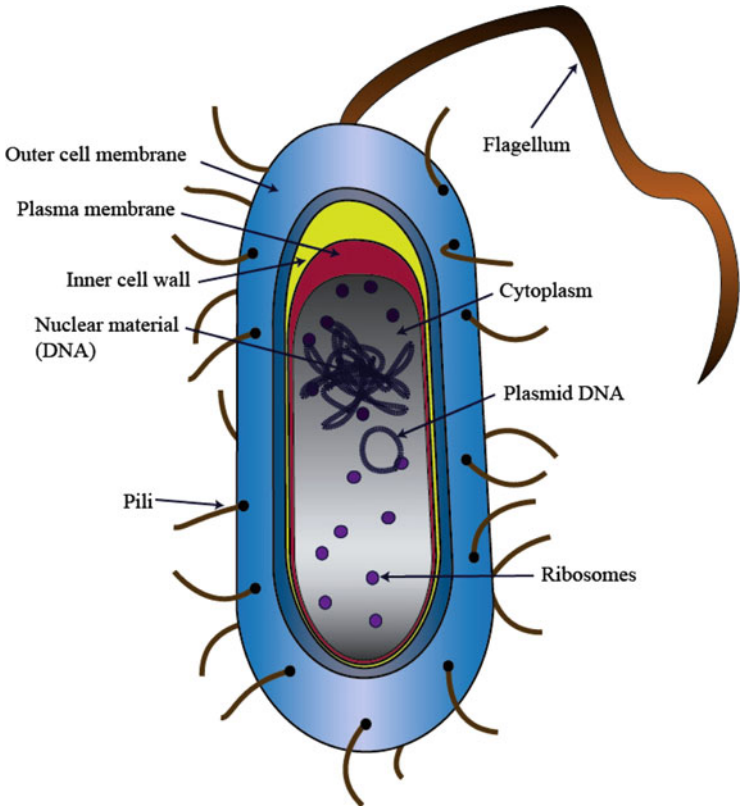

Fig. 1.1 Cartoon of a typical *E. coli* cell illustrating some of its more important components

5. *Ribosomes* are made up of ribonucleic acid (RNA) complexed with proteins and are the sites of protein biosynthesis.
6. Bacterial locomotion is provided by *flagella*. Most cells have more than a single flagellum, although only one is illustrated in Fig. 1.1.
7. Some bacterial cells adhere to their hosts by *pili* which are on the surface of the bacterium. Pili are also involved in cell adhesion during DNA transfer when bacterial cells undergo sexual activity.
8. *Plasmids*-satellite DNA distinct from the nucleoid DNA.

1.2 Archaea

Archaea are prokaryotes; however, they are distinctly different genetically from bacteria such as *E. coli*. It is believed that Archaea are among the most abundant life forms on Earth. They are thought to constitute approximately 40% of the organisms found in the sea.

1.3 Eukaryotic Cell (Non-Plant)

A typical eukaryotic cell and it components are illustrated in Fig. 1.2.

The eukaryotic cell is surrounded by a single plasma membrane. Features of eukaryotic cells are:

1. The *cell membrane (plasma membrane)* encloses the cell and separates one cell from the next. It allows for the entry and exit of cellular metabolites.
2. The *nucleus*, the cell's largest organelle, with the exception of the vacuole in plants, contains most, but not all, of the cell's DNA. Its surrounding membrane consists of two layers. DNA replication and transcription, which is the transmission of information from DNA to RNA, occurs in this organelle.
3. *Mitochondria* are the sites of energy and heat production in cells. They are deep red in color which reflects their high content of an iron-containing compound called heme. These organelles have both an inner and outer membrane and carry out a series of redox reactions which are coupled to the biosynthesis of ATP. Mitochondria also contain DNA.
4. The *rough endoplasmic reticulum* (ER) is closely associated with the nuclear membrane. The outer surface of the ER is in close proximity to ribosomes, the site of protein synthesis. Many of the ER-associated ribosomes synthesize

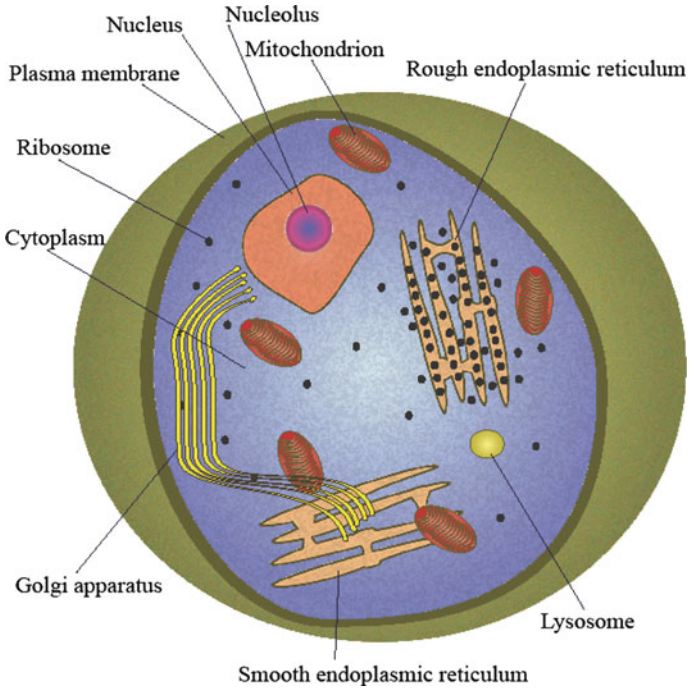

Fig. 1.2 Cartoon of a eukaryotic cell and its components

proteins that enter the interior or *lumen* of the ER where they may undergo modification. Some of these proteins form *vesicles* which are ultimately exported from the cell. Vesicles are membrane fragments that form a hollow shell. Substances may be contained within vesicles.

5. Some vesicles from the ER bud off and associate with the *Golgi apparatus*. These vesicles can be modified and transported to other cells within the organism or utilized within the cell in which they were synthesized.
6. *Lysosomes* are organelles that contain enzymes called *cathepsins* that hydrolyze proteins. These enzymes are not specific or selective in their action.
7. The internal milieu of the cell is the *cytosol* or *cytoplasm*.
8. *Nucleolus* is the site of ribosomal RNA (r-RNA) synthesis and assembly of the ribosome.
9. The *smooth endoplasmic reticulum* is the site of biosynthesis of steroids and lipids.
10. The *ribosomes* are the sites of protein synthesis.
11. The *cytoskeleton*, although not explicitly shown, provides the scaffolding of the cell and as such, its support. It consists of three filamentous proteins: *actin*, *tubulin*, and so-called *intermediate filaments*. In addition to physical support provided by the cytoskeleton, cytoskeleton components are involved in mitosis and sperm locomotion.

1.4 Eukaryotic Cell Components (Plant)

A plant cell is very similar to the cell shown in Fig. 1.2 except that it would contain three additional components: a rigid cell wall, chloroplasts and a vacuole.

1. The *cell wall* is composed mainly of cellulose. As is the case with *E. coli* this structure acts as a buffer between the cell and its environment.
2. The *chloroplast* is an energy-utilizing (from the sun) and energy-producing structure found primarily in the leaves of plants.
3. *Vacuoles* are fluid containing organelles that store a variety of compounds including water, ions, and nutrients. They are extremely large and in some plant cells may occupy as much as 90% of the cell's volume.

Chapter 2
Introduction to Biomolecules

The complexity of even the simplest of life forms, the single cell, cannot be overstated. Nevertheless, from a chemical perspective, cellular components can be segregated into macromolecules (DNA, RNA, proteins, etc.), relatively simple molecules (amino acids, monosaccharides, and lipids), and their precursors: CO_2, H_2O, and NH_3. In general, the macromolecules tend to be polymers of small biomolecules; however, each of these molecules, whether simple or complex, is involved in a myriad of intricate metabolic reactions. A case in point is the monosaccharide glucose which is synthesized from H_2O and CO_2. When degraded to its precursors, it provides the cell with its energy requirements for such diverse processes as macroscopic movement as well as the synthesis of complex macromolecules. In addition, glucose is the fundamental building block of macromolecules such as starch and cellulose. This basic theme, in which the cell uses a simple small molecule in a multitude of processes, is typical of how relatively small biomolecules are used in living systems.

In this chapter we will consider the chemistry and properties of four small biomolecules: amino acids, carbohydrates, lipids, and nucleotides and their roles in metabolism.

2.1 Amino Acids

Amino acids are the most versatile small biomolecules. They fulfill a number of extremely important roles in biology. These include: building blocks of proteins which are polymers of amino acids, precursors of hormones, and precursors of molecules with specialized physiological functions, e.g., the neurotransmitter dopamine and the hormone thyroxine are both derivatives of the amino acid tyrosine.

As the name implies, amino acids contain amino and carboxyl groups. They can be divided into groups based on acidic, basic, and neutral properties when dissolved in water. They are also classified according to solubility, e.g., hydrophilic and hydrophobic.

H.J. Fromm and M.S. Hargrove, *Essentials of Biochemistry*,
DOI 10.1007/978-3-642-19624-9_2,

Table 2.1 Amino acid structures, names and acid–base properties

			Acid and basic properties		
Amino acid	Abbreviations	Structure	pK_1	pK_2	pK_3
		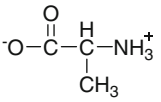			
Alanine	Ala, A		2.35	9.87	
		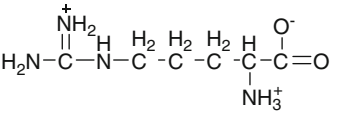			
Arginine	Arg, R		1.82	8.99	12.5
		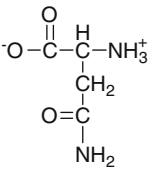			
Asparagine	Asn, N		2.14	8.72	
		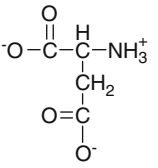			
Aspartic acid	Asp, D		1.99	3.90	9.90
		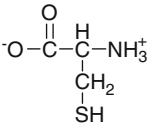			
Cysteine	Cys, C		1.92	8.37(SH)	10.7
		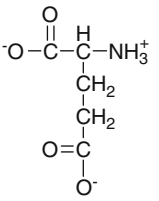			
Glutamic acid	Glu, E		2.10	4.07	9.47

(continued)

Table 2.1 (continued)

Amino acid	Abbreviations	Structure	Acid and basic properties		
			pK_1	pK_2	pK_3
		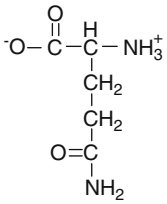			
Glutamine	Gln, Q		2.17	9.13	
		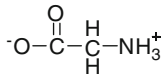			
Glycine	Gly, G		2.35	9.78	
		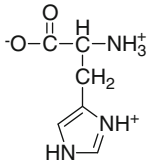			
Histidine	His, H		1.80	6.04	9.33
		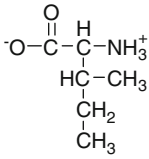			
Isoleucine	Ile, I		2.32	9.76	
		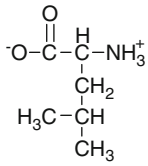			
Leucine	Leu, L		2.33	9.74	
		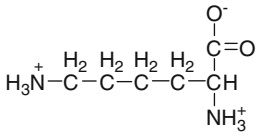			
Lysine	Lys, K		2.16	9.06 (α-NH_3^+)	10.5

(continued)

Table 2.1 (continued)

Amino acid	Abbreviations	Structure	Acid and basic properties		
			pK_1	pK_2	pK_3
		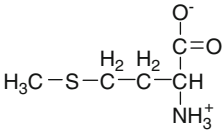			
Methionine	Met, M		2.13	9.28	
		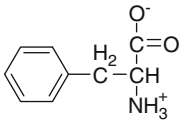			
Phenylalanine	Phe, F		2.20	9.31	
		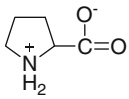			
Proline	Pro, P		1.95	10.6	
		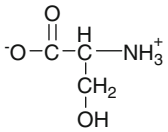			
Serine	Ser, S		2.19	9.23	
		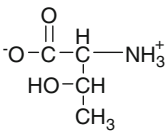			
Threonine	Thr, T		2.09	9.10	
		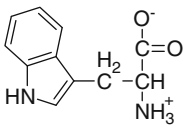			
Tryptophan	Trp, W		2.46	9.41	

(continued)

Table 2.1 (continued)

Amino acid	Abbreviations	Structure	Acid and basic properties		
			pK_1	pK_2	pK_3
Tyrosine	Tyr, Y	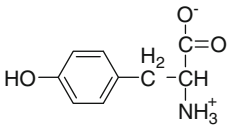	2.20	9.21	10.5 (phenol)
Valine	Val, V	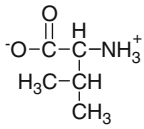	2.29	9.74	

There are 20 so-called amino acids in proteins; however, one of these, proline, is in fact an imino acid. Nineteen of the 20 amino acids are optically active, i.e., they are capable of rotating plane polarized light either to the right (*dextrorotary*) or left (*levorotary*). All 19 amino acids have an amino group at the α-position (C-2). Similarly, all amino acids have a carboxyl group in the 1-position.

Table 2.1 illustrates the amino acids found in proteins along with the pK values for the various functional groups associated with these molecules. Also included in the table are the one- and three-letter abbreviations for the individual amino acids.

2.1.1 Essential Amino Acids

Of the 20 amino acids found in proteins, 8 are said to be *essential amino acids*. These amino acids are: Met, Val, Leu, Ile, Lys, Phe, Thr, and Trp. Essential amino acids, as opposed to nonessential amino acids, are required in the diet for maintenance and sustenance. The elimination of a single essential amino acid from the diet will lead ultimately to death even on an otherwise nutritionally adequate ration. Children need two additional amino acids in their diets; His and Arg. The nutritionally essential nature of certain amino acids was determined by feeding healthy volunteer students synthetic diets lacking a single amino acid and measuring their nitrogen balance (N_B) which is equal to dietary nitrogen intake minus nitrogen excretion in the urine and feces. Thus

$$N_B = N_{Intake} - N_{Excretion},$$

in so-called normal human beings N_B equals 0, whereas it is positive in growing individuals and negative in the case of wasting diseases. Plants have the ability to synthesize all amino acids from CO_2, H_2O, NH_3, and inorganic salts including sulfate.

Bacteria, such as *Escherichia coli* are similar to plants in their nutritional requirements but also require an organic carbon source such as glucose.

2.1.2 Optical Properties

In 1874 Jacobus van't Hoff, who is referred to as the "father of stereochemistry" suggested that a carbon atom with four bound substituents exhibits tetrahedral geometry [1]. In addition, he surmised that if these substituents were different entities, two different stereoisomers (*enantiomers*) of this compound could exist. These enantiomers would also have different optical properties. Shortly after van't Hoff's discovery was made, the French chemist J.A. Le Bel came to the same conclusion independently. Although Le Bel did not win the Nobel Prize for his work (see below) he did share the Davey Medal with van't Hoff.

With the exception of glycine (amino acetic acid), all of the amino acids are optically active. Because the α-carbon atom of amino acids is a chiral center, with the exception of glycine whose α-carbon is bound to two hydrogen atoms, amino acids can exist as enantiomers (nonsuperimposable mirror images). Both isoleucine (2S,3S) and threonine (2S,3R) are diastereomers because they contain two chiral carbon centers. R and S nomenclature is rarely used in reference to amino acids; trivial names and D and L being the designations most frequently encountered.

As one may recall from organic chemistry, the D and L designations were first proposed by Emil Fischer using D- and L-glucose as examples (Fig. 2.1) [2]. In fact, his fundamental research on sugars proved, experimentally, the proposal of van't Hoff for the tetrahedral geometry of the carbon atom. Both van't Hoff and Fischer received the first and second Nobel prizes in chemistry, respectively.

These compounds are by definition enantiomers. By analogy with these aldohexose sugars, amino acids use identical nomenclature for enantiomers, e.g., alanine (Fig. 2.2).

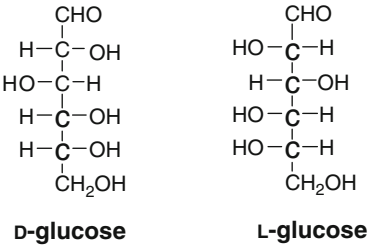

Fig. 2.1 The structures of the enantiomers, D- and L-glucose, as proposed by Emil Fischer

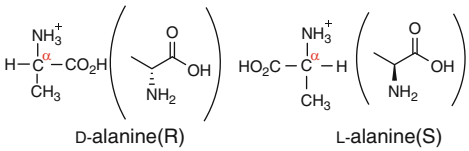

Fig. 2.2 The structures of D and L-alanine with carbon 2 designated the α-carbon atom. By placing the amino group up and the carboxyl group either to the right (D) or left (L) these structures are analogous to the D and L forms of sugars. In terms of R,S stereochemical nomenclature, D corresponds to (R) and L to (S). Abbreviated amino acids structures are shown in parenthesis.

It is important to note that although both D- and L-amino acids exist in nature, proteins are made up exclusively of L-amino acids.

Because of the p*K* values of amino and carboxyl groups, amino acids will always carry a charge, i.e., the uncharged form of amino acids *cannot* exist, e.g., the structure shown in Fig. 2.3.

Fig. 2.3 The structure of an uncharged amino acid

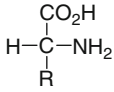

On the other hand, amino acids although charged, may not exhibit a net charge, e.g., in Fig. 2.4.

Fig. 2.4 The structure of an amino acid with no net charge

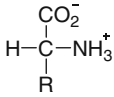

If we consider this structure, referred to as the *Zwitter ion* form, it is clear that amino acids can exist in net acid and net basic states (Fig. 2.5).

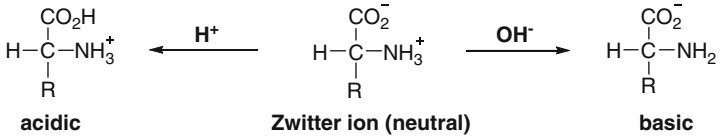

Fig. 2.5 The effect of acids and bases on the amino and carboxyl groups of an amino acid

The *Zwitter ion* form is said to be at the amino acid's *isoelectric point* (p*I*), i.e., it will not migrate in an electrical field. Depending upon the pH, the amino acid may be above (negative) or below (positive) its p*I*.

Obviously an amino acid below its p*I* will migrate to the cathode, and that above its p*I* will migrate to the anode when exposed to an electrical field. It is important to

note that the pK values for amino acids in solution may be markedly different for analogous functional groups in proteins where the dielectric constants are very different from that of water.

When a neutral amino acid such as glycine is placed in water, the resulting pH is 6.1. The equation used to calculate the pH of neutral amino acids in solution is:

$$\mathrm{pH} = \frac{\mathrm{p}K_1 + \mathrm{p}K_2}{2} = \frac{2.4 + 9.8}{2} = 6.1.$$

For a diacidic amino acid such as glutamate, pK_3, the pK of the amino group is not a factor

$$\mathrm{pH} = \frac{\mathrm{p}K_1 + \mathrm{p}K_2}{2},$$

in the calculation because the amount of the charged amino group (NH_3^+) is extremely small and does not contribute significantly to the solution pH.

In the case of dibasic amino acids in solution, the pH is:

$$\mathrm{pH} = \frac{\mathrm{p}K_2 + \mathrm{p}K_3}{2}.$$

Amino acids, because they are *weak* acids and bases, can act as *buffers*. Buffers are defined as weak acids or bases and their conjugate salts that resist changes in pH upon the addition of acids (H^+) or bases (OH^-). The rationale for the action of an acidic buffer (HA) and its salt (A^-) is as follows:

$$\mathrm{HA} = \mathrm{H}^+ + \mathrm{A}^-.$$

When an acid (H^+) is added to the buffer, it combines with the salt (A^-), thus effectively removing the added H^+ from solution, and the pH of the solution remains unchanged. When a base (OH^-) is added to the buffer, a proton (H^+) reacts with the added base (OH^-), and HA dissociates to maintain the equilibrium and H^+ concentration constant.

As a rule, buffers are effective when the [salt]/[acid] ratio is greater than 1/10 or less than 10/1. Buffering capacity decreases when these values are exceeded.

A very useful equation, when preparing a buffer, is the *Henderson–Hasselbach* equation:

$$\mathrm{pH} = \mathrm{p}K_\mathrm{a} + \log\frac{[\mathrm{salt}]}{[\mathrm{acid}]}.$$

The derivation of the Henderson–Hasselback equation is relatively straight forward:

$$\mathrm{HA} = \mathrm{H}^+ + \mathrm{A}^-,$$

$$K_\mathrm{a} = \frac{[\mathrm{H}^+][\mathrm{A}^-]}{[\mathrm{HA}]}.$$

Taking logs of both sides of this equation gives:

$$\log K_\mathrm{a} = \log \mathrm{H}^+ + \log \mathrm{A}^- - \log \mathrm{HA}.$$

Multiplying both sides of this equation by -1 and rearranging, gives the Henderson–Hasselbach equation.

2.2 Carbohydrates

Carbohydrates, also knows as sugars or saccharides, are defined as polyhydroxy aldehydes and ketones and/or their derivatives. They are the most abundant molecules found in nature and are involved in both dynamic and structural roles, e.g., they are focal points in energy metabolism and are major intermediates in plant structure and metabolism. They may exist in nature as carbohydrates per se, but they may also be associated chemically with lipids and proteins.

Simple carbohydrates are called sugars, whereas complex carbohydrates are referred to as glycoconjugates, i.e., glycolipids and glycoproteins.

2.2.1 Monosaccharides

1. By definition the simplest monosaccharides are the trioses; two glyceraldehydes, dihydroxyacetone, and glycerol (Fig. 2.6).
2. It is clear from these triose structures that monosaccharides can exist either as *aldo* or *keto sugars*.
3. The aldo and keto sugar carbons are numbered as illustrated for the trioses.

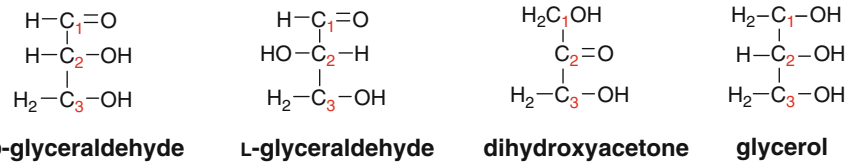

Fig. 2.6 The structures of the trioses glyceraldehyde and dihydroxyacetone and the numbering of their carbon atoms. D- and L-glyceraldehyde are enantiomers – nonsuperimposable mirror images

2.2.1.1 D and L Designation of Monosaccharides

The designation D or L has nothing to do with rotational properties of plane polarized light when it passes through a sugar solution, e.g., D-glucose rotates plane polarized light to the right whereas D-fructose rotates plane polarized light to the left, i.e., D-glucose is dextrorotary and D-fructose is levorotary.

The secondary hydroxyl group *farthest* from the aldo or keto group determines whether the sugar is D or L. If it is on the right-hand side, the sugar is D; on the left side, it is L. Examples are D- and L-glucose and D-fructose (Fig. 2.7).

Note that D-glucose is the mirror image of L-glucose. The D-sugars are the principal carbohydrates that occur naturally.

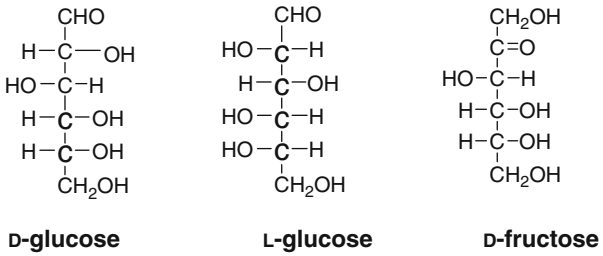

Fig. 2.7 Structures of the aldohexoses, D- and L-glucose and the ketohexose D-fructose

2.2.1.2 Monosaccharides that Play Important Roles in Metabolism

Three, four, five, six, and seven carbon monosaccharides and their derivatives play important roles in metabolism. Figure 2.6 illustrates the structures of important triose sugars. Other sugars that play significant metabolic roles are shown in Fig. 2.8.

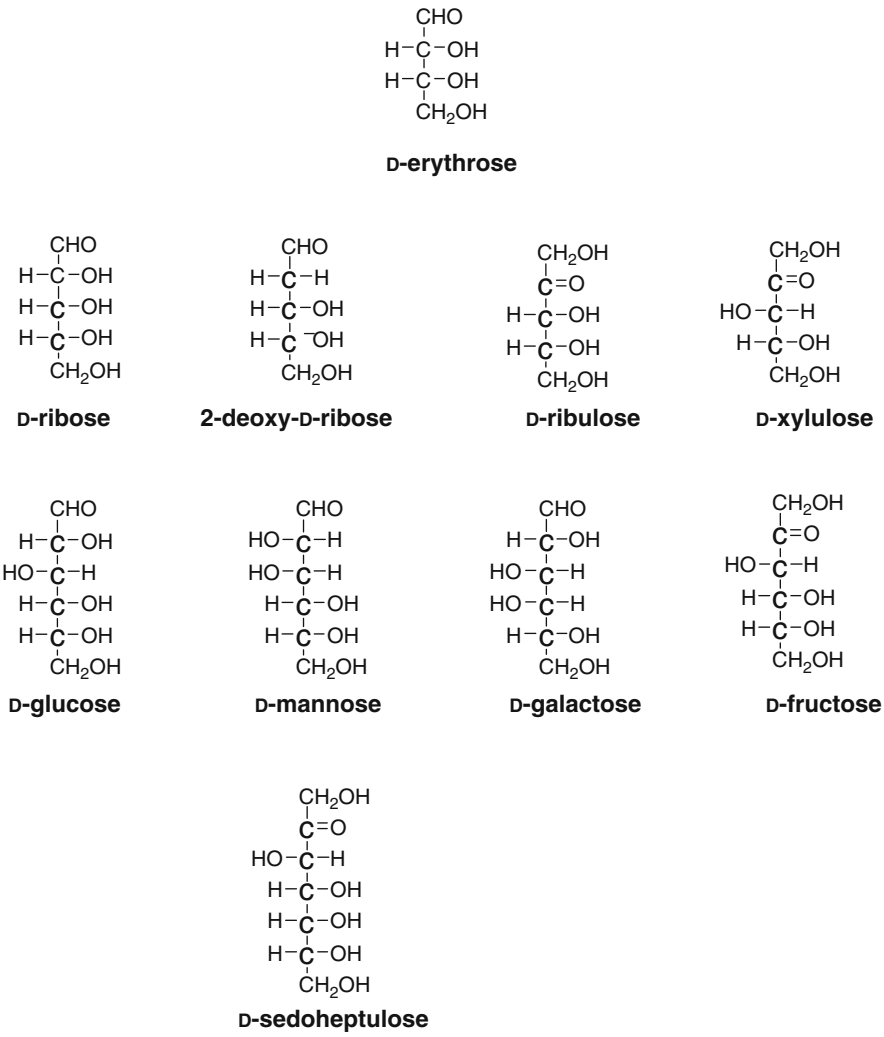

Fig. 2.8 The structures of biologically important four, five, six, and seven carbon sugars

2.2.1.3 Mutarotation: A Form of Tautomerization

If one views the straight chain form of glucose, it is clear that there are four chiral carbon centers. From the equation n^2 where n equals the number of chiral centers, there should be 16 isomers of glucose; however, there are 32 isomers of glucose. This was recognized by Emil Fischer [3] and is a result of mutarotation, which is base-catalyzed (Fig. 2.9).

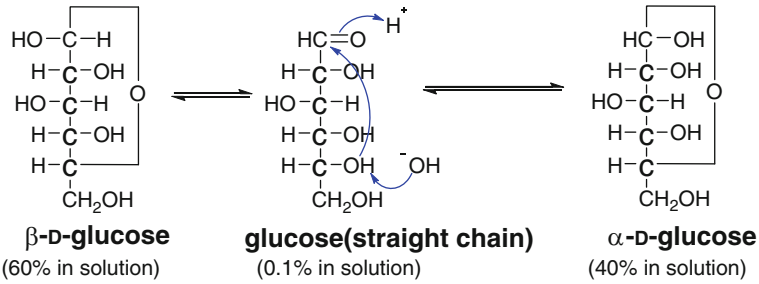

Fig. 2.9 Mechanism for the mutarotation of D-glucose in basic solution

The α and β forms of glucose are referred to as *anomers* and the C-1 carbons are called *anomeric carbons*. Both forms of glucose are *hemiacetals*. If the hydrogen atom of the C-1 hydroxyl is replaced by an R-group, the compound is an *acetal*.

2.2.1.4 Reducing Sugars

Sugars such as glucose form acids when exposed to strong bases and certain metal ions (Fig. 2.10).

In the case of Fehling's solution or Benedict's reagent, the Cu^{2+} is reduce to Cu^{1+} and the reddish color of copper oxide is observed. Such sugars are referred to as *reducing sugars*. It is important to note that the oxidation occurs at the anomeric carbon atom of the reducing sugar.

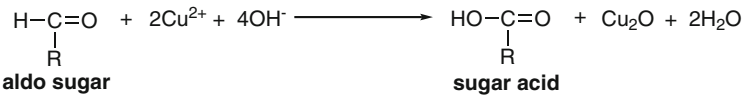

Fig. 2.10 The oxidation of an aldo sugar to a sugar acid by an alkaline solution of Cu^{2+}

2.2.1.5 Pyranoses and Furanoses

In solution, the straight chain forms of aldo and ketopentoses and hexoses represent a very small fraction of the sugars. Haworth used the pyranose and furanose rings to more correctly describe the structures of the sugars. The following glucose structures, α and β pyranoses, are illustrated by *Haworth projections* (Fig. 2.11). In the case of D-fructose, the Haworth projections are shown in Fig. 2.12.

The primary forms of D-fructose are pyranoses, unless the C-6 hydroxyl is substituted with a phosphoryl group. When the C-1 OH of glucopyranose or the C-2 OH of fructofuranose reacts with alcohols, the products are the acetals; glucopyranosides, and fructofuranosides, respectively.

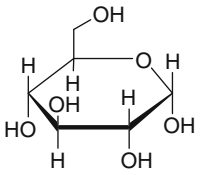

α-D-glucopyranose

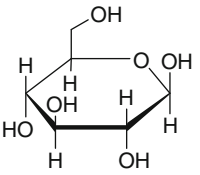

β-D-glucopyranose

Fig. 2.11 β-D-Glucopyranose, the primary structure of D-glucose in solution

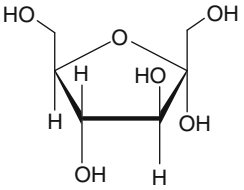

α-D-fructofuranose

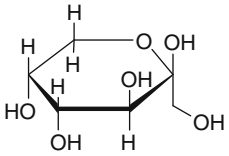

β-D-fructopyranose

Fig. 2.12 The pyranose and furanose forms of D-fructose. showing the hemiketal hydroxyl group in the α and β positions

The Haworth projections, as useful as they are, do not accurately depict the bond angles and structures of the sugars and therefore their conformations. Illustrated here is the C-1, or normal conformation of β-D-glucopyranose which is much more faithful to the true structure of D-glucose than the other projections. In this structure all of the hydroxyl groups are in the equatorial position (parallel to the nonadjacent side of the ring), whereas all of the hydrogen atoms are in the axial position (perpendicular to the ring's axis of symmetry) (Fig. 2.13).

Biochemists tend to use both Haworth projections and chair forms of sugars interchangeably, and this practice will be continued in this text.

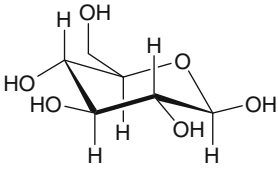

β-D-glucose

Fig. 2.13 The C-1, or normal conformation of β-D-glucopyranose. All of the hydroxyl groups, associated with the ring, are equatorial and all the hydrogens axial

2.2.1.6 Sugar Acids and Alcohols

Sugars can be oxidized either chemically or enzymatically. The nomenclature used to describe these acids is shown in Fig. 2.14(a):

In the case of glucose, the acids would be glucuronic, gluconic, and glucaric (saccharic) acids based on the general structures above. Sugars also form alcohols

when reduced either chemically or enzymatically. Some of the common sugar alcohols are illustrated in Fig. 2.14(b).

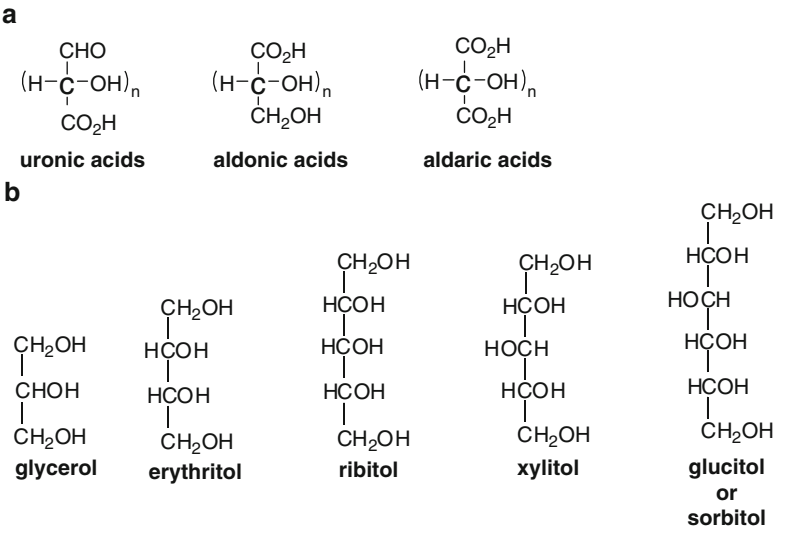

Fig. 2.14 The monocarboxylic and dicarboxylic forms of sugar acids **(a)** and some common sugar alcohols **(b)**

2.2.2 Disaccharides

Disaccharides are sugars containing two monosaccharides linked covalently through a glycosidic linkage. There are three disaccharides whose metabolism will be considered under the chapter on carbohydrate metabolism (Chap. 11): maltose, lactose, and sucrose. Their structures are illustrated in Fig. 2.15. Maltose and lactose contain acetal structures and have hemiacetal hydroxyl groups at their reducing ends. When these hemiacetal groups react with an alcohol, the product is referred to as a *glycoside*. Maltose is composed of two glucosyl units connected by an $\alpha 1 \rightarrow 4$ glycosidic linkage. The OH group at the reducing end of sugars, as illustrated for maltose and lactose, is not an alcohol but a hemiacetal (Fig. 2.15). In the case of sucrose, the linkage between the sugars is a glycosidic bond which is an acetal-ketal linkage. With no free hemiketal or hemiacetal hydroxyl group, sucrose is a nonreducing sugar.

Other oligo and polysaccharides have both reducing and non-reducing ends. This distinction will become important when carbohydrate metabolism is considered.

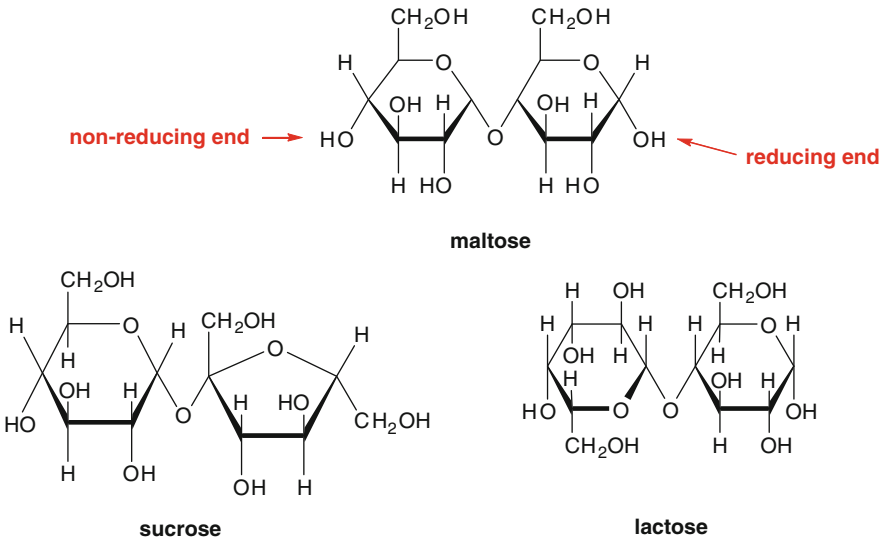

Fig. 2.15 The disaccharide maltose illustrating the reducing and nonreducing ends of the molecule. Also shown are the reducing sugar lactose and the non-reducing sugar sucrose

2.2.3 Polysaccharides

2.2.3.1 Glycogen

Glycogen is the storage form of glucose in animals. It is made up of a polymer of glucose units connected by glycosidic linkages. The glycosidic bonds are α-1 → 4, which produces a linear chain; however, a branch point (α-1 → 6) occurs approximately every 12–18 glucopyranosyl units. The end result is a branched chain between the linear polysaccharide chains (Fig. 2.16).

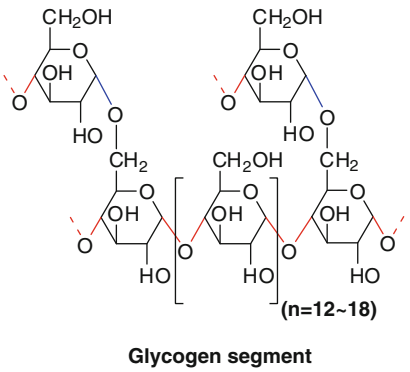

Fig. 2.16 A glycogen segment: α1 → 4 (red) and α1 → 6 (blue) glycosidic linkages in glycogen

2.2.3.2 Starch

Starch is the storage form of glucose in plants. Most starches are made up of two distinctly different molecules, *amylose* and *amylopeptin*. Segments of amylose and amylopectin are illustrated in Figs. 2.17 and 2.18, respectively.

(a) Amylose is a linear molecule composed of glucopyranosyl units connected by α1 → 4 glycosidic linkages.
(b) Amylopectin is similar to glycogen; however, the branch points (α1 → 6) occur much less frequently. Most starches are composed of approximately 20%-25% amylose and 75%-80% amylopectin; however, waxy rice and waxy maize are devoid of amylose and contain 100% amylopectin. The characteristics of starches vary depending upon the amylose to amylopectin ratio.

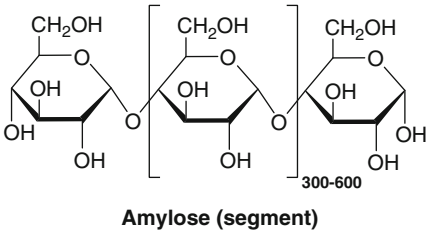

Fig. 2.17 A segment of amylose: α1 → 4 glycosidic linkages in a portion of amylose

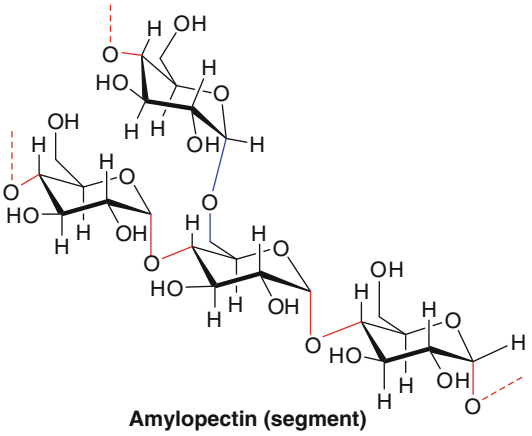

Fig. 2.18 A segment of amylopectin illustrating α1 → 4 (red) and α1 → 6 (blue) linkages

2.2.3.3 Cellulose

Cellulose is present in plants as a structural element. It is the most abundant molecule in nature. Wood and most plant cell walls are approximately 50% cellulose. Because of its highly hydrogen-bonded structure, cellulose is extremely

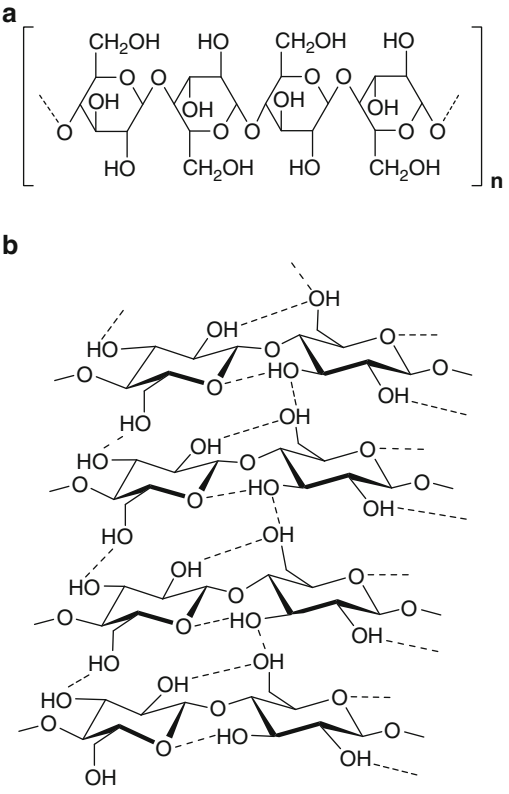

Fig. 2.19 Segments of a cellulose structure. A segment of cellulose: (**a**) β → 1,4 linkages between glucose units. (**b**) Interchain hydrogen bonding network between cellulose chains. Chains are not held together by 1,6-glycosidic lingages, but by interchain hydrogen bonding

difficulty to degrade either chemically or enzymatically to glucose. It is a linear chain of glucopyranosyl units joined by β1 → 4 glycosidic linkages. Cellulose chains are held together intermolecularly by hydrogen bonds between adjacent chains. The chains are believed to be among the tightest helices found in nature, called a twofold screw axis helix. The properties of the various celluloses are determined to a large degree by the number of glucose units in the linear chain. Segments of a cellulose structure are shown in Fig. 2.19.

2.2.3.4 Derived Carbohydrates

A large number of important biological molecules are *derived sugars*. Examples are D-glucose-6-P and 2-deoxy-*N*-acetyl-D-glucosamine (NAG) (Fig. 2.20).

Many membrane proteins are covalently bound to sugars through alcohol groups of L-serine (see Fig. 2.21) and L-threonine residues and the amide nitrogen of L-asparagine.

Heparin is a derived polysaccharide that is a powerful blood anticoagulant. Its structure is depicted in Fig. 2.22.

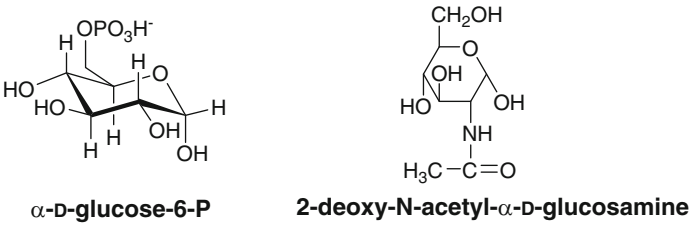

Fig. 2.20 Examples of derived sugars: α-D-glucose-6-P and 2-deoxy-*N*-acetyl-α-D-glucosamine (NAG)

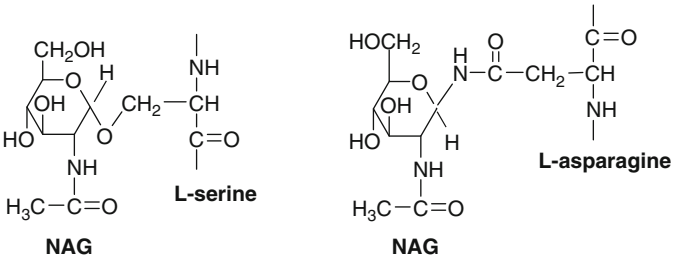

Fig. 2.21 NAG bound to a serine residue in a protein and through the amide group of an asparagine residue

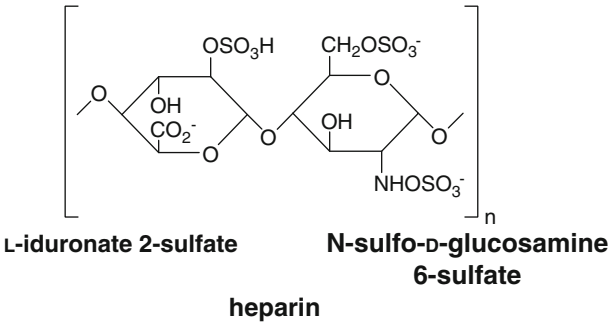

Fig. 2.22 The basic repeating unit in the heparin molecule

2.3 Lipids

Lipids, also known as fats, are biomolecules that are soluble in organic solvents but insoluble in aqueous solutions. They play essential roles in biological membranes in which they are the major components. All organelles from mitochondria to nuclei are surrounded by lipid membranes. They also play prominent roles in energy metabolism as components of adipose tissue. Finally, as hormones, they are essential to physiological regulation of cell metabolism.

There are a variety of compounds that fall into the lipid category. These include:

(a) Fatty acids
(b) Triacylglycerols
(c) Sphingolipids
(d) Phospholipids
(e) Glycolipids
(f) Lipoproteins
(g) Steroids and sterols
(h) Prostaglandins

2.3.1 Fatty Acids

Fatty acids are composed of a polar head (a carboxyl group) and a nonpolar aliphatic tail. Compounds that exhibit both polar and nonpolar properties are considered to be *amphiphathic*. There is essentially no free fatty acid in the cell; they exist either associated with other molecules, e.g., lipoproteins, or are short-lived metabolic intermediates. Fatty acids fall into two categories: saturated and unsaturated. Using 12 carbon atoms as the smallest fatty acid and 20 carbons as the largest, they are *lauric* (C_{12}), *myristic* (C_{14}), *palmitic* (C_{16}), *stearic* (C_{18}), and *arachidic* (C_{20}) (Fig. 2.23).

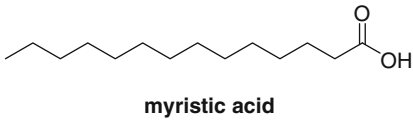

Fig. 2.23 Structure the saturated fatty acid myristic acid

Unsaturated fatty acids of physiological importance are *palmitoleic* (C_{16}; 16:1 *cis* Δ^9), *oleic* (C_{18}; 18:1 *cis* Δ^9), and *arachidonic* (C_{20}; 20:1 all *cis* Δ^5,Δ^8,Δ^{11},Δ^{14}). The nomenclature in parenthesis is self-evident, i.e., it lists the numbers of carbons in the fatty acid, the number and position of the double bonds, and the stereochemical relationship of the hydrogen atoms at the double bond (Fig. 2.24).

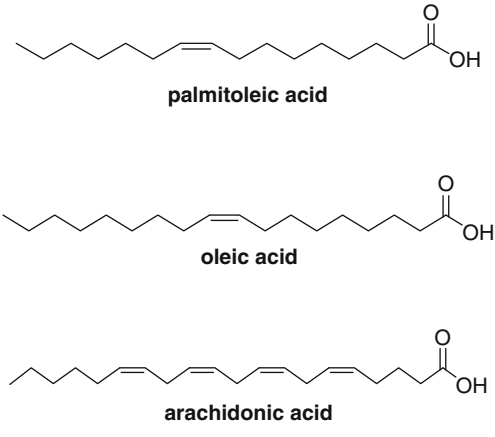

Fig. 2.24 Chemical structures of unsaturated fatty acids

2.3.2 Triacylglycerols

Triacylglycerols, also known as triglycerides and depot fats and stored as such in adipose tissue, are fatty acid esters of glycerol. A typical triacylglycerol is shown in Fig. 2.25

Note that C_2 of the substituted glycerol is chiral. The enantiomer illustrated is the prevalent form found in nature.

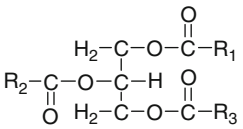

triacylglycerol

Fig. 2.25 The structure of triacylglycerol

2.3.3 Phosphoacylglycerols

Phosphoglycerols are glycerol esters of phosphoric acid. Examples of phosphoglycerols are shown in Fig. 2.26.

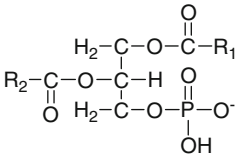

Phosphatidic Acid

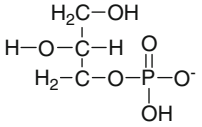

sn- glycerol-3 phosphate

Fig. 2.26 The structures of two phospholipids: phosphatidic acid and (2R)-2,3-dihydroxypropyl phosphate (*sn*-glycerol-3-P)

These molecules, like other phosphoglycerides, have a polar head and a hydrophobic tail. A number of important biological compounds are derivatives of *phosphatidic acid*.

These are represented by the structure in Fig. 2.27, where X is:

(a) Glycerol: $–CH_2–CHOH–CH_2OH$
(b) Ethanolamine: $–CH_2–CH_2–N^+H_3$
(c) Choline: $–CH_2–CH_2–N^+(CH_3)_3$
(d) Serine: $–CH_2–(CH–N^+H_3,CO_2H)$
(e) Inositol:

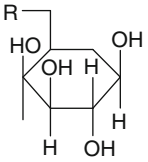

These compounds are referred to as phosphatidylglycerol, phosphatidylethanolamine, etc.

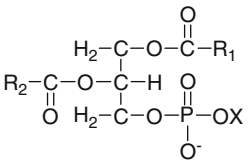

Fig. 2.27 Phosphatidic acid is where X = H. A variety of derivatives of phosphatic acid exist in nature

2.3.4 Sphingolipids

Sphingolipids are found in membranes and are derivatives of the base *sphingosine*. Note that the hydrogen atoms are *trans* at the double bond in sphingosine (Fig. 2.28).

Esterification of the hydroxyl group can occur to yield the compound *ceramide*, in which the R group of the fatty acid can vary from C_{16} to C_{20}. The concentration of ceramides in the cell is very low; they are precursors of other sphinolipids.

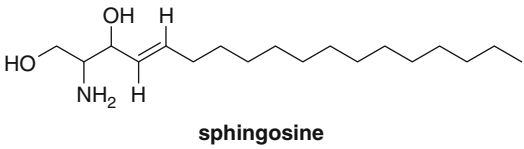

Fig. 2.28 The structure of the base sphingosine

2.3.4.1 Sphingomyelin

Note that the fatty acid is linked to the (Fig. 2.29) base in an amide linkage and also that sphingomyelin is a phospholipid.

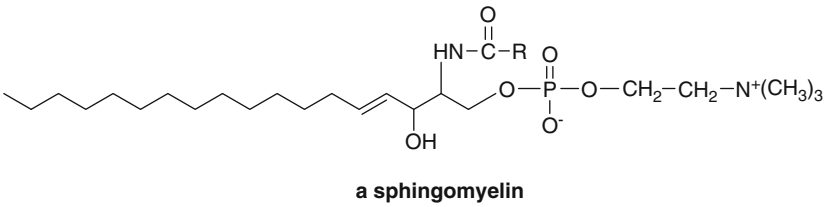

Fig. 2.29 Sphingomyelins are derivatives of sphingosine that contain a fatty acid and a phosphate ester

2.3.4.2 Cerebrosides

Cerebrosides are sphingolipids that contain sugars such as D-glucose or D-galactose (Fig. 2.30).

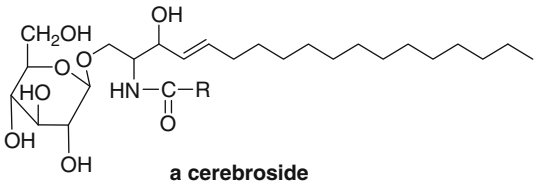

Fig. 2.30 Cerebrosides are derivatives of sphingosine that contain a fatty acid and a sugar

2.3.4.3 Gangliosides

Gangliosides are sphinoglipids that contain oligosaccharides rather than the monosaccharide as illustrated in the case of glucocerebrosides. They also contain *sialic acid*. The oligosaccharide portion of these molecules extends into the cytosol of the cell from the membrane anchor provided by the lipid moiety of the ganglioside and functions as hormone receptors.

2.3.5 Waxes

Waxes are esters of long-chain fatty acids and long-chain alcohols. Although the head of the wax is a polar (ester) group, it represents a small fraction of the remainder of the wax molecule which is hydrophobic. Waxes tend not to be permeable to water.

2.3.6 Terpenes

Terpenes are lipids formed by condensation of 2-methyl-1,3-butadiene (isoprene) resulting in long-chain unsaturated molecules (Fig. 2.31).

In the case of *cholesterol*, a linear terpene chain cyclizes to form a precursor of cholesterol. Cholesterol, a component of cell membranes in animals, is not found in plants.

Fig. 2.31 The structure of isoprene, the precursor of sterol and steroid structures

2.3.7 Sterols

Cholesterol is only one of the lipid compounds derived from terpenes. Others include testosterone (male sex hormone), estradiol (female sex hormone), cortisone (important in regulation of metabolism), and other sterols and steroids. Cholesterol is the precursor of many cellular sterols and steroids (Fig. 2.32).

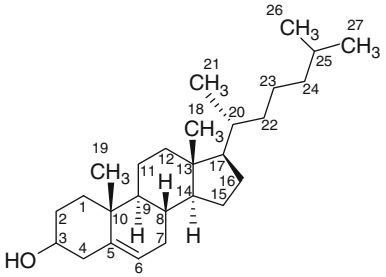

Fig. 2.32 The structure of the sterol cholesterol and its numbering system

2.3.8 Prostaglandins

Prostaglandins are hormone-like lipids that have a variety of physiological functions. But unlike hormones, which are transported throughout the body, prostaglandins function in the cells where they are synthesized. They were discovered by the Swedish scientist Ulf von Euler in the 1930s who believed that they originated in the prostate gland; hence the name prostaglandin. Their physiological roles involve control of blood pressure, smooth muscle contraction, and induction of inflammation. It is of interest that aspirin inhibits their biosynthesis. Prostaglandins are derivatives of the lipid prostanoic acid. They are synthesized in vivo from arachidonic acid. The structures of prostanoic acid and the prostaglandin PGH_2 are illustrated in Fig. 2.33.

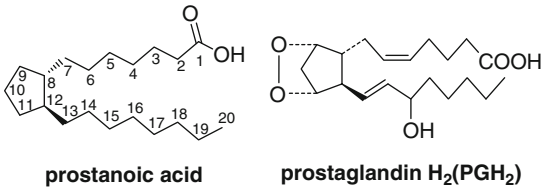

Fig. 2.33 Structures of prostanoic acid and prostaglandin H_2

2.3.9 Membranes

Lipids by definition are water insoluble; however, under certain conditions lipids and water are in fact miscible. Consider a typical water-insoluble fatty acid. At elevated

pH values, the fatty acid forms *soaps* with ions such as Na^+ and K^+. Fatty acids consist of a polar head and a hydrocarbon or nonpolar tail. Thus, salts of fatty acids are soluble in both polar and nonpolar solvents. These types of substances are called *amphiphatic* compounds, i.e., compounds with both polar and nonpolar components.

Amphiphatic substances form a number of different structures. Some of these structures are *monolayers*, *micells*, and *bilayers*.

1. A monolayer of lipid may form at the water–lipid interface (Fig. 2.34)
2. *Soaps* and *detergents* may form structures known as *micelles* when they reach a defined concentration in solution. This concentration of amphiphatic compound, known as the *critical micelle concentration* (CMC), is required before micelle formation can occur. The compounds that form micelles are made up of fatty acids with a single hydrophobic tail (Fig. 2.35)
3. *Lipid bilayers* may form from lipids that typically contain two hydrophobic tails. The most prominent members of this class are the sphingolipids and glycerophospholipids (Fig. 2.36).

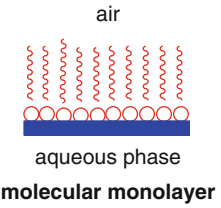

Fig. 2.34 Lipid monolayer illustrating the distribution of the fatty acids between the aqueous and gas (air) phases

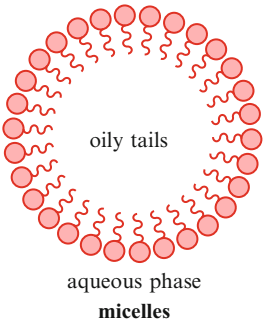

Fig. 2.35 The structure of a typical micelle illustrating the relationship between the fatty acids and the aqueous solution

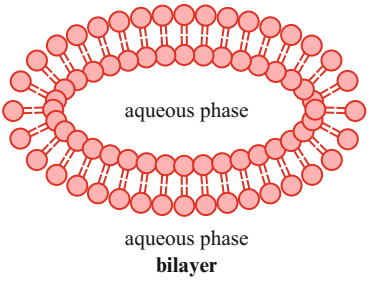

Fig. 2.36 The structure of a synthetic bilayer

Studies have indicated that the bilayer thickness is approximately 60 Å.
Lipid bilayers are structurally very similar to *biological membranes* and thus their properties have been studied extensively. Experimental bilayers, known as *liposomes*, have been prepared from phospholipids and sphingolipids by sonication.

4. Biological membranes will not be discussed in detail; however, simply stated, they are similar to liposomes in that they contain a lipid bilayer, but unlike liposomes they contain two types of proteins. One, the *integral proteins*, are embedded in the bilayer and the other, the *peripheral proteins*, are associated either with the surface of the bilayer or with the integral protein itself. Miscellaneous lipids such as cholesterol are also components of biological membranes and affect its fluidity (Fig. 2.37).

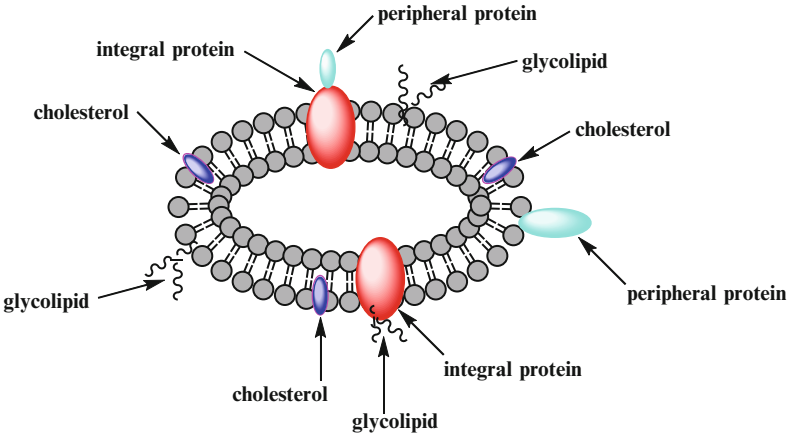

Fig. 2.37 Cartoon of a cell membrane and its many components. The basic structure of the cell membrane is the lipid bilayer

2.4 Nucleotides

Like amino acids which are the building blocks of proteins, nucleotides are the building blocks of the nucleic acids, RNA and DNA. Aside from these major biological roles, nucleotides are important players in energy metabolism, coenzymes, and intermediary metabolism.

Nucleotides are composed of a *nitrogenous base*, a *sugar*, and a *phosphoryl group*. Removal of phosphoryl group results in a compound known as a *nucleoside*.

There are two types of bases found in nucleotides, *purines* and *pyrimidines*. The sugars are either D-*ribose* or *2-deoxy*-D-*ribose*.

2.4.1 The Bases

2.4.1.1 Purines

Fig. 2.38 Purine and its numbering system

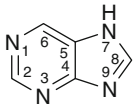

purine

There are two purine bases, *adenine(A)* and *guanine(G)* (Fig. 2.39).

Fig. 2.39 Guanine and adenine are both derivatives of the base purine

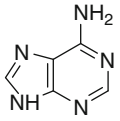

Adenine

6-aminopurine

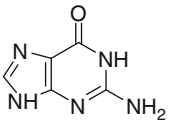

Guanine

2-amino-6-oxopurine

2.4.1.2 Pyrimidines

Fig. 2.40 The structure of pyrimidine along with its numbered atoms

pyrimidine

There are three pyrimidine bases, *uracil(U)*, *cytosine(C)*, and *thymine(T)*.

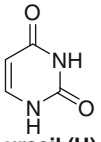

uracil (U)

2,4-dioxo pyrimidine

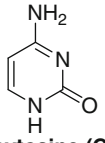

cytosine (C)

2-oxo-4-amino pyrimidine

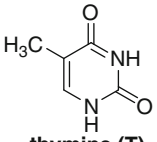

thymine (T)

2,4-dioxo-5-methyl pyrimidine

Fig. 2.41 The pyrimidine bases, uracil, cytosine, and uridine are derivatives of pyrimidine

2.4.2 The Sugars

The sugars found in nucleotides are D-*ribose* and *2-deoxy*-D-*ribose* (Fig. 2.42).

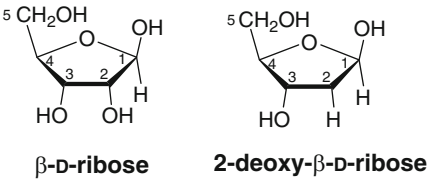

Fig. 2.42 The structures of D-ribose and 2-deoxy-D-ribose and their numbering systems

2.4.3 The Nucleosides

Examples of nucleosides which consist of either a purine or pyrimidine base and a sugar are illustrated in Fig. 2.43.

2.4.3.1 Structures

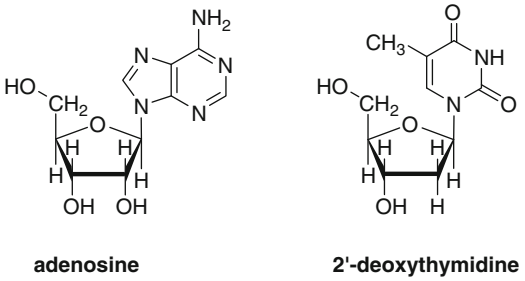

Fig. 2.43 The nucleosides, adenosine and thymidine. Note that besides the two different bases the sugars are also different

2.4.3.2 Nomenclature and Numbering the Bases and Sugars

The bases are numbered as illustrated in Figs. 2.38 and 2.40; however, the sugars when part of nucleosides or nucleotides have primed numbers, e.g., 5′.

Base	Nucleoside
Adenine(A)	Adenosine
Guanine(G)	Guanosine
Uracil (G)*	Uridine
Cytosine(C)	Cytidine
Thymine(T)**	Thymidine

*Uracil is found exclusively in RNA
**Thymine is found exclusively in DNA

2.4.4 *The Nucleotides*

Abbreviations are used to describe the various nucleotides, e.g., guanosine-5′-monophosphate, -diphosphate, and -triphosphate are referred to as GMP, GDP and GTP, respectively. Analogous deoxyribonucleotides are dGMP, dGDP, and dGTP.

Note that the linkage between the sugars and the purine bases is β1′ → 9, and between the pyrimidine bases and the sugar, β1′ → 1. The phosphoryl groups, in the case of a nucleoside-5′-triphosphate such as GTP, are labeled α, β, and γ. The γ phosphoryl is farthest from the ribose and the α, closest to the sugar (See Fig. 2.44).

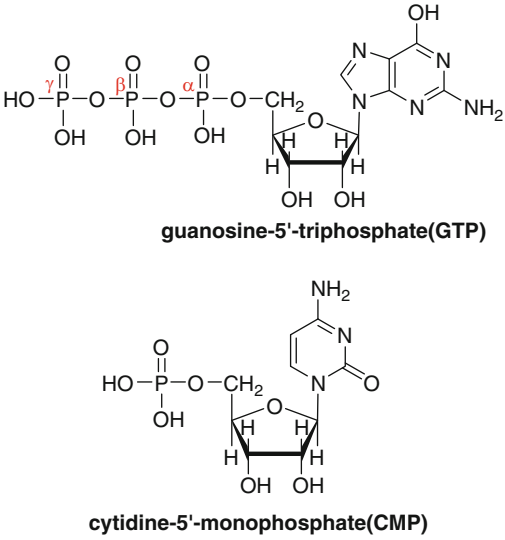

Fig. 2.44 The structures of the nucleotides GTP and CMP along with the numbering of the phosphoryl groups

2.4.4.1 *Syn* and *Anti* Conformations of Nucleosides and Nucleotides

Nucleosides and nucleotides can exist in one of two conformational states with the nitrogenous bases relative to the sugars. Although not at all clear in two-dimensional drawings, there is steric hindrance to free rotation around the bond connecting the sugars and the bases. These two conformations are *syn* and *anti* and are depicted in Fig. 2.45. In the *syn* conformation the base lies directly above the sugar, whereas in the *anti* conformation, positions 1, 2, and 6 of the purine ring are away from the sugar. Similarly, in the *anti* conformation, positions 2 and 3 of the pyrimidine ring lies away from the sugar.

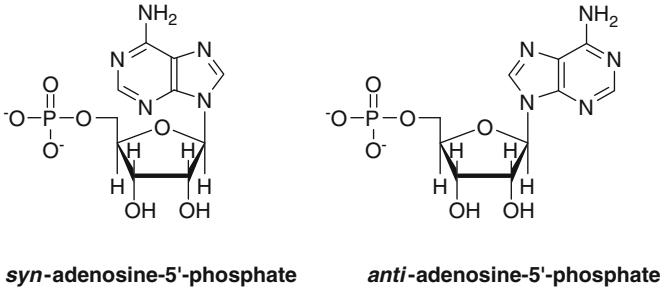

Fig. 2.45 The *syn* and *anti* forms of AMP

2.4.4.2 Tautomerism

The nitrogenous bases in nucleosides and nucleotides, with the exception of adenine and adenosine, undergo enol–keto tautomerism. Studies have shown that the predominant species in solution is the keto form. Examples are uracil and guanine (Fig. 2.46).

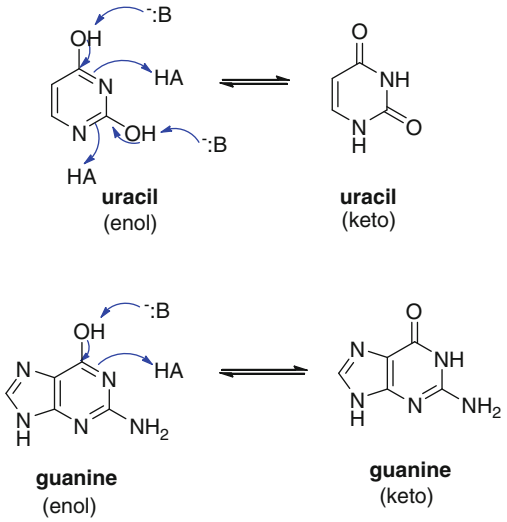

Fig. 2.46 Examples of tautomerism that occur with purines and pyrimidines. HA and B represent an acid and a base, respectively

Reference

1. Van't Hoff JH (1875) La chimie dan l'espace, P.M. Bazendijk, Rotterdam

Further Readings

Hudson CS (1941) Emil Fischer's discovery of the configuration of glucose. A semicentennial retrospect. J Chem Edu 18:353–357
Hudson CS (1953) The basic work of Fischer and Van't Hoff in carbohydrate chemistry. J Chem Educ 30:120–121

Chapter 3
Protein Structure and Function

The relationship between protein structure and function is the key interface between chemistry and life. The forces that dictate dynamic biochemical reactions inside cells more often involve transient weak molecular interactions than changes in covalent bonding. Just as two Lego's are held together by collective weak forces that work synergistically because of the complementary shape of the bocks, biological macromolecules use specific shapes to organize their collective weak chemical forces to direct molecular interactions. Thus, molecular shape is a principal determinant of biochemistry. The class of biomolecules called proteins provide an extremely diverse set of shapes, which form structures conferring activities ranging from chemical catalysis to the scaffolding that structures cells (Fig. 3.1). The diversity of protein structures is a direct result of the large variation in amino acid content and polymer length dictated by the coding regions of our genomes. This chapter will introduce amino acid polymerization and the forces that drive protein folding and structure.

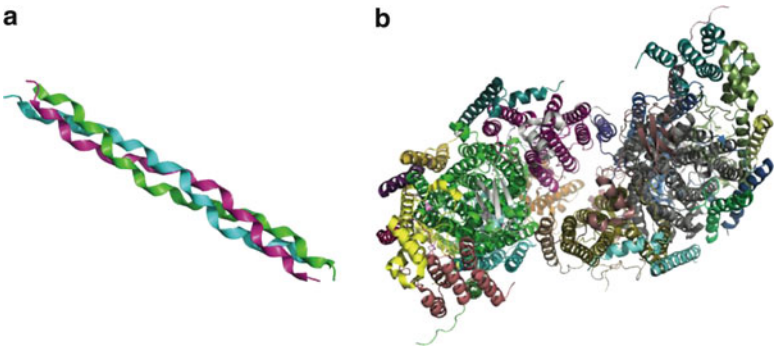

Fig. 3.1 The structures of the proteins collagen **(a)** and cytochrome oxidase **(b)** display diverse folds and degrees of complexity. Collagen is a structural protein found in mammalian connective tissue and skin, making up as much as 35% of the body weight in some species. Cytochrome oxidase is the enzyme that uses oxygen in the process of making ATP in the mitochondria

H.J. Fromm and M.S. Hargrove, *Essentials of Biochemistry*,
DOI 10.1007/978-3-642-19624-9_3, © Springer-Verlag Berlin Heidelberg 2012

3.1 Proteins Are Polymers of Amino Acids, Characterized by Four "Levels" of Structure

Proteins are polymers resulting from the formation of an amide bond between the carboxylic acid of one amino acid and the amino group of another (Fig. 3.2). Formation of this bond, called the peptide bond, requires energy but is very stable (with a half life of years) once formed. Peptide bond formation converts the

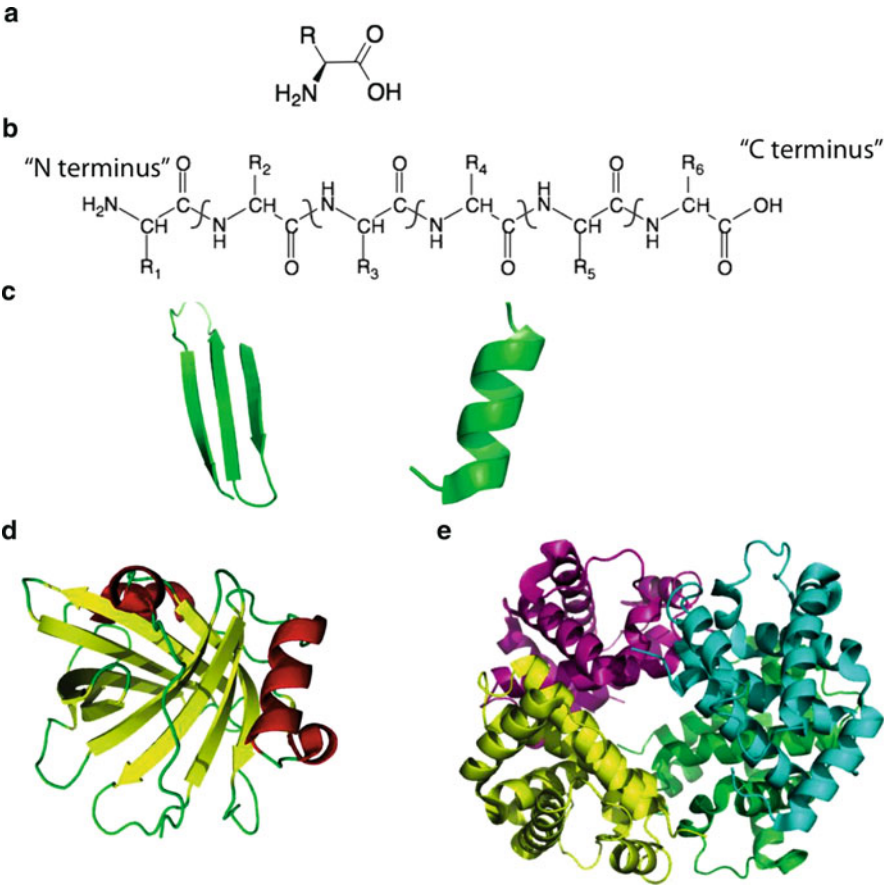

Fig. 3.2 (**a**) Proteins are polymers of amino acids. (**b**) Bonds between the carboxylic acid functional group of one amino acid and the amino group of another, called peptide bonds, allow amino acids to polymerize into sequences described as the "primary" structure of proteins. (**c**) The "secondary" structure of proteins describes common folds stabilized by localized amino acids within the polymer, including alpha helices (*left*) and beta sheets (*right*). (**d**) The "tertiary" structure of proteins results from the three-dimensional folding of the polymer, including the localization of secondary structural elements and the loops and turns that connect them. (**e**) "Quaternary" protein structure results from the combination of multiple polymer chains coming together in the folded protein

participating amino and carboxylic acids into amide and carbonyl groups no longer capable of rapidly exchanging protons with solvent water molecules. The order in which the amino acids are polymerized, called the primary structure of the resulting protein, is dictated by the cognate gene sequence and is assembled on the ribosome during translation. Because polymerization results from two different function groups, proteins have directionality and are usually written from the amino (N) to the carboxy (C) ends in reference to the remaining terminal function groups not participating in peptide bonds. The linkage of bonds consisting of the peptide bond, the Cα–CO, and the Cα–N, which constitute the continuous polymer are often referred to as the "main chain" of the protein.

Based on the interactions of the protein with its environment, the polymer will fold to maximize energetically favorable interactions with itself and the solvent. Local regions of common structures result from stabilizing interactions between amino acids proximal to one another in the primary structure. These structures, referred to as secondary structural elements, include alpha helices and beta sheets, which are stabilized through hydrogen bonding interactions between main chain carbonyl and amide functional groups (described below). The folding process continues with the packing of secondary structural elements, linked by loops and turns of amino acids, to give rise to the tertiary structure of the protein, defined as the three-dimensional structure of a single polypeptide chain. Many proteins are active in their tertiary structures, but others join together with one or more additional chains to form complexes containing multiple protein subunits. This level of structure is called "quaternary" structure, and can result from the same protein chain interacting with itself (referred to as having "homo" subunits), or from different chains coming together ("hetero" subunits). Protein quaternary structure is often mediated through weak force (noncovalent) interactions, but can also involve disulfide bonds between chains, usually in proteins that are found outside the cell.

3.2 The Protein "Main Chain" Controls Conformational Flexibility

There are three bonds that constitute the main chain of a protein: the peptide bond (N–CO), Cα–CO, and the Cα–N (Fig. 3.3). The peptide bond does not rotate because of double-bond character associated with the resonance structure of the amide bond. In fact, the peptide bond length is 1.33 Å, much closer to the value for the C–N double bond (1.27 Å) than that for the C–N single bond (1.49 Å), indicating that the double-bond resonance form is the predominate one. Because there is no rotation about the peptide bond, six atoms of the main chain are held in plane with one another: the two adjacent Cα atoms, the amide N and its proton, and CO of the peptide bond with its carbonyl oxygen.

Lacking the ability to rotate, the peptide bond is fixed into one of two potential conformations with respect to the locations of the flanking Cα atoms (Fig. 3.4).

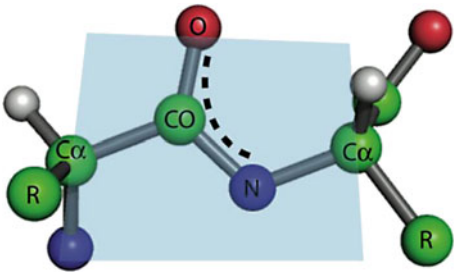

Fig. 3.3 The main chain bonds of a protein. The peptide bond does not rotate, keeping the two adjacent Cα atoms and the three atoms of the peptide bond in a plane

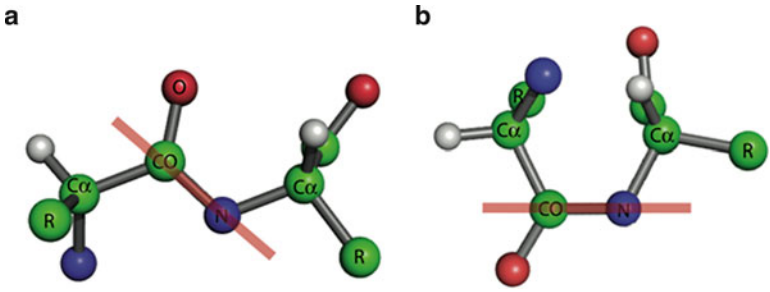

Fig. 3.4 (**a**) *Trans* and (**b**) *cis* peptide bonds. In the *cis* conformation, the functional groups on each alpha carbon experience increased steric hindrance. As a result, the vast majority of peptide bonds in proteins are *trans*. The only exceptions to this rule are proline, which experiences equal degrees of steric hindrance in both conformations, and glycine, which lacks a bulky R group

In the *trans* conformation, with the Cα atoms on opposite planes of the peptide bond, there is little steric hindrance between the R groups, amide nitrogens, and carbonyl carbons of the adjacent amino acids. The *cis* conformation, however, forces these atoms together, and therefore much less likely to be adopted. Greater than 95% of the peptide bonds in proteins are in *trans* conformations, with the exception of glycine and proline. Glycine lacks a bulky R group, and the conformationally restricted imide bond of proline experiences similar degrees of steric hindrance in both conformations, and thus is equally likely to occupy either one.

If the two adjacent Cα atoms of each peptide are fixed in a plane, how does the protein main chain have any flexibility? The answer lies in the other two bonds making up this polymer (Fig. 3.5). The single bonds between the Cα–N and Cα–CO can rotate, and have rotational bond angles defined as phi (ϕ) and psi (ψ), respectively. The effect of rotation about these bonds is that the planes of atoms defined by the peptide bonds have various "dihedral" angles between them, allowing the protein polymer to bend at each Cα–N and Cα–CO bond. Thus, even though the peptide bond is relatively rigid, rotation about the phi and psi bond angles allows the peptide to adopt a potentially large number of conformations.

In reality, phi and psi bond angles cannot adopt all combinations of values, but are restricted to combinations that avoid steric hindrance between R groups, amide

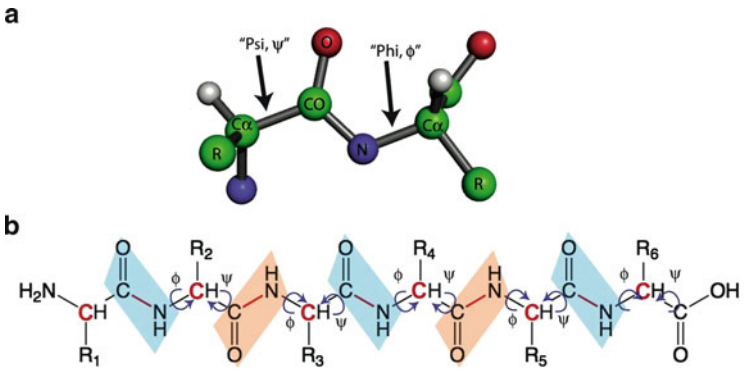

Fig. 3.5 (**a**) The phi and psi bonds of the main chain. Rotation about these bonds results in the protein polymer existing as a chain of planes, defined by the peptide bonds, with "dihedral" angles between them

nitrogens, and carbonyl oxygens. The great Indian biophysicist Gopalasamudram Narayana Ramachandran, using van der Waal's radii, the known bonding pattern of the protein main chain, and the geometries of organic bonds, made a predictive calculation of the allowed phi and psi bond angle combinations several years before the first atomic resolution protein structure was measured (Fig. 3.6). The resulting "Ramachandran plot," shows that the "allowed" phi and psi combinations in proteins are actually fairly limited, greatly reducing potential conformational flexibility. History has proven Ramachandran to have been correct; the tens of

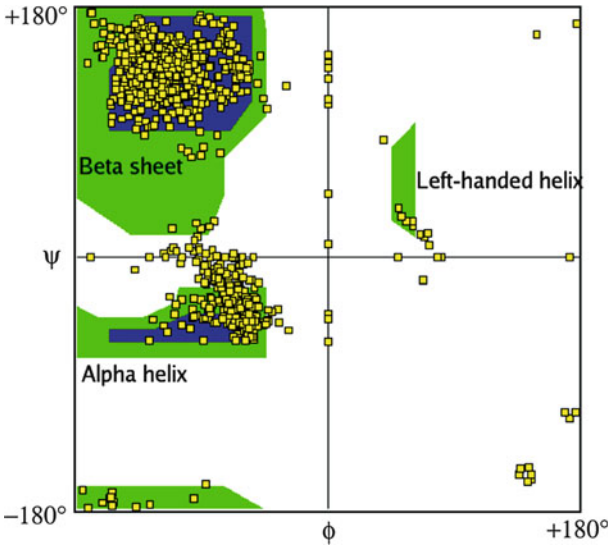

Fig. 3.6 The Ramachandran plot shows the allowed combinations of the phi and psi bond angles in proteins

thousands of protein structures solved to date show very few deviations from Ramachandran's predictions. In fact, Ramachandran geometry is considered to be an important check on newly-solved protein structures. Phi and psi combinations that lie outside the allowed regions of the Ramachandran plot are always subjected to scrutiny.

3.3 Common Secondary Structural Elements the Alpha Helix and the Beta Sheet

As the primary structure of a polypeptide collapses into allowed phi and psi combinations, there are some structures that are commonly adopted. These structures, the alpha helix and the beta strand, are considered "secondary" structure because they are often subelements of proteins that are packed together to form higher order structures, and because they are often stabilized through hydrogen bonding interactions between amino acids that are nearby in the primary structure.

The alpha helix is a very common secondary structural element stabilized by hydrogen bonding between main chain carbonyl oxygens and amide protons (Fig. 3.7). In the alpha helix, every carbonyl oxygen and amide proton are involved in a stabilizing hydrogen bonding interaction. Each carbonyl oxygen hydrogen bonds with the amide nitrogen of the fourth amino acid down the polymer.

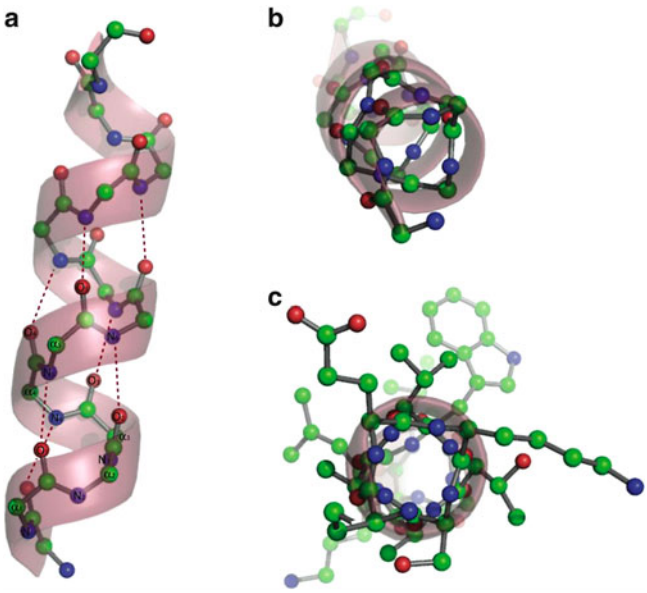

Fig. 3.7 The alpha helix. (**a**) The helix is stabilized by hydrogen bonding between the n to $n + 4$ carbonyl oxygen and amide nitrogen. (**b**) The helix is right-handed, with R groups radiating out from the helical axis (**c**)

The conformation necessary for this interaction is in the favorable region of Ramachandran space (Fig. 3.6). The resulting helix is right-handed, with the R groups pointing outward from the helical axis. In this way, the nature of the R groups themselves are not needed to stabilize the helix, although beta-branched amino acids and ones with small polar R groups tend to destabilize the alpha helix slightly more than the others.

Beta sheets are another common secondary structural element (Fig. 3.8). Beta sheets are made from beta strands, which are peptides with phi and psi angles extended at −180 and +180°, respectively. This creates a regular pattern of amide hydrogens and carbonyl oxygens pointing in the same direction, and perpendicular R groups, which alternate up and down on the strand. Like alpha helices, beta strands have directionality defined by the N and C termini of the protein. The stabilizing force for beta strands comes from interactions between more than one strand, forming beta "sheets." Beta sheets are held together by hydrogen bonding between the amide hydrogens and carbonyl oxygens across strands, made possible

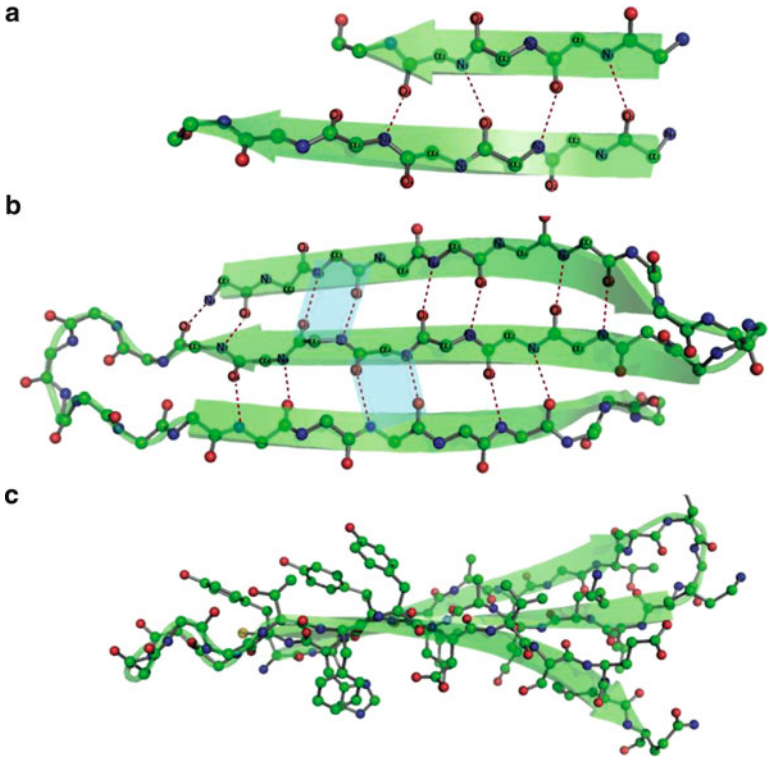

Fig. 3.8 Beta sheets. (**a**) The hydrogen bonding pattern in parallel beta sheets. (**b**) The hydrogen bonding pattern in antiparallel beta sheets. (**c**) The R groups are perpendicular to the amide hydrogens and carbonyl oxygens of the strand, and to the sheet

by the common direction of these functional groups on each strand, and the fact that the perpendicular R groups do not interfere with sheet formation.

Beta sheets can form from parallel or antiparallel strands. A defining distinction between the two is evident from the hydrogen bonding patterns between the strands. In antiparallel sheets, the hydrogen bonding capacity of an amino acid is met by a single amino acid on an adjacent strand (i.e., amino acids hydrogen bond in pairs). In parallel strands, the hydrogen bonding potential of the main chain of one amino acid requires an amide hydrogen and carbonyl oxygen from different amino acids on the adjacent strand. Beta sheets can consist of multiple strands, running parallel and antiparallel within the same sheet.

3.4 Tertiary Structure: Proteins Exhibit Common Folds

The folding of the polypeptide into a stable three-dimensional structure gives rise to the "tertiary" structure of proteins. This reaction is driven by the hydrophobic effect, which strives to burry hydrophobic protein surface area, to maximize constructive polar interaction between protein functional groups and water, and to minimize the ordering of water at the protein/solvent interface.

There are currently over 60,000 protein structures that have been measured using X-ray crystallography and NMR spectroscopy. However, not all of these are unique in shape. Many proteins, even with distinct functions, have shapes and folding patterns that are very similar. Thus it is believed that the number of protein folds is certainly much smaller than the number of sequences possible with 20 different amino acids, and probably limited to several hundred or a thousand different scaffolds that serve as stable housing for all of the unique active sites found in the proteins found in living organisms.

Several of these are shown in Fig. 3.9. Some are predominately helical or made of beta sheets, but many contain both types of structural elements folded into three dimensions by the inclusion of peptide loops and turns that bring the secondary structural elements together to form tertiary structure. A common feature of these folds is that, for water-soluble proteins, there are more amino acids with polar side chains on the surface, and more hydrophobic side chains in the interior (Fig. 3.10). This is of course a natural consequence of the hydrophobic effect driving the folding reaction, and an example of the power of collective weak forces in organizing macromolecular structure. One exception to this observation are membrane proteins, like porins, which have hydrophobic amino acids on the surface, which is imbedded in the hydrophobic cell membrane, and often have polar ones lining the inside pores if aqueous molecules pass through their channels. In this case the exception obviously supports the rule, as the protein fold is responding to the environment in which it must be stable.

Protein tertiary structures, particularly in eukaryotic organisms, often fold into discrete domains. Many enzymes that carry out multistep reactions, or binding domains that work in concert, can co exist on one polypeptide chain by folding into

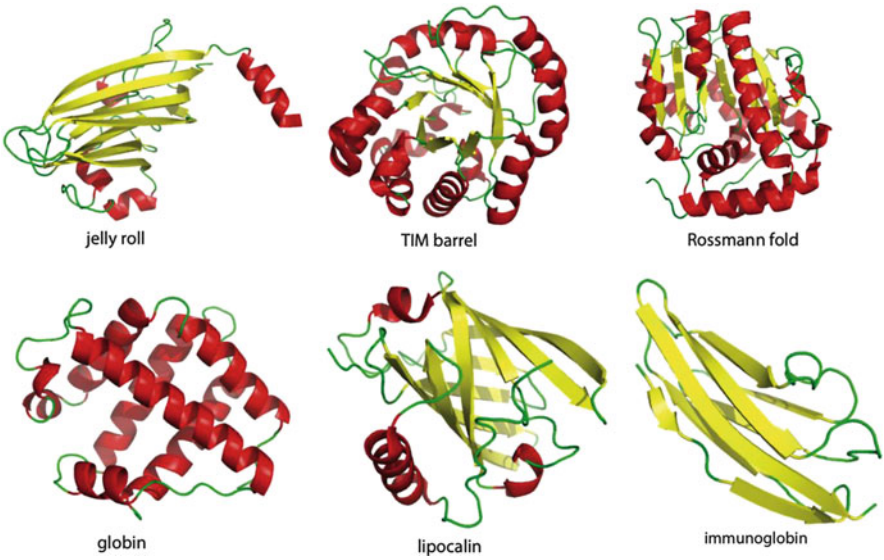

Fig. 3.9 Some common protein folds

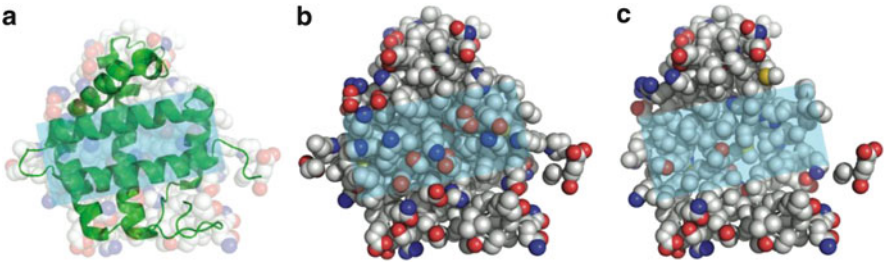

Fig. 3.10 (**a**) The structure of a globin reveals many polar groups (blue and red) on the surface. (**b**) If the surface is removed to reveal the inside of the protein, (**c**) there are predominately amino acids with hydrophobic side chains (grey) present

individual domains that are tethered together by short stretches of peptide. Domain structures are thought to result from the combination of gene products that work together toward a common goal into single coding regions.

An example of an enzyme with discrete domains is flavohemoglobin, which detoxifies nitric oxide (Fig. 3.11). This enzyme uses the "nitric oxide deoxygenase" reaction to convert nitric oxide to nitrate. This reaction requires oxygen binding, followed by reaction of nitric oxide with the oxygenated complex. The resulting ferric hemoglobin must be reduced to the ferrous state to continue the reaction. Flavohemoglobin has evolved a hemoglobin domain to bind oxygen and react with nitric oxide, and a flavoprotein domain to reduce the hemoglobin.

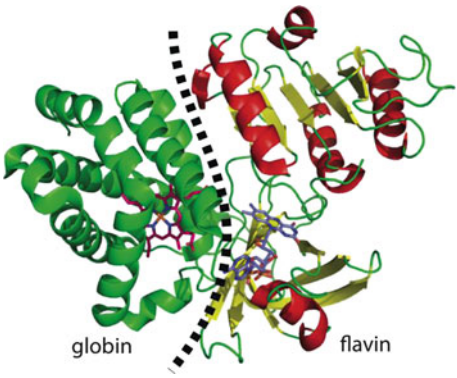

Fig. 3.11 Flavohemoglobin, a protein with two discrete folding domains. The hemoglobin domain is shown in *green*, and the flavoprotein in *red*. The *dashed line* shows the interface between the two domains

3.5 Quaternary Structure

Quaternary structure results from the combination of individual polypeptide chains into larger proteins with multiple subunits. The complexity of quaternary structure can range from homodimeric proteins, to large complexes making up viral coats, to megadalton combinations of protein and nucleic acid that constitute organelles like the ribosome. The forces that hold subunits together are the same that drive protein folding in the first place: multiple weak forces and the hydrophobic effect. Most proteins with quaternary structure are held together by buried hydrophobic surface at the subunit interfaces in combination with precisely placed electrostatic interactions. The special arrangement of hydrophobic and electrostatic regions on the subunit surface complement each other like pieces of a puzzle.

Sometimes quaternary structure is stabilized through disulfide bonds between subunits. This is relatively common in extracellular proteins which must remain intact outside of the protein-concentrated, controlled environment of the cell. Classic examples of these molecules include insulin and other peptide hormones, and many proteolytic enzymes.

3.6 What Are Protein Structures and How Are Protein Structures Measured?

All of the images we have seen in this chapter are artist's renditions of the structures of proteins. Are alpha helices and beta sheets really flat ribbons? Clearly not, but these representations are useful for helping students learn the important elements of the structures. All images of protein structures start as files containing the three-dimensional coordinates of every atom in the molecule. These coordinates are measured experimentally, and stored for use by scientists in the "Protein Data Bank," along with the file designation "pdb" (Fig. 3.12). These atomic coordinates can then be plotted and rendered artistically in many different ways, leading to the

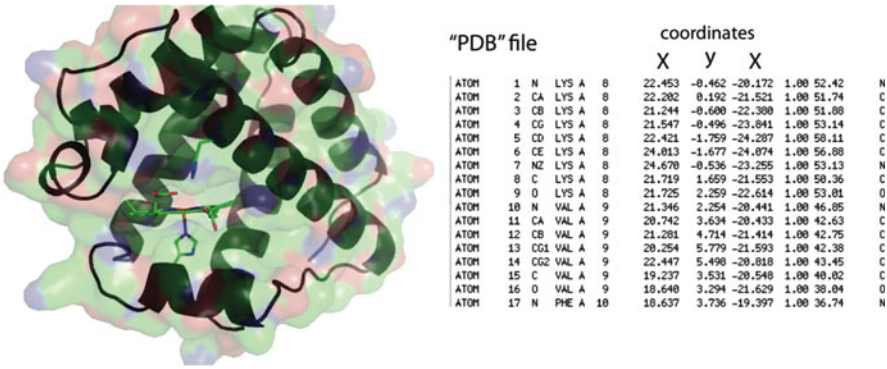

Fig. 3.12 Protein structures are artist's renditions of the molecular coordinates from a "pdb" file

wealth of molecular images that adorn the covers and pages of biology and biochemistry texts.

The first atomic resolution protein structure to be measured was that of myoglobin from sperm whale, in 1957. John Kendrew and Max Perutz received the 1962 Nobel Prize in chemistry for this contribution, and that of the first structure of red blood cell hemoglobin published in 1960. The technique of X-ray crystallography was used to measure these structures, and is still the technique most often used to solve new structures today. Two big problems that faced the first structural biologists were how to resolve objects as close together as organic chemical bonds (on the order of 1.5 Å), and how to prevent rotational averaging of the molecule during data collection.

The first problem concerns the fact that radiation used to resolve objects cannot be much longer in wavelength than the size of the objects to be resolved. For example, our eyes use visible light (~500 nm in wavelength) to see objects down to the size of ~1/10 of a millimeter. At that point, our retinas become limiting, but if we use a light microscope for magnification, we can see objects down to ~1 μM (approximately twice the wavelength of visible light). At that point, however, visible light can no longer resolve smaller objects. To resolve objects on the order of 1.5 Å, we need radiation with a wavelength near or shorter than this. X-rays, which are easy to produce and relatively inert, meet this need.

When molecules are present in solution, they exist in all manners of rotation and translation throughout the container. If such molecules were exposed to X-rays, the image taken would reveal rotationally averaged, lacking high-resolution information about the relative locations of each atom. To achieve this level of imaging, the molecules must be fixed into one or a small number of orientations. This requirement is met by the use of single crystals for X-ray diffraction studies. Molecules in the crystalline form are fixed in place in a regular, repeating fashion, facilitating atomic resolution imaging.

In the X-ray diffraction experiment, patterns of scattered X-rays from the protein crystal are compared to calculations of those that would result from potential structures inside the same crystal lattice. Good correlation between predicted and

observed scattering indicates an accurate structure. Once a source of high-concentration (usually millimolar), pure sample is available, the limit to the ability to solve macromolecular structures by X-ray crystallography is growing diffraction quality crystals. There are no limits brought by molecular size or complexity.

The other technique suitable for measuring atomic resolution structures of macromolecules is nuclear magnetic resonance (NMR) spectroscopy. NMR spectroscopy takes advantage of the fact that the unique molecular environment of each nucleus can be measured, and leaves a measurable fingerprint on neighboring nuclei. NMR experiments can measure these interactions to provide a collection of distance restraints that exist among the nuclei in the molecule. The process of solving the structure using NMR involves computationally manipulating the collection of bonded atoms into different conformations until one matching the observed contacts is found. Advantages of NMR for molecular structure solution include the ability to work in solution rather than the crystalline state, but there is a limit of approximately 50 kDa to the molecular size that can be studied at atomic resolution.

3.7 Hemoglobin: An Example of Protein Structure and Function

Prior to the development of recombinant genetic techniques, biochemists (and particularly structural biologists) were left to study proteins that were naturally available at relatively high concentrations. These included molecules that one could "grind and find," meaning that purification must have started from natural sources and tissues. One of these proteins is red blood cell hemoglobin (Fig. 3.13). Physiological studies had previously revealed that the function of hemoglobin is

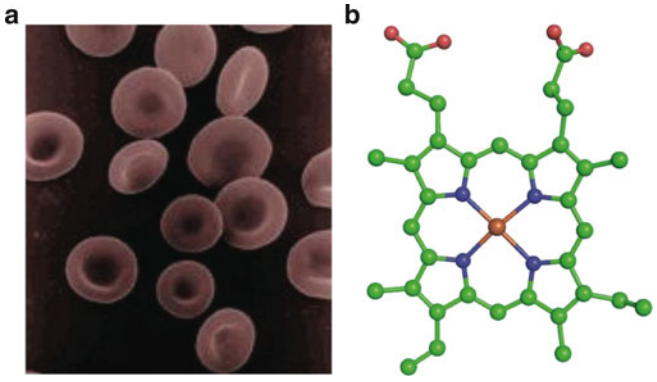

Fig. 3.13 (**a**) Red blood cells contain high (>30 mM) concentrations of the protein hemoglobin, which transports oxygen in mammals. The *red* color comes from the heme prosthetic group (**b**), which contains an iron atom (shown in *brown*) responsible for most of the color

oxygen transport, and the tools used to study protein structure and function were developed largely with the goal of learning how hemoglobin structure confers this function.

Unlike most enzymes, hemoglobin does not catalyze chemical reactions as part of its principal natural function. It simply binds and releases oxygen; it binds in the lungs where oxygen is plentiful, then releases it to tissues that would not otherwise have access to oxygen. Thus, while it is not catalyzing net chemical reactions, it is catalyzing oxygen transport. Under the simplest circumstances, the reversible binding of oxygen (O_2) to a protein (P) can be described by the following equation.

$$P + O_2 \rightleftharpoons PO_2. \tag{3.1}$$

The dissociation equilibrium constant for the reaction is:

$$K = \frac{[\mathrm{P}][\mathrm{O}_2]}{[\mathrm{PO}_2]}. \tag{3.2}$$

If we are interested in measuring the fraction of protein bound to oxygen at different oxygen concentrations, we can define the "fractional saturation" of protein as:

$$Y = \frac{[\mathrm{PO}_2]}{[\mathrm{P}] + [\mathrm{PO}_2]}. \tag{3.3}$$

Equation (3.3) will be zero if no oxygen is bound, and 1 if all of the protein is oxygenated. If we substitute for PO_2 in (3.3) with (3.2), we get the following expression for fractional saturation as a function of oxygen concentration and K.

$$Y = \frac{[\mathrm{O}_2]}{[K] + [\mathrm{O}_2]}. \tag{3.4}$$

Equation (3.4) tells us that the degree to which our protein is saturated with oxygen depends on the dissociation equilibrium constant and the oxygen concentration, both of which have units of concentration. A convenient way to think about (3.4) is to set $Y = 0.5$. At this value, K must be equation to oxygen concentration. Thus, K is the oxygen concentration at which P will be half-saturated.

The shape of the binding curve resulting from (3.4) is shown in Fig. 3.14a, using as an example hemoglobin with a value of $K = 26$ Torr (that of red blood cell hemoglobin).

(Torr is a unit of pressure measured by the level of mercury in a manometer. It can also be used as a unit of concentration for oxygen, along with the known value for oxygen solubility, as it reflects the oxygen concentration in solution

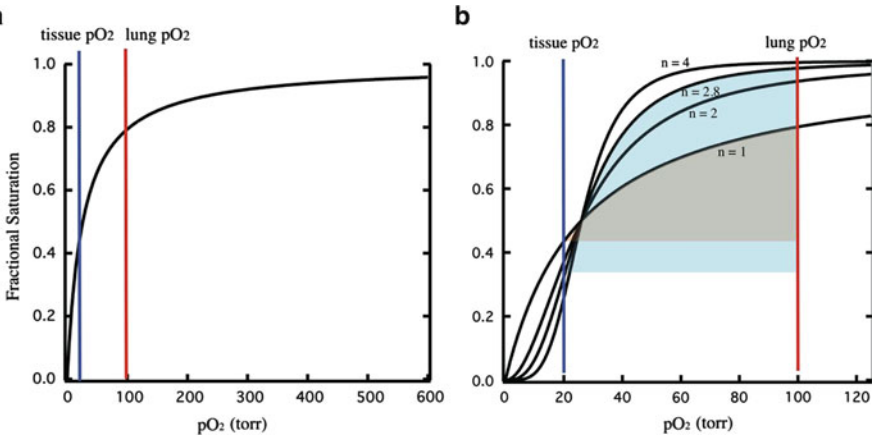

Fig. 3.14 (**a**) Oxygen binding to a monomeric protein (like Mb), and (**b**) a protein with various degrees of cooperativity. In each case, binding *curves* are calculated with the dissociation equilibrium constant K set to 26 Torr (the value for red blood cell hemoglobin). In (**b**), (3.3) is used, and in (**c**) (3.5) is used with various values of n. The *shading* in (**b**) indicates the amount of oxygen transported by the protein with $n = 2.8$ (the value for hemoglobin), and for $n = 1$ (the value for noncooperative protein)

at a given pressure. By saying that $K = 26$ Torr, we mean that at a gas pressure equal to 26 Torr, hemoglobin will be half-saturated with oxygen. As 760 Torr is atmospheric pressure at sea level, one can tell that hemoglobin would be saturated at this concentration.)

For this protein, half saturation is achieved at 26 Torr, as expected from (3.4). However, saturation to >90% requires several hundred Torr, revealing a shallow binding curve. In fact, as a transporter between the lungs and tissues, only a relatively small (38%) amount of oxygen would be transported.

Oxygen binding to hemoglobin, however, does not obey (3.4). Instead, the binding curve is much sharper, allowing for efficient transport between the lungs and tissues (66%). Deciphering the structural mechanism for oxygen transport has been a great achievement for biochemists. The principal feature of hemoglobin contributing to its sharp oxygen binding curve is the fact that it is a tetramer, made of two α and two β subunits, containing a total of four binding sites for oxygen (Fig. 3.15). The structure of each subunit is very similar to the monomeric oxygen storage protein, myoglobin, found in muscle tissue. Each has a single heme prosthetic group wrapped into a globin fold. But the surfaces of α and β subunits are modified for the formation of quaternary structure.

Having multiple binding sites presents the possibility of cooperative oxygen binding, wherein binding of the initial molecule or molecules affects the affinity of binding to subsequent sites. Such a model is described by a slight modification of (3.1):

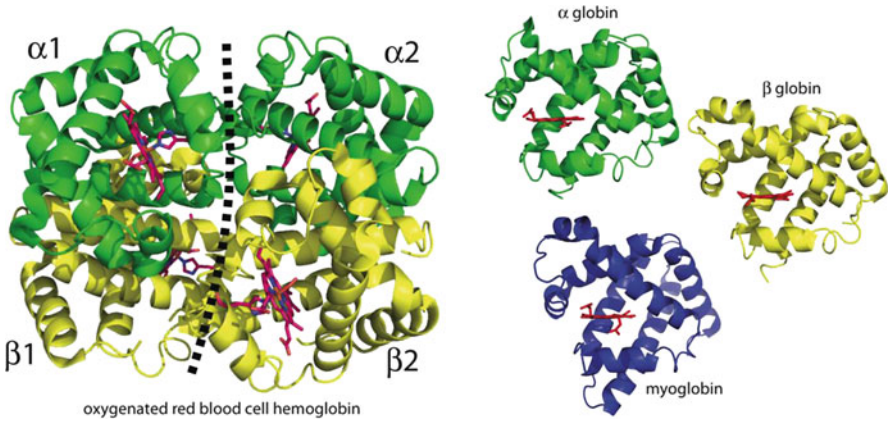

Fig. 3.15 The structure of hemoglobin is a heterotetramer composed of two α and two β subunits. These are arranged as a "dimer of dimers," in which the α1β1 and α2β2 dimers are symmetric. Each subunit is a myoglobin-like protein with a heme prosthetic group capable of reversible oxygen binding

$$nP + nO_2 \leftrightharpoons PO_2^n. \tag{3.5}$$

In this case, n is the number of binding sites for oxygen on P. Treatment of (3.5) in the same manner as (3.1) leads to an expression for fractional saturation under these conditions.

$$Y = \frac{[O_2]^n}{[K] + [O_2]^n}. \tag{3.6}$$

Plots of (3.6) with various values of n, and half-saturation set to 26 Torr, are shown in Fig. 3.14b. As n is increased to 4 (its maximum value for a protein with four binding sites), saturation occurs over a much sharper range of oxygen concentration, facilitating transport by losing oxygen transport more efficiently in the tissues, and gaining it with higher affinity in the lungs. Thus, cooperative oxygen binding has evolved in hemoglobin to transport oxygen over the relatively narrow range of concentrations that exist in our body. The n value for hemoglobin is near 2.8, representing a moderate degree of cooperativity compared to the maximum value of 4.

The molecular mechanism for cooperative oxygen binding in hemoglobin requires communication between subunits, and a structural transition between a low affinity state (the "T state", that exists when no oxygen is bound), and a higher affinity state (the "R state") that is triggered by oxygen binding. Initially, when oxygen concentrations are low, R state hemoglobin binds with low affinity. Binding of the first oxygen molecules converts the structure to the T state, and the remaining heme sites bind with higher affinity.

The structural transition associated with the change from the T state to the R state involves a ~15° rotation of the $\alpha_1\beta_1$ subunit with respect to the $\alpha_2\beta_2$ subunit (Fig. 3.16). This rotation is triggered by chemistry in the heme iron. In the absence of bound oxygen, the iron d-shell electrons exist in a high spin state, which has a larger atomic radius than the low spin state. This larger radius moves the iron atom out of the plan of the heme porphyrin in the direction of the coordinating histidine site chain. Binding of oxygen changes the iron to the low spin state, moving it into the plane of the porphyrin, brining with it the histidine, and pulling on the alpha helix to which it is connected. This subtle movement of the heme iron is leveraged to the rest of the subunit, and then to the entire hemoglobin molecule, causing the rest of the unbound subunits to convert the higher affinity R state.

Like most enzymes, hemoglobin activity (oxygen affinity) can be controlled by other molecules in its environment. One such molecule is 2,3 bisphosphoglycerate (BPG), which is present in relatively high (mM) concentrations in red blood cells (Fig. 3.17). BPB, having two phosphate groups, is negatively charge and binds to

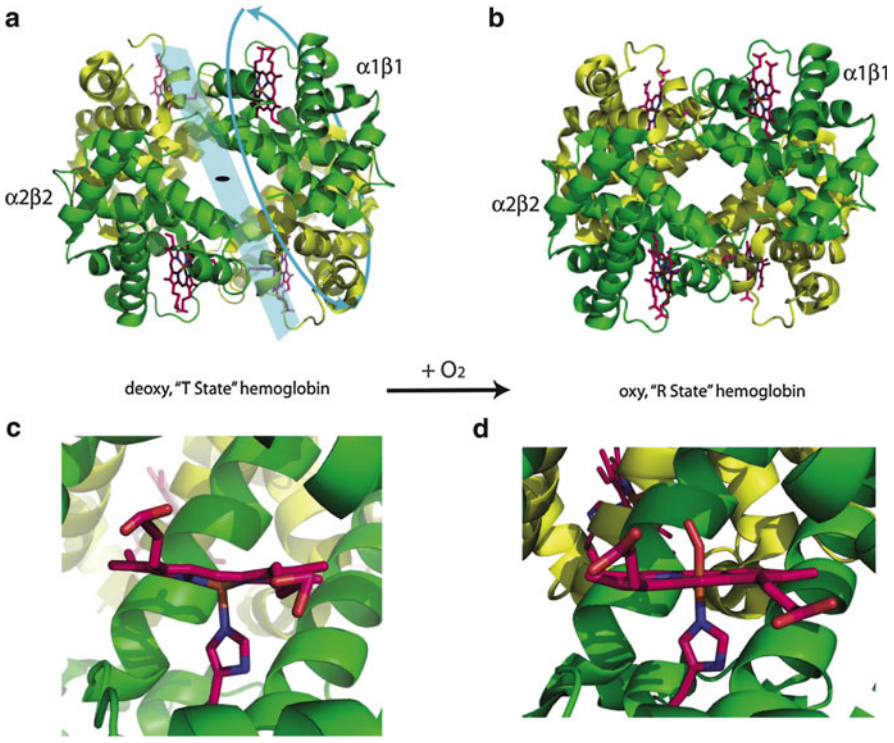

Fig. 3.16 (**a**) Upon oxygen binding, deoxygenated "T state" hemoglobin is converted to the higher affinity "R state" (**b**) by a 15° rotation of the α1β1 dimer with respect to the α2β2 dimer. (**c**) This conformational change is triggered by movement of the heme iron into the plane of the heme ring (**d**), pulling the coordinating histidine and its attached alpha helix

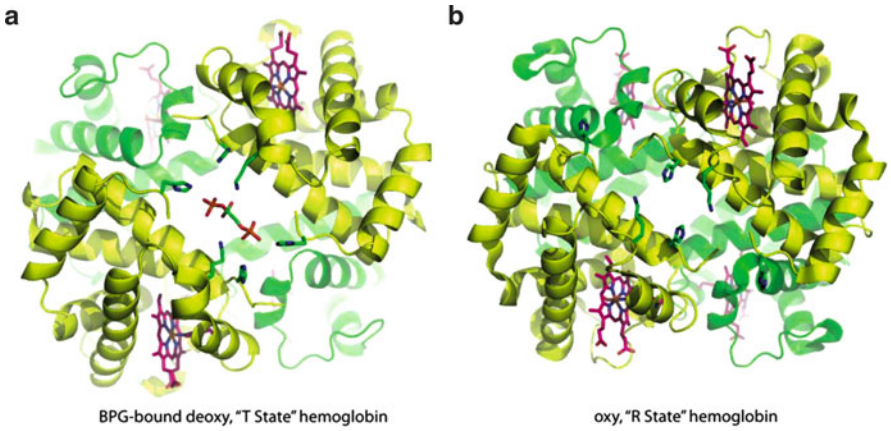

Fig. 3.17 Allosteric regulation of hemoglobin by BPG binding. BPG binds preferentially to the T state, lowering the affinity for oxygen binding by inhibiting the transition to the R state. A collection of positively charged amino acid side chains (shown in *green*) are grouped at the subunit interface in the T state, but are disrupted in the R state

a grouping of positive charges that form at the $\alpha_1\beta_1/\alpha_2\beta_2$ interface of T state hemoglobin. This interface is disrupted upon transition to the R state, which does not bind BPG. The effect of BPG binding is to lower hemoglobin affinity for oxygen. The physiological purpose of this regulation is to optimize oxygen affinity under different environmental or physiological conditions. The interplay between cooperativity and BPG binding is exploited in fetal hemoglobin, which has a γ subunit in the place of β subunits. The γ subunit lacks one of the charged side chains associated with BPG binding in adult hemoglobin, and thus fetal hemoglobin has a higher affinity for oxygen, resulting in its transport across the placenta.

3.8 Protein Folding and Stability

Protein structure results from a large number of offsetting weak forces that, on balance, stabilize the native fold. In most cases the net free energy of the native fold is only on the order of a few hydrogen bonds. Amino acid side chains on the surface are most often interacting favorably with solvent, and those buried inside are most often hydrophobic. The specific mechanism of protein folding is not yet understood, but many of the forces involved are clear.

1. Amino acid sequence dictates structure. Most proteins fold as they are translated, without the help of molecular chaperones, into a structure that results directly from the amino acid sequence. In fact, many amino acids might play little role in the native function of the protein, but be indelibly important in the folding process.

2. Folding is cooperative. The energy of the folded state is often only slightly lower than the extended unfolded state, but many folding intermediates are even less stabile than the extended unfolded state. Thus, as the protein folds, it rapidly transgresses these high energy states and moves cooperatively to the folded state.

3. Proteins often fold in milliseconds, thus, not every possible conformation of dihedral angles is sampled. Instead, an initial hydrophobic collapse into partially folded intermediates limits the number of conformations to be sampled. Correct structure within these intermediates is then retained, further limiting the number of subsequent conformations to be sampled in the search for the native structure. Iterations of such retention of correct structure are probably involved in the protein folding process.

Many small molecules disrupt native protein structure resulting in "denaturation" of the protein. A denatured protein is one that has lost organized structure along with any accompanying activity. The most common are urea, guanidinium chloride, and β-meraptoethanol (Fig. 3.18). High concentrations of urea and guanidinium chloride disrupt the weak forces holding proteins in their native states, and β-mercaptoethanol disrupts disulfide bonds. These chemicals have been used for decades in laboratory work with proteins, and in experiments to study protein folding.

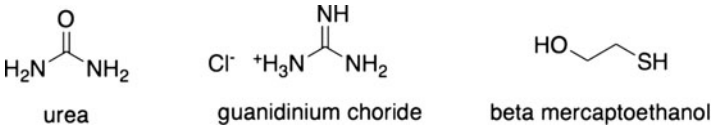

Fig. 3.18 Urea, guanidinium chloride, and beta mercaptoethanol are three chemicals that are used to denature proteins

Further Reading

1. Brändén C-I, Tooze J (2009) Introduction to protein structure, 2nd edn. Garland, New York
2. Creighton TE (1992) Protein folding. W.H. Freeman, New York
3. Dickerson RE, Geis I (1969) The structure and action of proteins. Harper & Row, New York
4. Fersht A (1999) Structure and mechanism in protein science: a guide to enzyme catalysis and protein folding. W.H. Freeman, New York
5. Kyte J (1995) Mechanism in protein chemistry. Garland, New York
6. Patthy L (1999) Protein evolution. Blackwell, Malden, MA
7. Perutz MF (1997) Science is not a quiet life: unravelling the atomic mechanism of haemoglobin. Imperial College Press/World Scientific, London/River Edge, NJ
8. Rhodes G (2006) Crystallography made crystal clear: a guide for users of macromolecular models, 3rd edn. Elsevier/Academic, Amsterdam/Boston, MA
9. Van Holde KE, Johnson WC, Ho PS (2006) Principles of physical biochemistry, 2nd edn. Pearson/Prentice Hall, Upper Saddle River, NJ
10. Wyman J, Gill SJ (1990) Binding and linkage: functional chemistry of biological macromolecules. University Science Books, Mill Valley, CA
11. Pain RH (2000) Mechanisms of protein folding, 2nd edn. Oxford University Press, New York

Chapter 4
Enzymes

Every living cell carries out thousands of chemical reactions. With few exceptions, such as neutralizations, spontaneous decompositions and rearrangements, all of these reactions are enzyme-catalyzed. It should be noted that not all biological catalysts are enzymes, e.g., ribozymes (RNA catalysts) and some metals, being exceptions.

The term enzyme was coined in 1876 by the German physiological chemist Kühne and comes from the Greek *in yeast*. Enzyme action in the nineteenth century was frequently studied in yeast extracts and enzymes were also referred to as *ferments*, a term that at that time was essentially synonymous with yeast. Over time, the term enzyme prevailed although its use was a point of controversy in the formative years of biochemistry.

4.1 Characteristics of Enzymes

1. Enzymes are biological catalysts that speed up rates of chemical reactions without appearing in the net final equation.
2. Catalysis occurs in a domain within the enzyme known as the *active site*.
3. There is universal agreement today that enzymes are proteins; however, until J.B. Summer crystallized the enzyme urease in 1926 [1], the chemical nature of enzymes was controversial. In the 1920s and even later, crystallization was recognized to be a criterion of chemical purity. It is ironic, however, that today, using techniques that were not available in the early part of the twentieth century, it is often found that crystalline enzymes are not homogeneous. It is an interesting coincidence that urease, the first enzyme recognized to be a protein, acts upon urea, the first organic compound to be synthesized.
4. Enzymes exhibit *high turnover numbers*. The turnover number (TN) is defined as:

H.J. Fromm and M.S. Hargrove, *Essentials of Biochemistry*,
DOI 10.1007/978-3-642-19624-9_4,

Table 4.1 A comparison of enzyme-catalyzed reaction rates with their theoretical uncatalyzed counterparts

Enzyme	Catalyzed rate k_{cat} (s^{-1})	Uncatalyzed rate[a] k_{cat} (s^{-1})	Catalyzed rate/uncatalyzed rate
Alcohol dehydrogenase	2.7×10^{-3}	$<6 \times 10^{-12}$	$>4.5 \times 10^{6}$
Creatine phosphokinase	4×10^{-3}	$<3 \times 10^{-9}$	$>1.3 \times 10^{6}$
Hexokinase	1.3×10^{-3}	$<1 \times 10^{-13}$	$>1.3 \times 10^{10}$
Glycogen phosphorylase	1.6×10^{-3}	$<5 \times 10^{-15}$	$>3.2 \times 10^{11}$

[a]Calculated from collision frequency theory

$$\mathrm{TN} = \frac{\text{Moles of substrate converted to product/s}}{\text{Moles of enzyme}}.$$

TN values vary from near unity with some enzymes (lysozyme's TN $= 0.5\ s^{-1}$) to rates approaching the diffusion-controlled limit with others, e.g., catalase exhibits a TN of $4 \times 10^{7}\ s^{-1}$. In general, the TN, often referred to as k_{cat}, is in the 10^{2}–$10^{3}\ s^{-1}$ range. The ability of enzymes to enhance rates of chemical reactions is enormous.

This point is illustrated in Table 4.1 from a paper by D.E. Koshland, Jr. which compares the rates of a few selected reactions with and without enzymes [2].

5. Enzymes do not alter the equilibrium constant of the reaction they catalyze; they merely speed up the rate to equilibrium. A simple chemical equation that an enzyme may catalyze is:

$$E + S \rightleftharpoons E + P,$$

where E, S and P represent enzyme, substrate and product, respectively, and where the equilibrium constant for the reaction (K_{eq}) is defined as:

$$K_{eq} = \frac{c(E)c(P)}{c(E)c(S)} = \frac{c(P)}{c(S)}.$$

Although a certain amount of product or substrate may be sequestered by the enzyme, e.g., in the *ES* complex (see below), the ratio of substrate and product relative to enzyme is very large and will therefore not affect the K_{eq}.

6. The one characteristic of enzymes that distinguishes them from other catalysts is their *specificity*. However, even enzymes exhibit a spectrum of specificities. Emil Fisher [3] was the first to attempt to explain specificity by proposing the "*key in lock*" hypothesis; the substrate being the key and the enzyme the lock. This idea failed when it was recognized that small substrate analogs could not substitute for large substrates, i.e., methanol is inactive with alcohol dehydrogenase, whereas ethanol, propanol, etc., are excellent substrates. It is currently believed that the substrate induces conformational changes in the enzyme that allows essentially "perfect" alignment between the substrate and the catalytic groups in the enzyme's active site. The energy for alterations in the enzyme

structure is provided by a loss of binding energy when the substrate and enzyme interact. This proposal was advanced in 1958 by D.E. Koshland, Jr. and is known as the "*induced-fit*" hypothesis [4]. Verification of the hypothesis has come from a number of physical studies of enzymes including X-ray crystallography.

7. Most enzymes function under mild physiological conditions, e.g., 37°C and pH ~7. Some, like enzymes from thermophiles, a bacterial class, function at temperatures in the 100C range, and enzymes such as pepsin are active in the acidic environment of the stomach.
8. Some enzyme's activities are sensitive to activation or inhibition by small molecules. Many enzymes in this class serve to regulate the activity or flux through metabolic pathways and as such are extremely important physiologically.
9. *Isozymes* are enzymes that differ in amino acid sequence within an organism, but which catalyze identical chemical reactions. The kinetic and regulatory properties of the isozymes may differ.
10. *Zymogens* or *proenzymes* are inactive proteins which undergo chemical alterations that lead to their activation. An example is chymotrypsinogen which is inactive until acted upon by the enzyme trypsin.
11. Some enzymes require a nonprotein factor for activity. This would be analogous to the prosthetic group heme in hemoglobin. The inactive protein is referred to as the *apoenzyme* and the active enzyme, the *holoenzyme*. Thus,

$$\text{apoenzyme} + \text{cofactor} = \text{holoenzyme}.$$

12. It is now becoming clear that some enzymes may play functional, rather than simply catalytic roles in the cell, e.g., brain and skeletal muscle hexokinase and creatine phosphokinase when associated with mitochondria, protect the cell against apoptosis (programmed cell death) [5].

4.2 Enzyme Classification

Enzymes can be segregated into six distinct classes. These are:

1. *Hydrolases*: Enzymes that hydrolyze substrates.
2. *Isomerases*: Enzymes involved in isomerization reactions.
3. *Ligases*: Enzymes involved in condensation reactions using nucleoside di- and triphosphates as an energy source. These enzymes are often called *synthetases*. Another class of ligases which use derivatives of nucleotides (UDP-α-D-glucose) are known as *synthases*.
4. *Lyases*: Enzymes that promote addition to double bonds.
5. *Oxidoreductases*: Enzymes involved in redox reactions.
6. *Transferases*: Enzymes that catalyze group transfer reactions.

Recently, the term *energase* has been used to describe enzymes that use the energy of nucleoside di- and triphosphate hydrolysis to do useful work.

4.3 Mechanisms of Enzyme Action

It was recognized late in the nineteenth century that enzymes facilitate catalysis by forming a loose complex with the substrate prior to catalysis [6]. This complex of enzyme and substrate is often referred to as a Michaelis-type or noncovalent complex.

In order to better appreciate how enzymes function as catalysts, it will be necessary to review briefly the concepts of activation energy and *transition state* theory.

In the latter part of the nineteenth century, the Swedish chemist Arrhenius proposed that an energy barrier exists for any chemical reaction and that the system must posses enough energy, *the activation energy* (E_a), for the reaction to occur.

1. For a multisubstrate reaction to occur, the substrates must come together (collide). As suggested by Arrhenius, not all collisions will be successful; rather, only those that possess the requisite amount of energy, E_a, will ultimately give rise to products. Successful collisions result in the formation of a short-lived complex, the *transition state*, proposed by Eyring, Evans, and Polanyi [7, 8], which breaks down very rapidly to form products. The least stable species along the reaction pathway is the transition state. It is in the transition state that chemical bonds are broken and new ones formed.

   A number of transition states occur in multistep reactions. The rate-limiting step in this sequence of reactions occurs at the transition state complex at the highest energy level. The *Hammond Postulate*, which is not applicable to multistep reactions attempts to correlate structures of intermediates with their stability, i.e., the transition state will tend to resemble the structure of the unstable intermediate.

   The sequence of events leading to the formation of the transition state is illustrated in Scheme 4.1 involving a typical S_N2 type reaction.

   The peak in the diagram is the transition state. The energy required to attain this activated state is the Gibbs free energy of activation, $\Delta G^{\ddagger}$. *The role of a catalyst is to decrease the* $\Delta G^{\ddagger}$.In the case of enzymes, the ground state is represented by E and S and the transition state by $ES^{\ddagger}$.
2. Molecules in the ground state, in this case $N:^{-}$ and A–X, are in equilibrium with those in the transition state, $[N–A–X]^{\ddagger}$, i.e.,

$$K_{eq}^{\ddagger} = \frac{[\text{Transition state molecules}]}{[\text{Ground state molecules}]}.$$

3. Once a molecule has attained the transition state, it breaks down immediately to form products.
   For the reaction $S \xleftrightarrow{k} P$, S, P and k represent substrate, product and rate constant, respectively.
4. The relationship, known as the *Arrhenius equation*, between the rate constant k and the energy of activation E_a is

$$k = Ae^{-E_a/RT}.$$

Scheme 4.1 Energy level diagram for an S_N2 reaction

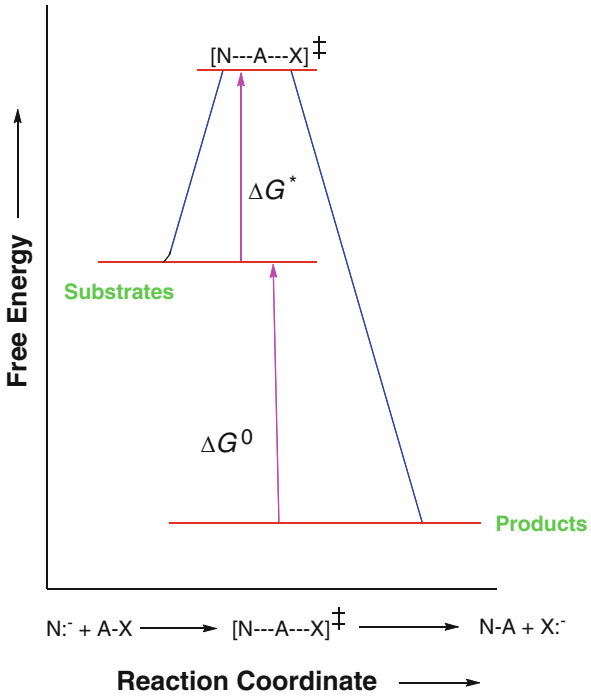

In the Arrhenius equation, A is a constant, the preexponential factor, E_a is the activation energy for the reaction, R the universal gas constant, and T the temperature.

5. Erying, in developing the concept of the transition state, showed that

$$k = \frac{[k_B T]}{h} K_{\text{eq}}^{\ddagger},$$

where k_B and h are the Boltzmann and Planck constants, respectively.

6. The equation relating the specific rate constant (k) to the equilibrium constant ($K_{\text{eq}}^{\pm}$) allows for the introduction of the Gibbs free energy of activation term (ΔG^*), as well as the specific rate constant for the reaction, $k(S \overset{k}{\longleftrightarrow} P)$, into a single equation. Using the relationship between free energy of activation and the equilibrium constant $K_{\text{eq}}^{\pm}$, and where

$$\Delta G^* = -RT \ln K_{\text{eq}}^{\pm} \quad \text{and} \quad \Delta G^* = \Delta H^* - T\,\Delta S^*.$$

k can also be expressed in terms of enthalpy and entropy of activation

$$k = \frac{[k_B T]}{h} e^{\left[\frac{\Delta S^*}{R} - \frac{\Delta H^*}{RT}\right]}.$$

7. A serious limitation in transition state theory occurs with reactions with loose transition states where tunneling occurs. In these cases, the highest peak in the

energy level diagram does not correspond to the activation energy, E_a calculated from the Arrhenius equation.

8. *Entropy* (S=kJ/K) describes the degree of disorder or randomness of a system is believed to play an extremely important role in catalysis. We will recall from elementary physical chemistry that the overall entropy of a system is given by the Boltzmann Law ($S=k_B\ lnW$) where the Boltzmann constant k_B is the per-molecule value of the gas constant and W is the number of ways that atoms or molecules are spatially arranged. Entropy, as we commonly refer to it, is actually made up of a number of factors. These include translational, rotational, and internal entropies.

   (a) *Translational entropy* describes the movement of a molecule in a single direction;
   (b) *Rotational entropy* represents the spinning of a molecule, similar to the spinning and wobbling of a toy top, whereas
   (c) *Internal entropy* is the movement of atoms relative to each other within a molecule

   As with enthalpy and Gibbs free energy, one best considers the change, ΔS, in this thermodynamic quantity. In this case; however, the quantity of interest is actually $T\Delta S$ which bears the very same units (kJ) as ΔH and ΔG.

   When two molecules come together, there is a loss of both translational and rotational entropies, i.e., the ΔS^* decreases. This concept is clearly at variance with the idea that entropy is an important factor in facilitating reaction rates. This follows from the universally held belief that the enzyme and substrate, or substrates, form a loose *ES* complex. On the other hand, substrate binding is in most cases highly exergonic and, in addition, dissociation of products from the enzyme–product complex leads to increased disorder of the system and the overall process is thus entropically favorable. It is important to point out that the unfavorable entropy effect noted above does not involve the transition state.

9. How catalysts and enzymes facilitate reaction rates.

   Organic chemistry often provides a clear understanding of reaction mechanisms involving, in most cases, relatively small molecules. These well-established mechanisms are often used to describe analogous mechanisms involving biomolecules.

   This point is illustrated by a comparison of the hydrolysis of aspirin and phenylacetate.

   (a) *Aspirin hydrolysis* – an example of *intramolecular catalysis*.
   (b) *Phenylacetate hydrolysis* (Fig. 4.1).

   The velocity expression for aspirin hydrolysis is $v_1 = k_1$[aspirin], whereas the equation for phenylacetate hydrolysis, which is base-catalyzed, is $v_2 = k_2$[phenylacetate][OH^-]. When the OH^- concentration is 13 M, $v_1 = v_2$, assuming the concentrations of aspirin and phenylacetate are equal. This analysis demonstrates the importance of intramolecular catalysis, i.e., of bringing

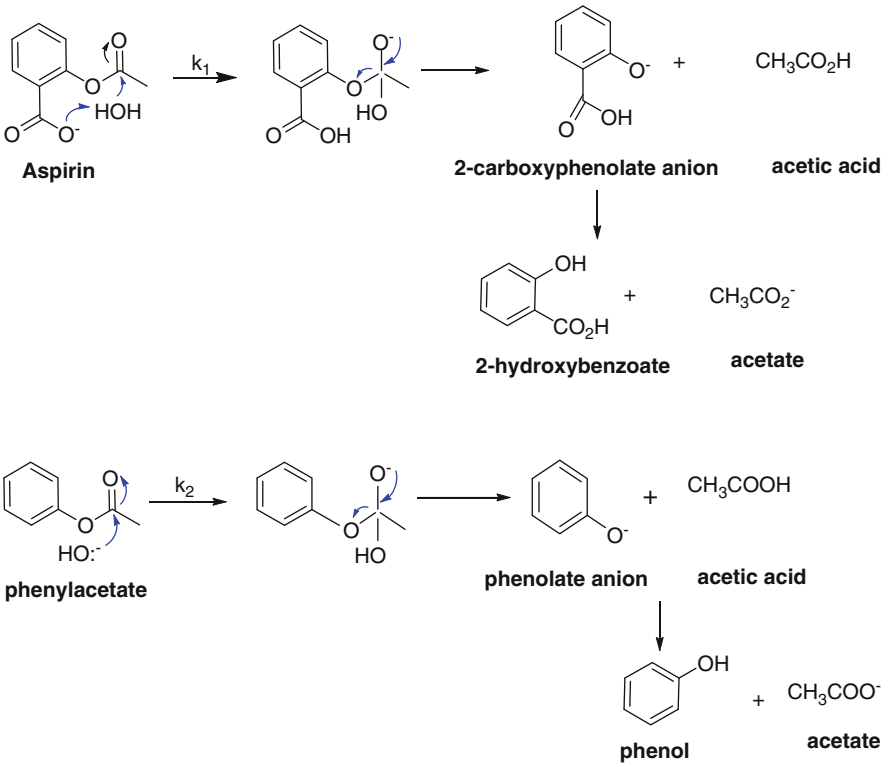

Fig. 4.1 Hydrolysis of aspirin and phenylacetate

substrates together in close proximity as a factor in enzyme catalysis [9]. This is precisely what happens in the enzyme–substrate complex.

The differences in the rates of intramolecular (aspirin) and intermolecular (phenylacetate) hydrolysis can be rationalized based on entropy differences between the two reactions. In the case of the intramolecular hydrolysis of aspirin, a single reactant, aspirin, forms two products, whereas in the case of phenylacetate hydrolysis, two reactants, phenylacetate and hydroxyl ion, form two products.

10. *Stabilization of the transition state* – the role of the catalyst in enhancing reaction rates.

In general, anything that stabilizes the transition state will facilitate the reaction. It is also generally true that the more closely the transition state resembles the substrates, the more rapid the reaction. Thus, if the substrates are neutral, a charged transition state will give rise to a relatively slow reaction. On the other hand, neutralization of the charge within the transition state will serve to enhance the reaction rate. Figures 4.2 and 4.3 serve to illustrate these points.

The mechanism shown in Fig. 4.2 is an example of an uncatalyzed, and thus extremely slow reaction, whereas that depicted in Fig. 4.3 illustrates acid

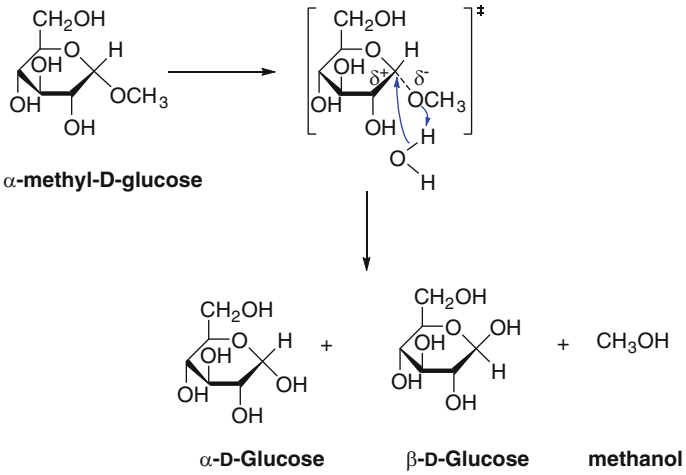

Fig. 4.2 Uncatalyzed hydrolysis of α-methyl-D-glucose. The partial charges are centered at the C-1 carbon

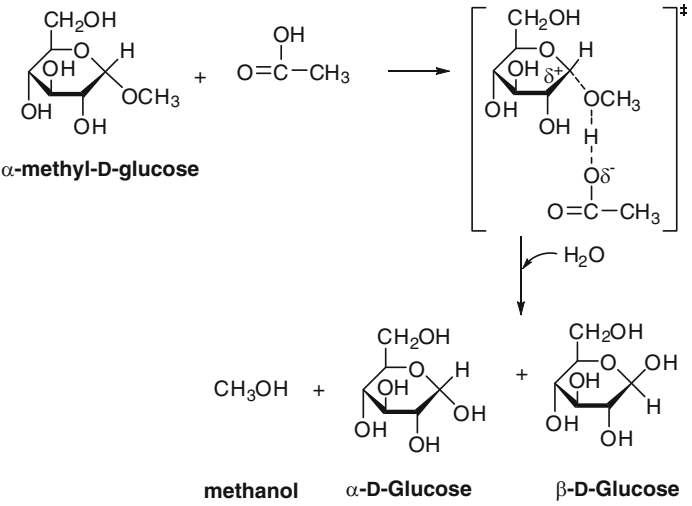

Fig. 4.3 Acid-catalyzed hydrolysis of α-methyl-D-glucose. The partial negative charge is distal to the C-1 carbon relative to that shown in Fig. 4.2

catalysis. In the transition state shown for the uncatalyzed reaction there are partial charges in close proximity to the C-1 carbon atom, whereas the ground state is neutral. In the case of the acid-catalyzed reaction, the transition state is charged; however, the partial negative charge developed on the leaving methanolate group is stabilized by the proton from acetic acid.

(a) Ester hydrolysis–base catalysis.
The most often encountered mechanism for ester hydrolysis involves the use of a base (see Fig. 4.4)

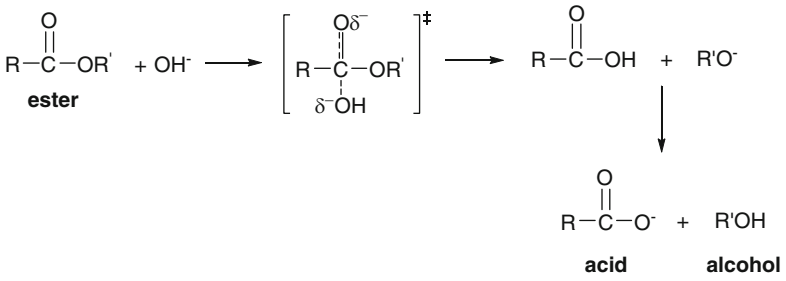

Fig. 4.4 The mechanism of base-catalyzed ester hydrolysis

In the mechanism shown in Fig. 4.4, both the ground and transition states exhibit negative charges. Hydrolysis can be accomplished at more neutral pH values with a base catalyst such as acetate as shown in Fig. 4.5.

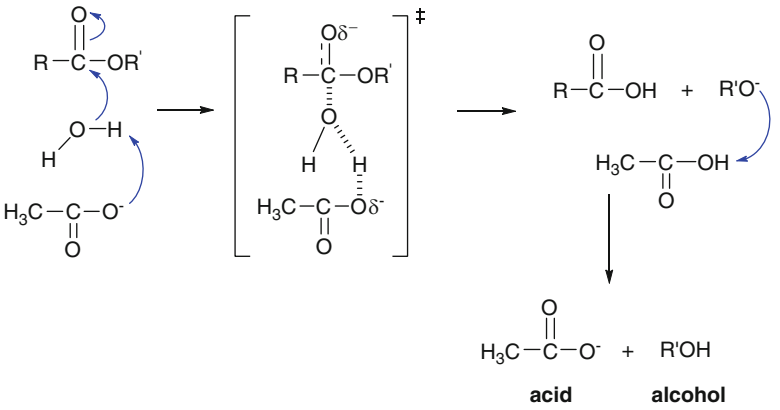

Fig. 4.5 Ester hydrolysis catalyzed by the weak base acetate which serves to stabilize the transition state by neutralizing the developing positive charge on the attacking water molecule proton

11. The strain or rack hypothesis.
Lumry and Eyring [10] were among the first to suggest that enzymes may function by causing bond distortion in the substrate. This point is illustrated by the hydrolysis of dimethyl phosphate (a) and ethylene phosphate (b) (Fig. 4.6). The rate of hydrolysis of ethylene phosphate is 10^7 times faster than that of dimethyl phosphate. This difference in hydrolysis rates is believed to be due to the bond strain caused by the five-membered ring associated with ethylene phosphate.

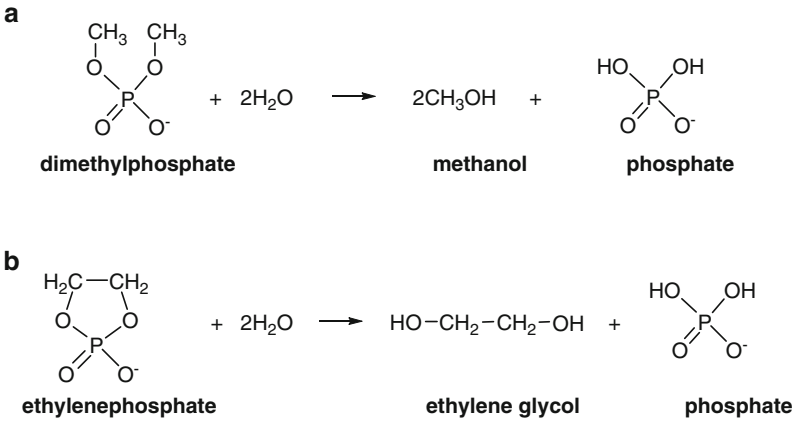

Fig. 4.6 An example of the strain hypothesis illustrated by the hydrolysis of dimethylphosphate (**a**) and ethylenephosphate (**b**)

12. Covalent catalysis.
    In some enzyme-catalyzed reactions, a covalent bond is formed between the enzyme and substrate after initiation of a loose Michaelis complex. An example of covalent catalyses is illustrated by a hypothetical kinase (Fig. 4.7):

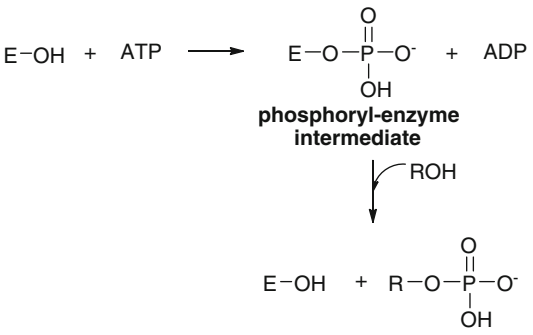

Fig. 4.7 An example of covalent catalysis where the enzyme is phosphorylated by ATP

    In the example cited there appears to be no chemical advantage to forming a covalent linkage between the enzyme and the substrate; however, many examples can be described in which covalent bonding between enzyme and substrate is clearly chemically advantageous, e.g., the formation of a Schiff base between pyridoxal phosphate coenzymes and an ε-amino group of the enzyme leading to the formation of what is in essence an electron sink (Chap. 6).
13. Cation catalyses (electrophilic catalysis).
    Metal ions are important activators of many enzymes. For example, ligases which require nucleoside triphosphates also require divalent metal ions for activity. Cited below are some of the functions of cations in enzyme catalysis.

(a) Polyphosphate–metal ion chelates.
Nucleoside di- and triphosphates bind divalent metal ions such as Mn^{2+} and Mg^{2+} as well as Ca^{2+}, all of which are physiologically important. Reactions of the type

$$Me^{2+} + ATP^{4-} = MeATP^{2-},$$

give the *formation constant* (K_f):

$$K_f = \frac{[MeATP^{2-}]}{[Me^{2+}][ATP^{4-}]}.$$

Mg^{2+} which is the activator most frequently encountered physiologically, because of its high intracellular concentration (~1 mM), has a K_f of approximately 70,000 M^{-1}. The interactions of the metal may be with the α, β, and γ phosphoryl groups, but bi (α–β) and tridentate (α–β–γ) ATP chelates form more easily. The metal may play at least two roles: First it may act as a bridge between the negatively-charged phosphoryl groups of the nucleotide and the enzyme, and second, it may serve to pull electrons away from the phosphorous atoms, thus enhancing their positive charge. This in turn will facilitate attack by a nucleophile on the phosphorous atom.
When nucleoside di- or triphosphates are involved in reactions it should be assumed that a divalent metal ion–nucleotide complex is the true substrate, unless explicitly stated otherwise.

(b) *Certain metals are capable of lowering the pK of water*. Although the hydroxyl ion is an excellent nucleophile, its concentrate is only 10^{-7} M at neutral pH. Both Zn^{2+} and Co^{2+} are capable of increasing the effective OH^- concentration in cases where the hydroxyl group functions as the nucleophile. An example involving Co^{2+} is as follows:

$$(NH_3)_5Co^{3+} + HOH = (NH_3)_5Co^{2+}OH + H^+.$$

(c) Cation catalysis is used by many enzymes to polarize groups other than phosphoryl groups cited in 13(a). Zn^{2+} is used by the pyridine-linked anerobic dehydrogenase, alcohol dehydrogenase, to enhance the positive charge on the carbonyl carbon atom of acetaldehyde (Fig. 4.8).

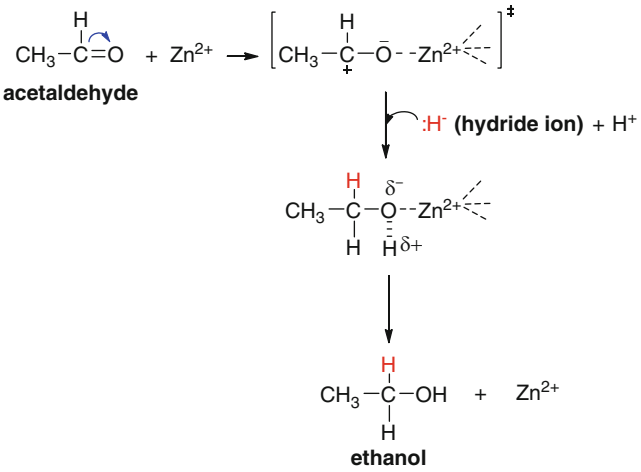

Fig. 4.8 The role of Zn^{2+} as an activator of alcohol dehydrogenase. Zn^{2+} is tightly bound to the enzyme. The reaction involves hydride ion transfer and proton transfer

4.4 Nucleophilic Substitution Reactions

4.4.1 S_N1 (Substitution, Nucleophilic, First Order Reaction)

(a) Hydrolysis of *t*-butyl bromide:
(b) $v = k$ (*t*-butyl bromide), where k is the rate constant for the slow, or rate-limiting, step (Fig. 4.9)
(c) If the substrate had a chiral carbon that formed the carbocation, the reaction would have led to two enantiomers, i.e., *racemization* would have occurred, e.g., see Fig. 4.10
(d) In enzyme-catalyzed reactions, there would be either a retention of configuration, or an inversion, *never a racemic mixture*

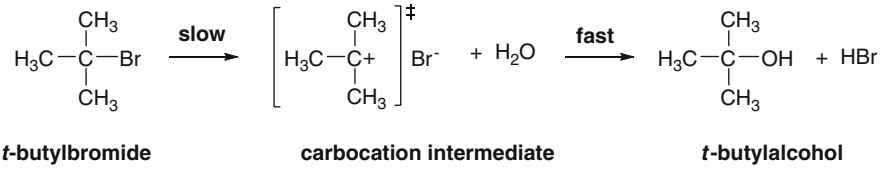

Fig. 4.9 An example of an S_N1 reaction: hydrolysis of *t*-butylbromide

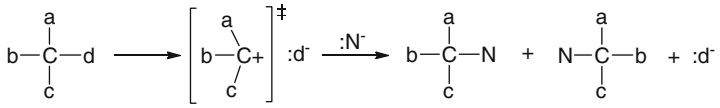

Fig. 4.10 Nonenzymatic S_N1 reaction leads to racemization of products

4.4.2 S_N2 (Substitution, Nucleophilic, Second Order)

(a) The base catalyzed hydrolysis of methyl bromide is a typical S_N2 reaction (Fig. 4.11)
(b) $v = k(CH_3\ Br)(OH^-)$, i.e., a second-order reaction
(c) Had the substrate been chiral, there would have been an inversion of configuration
(d) S_N2 reactions involving enzymes are stereochemically identical to nonenzymatic S_N2 reactions, i.e., there is an inversion of configuration

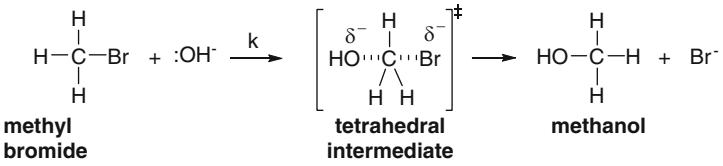

Fig. 4.11 Base-catalyzed hydrolysis of methyl bromide

4.4.3 Stereochemistry of Nucleophilic Substitution Reactions

Shown in Fig. 4.12 are the differences in S_N1 and S_N2 reaction stereochemistry.

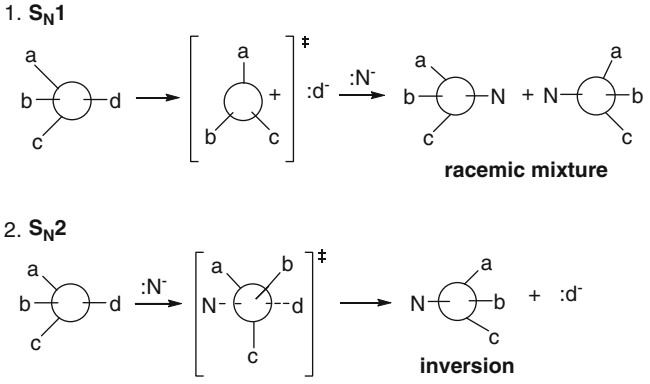

Fig. 4.12 Mechanism of S_N1 and S_N2 reactions illustrating their stereochemistry

4.5 Phosphorous Compounds and Their Chemistry

Phosphorous esters and anhydrides are commonplace in many of the most important biomolecules and biochemical reactions. In analogous organic compounds and reactions, carbon is the most frequently observed element. A fundamental question is why nature chose phosphorous rather than any other element as a substrate in biology. This point has been addressed by Westheimer [11], who suggested that

nature chose phosphorous for a number of reasons: Phosphoric acid in nucleic acids such as RNA and DNA, can link two nucleotides and still ionize, and the resulting negative charge can stabilize the diesters against hydrolysis and still allow the nucleotides to be contained within lipid membranes. Phosphates undergoing reaction can utilize metaphosphate, ($+PO_3^{-2}$), as an intermediate. The fact that phosphates are both negatively charged and stable make them excellent candidates in intermediary metabolism and as sources of energy (ATP). That phosphate esters and diesters are negatively charged enhances their stability and their resistance to hydrolysis. An excellent review on the mechanism of phosphorous compounds in both chemistry and biochemistry has been provided by Knowles [12].

4.5.1 Oxidation States of Phosphorous

The oxidation states of phosphorous vary from −3 to +5. The phosphorous atom can exhibit any one of five oxidation states (−3,−1,+1,+3, and +5) with +5 being the most common in biological systems.

4.5.2 Types of Reaction Involving Phosphorous

(a) Dissociative
(b) Associative

- Pentacoordinate transition state
- Pentacoordinate intermediate
- Pentacoordinate intermediate plus pseudorotation

4.5.2.1 Dissociative Mechanisms (S_N1)

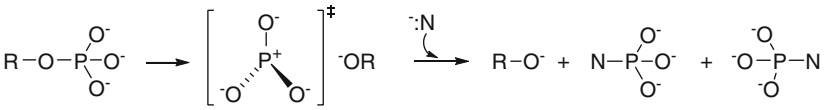

Fig. 4.13 A dissociative mechanism giving rise to a metaphosphate intermediate. Addition of a nucleophile, $^{-}$:N, leads to a racemic mixture of products

4.5.2.2 Associative Mechanisms (Inline Mechanisms)

Pentacoordinate Transition State.

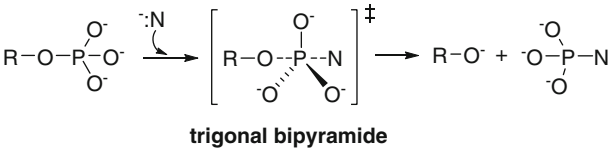

Fig. 4.14 The formation of a pentacoordinate transition state with subsequent inversion of configuration

Pentacoordinate Intermediate

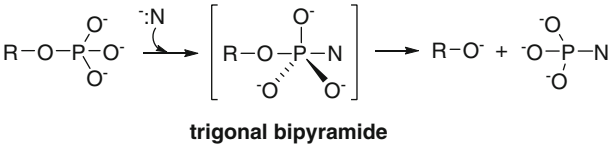

Fig. 4.15 The formation of a pentacoordinate intermediate with subsequent inversion of configuration of product

Pentacoordinate Intermediate and Pseudorotation

Pseudorotation occurs with a trigonal bipyramide structure when two equatorial bonds become apical bonds and vice versa. When elimination occurs to produce a tetravalent compound, there is a retention of configuration. Note that the intermediate(s) are pentacoordinate (Fig. 4.16).

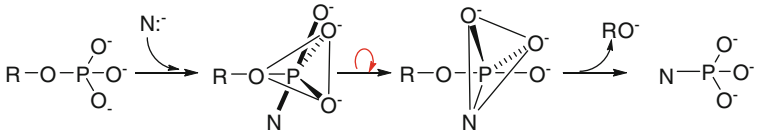

Fig. 4.16 The mechanism of pseudorotation leads to retention of configuration in the product

4.6 Studying the Stereochemistry of Enzyme-Catalyzed Reactions

4.6.1 The Use of Chiral Phosphorous Compounds

Chiral [^{16}O, ^{17}O, ^{18}O] γ-thio ATP is often a weak substrate for phosphotransferase enzymes. If one establishes the chirality of the reaction product, e.g., the

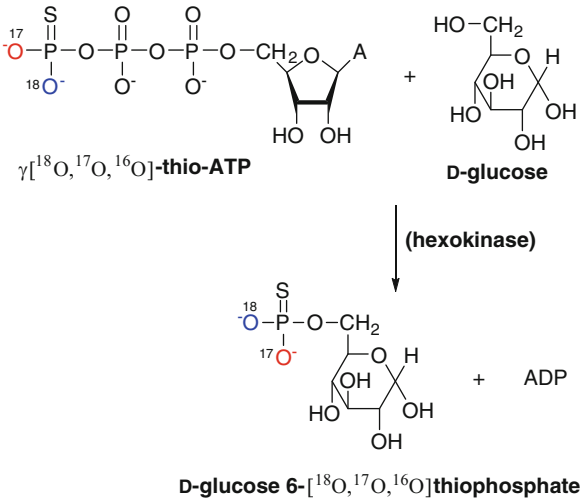

Fig. 4.17 Determining the stereochemical course of the hexokinase reaction

phosphoryl group in glucose-6-P in the yeast hexokinase reaction [13], then the stereochemical course of the hexokinase reaction can be determined (Fig. 4.17).

In this example, there is an inversion of configuration of the phosphoryl group. The hexokinase reaction is believed to be of the S_N2 type

4.6.2 Isotope Scrambling (Positional Isotope Exchange) [14]

If a metaphosphate or a covalent intermediate is suspected in a reaction, it is possible to use the technique of isotope scrambling to establish the mechanism. In these studies, one would use chemically synthesized [^{18}O] ATP in which all four oxygen atoms of the γ phosphoryl group contain the heavy isotope. The enzyme and the isotopic ATP are allowed to react in the *absence* of the second substrate. If a metaphosphate intermediate or a covalent intermediate is formed, and *if the β phosphoryl group of ADP can rotate*, the β,γ-^{18}O bridge oxygen will be replaced by ^{16}O. At equilibrium fully two-thirds of the oxygens will have been replaced. ^{31}P NMR can be used to analyze the resulting ATP. The mechanism of isotope scrambling is outlined in Fig. 4.18. A positive scrambling result will be considered significant; however a negative finding can always be attributed to a lack of rotation of the β phosphoryl group of ADP.

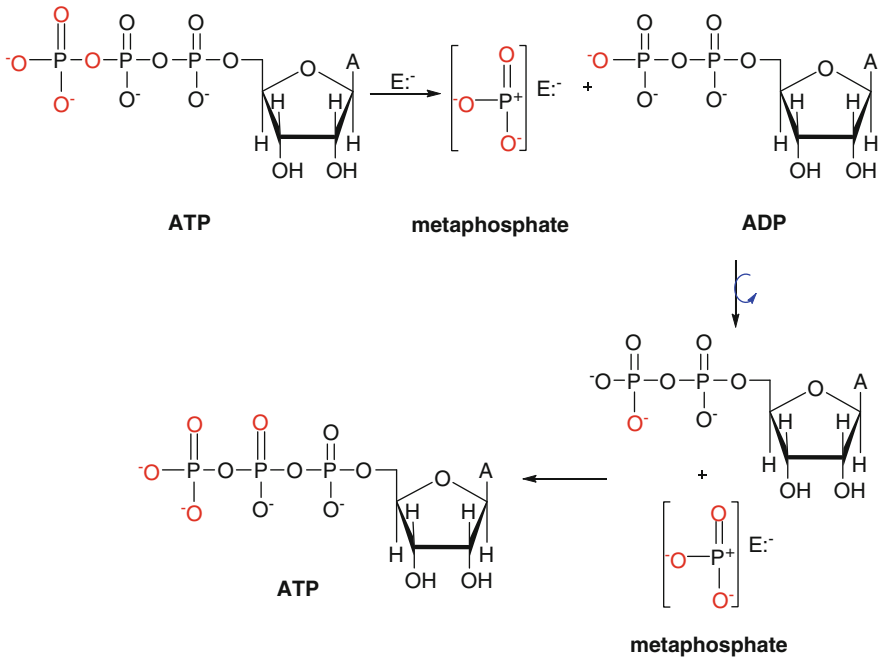

Fig. 4.18 Isotope scrambling or positional isotope exchange is used to determine whether a metaphosphate or covalent intermediate is involved in a transphosphorylase reaction

4.7 Studies on the Mechanism of Enzyme Action Using Transition State Analogs

4.7.1 Proline Racemase

The enzyme proline racemase interconverts the D(R) and L(S) isomers of the amino acid proline. Chemical and physical studies of the enzyme have demonstrated the involvement of a carbanion intermediate in the reaction mechanism [15]. One of the methods used to study the proline racemase reaction mechanism involved the use of *transition state analogs* [16]. Transition state analogs are stable compounds that mimic the structure of the transition state and thus are thought to bind more tightly to the enzyme than the substrate itself. The rationale behind this reasoning is that the binding energy that is normally used to alter the conformation of the substrate and enzyme in the transition state relative to the ground state, is not lost, simply because the transition state analog represents the structure of the activated complex more closely than does the substrate itself. Why transition state analogs bind more tightly to enzymes than do the substrates is illustrated in the following sequence of reactions:

$$E + S = ES \quad \Delta G^0 = -10\,\text{kJ/mol}\,(\text{binding phase}).$$

$$ES = ES^{\pm} \quad \Delta G^0 = +4\,\text{kJ/mol}\,(\text{conformational changes}).$$

$$E + S = ES^{\pm} \quad \Delta G^0 = -6\,\text{kJ/mol}\,(\text{overall}).$$

If the analog can go directly to the $ES^{\pm}$ state, i.e., by bypassing the conformational change required by the substrate and the enzyme to achieve the transition state, the binding energy will be preserved rather than being dissipated in step 2. These concepts are readily supported by the mechanism of the proline racemase reaction and binding studies of transition analogs [16].

Figure 4.19 illustrates the chemical mechanism of the proline racemase reaction. It can be seen that a cysteine thiolate anion abstracts hydrogen as a proton from proline giving rise to the carbanion intermediate. Thus, in the transition state the carbon atom exhibits sp^2 geometry, and the five-membered heterocyclic pyrrolidine ring is conformationally flat. In the last phase of the reaction, a hydrogen atom in the form of a proton is donated by another cysteine residue which acts as a catalytic acid.

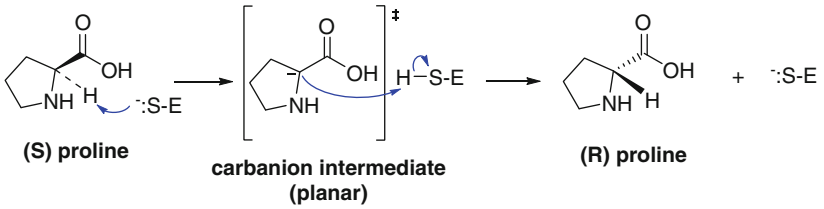

Fig. 4.19 Mechanism of the proline racemase reaction

A number of analogs have been found to mimic the flat geometry of the putative carbanionic transition state. One of the most effective is pyrroline-2-carboxylate (Fig. 4.20), which is structurally similar to the putative transition state. Kinetic studies reveal that this analog binds the enzyme 160 times more strongly than the substrate proline.

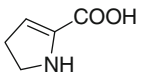

pyrroline-2-carboxylic acid

Fig. 4.20 Structure of pyrroline-2-carboxylic acid; a transition state analog of the proline racemase reaction

4.7.2 Adenylate Kinase

Adenylate kinase, also known as myokinase, is a ubiquitous enzyme in nature. The reaction catalyzed by the enzyme is,

$$\text{ATP} + \text{AMP} = 2\text{ADP}.$$

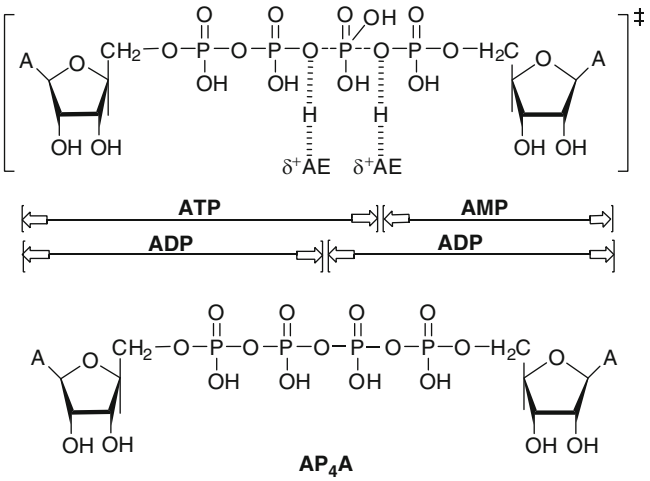

Fig. 4.21 The proposed transition state of adenylate kinase and the analog AP_4A

The kinetic mechanism was reported to be rapid-equilibrium random [17] and the transition state analog, P1,P4-di(adenosine-5′) tetraphosphate (AP_4A), was used to study and confirm the kinetic mechanism [18]. The transition state, based upon steady-state kinetics, is shown in Fig. 4.21.

The transition state analog, (AP_4A), is very similar structurally to the putative transition state, and not surprisingly, a very potent inhibitor of the adenylate kinase reaction ($K_d = 24$ μM).

4.7.3 Lysozyme

The enzyme lysozyme was discovered by Sir Alexander Fleming [19] and was the first enzyme structure to be solved by X-ray diffraction crystallography [20]. Lysozyme is found in human tears and egg white and its role in nature is as a bactericide. Catalytically, it functions as a hydrolase and destroys a polysaccharide that is essential to the maintenance of the cell walls of certain bacteria. The substrate for lysozyme is a β (1→4)-linked oligomer of alternating units of 2-acetamido-2-deoxy-D-muramic acid (NAM) and 2-acetamido-2-deoxy-D-glucose (NAG). [^{18}O]H_2O was used to determine that the hydrolysis of the polysaccharide occurs between the C-1 of NAM and the C-4 of NAG. A synthetic polymer of NAG may also serve as a substrate for lysozyme. The enzymatic reaction carried out by lysozyme is depicted in Fig. 4.22.

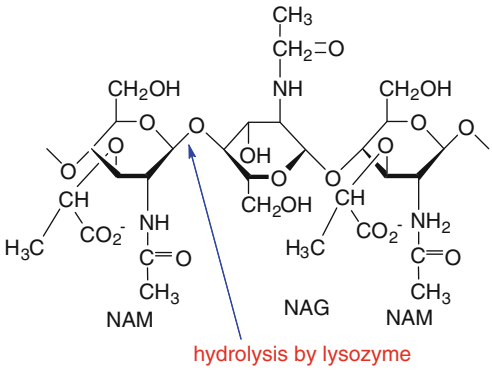

Fig. 4.22 The site of hydrolysis on the cell wall polysaccharide by lysozyme

The mechanism of the lysozyme reaction has been the subject of intense research since the pioneering studies of Phillips. A major finding in this context was the discovery by Lienhard and coworkers that the γ-lactone of tetra-*N*-acetyl-chitotetraose is a potent transition state analog of the substrate [21]. The reaction is believed to proceed via an alkoxycarbocation intermediate as depicted in Fig. 4.23. This intermediate has a half-chair conformation in which carbon atoms 1, 2, and 5 of the pyranose ring lie in the same plane as the ring oxygen and the C-1 carbon which are thought to be sp^2-hybridized.

In the putative lysozyme mechanism, shown in Fig. 4.23, Glu 35 is believed to donate a proton to the C-4 of the sugar residue designated as NAG-X.

It is clear from the examples sited here that transition state analogs are valuable tools for the study of enzyme reaction mechanisms.

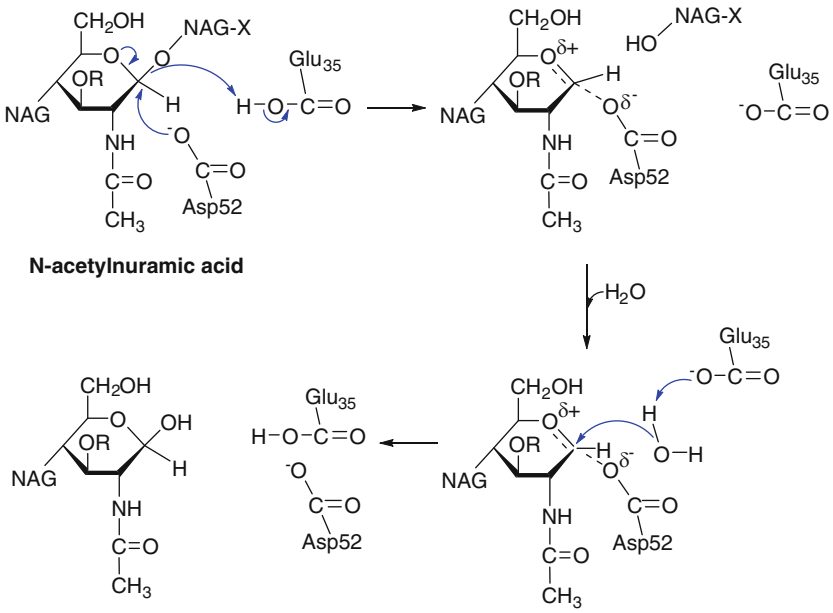

Fig. 4.23 The mechanism of the lysozyme reaction

4.8 Mechanism of Chymotrypsin

Chymotrypsin is a member of the serine protease family of enzymes. Serine proteases as a class are involved in blood clotting, peptide bond hydrolysis, nerve impulse transmission. and complement factors. Chymotrypsin, a digestive enzyme, is probably the best studied of the serine proteases. Its mechanism of action is typical of this class of enzymes.

The precursor of chymotrypsin, chymotrypsinogen, known as a zymogen or proenzyme, is synthesized in the pancreas as an inactive protein in order to preclude digestion of the parent tissue. Chymotrypsinogen, a polypeptide, comprised of 245 amino acids is excreted into the intestine where it is cleaved by trypsin, another serine protease, to π-chymotrypsin. π-Chymotrypsin is autocatalytic and hydrolyzes itself to produce the fully active enzyme, chymotrypsin. In the overall process, there is a loss of four amino acid residues in going from chymotrypsinogen to the active enzyme. Chymotrypsin is an enzyme consisting of three polypeptide chains held together by two disulfide linkages. This process is described in Fig. 4.24.

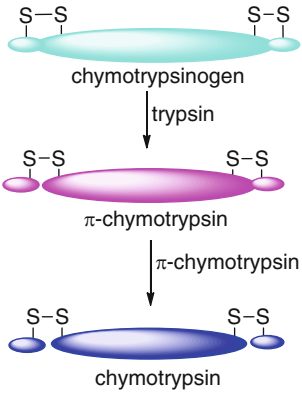

Fig. 4.24 The conversion of inactive chymotrypsinogen to the active form of the enzyme chymotrypsin

Best known as a protease, chymotrypsin also exhibits esterase activity. This fortuitous property greatly facilitated study of the enzyme, i.e., it is much more difficult to analyze protein fragments than to study the hydrolysis of an ester.

Kinetic studies of chymotrypsin involved the use of ρ-nitrophenylacetate as a substrate. The chemical reaction is:

$$\rho\text{-nitrophenylacetate} + H_2O \rightarrow \rho\text{-nitrophenol} + \text{acetate}.$$

Although the aromatic substrate and product are both choromophores they absorb light at distinctly different wave lengths. When the kinetics of the chymotrypsin reaction were carried out, a surprising result, illustrated in Fig. 4.25 was obtained.

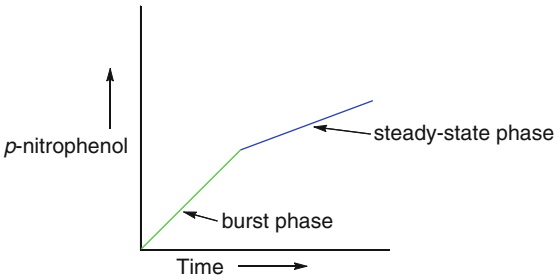

Fig. 4.25 *p*-Nitrophenol formation as a function of time in the chymotrypsin reaction using *p*-nitrophenylacetate as the substrate. The burst phase of the reaction (*green*) is followed by the slower steady-state phase (*blue*)

The biphasic curve incorporates not only the expected steady-state phase of the reaction, but also an initial accelerated rate called the "*burst*." In order to explain these findings, the following mechanism was proposed:

Fig. 4.26 All steps in the conversion of *p*-nitrophenylacetate to *p*-nitrophenol and acetate-E are rapid. The rate-limiting step in the chymotrypsin reaction is the dissociation of acetic acid from the enzyme

It is only in the very early phase of the reaction, i.e., during the first turnover of the enzyme that the burst is observed. The bottle-neck in the overall scheme is the conversion of the acetyl–enzyme intermediate to acetic acid and free enzyme. The kinetics are analogous to a train leaving a station at 8 A.M. and then traveling at 50 km/h. An hour later a second train, using the same track, leaves the station traveling at 100 km/h. At 10 A.M. the relatively fast (burst) second train will be forced to travel at 50 km/h (steady-state) behind the early departing train.

The chemical mechanism of the chymotrypsin reaction has been investigated in great detail by both kinetics and X-ray crystallography [22]. The mechanism itself has gone by a number of names, including the *charge relay system*, the *proton shuttle*, and the *triad*. There are three dynamic enzyme residues involved in the chemical mechanism: serine, aspartate, and histidine. The reaction mechanism is depicted in Fig. 4.27.

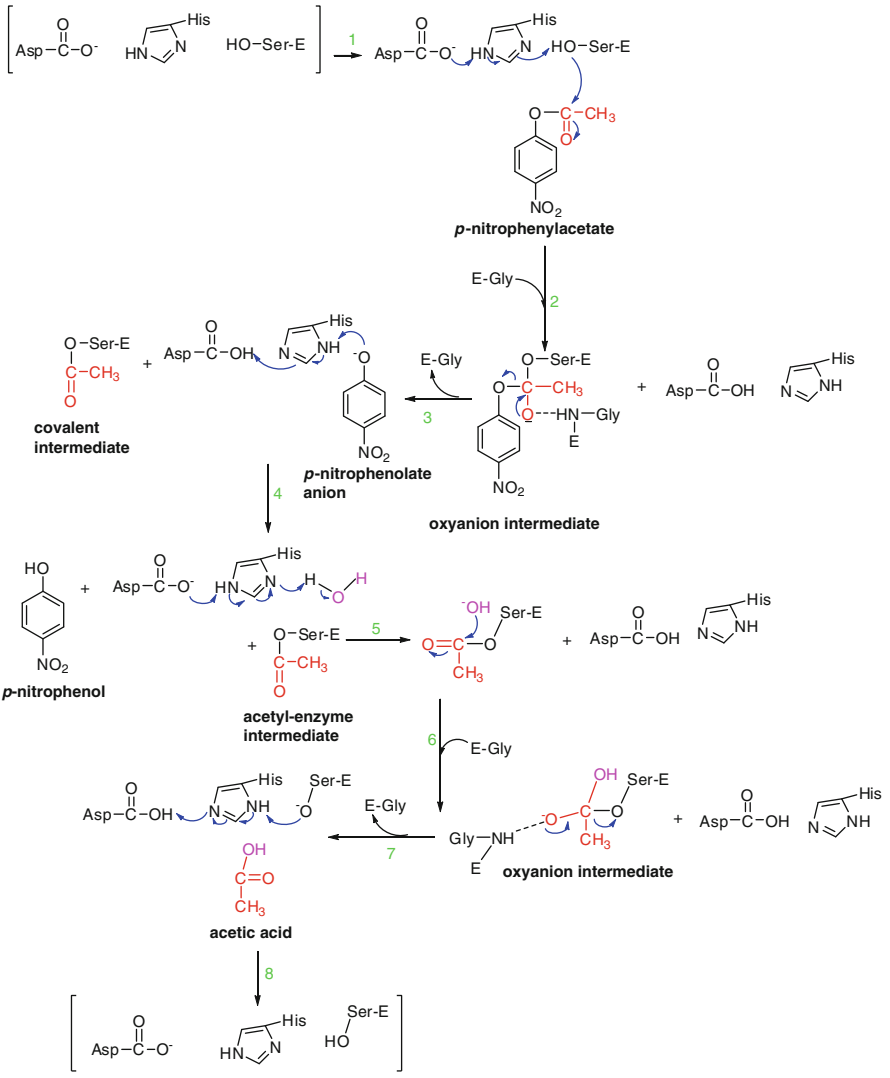

Fig. 4.27 The mechanism of the chymotrypsin reaction with the substrate *p*-nitophenylacetate

4.9 Specificity of the Serine Proteases

Among the serine proteases, the best known are chymotrypsin, elastase, and trypsin. All three enzymes display similar secondary and tertiary structures (they exhibit 40% amino acid sequence homology) and their chemical mechanisms are similar. What differentiates them from each other is their specificity. Consider the peptide sequence shown in Fig. 4.28 where R represents an amino acid side chain.

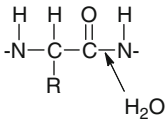

Fig. 4.28 The site of peptide bond cleavage by serine proteases

If R is aromatic (trp, phe, tyr) it will be acted upon by chymotrypsin; trypsin and elastase hydrolyze peptides where R is a basic amino acid (lys, arg) and a neutral amino acid, respectively. The X-ray structures have shown that there are nonpolar or hydrophobic residues in the active site of chymotrypsin. Acidic amino acids such as Asp are contained in the active site of trypsin, whereas neutral amino acid residues are part of the active site of elastase. Genetic studies strongly suggest that the various forms of the serine protease family have arisen by the process of *gene duplication followed by amino acid mutations*.

It should be pointed out that the serine proteases are not the only protein hydrolyases found in nature. Another class of proteases uses cysteine rather than serine at its active site. These are the so-called *thiol proteases*. The best known enzyme in this class is *papain* which is found in the papaya leaf.

4.10 Low-Barrier Hydrogen Bonds

The mechanism of chymotrypsin action in which proton abstraction by a histidine (pK 6.0) of a serine hydroxyl (p$K > 15$) seems unlikely; however, Cleland [23] and Gerlt et al. [24] have proposed that the concept of so-called low-barrier hydrogen bonds (LBHB) can explain how this might occur. If the enzyme can position the energetically unfavorable proton abstraction in the ground state, to an energetically favorable position in the transition state, e.g., a distance of say 2.8 Å between donor and acceptor, proton transfer could occur. The energy for this positioning of the catalytic groups would be supplied by substrate binding. It should be noted that the concept of LBHB is not universally accepted [25, 26].

4.11 Mechanism of Glucoamylase

Glucoamylase is an α-1,4-D-glucohydrolase (exohydrolase) that catalyzes the removal of β-D-glucose from the nonreducing end of starch and malto-oligosaccharides. The reaction mechanism is thought to involve an oxonium ion intermediate (Fig. 4.29). This conclusion was arrived at from the use of the very tight binding inhibitor acarbose (Fig. 4.30) in X-ray crystallography [27] and kinetic studies. A secondary isotope effect was observed [28] using ^{3}H which strongly supports the notion of a carbocation intermediate being involved in the transition state of glucoamylase.

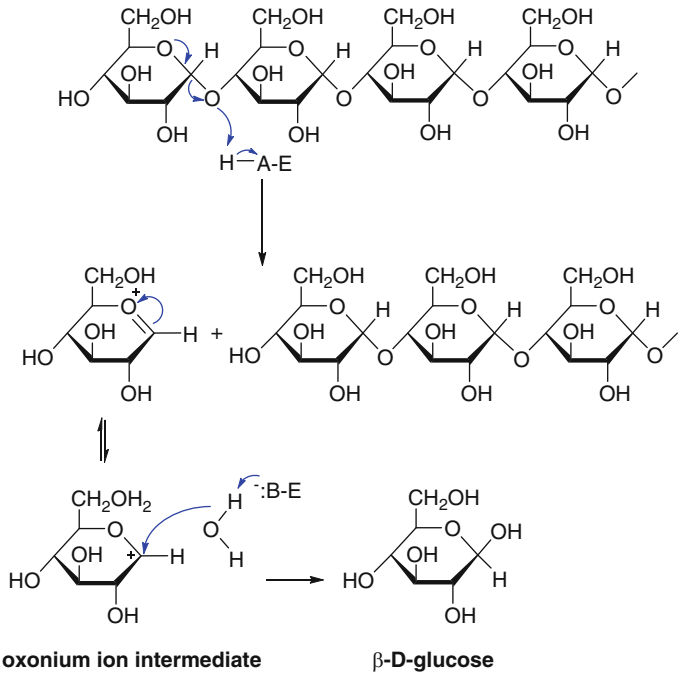

Fig. 4.29 The mechanism of the glucoamylase reaction

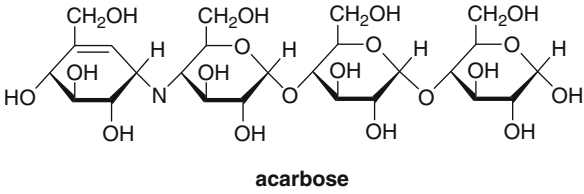

Fig. 4.30 The tight binding inhibitor acarbose was used in X-ray diffraction and kinetic studies to explain the mechanism of the glucoamylase reaction

4.12 Substrate Channeling

There are two types of substrate channeling: inter-enzyme and intra-enzyme channeling. In the former case, the product of one enzyme in a metabolic sequence is the substrate for the second enzyme in that sequence. The enzymes are in close proximity and the product of the first enzyme is precluded from entering the solvent where it may react with other enzymes or with the solvent itself.

In intra-enzyme channeling, the intermediates channel or "tunnel" between topologically distinct, and in some cases, widely separated active sites within a single enzyme.

The active site in most enzymes is a continuum, i.e., in the active site the substrates are juxtaposed just prior to reaction. In intra-channeling enzymes, however, the substrate undergoes a chemical reaction at an active site, active site-1, and the product is then transported or channeled some distance to another active site,

active site-2, where it undergoes a second reaction. An excellent review of some enzymes in this class is in an article by Raushel et al. [29].

The crystal structure of an enzyme that uses tunneling as part of its mechanism of action is carbamoyl phosphate synthetase (Fig. 4.31). The chemical mechanism of carbamoyl phosphate synthetase is shown in Fig. 4.32.

The hydrolysis of glutamine within the small subunit is enhanced when HCO_3^- is phosphorylated by ATP to form carboxyphosphate. Although H_2O molecules are present in the tunnel they do not react with the carboxyphosphate intermediate. The active sites are greater than 35 Å apart and the tunnel itself has a diameter of 3.4 Å which is large enough for passage of the intermediates.

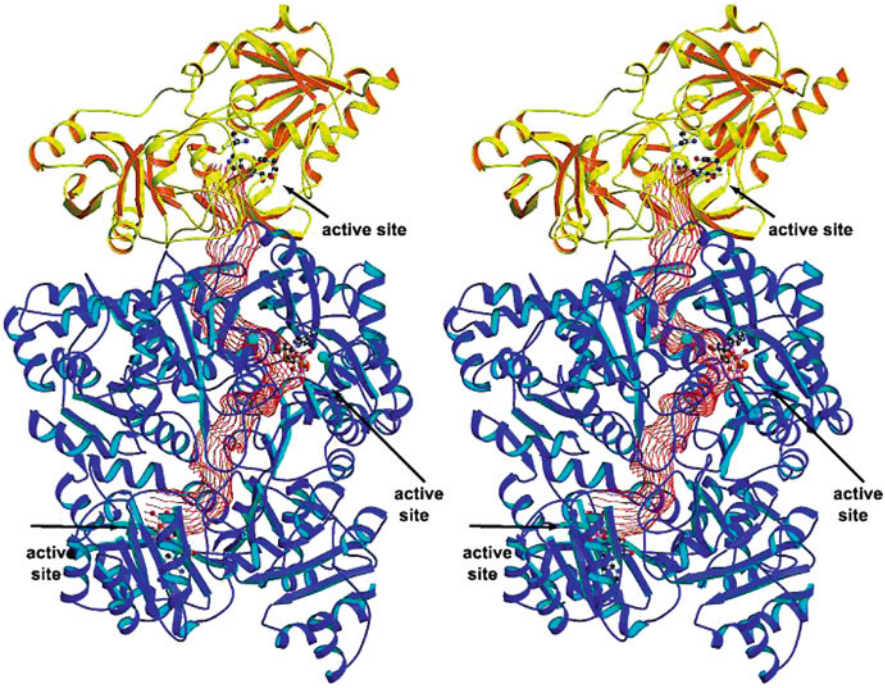

Fig. 4.31 Structural representation of carbamoyl phosphate synthetase. The small and large subunits are shown in *yellow* and *blue*, respectively. The location of the molecular tunnel connecting the three active sites is indicated in *red*

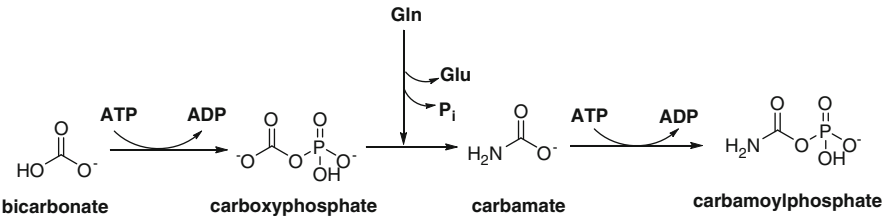

Fig. 4.32 The chemical mechanism of the carbamoyl phosphate synthetase reaction

References

1. Sumner JB (1926) The isolation and crystallization of the enzyme urease. J Biol Chem 69: 435–441
2. Koshland DE Jr (1956) Molecular geometry in enzyme action. J Cell Comp Physiol 47(S1): 217–234
3. Fischer E (1894) Einfluss der configuration auf die wirkung der enzyme. Ber Dtsch Chem Ges 27:2985–2993
4. Koshland DE Jr (1958) Application of a theory of enzyme specificity to protein synthesis. Proc Natl Acad Sci USA 44:98–104
5. Shoshan-Barmatz V, Zakar M, Rosenfethal K, Abu-Hamad S (2008) Key regions of VDAC1 functioning in apoptosis induction and regulation by hexokinase. Biochim Biophys Acta 1787:421–430
6. O'Sullivan C, Tompson FW (1890) Invertase: a contribution to the history of an enzyme or unorganized ferment. J Chem Soc (Trans) 57:834–931
7. Erying H (1935) The activated complex in chemical reactions. J Chem Phys 3:107
8. Evans MG, Polanyi M (1935) Some applications of transition state method to the calculation of reaction velocities, especially in solution. Trans Faraday Soc 31:875
9. Fersht A (1985) Enzyme structure and mechanism, 2nd edn. W.H. Freeman, New York
10. Lumry R, Eyring H (1954) Conformational changes in proteins. J Phys Chem 58:110–120
11. Westheimer FH (1987) Why nature chose phosphates. Science 235:1173–1178
12. Knowles JR (1980) Enzyme catalyzed phosphoryl transfer reactions. Annu Rev Biochem 49: 877–919
13. Lowe G, Potter BV (1981) The stereochemical course of the yeast hexokinase-catalyzed phosphoryl transfer by using adenosine 5′[gamma(S), 16O, 17O, 18O] triphosphate as a substrate. Biochem J 199:227–233
14. Midelfort CF, Rose IA (1976) A stereochemical method for detection of ATP terminal phosphate transfer in enzymatic reactions. Glutamine synthetase. J Biol Chem 261:5881–5887
15. Cardinale GJ, Abeles RH (1968) Purification and mechanism of action of proline racemase. Biochemistry 7:3970–3978
16. Wolfenden R (1976) Transition state analog inhibitors and enzyme catalysis. Ann Rev Biophys Bioeng 5:271–306
17. Rhoads DG, Lowenstein JM (1968) Initial velocity and equilibrium kinetics of myokinase. J Biol Chem 243:3963–3972
18. Purich DL, Fromm HJ (1972) Inhibition of rabbit skeletal muscle adenylate kinase by the transition state analogue P1, P4-di(adenosine-5′-tetraphosphate). Biochim Biophys Acta 276:563–567
19. Fleming A (1922) On a remarkable bacteriolytic element found in tissues and secretions. Proc R Soc Lond B 93:306–317
20. Blake CC, Koenig DF, Mair GA, North AC, Phillips DC, Sarma VR (1965) Structure of hen egg-white lysozyme. A three dimensional Fourier synthesis at 2 Angstrom resolution. Nature 206:757–761
21. Secemski II, Lehrer SS, Leinhard GE (1972) A transition state analog for lysozyme. J Biol Chem 247:4740–4748
22. Sigler PB, Jeffery BA, Matthews BW, Blow DM (1966) An X-ray diffraction study of inhibited derivatives of α-chymotrypsin. J Mol Biol 15:175–192
23. Cleland WW, Kreevoy MM (1994) Low-barrier hydrogen bonds and enzymic catalysis. Science 264:1887–1890
24. Gerlt JA, Kreevoy MM, Cleland WW, Frey PA (1997) Understanding enzymic catalysis: the importance of short, strong hydrogen bonds. Chem Biol 4:259–267
25. Usher KC, Remington SJ, Martin DP, Drueckhammer DG (1994) A very short hydrogen bond provides only moderate stabilization of an enzyme-inhibitor complex of citrate synthase. Biochemistry 28:7753–7759

26. Warshel A, Papazyan A (1996) Energy considerations show that low-energy hydrogen bonds do not offer a catalytic advantage over ordinary hydrogen bonds. Proc Natl Acad Sci USA 93: 13665–13670
27. Aleshin AE, Stoffer B, Firsov LM, Svensson B, Honzatko RB (1996) Crystallographic complexes of glucoamylase with maltooligosaccharide analogs: relationship of stereochemical distortions at the nonreducing end to the catalytic mechanism. Biochemistry 35:8319–8328
28. Tanaka Tao W, Blanchard JS, Hehre EJ (1994) Transition state structures for the hydrolysis of alpha-D-glucopyranosyll fluoride by retaining and inverting reactions by glycolases. J Biol Chem 269:32306–32312
29. Raushel FM, Thoden JB, Holden HM (2003) Enzymes with molecular tunnels. Acc Chem Res 36:539–548

Further Readings

Purich DL (2010) Enzyme Kinetics: Catalysis and Control. Academic Press, New York

Chapter 5
Enzyme Kinetics

Enzyme kinetics is arguably the most time and cost effective way to study enzymes. It is the primary way to study enzyme catalysis, because no other approach allows one to test whether a chemically or spectrophotometrically detected intermediate is formed and turned over on the catalytic timescale. Kinetic studies provide the investigator with information on the mechanism, mode of regulation, and kinetic parameters that are essential for an understanding of enzyme specificity and physiological function.

Enzymes are biological catalysts, and like all catalysts, their properties are studied by measuring their rates of reaction or kinetics. It was recognized in the late nineteenth century that enzymes and their substrates must come together to form a "complex" before a reaction can occur [1]. This complex, non-covalent in nature, is the essence of enzyme catalysis. Because in theory the enzyme is unaltered at the end of a reaction, the conversion of substrate to product as a function of time is normally investigated. In this chapter there will be a brief review of chemical kinetics before a discussion of enzyme kinetics is undertaken.

5.1 Nomenclature

1. The kinetic description of a chemical reaction is based upon the number of substrate and product molecules in the reaction. In deference to the designations used by Michaelis in the early part of the twentieth century, for one substrate–one product systems, the substrate will be designated S and the product P. For more complex reactions the terms Uni, Bi, Ter, etc., are used to describe the reaction order. Thus, a Uni Bi reaction involves one substrate (A) and two product molecules (P, Q), and a Bi Ter reaction two substrate (A, B) and three product (P, Q, R)molecules.
2. Rate constants, regardless of the reaction direction will have positive subscripts: thus k_2, k_4, etc., never k_{-2}, k_{-4}, etc.
3. Products of rate constants will be described as follows: $k_1k_2k_3$, never $k_1 \cdot k_2 \cdot k_3$ or $(k_1)(k_2)(k_3)$.

H.J. Fromm and M.S. Hargrove, *Essentials of Biochemistry*,
DOI 10.1007/978-3-642-19624-9_5, © Springer-Verlag Berlin Heidelberg 2012

5.2 Brief Review of Chemical Kinetics

One goal of thermodynamics is to predict whether chemical reactions will occur spontaneously. But a spontaneous reaction is of little use unless it occurs at a finite rate. The purpose of chemical kinetics, of which enzyme kinetics is a specific application, is to quantify rates of chemical reactions based on defined reaction conditions, and extract information that can be used to predict rates under a broad set of conditions. The Law of Mass Action states that reactions will proceed to equilibrium at a rate proportional to the concentrations of reactants. Thus, the equilibrium constant and reaction quotient will dictate *whether* a reaction will occur, and kinetic constants will describe the *rate* at which the reaction will occur. Thus, the kinetic view of "dynamic" equilibrium is the point at which the forward and reverse reaction rates are equivalent.

As a general example of the information considered in chemical kinetics, we can look at a reversible first-order reaction:

$$A \underset{k_2}{\overset{k_1}{\rightleftharpoons}} B, \tag{5.1}$$

The values k_1 and k_2 are called "rate constants," which tell you how fast the reaction will occur in each direction based on the concentrations of A and B. If a solution starts out containing only A, the initial reaction rate of conversion of A into B will be $k_1[A]$. Of course once the reaction starts, the concentration of A is lowered, and B starts to accumulate. This process continues until the equilibrium concentration is reached. At this point A is converted to B, and vice versa, at rates that maintain this equilibrium. For this reason, the equilibrium constant for the reaction is dictated by the rate constants.

$$K_{AB} = \frac{k_1}{k_2}. \tag{5.2}$$

For a reaction initiated with $[A] > [B]$, the velocity of the reaction could be measured by monitoring the disappearance of A, or the formation of B as the reaction proceeds to equilibrium:

$$\frac{-d(A)}{dt} = \frac{d(B)}{dt} = k_1(A) - k_2(B). \tag{5.3}$$

If the reaction is initiated with only $[A]$, and the velocity measured at very early time points before much $[B]$ is formed, then the measured (initial) velocity will be equal to $k_1[A]$, allowing measurement of k_1 directly. Alternatively, (5.1) can be integrated to calculate a time course for the concentration of either reactant (in this case A).

$$A_t = \Delta(A)\exp[-(k_1 + k_2)(t)]. \tag{5.4}$$

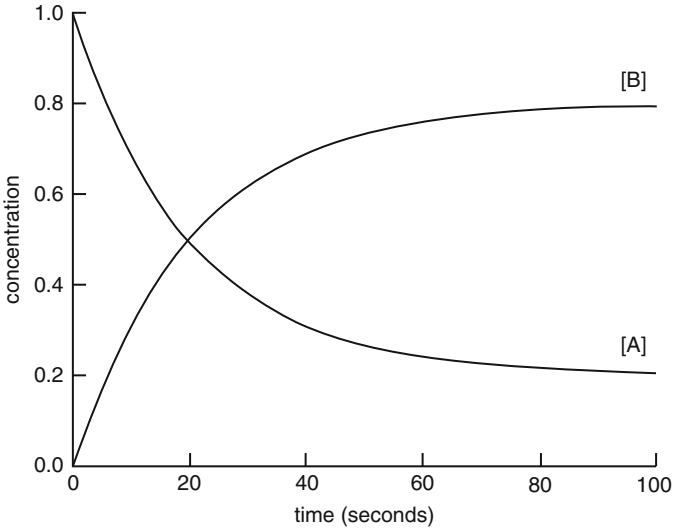

Fig. 5.1 Plot of concentration of species *A* and *B* as a function of time based upon the kinetic mechanism illustrated in (5.1)

In (5.4), ΔA is the change in $[A]$ from start of the reaction to the value at equilibrium. Figure 5.1 demonstrates the approach of $[A]$ and $[B]$ to equilibrium under conditions where the reaction is initiated with only A, $k_1 = k_2 = 0.05\ s^{-1}$, and $K_{AB} = 0.25$.

Plots of concentrations of species *A* and *B* as a function of time based upon the kinetic mechanism illustrated in (5.1) are shown in Fig. 5.1.

Equation 5.1 is a simple reversible first-order reaction. Many reactions schemes, including that derived below for enzyme catalysis are much more complex. In some cases integrated solutions for the differential equations describing reaction velocities have finite solutions [such as the relationship between (5.3) and (5.4)]. Often however, they do not, and reaction time courses must be analyzed by numerical integration or, as in the case with many enzyme-catalyzed reactions, through examination of initial velocities under controlled conditions.

5.3 The Evolution of Enzyme Kinetics

5.3.1 Historical

The idea that the enzyme and substrate must unite for a finite period of time before catalysis can occur is the recognized basis of contemporary enzyme kinetics. O'Sullivan and Tompson [1] were among the first to suggest such interaction.

These investigators also reported that the reaction rate is first order with respect to the substrate and they concluded that enzyme reactions follow the Law of Mass Action. In 1892, Brown found that enzymes also follow zero-order kinetics relative to their substrates and he was able to synthesize the concept in 1902 that when the velocity of an enzyme-catalyzed reaction is plotted against substrate concentration, the result is a rectangular hyperbola which incorporates both zero- and first-order kinetics [2]. Henri [3] in attempting to summarize the state of enzyme kinetics in 1903, pointed out that enzymes do not alter the equilibrium constant, but do enhance reaction rates in proportion to their concentration, and in addition, are present in kinetic studies at much lower concentrations than are the substrates. Using these concepts as the basis of his reasoning, Henri was able to propose a rate expression that is very similar to the well-known Michaelis–Menten Equation (see below). He also integrated his equation and showed how it might be used to study the full-time course of an enzyme-catalyzed reaction. Although his goal was to study the full-time course of enzyme-catalyzed reactions, he has received very little credit for his pioneering contributions to enzyme kinetics.

Michaelis and Menten [4], in order to explain enzyme kinetics mathematically, assumed that the enzyme and substrate are in equilibrium with the loose complex of enzyme and substrate. The reaction velocity was assumed to be governed by the decomposition of the enzyme–substrate complex to form product and release enzyme. In 1925, Briggs and Haldane [5] incorporated the concept of the steady-state into the derivation of the Henri–Michaelis–Menten Equation. In both the equilibrium and steady-state derivations the concentration of the enzyme–substrate complex remains constant, but for very different reasons.

5.3.2 *Time Course of Enzyme-Catalyzed Reactions*

After the initiation of an enzyme-catalyzed reaction as illustrated in (5.5), the concentrations of the various components change with time, as depicted by the computer simulation outlined in Fig. 5.2 of the full-time course of the reaction.

$$E + S \underset{k_2}{\overset{k_1}{\rightleftharpoons}} ES \overset{k_3}{\rightarrow} E + P. \tag{5.5}$$

Illustrated in Fig. 5.2 are the pre-steady-state and steady-state phases of an enzyme-catalyzed reaction using (5.28) to generate the simulations. The parabolic slope increase in product formation in the early phase of the reaction (pre-steady-state) is due to the exponential term in (5.28). During the steady-state phase of the reaction $d(ES)/dt \cong 0$ and P is a linear function of time.

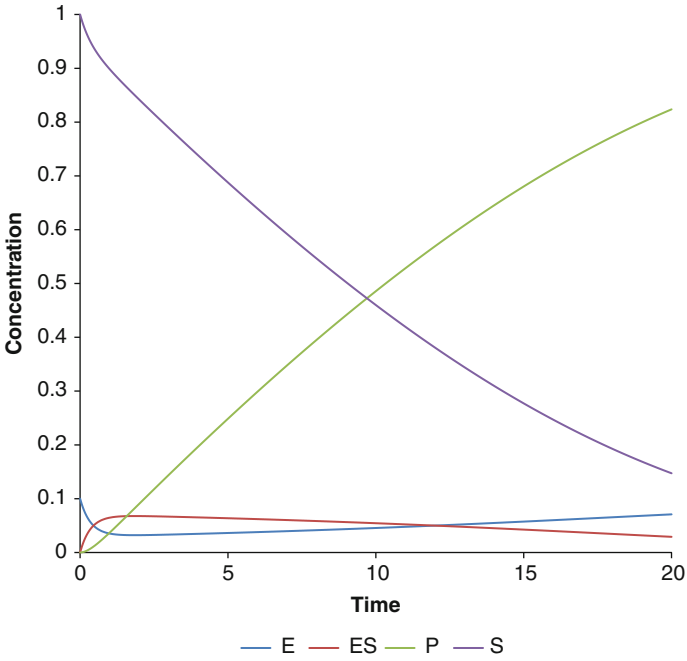

Fig. 5.2 Time course of an enzyme-catalyzed reaction. How the variables in (5.5) change with time is depicted in the figure based upon simulations using (5.28)

5.3.3 Derivation of the Henri–Michaelis–Menten Equation

Both the Michaelis–Menten Equation and the Henri equation were derived to explain the experimental observation that when reaction velocity for an enzyme-catalyzed reaction is plotted against substrate concentration the result is a rectangular hyperbola.

The basic assumption made in these derivations is illustrated by (5.5), where E, S, ES, and P represent free enzyme, substrate, enzyme–substrate complex, and product, respectively. The ks are taken to be rate constants for the individual steps in the mechanism.

In order to derive the rate equation, certain information is required:

(a) *A velocity expression* (v). This would be $v = k_3(ES)$ or $v = -k_1(E)(S) + k_2(ES)$.
(b) *A conservation of enzyme expression*, i.e., $E_0 = E + ES$.
(c) *The assumption that the substrate concentration does not change*, i.e., very little product is formed.
(d) *An equation for the equilibrium between the E, S, and the ES complex*, i.e.,

$$K_S = \frac{[E][S]}{[ES]}. \tag{5.6}$$

The K_S in (5.6) is a dissociation constant.

Because the velocity term $v = k_3[ES]$ is simpler than the alternative, it is used. In addition, using this expression, it is necessary to get all enzyme terms into the form $[ES]$, thus:

$$[E] = \frac{K_S[ES]}{[S]}. \tag{5.7}$$

Substituting this information into the *Conservation of Enzyme Equation* gives:

$$E_0 = [E] + [ES] = \frac{K_S[ES]}{[S]} + [ES]. \tag{5.8}$$

Dividing both sides of (5.8) by $[ES]$ yields:

$$\frac{[E_0]}{[ES]} = \frac{K_S}{[S]} + 1. \tag{5.9}$$

Multiplying the numerator and denominator on the left-hand side of (5.9) by k_3 gives:

$$\frac{k_3[E_0]}{k_3[ES]} = \frac{K_S}{[S]} + 1. \tag{5.10}$$

With the knowledge that $v = k_3[ES]$,

$$\frac{k_3[E_0]}{v} = \frac{K_S}{[S]} + 1 = 1 + \frac{K_S}{[S]}. \tag{5.11}$$

Reciprocating (5.11) gives the so-called Michaelis–Menten Equation or the Henri Equation.

$$v = \frac{k_3[E_0][S]}{K_S + [S]} \tag{5.12}$$

Equation 5.12 describes the rectangular hyperbola shown in Fig. 5.3 when velocity is plotted against substrate concentration.

(e) In the derivation of the Henri–Michaelis–Menten Equation it is assumed that the system is at equilibrium. The Briggs–Haldane derivation [5] of the rate equation for (5.5) assumes a steady-state, i.e., $d(ES)/dt = 0$ and $d(E)/dt = 0$ (see Fig. 5.2). The derivation using the steady-state assumption is similar to that described using the equilibrium assumption except that $(n - 1)$ differential equations are required for the solution (where n is the number of enzyme terms). In the case of (5.5), $n = 2$ and only one equation is necessary. The different differential equations are then set equal to zero, and the equations for

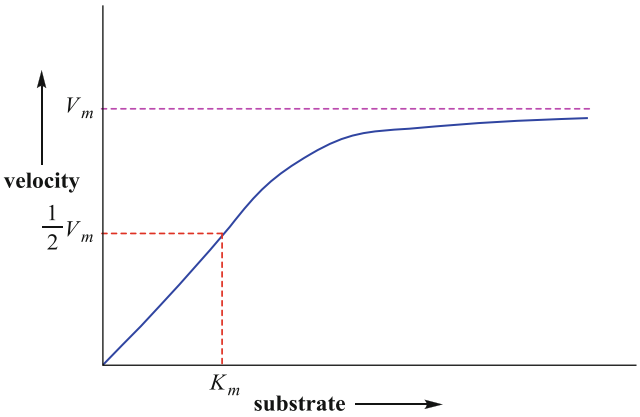

Fig. 5.3 Plot of velocity versus substrate concentration. The kinetic parameters V_m and K_m, or K_S, are described in the text

the different enzyme forms can then be evaluated as one would do in the case of solving simultaneous equation, e.g., algebraically, using matrix algebra, computers, etc. Thus,

$$d(ES)/dt = k_1(E)(S) - k_2(ES) - k_3(ES) = 0, \tag{5.13}$$

$$E = \frac{(k_2 + k_3)(ES)}{k_1(S)}. \tag{5.14}$$

Following the method already outlined for the derivation of the Henri–Michaelis–Menten Equation, the velocity expression is:

$$v = \frac{k_1 k_3 [E_0][S]}{k_1[S] + k_2 + k_3} \tag{5.15}$$

Reference to Fig. 5.3 suggests that at high levels of substrate a limiting velocity, the maximum velocity (V_m), is obtained. An expression for V_m can be obtained by first dividing the numerator and denominator of (5.15) by $k_1[S]$.

$$v = \frac{k_3[E_0]}{1 + \dfrac{(k_2 + k_3)}{k_1[S]}}. \tag{5.16}$$

At very high, or infinite concentrations of substrate, $v = k_3[E_0]$. Under these conditions, $v = k_3[E_0] = V_m$, and where $v = ½(V_m)$, $[S] = (k_2 + k_3)/k_1 = K_m$. Substituting these values for V_m and K_m into (5.16) yields (5.17).

$$v = \frac{V_m[S]}{K_m + S}. \tag{5.17}$$

In the case of the equilibrium derivation (5.12), $V_m = k_3[E_0]$, and K_S is a dissociation constant. Thus, (5.12) and (5.17) are *identical in form and are indistinguishable kinetically*.

V_m, K_S, and K_m are referred to as kinetic parameters that serve to define enzyme properties. The higher the V_m and the lower the K_S or K_m the more active and specific the enzyme. The ratio V_m/K_m is frequently used to define enzyme efficiency. This ratio is often characterized as k_{cat}/K_m, where $k_{cat} = k_3$.

At low substrate concentrations, i.e., where $S \ll K_m$, $v = V_m\ [S]/K_m$ or $v =$ a constant $[S]$. Under these conditions the reaction is first order with respect to substrate. At high substrate levels relative to the K_m, $v = V_m$, and the velocity is zero order with respect to substrate. The Henri–Michaelis–Menten Equation shows that the enzyme has a finite number of active sites and that when these sites are saturated with substrate the maximal velocity will be attained.

(f) The kinetic mechanism illustrated by (5.5) is an example of a one substrate system, also referred to as a Uni Uni mechanism-one substrate and one product. Examples of Uni Uni mechanisms are hydrolases, isomerases, lyases, and mutases. In the case of hydrolases, H_2O is a substrate; however, the concentration of H_2O does not change in the course of the reaction, i.e., $d(H_2O)/dt = 0$ and H_2O is therefore not part of the kinetic equation. The mechanism shown in (5.5) may also be described as depicted in Fig. 5.4.

Fig. 5.4 The kinetic mechanism of the Henri–Michaelis–Menten for enzyme and substrate interaction

It is very difficult to estimate the asymptote of the curve and thus evaluate the kinetic parameters from a plot of the type shown in Fig. 5.3 without a computer; however, this problem was solved many years ago by reciprocating (5.17) [6].

$$\frac{1}{v} = \frac{1}{V_m}\left(1 + \frac{K_m}{S}\right). \tag{5.18}$$

Equation (5.18) is in the form of a straight line: $y = m \times x + b$.
A plot of $1/v$ versus $1/S$, known as the, *Linweaver–Burk* [6], or *double reciprocal plot*, will be linear as shown in Fig. 5.5. It can be seen in Fig. 5.5 that the kinetic parameters are readily evaluated.

Examination of (5.5) which is the basis for the Henri–Michaelis–Menten Equation reveals that it does not provide a term for product formation, i.e., the point at which the chemistry of the reaction occurs. A more realistic mechanism includes both *ES* and *EP* terms (Fig. 5.6):

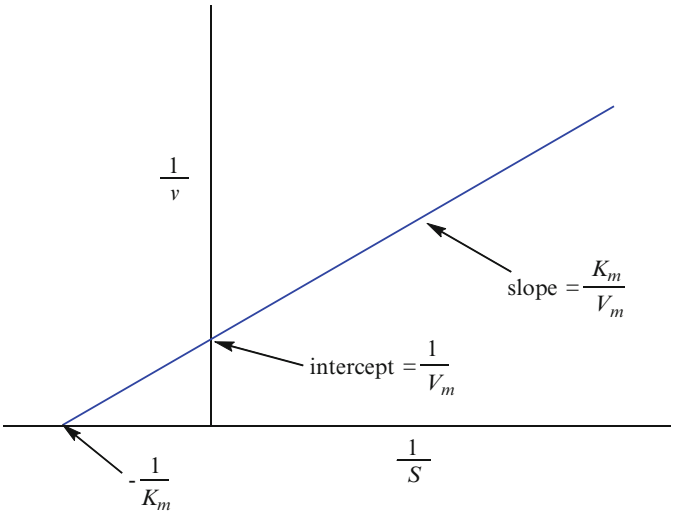

Fig. 5.5 Plot of $1/v$ versus $1/S$ for (5.12). The kinetic parameters can be evaluated directly from the plot as indicated

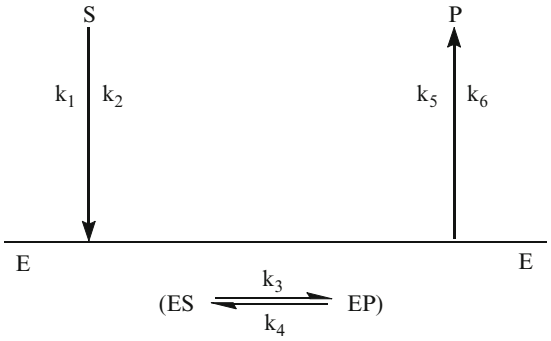

Fig. 5.6 One substrate system (Uni Uni) involving an enzyme–substrate and an enzyme–product complex

(g) The two binary complexes illustrated in Fig. 5.6 constitute "*central complexes*" in which the chemical transformations occur. The derivation of the rate equation for this mechanism, even assuming that $P = 0$, is much more complex than that involving a single enzyme–substrate complex (Fig. 5.4).

In this case two differential equations are required, both of which are set to zero, assuming the steady state. The three equations are:

$$d(E)/dt = -k_1(E)(S) + k_2(ES) + k_5(EP) - k_6(P)(E) = 0, \tag{5.19}$$

$$d(ES)/dt = k_1(E)(S) - (k_2 + k_3)(ES) + k_4(EP) = 0, \tag{5.20}$$

$$d(EP)/dt = k_3(ES) - (k_4 + k_5)(EP) + k_6(E)(P) = 0. \tag{5.21}$$

If it is assumed that P is very small, the $k_6(E)(P)$ term is eliminated. Solving the last two equations for E and ES gives:

$$ES = \frac{(k_4 + k_5)(EP)}{k_3}, \tag{5.22}$$

$$E = \frac{(EP(k_2k_4 + k_2k_5 + k_3k_5))}{k_1K_3(S)}. \tag{5.23}$$

When these enzyme term are substituted into the *Conservation of Enzyme Equation* and the velocity term, $v = k_5(EP)$ introduced, the following rate equation, in double reciprocal form, is obtained:

$$\frac{E_0}{v} = \frac{(k_3 + k_4 + k_5)}{k_3k_5} + \frac{(k_2k_4 + k_2k_5 + k_3k_5)}{k_1k_3k_5(S)}. \tag{5.24}$$

(h) To introduce the kinetic parameter terms, a universal shorthand method can be used instead of setting $[S] = \infty$ to determine V_m, and then solving for $K_m = [S]$, where $v = \frac{1}{2}V_m$. The procedure involves simply transforming (5.24) into one where the constant term is multiplied by its reciprocal to equal 1, e.g.,

$$\frac{k_3k_5E_0/k_3 + k_4 + k_5}{v} = 1 + \frac{(k_2k_4 + k_2k_5 + k_3k_5)}{(k_1k_3k_5)(S)} \times \frac{(k_3k_5)}{(k_3 + k_4 + k_5)}, \tag{5.25}$$

$$V_m = \frac{k_3k_5E_0}{(k_3 + k_4 + k_5)}, \quad K_m = \frac{(k_2k_4 + k_2k_5 + k_3k_5)}{k_1(k_3 + k_4 + k_5)}, \tag{5.26}$$

$$v = \frac{V_m(S)}{K_m + S}. \tag{5.27}$$

After canceling common terms in the numerator and denominator of (5.25), the V_m term is found on the left-hand side of the equation and the K_m term on the right-hand side.

Equations (5.27) and (5.17) are identical in form. Thus, it is not possible from kinetics alone to distinguish between the mechanisms depicted in Figs. 5.4 and 5.6.

(i) The velocity term in the Henri–Michaelis–Menten Equation, which is the basis of enzyme kinetics in general, is in fact *initial velocity* (see Fig. 5.2). It is only when initial velocity is measured that these equations are valid. This point is illustrated in Fig. 5.7. Too often replicate measurements are made at a *single* time point. The danger inherent in such assays should be obvious from the data illustrated in Fig. 5.7, e.g., note that after two time units the observed velocity deviates from the initial velocity.

If (5.19), (5.20), and (5.21) are *not* set equal to zero but are integrated, after substituting for the *Conservation of Enzyme Equation* between the limits of

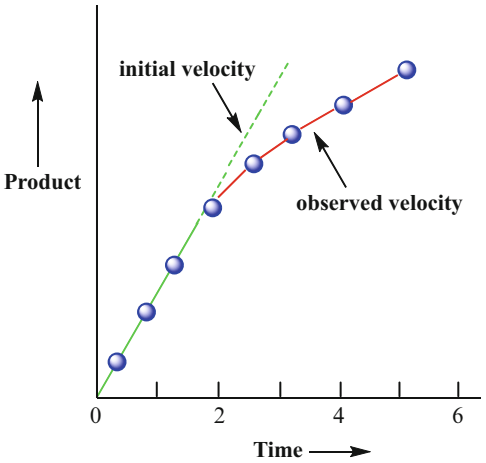

Fig. 5.7 Plot of product as a function of time

$[ES] = 0$ and $[ES]$, an equation for $[ES]$, $[ES]_t$, as a function of time is obtained. By substituting for $[ES]$ in the equation $v = dP/dt = k_3[ES]$, and integrating between the limits of $P = 0$ and P_t and time $= 0$ and time $= t$, (5.28) is obtained:

$$P_t = \frac{k_1 k_3 (S)(E_0)}{[k_1(S) + k_2 + k_3]} \left[t + \frac{1}{(k_1(S) + k_2 + k_3)} e^{-(k_1(S)+k_2+k_3)(t)} - 1 \right]. \tag{5.28}$$

Equation (5.28) predicts that in the early time phase in an enzyme catalyzed reaction there will be an exponential increase in the parabolic slope in the product–time progress curve (see Fig. 5.2), i.e., an *induction period* known as the pre-steady state phase of the reaction. At a still later time, when the exponential term in (5.28) approaches zero, $[P]$ will be a linear function of time, t, with a slope, $(\Delta P/\Delta t)$ of $k_1 k_3 (S)(E_0)/(k_1(S) + k_2 + k_3)$.

This is precisely the form of the steady-state rate equation for the kinetic mechanism illustrated in Fig. 5.4 and where $(\Delta P/\Delta t)$ equals initial velocity.

5.3.4 The Haldane Equation

There is a relationship, known as the Haldane Equation, that relates the equilibrium constant for a reaction and the kinetic parameters. Consider (Fig 5.6) where the reverse reaction is taken into account:

$$E + S \underset{k_2}{\overset{k_1}{\rightleftharpoons}} ES \underset{k_4}{\overset{k_3}{\rightleftharpoons}} E + P. \tag{5.29}$$

The equilibrium constant for the reaction is:

$$K_{\text{eq}} = \frac{k_1 k_3}{k_2 k_4}. \tag{5.30}$$

Multiplying the numerator and denominator of (5.30) by $E_0/(k_2 + k_3)$ and rearranging yields the Haldane Equation:

$$K_{\text{eq}} = \frac{V_{m,f}K_{m,r}}{V_{m,r}K_{m,f}}, \tag{5.31}$$

where f and r represent forward and reverse reaction parameters, respectively.

If a proton is generated in a reaction. the numerator on the right hand side of (5.30) would be multiplied by $[H^+]$. When using the Haldane relationship, $[H^+]$ is omitted and the equilibrium constant is referred to as the apparent equilibrium constant.

5.3.5 *Shorthand Method for Deriving Rate Equations for the Reverse Reaction*

It is possible to derive the rate equation for the reverse reaction of a kinetic mechanism, as was illustrated for the forward reaction; however, there is a less cumbersome way to achieve this goal. Simply write the rate constants in two rows, e.g., in the case of the simple Henri–Michaelis–Menten Equation (5.16):

$$k_1 \ldots\ldots k_4$$

$$k_2 \ldots\ldots k_3$$

Replace k_1 with k_4 and k_2 with k_3 and S with P. This shorthand method can be used with any symmetrical kinetic mechanism regardless of its complexity.

5.3.6 *Enzyme Inhibition*

The rates of enzyme-catalyzed reactions may be modulated by a variety of factors. One of these factors, and one of the most important, involves enzyme inhibitors. Enzyme inhibitors are widely used today in pharmaceuticals to target-specific enzymes. Thus, the study of enzyme inhibition is not only important from a pedagogical perspective, but from a practical one as well.

There are basically two types of enzyme inhibitors: irreversible and reversible. Irreversible inhibitors react with the enzyme and form a covalent bond with the enzyme which causes inhibition. Reversible inhibitors, unlike irreversible inhibitors, can be removed by dialysis or their effects ameliorated by dilution.

An example of an irreversible inhibitor is diisopropylphosphofluoridate, or nerve gas, in which the diisopropylphosphoryl moiety binds covalently to the active site of the serine protease acetylcholinesterase, an enzyme involved in nerve impulse transmission (Fig. 5.8).

How does dilution reverse the effects of the reversible inhibitor, I? Consider the addition of a reversible inhibitor (I) to an enzyme (E). The following equilibria then pertain assuming that only a small fraction of inhibitor is bound to the enzyme:

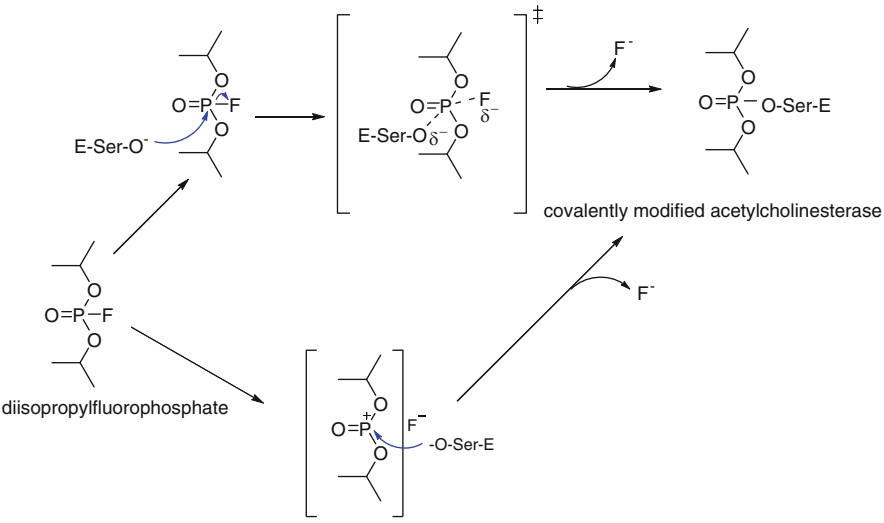

Fig. 5.8 The binding of diisopropylflurophosphate at the active site of acetylcholine esterase

$$E + I = EI \tag{5.32}$$

$$E_0 = E + EI \tag{5.33}$$

$$K_\mathrm{i} = \frac{[E][I]}{[EI]} = \frac{[E_0 - EI][I]}{[EI]}, \tag{5.34}$$

$$\frac{[EI]}{[E_0]} = \frac{[I]}{[K_\mathrm{i} + I]}. \tag{5.35}$$

If $K_\mathrm{i} = 10^{-3}$ M and the concentration of $I = 10^{-3}$ M, $[EI]/[E_0] = 0.5$, or 50% of the enzyme is complexed with inhibitor. If the system is then diluted so that the concentration of the inhibitor is 10^{-4} M, only 9% of the enzyme is complexed with the inhibitor. It is clear from this simple example that dilution of the inhibitor will serve to reverse the effects of inhibition.

5.3.7 Reversible Enzyme Inhibition

Although there are many types of inhibition that have been observed with enzymes, this text will consider only the three types of so-called classical reversible enzyme inhibition: *competitive, non-competitive* (*mixed*), *and uncompetitive*. In all cases the inhibitor(s) will be of the "*dead-end*" type, i.e., a complex of enzyme, substrate, and inhibitor will not produce products.

5.3.7.1 Competitive Inhibition

Outlined in Fig. 5.9 is the model for competitive inhibition within the context of the Henri–Michaelis–Menten mechanism.The derivation of the rate equation for a competitive inhibitor in a Uni Uni system is:

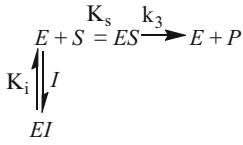

Fig. 5.9 Mechanism of competitive inhibition for a one substrate system

$$v = k_3[ES], \tag{5.36}$$

$$E_0 = E + ES + EI, \tag{5.37}$$

$$K_\mathrm{i} = \frac{[E][I]}{[EI]},\ EI = \frac{[E][I]}{K_\mathrm{i}}, \tag{5.38}$$

$$E_0 = E + ES + \frac{[E][I]}{K_\mathrm{i}} = ES + [E]\left(1 + \frac{[I]}{K_\mathrm{i}}\right), \tag{5.39}$$

$$E = \frac{K_S[ES]}{[S]}, \tag{5.40}$$

$$E_0 = ES + \frac{K_S[ES]}{[S]}\left(1 + \frac{[I]}{K_\mathrm{i}}\right), \tag{5.41}$$

$$\frac{E_0}{ES} = 1 + \frac{K_S}{[S]}\left(1 + \frac{[I]}{K_\mathrm{i}}\right), \tag{5.42}$$

$$\frac{k_3[E_0]}{k_3[ES]} = 1 + \frac{K_S}{[S]}\left(1 + \frac{[I]}{K_\mathrm{i}}\right) = \frac{V_m}{v}, \tag{5.43}$$

$$\frac{V_m}{v} = 1 + \frac{K_S}{[S]}\left(1 + \frac{[I]}{K_\mathrm{i}}\right), \tag{5.44}$$

$$\frac{1}{v} = \frac{1}{V_m}\left[1 + \frac{K_S}{[S]}\left(1 + \frac{[I]}{K_\mathrm{i}}\right)\right]. \tag{5.45}$$

It is important to note that there is no indication from Fig. 5.9 where on the enzyme the inhibitor binds. If the inhibitor and the substrate are structurally similar, the inhibitor *may* bind at the active site. A case in point involves mammalian liver

fructose-1,6-bisphosphatase ($FBPase_1$), an enzyme that requires divalent metal ions for activity. β-D-Fructose 2,6-bisphosphate, which is structurally similar to the substrate α-D-fructose 1,6-bisphosphate, is a competitive inhibitor and binds at the active site [7]. On the other hand, AMP, an allosteric inhibitor, is a competitive inhibitor of Mg^{2+} [8] which also binds at the active site; however, the AMP and metal-binding sites are 28Å apart [9].

Finally, the rate equation (5.45) suggests that at very high (infinite) substrate concentration, competitive inhibition is eliminated.

If one plots $1/v$ versus $1/substrate \pm$ inhibitor using (5.45), a family of lines is generated that intersect on the ordinate ($1/v$) axis. It can be seen that where $1/S = 0$ (infinite substrate concentration) competitive inhibition is eliminated (Fig. 5.10).

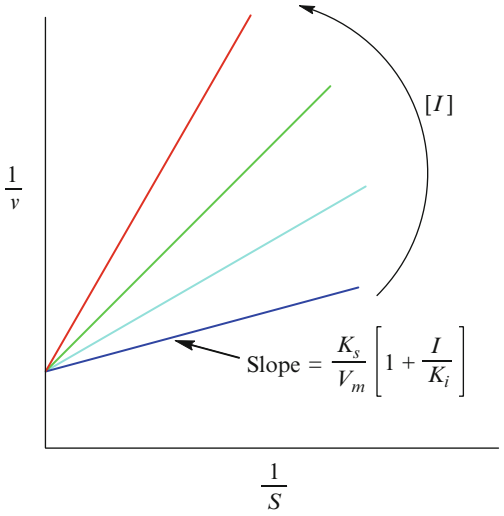

Fig. 5.10 Double reciprocal plot of $1/v$ versus 1/substrate concentration for a competitive inhibitor. Plot of slopes versus [*I*] allows for the calculation of K_i

5.3.7.2 Noncompetitive Inhibition

In noncompetitive inhibition the inhibitor binds at a site *other* than the active site. Binding of the inhibitor to the enzyme sends a signal to the active site, presumably via a conformational change, that causes a decrease in enzyme activity. Because the inhibitor binds at a site that is topologically distinct from the active site, the binding can be considered to be *allosteric* in nature.

Another feature of noncompetitive inhibition is that inhibitor and substrate binding are *not* mutually exclusive. Thus, noncompetitive inhibition is not totally reversible at infinite substrate concentration.

A model for noncompetitive enzyme inhibition is shown in Fig. 5.11.

In the typical derivation of noncompetitive inhibition it is assumed that all steps in the mechanism are rapid and in equilibrium relative to the k_3 step. Thus, the following equilibria hold:

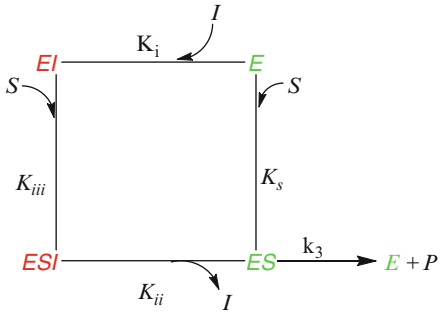

Fig. 5.11 Kinetic model of noncompetitive inhibition

$$K_{\mathrm{i}} = \frac{[E][I]}{[EI]}, K_{\mathrm{ii}} = \frac{[ES][I]}{[ESI]}, K_{\mathrm{iii}} = \frac{[EI][S]}{[ESI]}. \tag{5.46}$$

The Conservation of Enzyme Equation for this mechanism is: $E_0 = E + ES + EI + ESI$.

The *ESI* term can come from either the K_{ii} or the K_{iii} relationship, thus:

$$E_0 = (E)\left(1 + \frac{[I]}{K_{\mathrm{i}}}\right) + (ES)\left(1 + \frac{[I]}{K_{\mathrm{ii}}}\right). \tag{5.47}$$

Finally, the equation for noncompetitive inhibition is:

$$\frac{1}{v} = \frac{1}{V_m}\left[\left(1 + \frac{[I]}{K_{\mathrm{ii}}}\right) + \frac{K_S}{[s]}\left(1 + \frac{[I]}{K_{\mathrm{i}}}\right)\right]. \tag{5.48}$$

A plot of data for (5.48) is shown in Fig. 5.12. It is possible to calculate K_{i} and K_{ii} as indicated in Fig. 5.11 by plotting both slopes and intercepts against inhibitor concentration. A knowledge of K_S and V_m, which can be obtained from a plot of $I = 0$, is required for these determinations. Inspection of Fig. 5.11 reveals that K_{iii} can be determined from the relationship $K_S K_{\mathrm{ii}} = K_{\mathrm{i}} \cdot K_{\mathrm{iii}}$.

It can be seen from Fig. 5.12 that the lines converge above the *abscissa*. Where convergence occurs depends upon the relationship between K_{i} and K_{ii}. The $1/v$ coordinate for the noncompetitive double reciprocal plot is shown in Fig. 5.12. If $K_{\mathrm{i}} > K_{\mathrm{ii}}$, intersection will be below the 1/[*substrate*] axis. If $K_{\mathrm{i}} < K_{\mathrm{ii}}$, intersection will be above the 1/[*substrate*] axis. In the case where $K_{\mathrm{i}} = K_{\mathrm{ii}}$ intersection of the lines will be on the axis. The term "mixed" inhibition is often seen in books and the literature. It refers to noncompetitive inhibition plots that intersect *above* or *below* the 1/[*substrate*] axis. In this text noncompetitive inhibition will be used regardless of where the intersection occurs as long as the convergence point is to the left of the ordinate axis.

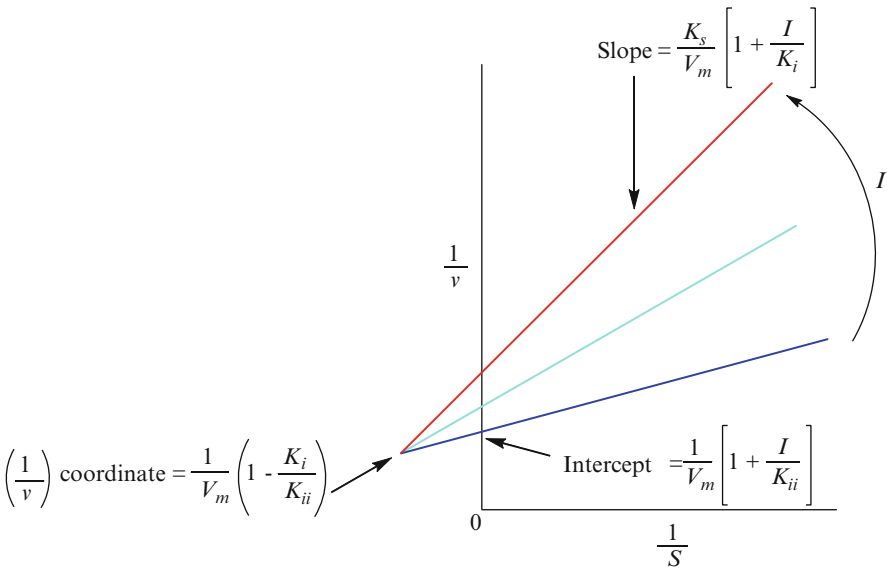

Fig. 5.12 Plot of 1/*velocity* (1/*v*) versus 1/*substrate* (1/*S*) concentration for noncompetitive inhibition

5.3.7.3 Uncompetitive Inhibition

In uncompetitive inhibition the inhibitor binds exclusively to the enzyme–substrate (*ES*) complex. Uncompetitive inhibition is seen infrequently in one substrate systems (Fig. 5.13).

The derivation of the rate equation for uncompetitive inhibition involves the following relationships:

Fig. 5.13 The kinetic model for uncompetitive inhibition

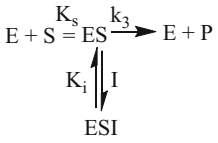

$$K_i = \frac{(ES)(I)}{(ESI)}, K_S = \frac{(E)(S)}{(ES)}, \tag{5.49}$$

$$\frac{E_0}{(ES)} = \left(1 + \frac{I}{K_i}\right) + \frac{K_S}{S}, \tag{5.50}$$

$$v = k_3(ES), V_m = k_3(E_0), \tag{5.51}$$

$$\frac{V_m}{v} = \left(1 + \frac{I}{K_i}\right) + \frac{K_S}{S}. \tag{5.52}$$

If one plots $1/v$ versus $1/S$ for uncompetitive inhibition, (5.52) predicts that a family of parallel lines will be observed (see Fig. 5.14). The inhibition constant can be obtained from a replot of the intercepts in Fig. 5.14. V_m can be evaluated from data where $I = 0$.

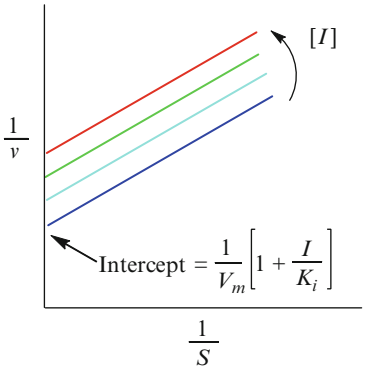

Fig. 5.14 Plot of $1/v$ versus $1/S$ for uncompetitive inhibition

5.3.7.4 Substrate Inhibition

Another type of enzyme inhibition frequently encountered in kinetic studies is substrate inhibition. This is a phenomenon that tends to cloud the interpretation of kinetic data and is to be avoided, unless this effect is itself a subject of study. In the case of substrate inhibition, high levels of substrate tend to react with the enzyme–substrate complex to produce an inactive ternary complex of the type [*S*–*E*–*S*]. The kinetic mechanism for substrate inhibition is described in Fig. 5.15.

The rate equation that accounts for substrate inhibition is shown in (5.53).

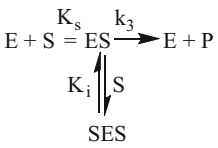

Fig. 5.15 Kinetic mechanism describing substrate inhibition

$$\frac{V_m}{v} = \left(1 + \frac{S}{K_i}\right) + \frac{K_S}{S}. \tag{5.53}$$

The derivation of (5.53) is identical to that shown for uncompetitive inhibition (5.52), except that [*S*] is substituted for [*I*]. A plot of [*velocity*] versus [*substrate*] based upon (5.53) exhibits inhibition as illustrated in Fig. 5.16.

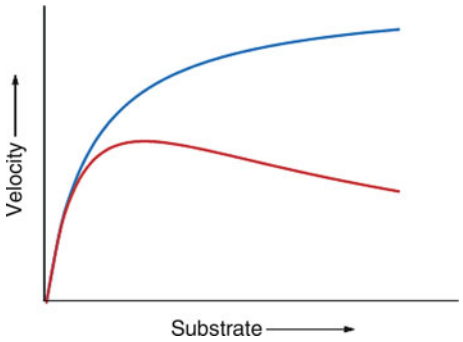

Fig. 5.16 Plot of velocity versus substrate concentration illustrating substrate inhibition. The curve describing substrate inhibition in *red* and the uninhibited curve in *blue*

5.3.8 The Effect of pH on Enzyme Kinetics

pH has a profound effect on enzyme activity. In almost all cases involving kinetic assays the pH of the reaction is controlled by a buffer. The buffer itself should act as a "spectator," i.e., it should not affect the reaction being measured. The optimum pH may or may not be the physiological pH. It is very tenuous to attempt to correlate the pK values for V_m and K_m with acidic and basic groups on the enzyme. The environment of the interior of proteins, including enzymes, is obviously very different from that of aqueous solutions where pK values for functional acidic and basic groups of amino acids are determined. Even when pK values are determined for "typical" proteins they may differ markedly from analogous groups in enzymes.

Michaelis and his coworkers were the first to attempt to explain how enzyme activity varies with pH [10]. They proposed mechanisms to account for the behavior of enzymes as the pH of the environment changes. The simplest model on the effect of pH on the kinetics of a one substrate system is outlined in Fig. 5.17. It is assumed that the substrate is unaffected by pH.

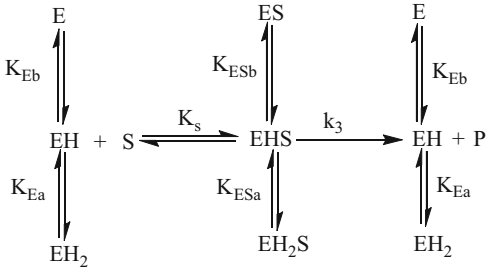

Fig. 5.17 A model for the effect of pH on the kinetics of a Uni Uni system

The derivation of the rate equation, (5.54), for the mechanism depicted in Fig. 5.17, is straight forward: The conservation of enzyme equation has six terms: $E_0 = E + EH + EH_2 + ES + EHS + EH_2S$. E and EH_2 are solved in terms of EH, and ES and EH_2S are expressed in terms of EHS. As can be seen from Fig. 5.17 $v = k_3[EHS]$, and $K_S = [EH][S]/[EHS]$. Thus,

$$v = \frac{V_m}{\left[1 + \frac{H}{K_{ESa}} + \frac{K_{ESb}}{H}\right] + \frac{K_S}{(S)}\left[1 + \frac{H}{K_{Ea}} + \frac{K_{Eb}}{H}\right]}, \tag{5.54}$$

where $V_m = k_3 \times E_{0.}$

When velocity is plotted as a function of pH, the result is a *bell-shaped* curve similar to that shown in Fig. 5.18.

The plot shown in Fig. 5.18 is based on the equation for V_m, pH (5.55):

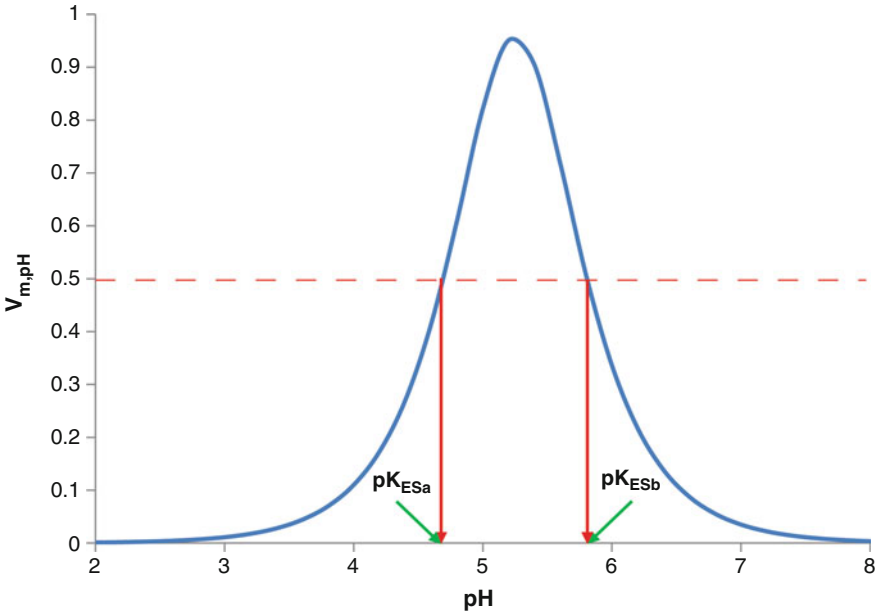

Fig. 5.18 Plot of velocity versus pH for an enzyme-catalyzed reaction. The plot allows one to calculate pK_{ESa} and pK_{ESb}

$$V_{m,\mathrm{pH}} = \frac{V_m}{\left[1 + \frac{H}{K_{ESa}} + \frac{K_{ESb}}{H}\right]}. \tag{5.55}$$

Equation (5.54) can also be used to evaluate K_S, pH (5.56). A bell-shaped curve similar to that shown in Fig. 5.18 is obtained when K_S, pH/V_m, pH is plotted against pH. This protocol allows one to evaluate K_{EA} and K_{EB} as shown in (5.56), when (5.54) is divided by (5.55).

$$K_{S,\mathrm{pH}} = \frac{K_S\left[1 + \frac{H}{K_{Ea}} + \frac{K_{Eb}}{H}\right]}{\left[1 + \frac{H}{K_{ESa}} + \frac{K_{ESb}}{H}\right]}. \tag{5.56}$$

5.3.9 The Effect of Temperature on Enzyme Kinetics

Temperature can be expected to have an effect on enzyme-catalyzed reactions as it does on virtually all chemical reactions. Shown in Fig. 5.19 is the effect of temperature on the velocity of an enzyme-catalyzed reaction. The bell-shaped curve is explained by two effects; the increase in reaction rate as the temperature increases followed by a decreased rate as the enzyme is heat-denatured. It should be noted that the optimum temperature is not necessarily the physiological temperature.

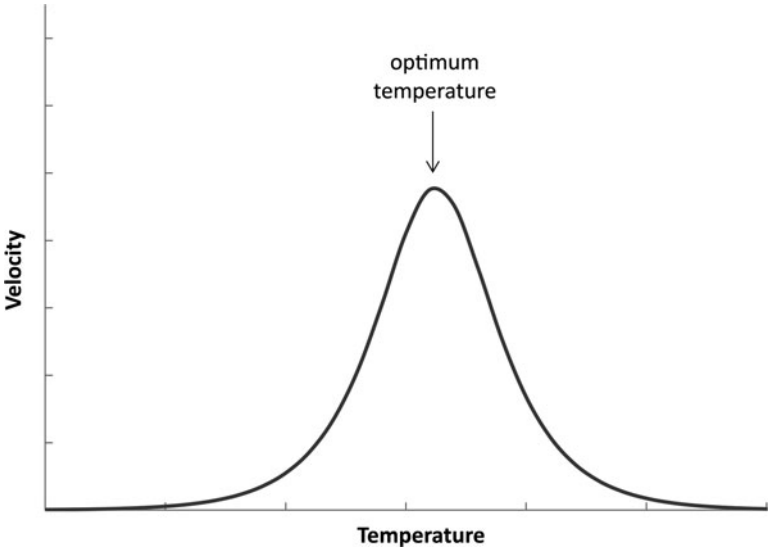

Fig. 5.19 Plot of velocity versus temperature for an enzyme-catalyzed reaction

5.3.10 The Integrated Henri–Michaelis–Menten Equation

The overwhelming majority of kinetic studies involve measurements of initial velocity (see Fig. 5.7). It is sometimes necessary, however, to study the full-time course of an enzyme-catalyzed reaction minus the pre-steady-state phase. One reason for using this protocol might involve the insensitivity of small amounts of product for analysis. It is possible to study the course of the reaction in which relatively large amounts of substrate are converted to product (note that in initial-rate experiments it is assumed that the substrate concentration remains unchanged throughout the reaction). This end can be achieved by using the integrated form of the Henri–Michaelis–Menten Equation. This approach was suggested by Henri in 1902 [3].

$$v = \frac{V_m(S)}{K_m + S} = \frac{dP}{dt} = \frac{V_m(S_0 - P)}{K_m + (S_0 - P)} \text{ where } S_0 = S + P. \tag{5.57}$$

Collecting variables gives:

$$\int_0^P \frac{dP}{V_m(S_0 - P)/K_m + S_0 - P} = \int_0^t dt. \tag{5.58}$$

and integrating yields the so-called integrated form of the Michaelis–Menten Equation:

$$V_m(t) = P + K_m \ln \frac{S_0}{(S_0 - P)}, \tag{5.59}$$

where S_0 is the substrate concentration at $t = 0$.

A convenient method for plotting full-time course data is to use the following equation (Fig. 5.20):

$$\frac{2.303}{t} \log \frac{S_0}{(S_0 - P)} = \frac{V_m}{K_m} - \frac{1}{K_m}\left[\frac{P}{t}\right]. \tag{5.60}$$

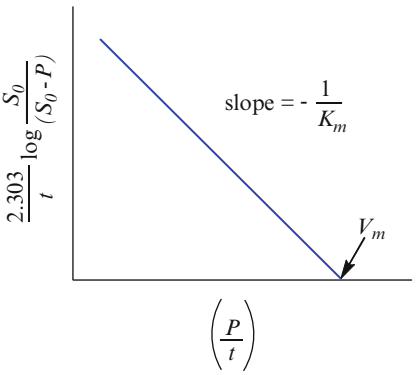

Fig. 5.20 Plot of the integrated form of the Henri–Michaelis–Menten Equation allows evaluation of kinetic parameters

Because the Henri–Michaelis–Menten Equation is based on the premise that the velocity (dP/dt) is the *initial velocity*, and where $S = S_0$, the question arises regarding the validity of the integrated form of the Henri–Michaelis–Menten Equation. It has been shown using computer simulations that the integrated form of the Henri–Michaelis–Menten Equation is valid even when a very large fraction of substrate is converted to product [11].

5.3.11 *Kinetic Isotope Effects*

Although initial-rate enzyme kinetics is a valuable tool in the biochemist's arsenal, it does have one very serious limitation; it provides almost no information on the nature of the transition state of enzyme-catalyzed reactions. Another kinetic method, kinetic isotope effects (KIE); however, does allow one to come to definitive conclusions on the nature of the transition state. KIE protocols involve substituting heavy isotopes such as ^{2}H, ^{3}H, ^{13}C, ^{15}N, ^{18}O, etc., for high abundance natural or light isotopes. Here we will consider the ways in which these atomic substitutions are used to investigate the nature of transition states. The interpretation of KIE data for enzymes is based largely on studies of model chemical reactions. The two most common KIE type studies involve *primary* and *secondary* kinetic isotope effects. Figure 5.21 indicates bond cleavage and isotope replacements that lead to KIEs.

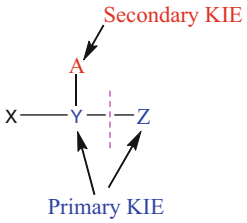

Fig. 5.21 Structure where KIEs may occur. Cleavage occurs at the Y–Z bond. Replacement of atoms Y or Z with heavy isotopes may lead to a Primary KIE. Replacement of atom A may cause a Secondary KIE

5.3.11.1 Primary Kinetic Isotope Effects

Primary kinetic isotope kinetic experiments involve substituting a heavy atom at the point of bond cleavage. Thus, if a C–H bond is cleaved, a kinetic isotope experiment will involve a comparison of the rates of C–H and C–D bond cleavage, k_H/k_D. One could also use ^{13}C and ^{12}C, but the Primary KIEs will be much less when carbon as opposed to hydrogen is used.

If a C–H or C–D bond is broken in the transition state, the C–D bond will break much more slowly. This will appear as a Primary KIE provided that the cleavage step is rate limiting. The difference in reaction rates between the C–H and C–D bonds is a result of differences in *zero point energies* (ZPE) between the two bonds rather than energy differences in their transition states, i.e., a greater energy of activation is required to break the C–D bond than the C–H bond. These effects are summarized in Fig. 5.22.

Based on quantum theory, the lowest energy level of the well shown in Fig. 5.22 is the ZPE. For the C–H and C–D bonds the lowest energy level is $\frac{1}{2}hv$ (here v is the frequency of vibration) above the lowest point of the well. The energy level of the transition states for C–H and C–D bond cleavage is identical. Thus, the energy

difference between the two bonds is a result of differences in ZPEs. Theoretically, the k_H/k_D is 6.44; however, higher values have been reported due to quantum mechanical tunneling, and lower values are a result of compensating bending motions in the transition state.

Using model chemical systems as a guide, it has been possible to attribute Primary KIEs as being due to rate-limiting formation and/or breakdown of *tetrahedral intermediates* in enzyme-catalyzed reactions.

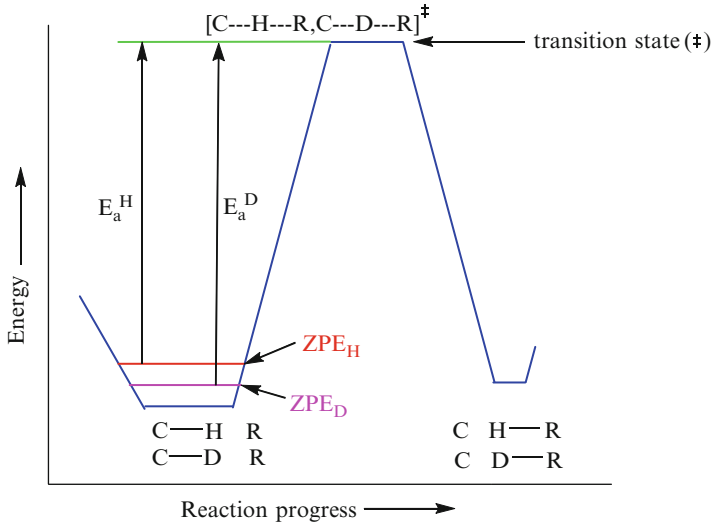

Fig. 5.22 Plot of energy of activation versus reaction coordinate for a Primary KIE. The well represents the ZPEs of the C–H and C–D bonds

5.3.11.2 Secondary Kinetic Isotope Effects

Secondary KIEs arise when a heavy atom is adjacent to the bond cleaved in the reaction. When the hybridization changes from sp^3 to sp^2 a number of vibrational modes in the transition state are altered. Assuming that the Secondary KIEs involve hydrogen and deuterium, the Secondary KIE, k_H/k_D, may be as great as 1.2. An *inverse isotope* effect may be observed when carbon hybridization changes from sp^2 to sp^3. In this case the isotope effect may be as low as 0.8.

Figure 5.23 describes an energy level diagram illustrating a secondary isotope effect.

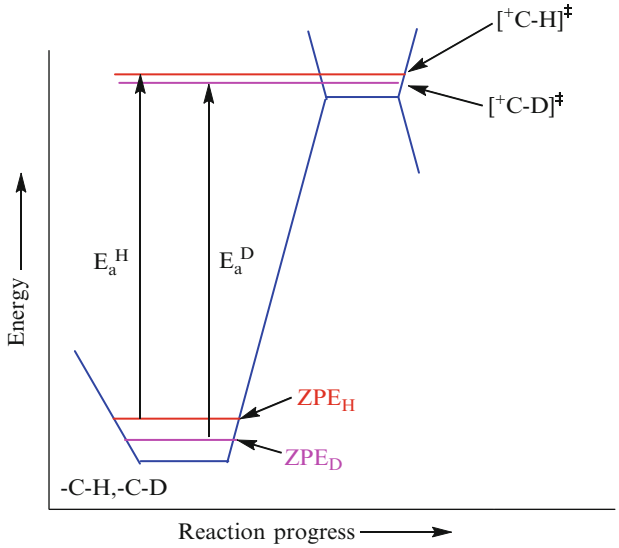

Fig. 5.23 Plot of energy of activation versus the reaction coordinate for a Secondary KIE. The well represents ZPEs for the C–H and C–D bonds. The energy required to reach the [H-C+] transition state is less than that required to attain the [D-C+] state

5.3.12 Miscellaneous Methods for Studying Enzyme Kinetics

A number of procedures are available for studying the mechanism of enzyme action in addition to those already described. These include *stopped-flow* and *NMR* kinetic studies. To demonstrate the application of these methods, consider the proposed mechanism for adenylosuccinate synthetase [12]:

$$\text{IMP} + \text{GTP} \rightarrow 6\text{-phosphoryl-IMP} + \text{GDP},$$

$$6\text{-phosphoryl-IMP} + \text{L-aspartate} \rightarrow \text{adenylosuccinate} + \text{phosphate } (\text{P}_\text{i}).$$

IMP is inosine-5′-monophosphate (6-hydroxypurine-5′-monophosphate).

Support for this mechanism could be obtained if it could be demonstrated that that the rate of conversion of 6-phosphoryl-IMP to adenylosuccinate is as fast or faster than the rate of conversion of IMP to adenylosuccinate. Both stopped flow kinetics and saturation transfer kinetics using [^{31}P] NMR could be used to come to a definitive conclusion regarding the reaction mechanism.

5.3.12.1 Stopped-Flow Studies

First, mixing IMP, GTP, and enzyme would lead to the formation of 6-phosphory-IMP. One could then measure the rate of adenylosuccinate formation following addition of L-aspartate. Second, one could measure the rate of adenylosuccinate formation when IMP, GTP, L-asparate, and enzyme are mixed. The rate of adenylosuccinate formation should be equal to or more rapid in the first experiment than in the second study involving the complete reaction mixture, if the proposed mechanism is correct, and if the first step is rate limiting.

5.3.12.2 Saturation Transfer Studies [13, 14]

An equilibrium mixture of enzyme, substrate, and product is subjected to [^{31}P] NMR analysis. Assuming that the [^{31}P] resonance of 6-phosphory-IMP, if it forms, is separated from the other [^{31}P] resonances, it is then "saturated" with radiation to eliminate its signal. (This procedure is analogous to decoupling the proton H_2O signals in [^{1}H] NMR experiments). This magnetization (loss of the resonance) is then carried over to the product, P_i which will decrease in amplitude. Likewise, the γ[^{31}P] resonance of GTP is irradiated and the diminution in the amplitude of the P_i resonance is determined. These data are then used to calculate the kinetics of the transfer reactions [14]. If the mechanism proposed is correct, the rate of transfer of 6-phosphoryl-IMP to P_i should be equal to, or greater, than the rate of transfer of GTP to P_i.

5.3.13 Cooperativity and Sigmoidal Kinetics

Almost all enzymes exhibit "Henri–Michaelis–Menten kinetics," i.e., plots of initial velocity versus substrate concentration are hyperbolic. A few, and these are usually regulatory enzymes, display *sigmoidal kinetics or positive cooperativity*. The term "positive cooperativity" means that for enzymes with multiple active sites, the first substrate adds with difficulty, the next, less so, and so on. The earliest studies that attempted to explain this phenomenon were binding, and not kinetic investigations, associated with oxygen binding to hemoglobin. A number of models, both kinetic and binding, are now available; however, this discussion will be limited to the earliest attempt to understand sigmoidicity; the work of Hill [15]. The model, which is the basis for the so-called *Hill Equation* is as follows:

The rate equation (5.61) which is derived based on Fig. 5.24 is analogous to that derived for the Henri–Michaelis–Menten Equation (5.12).

Fig. 5.24 The kinetic model for the Hill Equation

$$E + nS = ESn \xrightarrow{k_3} E + nP$$

$$v = \frac{V_m S^n}{[K_m + S^n]}. \tag{5.61}$$

Rearranging (5.57) and taking logs of both sides of the equation yields:

$$\log\left[\frac{V_m}{v} - 1\right] = \log K_m - (n_H)\log(S). \tag{5.62}$$

A plot of $\log\left[\frac{V_m}{v} - 1\right]$ versus $\log(S)$, known as the Hill Plot, can be used to calculate the *Hill coefficient*, η_H (Fig. 5.25).

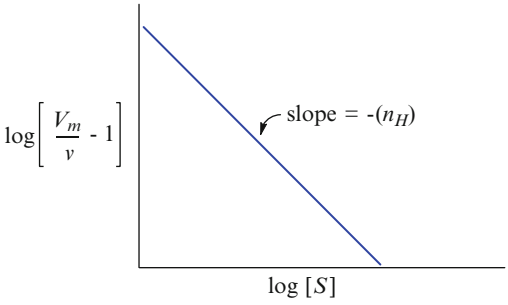

Fig. 5.25 The Hill Plot, based upon (5.58), is used to calculate the Hill coefficient, $n(\eta_H)$

Plotting velocity (v) against [S] according to (5.61) will yield a sigmoidal rather than a hyperbolic plot. This phenomenon is also referred to as positive cooperativity. The Hill equation is said to be completely, or 100%, cooperative. In the case of hemoglobin, plotting fractional saturation (ES_n/E_0) against O_2, gives a Hill coefficient (η_H) of 2.8. If the Hill Equation was faithful to the hemoglobin data, the Hill coefficient would be 4.0 as there are four O_2 binding sites in hemoglobin. Other models, discussed in Chap. 3, give results more closely associated to the true oligomeric state of hemoglobin [16, 17].

One of the most frequently invoked models used to explain cooperativity is the *Symmetry* or *Monod Model* [17]. The fundamental premise of the model is that the protein exists in two states, the R (active) and the T (inactive) state. Different factors can shift the protein from one state to the other. These factors include substrates (*homotrophic*) and other small molecules (*heterotrophic effectors*). Some modifiers affect the K_m of the system if an enzyme is involved (*K-system*) and others the V_m (*V-system*). Additionally, some effectors may cause both K_m and V_m effects.

Most enzymes are oligomeric, e.g., dimers, trimers, etc., yet they do *not* exhibit cooperativity. Cooperativity will not be observed if the subunits act *independently* of each other. Thus, they function kinetically as monomers even when their quaternary structure is required for activity.

Supplement to Enzyme Kinetics

The vast majority of enzyme systems involve two or more substrates. No biochemistry textbook would be complete without considering multisubstrate enzyme kinetics; however, most biochemistry texts do not cover this important topic in detail. Material on multisubstrate systems will be considered in this supplement with the hope that students will find the material of interest.

S5.1 Two Substrate Systems

There are two types of two substrate systems, *Sequential* and *Ping-Pong* and they are segregated based upon initial-rate kinetic plots. The substrates are represented by *A* and *B* and the products by *P* and *Q*.

S5.1.1 Ping-Pong Mechanism

The rate equation for the Ping-Pong mechanism in double reciprocal form is:

$$\frac{1}{v} = \frac{1}{V_m}\left[1 + \frac{K_a}{A} + \frac{K_b}{B}\right]. \tag{5.63}$$

K_a and K_b are Michaelis constants for substrates *A* and *B*, respectively.

In the Bi Bi Ping-Pong mechanism, shown in Fig. 5.26, substrate *A* reacts with the enzyme to form an intermediate that may or may not be covalent. The cardinal feature of this mechanism is that the product (*P*) *dissociates from the enzyme before the addition of the second substrate*. Double reciprocal plots, of the type illustrated in Fig. 5.27, yield a family of parallel lines. If product release does not occur, the mechanism will produce sequential kinetics as illustrated in Fig. 5.30.

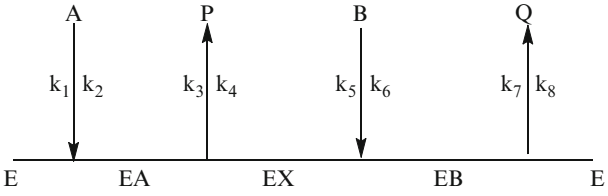

Fig. 5.26 Bi Bi Ping-Pong kinetic mechanism

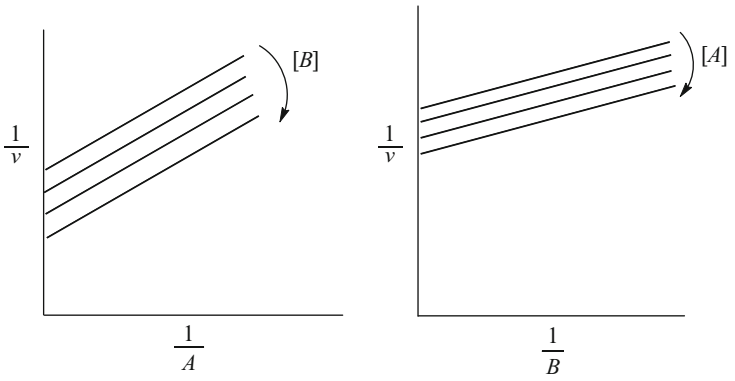

Fig. 5.27 Double reciprocal plot of a Ping-Pong mechanism

S5.1.2 Sequential Mechanisms

Sequential mechanisms are of two types, *Ordered* (Fig. 5.28) and *Random* (Fig. 5.29).

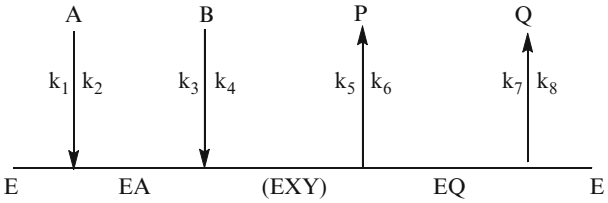

Fig. 5.28 Example of an ordered Bi Bi sequential mechanism

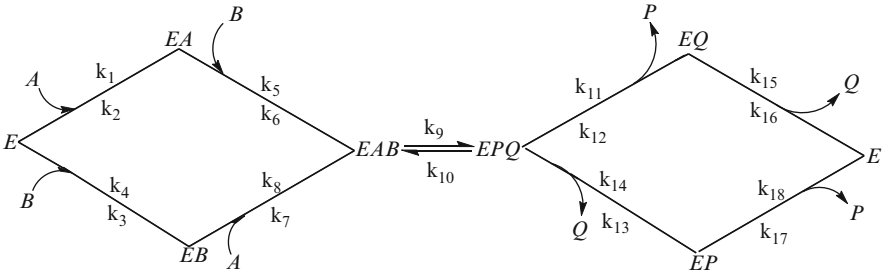

Fig. 5.29 Example of a random Bi Bi sequential mechanism

The rate equation, in double reciprocal form, for the Ordered Bi Bi mechanism (5.64) using the steady-state assumption, is:

$$\frac{1}{v} = \frac{1}{V_m}\left[1 + \frac{K_a}{A} + \frac{K_b}{B} + \frac{K_{ia} \times K_b}{[A][B]}\right], \tag{5.64}$$

where K_a, K_b, and K_{ia} in (5.64) represent, Michaelis constant for A, Michaelis constant for B, and dissociation constant for the EA complex, k_2/k_1.

Note that both substrates interact with the enzyme before a product is formed. In the Ordered mechanism only a site for substrate A exists on the free enzyme. Once A binds to form the EA complex, a site is created for substrate B.

In the case of the Random Bi Bi mechanism, sites exist on the free enzyme for both substrates A and B and thus they can bind independently of each other (Fig. 5.29). Both the Random Bi Bi mechanism when derived using the rapid-equilibrium assumption and the Order Bi Bi mechanism,using the steady-state assumption, give rate equation (5.64).

It is clear from Figs. 5.27 and 5.30, as inferred from (5.63) and (5.64), respectively, that the double reciprocal Ping-Pong plots give a family of parallel lines whereas the Sequential plots converge at a common point. These plots are obviously a consequence of the different kinetic mechanisms and the resulting rate equations and allow one to distinguish between Sequential and Ping-Pong mechanism by *inspection*.

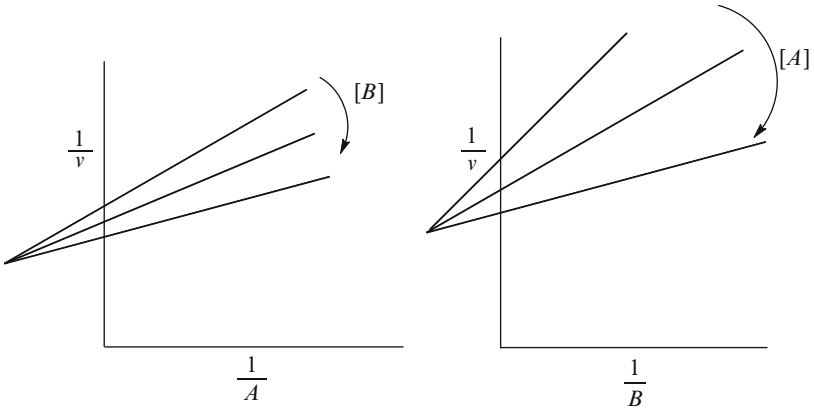

Fig. 5.30 Double reciprocal plot of a Sequential mechanism

S5.2 Evaluation of the Kinetic Parameters from Lineweaver–Burk Plots

Florini and Vestling [S1] were the first to show that Figs. 5.27 and 5.30, referred to as *Primary Plots*, can be used to determine the kinetic parameters found in (5.63) and (5.64). So-called *Secondary Plots* are then made from the slopes and intercepts of the Primary Plots and the various kinetic parameters determined (Fig. 5.31). Today these determinations are made by computer.

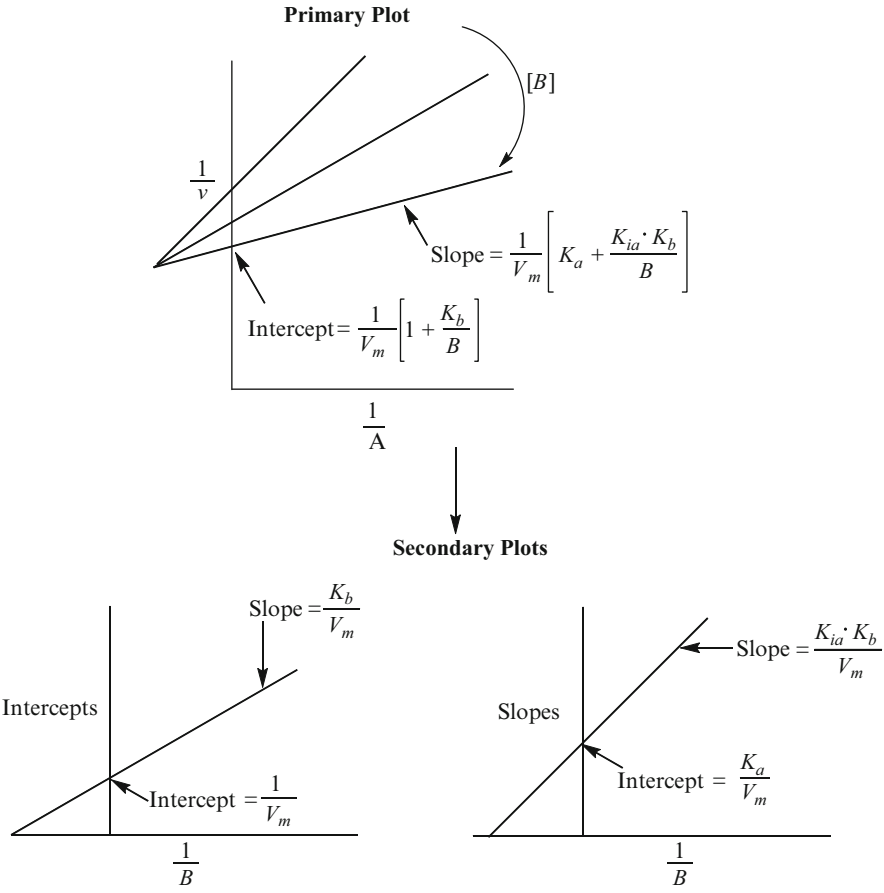

Fig. 5.31 Primary and secondary plots of kinetic data for evaluation of kinetic parameters

S5.3 Derivation of Rate Equations for Complex Mechanisms

S5.3.1 Derivations Assuming the Steady State

The difficulty involved in deriving rate equations is directly proportional to the complexity of the kinetic mechanism. A number of methods are available in the literature that allows one to reduce the effort required for the derivations [S2]. One method that relies almost exclusively on simple algebra and inspection will be presented in this text [S3].

Consider the mechanism described in Scheme 5.1 using a somewhat different notation as illustrated in Scheme 5.2.

Scheme 5.1 Random Bi Bi mechanism in which breakdown of the EAB complex is rate-limiting

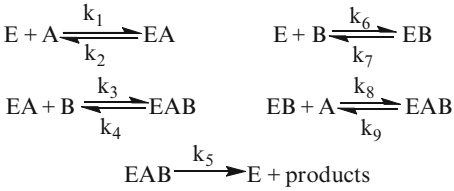

Scheme 5.2 Mechanism in Scheme 5.1 cast in the form of a square

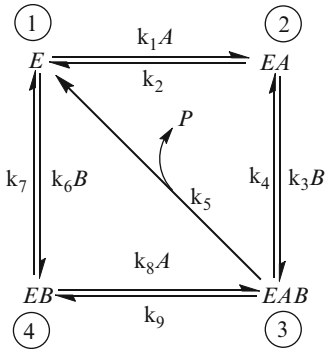

Rules for the Derivation

1. The kinetic mechanism (Scheme 5.2) is set up in geometric form; in this case a square.
2. Each enzyme form is numbered as illustrated in Scheme 5.2; *E* is 1, *EA* is 2, etc.
3. Each circled number above the enzyme form in Scheme 5.2 is characterized by one or more arrows that lead *away* from that node. These are listed in parenthesis as a summation of rate constants.

$$(1) = (k_1[A] + k_6[B]) \qquad (3) = (k_4 + k_5 + k_9)$$
$$(2) = (k_2 + k_3[B]) \qquad (4) = (k_7 + k_8[A]).$$

4. To obtain the determinant for an enzyme form, the shortest *one-step* paths to that form from the other enzyme species that contribute directly to it are written down. Thus, for *E* or 1, we would have 2 → 1, 3 → 1, and 4 → 1. Each path is characterized by a rate constant. For the paths illustrated they would be k_2, k_5, and k_7, respectively.
5. Next to each of these one-step routes is written in parentheses the number in the geometric figure that does *not* appear in the one-step path; e.g., 2 → 1(3)(4), 3 → 1(2)(4), and 4 → 1(2)(3).
6. The determinant for *E* is then, $E = 2 \rightarrow 1(3)(4) + 3 \rightarrow 1(2)(4) + 4 \rightarrow 1(2)(3)$, and thus $E = k_2(k_4 + k_5 + k_9)(k_7 + k_8A) + k_5(k_2 + k_3B)(k_7 + k_8A) + k_7(k_2 + k_3B)(k_4 + k_5 + k_9)$

7. The determinant is next expanded, and certain terms are eliminated by inspection. These are:
   (a) *Redundant terms* – only one particular term is permitted in each determinant, and
   (b) *Forbidden terms* – these are of the type $k_1k_2(A)$, $k_3k_4(B)$, $k_6k_7(B)$, *and* $k_8k_9(A)$. Whenever they appear in a product of rate constants, the entire term is eliminated. These terms contain rate constants whose reactions go in opposite directions.
   (c) If a *closed loop* is generated, it is not included in the determinant. Although mechanisms that produce closed loops are rare, the terms would be of the type $k_5k_6k_8(A)(B)$ for the mechanism above
8. Expansion of E gives:
   (a) $E = k_2k_4k_7 + k_2k_4k_8(A) + k_2k_5k_7 + k_2k_5k_8(A) + k_2k_7k_9 + k_2k_8k_9(A) + k_2k_5k_7 + k_2k_5k_8(A) + k_3k_5k_7(B) + k_3k_5k_8(A)(B) + k_2k_4k_7 + k_2k_5k_7 + k_2\,k_7\,k_9 + k_3k_4k_7(B) + k_3k_5k_7(B) + k_3k_7k_9(B)$.
   (b) The eliminated terms are either redundant or forbidden.
   (c) $E = k_2k_4k_7 + k_2k_4k_8(A) + k_2k_5k_7 + k_2k_5k_8(A) + k_2k_7k_9 + k_3k_5k_7(B) + k_3k_5\,k_8(A)(B) + k_3k_7k_9(B)$
9. Determinants for the other enzyme forms are:

$$\begin{aligned} EA &= k_2k_4k_7(A) + k_1k_4k_8(A)^2 + k_1k_5k_7(A) + k_1k_5k_8(A)^2 + k_1k_7k_9(A) \\ &\quad + k_4k_6k_8(A)(B), \\ EAB &= k_1k_3k_7(A)(B) + k_1k_3k_8(A)^2(B) + k_3k_6k_8(A)(B)^2 + k_2k_6k_8(A)(B), \\ EB &= k_2k_4k_6(B) + k_2k_5k_6(B) + k_2k_6k_9(B) + k_3k_5k_6(B)^2 + k_3k_6k_9(B)^2 \\ &\quad + k_1k_3k_9(A)(B). \end{aligned}$$

10. The rate equation for this mechanism is: $v = k_5(EAB)$, dividing both sides of the equation by E_0,

$$\frac{v}{E_0} = \frac{k_5(EAB)}{E_0} = \frac{k_5(EAB)}{[E + EA + EB + EAB]}, \tag{5.65}$$

$$v = \frac{E_0[k_5(EAB)]}{[E_0 + EA + EB + EAB]}, \tag{5.66}$$

    where v, E_0, E, EA, and EAB represent velocity, total enzyme, determinant for E, determinant for EA, determinant for EB, and determinant for EAB, respectively.
11. The values for the different enzyme forms from Rule 9 are finally substituted into (5.66) to yield the final rate equation.

S5.3.2 Derivations Making the Equilibrium Assumption

Consider the mechanism outlined in Scheme 5.3 in which it is assumed that all steps equilibrate rapidly relative to the breakdown of the ternary (*EAB*) complex to products. The mechanism now becomes:

Scheme 5.3 Mechanism shown in Scheme 5.1 in which all steps equilibrate rapidly relative to the breakdown of the EAB complex to products

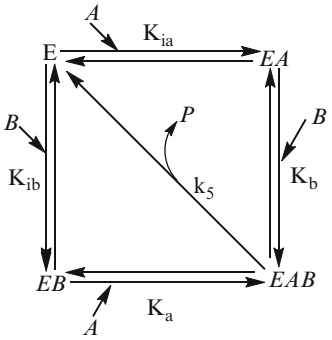

The velocity expression is, $v = k_5(EAB)$, as the k_5 step is rate limiting. Thus all enzyme forms in the Conservation of Enzyme Equation (E_0 + EA + EB + EAB) must be in terms of EAB. The various equilibrium expressions are:

$$K_{\mathrm{ia}} = \frac{(E)(A)}{(EA)}, \quad K_{\mathrm{ib}} = \frac{(E)(B)}{(EB)}, \quad K_{\mathrm{a}} = \frac{(EB)(A)}{(EAB)}, \quad K_{\mathrm{b}} = \frac{(EA)(B)}{(EAB)}. \tag{5.67}$$

Note that K_{ia}, K_{ib} are dissociation constants, whereas K_{a} and K_{b} are Michaelis constants. Inspection of the last two terms indicates that EA and EB are already expressed in terms of EAB,

$$EA = \frac{K_{\mathrm{b}}(EAB)}{B} \quad \text{and} \quad EB = \frac{K_{\mathrm{a}}(EAB)}{A}. \tag{5.68}$$

The expression for E in the Conservation of Enzyme Equation can be in terms of *either* K_{ia} or K_{ib} as all four dissociation constants are not independent of each other but are related by the expression, $K_{\mathrm{ia}} \times K_{\mathrm{b}} = K_{\mathrm{a}} \times K_{\mathrm{ib}}$. Substituting these enzyme forms into the Conservation of Enzyme equation gives,

$$E_0 = \left[1 + \frac{K_a}{A} + \frac{K_b}{B} + \frac{K_{ia} \times K_b}{A \times B}\right](EAB). \tag{5.69}$$

Because $(\mathrm{EAB}) = v/k_5$ (5.69) can be rearranged to

$$E_0 = \left[1 + \frac{K_{\mathrm{a}}}{A} + \frac{K_{\mathrm{b}}}{B} + \frac{K_{\mathrm{ia}} \times K_{\mathrm{b}}}{A \times B}\right]\left[\frac{v}{k_5}\right], \tag{5.70}$$

$$v = \frac{k_5 \times E_0}{\left[1 + \frac{K_a}{A} + \frac{K_b}{B} + \frac{K_{ia} \times K_b}{A \times B}\right]} = \frac{V_m}{\left[1 + \frac{K_a}{A} + \frac{K_b}{B} + \frac{K_{ia} \times K_b}{A \times B}\right]}. \tag{5.71}$$

It can be seen that (5.64) and (5.71) are identical in form and thus it is *not* possible from initial rate experiments alone to differentiate between the Ordered Bi Bi and the Rapid-Equilibrium Random Bi Bi mechanisms. On the other hand, it is possible to make a choice from among a very large number of three substrate mechanisms from inspection of Lineweaver–Burk plots alone [S4].

S5.4 Making a Choice Between the Ordered Bi Bi and Rapid Equilibrium Random Bi Bi Mechanisms

There are a few kinetic protocols that allow one to make a choice between the Rapid-Equilibrium Random Bi Bi mechanism and the steady-state Ordered Bi Bi mechanism. These methods include isotope exchange at chemical equilibrium and the use of dead-end inhibitors.

1. Isotope exchange at chemical equilibrium [S5].

The isotope exchange method was introduced by Nobel Laureate P.D. Boyer in 1959. We will not attempt to illustrate the rigorous mathematical treatment advanced by Boyer, rather, the discussion will attempt to provide an intuitive understanding of the method. The experimental protocol involves first bringing a system, e.g., a bireact system to *chemical equilibrium*. Then a tracer amount of substrate *A*, *A**, is added, at a concentration that will not perturb the equilibrium, and its rate of conversion, or exchange, with product *Q* is monitored. This is referred to as the A ↔ Q exchange. Similar exchanges may occur with other substrate–product pairs.

Consider first, the case of the Ordered Bi Bi mechanism (Fig. 5.32).

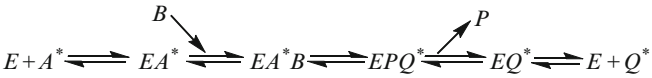

Fig. 5.32 The addition of radioisotope A, A*, to an Ordered Bi Bi system at chemical equilibrium

If the concentration of the *B–P* pair is increased in an equilibrium ratio so as not to disturb the equilibrium of the system, the exchange rate would be expected to increase; however, a concentration range will be approached where free enzyme will not be available for reaction with *A* or *Q*. At infinite *B* and *P* all the enzyme will exist as the ternary complexes *EAB* and *EPQ* and the *A*↔*Q* exchange will fall to zero.

On the other hand, if one were to measure the *B*↔*P* exchange, and *A* and *Q* were increased in an equilibrium ratio, the enzyme would be forced into the binary

complexes *EA* and *EQ*. These complexes can react with both substrate *B* and product *P* to form productive ternary complexes *EAB* and *EPQ* and the *B*↔*P* exchange will not be inhibited at elevated levels of *A* and *Q* (Fig. 5.33).

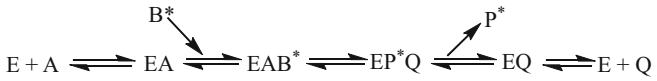

Fig. 5.33 The addition of radioisotope B, B*, to an Ordered Bi Bi system at chemical equilibrium

Other types of exchanges may be visualized for the Ordered Bi Bi mechanism i.e., *B*↔*Q* and *A*↔*P*; however, all four exchanges are not to be expected. For example, with lactate dehydrogenase, the exchangeable pairs are: lactate–pyruvate, NAD^+–NADH, and lactate–NADH, but not NAD^+–pyruvate. At any rate, if the *B*↔*Q* exchange could be measured for this mechanism, it would be inhibited and finally decrease to zero as the levels of *A* and *P* are elevated because of the decrease in the concentration of free enzyme available to react with *Q*. The exchange patterns to be expected for the Ordered Bi Bi mechanism are illustrated in Figs. 5.34 and 5.35.

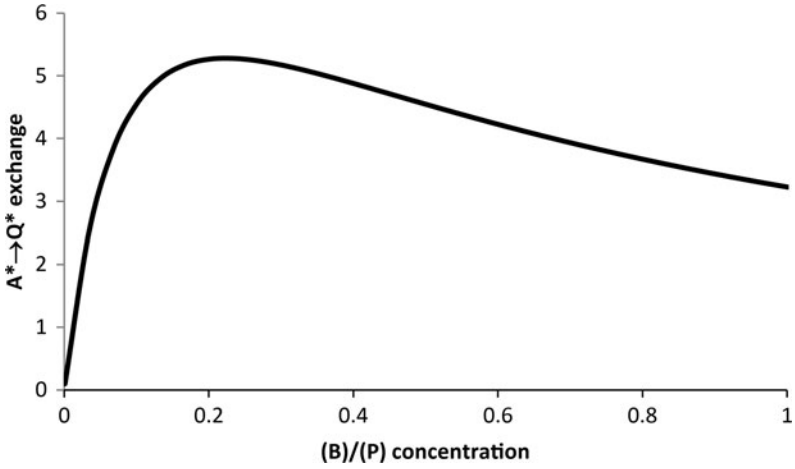

Fig. 5.34 Rate of isotope exchange at equilibrium for the A↔Q exchange of an ordered mechanism as a function of the concentration of B and P which are maintained in an equilibrium ratio

How the isotope exchange rate at equilibrium of a substrate–product pair is affected in branched mechanisms is best illustrated by using the Random Bi Bi mechanism (Fig. 5.29) as an example. Here if one determines the *A*↔*Q* exchange as *B* and *P* are raised, the exchange rate reaches a maximal velocity, levels off, and is not depressed at elevated concentrations of the *B*–*P* pair. The exchange of *A*↔*Q* is

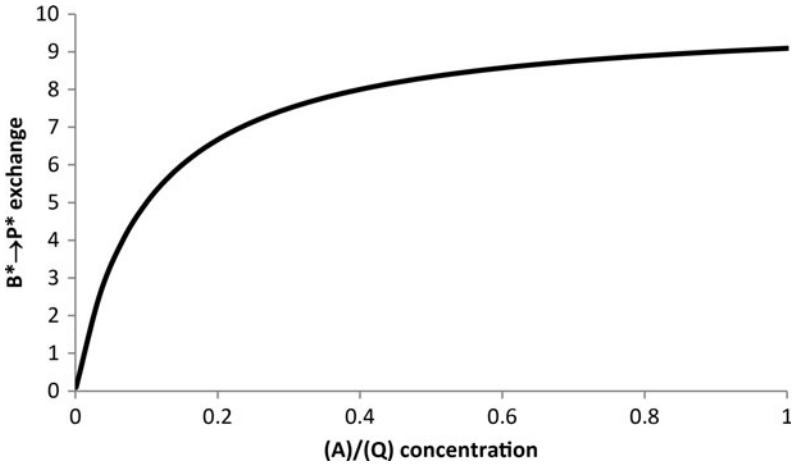

Fig. 5.35 Rate of the B↔P isotope exchange for an ordered mechanism as the concentrations of A and Q are raised in an equilibrium ratio

not reduced as in the case of the Ordered Bi Bi mechanism, because there are alternative reaction pathways that the labeled substrate can follow in its conversion to product. When B and P approach infinity, the enzyme will exist as EB and EP; however, both A^* and Q^* can add to these binary complexes to form the productive ternary complexes that permit the conversion of A^* to Q^* and vice versa. By analogy, the $B \leftrightarrow P$ exchange is not inhibited as the concentration of the A–Q substrate–product pair approaches saturation. Both exchange patterns for the random mechanism would resemble the results of Fig. 5.35.

When considering the Random Bi Bi interaction pathway mechanism illustrated in Fig. 5.36, it is assumed that all steps in the sequence equilibrate rapidly relative to the central ternary complexes. Because this isomerization step is rate limiting, it follows that all substrate ↔ product exchange rates should be the same. This has been found to be true in some Random Bi Bi cases (creatine kinase) [S6], but not in others (yeast hexokinase) [S7]. For the latter system, it was observed that

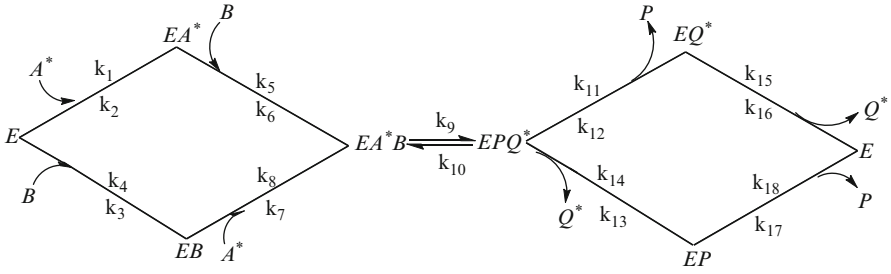

Fig. 5.36 The addition of radiolabeled A, A*, to a Random Bi Bi system which is at chemical equilibrium

the glucose–glucose-6-phosphate exchange exceeds the ADP↔ATP exchange by approximately 50%. These results suggest that the interconversion of the ternary complexes is not rate limiting, and that, although the kinetic mechanism is Random Bi Bi, the equilibrium assumption is not correct. Isotope exchange thus permits one to gain insight into the relative flux rates of the alternative pathways in Random mechanisms and also to obtain information on the relative magnitudes of certain portions of the kinetic mechanisms. These ends can be achieved to some extent by studies of the $A \leftrightarrow Q$, $B \leftrightarrow P$ exchanges and the $A \leftrightarrow P$ or $B \leftrightarrow Q$ exchanges where applicable.

Another advantage of using isotope exchange at equilibrium to study kinetic mechanisms is that it will identify substrates A and B and products P and Q in the Ordered mechanism. In the case of lactate dehydrogenase, for example, the mechanism of which is Ordered Bi Bi, substrate A is NAD^+ and product Q is NADH. It was found that the NAD^+–NADH exchange is depressed as the concentration of lactate and pyruvate increase to very high levels [S8], i.e., the results are similar to those described in Fig. 5.34.

S5.5 The Use of Dead-End Competitive Inhibitors to Choose Between the Ordered Bi Bi and Rapid-Equilibrium Random Bi Bi Mechanism

Dead-end competitive inhibitors were used for the first time in 1962 to determine a kinetic mechanism [S9]. Consider first, the Random mechanism illustrated in Scheme 5.3. A competitive inhibitor for substrate A (I_a) would bind at every step in the mechanism in place of substrate A. Thus the following complexes would form: EI_a and EI_aB. The Conservation of Enzyme Equation would then be modified to accommodate these new terms:

$$E_0 = E + EA + EB + EAB + EI_a + EI_aB, \tag{5.72}$$

$$K_i = \frac{(E)(I_a)}{(EI_a)}, \quad K_{ii} = \frac{(EB)(I_a)}{(EBI_a)} \text{ and } K_{iii} = \frac{(EI_a)(B)}{(EI_aB)}. \tag{5.73}$$

Using the first two terms and substituting into the Conservation of Enzyme Equation gives:

$$E_0 = (E)\left[1 + \frac{I_a}{K_i}\right] + EA + (EB)\left(1 + \frac{I_a}{K_{ii}}\right) + EAB. \tag{5.74}$$

Remembering that $v = k_5(EAB)$, the final rate equation in double reciprocal form, for the effect of a dead-end competitive inhibitor for A, I_a, is:

$$\frac{1}{v} = \frac{1}{V_m}\left[1 + \frac{K_a}{A}\left(1 + \frac{I_a}{K_{ii}}\right) + \frac{K_b}{B} + \frac{K_{ia} \times K_b}{A \times B}\left(1 + \frac{I_a}{K_i}\right)\right]. \tag{5.75}$$

A similar rate expression can be derived using a competitive inhibitor for substrate B, I_b. Making analogous assumptions for I_b that were made for I_a the modified rapid-equilibrium Randon Bi Bi mechanism is:

$$\frac{1}{v} = \frac{1}{V_m}\left[1 + \frac{K_a}{A} + \frac{K_b}{B}\left(1 + \frac{I_b}{K_{ii}}\right) + \frac{K_{ia} \times K_b}{A \times B}\left(1 + \frac{I_b}{K_i}\right)\right] \tag{5.76}$$

A plot of $1/v$ versus $1/A$ at different concentrations of I_a is typically competitive, whereas a double reciprocal plot of $1/v$ versus $1/B$ at different levels of I_a gives noncompetitive inhibition. These findings are predicted from (5.75) (Fig. 5.37).

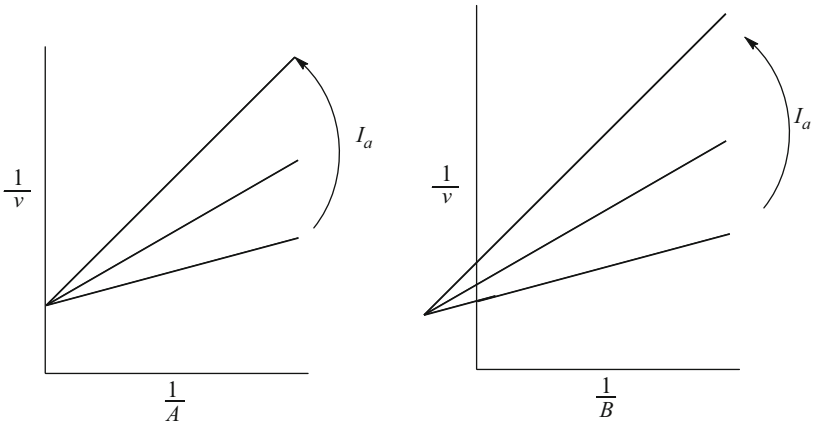

Fig. 5.37 Lineweaver–Burk plots of $1/v$ versus 1/Substrate at different concentrations of the inhibitor I_a

If one were to plot data for (5.76), using a competitive inhibitor for B, I_b, inhibition would be competitive with respect to substrate B and noncompetitive relative to substrate A.

When dead-end competitive inhibitors are used in the case of the Ordered Bi Bi kinetic mechanism different inhibition patterns emerge. For the Ordered Bi Bi mechanism, substrate A adds only to the free enzyme and substrate B adds only to the binary EA complex. Thus, a competitive dead-end inhibitor for substrate A would add exclusively E. On the other hand, I_b, a competitive dead-end inhibitor for B, will add only to the EA complex to form the ternary complex, EAI_b. These concepts can then be used to derive the rate equations that incorporate dead-end inhibition for I_a and I_b for the mechanism shown in Fig. 5.28.

First the case where the inhibitor I_a adds to the free enzyme, E:

$$E + I_a = EI_a, \tag{5.77}$$

$$K_i = \frac{(E)(I_a)}{EI_a}, \tag{5.78}$$

$$E_0 = E + EA + EXY + EI_a = (E)\left[1 + \frac{I_a}{K_i}\right] + EA + EXY, \tag{5.79}$$

$$\frac{1}{v} = \frac{1}{V_m}\left[1 + \frac{K_a}{A}\left(1 + \frac{I_a}{K_i}\right) + \frac{K_b}{B} + \frac{K_{ia} \times K_b}{A \times B}\left(1 + \frac{I_a}{K_i}\right)\right]. \tag{5.80}$$

Equation (5.80) predicts that the dead-end competitive inhibitor for substrate A, I_a, will be noncompetitive relative to substrate B. On the other hand, a dead-end competitive inhibitor for B, I_b, when added to this system will exhibit the following interactions:

$$EA + I_b = EAI_b, \tag{5.81}$$

$$K_i = \frac{(EA)(I_b)}{(EAI_b)}, \tag{5.82}$$

$$E_0 = E + EA + EXY + EAI_b = E + (EA)\left[1 + \frac{I_b}{K_i}\right] + EXY, \tag{5.83}$$

$$\frac{1}{v} = \frac{1}{V_m}\left[1 + \frac{K_a}{A} + \frac{K_b}{B}\left[1 + \frac{I_b}{K_i}\right] + \frac{K_{ia} \times K_b}{A \times B}\right]. \tag{5.84}$$

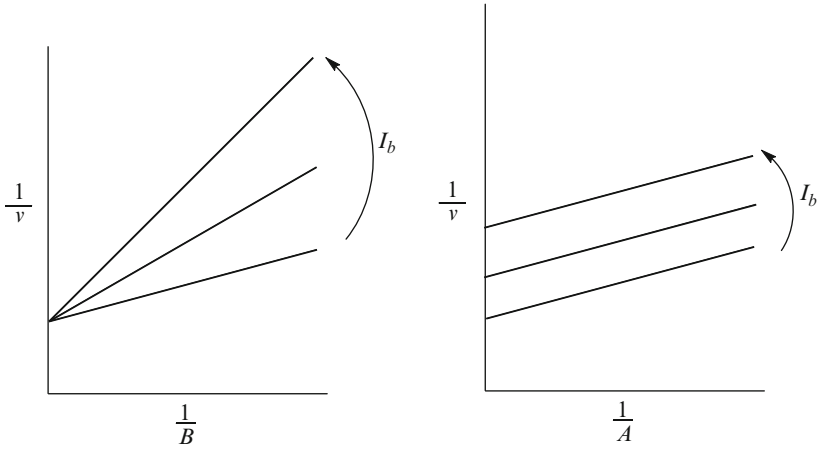

Fig. 5.38 Double reciprocal plot of (5.75) in which a competitive inhibitor for substrate [B] (I_b) produces uncompetitive inhibition relative to substrate [A]

Equation (5.84) predicts that a dead-end competitive inhibitor for substrate B (I_b) will be an uncompetitive inhibitor in a 1/[A] plot. This is a unique inhibition pattern (see Fig. 5.38) and allows one to choose between the Ordered and the rapid equilibrium Random Bi Bi kinetic mechanisms. In addition, if the mechanism is Ordered Bi Bi the identity of substrates A and B can be established.

As expected, the Ping-Pong mechanism also gives unique inhibition patterns with dead-end competitive inhibitors.

The types of data to be expected for the three bireactant systems seen most frequently are summarized in Table 5.1. This treatment has been extended to three substrate systems and can be found in the literature [S10].

Table 5.1 Use of competitive inhibitors for determining bireactant kinetic mechanisms

Mechanism	Competitive inhibitor for substrate	1/A plot	1/B plot
Random Bi Bi and	A	Competitive	Noncompetitive
Random Bi Uni	B	Noncompetitive	Competitive
Ordered Bi Bi and	A	Competitive	Noncompetitive
Ordered Bi Uni	B	Uncompetitive	Competitive
	A	Competitive	Uncompetitive
Ping-Pong Bi Bi	B	Uncompetitive	Competitive

References

S1. Florini JR, Vestling CS (1957) Graphical determination of the dissociation constants for two-substrate enzyme systems. Biochim Biophys Acta 25:575–578

S2. Huang C (1979) Derivation and initial velocity and isotope exchange rate equations. Methods Enzymol 63:54–84

S3. Fromm HJ (1970) A simplified schematic method for deriving steady-state rate equations using a modification of the theory of graphs procedure. Biochem Biophys Res Commun 40:692–697

S4. Rudolph FB and Fromm HJ (1969) Initial rate studies of adenylosuccinate synthetase with product and competitive inhibitors J Biol Chem 244:3832–3839

S5. Boyer PD (1959) Uses and limitations of measurements of rates of isotopic exchange and incorporation in catalyzed reactions. Arch Biochem Biophys 82:387–410

S6. Morrison JF and Cleland WW (1966) Isotope exchange studies of the mechanism of the reaction catalyzed by adenosine triphosphate: creatine phosphotransferase. J Biol Chem 241:673–683

S7. Fromm HJ, Silverstein E, and Boyer PD (1964) Equilibrium and net reaction rates in relation to the mechanism of yeast hexokinase. J Biol Chem 239:3645–3652

S8. Silverstein E and Boyer PD (1964) Equilibrium and net reaction rates and the mechanism of bovine heart and rabbit muscle lactate dehydrogenase. J Biol Chem 239:3901–3907

S9. Zewe V and Fromm HJ (1962) Kinetic studies of yeast hexokinase J Biol Chem 237:3027–2032

S10. Fromm HJ (1979) Use of competitive inhibitors to study substrate binding order. Methods Enzymol 63:467–486

References

1. O'Sullivan C, Tompson FW (1890) Invertase: a contribution to the history of an enzyme or unorganized ferment. J Chem Soc (London) 57:834–931
2. Brown AJ (1902) Enzyme action. J Chem Soc (Trans) 81:373–388
3. Henri V (1903) Lois generals de l'action des diastases. Hermann, Paris
4. Michaelis L, Menten ML (1913) Kinetics of invertase action. Biochem Z 49:333–369
5. Briggs GE, Haldane JBS (1925) A note on the kinetics of enzyme action. Biochem J 19: 338–339
6. Lineweaver H, Burk D (1934) The determination of enzyme dissociation constants. J Am Chem Soc 56:658–666
7. Ganson NJ, Fromm HJ (1985) Nuclear magnetic resonance studies of fructose 2,6-bisphosphate and adenosine-5′-monophosphate interaction with bovine liver fructose-1,6-bisphosphatase. J Biol Chem 260:2837–2843
8. Liu F, Fromm HJ (1990) Kinetic studies on the mechanism and regulation of rabbit liver fructose-1,6-bisphosphatase. J Biol Chem 265:7401–7406
9. Liang JY, Huang S, Zhang Y, Ke H, Lipscomb WN (1992) Crystal structure of the neutral form of fructose-1,6-bisphosphatase complexed with the regulatory inhibitor fructose 2,6-bisphosphate at 2.6Å resolution. Proc Natl Acad Sci USA 89:2404–2408
10. Michaelis L, Davidsohn H (1911) The theory of the isoelectric effect. Biochem Z 30:143–150
11. Stayton MM, Fromm HJ (1979) A computer analysis of the validity of the integrated Michaelis-Menten equation. J Theor Biol 78:309–323
12. Cooper BF, Fromm HJ, Rudolph FB (1986) Isotope exchange at equilibrium studies with rat muscle adenylosuccinate synthetase. Biochemistry 25:7323–7327
13. Forsen S, Hoffman RA (1963) Study of moderately rapid chemical exchange reactions by means of nuclear magnetic double resonance. J Chem Phys 39:2892–2901
14. Brown TR, Ugurbil K, Shulman RG (1977) ^{31}P nuclear magnetic resonance of ATPase kinetics in aerobic *Escherichia coli* cells. Proc Natl Acad Sci USA 74:5551–5553
15. Hill AV (1910) The possible effects of the aggregation of the molecules of haemoglobin on its dissociation constant. J Physiol (London) 40:iv–vii
16. Koshland DE Jr (1970) The molecular basis for enzyme regulation. The Enzymes 1:341–396, Academic Press
17. Monod J, Wyman J, Cangeux J-P (1965) On the nature of allosteric transitions: a plausible model. J Mol Biol 12:88–118

Further Readings

Fromm HJ (1975) Initial Rate Enzyme Kinetics, Springer-Verlag, New York
Purich DL (2010) Enzyme Kinetics: Catalysis and Control, Academic Press, New York

Chapter 6
Coenzymes and Vitamins

Coenzymes are organic substances that participate like substrates in enzymatic reactions; however, unlike normal products the coenzymes are regenerated in subsequent reactions. Many, but not all coenzymes are vitamin derivatives. Vitamins are the dietary micronutrients that are required to produce these coenzymes.

6.1 Coenzymes

6.1.1 NAD^+ and $NADP^+$

NAD^+ (nicotinamide adenine dinucleotide) and $NADP^+$ (nicotinamide adenine dinucleotide phosphate) participate in redox-type reactions. Their structures are presented in Fig. 6.1.

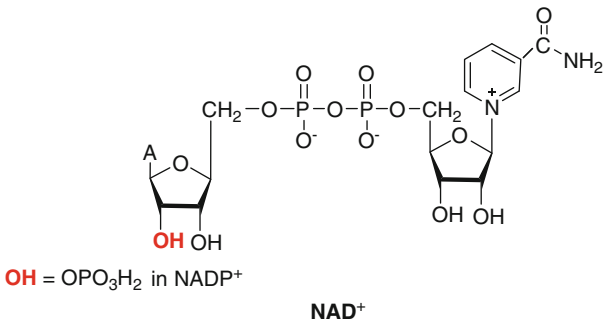

Fig. 6.1 The structures of NAD^+ and $NADP^+$

H.J. Fromm and M.S. Hargrove, *Essentials of Biochemistry*,
DOI 10.1007/978-3-642-19624-9_6, © Springer-Verlag Berlin Heidelberg 2012

These compounds are synthesized in vivo from the vitamin nicotinic acid (Fig. 6.2).

Fig. 6.2 The structure of the vitamin nicotinic acid

Enzymes that utilize these compounds are quite specific for their coenzyme. Exactly how NAD^+ and $NADP^+$ are involved in redox reactions is illustrated in the case of the well-studied enzyme alcohol dehydrogenase which utilizes NAD^+ exclusively. Alcohol dehydrogenase is a member of a large class of catalysts known as *pyridine-linked anerobic dehydrogenases*. The alcohol dehydrogenase reaction is shown in Fig. 6.3.

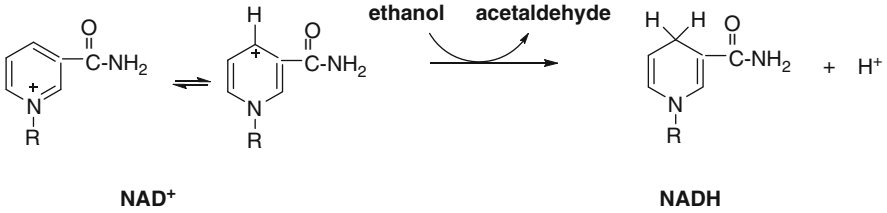

Fig. 6.3 The reaction catalyzed by alcohol dehydrogenase

The activator ion, Zn^{2+}, is tightly bound to the enzyme and plays an important role in catalysis. Enzyme-bound Zn^{2+} interacts with ethanol to form a Zn^{2+}-polarized hydroxyl group. This interaction markedly decreases the p*K* of the hydroxyl group and allows it to act as a typical Lewis acid, thus facilitating proton abstraction.

Westheimer and Vennesland and their colleagues [1] at the University of Chicago prepared 2,2-dideuteroethanol and incubated it with NAD^+ and alcohol dehydrogenase. After terminating the reaction they found one deuterium atom in acetaldehyde and the other in NADH. When this [^{2}H] NADH was incubated with unlabeled acetaldehyde and enzyme, the reaction products were monodeuterated ethanol and NAD^+ devoid of deuterium. On the basis of these findings, it was concluded that:

(a) There is a direct transfer of deuterium from ethanol to NAD^+ to form [^{2}H] NADH.
(b) That the transfer must be stereospecific. It was also concluded that deuterium is transferred as the deuteride ion ($^2H{:}^-$). Thus, the alcohol dehydrogenase reaction proceeds as follows in Fig. 6.4.

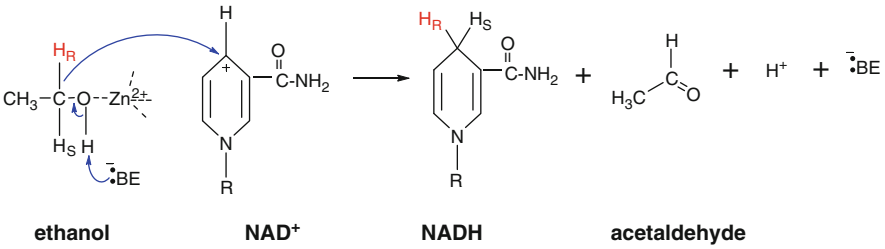

Fig. 6.4 The mechanism of the alcohol dehydrogenase reaction. Zn^{2+} labilizes the ethanol hydroxyl proton by polarizing the hydroxyl oxygen electrons thus promoting aldehyde and hydride ion formation

These studies demonstrated that enzymes exhibit specificity for both sp^2 and sp^3 prochiral centers:

1. sp^3 prochiral center specificity
   The C-1 of ethanol is an example of a prochiral sp^3 center (Fig. 6.5):

Fig. 6.5 The structure of ethanol illustrating the pro-R and pro-S hydrogen atoms

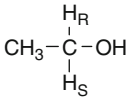

In the alcohol dehydrogenase reaction, the pro-R hydrogen is removed from the C-1 carbon atom as a hydride ion ($H:^-$). The same is true at the C-4 carbon atom of the pyrididium ring of NADH where the pro-R hydrogen is abstracted as a hydride ion (Fig. 6.6).

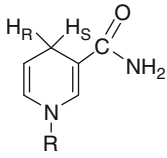

Fig. 6.6 NADH illustrating the pro-R and pro-S hydrogen atoms

2. sp^2 prochiral center specificity
   In the reverse reaction, starting with acetaldehyde, a hydride ion from NADH is added stereospecifically to the *re* face of acetaldehyde (Fig. 6.7).

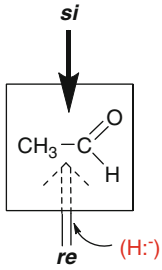

Fig. 6.7 Addition of the hydride ion to the *re* face of acetaldehyde

Mechanistically, the carbonyl carbon electrons of acetaldehyde are polarized by Zn^{2+}. The effect of the polarization increases the positive nature of the C-1 carbon atom and thus makes it more susceptible to nucleophilic attack.

In the forward reaction, addition of the hydride ion to NAD^+ occurs on the *re* face of the pyridinium ring (Fig. 6.8).

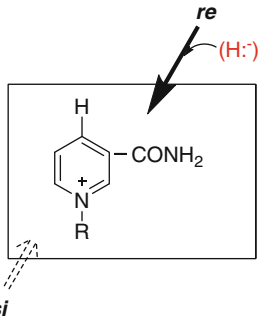

Fig. 6.8 Hydride ion addition to NAD^+ occurs on the *re* face of the pyridinium ring

It is important to note that the stereospecificity exhibited by the alcohol dehydrogenase reaction relative to hydride addition to NAD^+ and removal from NADH is not universal among all pyridine-linked anerobic dehydrogenases. Some of these enzymes do in fact add the hydride ion to the *si* face of NAD^+, also known as the *B* face. An example of such an enzyme is glucose-6-phosphate dehydrogenase. In the case of alcohol dehydrogenase, hydride ion addition is to the *A* or *re* face as indicated.

6.1.2 Biotin

Biotin, when it functions as a coenzyme is a carboxyl group carrier. It is covalently bound to the protein through an amide (peptide-like bond). The biotin side chain has a terminal carboxyl group that is covalently linked to an ε-amino group of a lysyl residue. The vitamin biotin and the coenzyme are identical in structure shown in Fig. 6.9.

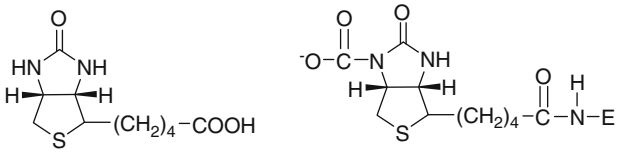

Fig. 6.9 The vitamin biotin (*left*) and carboxybiotin covalently bound to an enzyme

If biotin was not linked covalently to its conjugate enzyme, the reaction being catalyzed would lie far in the direction of decarboxylation. Biotin is involved in a variety of reaction types. These include: carboxylation coupled to ATP hydrolysis, transcarboxylation reactions which do not involve an energy source, and biotin-dependent sodium pumps. Pyruvate carboxylase (Chap. 8) is a typical example of

how biotin functions as a coenzyme in a reaction involving ATP. Methylmalonyl-oxaloacetate transcaboxylase [2] is an example of a system not coupled to ATP cleavage (Fig. 6.10).

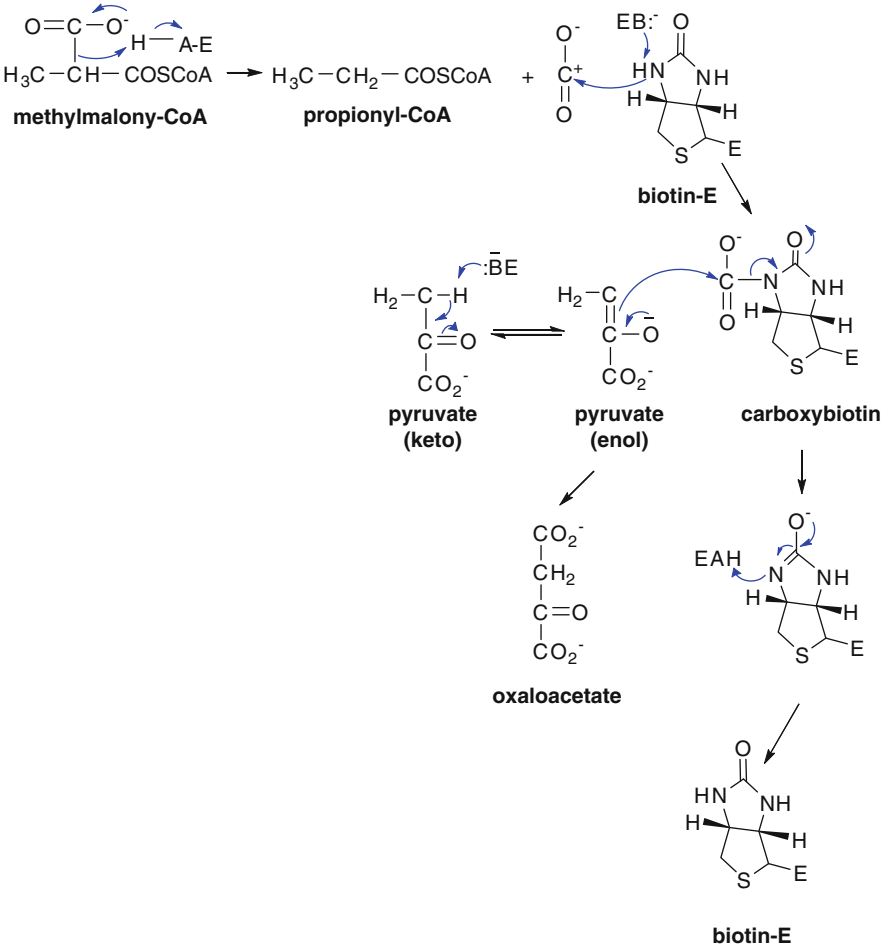

Fig. 6.10 The role of biotin in a non-ATP requiring transcarboxylation reaction

The protein *avidin*, found in eggs, binds very tightly to biotin with a K_{eq} of $10^{15}\ M^{-1}$. A diet of raw eggs over a prolonged period of time could lead to a biotin deficiency. Fortunately for egg lovers, the boiling, scrambling, or frying of eggs causes denaturation of avidin and its ability to sequester biotin.

6.1.3 Thiamine Pyrophosphate

Thiamine pyrophosphate (TPP) is a coenzyme involved in both oxidative and nonoxidative decarboxylation reactions. The vitamin thiamine lacks the

pyrophosphoryl group shown in the structure of TPP. A deficiency in thiamine leads to the nutritional disease *Beri Beri* (Fig. 6.11).

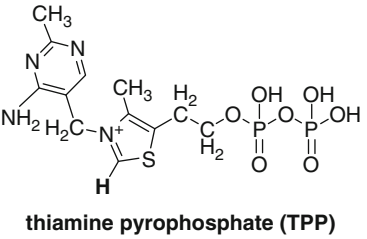

Fig. 6.11 The structure of the coenzyme thiamine pyrophosphate (TPP)

The hydrogen atom at the 2-position of the thiazolium ring is highly acidic as the C-2 is sandwiched between two strong electron-withdrawing groups. TPP forms a dipolar thiazolium ion or *ylid*. How TPP functions as a coenzyme is illustrated by the pyruvate decarboxylase reaction [3] (Fig. 6.12).

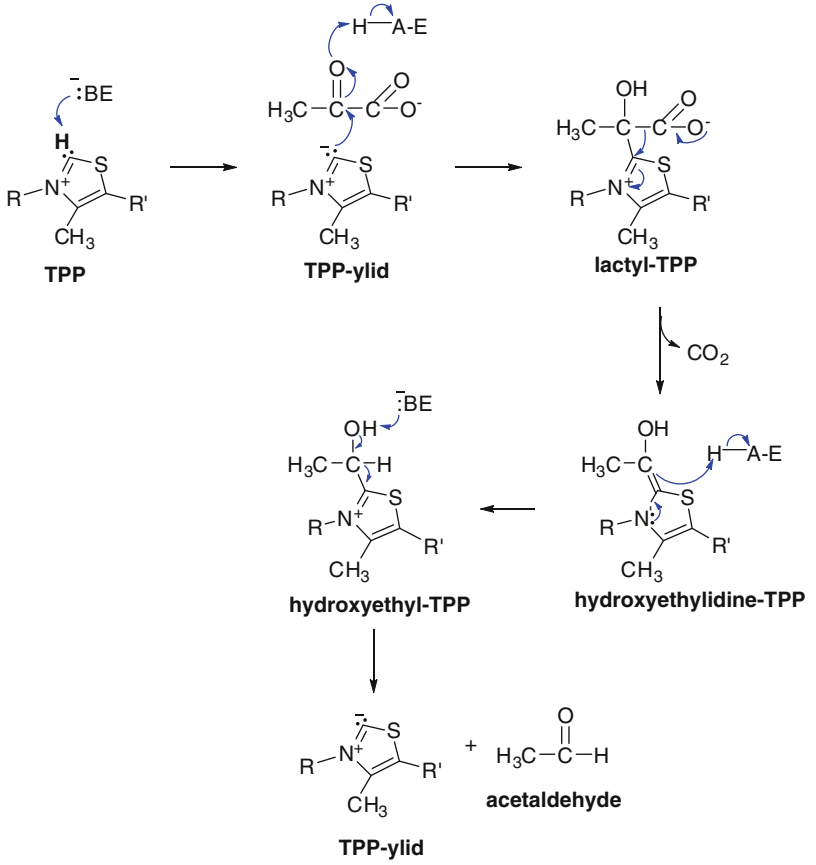

Fig. 6.12 The role of TPP in the pyruvate decarboxylase reaction

6.1.4 Coenzyme A

Coenzyme A (CoASH) functions as a *carrier* of acyl and acetyl groups. It is a derivative of the B-vitamin *pantothenic acid*. Acyl-CoA has the structure shown in Fig. 6.13.

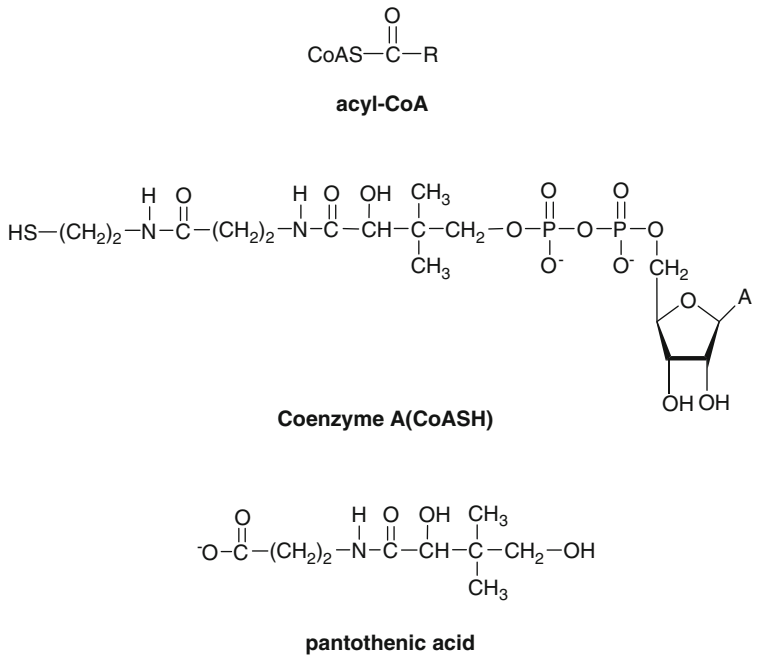

Fig. 6.13 Structures of acyl-CoA, CoASH, and the vitamin pantothenic acid

It functions as a coenzyme in two ways:

1. It facilitates activation of the acyl group for displacement by a nucleophile (Fig. 6.14).

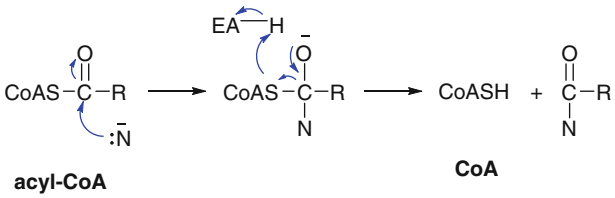

Fig. 6.14 Nucleophilic attack by a nucleophile ($^{-}$:N) on acyl-CoA

2. The acetyl group can act as a nucleophile by first labilizing a hydrogen atom adjacent to the keto group (Fig. 6.15).

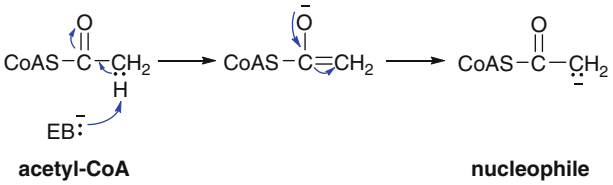

Fig. 6.15 The removal of a proton from the methyl group of acetyl-CoA

In the *acetyl-CoA carboxylase* reaction [4], the first step in fatty acid biosynthesis, acyl-CoA acting as a nucleophile accepts CO_2 from *carboxybiotin* (Fig. 6.16).

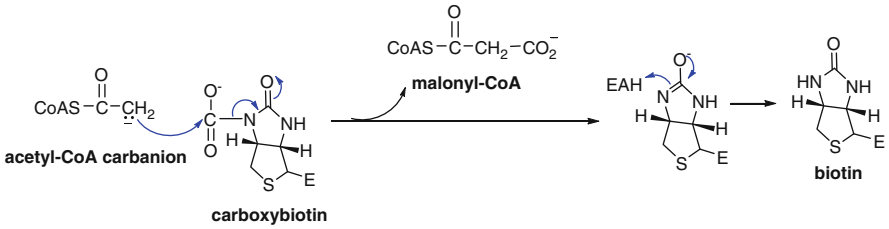

Fig. 6.16 The mechanism of the acetyl-CoA carboxylase reaction

6.1.5 *Pyridoxal Phosphate*

Pyridoxal phosphate (PLP) is one of the most versatile coenzymes. Aside from its role in the glycogen phosphorylase reaction where it functions as an acid–base catalyst (Chap. 11), it is involved in racemization, cyclization, transamination, decarboxylation, and side-chain removal reactions.

PLP is derived from *pyridoxine* (Vitamin B_6) (Fig. 6.17).

PLP is best known for its role in *transamination* reactions where an α-amino acid transfers its amino group to an α-keto acid. Reactions of this type are essential in the *de novo* biosynthesis of amino acids. Formally, a generic transamination reaction is as follows:

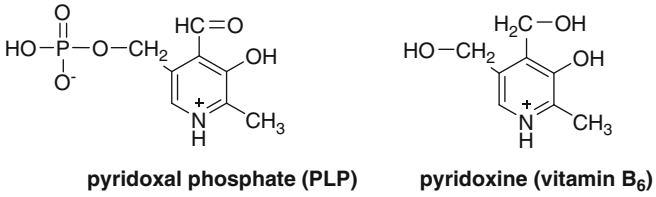

Fig. 6.17 The structures of the vitamin pyridoxine and the coenzyme pyridoxal phosphate

$$\alpha\text{-amino acid}_1 + \alpha\text{-keto acid}_2 = \alpha\text{-amino acid}_2 + \alpha\text{-keto acid}_1.$$

A typical transamination mechanism involving the first half of the sequence of reactions is depicted in Fig. 6.19 [5]. In the transamination reaction PLP is bound initially to the transaminase through a lysyl residue. Reversal of the illustrated steps leads to the entire transamination mechanism. Schiff base formation, shown in Figs. 6.18 and 6.19, is a prerequisite for transamination.

Another example of how PLP functions as a coenzyme is described by the *decarboxylation* mechanism shown in Fig. 6.20. The end result of amino acid decarboxylation is the formation of a primary amine.

Carbon–carbon bond cleavage reactions also utilize the coenzyme PLP. Schiff base formation is one prerequisite for reactions of this type, e.g., aldolase (Chap. 8) and the enzyme *threonine aldolase* [6, 7], a PLP enzyme that converts L-threonine to glycine and acetaldehyde. This is an example of the biosynthesis of a nonessential amino acid from an essential amino acid (Fig. 6.21).

Schiff base formation is not limited to the coenzyme PLP. Approximately 5% of hemoglobin is glycosylated. It is well established that this glycosylation is the result of an amino group on *hemoglobin* A_{1c} forming a Schiff base with glucose in the red blood cell [8].

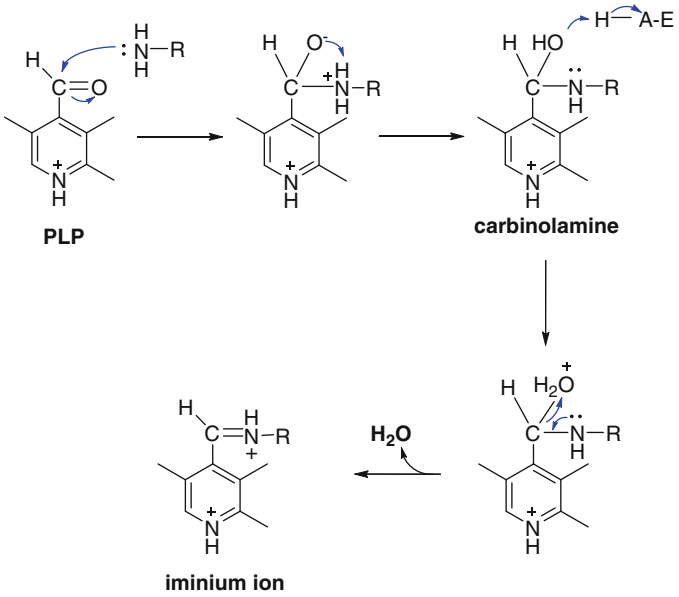

Fig. 6.18 The mechanism of Schiff base formation: reaction of PLP with an amino acid

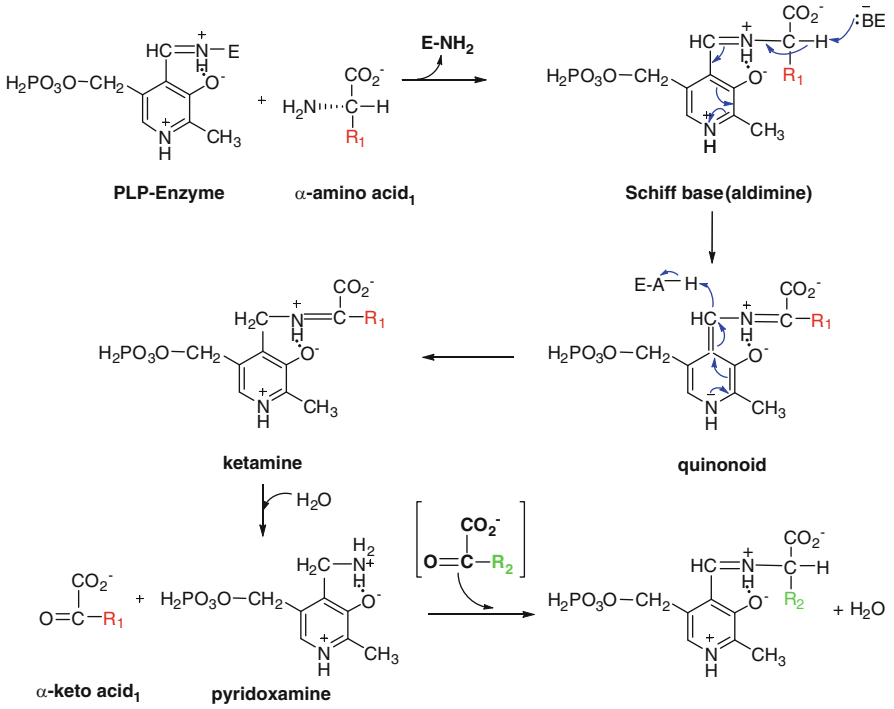

Fig. 6.19 The first half of a transamination reaction involving the deamination α-amino acid$_1$ to α-keto acid$_1$ and the addition of α-keto acid$_2$ to the transaminase

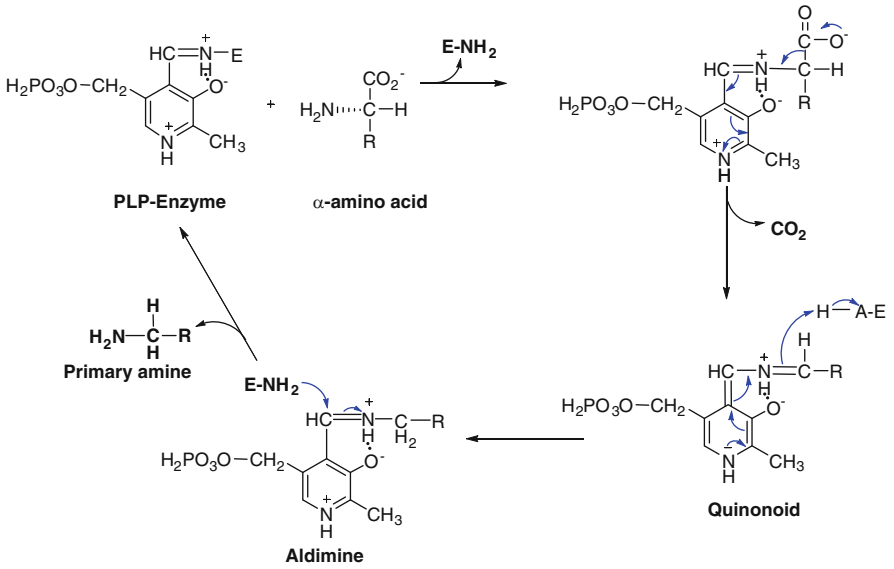

Fig. 6.20 Participation of PLP in amino acid decarboxylation

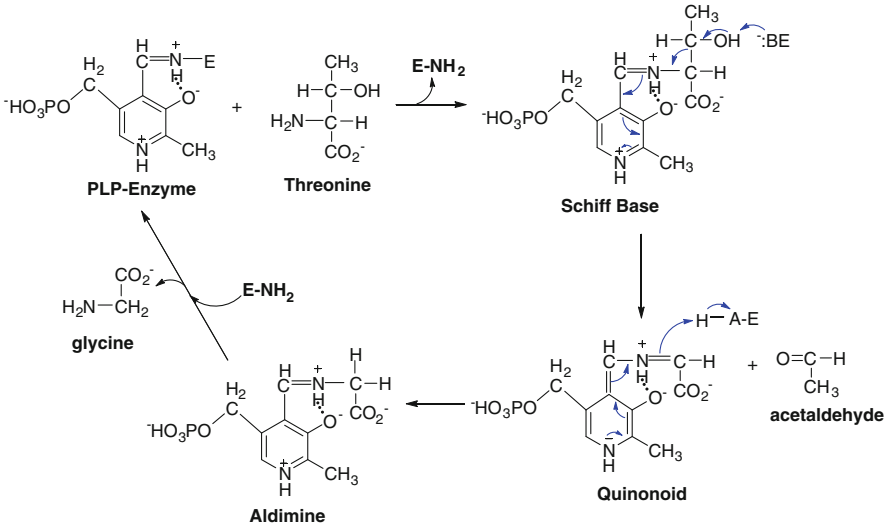

Fig. 6.21 The biosynthesis of glycine from L-threonine by threonine aldolase

6.1.6 Flavin Coenzymes

Flavins function as coenzymes in redox reactions. There are two flavin coenzymes: flavin mononucleotide (FMN) and flavin adenine dinucleotide (FAD). Both coenzymes are derivatives of the B-vitamin *riboflavin*. Flavoprotein enzymes are specific for either FAD or FMN (Fig. 6.22).

Both FAD and FMN can be reduced by reactions involving a single two-electron transfer or two one-electron transfer reactions.

A typical two-electron transfer reaction can occur when NADH donates a hydride ion to a flavin coenzyme to produce the reduced flavin, e.g., in Fig. 6.23.

The following redox reaction (Fig. 6.24) is an example of two one-electron transfer reactions.

As a rule, flavin coenzymes are bound very tightly, but not covalently, to their conjugate proteins. There are however, a few known examples in which the flavin is

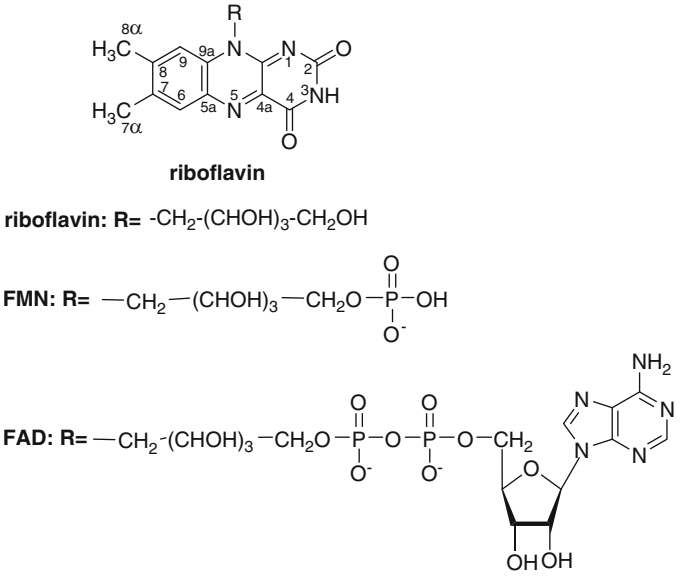

Fig. 6.22 Structures of riboflavin, FAD and FMN

covalently bound to an enzyme. This may occur at the C-8α where the hydrogen on the methyl group is replaced by a nitrogen atom from a histidyl residue in the protein, and at the C-6 where the hydrogen is replaced by a sulfur atom from a cysteinyl residue of the enzyme.

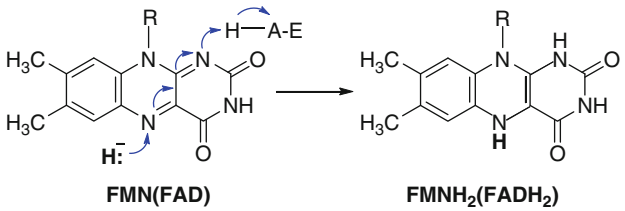

Fig. 6.23 Mechanism of a two-electron transfer reaction involving FAD and FMN

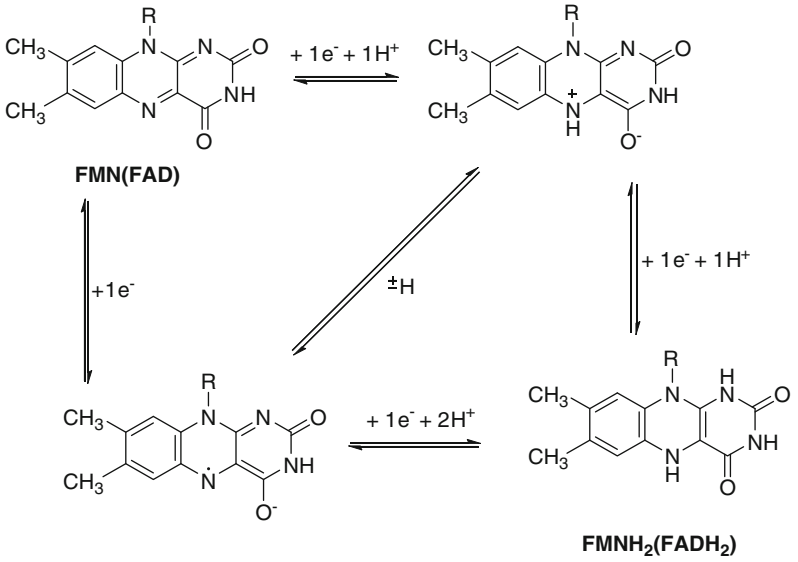

Fig. 6.24 One-electron redox reaction involving FAD and FMN

6.1.7 Lipoic Acid

Lipoic acid is by definition a coenzyme; however, it is not a vitamin derivative, i.e., it is synthesized in vivo (Fig. 6.25).

Functioning as a coenzyme, lipoic acid is bound to the enzyme through an amide linking. In the pyruvate dehydrogenase reaction [9], the coenzyme accepts an acyl group from TPP and ultimately passes it on to CoASH (Fig. 6.26).

The reoxidation of reduced lipoamide will be considered in Chap. 9.

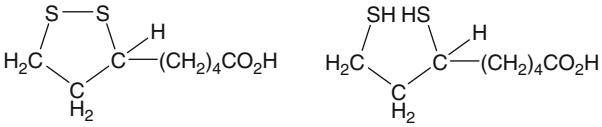

lipoic acid (oxidized) **lipoic acid** (reduced)

Fig. 6.25 The oxidized and reduced forms of lipoic acid

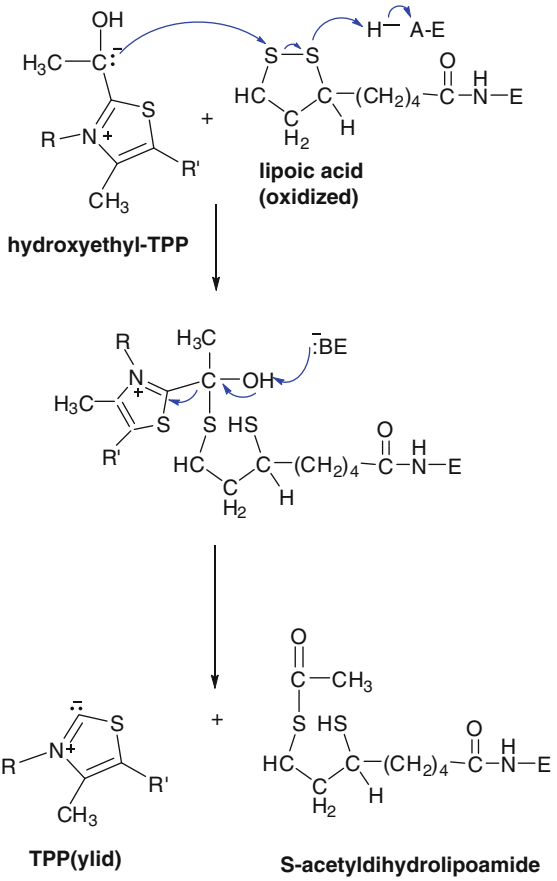

Fig. 6.26 The participation of enzyme-bound lipoamide in the pyruvate dehydrogenase reaction

6.1.8 Folic Acid Coenzymes

Folic acid functions in *one-carbon metabolism*, i.e., it transfers a number of different one-carbon units to a myriad of biological compounds and is considered to be the most versatile of the coenzymes. For example, it is essential for the biosynthesis of DNA, formylmethionine, purines, glycine, methionine, methane, and many other essential biomolecules.

The primary coenzyme derivative of folic acid is 5,6,7,8-tetrahydrofolic acid (FH_4). Although the vitamin has a single glutamyl residue as part of its structure (see below) FH_4 has a polyglutamyl side chain containing five or six glutamyl units. Folic acid itself contains a *pterin* moiety, glutamate, and ρ-aminobenzoic acid. Aside from the size of the glutamyl side chain, folic acid and TH_4 differ in the state of oxidation of the pterin moiety as can be seen from a comparison of their structures (Fig. 6.27).

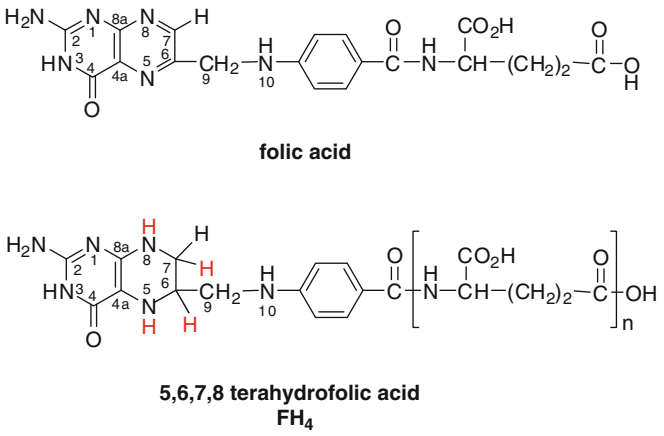

Fig. 6.27 The vitamin folic acid and the reduced form of the coenzyme, FH_4

The enzyme *dihydrofolate reductase*, an $NADP^+$-linked anerobic dehydrogenase, reduces folic acid to FH_4 in a two-step reaction, first to 7,8-dihydrofolate and then to the tetrahydrofolate (FH_4) (Fig. 6.28).

There are five different one-carbon units carried by the coenzyme:

(a) Methyl ($-CH_3$)
(b) Methylene ($-CH_2-$)
(c) Methenyl ($-CH=$)
(d) Formyl ($-CHO$)

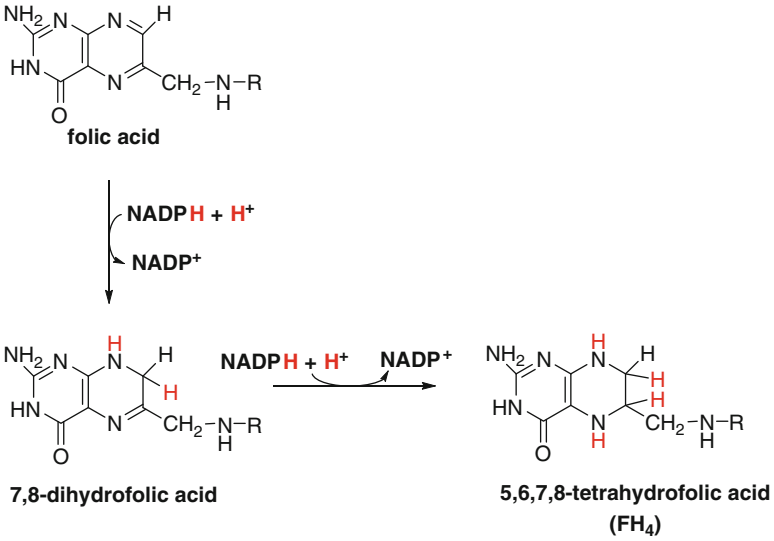

Fig. 6.28 The reduction of dihydrofolate to tetrahydrofolate

(e) Formimino (−CH=NH)

The following sequence of reactions illustrates some of the one-carbon derivatives of TH_4 and their interconversions. The enzyme names are omitted (Fig. 6.29).

One of the first antibiotics synthesized in the laboratory was sulfanilamide which is an inhibitor for the synthesis of *p*-aminobenzoic acid (Fig. 6.30).

Note the similarity between the structure of the synthetic drug and ρ-amino-benzoic acid, a precursor of TH_4 synthesis in certain bacteria. In these bacteria sulfanilamide acts as an inhibitor of TH_4 synthesis.

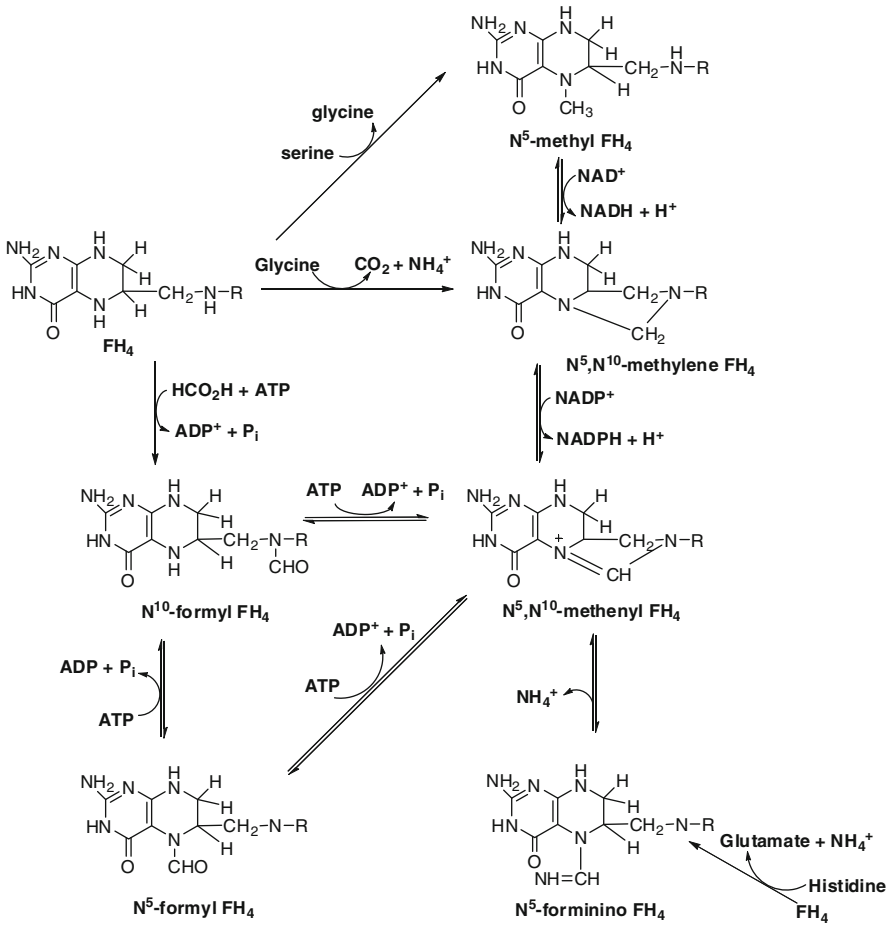

Fig. 6.29 The interconversion of the folate coenzymes

Because folic acid coenzymes are involved in DNA synthesis, FH_4 inhibitors have been used in cancer chemotherapy. One such compound, *methotrexate* is

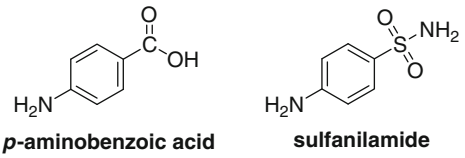

Fig. 6.30 Sulfanilamide is an inhibitor for the synthesis of *p*-aminobenzoic acid

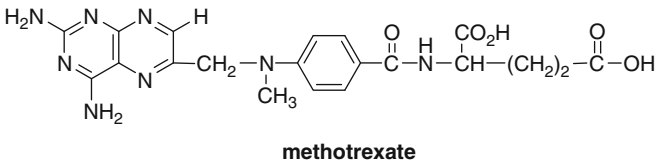

Fig. 6.31 The structure of methotrexate an inhibitor of folic acid metabolism

used for the treatment of leukemia; however, the drug itself is extremely toxic (Fig. 6.31) [10].

6.1.9 Vitamin B_{12} Coenzymes

Thomas Addison reported a lethal form of anemia (pernicious) in the 1850s, and in 1934 Minot, Murphy, and Whipple were awarded the Nobel Prize for finding that raw liver cured the symptoms of *pernicious anemia*. In 1948, Karl Folkers isolated the crystalline form of the so-called "extrinsic factor" from liver and named it vitamin B_{12}. The Nobel Prize was awarded to Dorothy Crowfoot-Hodgkin for solving the structure of vitamin B_{12} and in 1971 Robert Woodward published its synthesis.

Vitamin B_{12} or cobalamin, when chemically modified, is a coenzyme in a relatively small number of very important enzyme-catalyzed reactions. Although the human body contains only 1.5 mg of cobalt, lack of vitamin B_{12} in the diet leads to pernicious anemia, a potentially fatal disease.

Cobalamin contains a *corrin* ring structure containing four pyrrole rings in which two pyrrole rings are directly linked to each other. The vitamin contains Co(III) which is held at the center of the corrin ring system by coordination to the four nitrogen atoms of the pyrrole rings. One other cobalt bond is to the nitrogen of 5,6-dimethylbenzimidazole ribonucleotide. The remaining coordination bond of cobalt can be to a number of different ligands such as CN in Vitamin B_{12}, the form in which it is commercially isolated, a methyl group, or the *5′-deoxyadenosyl* moiety in the coenzyme. The structure of coenzyme B_{12} is shown in Fig. 6.32.

The cobalt in cobalamin undergoes oxidation state changes in the course of the reactions in which it is involved and in a sense these transformations are in

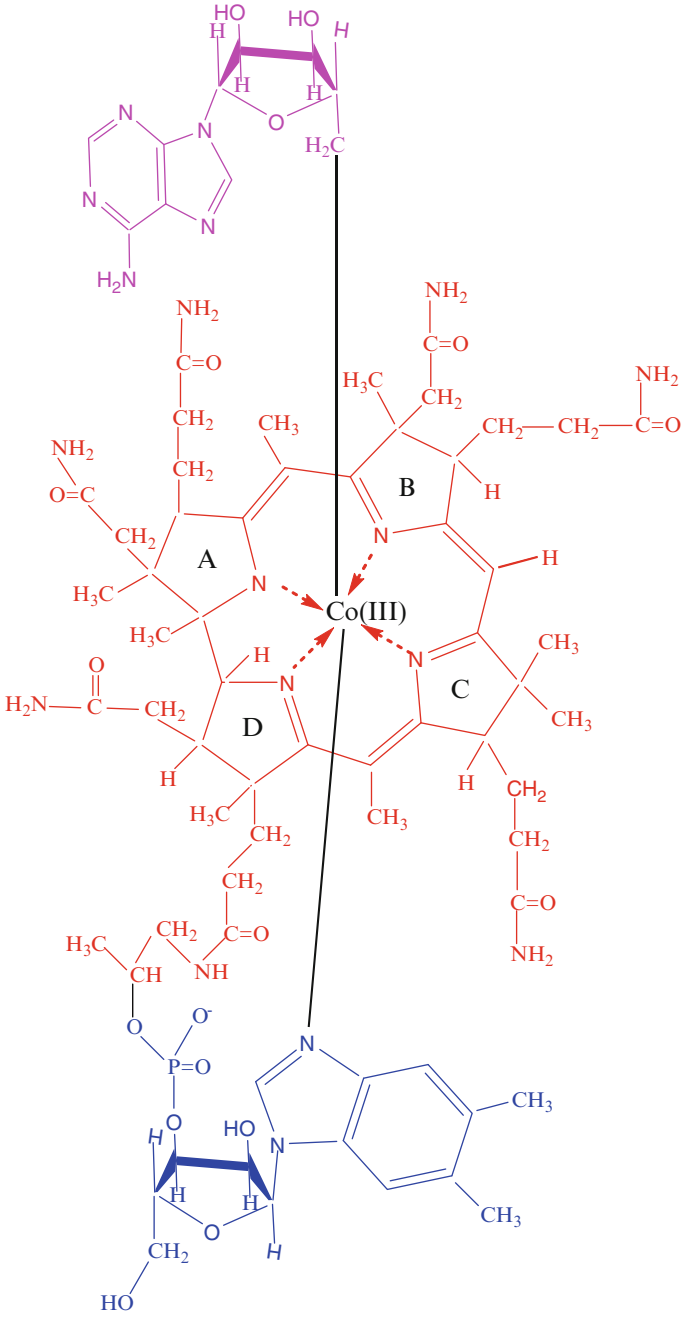

Fig. 6.32 The structure of Vitamin B_{12} (5′-deoxyadenosylcobalamin). The 5,6-dimethylbenzimidazole ribonucleotide and 5′-deoxyadenosyl moieties are colored *blue* and *purple*, respectively

fact redox reactions. Free radical intermediates are also commonplace in Vitamin B_{12} reactions.

The B_{12} coenzymes are involved in three different types of enzyme-catalyzed reactions:

1. The reduction of ribonucleotides to deoxyribonucleotides by a ribonucleotide reductase.
2. Isomerization reactions in which two groups on adjacent carbons exchange positions.
3. Methyl group transfer from methyl cobalamin.

There are at least three classes of ribonucleotide reductases found in nature. One of them (Class II), uses 5′-deoxyadenosylcobalamin as a coenzyme in these reactions (Fig. 6.33).

A well-studied example of a B_{12} coenzyme in an isomerization reaction involving hydrogen transfer is illustrated by the enzyme *methylmalonyl-CoA mutase* (Fig. 6.34).

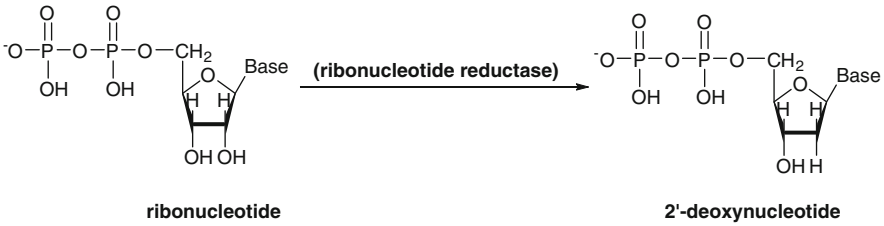

Fig. 6.33 The reaction catalyzed by ribonucleotide reductase reduces the 2′ hydroxyl to a hydrogen atom

The mechanism of the *propanediolhydratase* reaction, another isomerization, is shown in Fig. 6.35.

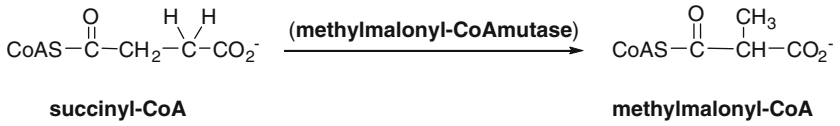

Fig. 6.34 The isomerization of succinyl-CoA to methylmalonyl-CoA by methylmalonyl-CoA mutase

The mechanism shown in Fig. 6.36 is one of a number proposed for B_{12}-type isomerization reactions.

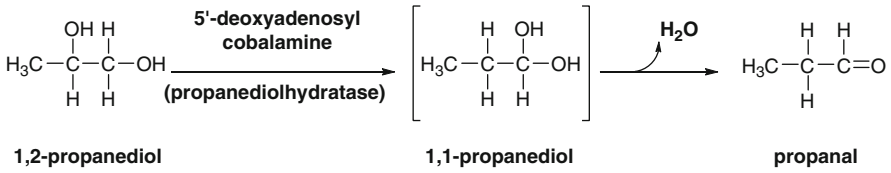

Fig. 6.35 The isomerization of 1,2-propanediol to form the intermediate 1,1-propanediol is the first step in the formation of 1,1-propanediol

Certain methylation reactions use the B_{12} coenzyme methylcobalamin. Both *Escherichia coli* and humans use this form of the coenzyme for some methylation

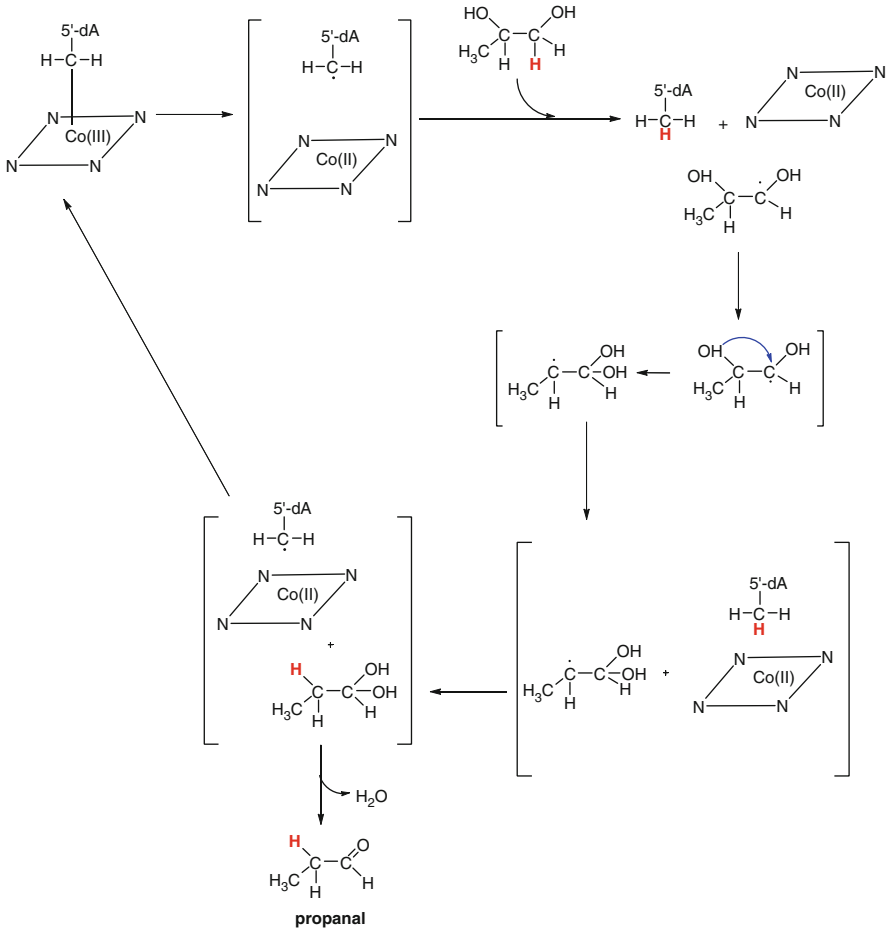

Fig. 6.36 One mechanism proposed to explain the function of cobalamin in the isomerization of 1,2-propanediol

reactions. N^5-methylFH_4 passes its methyl group on to cobalamin to yield the methylating agent, methylcobalamin. An example of such a system involves the conversion of homocysteine to methionine by the enzyme *methionine synthase* (Fig. 6.37).

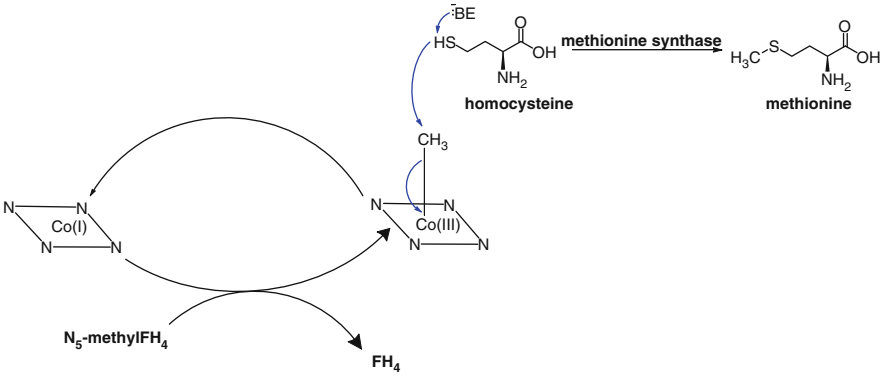

Fig. 6.37 The role of methylcobalamin in the methionine synthase reaction

6.2 Vitamins

6.2.1 Vitamin A

Vitamin A or *retinol* is a 20-carbon polyprenyl alcohol derived by the cleavage of 40-carbon β-carotene. β-Carotene is synthesized in plants and is converted in the gut to retinal which is reduced by dehydrogenases using NADH as the reductant. The resulting alcohol is esterified and absorbed as chylomicrons by the liver where it can be stored for long periods of time. Retinol is released from liver bound to a *retinol-binding protein* into blood where it is transported throughout the body as needed. Vitamin A is essential in preventing night blindness, sterility, and is required for the maintenance of epithelial tissue integrity (Fig. 6.38).

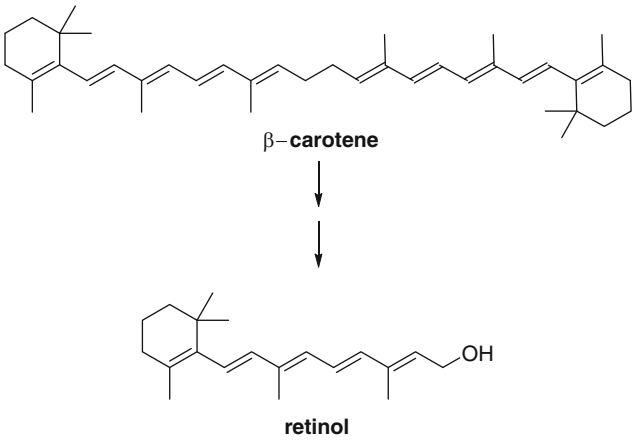

Fig. 6.38 Conversion of dietary β-carotene to retinol, Vitamin A

6.2.2 Vitamin C

Vitamin C, or ascorbic acid, is a cofactor for the enzyme *prolyl hydroxylase* which converts proline in collagen to *4-hydroxyproline* in a post-translational reaction. Normal collagen has a triple-stranded helical structure of enormous tensile strength. It is found in high concentrations in skin, tendons, cartilage, blood vessels and bone where it is the matrix of bone tissue. In quantitative terms, it is the most abundant protein in vertebrates. A lack of dietary ascorbic acid leads to the potentially fatal disease, *scurvy*, in which collagen is weakened by being either deficient or lacking in 4-hydroxyproline. Structures of ascorbic acid and 4-hydroxyproline bound to collagen are shown in Fig.6.39.

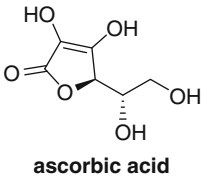

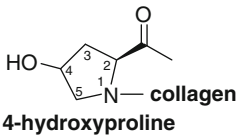

Fig. 6.39 Ascorbic acid (Vitamin C) is a cofactor in the synthesis of hydroxyproline from proline

6.2.3 Vitamin D

Vitamin D makes up a family of compounds that are capable of preventing *rickets*, a bone deformity in children, and *osteomalacia* a syndrome involving fragile bones in adults. Chemically, the D vitamins are sterol derivatives and may be considered hormones.

Vitamin D_3 (cholecalciferol) is hydroxylated in liver to produce 25-hydroxycholecalciferol and then further hydroxylated by an oxygenase in kidney to form the hormone which is *1-α,25-dihydrocholecalciferol*. It is this hormone that is responsible for increased absorption of dietary Ca^{2+} in the intestine. Phosphate is absorbed as the counter ion and both Ca^{2+} and phosphate are deposited in bone tissue (Fig. 6.40).

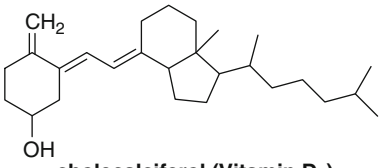

cholecalciferol (Vitamin D_3)

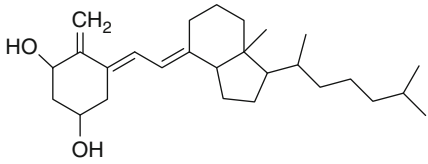

1-α,25-dihydroxycholecalciferol

Fig. 6.40 Cholecalciferol (Vitamin D_3) is the precursor of the hormone 1-α, 25-dihydroxycholecalciferol which is involved in Ca^{2+} absorption in the intestine

6.2.4 Vitamin E

Vitamin E (α-tocopherol) is thought to function as an antioxidant, i.e., it protects the cell against free radicals. Because it is so widespread in nature it is difficult to suffer from a vitamin E deficiency. Like other lipid soluble vitamins, its absorption is aided by bile salts, which are synthesized in the liver, stored in the gall bladder, and excreted into the small intestine. *Glycocholate* is a typical bile salt (Fig. 6.41).

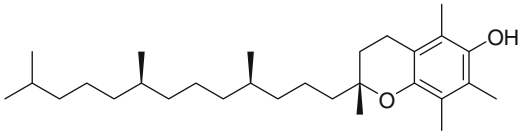

vitamin E

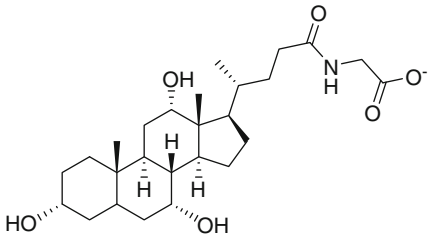

glycocholate

Fig. 6.41 α-tocopherol (Vitamin E) absorption from the gut is aided by salts of the bile acid glycocholate

6.2.5 *Vitamin K*

Vitamin K (*menaquinone*) is an essential factor in blood clotting (Fig. 6.42).

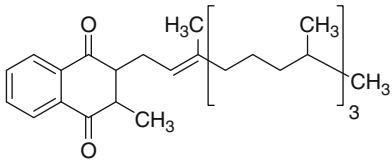

Vitamin K_2 (menaquinone)

Fig. 6.42 Vitamin K_2 (menaquinone) is a cofactor in blood clotting

After a cut or injury, blood platelets are activated and form a "plug." This plug, which slows bleeding, is made up of the protein fibrin which grows and hardens on the surface of blood platelets. Two separate, but converging pathways exist in humans to produce the fibrin clot. One, the *extrinsic* or *tissue factor pathway* is initiated by injured tissue by a glycoprotein, called tissue factor. The extrinsic pathway's response to injury is rapid. The other or slower pathway to clot formation is the *intrinsic* pathway which is triggered when blood comes in contact with abnormal surfaces such as glass.

As shown in Scheme 6.1, both pathways converge to form *thrombin*, a serine protease that converts the soluble blood protein *fibrinogen* to the fibrin clot. Ca^{2+}, an essential component of the clotting mechanism, is required at the convergence point of the two pathways.

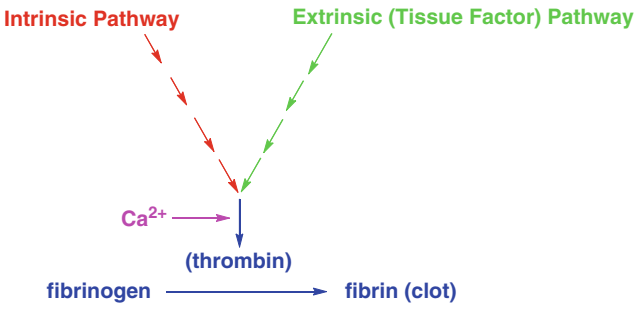

Scheme 6.1 Two pathways, the intrinsic and extrinsic pathways, are involved in blood clotting

Blood clotting in vertebrates occurs by a pathway known as a *biological cascade*. In the case of the blood clotting cascade, the enzymes exist as zymogens in blood until activation of one of the zymogens is triggered by injury. This enzyme then activates a second zymogen which in turn activates a third and so on until the final zymogen, *prothrombin*, is converted to *thrombin*. The soluble plasma protein *fibrinogen* is then acted upon by thrombin to form the insoluble *fibrin* clot.

Overall, the blood clotting cascade represents a series of reactions that lead to *amplification* of the number of enzymes at each step in the cascade. If ten molecules

of zymogen are activated by the injury and each enzyme in the sequence activates ten new zymogen molecules, the number of active enzyme molecules will increase as follows: 10, 100, 1000, etc.

The blood clotting enzymes are for the most part serine proteases. As we saw, each step in the cascade generates large quantities of enzymes and this amplification phenomenon ultimately produces a large amount of the enzyme thrombin. In addition, the cascade allows for precise regulation of clot formation at various steps in the coagulation process and thus prevents either hemorrhaging or thrombosis.

Vitamin K is a cofactor in the carboxylation of glutamate residues in a number of proteins involved in blood clotting. These carboxylations are absolutely essential to the formation of the fibrin clot. Although the exact mechanism of action of Vitamin K in the carboxylation reactions is not known, there is excellent evidence for the existence of the intermediates outlined in Fig. 6.43.

A number of compounds have *anti-vitamin K* activity. These compounds resemble vitamin K structurally and compete with the coenzyme for the carboxylase. One of these is *warfarin* which is an ingredient in rat and mouse poison. After warfarin ingestion animals will tend to hemorrhage and eventually die even after

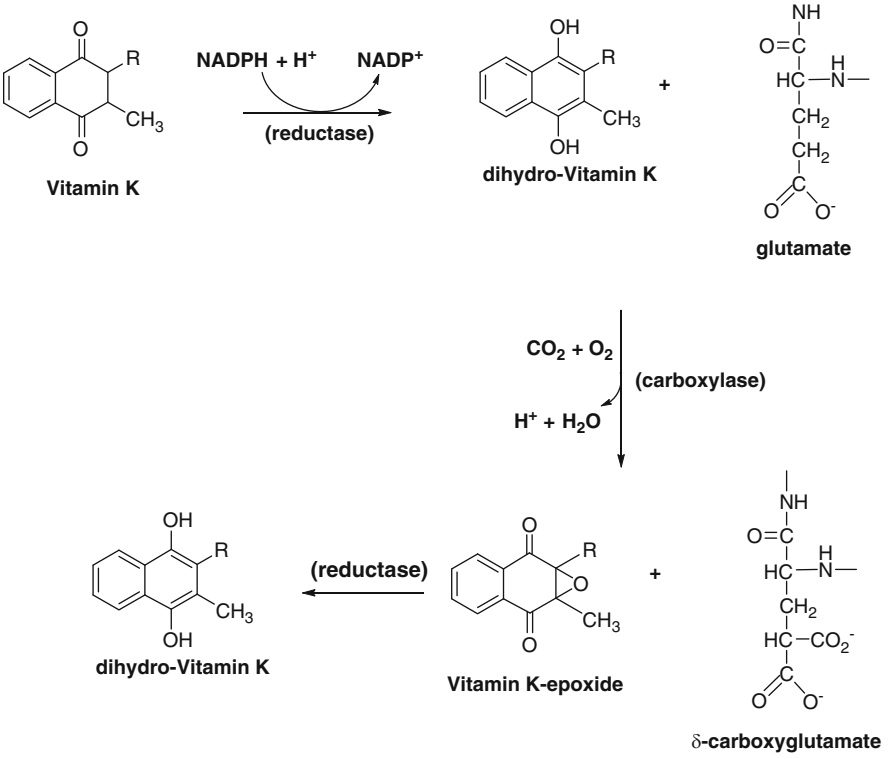

Fig. 6.43 A proposed role for Vitamin K in the synthesis of δ-carboxyglutamate, a key factor in clot formation

a superficial injury. On the other hand, anticoagulant drugs such as *coumarol* are used to prevent blood clotting in individuals who have had heart attacks (Fig. 6.44).

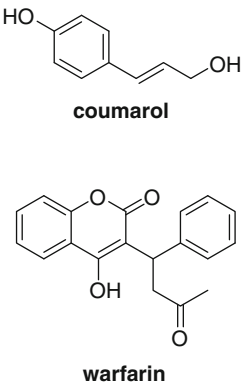

Fig. 6.44 The anti-vitamin K compounds coumarol and warfarin prevent blood clotting

References

1. Fisher HF, Conn EE, Vennesland B, Westheimer FH (1953) The enzymatic transfer of hydrogen. I. The reaction catalyzed by alcohol dehydrogenase. J Biol Chem 202:687–697
2. Wood HG, Allen SH, Stjerholmr R, Jacobson B (1963) Transcarboxylase. III. Purification and properties of methylmalonyl-oxaloacetic transcarboxylase containing tritiated biotin. J Biol Chem 238:547–556
3. Dyda F, Furey W, Swaminathan S, Sax M, Farrenkopf B, Jordan F (1993) Catalytic centers in the thiamin diphosphate dependent enzyme pyruvate decarboxylase at 2.4-Å resolution. Biochemistry 32:6165–6170
4. Moss J, Lane MD (1972) IV. Biotinyl prosthetic group-independent malony Coenzyme A decarboxylation and carboxyl transfer: Generalization to other biotin enzymes. J Biol Chem 247:4952–4957
5. Snell EE, Jenkins WT (1959) The mechanism of the transamination reaction. J Cell Comp Physiol 54:161–177
6. Karasek MA, Greenberg DM (1957) Studies on the properties of threonine aldolases. J Biol Chem 227:191–205
7. Kielkorpf CL, Burley SK (2002) X-ray structures of threonine aldolase complexes: structural basis of substate recognition. Biochemistry 41:11711–11720
8. Haney DN, Bunn HF (1976) Glycosylation of hemoglobin in vitro: labeling of hemoglobin by glucose-6-phosphate. Proc Natl Acad Sci USA 73:3534–3538
9. Reed LJ (1974) Multienzyme complexes. Acc Chem Res 7:40–46
10. Huennekens FM (1994) The methotrexate story: a paradigm for development of cancer chemotherapeutic agents. Adv Enzym Regul 34:399–419

Chapter 7
Introduction to Metabolism

Metabolism is defined as the sum total of all reactions that occur in the cell. It consists of two phases: catabolism and anabolism. Catabolism is the degradation of complex molecules to simpler ones with the liberation of Gibbs free energy, i.e., catabolic reactions are exergonic. Anabolism is the antithesis of catabolism, i.e., the synthesis of complex molecules from simpler ones with the utilization of Gibbs free energy, i.e., anabolic reactions are endergonic. The simple equation:

$$M = A + C,$$

where M is metabolism and A and C are anabolism and catabolism, respectively, aptly describes biosynthesis, biodegradation, and energy flux in the biology of living organisms.

When considering free energy produced and utilized in metabolism, it is necessary to focus on energy currency, ATP. During catabolism, the Gibbs free energy generated is utilized to drive the highly endergonic synthetic reactions. In many, but certainly not all cases, the driving force is ATP. The relationships between anabolism and catabolism can readily be appreciated by a few simple analogies, i.e., the inclined plane and the pulley (Scheme 7.1).

It is clear from this example that baring frictional forces, the weight on plane A will slide down the inclined plane (catabolism), whereas the weight on plane B will not move up plane B spontaneously (anabolism). However, if a pulley system is installed, the energy from system A can be harnessed to move the weight on plane B upward; thus, the systems are said to be "coupled." This is illustrated in Scheme 7.2.

The common factor between exergonic and endergonic reactions in living organisms, by analogy with the pulley, is ATP and other so-called "energy-rich compounds" [1] and enzymes. Enzymes are also capable of harnessing energy from

H.J. Fromm and M.S. Hargrove, *Essentials of Biochemistry*,
DOI 10.1007/978-3-642-19624-9_7,

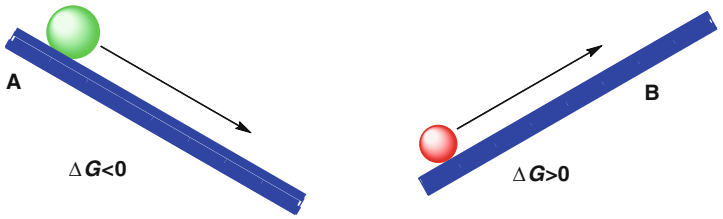

Scheme 7.1 The inclined plane as an analogy for endothermic and exothermic reactions

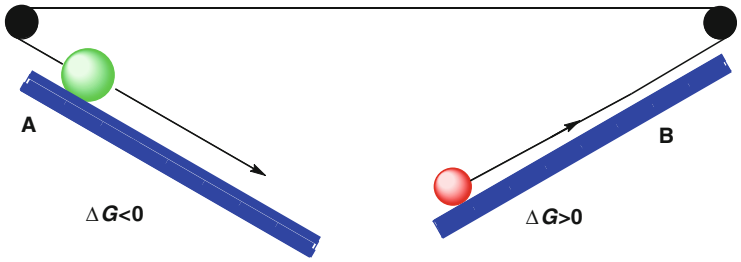

Scheme 7.2 The inclined plane illustrates the concept of coupled reactions

exergonic reactions to drive endergonic reactions. An example is the enzyme hexokinase which catalyzes the reaction:

$$\text{D-glucose} + \text{ATP} \rightarrow \text{D-glucose 6 - phosphate} + \text{ADP}. \tag{7.1}$$

Absent the enzyme, the phosphorylation of D-glucose by phosphate is endergonic, if it occurs at all. On the other hand, the hydrolysis of ATP is highly exergonic. By coupling these two reactions, the desired product D-glucose 6-phosphate is obtained. This is better understood by considering the two reactions, phosphorylation and hydrolysis separately:

$$\begin{aligned}\text{D - glucose} + \text{phosphate } (P_i) \rightarrow \text{D - glucose - 6 - P} + H_2O, \Delta G^0 \\ = +13.8\,\text{kJ/mol},\end{aligned} \tag{7.2}$$

$$\text{ATP} + H_2O \rightarrow \text{ADP} + P_i, \Delta G^0 = -30.5\,\text{kJ/mol}. \tag{7.3}$$

Thus the ΔG^0 for overall reaction is -16.7 kJ/mol.

Huge amounts of ATP are produced in living systems. One example, cited by P. D. Boyer, involves a student whose typical caloric intake is 2,000 kcal or 8,360kJ/day. If the efficiency of ATP production is approximately 40%, then 3,344kJ/day may be utilized for ATP production. If we assume that the ΔG^0 of ATP hydrolysis is -30.5kJ/mol, it follows that 111 mols of ATP are synthesized by the student the day that he/she ingests 8360kJ of food. The molecular weight of

ATP is 550, thus 61 kg (134 pounds) of ATP/day are produced by the student to do work. It should be pointed out that a very large fraction of the ATP synthesized is utilized for brain activity.

Why are ATP and similar compounds so effective, energetically, in anabolic reactions when their hydrolysis yields relatively small amounts of energy? The answer is that the bonds that they help synthesize in enzymatic reactions are even less energetic. A case in point is the synthesis of a peptide bond, which when hydrolyzed yields approximately 10kJ/mol of Gibbs free energy. In other cases, such as the synthesis of phosphoenolpyruvate, whose ΔG^0 of hydrolysis is approximately -67kJ/mol, two ATP or equivalent molecules are used in successive steps for its synthesis.

When the importance of ATP was first recognized in synthetic reactions, it was referred to as a "*high energy*" compound. In reality, there is nothing unusual about ATP; rather the products of ATP hydrolysis are at relatively low energy levels for a variety of reasons. These include *resonance*, *tautomerism*, substrate *bond strain*, and effects of *entropy*. Two energy level diagrams depicted in Scheme 7.3 illustrate these points.

It should be noted that in many of the examples of high energy compounds cited below a proton is generated in the reaction. Reactions such as these are obviously pH sensitive and the ΔG^0 values indicated will vary with pH.

The difference in ΔG^0 values between these two reactions (see Scheme 7.3) is a result of low energy levels displayed by the products, i.e., the energy levels of the two transition states are equal.

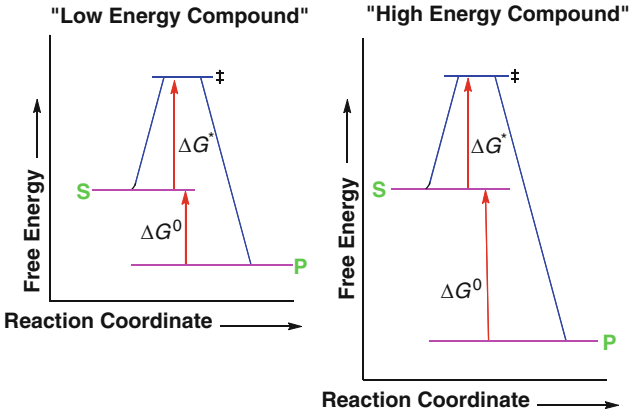

Scheme 7.3 Energy level diagrams illustrate differences between "low" and "high energy" compounds

7.1 High Energy Compounds

"*High Energy*" compounds are defined as those that release more than 20kJ/mol of free energy [1] when hydrolyzed.

7.1.1 ATP *(as Well as Other Nucleoside Di-and Triphosphates),* $\Delta G^0 = -30.5$ *kJ/mol*

ATP is a tripolyphosphate of the following abbreviated structure, which when hydrolyzed produces $ADP^{3-} + P_i^{2-} + H^+$. It should be noted that a divalent ion, such as Mg^{2+}, enhances the rate of hydrolysis of ATP in solution, and in enzyme-catalyzed reactions is essential for very rapid hydrolysis (Fig. 7.1).

The tripolyphosphate substrate structure is less stable than the diphosphate product due to the repulsion of the negatively charged oxygen atoms between the β and γ phosphoryl groups of ATP. Second, there is more resonance associated with $ADP^{3-} + P_i^{2-}$ than with ATP^{4-}. Finally, the hydrolysis reaction produces three products compared to the single substrate, ATP. This favorable entropy effect also serves to decrease the energy inherent in the products relative to that of the substrate. It is these factors that contribute to the overall loss of Gibbs free energy when ATP undergoes hydrolysis. In so-called synthetase reactions, the energy inherent in the cleavage of the β–γ or α–β phosphoryl bonds is used to drive endergonic reactions, i.e., the energy is not lost as it would be in the example cited in Fig. 7.1.

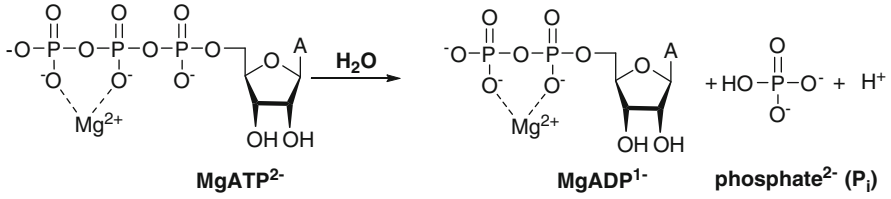

Fig. 7.1 The hydrolysis of ATP yields ADP, P_i, and a proton. Mg^{2+} binds much less tightly to ADP than to ATP and even less tightly to P_i

7.1.2 *Acetyl Phosphate,* $\Delta G^0 = -43$*kJ/mol*

Acetyl phosphate (Fig. 7.2) is found in abundant quantities in bacteria. The hydrolysis of acetyl phosphate yields significant quantities of energy for a number of reasons; these include the highly-resonating carboxylate group of acetate, increased resonance of orthophosphate compared to the phosphate anhydride (acetyl phosphate), and the favorable entropic effect when the substrate breaks down to form three products.

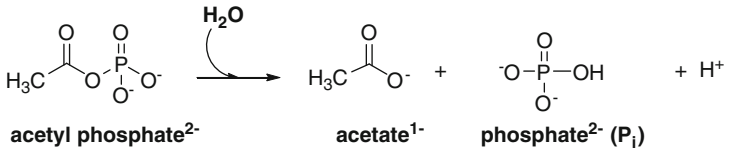

Fig. 7.2 The hydrolysis of acetyl phosphate

7.1.3 Creatine Phosphate, $\Delta G^0 = -43 kJ/mol$

Creatine phosphate (Fig. 7.3) is found in high concentrations in animals, particularly in muscle tissue. Creatine phosphate falls into the "high energy" phosphate category because of the high degree of resonance stabilization exhibited by creatine relative to creatine phosphate, e.g., there are two resonance forms of creatine involving the guanidino group (see Fig. 7.3). Entropy plays only a small role as two products are produced in the hydrolysis reaction, but free phosphate exhibits greater resonance than the phosphoryl group in creatine phosphate.

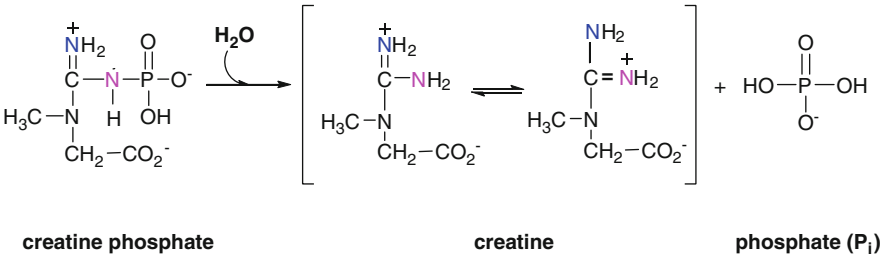

Fig. 7.3 The hydrolysis of creatine phosphate yields the highly resonating structures creatine and P_i

7.1.4 Phosphoenolpyruvate, $\Delta G^0 = -62 kJ/mol$

Phosphoenolpyruvate (Fig. 7.4) is a ubiquitous biomolecule and is found in all life forms. The hydrolysis of phosphoenolpyruvate produces roughly two ATP equivalents of Gibbs free energy. The major role played by tautomerism in the reaction products, i.e., the enol–keto–pyruvate interconversion is responsible for this highly exergonic reaction. Increased resonance of the released phosphate and proton formation are significant but minor relative to tautomerism.

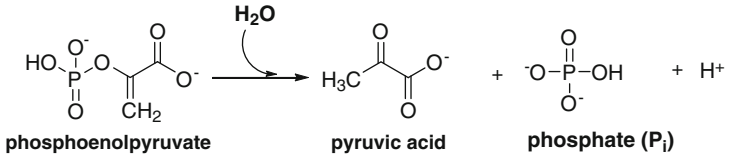

Fig. 7.4 The hydrolysis of phosphoenolpyruvate yields approximately two ATP energy equivalents

7.1.5 Pyrophosphate, $\Delta G^0 = -33.5 kJ/mol$

The hydrolysis of pyrophosphate yields more energy than the hydrolysis of ATP. The rationale behind this observation is that $2P_i$ molecules resonate more than do an ADP and a single P_i molecule (Fig. 7.5).

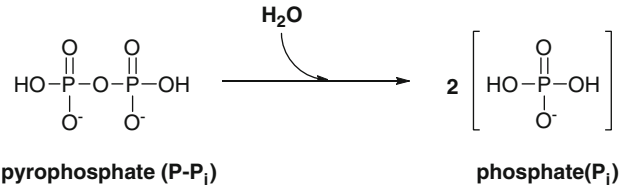

Fig. 7.5 The hydrolysis of pyrophosphate produces two molecules of P_i

7.1.6 Acetyl-Coenzyme A (Acetyl-CoA), $\Delta G^0 = -32.2$kJ/mol

Acetyl-coenzyme A (acetyl-CoA) (Fig. 7.6), like phosphoenolpyruvate, is ubiquitous in nature. The explanation for the exergonic nature of the acetyl-CoA hydrolysis reaction is similar to that outlined for the hydrolysis of acetyl phosphate, except that acetyl-CoA is a thioester [2].

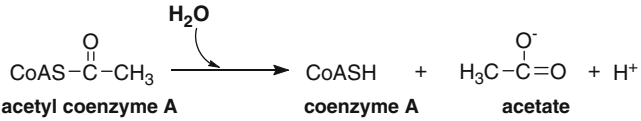

Fig. 7.6 Acetyl-CoA can be hydrolyzed to yield CoA and acetate. It is one of a small number of high energy compounds that are not phosphate esters or anhydrides

7.2 Intermediate Energy Compounds

Intermediate energy compounds are those that liberate somewhat less than 19kJ/mol of Gibbs free energy when hydrolyzed. D-Glucose 1-phosphate is an example of an intermediate energy compound. The hydrolysis of this ester gives rise to two anomers of glucose, the α and β forms as well as phosphate. Thus, it is mutarotation, a form of tautomerism, as well as the increased resonance of orthophosphate along with the favorable entropy effect that is responsible for the exergonic nature of this reaction (Fig. 7.7).

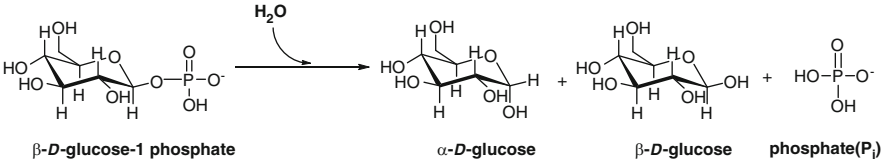

Fig. 7.7 The hydrolysis of the "intermediate energy" phosphate compound β-D-glucose-1 phosphate

7.3 Low Energy Compounds

Most phosphate esters found in nature fall into the class of low energy compounds. When hydrolyzed they liberate approximately 8.4 to 12.6 kJ/mol of Gibbs free energy. One example of this class of substances is glyceraldehyde-3-P (Fig. 7.8).

The favorable energetics of this reaction is a result of the increased resonance of the product (orthophosphate) relative to the substrate as well as a favorable entropy effect.

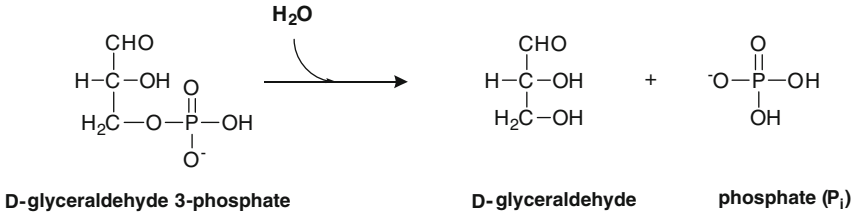

Fig. 7.8 Hydrolysis of the "low energy" phosphate compound D-glyceraldehyde 3-phosphate

7.4 Regeneration of Nucleoside Di- and Tri-Phosphates

ATP when used in metabolic reactions as an energy source is converted to either ADP or AMP. ATP is regenerated from ADP via glycolysis and oxidative phosphorylation. AMP can be phosphorylated to ADP in the myokinase (adenylate kinase) reaction:

$$\mathrm{AMP} + \mathrm{ATP} \leftrightarrow 2\mathrm{ADP},$$

and ADP can then be phosphorylated to yield ATP by this same enzyme.

Other nucleoside mono- and diphosphates can follow a similar biosynthetic route with ATP as the phosphoryl donor and nucleoside mono- and diphosphates as acceptors. The enzymes that catalyze these reactions are referred to as nucleoside mono- and nucleoside diphosphokinases. The following reactions illustrate these points:

$$\mathrm{XMP} + \mathrm{ATP} \leftrightarrow \mathrm{XDP} + \mathrm{ADP}(\text{nucleoside monophosphate kinase}),$$

$$\mathrm{XDP} + \mathrm{ATP} \leftrightarrow \mathrm{XTP} + \mathrm{ADP}(\text{nucleoside diphosphate kinase}),$$

where X is a nitrogenous base such as: G, C, U, or T.

7.5 Metabolic Pathways and Their Regulation

The goal of every metabolic pathway is to produce one or more end products required by the cell for sustenance. These end products of metabolism may be used as such or alternatively they may feed into other pathways. A case in point is the ubiquitous glycolysis pathway. The substrate for glycolysis is glucose and the end product pyruvic acid which itself may be converted to alanine or, alternatively, may be oxidized to CO_2 and H_2O. Intermediates for glycogen and lipid biosynthesis are also produced in the glycolytic pathway.

Metabolic pathways in which the same end product is produced may differ from kingdom to kingdom and indeed from species to species; however, many of the enzymes within the pathway are expected to be similar. Nature, rather than synthesize new enzymes *de novo*, modifies existing enzymes through evolution to meet the biological needs of the organism. The goal of any organism is to survive in the environment it finds itself in. An organism's response to environmental pressures is largely responsible for the myriad of metabolic pathways seen in nature.

Some metabolic pathways are both anabolic and catabolic in nature. These pathways are referred to as *amphibolic*. An example of an amphibolic pathway is the Tricarboxylic Acid Cycle in which citric acid is synthesized from oxaloacetate (anabolic) and isocitrate is converted to α-ketoglutarate (catabolic).

In other metabolic pathways carbon compounds that have been removed to produce cellular constituents are replaced by other compounds. These reactions are referred to as *anaplerotic* or "filling in" (Gr.) reactions. A typical anaplerotic reaction involves the enzyme pyruvate carboxylase which is involved in the conversion of pyruvate to oxaloacetate which may be removed by the cell to form aspartate or phosphoenolpyruvate.

7.5.1 The Concept of the "Committed Step" in a Metabolic Pathway

A typical metabolic pathway is described in Scheme 7.4.

Each of the steps depicted in Scheme 7.4 is enzyme-catalyzed. How is this pathway regulated (inhibited) if the concentration of metabolite increases beyond the amount required by the cell? The first step committed *exclusively* to the production of F is E_4. Inhibition of E_5 would also serve the purpose of either turning off the production of F or decreasing it; however, the level of E would continue to rise, a situation the cell cannot tolerate. Step E_4 is thus the *first committed step* for the production of metabolite F. Analogous arguments suggest that E_6 is the committed step for the production of G and E_7 the committed step for the formation of I. The committed steps are indicated in red. Inhibition at steps E_1 and E_2 will also serve to decrease or eliminate the formation of the end products; however, situations can be envisioned where the cell requires metabolites G and F,

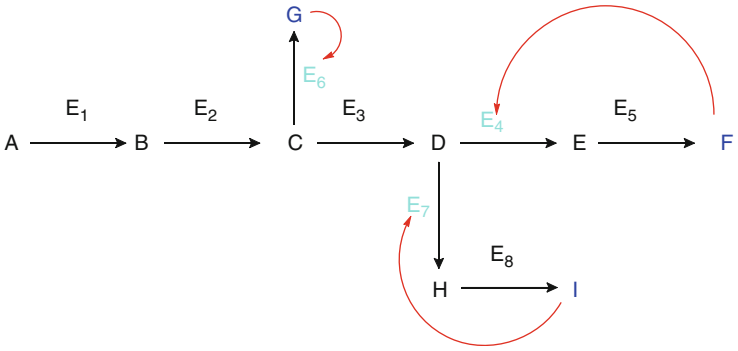

Scheme 7.4 The concept of committed steps in metabolic pathways

but not I. Inhibition at steps E_1 and E_2 under these circumstances would be detrimental to the cell's survival. The inhibition illustrated in Fig. 7.4 is of the *feed-back* type.

7.5.2 *Metabolic Pathways Are Highly Exergonic*

All cells are relatively-small entities and as such they guard judiciously against increases in metabolites other than the required end products. Consider the equilibrium for the reaction: $A = B$, where the ratio of B/A will be assumed to be 1,

$$K_{\text{eq}} = \frac{c[B]}{c[A]}. \tag{7.4}$$

Thus, a requirement for high concentrations of B by the cell will also assure that the concentration of A will also be high. On the other hand, if $K_{\text{eq}} = 1{,}000$, the ratio of B:A would be 1,000:1. This requirement that the pathway be highly exergonic in order to keep the substrates and non-end products low is illustrated using the bacterium *Escherichia coli* as an example. Data from the *E. coli* data base at the University of Alberta, Canada [3] suggests that the *E. coli* cell volume is 7×10^{-16} L and that 70% of the cell is water. Using this information as well as Avogadro's number, a *single* ion or compound will yield a concentration of 3.3 nM in *E. coli*. This would represent the minimal concentration of a single metabolite molecule. In terms of pH, a single free proton would produce a pH of 8.5.

7.5.3 *Pathways Are Not Thermodynamically Reversible, But They Are Physiologically Reversible*

In Scheme 7.5, the conversion of substrate A to end product F is highly exergonic, i.e., irreversible. It is possible to go from F back to A; however, this will require the input of energy and the use of different enzymes, e.g., in Scheme 7.5.

In Scheme 7.5, both the A → F and F → A pathways are energetically exergonic. Of equal importance is the fact that both the A → F and the F → A pathways, because they require different enzymes, can be regulated differently, i.e., A → F may be inhibited at the same time that F → A is functional.

Scheme 7.5 The exergonic nature of metabolic pathways that run in opposite directions

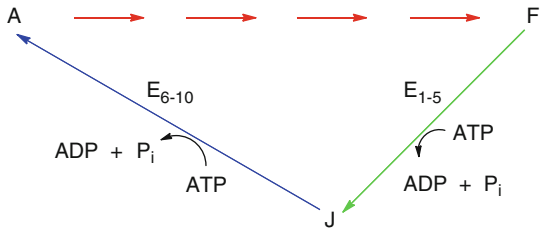

7.5.4 *Feed Forward Activation and Feed-Back Inhibition*

We have seen that a rise in the concentration of product F can lead to inhibition of the enzyme committed exclusively to its formation (Scheme 7.4). This phenomenon is known as feed-back inhibition [4]. Alternatively, it is possible that an intermediate in a metabolic pathway may actually activate (feed forward) an enzyme down the metabolic chain [5]. These concepts are extremely important in understanding the role of physiological regulators in the flux of metabolites in metabolic pathways.

7.5.5 *Equilibrium Versus Nonequilibrium Enzymes as Sites of Regulation*

The flux through a metabolic pathway is controlled by one or more rate-limiting enzyme activities. There is general, but certainly not universal agreement that regulation in metabolic pathways occurs at steps that are *irreversible*. A clue as to which step may be rate-limiting can be determined by examination of the *mass action ratio* and K_{eq} for each enzyme and comparing the two. If the two are equal, the system is said to be at equilibrium and not a regulated enzyme; however, a large discrepancy between the mass action ratio and K_{eq} indicates the system is not at equilibrium. The mass action ratio, Γ, for a system such as:

$$A + B = C + D,$$

is defined as:

$$\Gamma = \frac{c[\Sigma\ C \text{ species}] \times c[\Sigma\ of\ D \text{ species}]}{c[\Sigma\ of\ A \text{ species}] \times c[\Sigma\ of\ B \text{ species}]}. \tag{7.5}$$

The terms in brackets are in molarity and represent free substrates and products. The K_{eq} and Γ are equal when time $= \infty$.

Steps prior to the rate-limiting step produce substrate more rapidly than the rate-limiting enzyme can utilize, whereas steps subsequent to that step also utilize product at a rapid rate relative to the rate-limiting step. The enzymes prior to, and subsequent to, the rate-limiting step in a metabolic pathway are thus in equilibrium, whereas the mass action ratio at the rate-limiting step in vivo is much less than what one would expect from the enzyme's mass action ratio or K_{eq} in vitro. Recall that for a system at equilibrium the rates of all steps, both forward and reverse, are equal.

Lunn and Rees [6] used this protocol to show that sucrose–phosphate synthase is a nonequilibrium enzyme, and the probable site of regulation of sucrose synthesis in plant seeds.

The notion that regulation always takes place at thermodynamically irreversible steps in a metabolic pathway is clearly an overstatement. As pointed out above, one must focus instead on the mass action ratio of enzymes in the cell and in the test tube, and not on their equilibrium constants in vitro exclusively. For example, hexokinase I is the so-called "pacemaker of glycolysis" in brain tissue and the erythrocyte, but not in liver or muscle. Similarly, yeast hexokinase is not a regulated enzyme. Obviously, the equilibrium constant, and the highly exergonic nature of the reaction is the same for all hexokinase isozymes, but the concentrations of the substrates and products (the mass action ratio) will vary with different cells.

7.5.6 *Modulation of Enzyme Activity*

Enzyme activity within the cell can be modulated by a large number of factors. These include:

(a) *Synthesis and degradation of the enzyme itself*: This is one type of genetic control. Examples include the adaptive enzyme ribitol dehydrogenase from *Aerobacter areogenes*, muscle hexokinase, and glucose-6-phosphatase. Extremely small quantities of ribitol dehydrogenase exist in the bacterium until the organism is fed ribitol (reduced D-ribose) after which the enzyme is synthesized in large amounts [7]. Muscle hexokinase requires insulin to prevent its degradation, and glucose-6-phophatase deceases upon fasting but is synthesized after a glucose-rich diet.

(b) *Positive cooperativity*: Enzymes that exhibit positive cooperativity or sigmoidicity are not functional at low substrate levels but exhibit accelerated activity after the lag phase in the velocity versus substrate plot [8, 9].
(c) *Allostery*: Some enzymes contain sites that are topologically distinct from the active site. When these so-called allosteric sites are occupied by effector ligands, information is conveyed to the active site, usually through conformational changes in the enzyme's structure, which results in an alteration of substrate affinity or activity or both. The simplest example of allostery is noncompetitive inhibition; however, much more sophisticated models have been proposed [8, 9].
(d) *Covalent modification*: Some enzymes undergo covalent modification as a response to a signal, e.g., the release of a hormone resulting indirectly in an alteration of the enzyme's properties. As will be shown in Chap. 11, phosphorylation of glycogen phosphorylase activates the enzyme [10]. On the other hand, protein kinase-catalyzed phosphorylation of glycogen synthase results in its loss of activity [11].
(e) *Association–dissociation of subunits*: Many examples exist in the literature where association of enzyme subunits converts an inactive enzyme to one that is active. There are also examples where the reverse phenomenon leads to enzyme activation. The following examples serve to illustrate these points: The enzyme adenylosuccinate synthetase from *E. coli* is converted to the active dimer from the inactive monomer in the presence of substrates [12]. At the other extreme, dissociation of inactive protein kinase A caused by 3′:5′-cylic AMP activates the enzyme [13].
(f) *Ligand binding – activation and inhibition*: The binding of small molecules or ions alters the kinetic properties of some enzymes, e.g., K^+ is required to activate the enzyme pyruvate kinase [14] and is required along with a divalent metal ion for the complete activation of $FBPase_1$ [15]. An example of enzyme inhibition by a small molecule involves the enzyme $FBPase_1$ which binds AMP at an allosteric site [16]. There are numerous examples in the literature of both inhibition and activation of enzyme activity caused by small molecules and ions.
(g) *Signal transduction*: Some metabolic processes in higher organisms are regulated by signal transduction. A ligand, referred to as the *first messenger*, binds to a membrane receptor. The signal is then transmitted through the membrane to an effector enzyme which synthesizes a compound known as the *second messenger*. The second messenger then diffuses to its site(s) of action where it elicits a specific response, usually at the enzyme level.

There are a number of different signaling pathways, the most prominent of which are: the cyclic-AMP-adenylate cyclase pathway, the inositol-phospholipid pathway, and the tyrosine kinase receptor pathway. One of these, the cyclic-AMP-adenylate cyclase pathway is considered in detail in the regulation of carbohydrate metabolism (Chap. 8).

References

1. Lipmann F (1941) Metabolic generation and utilization of phosphate bond energy. Adv Enzymol 1:99–162
2. Jencks WP, Cordes S, Carriuolo J (1960) The free energy of thiol ester hydrolysis. J Biol Chem 235:3608–3614
3. *E. coli* statistics: http://www.gchelpdesk.ualberta.ca/CCDB/cgi-bin/STAT_NEW.cgi
4. Gerhart JC, Pardee AB (1962) The enzymology of control by feedback inhibition. J Biol Chem 237:891–896
5. Taylor CB, Bailey E (1967) Activation of liver pyruvate kinase by fructose 1,6-diphosphate. Biochem J 102:32c–33c
6. Lunn JE, Rees T (1990) Apparent equilibrium constant and mass-action ratio for sucrose-phosphate synthase in seeds of *Pisum sativum*. Biochem J 267:739–743
7. Fromm HJ (1958) Ribitol dehydrogenase. I. Purification and properties of the enzyme. J Biol Chem 233:1049–1052
8. Monod J, Wyman J, Cangeux J-P (1965) On the nature of allosteric transitions: a plausible model. J Mol Biol 12:88–118
9. Koshland DE Jr, Neet KE (1968) The catalytic and regulatory properties of enzymes. Annu Rev Biochem 37:359–410
10. Fischer EH, Krebs EG (1955) Conversion of phosphorylase b to phosphorylase a in muscle extracts. J Biol Chem 216:121–132
11. Embi N, Rylatt DB, Cohen P (1980) Glycogen synthase kinase-3 from rabbit skeletal muscle. Separation from cyclic-AMP-dependent protein kinase and phosphorylase kinase. Eur J Biochem 107:519–527
12. Kang C, Kim S, Fromm HJ (1996) Subunit complementation of *Escherichia coli* adenylosuccinate synthetase. J Biol Chem 271:29722–29728
13. Hofmann F, Beavo JA, Bechtel PJ, Krebs EG (1975) Comparison of adenosine 3′:5′-monophosphate – dependent protein kinases from rabbit skeletal muscle and bovine heart muscle. J Biol Chem 250:7795–7801
14. Kachmar JF, Boyer PD (1953) Kinetic analysis of enzyme reactions:II. The potassium activation and calcium inhibition of pyruvate phosphoferase. J Biol Chem 200:669–682
15. Zhang R, Villeret V, Lipscomb WN, Fromm HJ (1996) Kinetics and mechanisms of activation and inhibition of porcine liver fructose-1,6-bisphosphatase by monovalent cations. Biochemistry 35:3038–3043
16. Tejwani GA (1983) Regulation of fructose-bisphosphatase activity. Adv Enzymol Relat Areas Mol Biol 54:121–194

Chapter 8
Carbohydrate Metabolism A: Glycolysis and Gluconeogenesis

Glycolysis is defined as the anerobic conversion of glucose to pyruvic acid. The glycolytic pathway, which is ubiquitous in nature, is also known as the Meyerhoff, Embden, Parnas pathway, named after the three biochemists who made major contributions to its formulation. The physiological role played by glycolysis in the cell far exceeds just the biosynthesis of pyruvate, e.g., it provides the cell with ATP under anerobic conditions and it also supplies precursors for the biosynthesis of proteins, lipids, nucleic acids, and polysaccharides.

The enzymes involved in glycolysis, ten in number, are water soluble and are found in the cell cytoplasm. Historically, these enzymes have received more scrutiny by biochemists than any other class of biochemical catalysts. As in all biochemical pathways, a number of glycolytic enzymes are regulated by small molecules. The primary regulatory enzymes in this pathway are phosphofructokinase$_1$ (PFK_1) and pyruvate kinase. In some tissues hexokinase is also a regulated enzyme, e.g., it has been called the "*pacemaker of glycolysis*" in brain and the red blood cell. In most mammalian tissues, however, hexokinase is not a regulated enzyme.

8.1 Glycolysis

Figure 8.1 illustrates the glycolytic metabolic pathway.

In Fig. 8.1 there are three thermodynamically irreversible steps, i.e., reactions where the ΔG^0 is highly negative. These reactions involve the enzymes hexokinase, phosphofructokinase$_1$ (PFK_1), and pyruvate kinase (all indicated in red).

The overall reaction for glycolysis is:

$$\text{glucose} + 2\text{NAD}^+ + 2\text{ADP}^{3-} + 2\text{P}_\text{i}^{2-} \rightarrow 2\text{pyruvate}^{1-} + 2\text{NADH} + 2\text{ATP}^{4-} + 2\text{H}^+.$$

In terms of energetics, four ATP molecules are synthesized; two at the phosphoglycerate kinase step and two more when phosphoenolpyruvate is converted to

H.J. Fromm and M.S. Hargrove, *Essentials of Biochemistry*,
DOI 10.1007/978-3-642-19624-9_8,

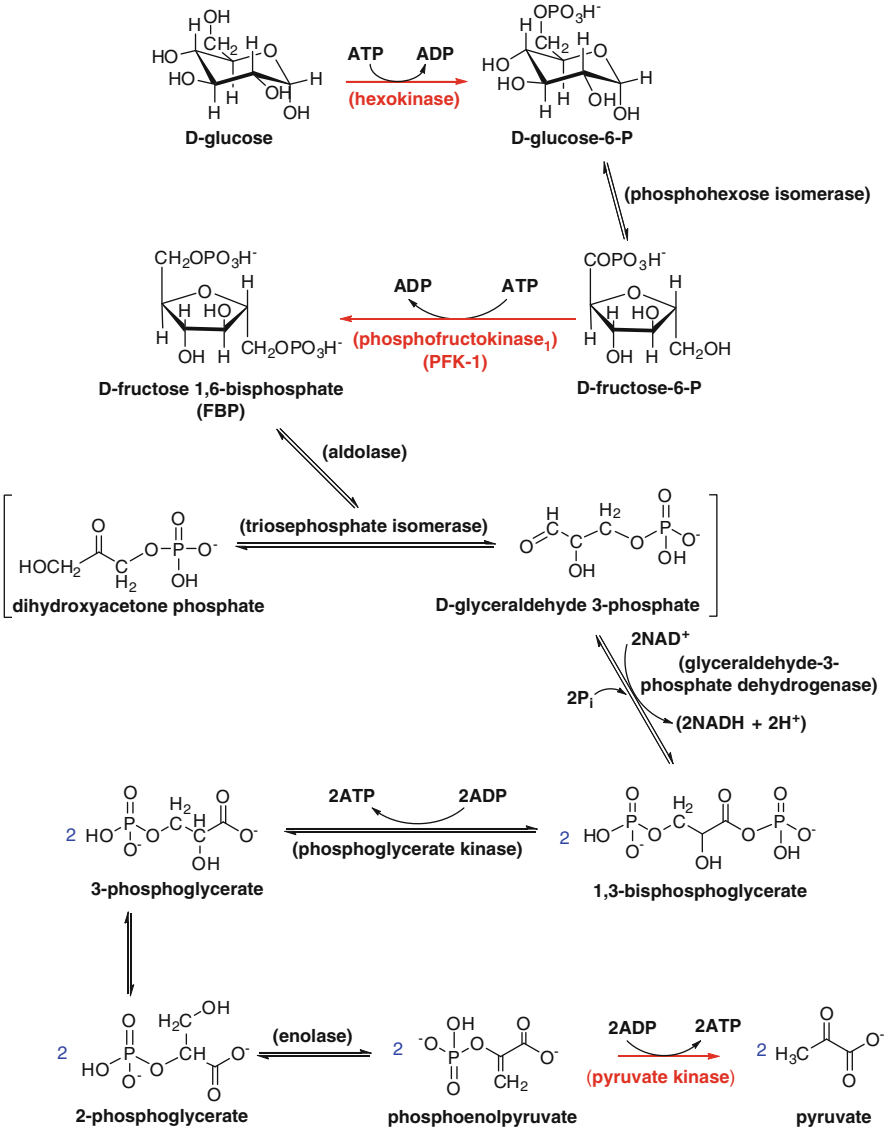

Fig. 8.1 The sequence of reactions involved in glycolysis. Included are the names of the glycolytic enzymes

pyruvate. On the other hand, one ATP molecule is utilized at the hexokinase step and another in the PFK_1 reaction. The end result is that glycolysis produces two ATP molecules for every molecule of glucose that undergoes catabolism. Glycolysis itself is anaerobic.

There are two triose sugars formed in the aldolase reaction, but only one of them, glyceraldehyde-3-P, is utilized in glycolysis. The other aldolase reaction product, dihydroxyacetone phosphate, is readily converted to the aldehyde by triosephosphate isomerase. To maintain the correct stoichiometry for glycolysis, the triose sugars are multiplied by the number two in Fig. 8.1.

Scrutiny of the reactions in glycolysis reveals that NAD^+ is converted to NADH by glyceraldehydes-3-phosphate dehydrogenase. Because NAD^+ is a coenzyme, its intracellular concentration is limited. Absent a mechanism for its regeneration, glycolysis would cease when the supply of NAD^+ is exhausted. In highly aerobic tissues, such as brain, oxidative mechanisms are available for the regeneration of NAD^+ from NADH. This problem is circumvented in anerobic tissues, tissues that do not readily regenerate NAD^+ from NADH, such as white skeletal muscle, by the presence of the enzyme lactate dehydrogenase and the end-product of glycolysis, pyruvate:

$$\text{NADH} + \text{H}^+ + \text{pyruvate} \rightarrow \text{lactate} + \text{NAD}^+.$$

In many microorganisms and yeast, the reoxidation of NADH is accomplished by the enzyme alcohol dehydrogenase:

$$\text{NADH} + \text{H}^+ + \text{acetaldehyde} \rightarrow \text{ethanol} + \text{NAD}^+.$$

It is of interest that alcohol dehydrogenase is also present in mammalian liver where it acts as a detoxifying agent when alcohols, not ethanol exclusively, are presented to it. The acetaldehyde, another toxic agent, is rendered harmless by another liver enzyme, aldehyde dehydrogenase, which converts the aldehyde to the corresponding acid. In the case of ethanol, the end-product is acetate, an innocuous compound that is readily metabolized.

8.1.1 Glycolytic Enzymes and Their Mechanisms of Action

8.1.1.1 Hexokinase ($\Delta G^0 = -16.7$kJ/mol)

The enzyme hexokinase, discovered by Otto Meyerhoff [1], has been studied from a variety of organisms. The best known sources of the enzyme are yeast and mammalian brain and skeletal muscle. Crystal structures are available for both the yeast and brain enzymes (see below). Hexokinase is best known for its phosphorylation of D-glucose; however, other physiologically important hexoses such as D-mannose and D-fructose are also good substrates for the enzyme.

Kinetic studies of hexokinase suggest that the kinetic mechanism is sequential and of the rapid equilibrium random type [2, 3]. There is strong evidence, however, that with yeast and muscle hexokinase there is a preference for glucose to add to

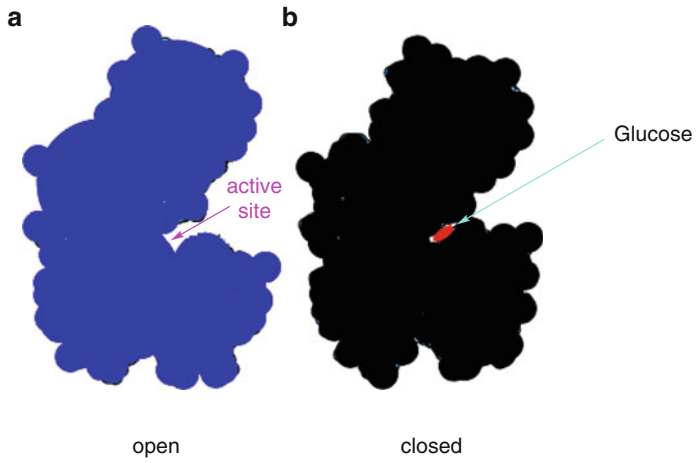

Fig. 8.2 The open (*left*) and closed (*right*) forms of yeast hexokinase are depicted in the figure. The ligand in *red* at the active site is D-glucose. The active site is in the area designated by the *arrow*. The closed form of hexokinase is induced by D-glucose

hexokinase prior to the addition of ATP [4, 5]. Steitz and coworkers [6] demonstrated that when glucose adds to the yeast enzyme, hexokinase goes from an "open" to a "closed" structure (see Fig. 8.2). This was one of the first examples in support of the *Induced Fit* hypothesis of enzyme specificity [7].

There are four hexokinase isozymes: Hexokinase I from brain (HKI), hexokinase II from skeletal muscle (HKII), hexokinase III, and hexokinase IV, also known as glucokinase, which is found primarily in mammalian liver and to some extent in brain and pancreas. In the latter tissue, it acts as a glucose sensor for insulin secretion. HK IV differs from the other isozymes most significantly in its kinetic characteristics; its $S_{0.5}$ is in the 5 mM range, more than an order of magnitude greater than the K_m values of the other isozymes, and it exhibits cooperative kinetics with respect to D-glucose. How these enzymes are involved in the regulation of glycolysis will be discussed below.

The chemical mechanism and transition state structure for hexokinase assuming an in-line associative mechanism is shown in Fig. 8.3.

The inability of hexokinase to catalyze isotope scrambling (positional isotope exchange) when the enzyme is incubated with $MgATP^{2-}$ alone [8] is consistent with the hypothesis that hexokinase involves an associative mechanism of phosphate addition to glucose. Nevertheless, it could be argued that the mechanism does involve a metaphosphate intermediate, but that scrambling does not occur because of restricted rotation of the β phosphoryl group of ADP in the scrambling studies. The work of Lowe and Potter using adenosine 5′-[γ(S)-^{16}O,^{17}O,^{18}O] triphosphate demonstrated an inversion of configuration in the yeast hexokinase reaction [9]. These findings, along with the isotope scrambling studies, imply that the reaction mechanism is an associative in-line S_N2 reaction. Finally, there is no evidence from X-ray diffraction studies with glucose-6-P to suggest that the mechanism is of the

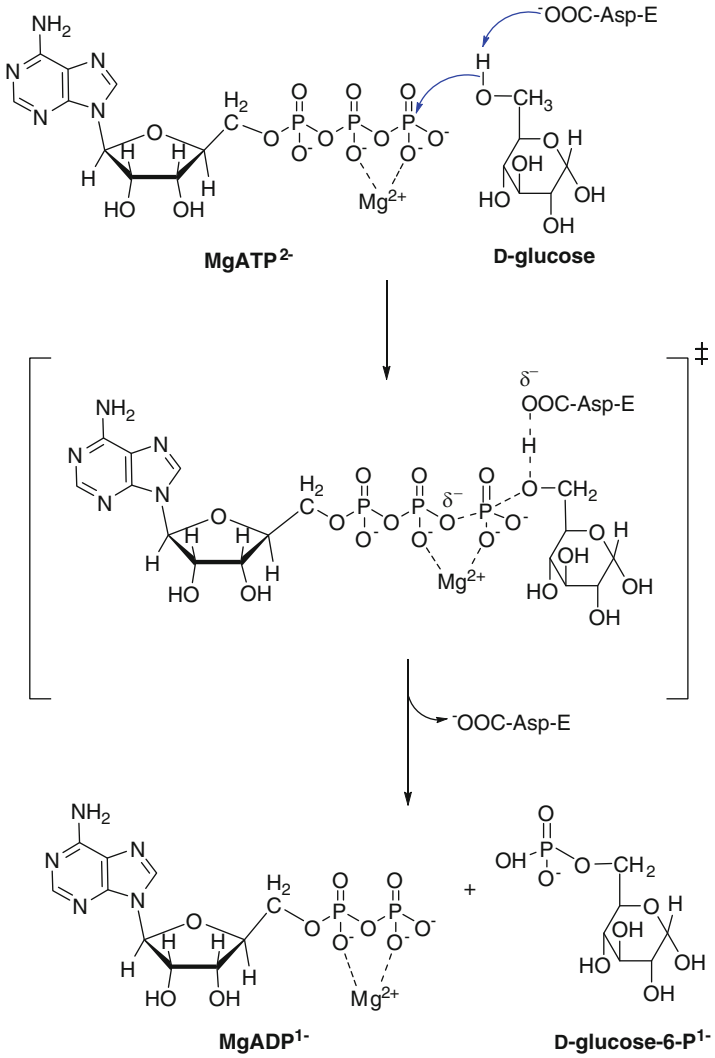

Fig. 8.3 The chemical mechanism and transition state structure of the hexokinase reaction

dissociative type. The putative hexokinase reaction mechanism can be found in Chap. 4.

Yeast hexokinase is a functional dimmer of subunit $M_W \sim 50$ kDa. On the other hand, mammalian hexokinases, such as brain and muscle hexokinase are functional monomers of M_W ~100 kDa with the exception of glucokinase (M_W ~50 kDa) which is also a functional monomer. It is believed that the mammalian enzymes are products of *gene duplication and fusion*, where each gene coded for a 50 kDa subunit protein prior to fusion of the two genes. Subsequent to gene fusion, mutations occurred in both halves of hexokinase producing the different isozymes

we see today. In the mammalian enzymes both the C- and N-terminal halves are joined by a connecting helix. In the case of brain hexokinase, the connecting helix is essential for N- and C-half communication. An interesting characteristic of both the brain and muscle enzyme is that they are potently inhibited by their product glucose-6-P.

In brain hexokinase the active site is found in the C-half of the enzyme; the site in the N-half having mutated to a regulatory function. This latter site contains a glucose-6-P inhibitory site, a P_i site that when associated with P_i can reverse glucose-6-P inhibition, and a hexokinase-mitochondrial release site. Figure 8.4 illustrates the ligand-complexed structures as determined from X-ray diffraction crystallography. Muscle hexokinase, on the other hand contains two active sites, one in each half of the enzyme. Both mammalian enzymes are bound to the outer mitochondrial membrane and are thought to protect the organelle against *apoptosis* (programmed cell death). A hydrophobic sequence of about 15 residues at the N-terminus is inserted into the outer mitochondrial membrane where it is in contact with porin, a membrane protein. It is this complex of hexokinase, porin, and the lipid membrane bilayer that exists on the surface of mitochondria.

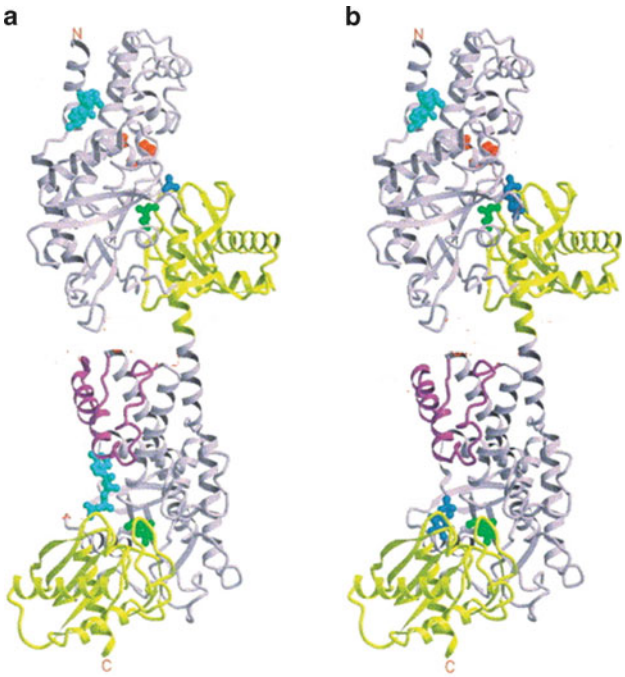

Fig. 8.4 Data from the crystal structure of brain hexokinase [10]. Overview of (**a**) the ADP/Glc-monomer complex and (**b**) the G6P/Glc-monomer complex of hexokinase I. The large and small domains of the N- and C-halves are *purple* and *yellow*, respectively. ADP molecules are cyan, glucose molecules are green, the phosphate and G6P molecules are *dark blue*

8.1.1.2 Phosphoglucose Isomerase (Phosphohexose Isomerase) ($\Delta G^0 = +1.7$kJ/mol)

The enzyme phosphoglucose isomerase catalyzes the second step in glycolysis. Because the product of the hexokinase reaction is in the pyranose form, the ring must open prior to its conversion to D-fructose-6-P. The mechanism of ring opening by phosphoglucoisomerase is analogous to base-catalyzed mutorotation. The two-step reaction leading to the formation of fructose-6-P is illustrated in Fig. 8.5. It is important to note that the intermediate in the second phase of the reaction is a *1,2-enediol*.

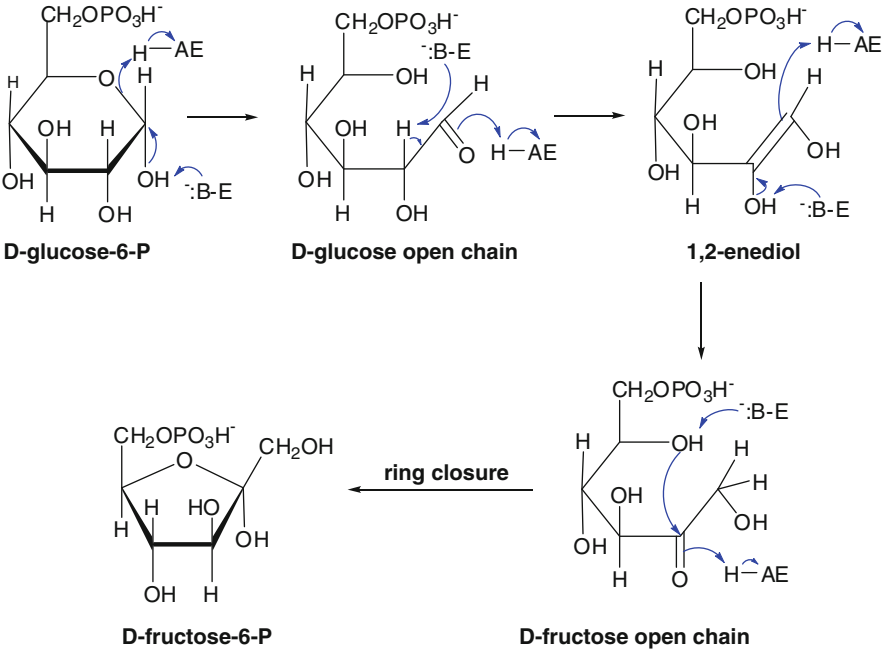

Fig. 8.5 The mechanism of the phosphoglucoisomerase reaction; the conversion of D-glucose-6-P to D-fructose-6-P

8.1.1.3 Phosphofructokinase-1 (PFK_1) ($\Delta G^0 = -14.2$kJ/mol)

PFK_1 is a tetrameric protein that catalyzes the phosphorylation at the C-1 position of D-fructose 6-P to produce D-fructose 1,6-bisphosphate. The enzyme is a control point in glycolysis and there are a number of small molecules that activate and inhibit this kinase. The activators include *D-fructose 2,6-bisphosphate* and AMP. Citrate and elevated levels of ATP are effective inhibitors. D-Fructose

2,6-bisphosphate activates PFK_1 approximately 100-fold in vitro and at the same time serves to inhibit gluconeogenesis, the pathway leading to the formation of glucose from pyruvate. Increased levels of AMP are a signal to the cell that the concentration of ATP is falling and its replenishment, via increased rates of glycolysis, is required. When levels of ATP are high, glycolysis is slowed by the direct action of ATP on PFK_1. Elevated concentrations of citrate, a metabolic product of pyruvate that produces large quantities of ATP in the Krebs Cycle is a signal that ATP levels are sufficient and inhibition of glycolysis is required.

The mechanism of the PFK_1 reaction is very similar to that described for hexokinase (see Fig. 8.3).

8.1.1.4 Aldolase ($\Delta G^0 = +24$kJ/mol)

It is at the aldolase step in glycolysis that carbon–carbon bond cleavage occurs and two triose sugars are produced from D-fructose 1,6-bisphosphate. There are two classes of aldolase: Class I is found in higher organisms and Class II is found in fungi and algae. The Class I enzymes use the ε-amino group of a lysine residue at the enzyme's active site to form a *Schiff base* which acts as an electrophile, whereas this function is performed by Zn^{2+} in the Class II enzymes.

Class I Aldolases

The pioneering work of Bernard Horecker helped establish the mechanism of the aldolase reaction (Fig. 8.6). He allowed the back reaction substrate [^{14}C]dihydroxyacetone phosphate to react with the enzyme and then added $NaBH_4$ to reduce the Schiff base. The enzyme was then subjected to hydrolysis and amino acids analysis. The results revealed that a lysine residue was covalently bound to the radioactive substrate.

Stereochemical studies with aldolase demonstrated that there is a stereospecific removal of a proton (H_S) from the Schiff base by a basic group on the enzyme in the course of the formation of the *eneamine intermediate*. It was shown that the addition of the eneamine to glyceraldehydes 3-P is also stereospecific.

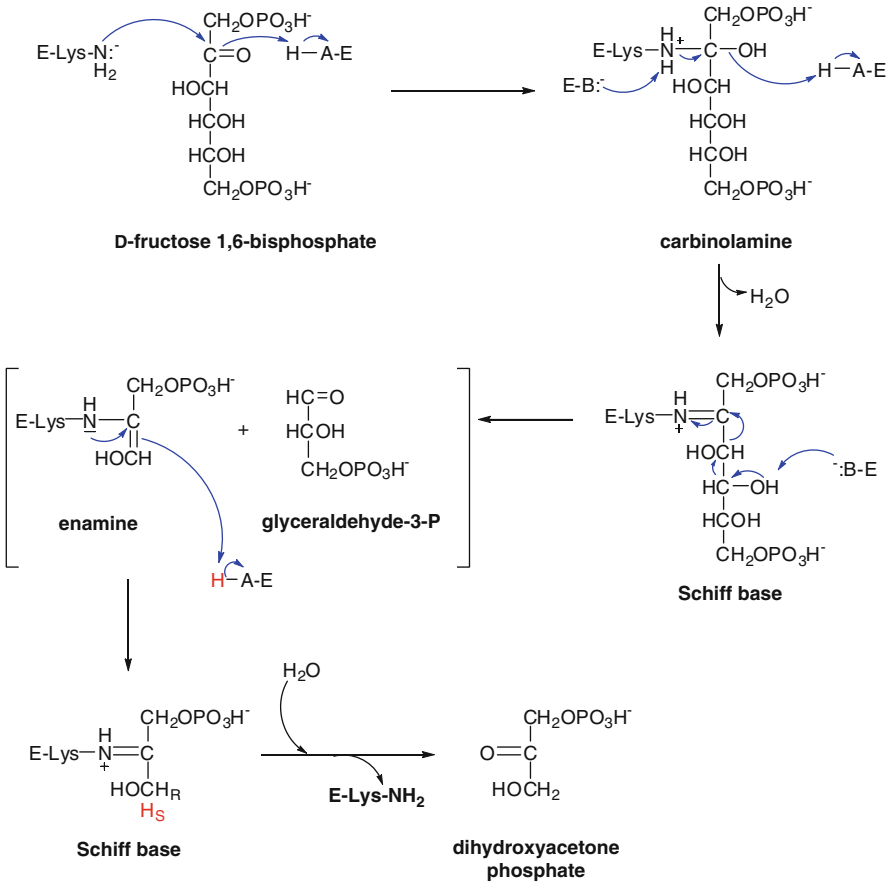

Fig. 8.6 Schiff base formation is a prerequisite for the catalysis of the Class I aldolases

Class II Aldolases

The Class II aldolases use Zn^{2+} to polarize the carbonyl oxygen electrons of the substrate instead of forming a Schiff base as is the case with the Class I aldolases (Fig. 8.7). The metal also serves to stabilize the *enolate anion intermediate*. It should be noted that the removal of the proton from dihydroxyacetone phosphate is stereospecific.

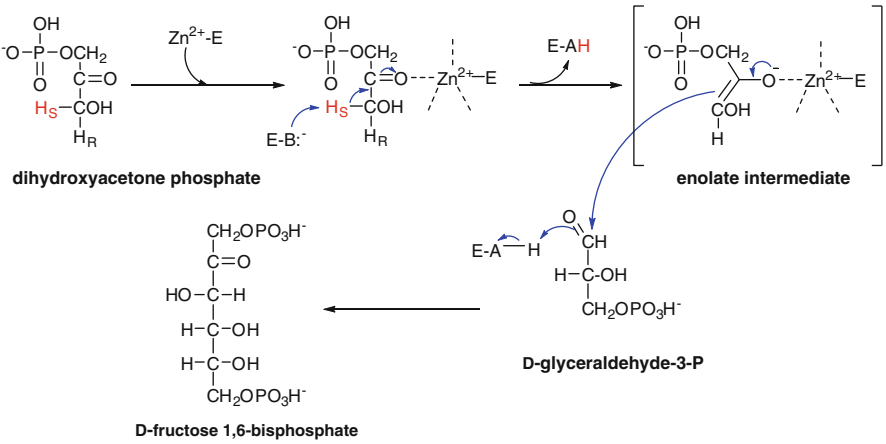

Fig. 8.7 Mechanism of action of a Class II aldolase

8.1.1.5 Triosephosphate Isomerase ($\Delta G^0 = +7.6$ kJ/mol)

The function of triosephosphate isomerase is to interconvert the two trioses formed in the aldolase reaction. The equilibrium constant for the triosephosphate isomerase reaction lies in the direction of dihydroxyacteone phosphate; however, the next enzyme in glycolysis, glyceraldehyde-3-phosphate dehydrogenase, cannot utilize the phosphoketone as a substrate. Thus, as a manifestation of Le Chatelier's principle, the metabolic flux is shifted to glyceraldehyde-3-P. The chemical mechanism of the triosephosphate isomerase reaction is similar to that described for phosphoglucose isomerase, i.e., an enediol intermediate participates in the reaction. Support for this mechanism comes from use of transition state analogs such as phosphoglycohydroximate, a powerful inhibitor of the triosephosphate isomerase reaction (Fig. 8.8).

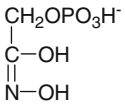

Fig. 8.8 Phosphoglycohydroximate. The structure is similar to that of the enediol intermediate in the triosephosphate isomerase reaction

8.1.1.6 Glyceraldehyde-3-Phosphate Dehydrogenase ($\Delta G^0 = +6.3$kJ/mol)

Glyceraldehyde-3-phosphate dehydrogenase is a pyridine-linked anerobic dehydrogenase; however, it carries out more than just a redox reaction. Although the initial phase of the reaction involves an oxidation of the substrate, this is followed by

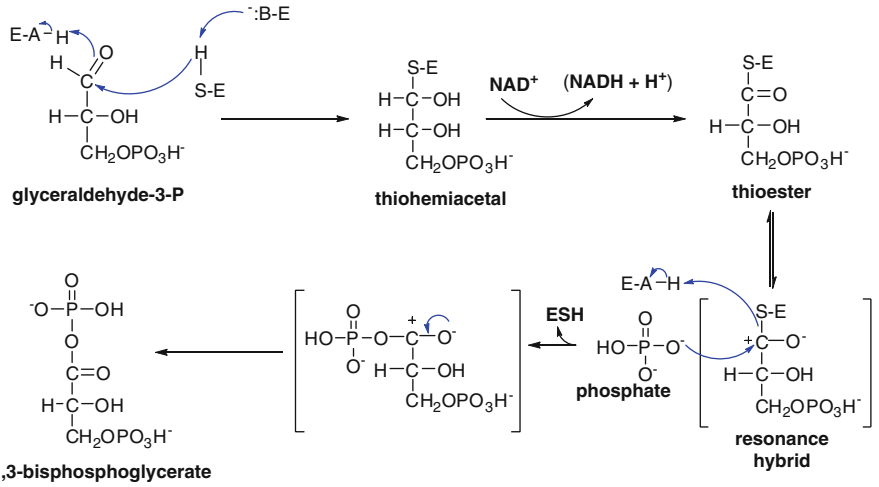

Fig. 8.9 The glyceraldehyde-3-phosphate dehydrogenase reaction involves a "high-energy" thioester intermediate

a substrate-level phosphorylation. Ultimately, glyceraldehyde-3-P is converted to 1,3-bisphosphoglycerate. The reactions involved are outlined in Fig. 8.9.

The addition of iodoacetate to the enzyme results in carboxymethylation of the cysteine sulfhydryl that makes the nucleophilic attack on the carbonyl carbon of the substrate. It was recognized in the early part of the twentieth century that the addition of sulfhydryl reagents such as iodoacetate to skeletal muscle did not eliminated its ability to contract, yet it was understood that iodoacetate was an inhibitor of glycolysis and thus ATP production. At that time it was recognized that ATP hydrolysis provided the energy for muscular contraction. This conundrum was reconciled with the discovery of creatine phosphate in muscle and the enzyme creatine phosphokinase which allows for the synthesis of ATP from ADP.

$$\text{creatine phosphate} + \text{ADP} \rightleftharpoons \text{creatine} + \text{ATP}.$$

8.1.1.7 Phosphoglycerate Kinase ($\Delta G^0 = -18.9$kJ/mol)

The phosphoglycerate kinase reaction has been studied in detail from a number of perspectives including X-ray crystallography [11] of the enzyme from the thermophilic bacterium *Thermatoga maritime* and pig muscle [12]. A ternary complex of enzyme, 3-phosphoglycerate, and the ATP analog AMP-PNP (*adenylylimidodiphosphate*) was observed in the crystallographic studies. From these results, it was concluded that the chemistry of the phosphoglycerate kinase reaction is an

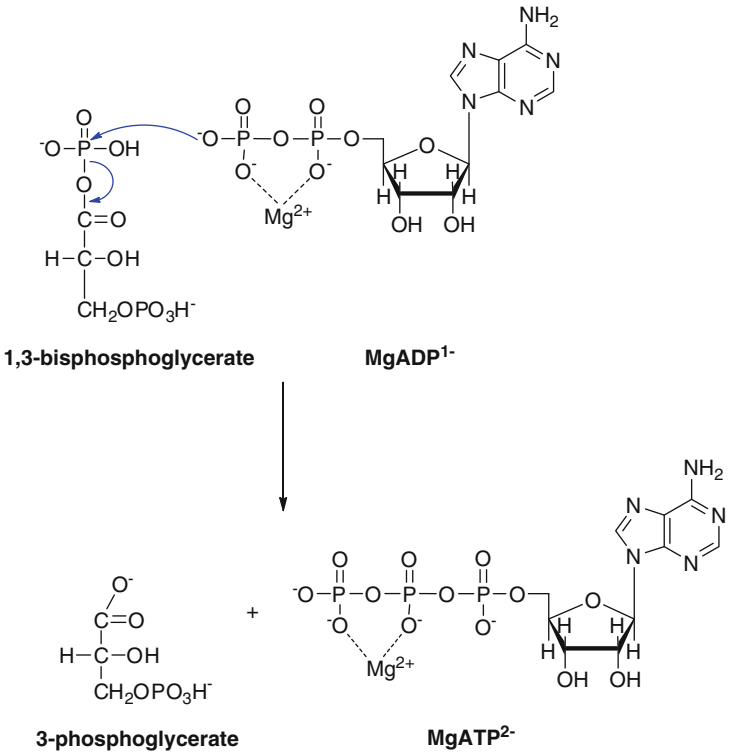

Fig. 8.10 The mechanism of the phosphoglycerate kinase reaction involves the synthesis of ATP. Bidentate $MgATP^{2-}$ and $MgADP^{1-}$ are illustrated

in-line associative S_N2 mechanism involving a pentacoordinate transition state (Fig. 8.10).

8.1.1.8 Phosphoglycerate Mutase ($\Delta G^0 = +4.4$kJ/mol)

Phosphoglycerate mutase has been investigated from a variety of sources and in all cases it has been found that the enzyme is involved mechanistically in covalent catalysis. The sites of covalent bond formation are histidine residues that undergo phosphorylation and dephosphorylation. The consensus mechanism that arose from a variety of biochemical [13] and biophysical [14] studies is shown in Fig. 8.11.

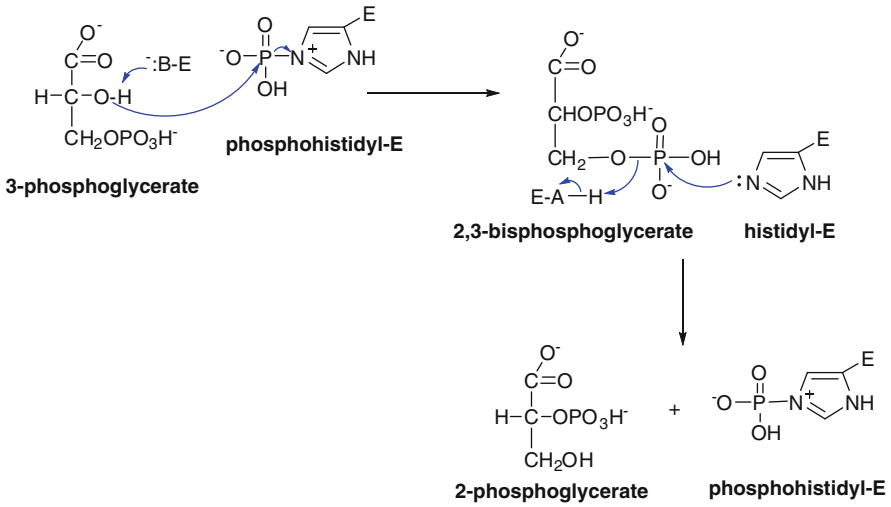

Fig. 8.11 The phosphoglycerate mutase reaction illustrating the participation of phosphohistidine: An example of covalent catalysis

8.1.1.9 Enolase ($\Delta G^0 = +1.8$kJ/mol)

The enzyme enolase catalyzes the dehydration of 2-phosphoglycerate. It was recognized early in investigations on the mechanism of the enolase reaction that the hydrogen at the 2-position is relatively acidic because of the large number of electron-withdrawing groups associated with the substrate. The chemical mechanism obtained from its crystal structure and EPR studies [15] is depicted in Fig. 8.12.

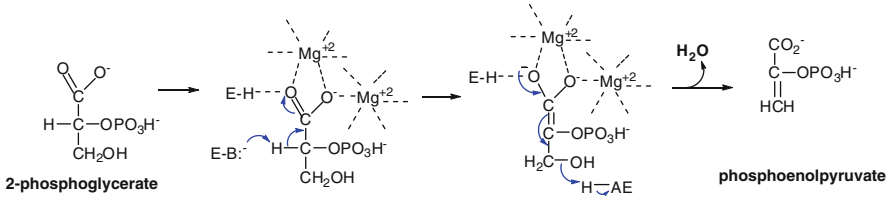

Fig. 8.12 The dehydration of 2-phosphoglycerate by the enzyme enolase

8.1.1.10 Pyruvate Kinase ($\Delta G^0 = -31.7$kJ/mol)

Pyruvate kinase is the final step in glycolysis. The favorable ΔG^0 for the reaction is one of the primary reasons that glycolysis is highly exergonic overall. The kinetics of the reaction was investigated by Reynard et al. [16] and Ainsworth and Macfarlane [17] who concluded that the kinetic mechanism for the rabbit skeletal muscle enzyme is rapid equilibrium Random Bi Bi. Orr et al. [18] demonstrated that

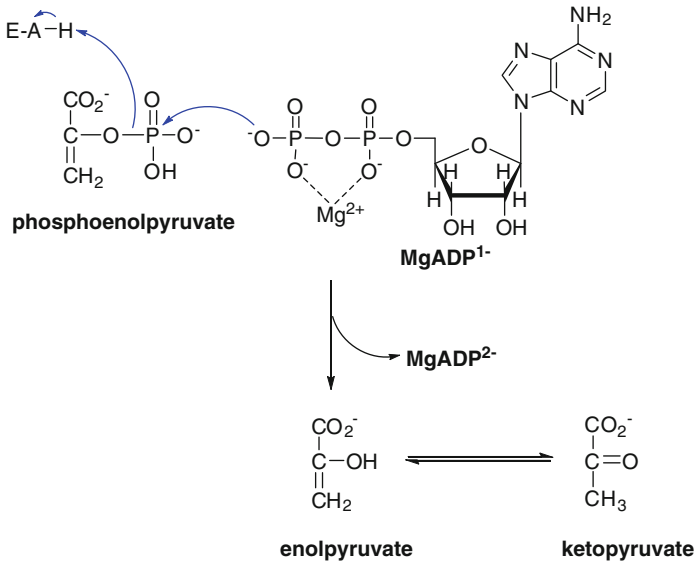

Fig. 8.13 The mechanism of the pyruvate kinase reaction: The generation of ATP from phosphoenolpyruvate. Proton addition at the last step is stereospecific

the stereochemistry of the reaction involved an inversion of configuration which they attributed to an associative in-line S_N2 mechanism. In the context of stereochemistry, Rose [19] using 3-[^{2}H],3[^{3}H]phosphoenol-pyruvate showed that a proton adds to the *si* face of the C-3 of phosphoenolpyruvate in its conversion to pyruvate. The mechanism of the pyruvate kinase reaction is shown in Fig. 8.13.

8.1.2 Metabolism of D-Mannose and D-Galactose

8.1.2.1 D-Mannose

D-Mannose is found in a variety of foods because of its distribution in cell membranes. After ingestion and digestion, it is carried to the liver where it is phosphorylated by ATP in the presence of hexokinase. The product of this reaction, D-mannose-6-P, is then converted to D-fructose-6-P by *phosphomannose isomerase* (the mechanism for the isomerase reaction is virtually identical to that described for phosphoglucose isomerase). Thus mannose enters glycolysis at the D-fructose-6-P step.

$$\text{D-mannose} + \text{ATP} \xrightarrow{\text{(hexokinase)}} \text{D-mannose-6-P} + \text{ADP}$$

$$\text{D-mannose-6-P} \xrightarrow{\text{(phosphomannoisomease)}} \text{D-fructose-6-P.}$$

8.1.2.2 D-Fructose

D-fructose is a common dietary constituent. It exists as a monosaccharide in many foods such as fruit and honey and as a disaccharide in sucrose. It enters the liver as a monosaccharide. In the case of sucrose ingestion, it is hydrolyzed through the action of sucrase, an enzyme found in the intestine, to D-glucose and D-fructose.

Liver contains the enzyme fructokinase which has a far lower K_m for D-fructose than does hexokinase. After the series of reactions depicted below, D-fructose enters the glycolytic pathway as shown in Fig. 8.14.

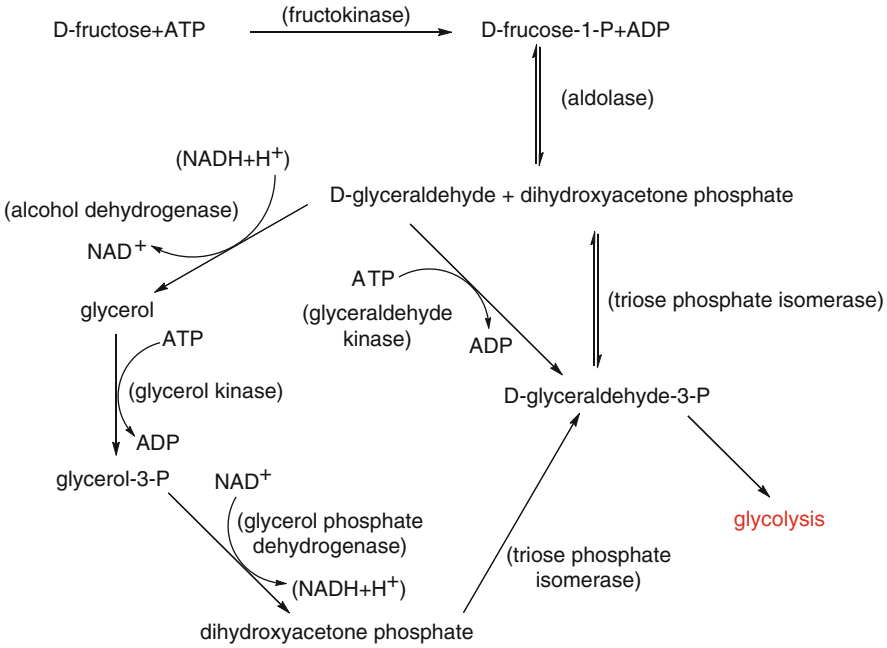

Fig. 8.14 The metabolism of D-fructose in mammalian liver

8.1.2.3 D-Galactose

D-Galactose is found in all living cells primarily conjugated with lipids and proteins. Infants, whose sole source of nutrients is mother's milk, receive ample quantities of the sugar from the disaccharide lactose, found exclusively in milk. After digestion in the intestine, from whatever source, D-galactose is metabolized in liver. D-Galactose is not a substrate for hexokinase; however, it is phosphorylated by ATP in the presence of the enzyme *galactokinase* to D-galactose-1-P. D-Galactose-1-P is further metabolized to UDP-D-galactose, a precursor of galactolipids, galactoproteins, and galactosaccharides including lactose. The sequence of events involving D-galactose metabolism is as follows (Fig. 8.15):

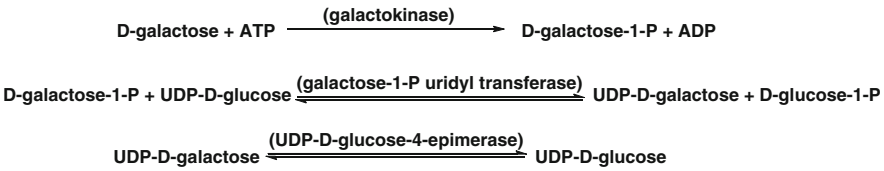

Fig. 8.15 The conversion of D-galactose to UDP-D-galactose and UDP-D-glucose

Enzymes of Galactose Metabolism

Galactokinase

The kinetic mechanism of the *Escherichia coli* galactokinase reaction has been studied by Gulbinsky and Cleland [20] who found it to be very similar to the yeast hexokinase reaction, i.e., Random Bi Bi from initial-rate kinetics, but with a preference for D-galactose to add before ATP and with D-galactose-6-P to dissociate from the kinase after ADP.

The Mechanism of the Galactose-1-Phosphate Uridyltransferase Reaction

The chemical mechanism of the *E. coli* D-galactose-1-phosphate uridyltransferase reaction has been investigated by Arabshahi et al. [21] and is shown in Fig. 8.16. They found the first step of the reaction to be the transfer of the uridylyl group from UDP-D-glucose to the N3 of a histidine residue to form a covalent uridylyl-enzyme intermediate and D-glucose-1-P. The uridylyl-enzyme intermediate then reacts with D-galactose-1-P to form UDP-D-galactose. Each of the two steps involves an S_N2 reaction.

The substrate UDP-D-glucose can be formed by the reaction of UTP and D-glucose-1-P in the presence of the enzyme *UDP-glucose pyrophosphorylase*:

$$\text{D-glucose-1-P} + \text{UTP} \rightleftharpoons \text{UDP-D-glucose} + \text{P-P}_i.$$

Although the reaction lies to the left, the presence of pyrophosphatases insures the synthesis of UDP-D-glucose.

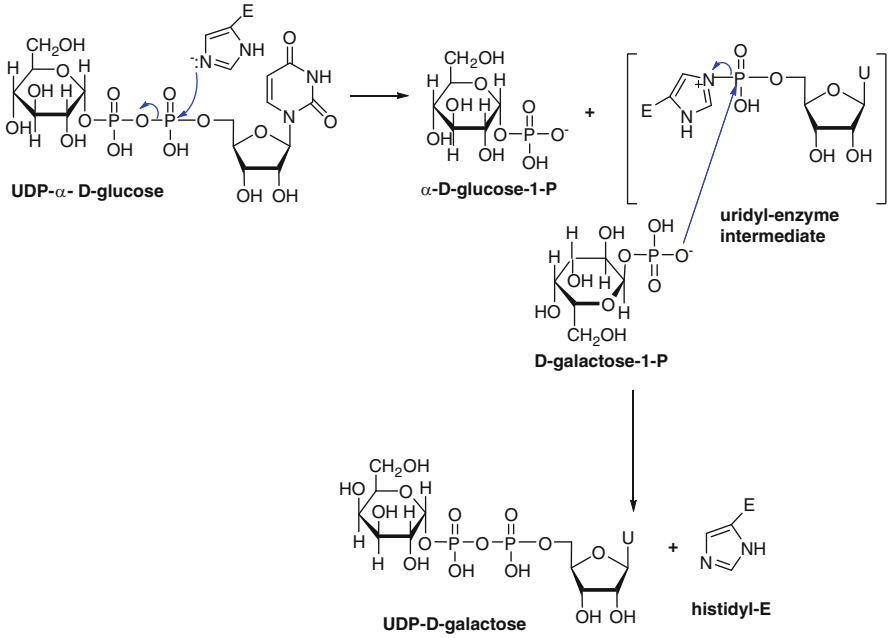

Fig. 8.16 The mechanism of the galactose-1-phosphate uridyl transferase reaction involves a histidyl residue on the enzyme

The UDP-Glucose-4-Epimerase Reaction

UDP-glucose 4-epimerase converts UDP-D-galactose to D-UDP-glucose. The conversion involves two redox reactions involving the coenzymes NAD^+ and NADH. The intermediate in the reaction is UDP-4-ketoglucose. The coenzymes are extremely tightly bound to the enzyme and it was unclear for many years how the isomerization of the sugars occurred. The solution to the problem involved first removing the bound coenzymes. When this was accomplished it became clear that the cofactors in the epimerase reaction were NAD^+ and NADH (Fig. 8.17) [22].

A mutation in the gene that codes for galactose-1-phosphate uridyltransferase leads to the potentially fatal illness *galactosemia* in infants in which very high levels of blood D-galactose leads to damage of vital organs. It can be seen from Fig. 8.15 that inhibition of the uridyltransferase will cause a buildup of D-galactose-1-P which will product-inhibit the galactokinase reaction. Once galactosemia is recognized, the newborn can be placed on a milk-free diet, thus eliminating the source of D-galactose. UDP-D-galactose is required for sustenance and can be supplied by UDP-D-glucose (Fig. 8.15). Adults with the defective uridyltransferase gene can utilize dietary D-galactose with the enzyme *UDP-galactose*

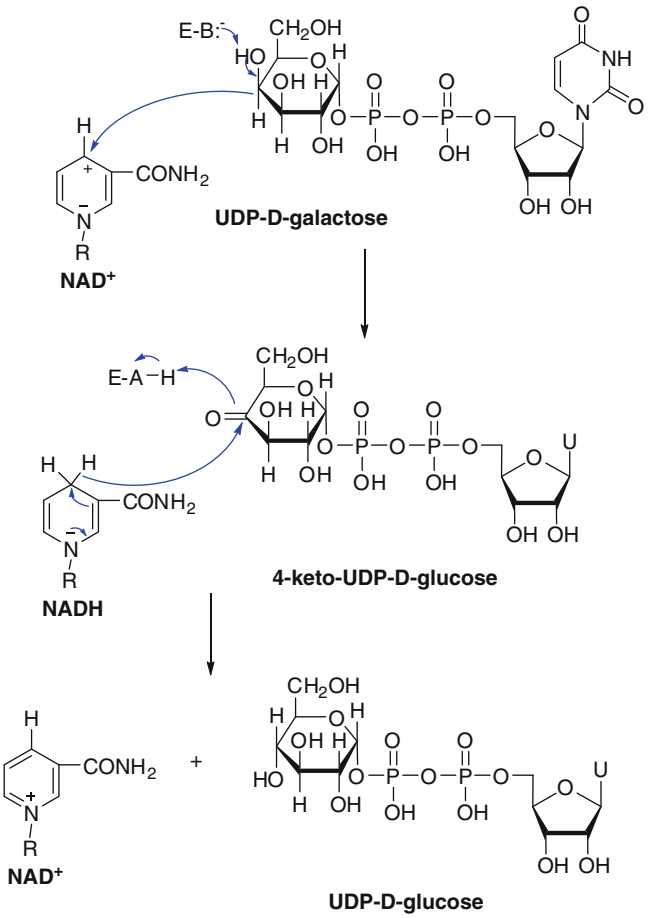

Fig. 8.17 The mechanism of the UDP-D-glucose-4-epimerase reaction involves two redox reactions using the coenzymes NADH and NAD^+

pyrophosphorylase which is synthesized in older humans. The reaction is as follows:

$$\text{UTP} + \text{D-galactose-1-P} \rightleftharpoons \text{UDP-D-galactose} + \text{P-P}_\text{i}.$$

8.1.3 Regulation of Glycolysis

At least two, and in some organisms and tissues three, glycolytic enzymes are regulated by small molecules. These enzymes are hexokinase I and IV (glucokinase), PFK_1, and pyruvate kinase. It is noteworthy that all of these enzymes

catalyze highly exergonic reactions and are therefore good candidates to be considered regulatory enzymes with the reservations suggested in Chapter 7.

8.1.3.1 Hexokinase

Hexokinase (HKI) is not normally a regulated enzyme; however, it is the first committed step in neuronal tissue glycolysis and in the red blood cell. In brain, HKI exists in the cytosol as the free enzyme where it constitutes approximately 25% of the total HKI. The majority of the enzyme is bound to the outer mitochondrial membrane by a hydrophobic tail at its N-terminus. HKI is noncovalently bound to the membrane protein *porin* or *VDAC* (voltage-dependent anion channel). The association of HKI with mitochondria prevents *apoptosis*. HKI contains an active site in the C-half and an allosteric site in the N-half of the enzyme. The relationship of HKI to other elements involved in preventing apoptosis is shown in Fig. 8.18.

The enzyme is thought to be about 95% inhibited by its product D-glucose-6-P. D-Glucose-6-P is also capable of releasing HKI from the mitochondrion; however, this process is opposed by inorganic orthophosphate (P_i). P_i is also capable of ameliorating inhibition of D-glucose-6-P-inhibited HKI.

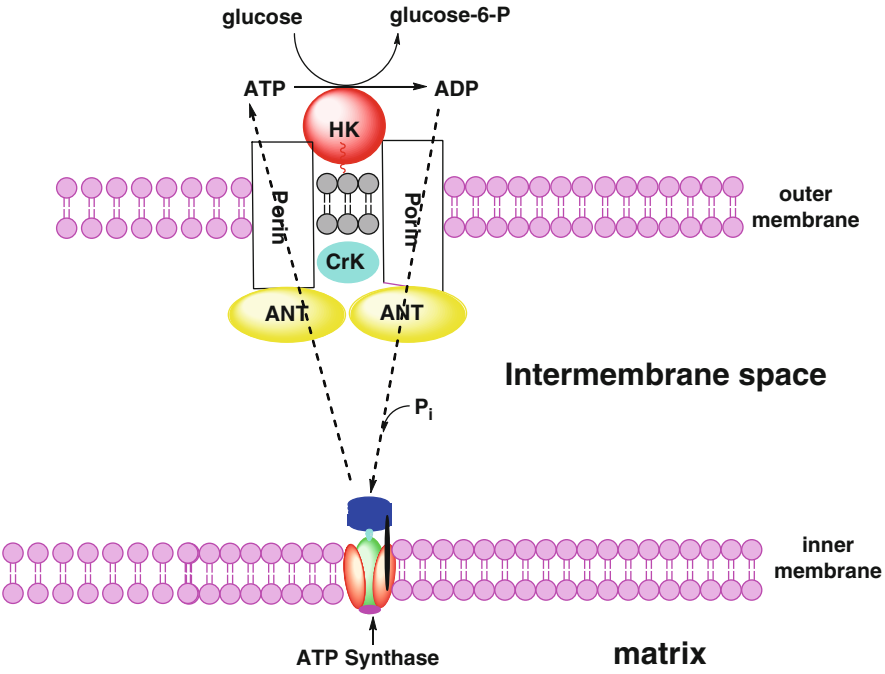

Fig. 8.18 Cartoon of a mitochondrion. Abbreviations are *hexokinase* HK, *creatine kinase* CrK, *ATP synthase* ATP Syn, and *adenine nucleotide transporter* ANT

8.1.3.2 Hexokinase IV (Glucokinase)

Glucokinase has a subunit M_W of 50,000 and exists as a monomer in the hepatic cells of the liver and in the pancreas where it functions as a glucose sensor for insulin release. Plots of velocity versus glucose concentration reveal that glucokinase does not exhibit classical Michaelis–Menten kinetics but rather displays cooperative kinetics with a Hill coefficient (η_H) of 1.7. The enzyme has an $S_{0.5}$ for D-glucose of approximately 5 mM, the concentration of the sugar in blood. Because glucokinase has a single binding site, in an attempt to rationalize its cooperativity, it was suggested that the enzyme exists in two different activity states and that there is a slow transition between these two states that allows for cooperativity to occur [23]. A second explanation is that the kinetic mechanism is steady-state Random Bi Bi [24]. The rate equation for this mechanism generates $(\text{substrate})^2$ terms, a value close to the observed Hill coefficient of 1.7.

Glucokinase in liver can undergo activation/deactivation by *compartmentation*. A regulatory protein, known as the *glucokinase regulatory protein* (*GKRP*), binds glucokinase in the nucleus when the level of D-glucose decreases, effectively removing the enzyme from its site of action, the cytosol. The presence of elevated levels of D-glucose serve to cause release of glucokinase from GKRP as does D-fructose-1-P, a product of the fructokinase reaction. This results in migration of the enzyme from the nucleus to the cytosol of the cell. On the other hand, D-fructose-6-P, a byproduct of gluconeogenesis, enhances glukokinase binding to GKBP.

In the β cells of the pancreas, increased levels of D-glucose produce increased concentrations of D-glucose-6-P through the action of glucokinase. Elevated levels of D-glucose-6-P in turn give rise to elevated levels of NADPH from the *Pentose Phosphate Shunt*. These alterations in the redox potential cause numerous changes within the β cells, with the ultimate production and secretion of insulin. This increase in insulin levels causes multiple effects including removal of D-glucose from blood and its storage as glycogen.

8.1.3.3 Phosphofructokinase$_1$

The enzyme phosphofructokinase$_1$ (PFK_1) is a major control point in glycolysis and there are a number of small molecules that activate and inhibit the enzyme. The activators include D-fructose 2,6-bisphosphate and AMP. Citrate and elevated levels of ATP are effective inhibitors. D-Fructose 2,6-bisphosphate activates PFK_1 approximately 100-fold in vitro and at the same time serves to inhibit gluconeogenesis, the pathway leading to the formation of D-glucose from pyruvate. Increased levels of AMP are a signal to the cell that the ATP concentrations are falling and its replenishment, via increased rates of glycolysis, is required. When levels of ATP are high, glycolysis is slowed by the direct action of ATP on PFK_1. Elevated concentrations of citrate, a metabolic product of pyruvate that produces large quantities of ATP in the Krebs Cycle is a signal that ATP levels are sufficient and inhibition of glycolysis is required.

8.1.3.4 Pyruvate Kinase

Pyruvate kinase is found in all cells, primarily as isozymes. The enzyme from all sources that have been studied is a homotetramer. Pyruvate kinase is one on the control points in glycolysis and has a requirement for K^+ for activity. A divalent cation such as Mg^{2+} is also needed for chelation to ATP.

The liver (L-type) isozyme is affected by small molecules such as D-fructose 1,6-bisphosphate, which acts as a *feed-forward activator*. On the other hand, elevated levels of ATP and L-alanine serve to inhibit the kinase. The enzyme is also under hormonal control. Insulin enhances enzyme activity whereas glucagon causes inhibition. Glucagon activates adenylate cyclase which leads to the production of 3′,5′-cyclic AMP, an activator of cyclic-AMP-dependent protein kinase. It is activation of this protein kinase that leads to phosphorylation of L-type pyruvate kinase. In this case covalent modification causes enzyme inhibition.

Dobson et al. [25] determined the *mass action ratio* of the pyruvate kinase reaction, i.e., c[pyruvate]·c[ATP]/c[PEP]·c[ADP], where each reactant is the sum of all ionic and metal complex species [in M], and found the pyruvate kinase system to be near equilibrium in skeletal muscle. The significance of this finding is obvious: phosphoenolpyruvate synthesis from pyruvate and ATP may be possible in skeletal muscle [26].

8.2 Gluconeogenesis

Gluconeogenesis is the synthesis of D-glucose from noncarbohydrate sources. In animals these sources are proteins; lipids are not converted to carbohydrate. In plants and certain bacteria on the other hand, both proteins and lipids are precursors of carbohydrates. The enzymes of gluconeogenesis are found primarily, but not exclusively, in the cytoplasm of the cell. Seven of the ten glycolytic enzymes are part of the gluconeogenesis pathway; the three exceptions being enzymes that catalyze the irreversible steps in glycolysis, i.e., hexokinase, PFK_1, and pyruvate kinase. Because of the unfavorable thermodynamics at these points, nature has provided a scenario that allows for their circumvention. These three enzymes are replaced by four enzymes, which when active, provide thermodynamically irreversible reactions in gluconeogenesis.

Two enzymes, pyruvate carboxylase and phosphoenolpyruvate carboxykinase (PEPCK), are used to reverse the pyruvate kinase step in glycolysis. D-Fructose-1,6-bisphosphatase$_1$ ($FBPase_1$) reverses the PFK_1 reaction, and D-glucose-6-phosphatase bypasses the hexokinase reaction. Thus, no laws of thermodynamics are violated in the reversal of glycolysis. In fact, like glycolysis, gluconeogenesis is highly exergonic.

The sequence of reactions involved in gluconeogenesis is described by Scheme 8.1.

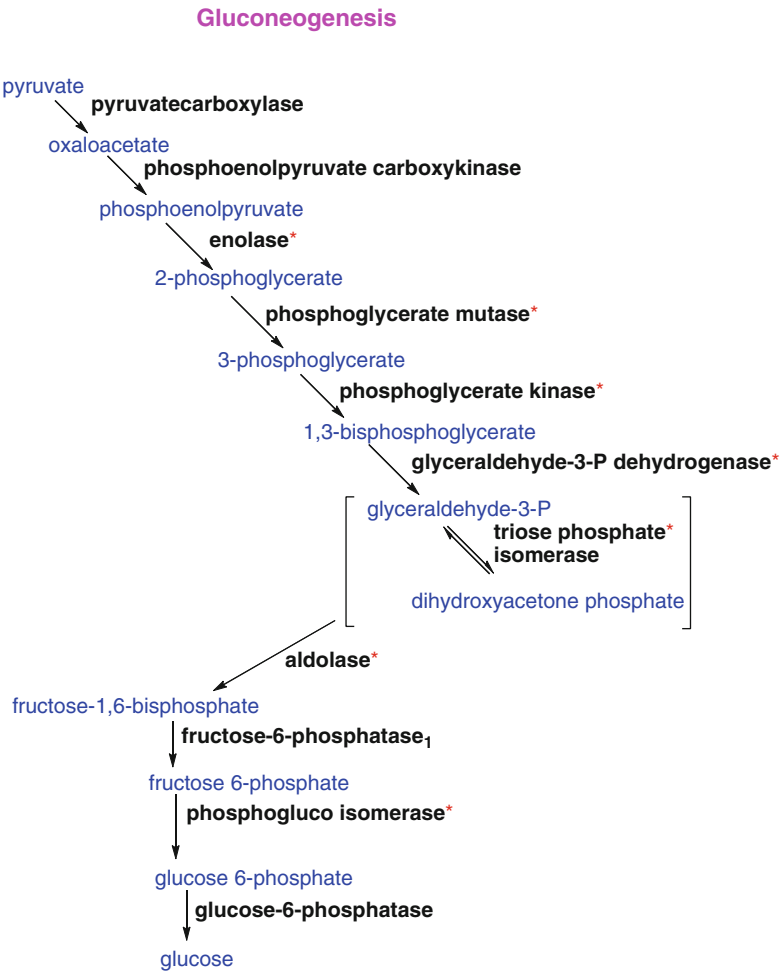

Scheme 8.1 Enzymes that catalyze reactions in glycolysis and gluconeogenesis. The * represents enzymes found in both pathways

8.2.1 Pyruvate Carboxylase

Utter and Keech were the first to isolate and characterize pyruvate carboxylase, the enzyme that initiates the gluconeogenesis pathway [27]. They subsequently found that acetyl-CoA was a necessary cofactor with mammalian enzymes, but not for the carboxylase found in bacteria. It is now recognized that the mechanism of the pyruvate carboxylase reaction involves the coenzyme biotin (Fig. 8.19). Pyruvate carboxylase is found in mitochondria whereas the other ten enzymes involved in gluconeogenesis reside in the cytosol of the cell. Pyruvate has relatively easy access to the mitochondrion; however, oxaloacetate, the product of the carboxylation

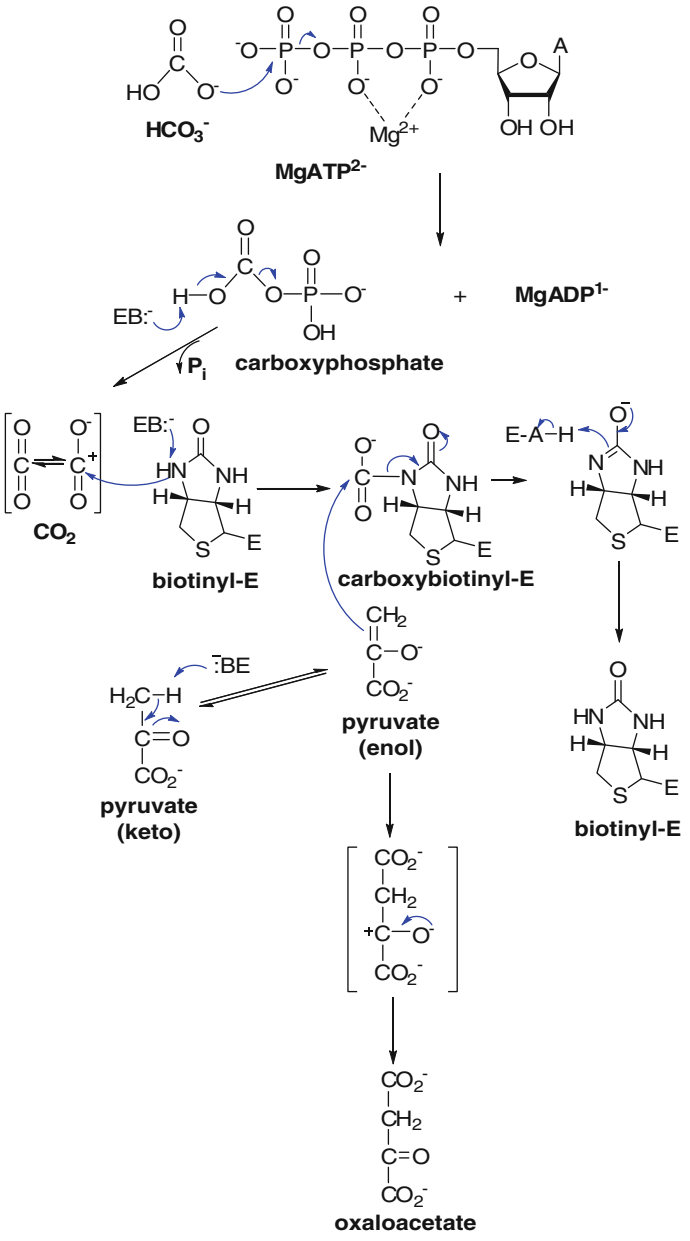

Fig. 8.19 The mechanism of action of pyruvate carboxylase involves enzyme-bound biotin. The conversion of (keto) pyruvate to (enol) pyruvate is enzyme catalyzed

reaction is incapable of leaving this organelle. How oxaloacetate enters the cytosol will be considered prior to the discussion on the coordinated regulation of glycolysis and gluconeogenesis (Scheme 8.6).

8.2.2 *Phosphoenolpyruvate Carboxykinase*

Phosphoenolpyruvate carboxykinase (PEPCK) exists in both the cytosol and mitochondrion. It catalyzes the conversion of oxaloacetate to phosphoenolpyruvate. Thus, two enzymes, pyruvate carboxylase and PEPCK, are required to reverse the highly exergonic pyruvate kinase reaction. If we assume for simplicity that CO_2 and HCO_3^- are the same and that ATP and GTP are equivalent, the summation of the PEPCK and pyruvate carboxylase reactions is:

$$2\text{ATP} + \text{pyruvate} \rightleftharpoons 2\text{ADP} + \text{phosphoenolpyruvate} + \text{P}_\text{i}.$$

It is not clear what the role is for mitochondrial PEPCK when it is recognized that mitochondrial phosphoenolpyruvate cannot migrate from the mitochondria to the cytoplasm. The importance of PEPCK in gluconeogenesis cannot be underestimated: When the enzyme is overexpressed in mice, the animals acquire *Type 2 diabetes*.

The mechanism of the PEPCK reaction is shown in Fig. 8.20.

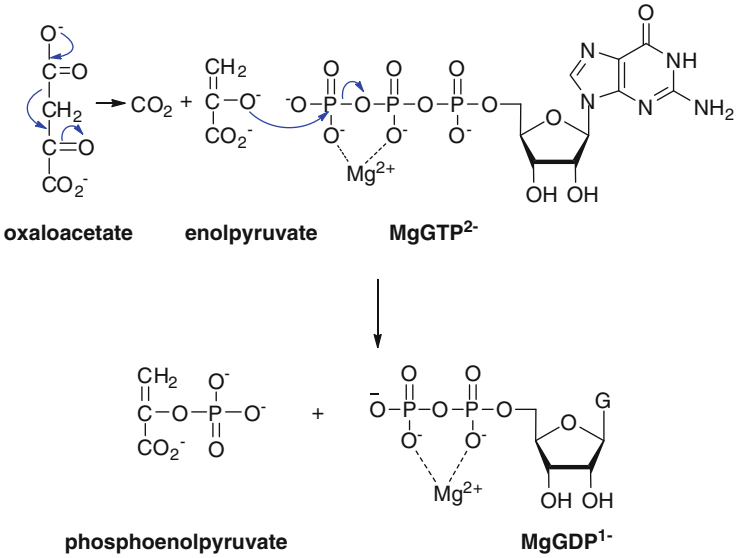

Fig. 8.20 The PEPCK reaction requires the involvement of the enol form of pyruvate and GTP

8.2.3 *Fructose-1,6-Bisphosphatase$_1$*

FBPase$_1$ is a major control point in gluconeogenesis and is used by the cell to override the unfavorable energetics of the PFK$_1$ reaction. The principle regulators of FBPase$_1$ are AMP and D-fructose 2,6-bisphosphate, both potent inhibitors of the enzyme. D-Fructose 2,6-bisphosphate is a competitive inhibitor of the substrate and binds at the active site, whereas AMP is an allosteric inhibitor of FBPase$_1$. FBPase$_1$ exists in three conformational states, the usual R-(active) and T-(inactive) states as well as a *hybrid state* [28]. The T-state is induced by AMP. The enzyme has an absolute requirement for divalent metal ions such as Mg^{2+} or Zn^{2+}which are necessary for substrate binding. Maximal activity requires K^+ ions. AMP causes release of enzyme bound metal and functions as a competitive inhibitor of enzyme-bound cations. It is of interest that the AMP allosteric site is 28 Å from the active site, nevertheless AMP and divalent cations are mutually exclusive in their binding.

The chemical mechanism of the FBPase$_1$ reaction has been studied in great detail. The stereochemical course of the reaction involves an inversion of configuration, exactly what might be expected for a typical S_N2 reaction; however, X-ray diffraction crystallography of the system indicates that a *metaphosphate*

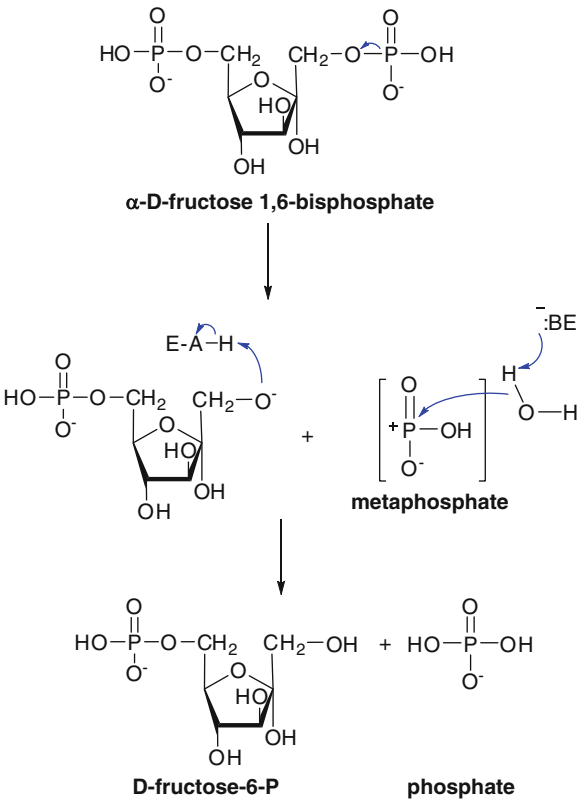

Fig. 8.21 The mechanism of the FBPase$_1$ reaction implicating a metaphosphate intermediate

intermediate participates in the reaction [29]. This was the first demonstration of a dissociative mechanism in biochemistry using physical methods as opposed to kinetic protocols (KIE). The chemical mechanism as gleaned from X-ray diffraction studies is presented in Fig. 8.21.

8.2.4 Glucose-6-Phosphatase

Glucose-6-phosphatase catalyzes the last step in gluconeogenesis, and circumvents the unfavorable energy barrier provided by the hexokinase reaction. The enzyme is highly hydrophobic and is found primarily in the *endoplasmic reticulum* of the liver cell. Its location in the liver of animals allows this organ to control the level of glucose in blood (see Cori Cycle and the Glucose-Alanine Cycle). The enzyme itself is under both dietary and hormonal control. Shown in Scheme 8.2 is a representation of the glucose-6-phosphatase complex involving D-glucose-6-P transport and hydrolysis of D-glucose-6-P as well as the transport of the reaction products, D-glucose and P_i [30, 31].

The chemical mechanism of the glucose-6-phosphatase reaction has been studied extensively [32]. Phosphohistidine, a covalent intermediate, plays a role in the chemical mechanism of the enzyme (Fig. 8.22) [33].

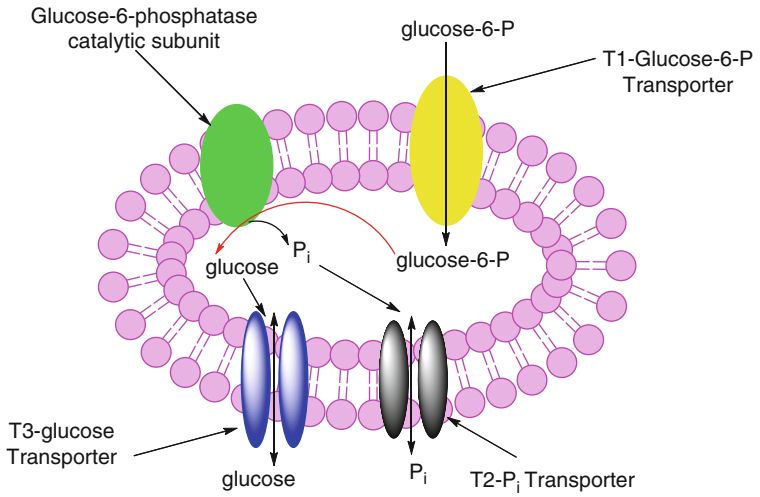

Scheme 8.2 Cartoon of the glucose-6-phosphatase complex

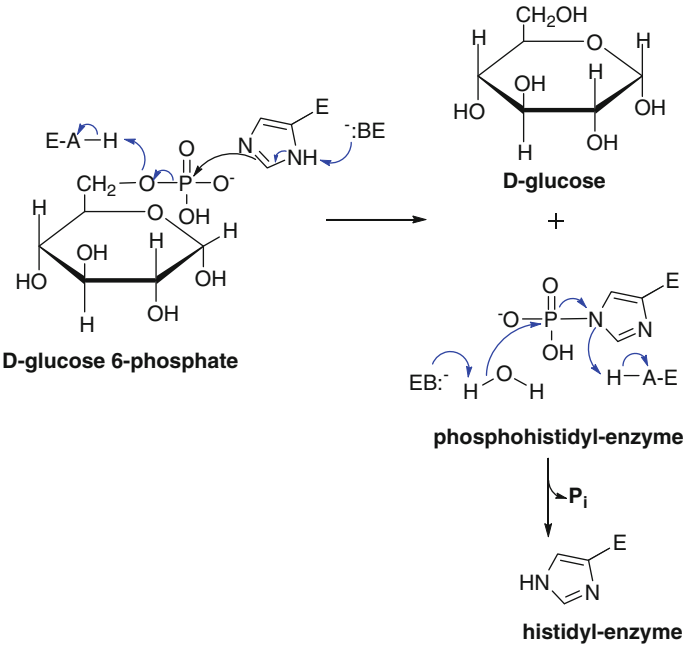

Fig. 8.22 The mechanism of the glucose-6-phosphatase reaction involves the participation of a phosphohistidine intermediate

8.3 Coordinated Regulation Between Glycolysis and Gluconeogenesis

Two crucial steps in glycolysis and gluconeogenesis involve D-fructose 1,6-bisphosphate (FBP): In glycolysis fructose-6-P + ATP = FBP + ADP, whereas in gluconeogenesis FBP + H_2O → D-Fructose-6-P + P_i. The sum of these two reactions is: ATP + H_2O → ADP + P_i and is referred to as a *futile cycle*. If these two processes were left unregulated, the cell would use its supply of ATP until it was exhausted. To circumvent this possibility, which would be catastrophic, controls are in place so that when glycolysis occurs, gluconeogenesis activity is diminished and vice versa. The key element in this metabolic coordination is the compound D-fructose 2,6-bisphosphate (Fru-2,6-P_2).

The synthesis and degradation of Fru-2,6-P_2 is under hormonal control; specifically, epinephrine from the adrenal cortex in the case of skeletal muscle and glucagon, a small protein from the α cells of the pancreas. Membrane protein receptors exist in muscle and liver cells for the hormones epinephrine and glucagon and are associated with a guanosine-5′-P nucleotide binding protein (G-protein). The G-protein has three different types of subunits: α, β, and γ. The β and γ subunits are always associated with the receptor; the α subunit, when associated with GDP, is also bound to the hormone receptor. When the hormone binds to its receptor, GDP is replaced by cytosolic GTP and the GTP-bound α-subunit migrates to

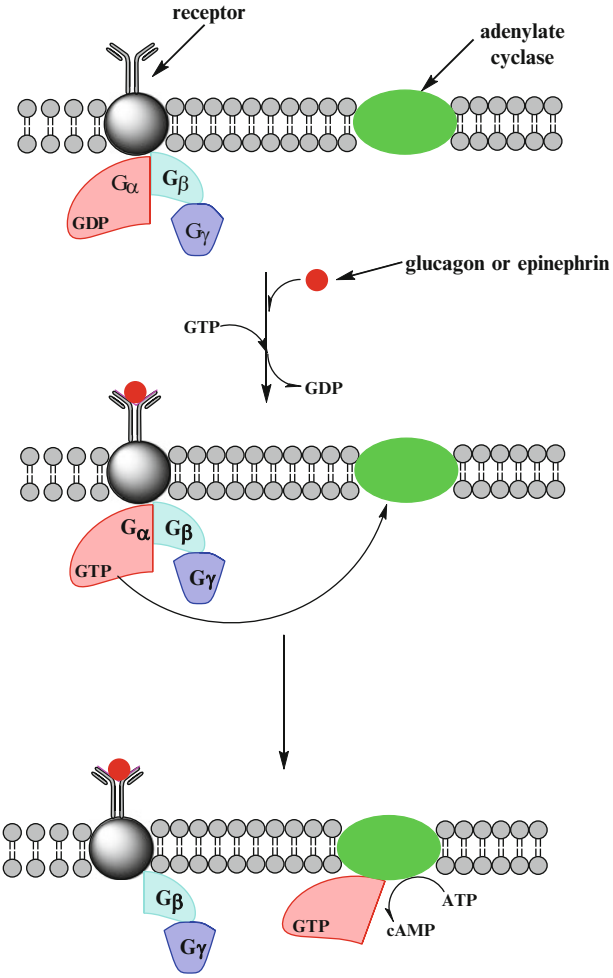

Scheme 8.3 The synthesis of 3′,5′-cyclic AMP is under hormonal control. The binding of glucagon or epinephrin to a membrane receptor results in the activation of adenylate cyclase

another membrane protein, adenylate cyclase. Absent the GTP-bound α-subunit, adenylate cyclase is inactive; however, when the GTP-bound α-subunit binds adenylate cyclase, the enzyme becomes active and uses ATP to produce 3′,5′-cyclic AMP (C-AMP). This process is turned off when GTP is hydrolyzed to GDP by the α-subunit itself, in which case the GDP-bound α-subunit migrates back to its receptor site as shown in Scheme 8.3.

Shown in Fig. 8.23 is the chemical mechanism of the adenylate cyclase reaction.

Cytoplasm contains a number of specific protein kinases, one of which is a 3′,5′-cyclic-AMP-dependent protein kinase, protein kinase A. The enzyme in

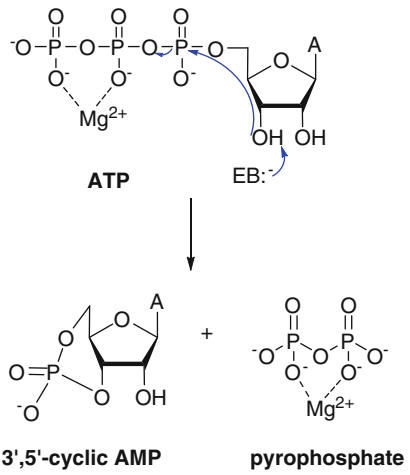

Fig. 8.23 The reaction catalyzed by adenylate cyclase. Activation of the enzyme requires its association with the α subunit of the G-protein from the glucagon or epinephrine receptor site

the absence of 3′,5′-cyclic-AMP is an inactive heterotetramer consisting of two catalytic and two regulatory subunits. When exposed to 3′,5′-cyclic-AMP, the enzyme dissociates into active catalytic subunits (C) and 3′,5′-cyclic-AMP bound regulatory (R) subunits:

$$\underset{\text{inactive}}{2[\text{C-R}]_2} + 4\text{C-AMP} \leftrightarrow 2\text{C} + \underset{\text{active}}{2\text{R}[\text{C-AMP}_2]}.$$

Also present in human liver is a protein with two distinctly different activities. One catalyzes the synthesis of Fru-2,6-P_2, the other, the degradation of Fru-2,6-P_2. The transphosphorylase, known as PFK_2, is involved in the phosphorylation of Fru-6-P at the C-2-position of Fru-6-P (Fig. 8.24).

The second enzyme activity involves the hydrolysis of Fru-2,6-P_2 by the enzyme $FBPase_2$ (Fig. 8.25).

Like their counterparts PFK_1 and $FBPase_1$, these enzymes if uncontrolled, form a *futile cycle*. This potential futile cycle is precluded by covalent modification of the dual function protein in which PFK_2 is inhibited and $FBPase_2$ is activated. Covalent modification is mediated by the enzyme *protein kinase A* in which ATP is used as the phosphorylating agent. Thus, it is the hormones epinephrine and glucagon that lead to the synthesis of 3′,5′-cyclic-AMP that results in the degradation of Fru-2,6-P_2. The end result of these events is that gluconeogenesis is allowed to proceed because of the loss of the $FBPase_1$ inhibitor, Fru-2,6-P_2, whereas glycolysis is diminished because of the loss of PFK_1 activity in the absence of Fru-2,6-P_2. Ultimately, insulin causes the dephosphorylation, probably through the action of a phosphoprotein phosphatase, of the dual functional protein and glycolysis is enhanced and gluconeogenesis is diminished.

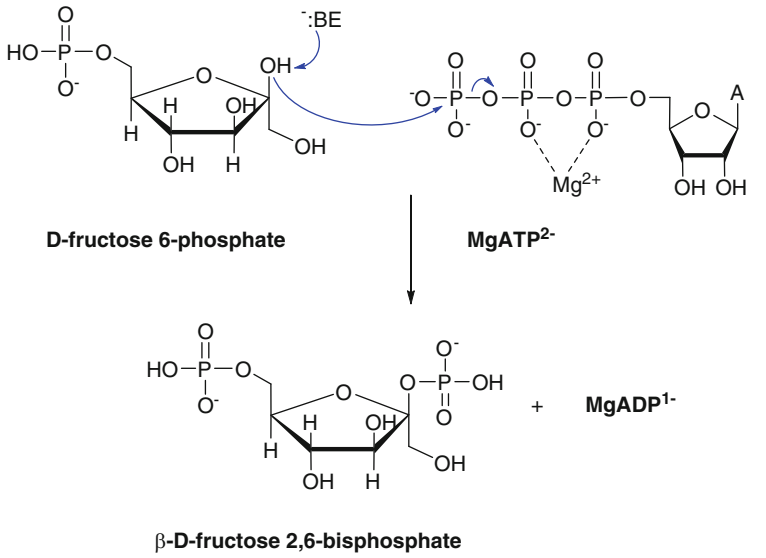

Fig. 8.24 The synthesis of β-D-fructose 2,6-bisphosphate (Fru-2,6-P_2) by PFK_2

Fig. 8.25 The hydrolysis of β-D-fructose 2,6-bisphosphate (Fru-2,6-P_2) catalyzed by $FBPase_2$

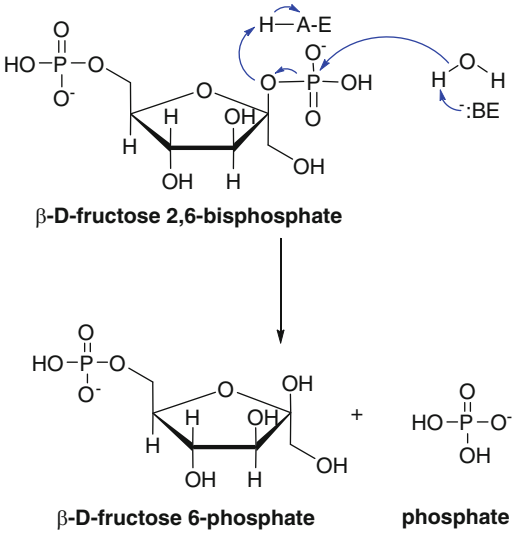

It has been recognized for many years that lower life forms do not produce Fru-2,6-P_2. On the other hand, plants and bacteria do carry out both glycolysis and gluconeogenesis. The obvious question then is, how is the balance between these two pathways maintained in the absence of hormonal control and Fru-2,6-P_2? This question was recently addressed by Hines et al. using *E. coli* as their experimental system [34]. They found that the bacterial $FBPase_1$ enzyme, like the mammalian enzyme, is strongly inhibited by AMP and that inhibition is exacerbated by the

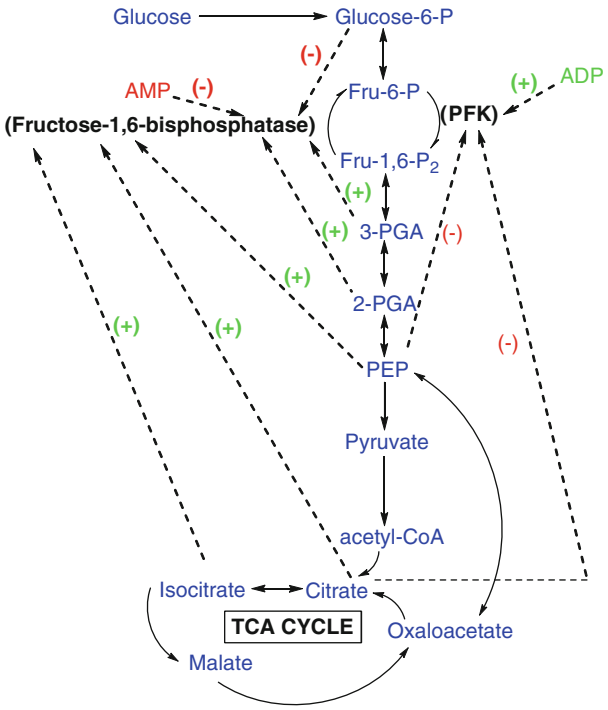

Fig. 8.26 Regulation of glycolysis and glucogenesis in *E. coli*. The abbreviations are as follows: *F-6-P* fructose-6-P, *Fru-1,6-P*$_2$ fructose 1,6-bisphosphate, *3-PGA* 3-phosphoglycerate, *2-PGA* 2-phosphoglycerate, *PEP* phosphoenolpyruvate, and *PFK* phosphofructkinase

penultimate product of gluconeogenesis, D-glucose-6-P. D-Glucose-6-P binds to allosteric sites on *E. coli* FBPase$_1$, sites that do not exist in the mammalian enzyme. The enzyme, when ligated with AMP and D-glucose-6-P exists in a T-like state. Phosphoenolpyruvate is a feed-forward activator of FBPase$_1$; however, AMP and D-glucose-6-P acting synergistically are able to overcome FBPase$_1$ activation. Figure 8.26 illustrates the relationships between glycolysis and gluconeogenesis in *E. coli* and how the activities of these two pathways are modulated by small metabolite molecules.

8.4 The Cori Cycle

Exercising skeletal muscle generates significant quantities of pyruvate anerobically. Reoxidation of NADH to NAD$^+$ by lactate dehydrogenase is required to maintain glycolysis at the glyceraldehyde-3-P dehydrogenase step. The end-product of this sequence of events is lactate which diffuses into the blood and is eventually absorbed by the liver. Here, the lactate is converted back to pyruvate by lactate

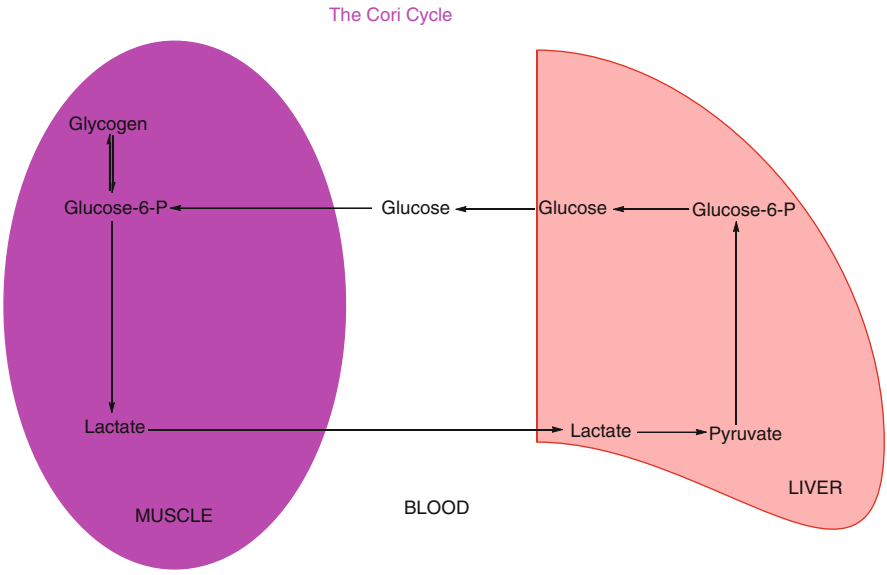

Scheme 8.4 Outline of the Cori Cycle in which lactate produced in skeletal muscle tissue is converted back to D-glucose in liver before it returns to muscle

dehydrogenase, a reaction that strongly favors lactate formation rather than pyruvate synthesis. The unfavorable equilibrium of the lactate dehydrogenase reaction is overcome by gluconeogenesis that shifts the equilibrium from lactate to pyruvate. Ultimately, D-glucose-6-P is formed and the liver enzyme glucose-6-phosphatase catalyzes the formation of glucose. The glucose thus produced can enter the blood and ultimately end up in skeletal muscle where it can be used either immediately or stored as glycogen. It has been suggested that approximately 80% of the glycogen that is used in severe muscle exercise is regenerated in the Cori cycle. An outline of the Cori cycle is presented in Scheme 8.4.

8.5 The Glucose–Alanine Cycle

The Cori cycle is not the only way in which the liver and skeletal muscle cooperate to regenerate muscle glucose. In muscle tissue, pyruvate is not only a precursor of lactate, it may also form L-alanine in a transamination reaction using L-glutamate as the amino group donor (see Chap. 6). The alanine can then diffuse into the blood stream where it may be picked up by the liver. In liver tissue, the alanine can be converted back to pyruvate which can then undergo gluconeogenesis to form glucose. This glucose may then replenish the muscle's supply of either glucose or glycogen. This cycle, known as the Glucose–Alanine Cycle, is outlined in Scheme 8.5.

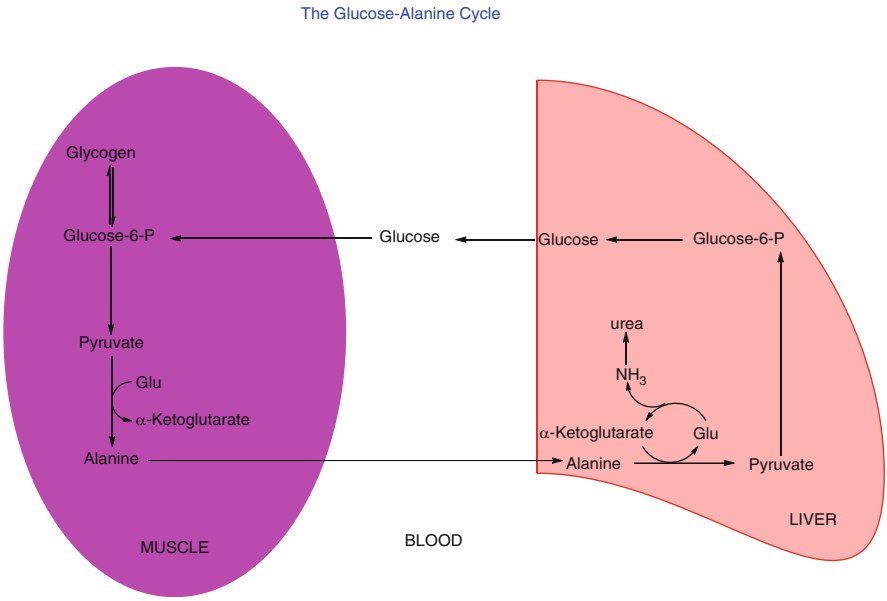

Scheme 8.5 Outline of the Glucose-Alanine Cycle:A mechanism for regenerating D-glucose and removing ammonia from muscle

Protein degradation in muscle produces alanine which may also be part of the Glucose–Alanine Cycle. The amino group generated in this process may form glutamate which may ultimately give rise to urea (Chap. 13). This cycle is thus a means of ridding the muscle tissue of ammonia.

8.6 Shuttle Mechanisms Allow Oxaloacetate Transport from Mitochondria to the Cytosol

Oxaloacetate, once it is synthesized in the pyruvate carboxylase reaction, must enter the cytosol where it can be converted to phosphoenolpyruvate if gluconeogenesis is to occur. However, oxaloacetate is not permeable to the mitochondrion. Nevertheless, oxaloacetate does enter the cytosol from its site of synthesis via shuttle mechanisms; two of which are shown in Scheme 8.6. One involves a oxaloacetate–aspartate shuttle in which oxaloacetate undergoes transamination to aspartate. The aspartate is then transported from the mitochondrion to the cytosol where it undergoes transamination to produce oxaloacetate. Another shuttle mechanism involves the conversion of oxaloacetate to malate which is then transported

from the mitochondrion to the cytosol. Oxidation of the malate yields the desired oxaloacetate.

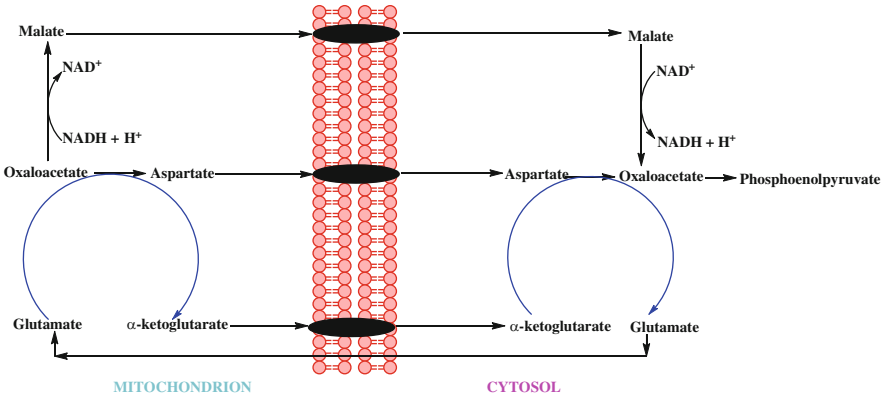

Scheme 8.6 Shuttle mechanism for the transport of oxaloacetate from the mitochondria to the cytosol

8.7 The Pentose Phosphate Shunt

The Pentose Phosphate Shunt also known as the Hexose Monophosphate Pathway is found in the cytoplasm of most life forms. Its purpose is twofold; one, to produce NADPH which is required for many anabolic reactions, and second to provide the cell with D-ribose and ultimately 2-deoxy-D-ribose, precursors of nucleotides, coenzymes, RNA, and DNA. Approximately one-third of the glucose oxidized in the liver occurs in the Shunt. Shunt enzymes are high in fat-producing tissues and adipose tissue where there is a requirement for NADPH for fatty acid biosynthesis.

Many of the Shunt enzymes participate in the Calvin cycle in organisms that carry out photosynthesis (Chap. 15).

The pathway is shown in Fig. 8.27.

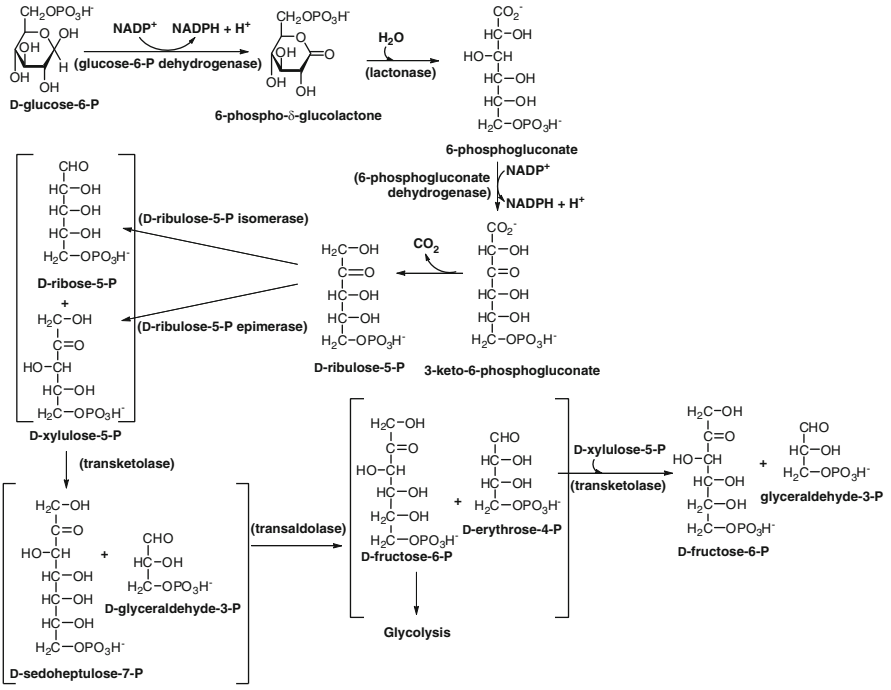

Fig. 8.27 The reactions involved in the pentose monophosphate shunt starting with glucose-6-P and ending with glyceraldehydes-3-P and D-fructose-6-P

8.7.1 The Enzymes of the Pentose Phosphate Shunt

8.7.1.1 Glucose-6-Phosphate Dehydrogenase

Glucose-6-phosphate dehydrogenase is a pyridine-linked anerobic dehydrogenase that is specific for $NADP^+$. The hydride ion from the C-1 of glucose adds to the *si*-face of $NADP^+$. In the reverse reaction, the *pro*-S hydrogen is removed from NADPH (Fig. 8.28).

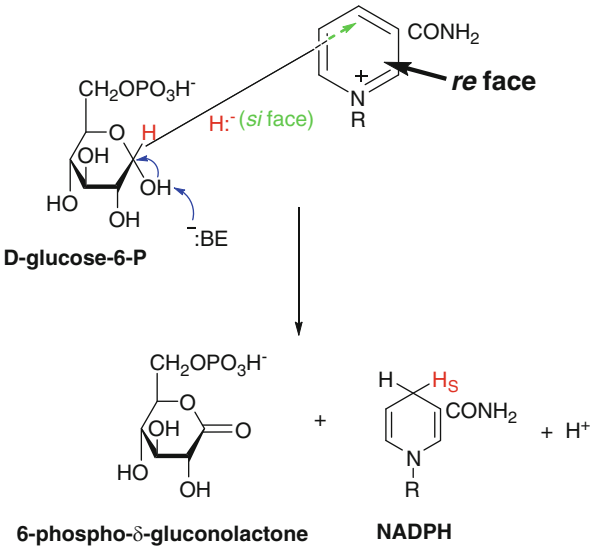

Fig. 8.28 The mechanism and stereochemistry of the glucose-6-phosphate dehydrogenase reaction. The hydride ion extracted from the C-1 position of D-glucose-6-P adds to the *si* face of $NADP^+$ and appears as the H_S hydrogen in NADPH

8.7.1.2 Lactonase

The lactonase reaction and its mechanism of action is shown in Fig. 8.29

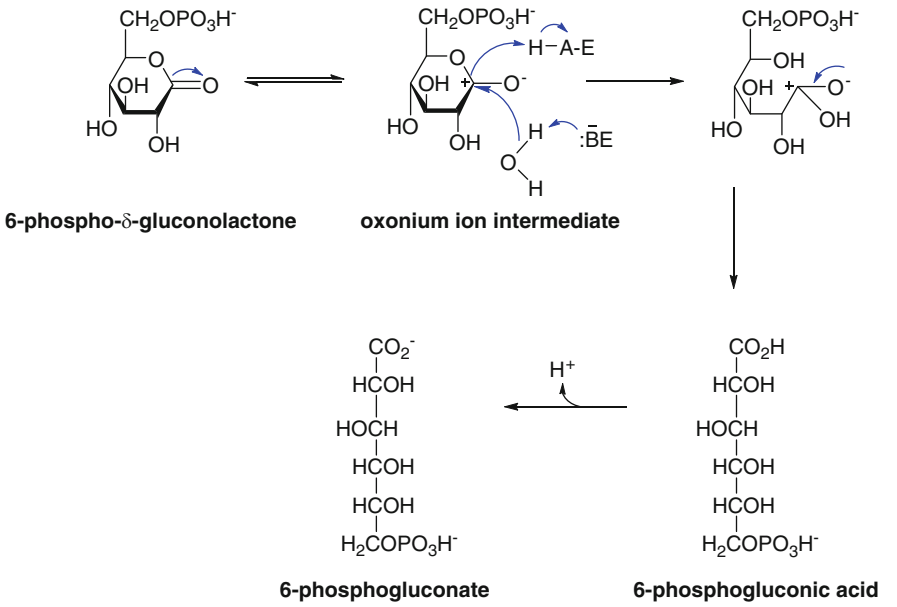

Fig. 8.29 The mechanism of the lactonase reaction involves the opening of the pyranose ring of 6-phospho-δ-glucolactone. The end-product of the reaction is 6-phosphogluconate

8.7.1.3 6-Phosphogluconate Dehydrogenase

6-Phosphogluconate is oxidized to 3-keto-6-phosphogluconate by 6-phosphogluconate dehydrogenase. The keto product then undergoes decarboxylation to produce the ketopentose, D-ribulose-5-P. The Pentose Phosphate Pathway at this step has generated two equivalents of NADPH for each molecule of D-glucose-6-P oxidized (Fig. 8.30).

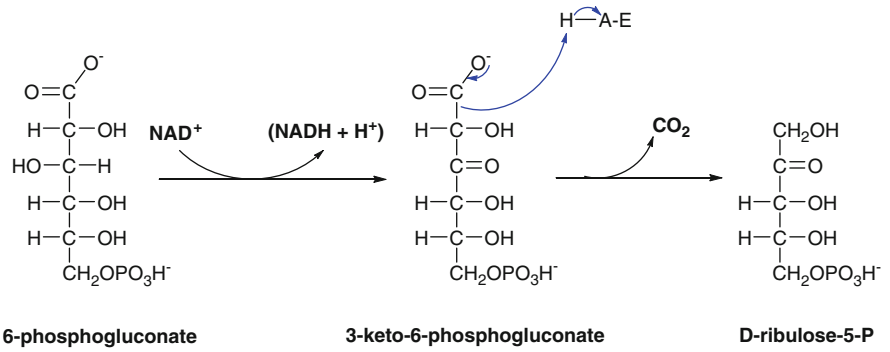

Fig. 8.30 The 6-phosphogluconate dehydrogenase reaction generates NADPH and the ketopentose, D-ribulose-5-P

8.7.1.4 Phosphopentose Isomerase

At this point in the pathway, D-ribulose-5-P is the precursor of two pentose phosphates, D-ribose-5-P which can continue in the Pentose Phosphate Pathway or be utilized for nucleotide biosynthesis, and D-xylulose-5-P. Phosphopentose isomerase converts D-ribulose-5-P to D-ribose-5-P. The intermediate in this process is thought to be the 1,2-enediol (Fig. 8.31).

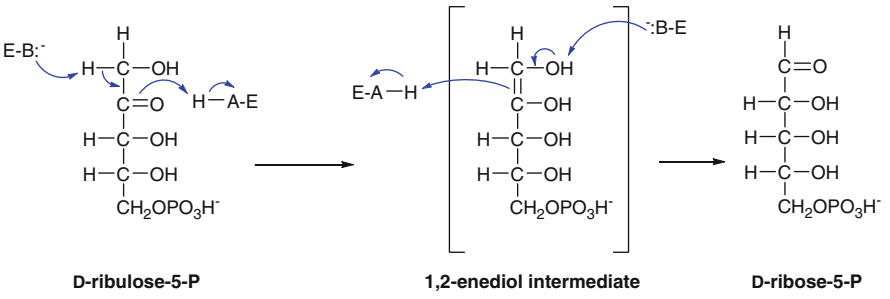

Fig. 8.31 The isomerization of D-ribulose-5-P to D-ribose-5-P involves an enediol intermediate

8.7.1.5 Phosphopentose Epimerase

D-Ribulose-5-P is also the substrate for phosphopentose epimerase. The mechanism is similar to that described for phosphopentose isomerase except that the intermediate is a 2,3-enediol (Fig. 8.32).

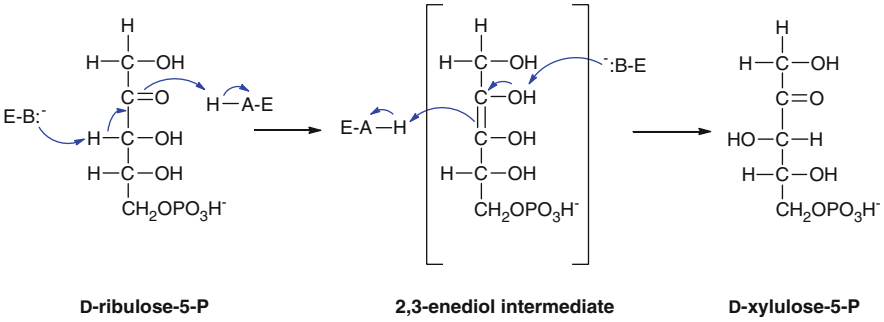

Fig. 8.32 D-Xylulose-5-P, an epimer of D-ribulose-5-P, is synthesized in the phosphopentose epimerase reaction. A 2,3-enediol intermediate is involved in the epimerization reaction

8.7.1.6 Transketolase

Transketolase uses TPP as a coenzyme. The substrates are D-ribose-5-P and D-xylulose-5-P and the products D-sedoheptulose-7-P and glyceraldehydes-3-P. *Ylid* formation by the coenzyme is an essential feature of the reaction mechanism (Fig. 8.33).

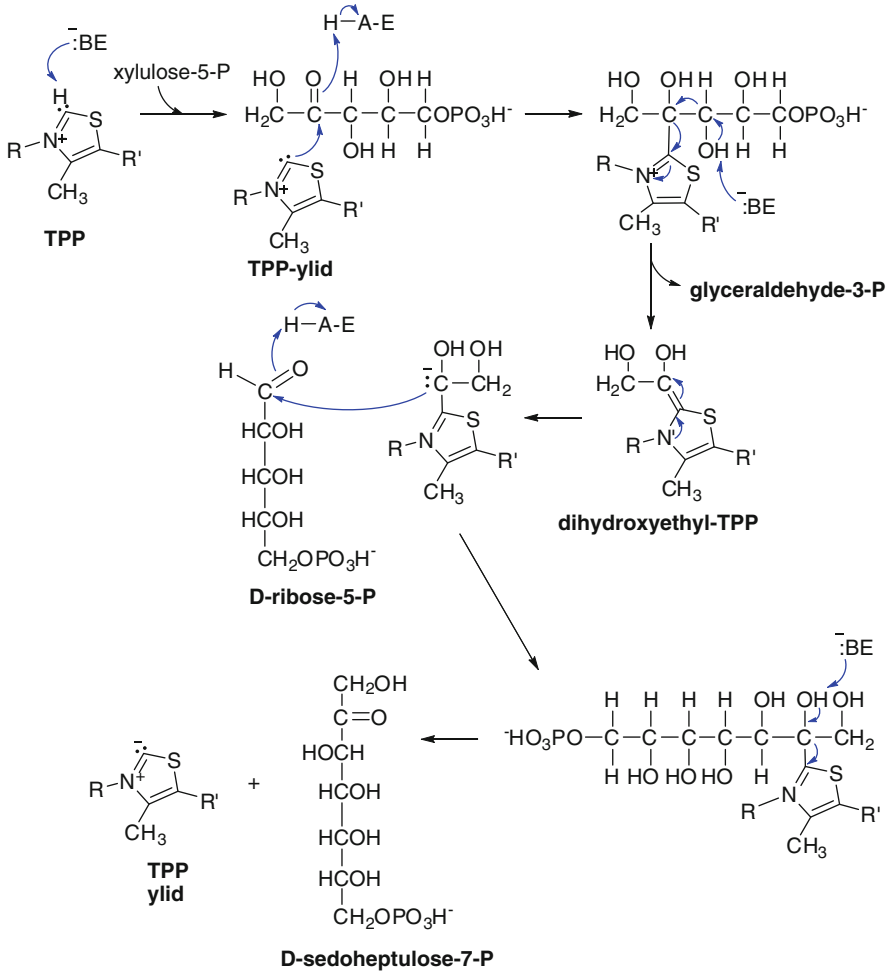

Fig. 8.33 Two five-carbon sugar phosphates produce a seven- and a three-carbon sugar phosphate in the transketolase reaction

8.7.1.7 Transaldolase

The products of the transketolase reaction (D-sedoheptulose-7-P and D-glyceraldehyde-3-P) are substrates for the next enzyme in the pathway, transaldolase. The products of the transaldolase reaction are D-fructose-6-P which can enter the glycolytic or gluconeogenic pathways and D-erythrose-4-P. Transaldolase is classified as a Class I aldolase as a Schiff base is an intermediate in the reaction mechanism (Fig. 8.34).

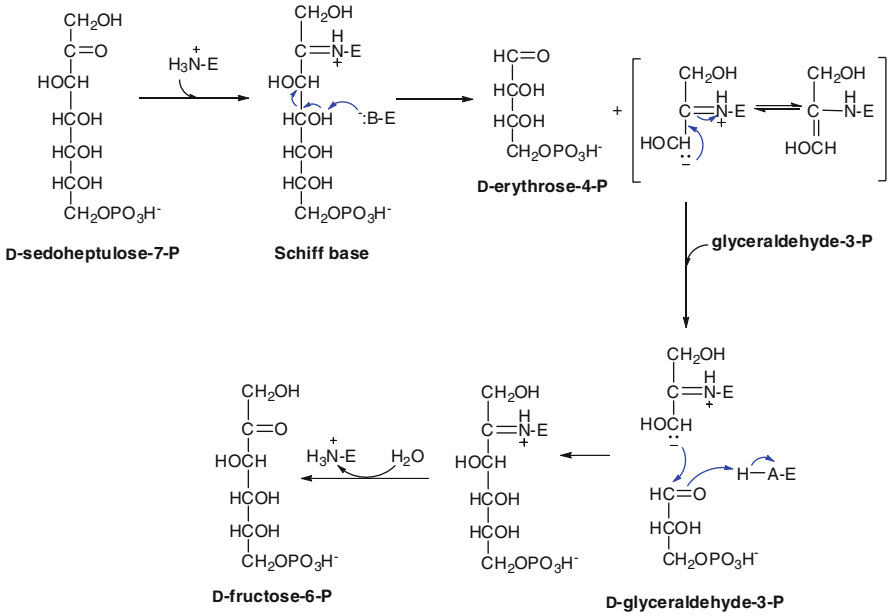

Fig. 8.34 A Schiff base is an essential feature of the transaldolase reaction. In this reaction, seven- and three-carbon sugars form a six- and a four-carbon sugar phosphate

8.7.1.8 Transketolase

The terminal reaction in the Pentose Phosphate Pathway involves the conversion D-erythrose-4-P and D-xylulose-5-P to D-fructose-6-P and D-glyceraldehyde-3-P. The enzyme that catalyzes this reaction is TPP-dependent transketolase. The reaction mechanism is identical to that depicted in Fig. 8.33.

8.7.2 Regulation of the Pentose Phosphate Pathway

Control of the Pentose Phosphate pathway occurs at the *first committed step* in the pathway, D-glucose-6-P dehydrogenase. The flux through this step in the pathway is determined by the NADPH/$NADP^+$ ratio. When the concentration of NADPH within the cell is high, the level of $NADP^+$ will be low and there will be a decrease in the flux through the pathway. The reverse will be true when levels of $NADP^+$ are elevated.

References

1. Meyerhoff O (1930) Lancet 2:1415–1421
2. Fromm HJ, Zewe V (1962) Kinetic studies of yeast hexokinase. J Biol Chem 237:3027–3032
3. Fromm HJ, Ning J (1968) Kinetic studies of solubilized brain hexokinase with D-fructose as a substrate. Biochem Biophys Res Commun 32:672–677
4. Fromm HJ, Silverstein E, Boyer PD (1964) Equilibrium and net reaction rates in relation to the mechanism of yeast hexokinase. J Biol Chem 239:3645–3652
5. Ganson NJ, Fromm HJ (1984) Initial rate and isotope exchange studies of rat skeletal muscle hexokinase. J Biol Chem 260:12099–12105
6. Fletterick RJ, Bates DJ, Steitz TA (1975) Structure of a yeast hexokinase monomer and its complexes with substrates at 2.7 Å resolution. Proc Natl Acad Sci USA 72:38–42
7. Koshland DE Jr (1958) Application of a theory of enzyme specificity to protein synthesis. Proc Natl Acad Sci USA 44:98–104
8. Rose IA (1980) Mechanism of phosphoryl transfer by hexokinase. Biochem Biophys Res Commun 94:573–578
9. Lowe G, Potter BV (1981) The stereochemical course of yeast hexokinase-catalysed phosphoryl transfer by using adenosine 5'[gamma(S)-16O,17O,18O]triphosphate as substrate. Biochem J 199:227–233
10. Aleshin AE, Kirby C, Liu X, Bourenkov GP, Bartunik HD, Fromm HJ, Honzatko RB (2000) Crystal structure of mutant monomeric hexokinase I reveal multiple ADP binding sites and conformational changes relevant to allosteric regulation. J Mol Biol 296:1001–1015
11. May A, Vas M, Harlos K, Blake C (1996) 2.0 Å resolution structure of a ternary complex of pig muscle phosphoglycerate kinase containing 3-phospho-D-glycerate and the nucleotide Mn adenylylimidodiphosphate. Proteins 24:292–303
12. Auerbach G, Huber R, Grättinger M, Zaiss K, Schurig H, Jaenicke R, Jacob U (1997) Closed structure of phosphoglycerate kinase from Thermotoga maritime reveals the catalytic mechanism and determinants of thermal stability. Structure 5:1475–1483
13. Britten HG, Clark JB (1972) Mechanism of the 2,3-diphosphoglycerate-dependent phosphoglycerate mutase from rabbit muscle. Biochem J 130:397–410
14. Rigden DJ (1998) The 2.3 A X-ray crystal structure of *S. cerevisiae* phosphoglycerate mutase. J Mol Biol 276:449–459
15. Reed GH, Poyer RP, Larse, JE, Wedekind JE, and Rayment I (1996) Structural and mechanistic studies of enolase. Curr Opin Struct Biol 6:736–743
16. Reynard AM, Hass LF, Jacobsen DD, Boyer PD (1961) The correlation of reaction kinetics and substrate binding with the mechanism of pyruvate kinase. J Biol Chem 236:2277–2283
17. Ainsworth S, MacFarlane N (1973) A kinetic study of rabbit musclepyruvate kinase. Biochem J 131:223–236
18. Orr GA, Simon J, Jones SR, Chin GJ, Knowles JR (1978) Adenosine 5′-O-([gamma-18O] gamma-thio)triphosphate chiral at the gamma-phosphorus: stereochemical consequences of reactions catalyzed by pyruvate kinase, glycerol kinase, and hexokinase. Proc Natl Acad Sci USA 75:2230–2233
19. Rose IA (1970) Stereochemistry of pyruvate kinase pyruvate carboxylase, and malate enzyme reactions. J Biol Chem 245:6052–6056
20. Gublinsky JS, Cleland WW (1968) Kinetic studies of *Escherichia coli* galactokinase. Biochemistry 7:566–575
21. Arabshahi A, Brody RS, Smallwood A, Tsai TC, Frey PA (1986) Galactose-1-phosphate uridyltransferase. Purification of the enzyme and stereochemical course of each step of the double displacement mechanism. Biochemistry 25:5583–5589
22. Nelsestuen GL, Kirkwood SJ (1971) The mechanism of action of uridine diphosoglucose dehydrogenase. Uridine diphosphohexodialdoses as intermediates. J Biol Chem 246: 7533–7543

23. Storer AC, Cornish-Bowden A (1977) Kinetic evidence for a 'mnemonical' mechanism for rat liver glucokinase. Biochem J 165:61–69
24. Pettersson G (1986) Mechanistic origin or the sigmoidal rate behavior of galactokinase. Biochem J 233:347–350
25. Dobson GP, Hitchins S, Teague WE Jr (2002) Thermodynamics of the pyruvate kinase reaction and the reversal of glycolysis in heart and skeletal muscle. J Biol Chem 277: 27176–27182
26. Lardy HA, Ziegler JA (1945) The enzymatic synthesis of phosphopyruvate from pyruvate. J Biol Chem 159:343–351
27. Utter MF, Keech DB (1960) Formation of oxolo-acetate from pyruvate and CO_2. J Biol Chem 235:PC17–PC18
28. Iancu CV, Mukund S, Fromm HJ, Honzatko RB (2005) R-state AMP complex reveals initial steps of the quarternary transition of fructose-1,6-bisphosphatase. J Biol Chem 280: 19737–19745
29. Choe JY, Nelson SW, Fromm HJ, Honzatko RB (2003) Metaphosphate in the active site of fructose-1,6-bisphosphatase. J Biol Chem 278:16015–16020
30. Arion WJ, Wallin BK, Lange AJ, Ballas LM (1975) On the involvement of a glucose 6-phosphate transport system in the function of microsomal glucose 6-phosphatase. Mol Cell Biochem 6:75–83
31. van Schaftingen E, Gerin I (2002) The glucose-6-phosphatase system. Biochem J 362: 513–532
32. Arion WJ, Nordlie RC (1964) Liver microsomal glucose 6-phosphatase. Inorganic pyrophosphatase, and pyrophosphate-glucose phosphotransferase. II. Kinetic studies. J Biol Chem 239:2752–2757
33. Ghos A, Shieh J-J, Pan C-J, Sun M-S, Chou JY (2002) The catalytic center of glucose-6-phosphatase: His^{176} is the nucleophile forming the phosphohistidine-enzyme intermediate during catalysis. J Biol Chem 277:32837–32842
34. Hines JK, Kruesel CE, Fromm HJ, and Honzatko RB (2007) Structure of inhibited fructose-1,6-bisphosphatase from Escherichia coli : distinct allosteric inhibition sites for AMP and glucose 6-phosphate and characterization of a gluconeogenic switch. J Biol Chem 282: 24697–24706

Chapter 9
The Tricarboxylic Acid Cycle

Named for its metabolism of the conjugate bases (citrate, isocitrate, and *cis*-aconitate) of three tricarboxylic acids in the early steps of the pathway, the *Tricarboxylic Acid Cycle* (or TCA cycle) is known simply as the *Citric Acid Cycle*. The term "cycle" refers to the fact that the initial six-carbon substrate (citrate) is oxidatively decarboxylated twice to form the pathway's ultimate four-carbon product (oxaloacetate), which then combines with two-carbon units (as acetyl-CoA) to regenerate citrate, thereby allowing the cycle to begin anew. This same pathway is also known as the *Krebs Cycle* in honor of Sir Hans Krebs, the German-born British biochemist, who proposed the pathway in the late 1930s and later earned the Nobel Prize for demonstrating its key properties.

Although the Citric Acid Cycle involves the oxidation of two carbon atoms, supplied initially as acetyl-CoA, pyruvate is the precursor of acetyl-CoA in a noncyclic reaction that supplies two-carbon units to the cycle. When viewed as the continuation of glycolysis, the overall process oxidizes two molecules of pyruvate:

$$2\text{Pyruvic Acid} + 5O_2 \rightarrow 6CO_2 + 4H_2O + \text{Gibbs Free Energy}.$$

The cycle successfully captures the resulting Gibbs free energy as P–O–P bonds and as hydrides in the form of ATP (or GTP) and NADH, respectively. In eukaryotes, this series of reactions occurs in mitochondria, the small organelles roughly the size of *Escherichia coli,* wherein the Gibbs energy of NADH oxidation is later captured as P–O–P bonds, again in the form of ATP, by the action of the energy-transducing Electron Transport System (ETS).

Pyruvate itself has metabolic fates other than oxidation. These include amination to alanine and conversion to phosphoenolpyruvate in gluconeogenesis. Generated in the cell from D-glucose (via glycolysis) and glycogen (via glycogenolysis), pyruvate enters the mitochondrion by passing through its outer membranes,

H.J. Fromm and M.S. Hargrove, *Essentials of Biochemistry*,
DOI 10.1007/978-3-642-19624-9_9,

which are leaky or porous to many ions and small molecules. The inner mitochondrial membrane, however, is highly selective and contains a pyruvate transporter protein that allows pyruvate to enter the mitochondrion's innermost compartment, the matrix. Once within the mitochondrial matrix, pyruvate is ultimately degraded to CO_2 and H_2O.

9.1 The Conversion of Pyruvate to Acetyl-CoA

The first step in the oxidation of pyruvate involves the pyruvate dehydrogenase enzyme complex. It should be noted that the pyruvate dehydrogenase complex is not part of the TCA cycle. The pyruvate dehydrogenase complex from *E. coli* consists of 60 copies of E_2, which is the core of the complex, 30 copies of E_1, 12 copies of E_3, and 12 copies of the E_3 binding protein. Proteins E_1, E_2, and E_3 are associated with TPP, lipoamide, and FAD, respectively. The pyruvate dehydrogenase complex is believed to be the largest multienzyme complex in cells and is larger than the ribosome. It is found in the cytosol in bacterial, in the mitochondria in eukaryotic cells, and in the chloroplast in plants.

A reproduction of the complex from *Sacromycetes cerevisiae* is shown in Fig. 9.1 [1].

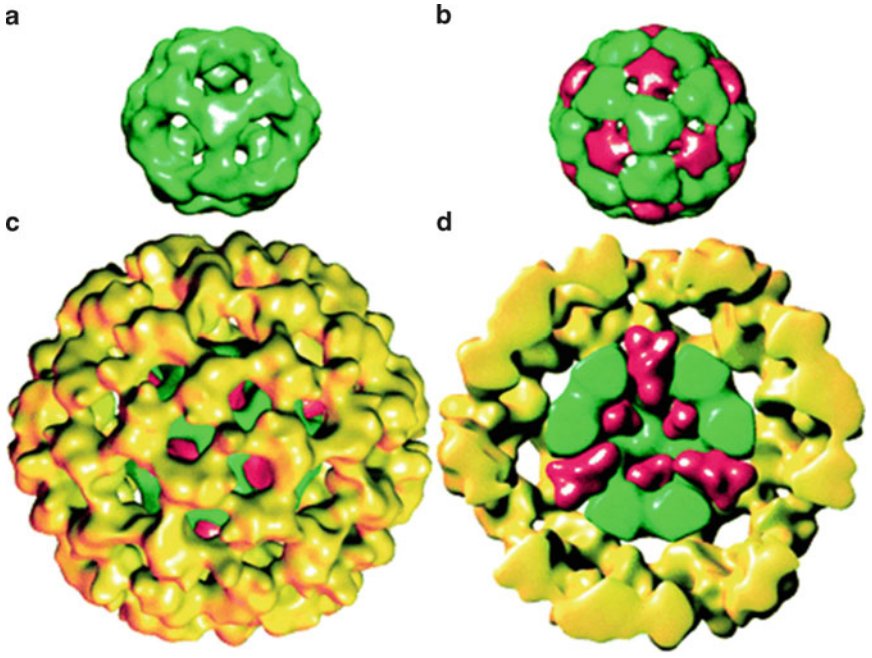

Fig. 9.1 *Surface shaded* representations of three-dimensional reconstructions of the *S. cerevisiae* pyruvate dehydrogenase complex and its subcomplexes viewed along a threefold axis of

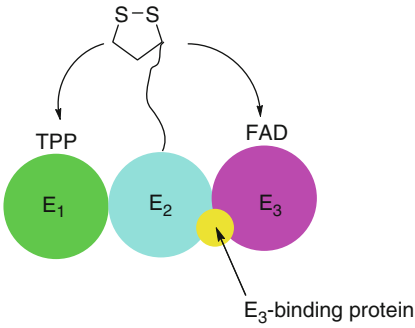

Fig. 9.2 Cartoon of the functional portion of the pyruvate dehydrogenase complex

The simplest representation of the pyruvate dehydrogenase complex trimer, along with its compliment of coenzymes, is shown in Fig. 9.2.

The lipoamide in the pyruvate dehydrogenase complex, as can be seen in Fig. 9.2, is capable of interacting with both TPP on E_1 and FAD on E_3. This is because its hydrophobic side chain, known as a *swinging arm*, is 14 Å long.

E_1, E_2, and E_3 are referred to as pyruvate dehydrogenase, dihydrolipoyl transacylase, and dehydrolipoyl dehydrogenase, respectively.

The overall reaction of pyruvate dehydrogenase (E_1) is:

$$\text{Pyruvate} + H^+ + \text{TPP-E}_1 \rightarrow \text{hydroxyethylidine(hydroxyethyl)TPP-E}_1 + CO_2.$$

In the following step of the pyruvate dehydrogenase complex reactions, the hydroxyethylidine group is transferred to lipoamide as an acetyl group and forms a thioester.

$$\text{hydroxyethylidine TPP-E}_1 + \text{lipoamide-E}_2 \rightarrow \text{acetyl lipoamide-E}_2 + \text{TPP-E}_1.$$

Next, the acetyl moiety is passed on to CoASH by dihydrolipoamide transacetylase forming acetyl-CoA and fully reduced lipoamide-E_2 (dihydrolipoamide-E_2).

In the final steps in the sequence of reactions involving the pyruvate dehydrogenase complex, dihydrolipoamide is oxidized by FAD-E_3, which is reduced to $FADH_2$-E_3. $FADH_2$-E_2 is then reoxidized by NAD^+, which is converted to NADH.

Fig. 9.1 (continued) symmetry. (**a**) truncated-E_2; (**b**), the truncated-E_2·Binding Protein-E_3 subcomplex has 12 copies of Binding Protein-E_3 (*red*) buried deep inside the 12 pentagonal openings of the truncated-E_2 scaffold (*green*); (**c**) structure of the pyruvate dehydrogenase complex consisting of the truncated-E_2 inner core (*green*) with the Binding Protein-E_3 components (*red*) bound on the inside and the tetrameric E_1 molecules (*yellow*) bound on the outside. (**d**), cutaway reconstruction of the pyruvate dehydrogenase complex from **c** showing the disposition of Binding Protein-E_3 and E_1 relative to truncated-E_2

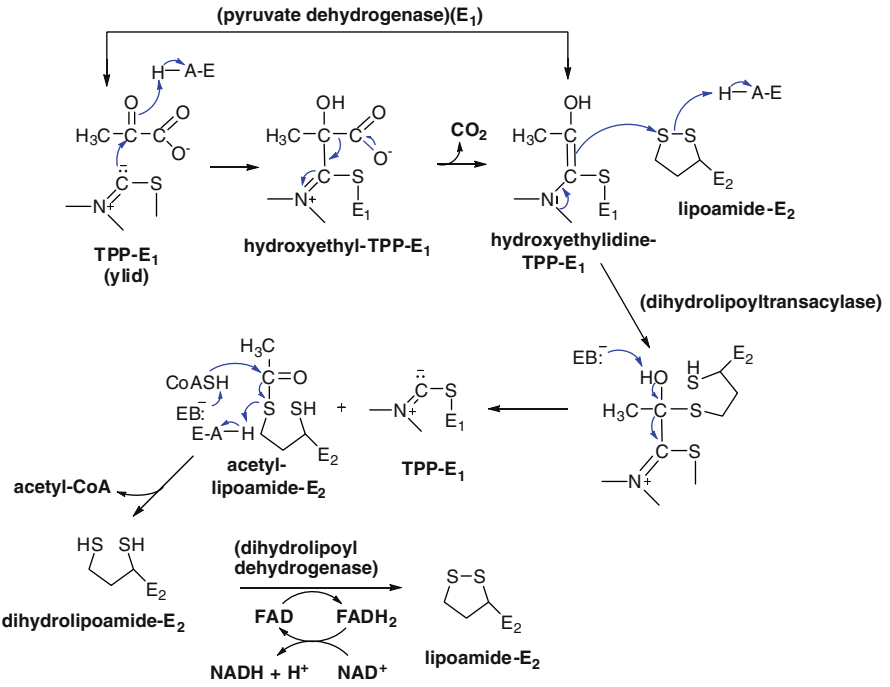

Fig. 9.3 Reactions carried out by the pyruvate dehydrogenase complex

Ultimately, NADH is oxidized to NAD^+ by an ETS on the inner mitochondrial membrane. This redox reaction is coupled to ATP biosynthesis from ADP and Pi, and is referred to as *oxidative phosphorylation* (Chap. 10).

The three enzymes that make up the pyruvate dehydrogenase complex carry out the reactions shown in Fig. 9.3.

How the lipoamide functions as the "*swinging arm*" is illustrated in Fig. 9.4.

Dihydrolipoamide dehydrogenase utilizes FAD which is reduced in order to reoxidize dihydrolipoamide. The $FADH_2$ is in turn oxidized at the expense of NAD^+ as described in Fig. 9.4. NADH, the ultimate electron acceptor, is itself reoxidized by the ETS associated with oxidative phosphorylation (Fig. 9.5).

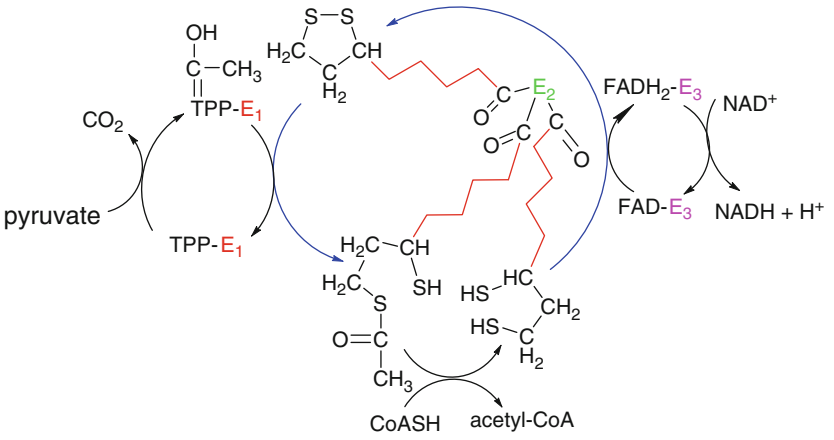

Fig. 9.4 The long hydrophobic side chain associated with lipoamide-E_2 is capable of interacting with TPP on E_1 and FAD on E_3

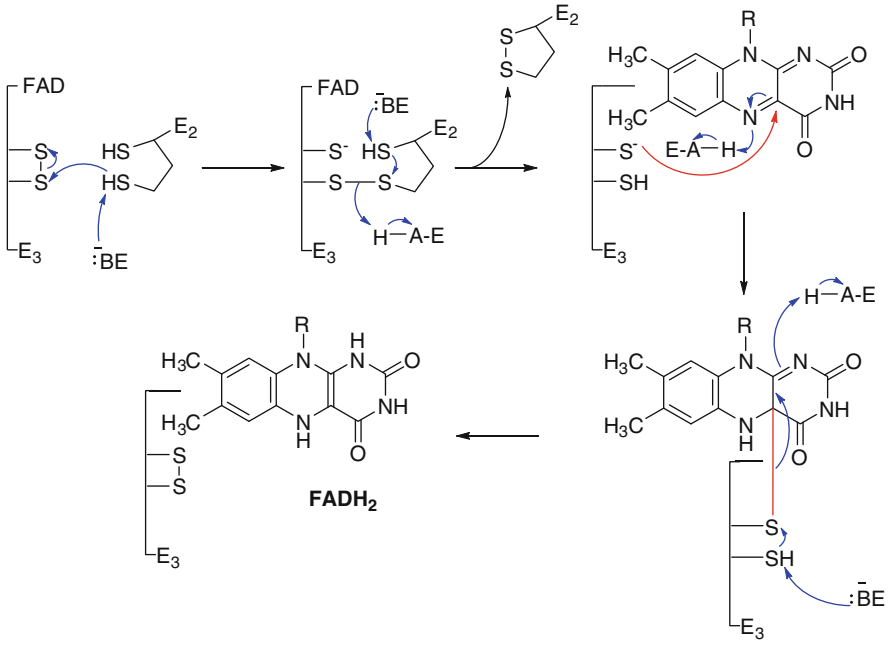

Fig. 9.5 The reactions leading to the reoxidation of reduced lipoamide. Involved is the coenzyme FAD. $FADH_2$ is itself reoxidized by NAD^+ which is reduced to NADH as illustrated in Fig. 9.4

9.2 The TCA Cycle: The Fate of Acetyl-CoA

The TCA cycle converts acetyl-CoA to CO_2 and energy, primarily in the form of reduced coenzymes. A cursory examination of the reactions of the TCA cycle does not overtly explain the production of energy nor does it indicate how H_2O is produced from the oxidation of acetyl-CoA. Exactly how energy in the form of ATP is produced, and where the product H_2O arises, will be considered when the topic of oxidative phosphorylation is discussed (Chap. 10).

The TCA cycle may be considered a metaphor for a steam engine. Acetyl-CoA, the energy source is analogous to coal, and the steam, capable of doing useful work, is analogous to ATP. ATP production in mitochondria is a relatively efficient process and is believed to exceed 60% efficiency. Steam engine efficiency is less than 20%, however, the energy lost in terms of heat in the living cell is used for heating the cell itself.

It may be possible to consider the TCA cycle as a metabolic end-product incinerator. Not only are glucose- and glycogen-derived molecules oxidized in the TCA cycle, but many amino acids and fatty acids share a similar fate.

Figure 9.6 describes the TCA cycle in detail. In only one step, succinyl-CoA synthetase, is there overt formation of an energy rich compound (GTP), nor is it obvious that H_2O is produced in the cycle.

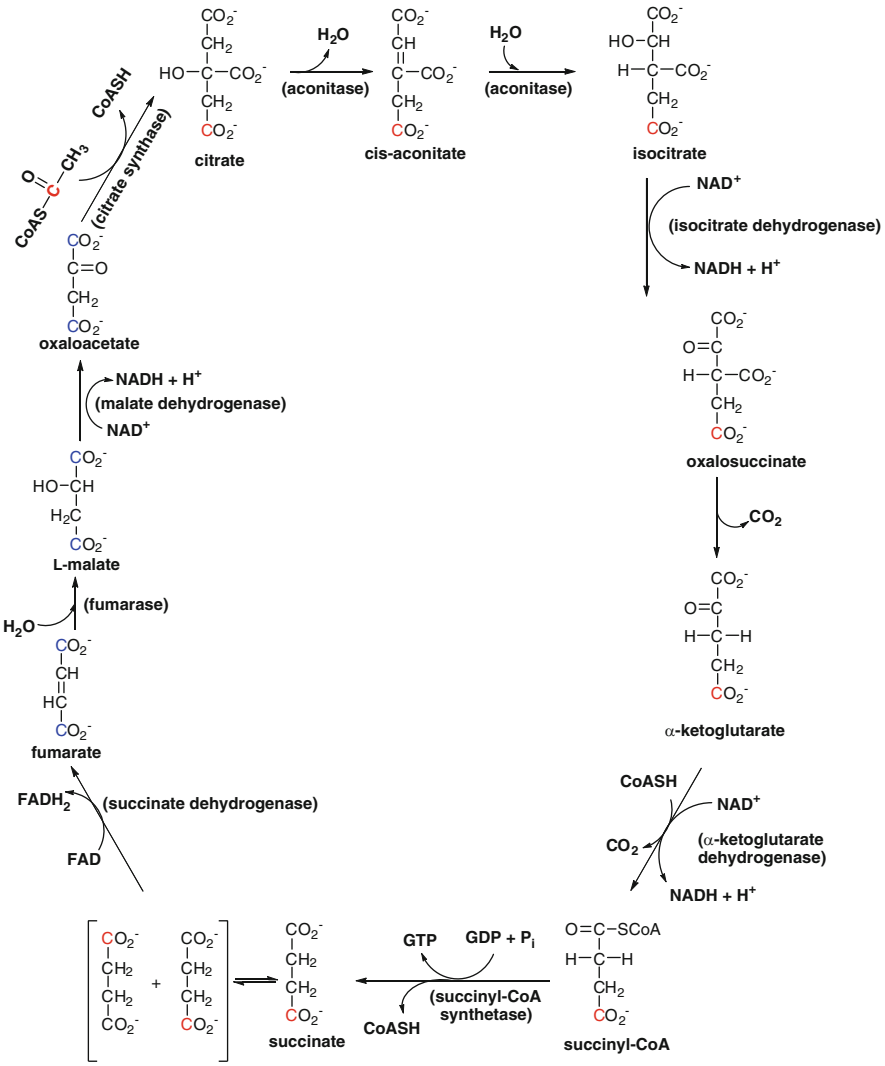

Fig. 9.6 The reactions involved in the TCA Cycle. Acetyl-CoA is fed into the cycle, and its two carbon atoms are converted to oxaloacetate in a single cycle. The carbon atom(s) are traced by color coding the carbonyl carbon atom (*red*) of acetyl-CoA which is introduced into the cycle. At the succinyl-CoA synthetase step the labeled carbonyl carbon atom from acetyl-CoA appears exclusively in one of the carboxyl groups of succinate; however, because succinate has a twofold axis of symmetry, it is not possible to distinguish one carboxylate group from the other. Thus, each carboxylate will appear to contain 50% (*blue*) of the label from succinyl-CoA

9.3 Energetics of Pyruvate Oxidation

The reoxidation NADH and $FADH_2$ in mitochondria involve redox reactions that occur with the release of Gibbs free energy which is captured in oxidative-phosphorylation as ATP.

When one molecule of NADH is reoxidized to NAD^+, 2.5 ATP molecules are synthesized from $ADP + P_i(\frac{1}{2}O_2 + NADPH + H^+ \rightarrow NAD^+ + H_2O)$. In the case of $FADH_2$ reoxidation, 1.5 ATP molecules are synthesized $(FADH_2 + \frac{1}{2}O_2 \rightarrow FAD + H_2O)$.

The energetics of specific TCA Cycle reactions are shown in Table 9.1.

Table 9.1 The production of energy (ATP) in mitochondria from pyruvate

Enzyme system	Coenzyme (or nucleotide)	ATP equivalence
Pyruvate dehydrogenase[a]	NADH	2.5
Isocitrate dehydrogenase	NADH	2.5
α-ketoglutarate dehydrogenase	NADH	2.5
Succinate thiokinase	GTP	1
Succinate dehydrogenase	$FADH_2$	1.5
Malate dehydrogenase	NADH	2.5

[a]The pyruvate dehydrogenase complex is not part of the TCA cycle

Thus, when one molecule of pyruvate is oxidized in the TCA cycle, by the pyruvate dehydrogenase complex, and its electrons passed on to O_2 via oxidative phosphorylation, 12.5 ATP molecules are produced. Because glucose produces two pyruvates, 25 ATP molecules are formed in the process of oxidative phosphorylation. In glycolysis, two ATP molecules are produced from glucose. Thus when glucose is oxidized, a total of 27 ATP molecules are synthesized. Because oxidative phosphorylation is responsible for 25 of these molecules, 93% of the ATP molecules generated when glucose is oxidized to CO_2 and H_2O come from the pyruvate dehydrogenase complex and the TCA cycle.

The energetics, in terms of redox reactions are illustrated in the following example: Consider the pyruvate dehydrogenase reaction in which a single NADH molecule is generated.

The overall reaction for the reoxidation of NADH is:

$$NADH + H^+ + \frac{1}{2}O_2 \rightarrow NAD^+ + H_2O; \quad \varepsilon^o = +1.155\ V.$$

Table 9.2 Reduction potentials for redox systems

Reaction	Reduction potential (V)
$^1/_2O_2 + 2H^+ + 2e^- \rightarrow H_2O$	+0.815
$NAD^+ + H^+ + 2e^- \rightarrow NADH$	−0.34

The *Nernst equation* which allows one to convert voltage generated in a redox reaction to Gibbs free energy is, $\Delta G^0 = -\eta \times F \times \varepsilon^o$, where η is the number of electrons transferred per mole of reactants, F the Faradays (96.5kJ/Vxmol), and ε^o the voltage of the system. Table 9.2 provides the half-cell reduction potentials. Thus, $\Delta G^0 = -2 \times 96{,}500 \times 1.155 = -223$kJ/mol. The ΔG^0 of ATP hydrolysis is −30.5kJ/mol. Because 2.5 ATP molecules are synthesized per NADH oxidized, the theoretical efficiency of the phosphorylation coupled to oxidation is 34%. In the living cell, as opposed to the test tube where equilibrium thermodynamics prevail, the efficiency of oxidation coupled to ATP synthesis is believed to exceed 60%.

9.4 Stereochemistry of the TCA Cycle

Wood and Werkman [2] showed in 1936 that [^{13}C]CO_2 was fixed (incorporated) into biomolecules in bacteria. This was an extremely important discovery because until then it was believed that only plants could fix CO_2. It was later demonstrated that the isotopic CO_2 was incorporated *exclusively* into one of the carboxyl groups of α-ketoglutarate. It was concluded from these results that citrate, a symmetrical molecule, with a onefold axis of symmetry, could not be a member of the Citric Acid Cycle [3]. Examination of the TCA cycle, if this idea was correct, would predict that in the aconitase reaction, dehydration could occur either at the top or at the bottom end of citrate. Thus, there should be a 50–50% distribution of the [^{13}C] in isocitrate and α-ketoglutarate, and 50% of the synthesized succinate should be labeled. This conclusion was generally accepted by the biochemical community until 1948 when Ogston [4] showed that asymmetric attack could occur on a symmetrical molecule such as citrate. This hypothesis, known as the "*Polyaffinity Theory*," asserts that a symmetrical molecule can be attacked asymmetrically if the enzyme (itself asymmetrical) makes a three-point attachment to the substrate, i.e., this *precise three-point attachment* is a prerequisite for catalysis. How then does the Polyaffinity Theory account for asymmetric attack on citrate? Consider the prochiral carbon center shown in Fig. 9.7.

If the molecule is rotated 109.5° the following interactions between the enzyme and substrate are obtained.

Thus, making the assumptions described by the Polyaffinity Theory, the enzyme can discriminate between the two "b" groups on the substrate, i.e., only the orientation between the substrate and the enzyme described by interaction A, will allow catalysis to occur. Complexes B and C do not describe a three point attachment between enzyme and substrate, and are therefore not productive.

It should be pointed out that the Polyaffinity Theory is *not* valid for symmetrical molecules that have a twofold or greater axis of symmetry, e.g., succinate.

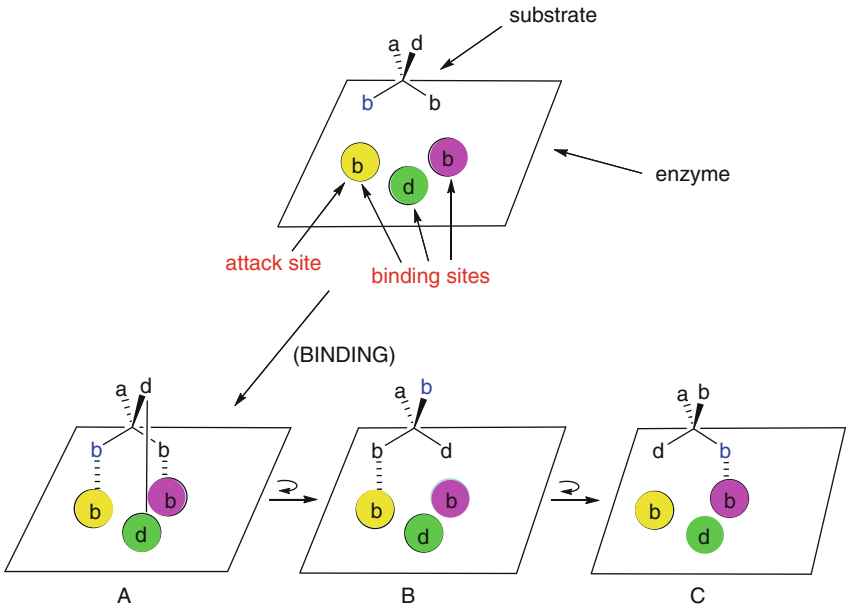

Fig. 9.7 A prochiral center can be attacked asymmetrically if the enzyme makes a precise three-point (A) attachment to the substrate. Other binding modes between the enzyme and substrate are unproductive

9.5 TCA Cycle Enzymes and Their Mechanisms

9.5.1 Citrate Synthase ($\Delta G^0 = -31.4$ kJ/mol)

One of the substrates for citrate synthase, oxaloacetate, has an sp^2 prochiral center. The other substrate, acetyl CoA, adds to the *si* face of oxaloacetate (Fig. 9.8).

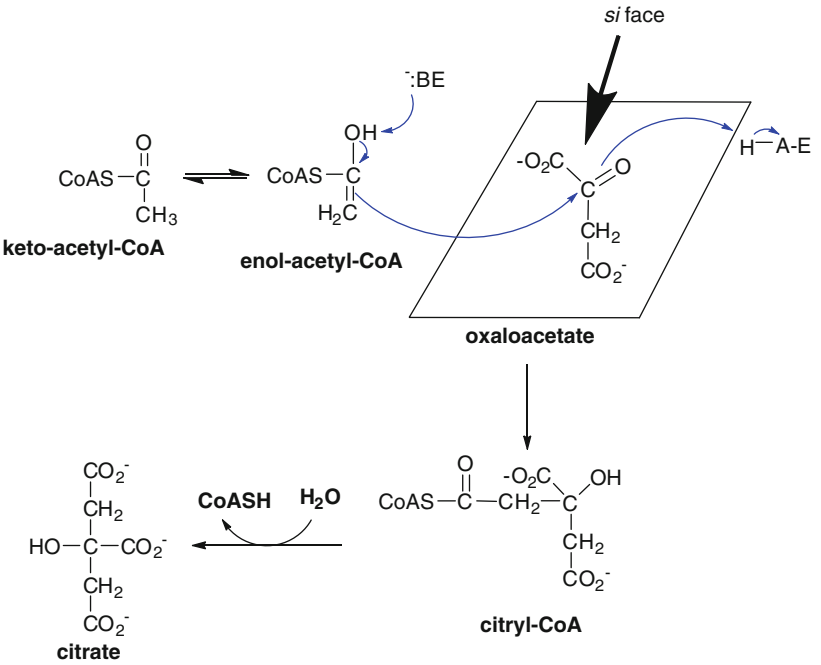

Fig. 9.8 The stereochemistry of the citrate synthase reaction: addition of acetyl-CoA to the *si* face of oxaloacetate

9.5.2 Aconitase ($\Delta G^0 = +5.0$ kJ/mol)

Aconatase catalyzes a two step reaction. First, it causes dehydration of citrate to form *cis*-aconitate. The second step involves hydration of *cis*-aconitate to yield isocitrate. The overall sequence of reactions results in an isomerization of the symmetrical citrate molecule to isocitrate in which there is no axis of symmetry.

Citrate has a onefold axis of symmetry, and dehydration occurs specifically at the pro-R arm of the substrate.

In order to maintain the correct stereochemistry of the isomerization reaction, it is assumed that *cis*-aconitate dissociates from aconitase, rotates or flips 180° and then rebinds. The *iron–sulfur cluster* interacts with the hydroxyl group so as to weaken the carbon–oxygen bond, thus enhancing the hydroxyl group's ability to act as a leaving group. The iron–sulfur cluster and the catalytic base that removes the H_R proton are not believed to move significantly. The function of the iron–sulfur cluster in aconitase is to bind the hydroxyl group that is first removed, and water that is added back to the substrate. It is not believed to be involved in a redox-type reaction in the case of aconitase (Fig. 9.9).

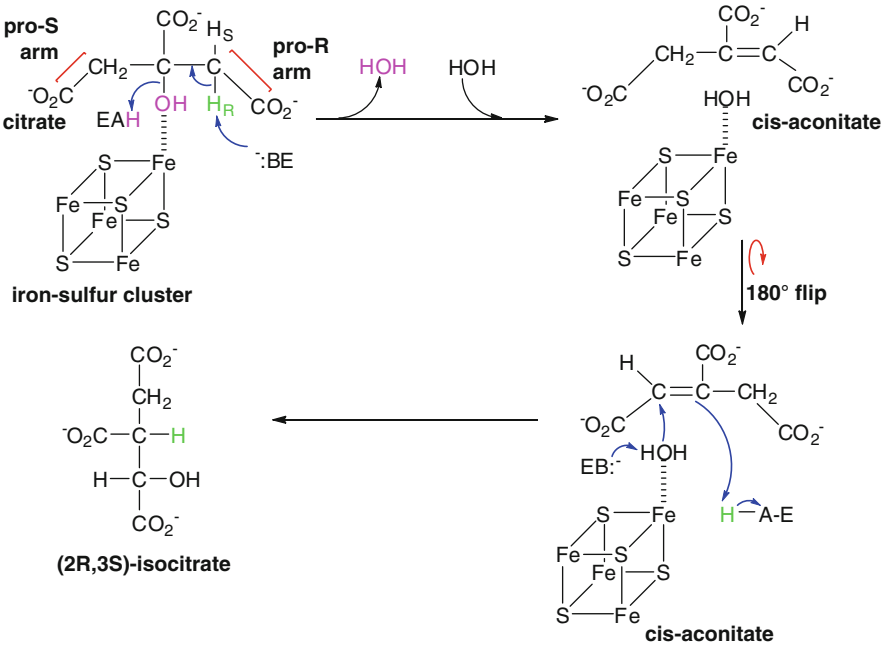

Fig. 9.9 The stereochemistry and mechanism of action of aconitase. The enzyme makes an asymmetrical attack on the symmetrical substrate citrate. The proton abstracted from citrate appears in isocitrate, and the hydroxyl group removed from citrate appears in water

9.5.3 Isocitrate Dehydrogenase ($\Delta G^0 = -20.9 kJ/mol$)

Isocitrate dehydrogenase is a typical pyridine-linked anerobic dehydrogenase; however, one of its reaction products oxalosuccinate is unstable in the presence of Mn^{2+}, a ubiquitous cation, and spontaneously decarboxylates to form α-ketoglutarate. Studies with enzyme mutants suggest that the decarboxylation occurs on the enzyme (Fig. 9.10).

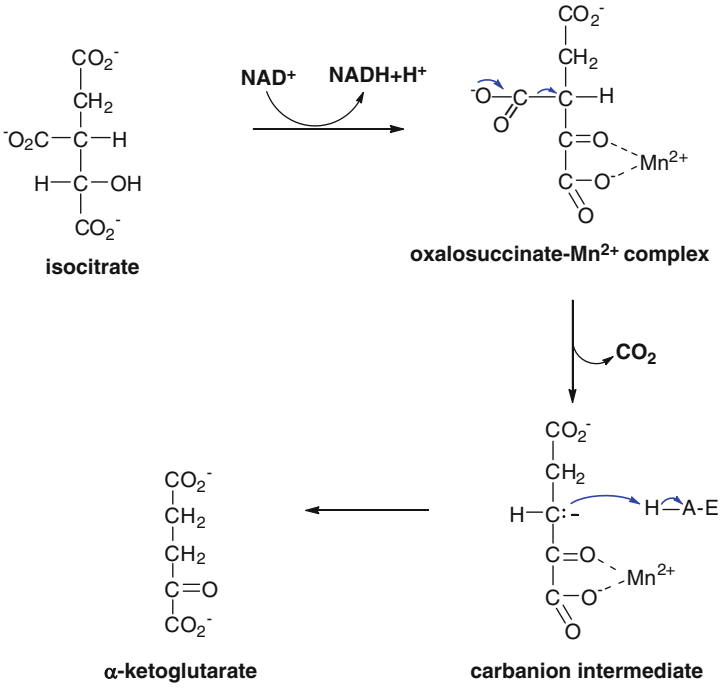

Fig. 9.10 The isocitrate dehydrogenase reaction involves both a redox and a decarboxylation reaction

9.5.4 α-Ketoglutarate Dehydrogenase ($\Delta G^0 = -32.9 kJ/mol$)

α-Ketoglutarate dehydrogenase is not a single enzyme but rather a complex similar to the pyruvate dehydrogenase complex. Like pyruvate dehydrogenase, the basic unit of the α-ketoglutarate dehydrogenase complex is a trimer, and the coenzymes are identical to those described for pyruvate dehydrogenase, as is the mechanism. After completion of the α-ketoglutarate dehydrogenase reaction, acetyl-CoA would have lost both of its carbon atoms in the form of CO_2.

9.5.5 Succinyl-CoA Synthetase ($\Delta G^0 = -2.1$ kJ/mol)

One of the products of the α-ketoglutarate dehydrogenase reaction is succinyl-CoA. In the presence of GDP and P_i, succinyl-CoA synthetase catalyzes a *substrate level* phosphorylation, i.e., GDP is phosphorylated by P_i to form GTP at the expense of succinyl-CoA, which like acetyl-CoA is a "high energy compound" (Chap. 7).

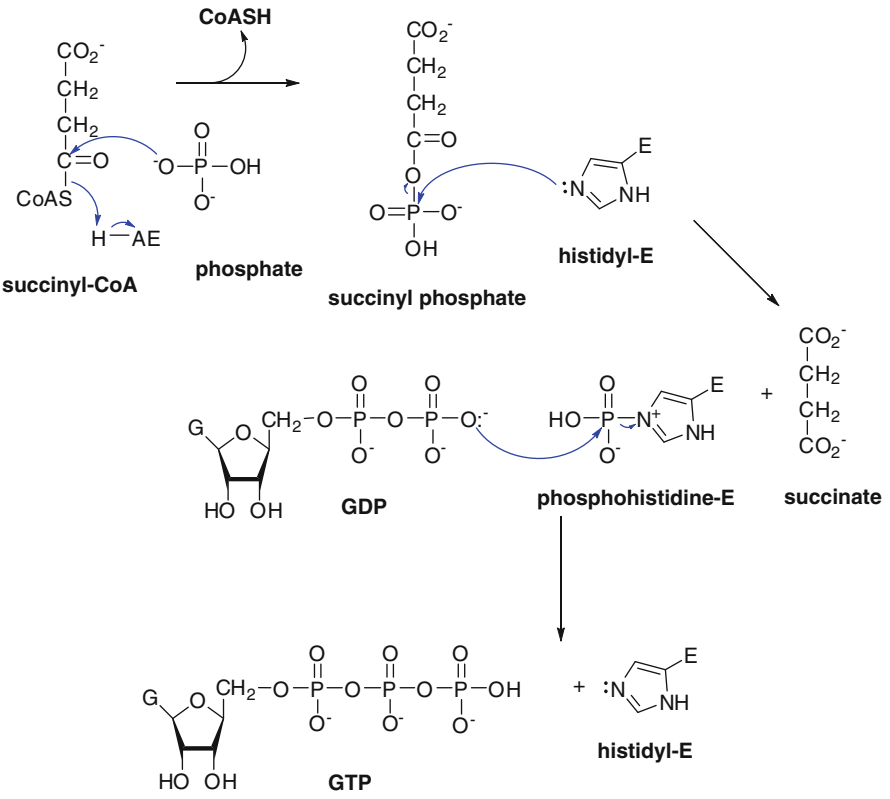

Fig. 9.11 Succinyl-CoA synthetase (succinate thiokinase) is involved in a substrate level phosphorylation. Enzyme-bound phosphohstidine is involved in covalent catalysis

The succinyl-CoA synthetase reaction involves the participation of a *phosphohistidine* intermediate, an example of covalent catalysis. Investigation of this enzyme in Boyer's laboratory in 1964 was the first example of the involvement of phosphohistidine as an intermediate in an enzyme catalyzed reaction [5] (Fig. 9.11).

9.5.6 Succinate Dehydrogenase ($\Delta G^0 = +6.0$ kJ/mol)

Succinate dehydrogenase oxidizes the symmetrical molecule succinate to fumarate by removing a pro-H_R from one carbon atom and a pro-H_S from the other. The hydrogens on the product are thus *trans*. One of the hydrogens leaves succinate as a proton and the other as a hydride ion. FAD is covalently bound to the enzyme in yeast through a histidine residue [6]. The reduced coenzyme $FADH_2$ is reoxidized by the electron transport chain (Fig. 9.12).

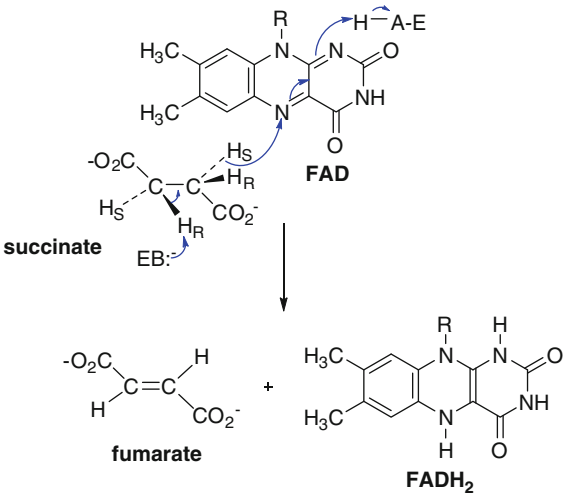

Fig. 9.12 The mechanism of the FAD-linked enzyme succinate dehydrogenase

9.5.7 *Fumarase ($\Delta G^0 = -3.4$ kJ/mol)*

The fumarase mechanism of action is not a settled issue at this time. Two proposals have been advanced that accord with data available in the literature. One involves a carbocation intermediate and the other a carbanion intermediate. The two mechanisms are illustrated in Fig. 9.13.

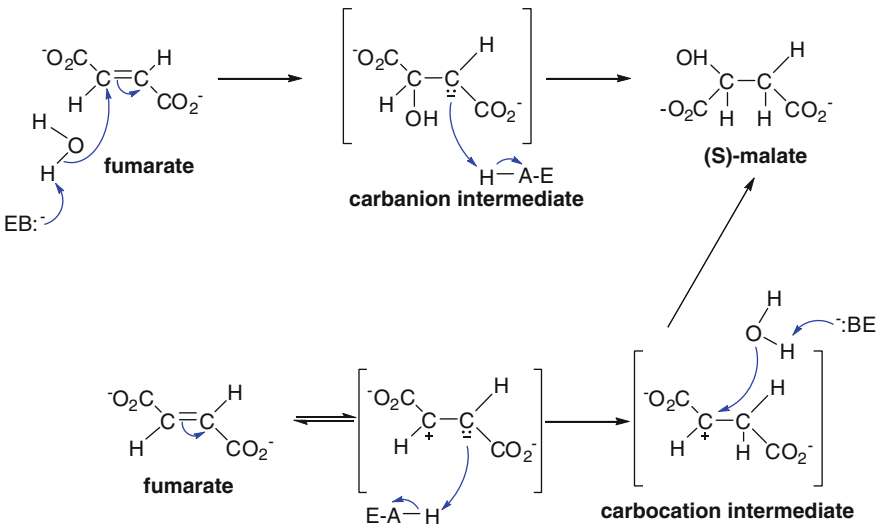

Fig. 9.13 Shown here are two proposals that have been advance as mechanisms for fumarase. The *upper mechanism* represents a hydration reaction involving a carbanion intermediate, whereas the intermediate in the *lower mechanism* is a carbocation

9.5.8 *Malate Dehydrogenase ($\Delta G^0 = +29.6$ kJ/mol)*

Malate dehydrogenase is the last enzyme in the TCA cycle. In this step malate is oxidized to oxaloacetate at the expense of NAD^+. The NADH produced in all of the TCA cycle reactions as well as $FADH_2$ generated at the succinate dehydrogenase step are reoxidized by the ETS, which is on the surface of the inner mitochondrial membrane, and thus in close proximity to the enzymes and products of the TCA cycle. With the formation of oxaloacetate from malate, the TCA cycle is completed and poised to accept a new molecule of acetyl-CoA for oxidation.

9.6 Regulation of Acetyl-CoA Oxidation

Control of acetyl-CoA degradation occurs at the pyruvate dehydrogenase and TCA cycle levels.

9.6.1 *Pyruvate Dehydrogenase Regulation*

The pyruvate dehydrogenase complex can be inhibited by covalent modification (phosphorylation of a serine residue on E_1), and by products NADH and acetyl-CoA. The enzyme responsible for phosphorylation of E_1, pyruvate dehydrogenase kinase, is activated by high levels of ATP, acetyl-CoA, and NADH and inhibited by pyruvate, and ADP. The fundamental role of the pyruvate dehydrogenase complex and the TCA cycle is to produce ATP from NADH and $FADH_2$. When ATP, NADH, and acetyl-CoA levels are high, pyruvate dehydrogenase kinase activity is activated and the flux through the pyruvate dehydrogenase complex is inhibited. Pyruvate dehydrogenase phosphatase, the enzyme that dephosphorylates phosphorylated E_1, is itself activated by the hormone insulin [7] and Mg^{2+}. The end result of phosphatase activation is the enhancement of acetyl-CoA degradation (Fig. 9.14).

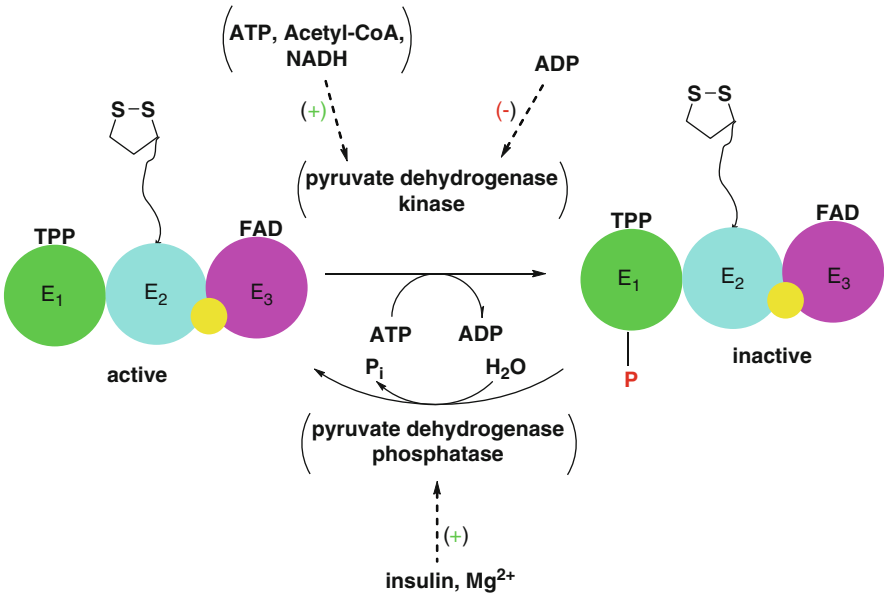

Fig. 9.14 Regulation of pyruvate dehydrogenase by phosphorylation and dephosphorylation of subunit E_1

9.6.2 TCA Cycle Regulation

The metabolic flux through the TCA cycle is controlled by factors such as the availability of acetyl-CoA, the rates of reoxidation of NADH and $FADH_2$, and the level of TCA cycle intermediates. It has been suggested that regulation of the TCA cycle depends upon those enzymes, such as citrate synthase, which are highly exergonic and catalyze "irreversible steps" in the cycle. As was shown earlier (Chap. 7), it is the mass action ratio and not exclusively the equilibrium constant of enzymes that determines whether they are potential regulatory steps in a metabolic pathway.

In vitro studies with various TCA cycle enzymes indicate that citrate is a competitive inhibitor of oxaloacetate in the citrate synthase reaction and that succinyl-CoA competes with acetyl-CoA in the citrate synthase reaction. In addition, Ca^{2+} is an activator of both pyruvate and α-ketogluterate dehydrogenase reactions.

The regulation of the TCA Cycle is summarized in Fig. 9.15.

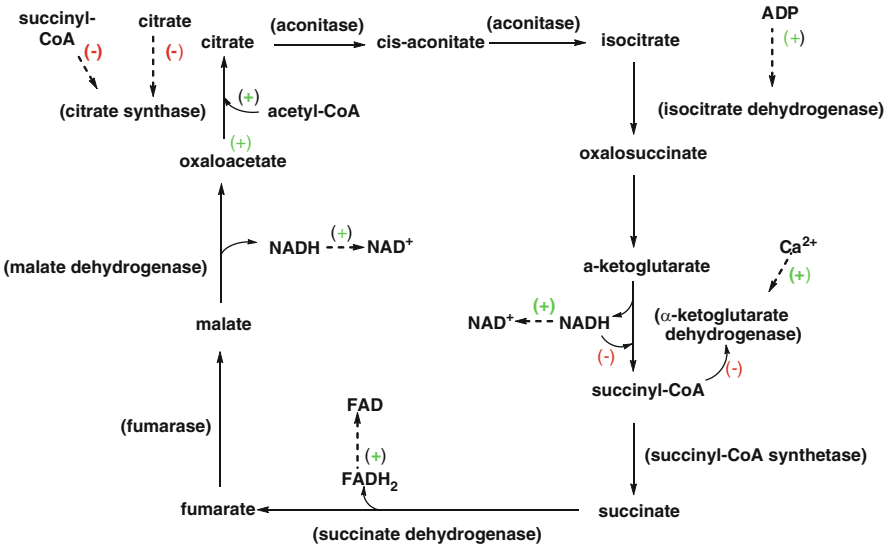

Fig. 9.15 Regulation of the TCA cycle by low molecular weight metabolites and ions

References

1. Reed LJ (2001) A trail of research from lipoic acid to α-keto acid dehydrogenase complexes. J Biol Chem 276:38329–38336
2. Wood HG, Werkman CH (1936) The utilisation of Co_2 in the dissimilation of glycerol by the propionic acid bacteria. Biochem J 30:48–53
3. Wood HG, Werkman CH, Hemingway A, Nier AO (1941) Mechanism of fixation of carbon dioxide in the Krebs cycle. J Biol Chem 139:483–484
4. Ogston AG (1948) Interpretation of experiments on metabolic processes using isotopic tracer elements. Nature 162:963
5. Mitchell RA, Butler LG, Boyer PD (1964) The association of readily-soluble bound phosphohistidine from mitochondria with succinate thiokinase. Biochem Biophys Res Commun 16: 545–550
6. Robinson KM, Lemire BD (1996) Covalent attachment of FAD to yeast succinate dehydrogenase flavoproteins requires import into mitochondria, presequence removal, and folding. J Biol Chem 271:4055–4060
7. Denton RM, McCormac K, Rutter GA, Burnett NJ, Edgill SK, Diggle TA (1996) The hormonal regulation of pyruvate dehydrogenase complex. Adv Enzyme Regul 36:183–198

Chapter 10
Electron Transport and Oxidative Phosphorylation

Cursory consideration of the TCA cycle (Chap. 9) reminds us that absent NADH and $FADH_2$ reoxidation, this cycle would quickly become substrate-limited and would promptly cease to function. Likewise, ATP is essential to drive biosynthesis and fuel the molecular motors that translocate macromolecules and transport metabolites. How then do cells prevent massive accumulation of NADH and $FADH_2$, while continually resupplying sufficient ATP? This conundrum is circumvented in mitochondria, not by substrate-level reactions analogous to glyceraldehyde-3-phosphate dehydrogenase and phosphoglycerate kinase within the cytosol, but by a series of redox reactions that electrochemically generate transmembrane proton gradients that are ultimately mechanochemically coupled to ATP synthesis. The latter reactions take place within mitochondria, and this chapter focuses on the logical arrangement and operation of the electron transport system and oxidative phosphorylation. A similar system allows chloroplasts to harvest photic energy electrochemically, again generating transmembrane proton gradients that are likewise coupled to ATP synthesis (Chap. 15).

When catabolic products of carbohydrates, lipids, and amino acids are oxidized in mitochondria, there is a concomitant release of large quantities of Gibbs free energy (ΔG). For example, the free energy of glucose oxidation to CO_2 and H_2O is -2867kJ/mol. Because the cell is not 100% efficient, not all of the energy released is transformed into useful work or ATP production; however, approximately 95% of the energy of glucose oxidation that is captured by the cell occurs by coupling the TCA cycle to the process known as oxidative phosphorylation.

For nearly a century, biochemists struggled to understand how mitochondria transform redox energy of NADH and $FADH_2$ in the reactions of the respiratory chain or electron transport system and how such energy is utilized or coupled at the molecular level to synthesize ATP. It is now known, even if not entirely understood, that the energy from electron transport, via a series of redox reactions, establishes a proton gradient between the mitochondrial matrix and the intermitochondrial membrane space. These translocated protons eventually flow back to the matrix, allowing ATP synthase to catalyze the synthesis of ATP from ADP and P_i.

H.J. Fromm and M.S. Hargrove, *Essentials of Biochemistry*,
DOI 10.1007/978-3-642-19624-9_10,

The process that couples electron transport and ATP synthesis can be separated into three phases. The first involves the respiratory or electron transport chain, the second proton translocation, and the third ATP synthesis.

Our understanding of how oxidative phosphorylation occurs at the molecular level is directly attributable to a number of pioneering investigators, among them Paul Boyer, Britton Chance, David Green, Peter Mitchell, Efraim Racker, John Walker, and Otto Warburg.

10.1 Electron Transport

We saw in Chap. 9 that the oxidation of NADH with the simultaneous reduction of oxygen produces 223 kJ/mol of free energy. Because the free energy of ATP hydrolysis is −30.5 kJ/mol, it would be disadvantageous to have a single coupling site when NADH is oxidized and ATP synthesized. There are in fact three such sites in mitochondria, when NADH is oxidized and 2.5 ATP molecules are synthesized for every NADH oxidized. In oxidative phosphorylation terms, this is referred to as a [*P*/*O*] ratio of 2.5. In the case of $FADH_2$ oxidation, the [*P*/*O*] ratio is 1.5 and examples exist for compounds, e.g., ascorbate, where the ratio is approximately 1.

There are five membrane-associated complexes involved in electron transport and ATP synthesis. Complexes I and II are involved in the oxidation of NADH and $FADH_2$, respectively, which are produced in the TCA cycle. They are also involved in electron transport, and in the case of Complex I, proton transport. Complexes III and IV transport electrons and protons, and in addition, Complex IV reduces O_2 to H_2O. Complex V, known as ATP-synthase, catalyzes the synthesis of ATP from ADP and Pi. The relationship among these complexes is shown in Fig. 10.1.

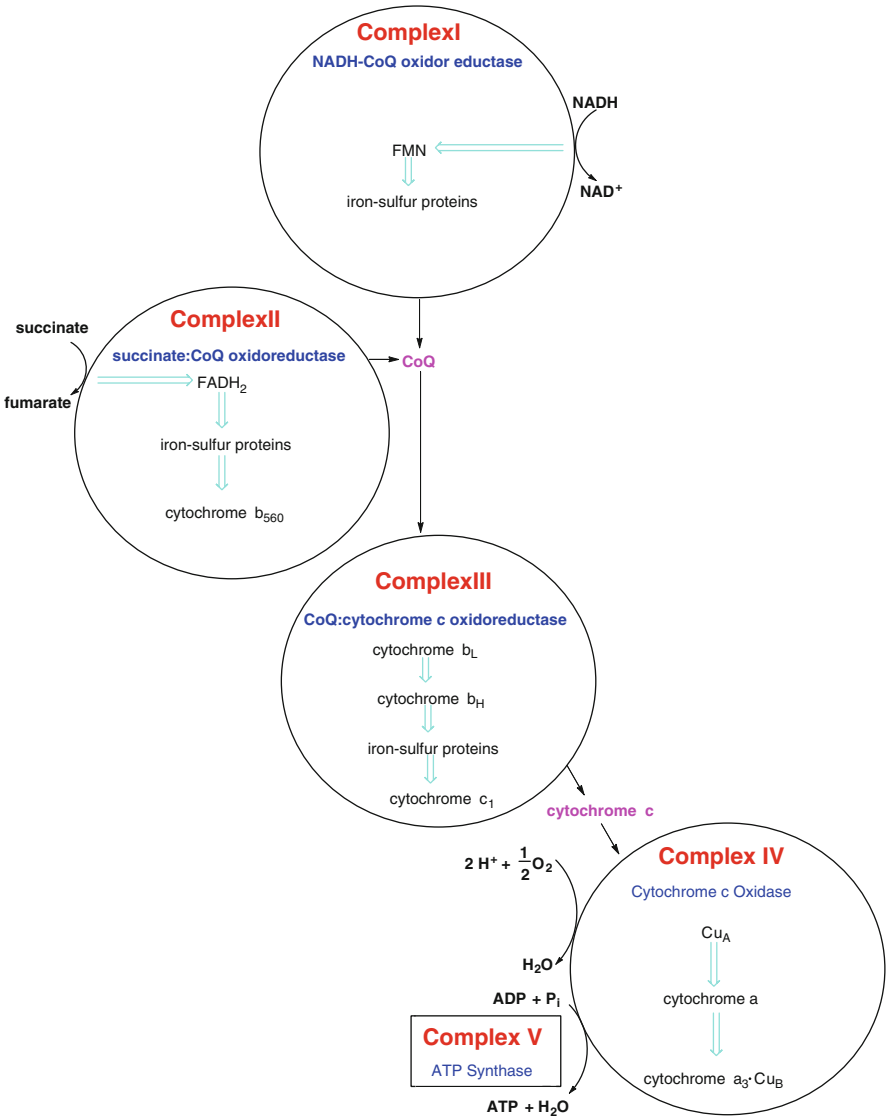

Fig. 10.1 The five complexes involved in electron transport and oxidative phosphorylation. The *arrows* indicate electron flow from the complex with the highest reduction potential to the complex with the lowest reduction potential. Electron flow within each complex is indicated by the large *bluish-green arrows*. The components within each complex are indicated within the *circles*

Table 10.1 contains the reduction potentials of some members of the electron transport chain. It is clear that electron flow along the respiratory chain is correlated with the reduction potentials in Table 10.1.

Table 10.1 Standard reduction potentials

System	n[a]	$E'_{0,}$ v
$NAD^+/NADH + H^+$	2	−0.32
$NADP^+/NADPH + H^+$	2	−0.32
$FMN/FMNH_2$	2	−0.30
$FAD/FADH_2$	2	−0.04
Cytochrome $b_L(Fe^{+3})$/Cytochrome $b_L(Fe^{+2})$	1	0.03
Cytochrome $b_H(Fe^{+3})$/Cytochrome $b_H(Fe^{+2})$	1	0.03
$CoQ/CoQH_2$	2	0.04
Cytochrome $c_1(Fe^{+3})$/Cytochrome $c_1(Fe^{+2})$	1	0.22
Cytochrome $c(Fe^{+3})$/Cytochrome $c(Fe^{+2})$	1	0.24
Cytochrome $a(Fe^{+3})$/Cytochrome $a(Fe^{+2})$	1	0.21
Cytochrome $a_3(Fe^{+3})$/Cytochrome $a_3(Fe^{+2})$	1	0.39
$½\ O_2 + 2H^+/H_2O$	2	0.82

[a] n represents the number of electrons involved in the reaction

10.2 Components of the Electron Transport Chain

10.2.1 Coenzyme Q

Coenzyme Q (CoQ) or *ubiquinone* is a membrane-associated redox-active metabolite that undergoes redox reactions of the type shown in Fig. 10.2. In animals, CoQ has ten isoprenoid units ($n = 10$), hence its often-abbreviated name is Co-Q_{10}.

CoQ is a mobile electron and proton carrier, able to leave the inner membrane and associate with Complex I, where it accepts electrons from $FMNH_2$ and the iron–sulfur proteins of Complex I in two successive one-electron transfers, as indicated in Fig. 10.3. Protons from the mitochondrial matrix provide the protons for $CoQH_2$ formation. CoQ is also reduced through the action of succinate dehydrogenase, which itself is a component of Complex II, by which succinate is oxidized to fumarate. It should be noted that Complex II does not pump protons. Oxidation of $CoQH_2$ takes place in Complex III.

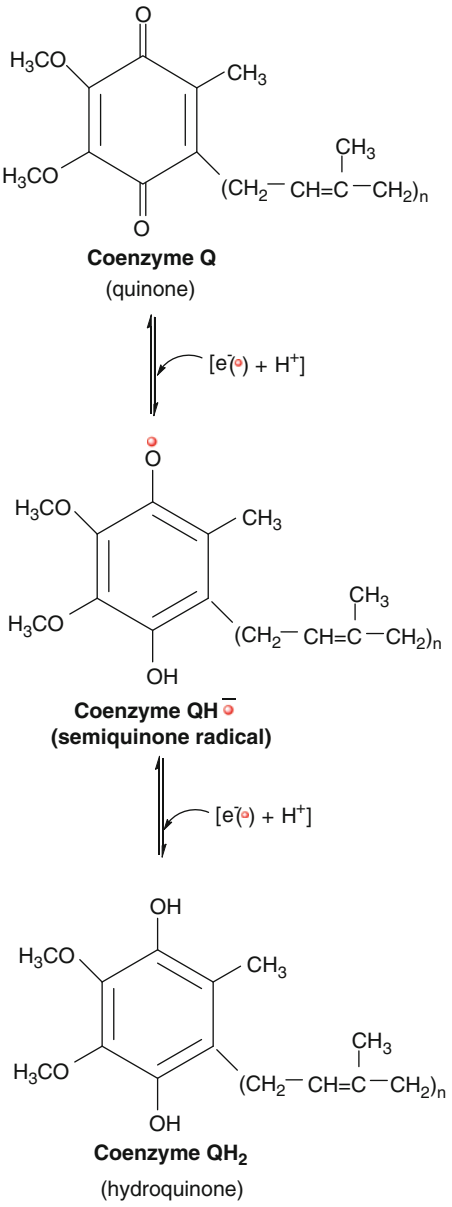

Fig. 10.2 The reduction of CoQ involves two successive one electron transfers

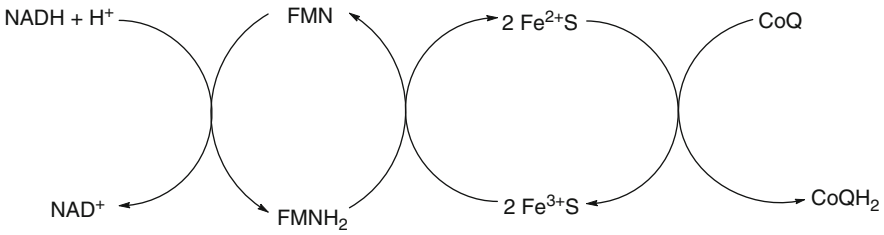

Fig. 10.3 Electrons in Complex I are passed on to CoQ in steps involving FMN and an iron–sulfur protein

10.2.2 Iron Sulfur Proteins

Iron–sulfur centers are associated with proteins as indicated in Fig. 10.4. All three iron–sulfur centers undergo redox-type reactions, involving both the ferrous and ferric states of the iron atom. These proteins are referred to as non-heme iron proteins, as opposed to other iron-containing proteins associated with the iron-containing prosthetic group heme.

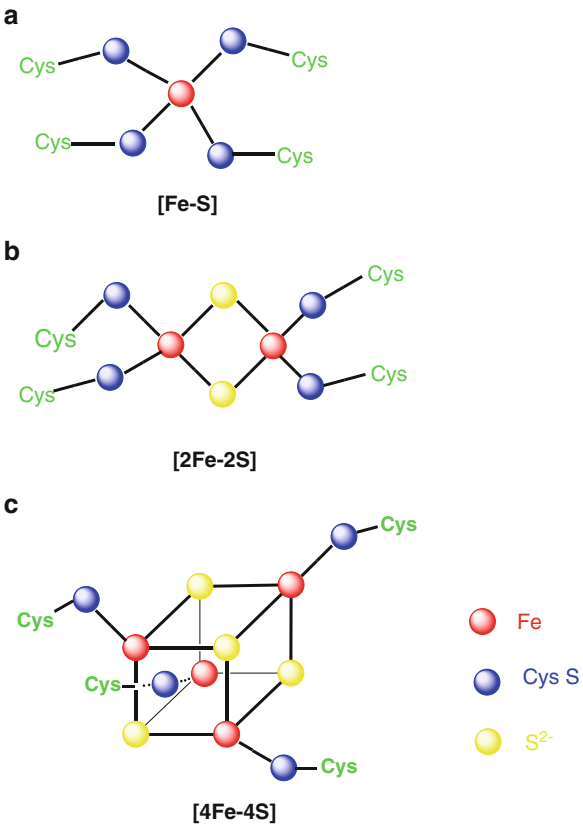

Fig. 10.4 Cartoon of the three types of iron–sulfur centers found in proteins. In all three centers the prosthetic groups are bound to the protein through the sulfur atom of a cysteinyl residue. The non-cysteinyl sulfur atoms have a -2 oxidation state. The structures are not intended to exhibit the exact geometry found with iron–sulfur centers in proteins

10.2.3 The Cytochromes

The cytochromes are a group of proteins that contain the heme prosthetic group; however, unlike heme in hemoglobin, the iron atom undergoes redox reactions involving both the ferrous and ferric states. These heme proteins are either red or brown in color and exhibit intense absorption spectra in the visible region.

The cytochromes were discovered by the British scientist David Keilin, who correctly inferred that the cytochromes were electron carriers involved in respiration [1].

Shown in Fig. 10.5 is Heme *a*, the prosthetic group found in cytochromes *a* and a_3. Note that Heme *a* is not covalently bound to its protein. On the other hand, the heme found in cytochromes *c* and c_1 (Fig. 10.6) is covalently bound to the protein through the cysteinyl sulfur atom.

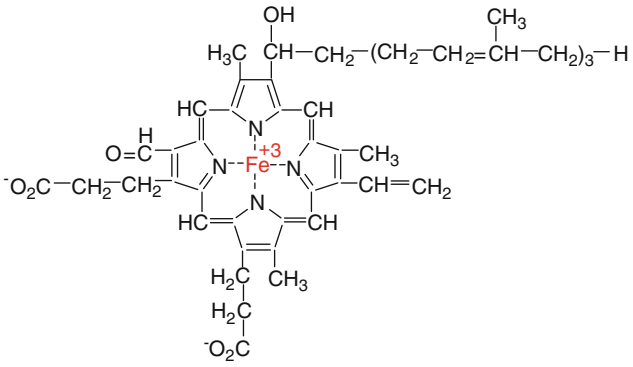

Heme *a*

Fig. 10.5 The structure of Heme *a* that is found in cytochromes *a* and a_3

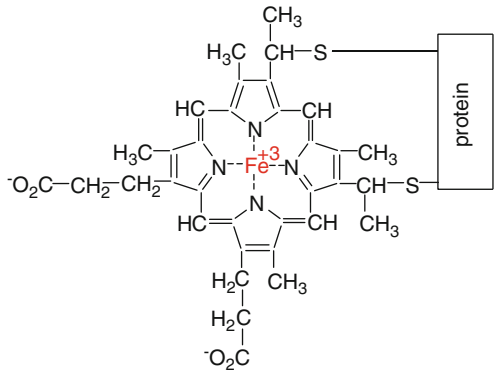

Heme *c*

Fig. 10.6 The structure of heme found in cytochromes *c* and c_1 is bound covalently to the protein

Like CoQ, cytochrome *c* is a mobile carrier of electrons between Complexes III and IV.

10.3 Electron and Proton Transport

Figure 10.1 illustrates the transport of electrons from NADH and $FADH_2$ down the respiratory chain to O_2. Three of the five complexes of the electron transport system also "pump" (or translocate) protons from the mitochondrial matrix to the intermembrane space (IMS); the exceptions being Complex II, which passes its protons on to CoQ and ATP synthase. It is through the latter complex that the protons flow back into the matrix from the IMS. The pumping of protons from the matrix to the IMS occurs against a concentration gradient and requires Gibbs free energy supplied by the electron transport chain. The stoichiometry of proton transport for Complexes I, III, and IV is as follows:

$$\text{Complex I: } \mathrm{NADH} + \mathrm{CoQ} + 5\mathrm{H}^{+}_{\text{matrix}} \rightarrow \mathrm{NAD}^{+} + \mathrm{CoQH_2} + 4\mathrm{H}^{+}_{\text{IMS}},$$

$$\text{Complex III: } \mathrm{CoQH_2} + 2\mathrm{H}^{+}_{\text{matrix}} + 2\text{Cyto } c\left(\mathrm{Fe}^{+3}\right) \rightarrow \mathrm{CoQ} + 4\mathrm{H}^{+}_{\text{IMS}} + 2\text{Cyto } c\left(\mathrm{Fe}^{+2}\right),$$

$$\text{Complex IV: } 4\text{Cyto } c\left(\mathrm{Fe}^{+2}\right) + 8\mathrm{H}^{+}_{\text{matrix}} + \mathrm{O_2} \rightarrow 2\mathrm{H_2O} + 4\text{Cyto } c\left(\mathrm{Fe}^{+3}\right) + 4\mathrm{H}^{+}_{\text{IMS}}.$$

The reaction shown in Complex III represents the overall reaction for the so-called Q Cycle which is composed of two separate reactions:

(a)
$$\mathrm{CoQH_2} + \text{Cyto } c\left(\mathrm{Fe}^{+3}\right) \rightarrow \mathrm{CoQ}^{-} + 2\mathrm{H}^{+}_{\text{IMS}} + \text{Cyto } c\left(\mathrm{Fe}^{+2}\right),$$

(b)
$$\mathrm{CoQH_2} + \mathrm{CoQ}^{-} + 2\mathrm{H}^{+}_{\text{matrix}} + \text{Cyto } c\left(\mathrm{Fe}^{+3}\right) \rightarrow \mathrm{CoQH_2} + 2\mathrm{H}^{+}_{\text{IMS}} + \mathrm{CoQ} + \text{Cyto } c\left(\mathrm{Fe}^{+2}\right)$$

The Q Cycle is not restricted exclusively to the electron transport chain in oxidative phosphorylation but also occurs in photosynthesis (Chap. 15).

We will see in the next section that this proton differential between the IMS and the mitochondrial matrix produces a ΔpH that provides the energy for ATP synthesis from ADP and P_i.

10.4 The Chemiosmotic Hypothesis

Scientists in the oxidative phosphorylation field spent many years fruitlessly attempting to detect chemical intermediates that might be involved in the process. These efforts proved to be uniformly unsuccessful, but in 1961, Peter Mitchell proposed a radically new hypothesis, termed the Chemiosmotic Theory, to explain

how electron transport might be coupled to ATP synthesis [2]. Although disputed for nearly two decades, his ideas are widely accepted today and Mitchell was awarded the Nobel Prize for his research.

The chemiosmotic hypothesis states that electron transport along the respiratory chain provides the energy for "*active transport*" (transport of a solute against a concentration gradient) of protons from the matrix of the mitochondrion across the inner-membrane to the IMS. This "pumping" of protons results in a lowering of the pH of the IMS relative to the matrix. Because of the establishment of this pH gradient, protons would be thermodynamically inclined to flow back across the inner membrane so as to neutralize the pH gradient. This is a manifestation of "*passive transport*" as opposed to active transport; transport that requires the input of energy. In so doing, they provide the energy required, for conformational changes in ATP synthase, that allow for the synthesis of ATP from ADP and P_i.

When measurements were made to test the chemiosmotic hypothesis, it was found that the pH of the IMS in mitochondria is less, by a factor of 1.4 units, than the pH of the matrix. This pH differential, or gradient, generates an electrical potential across the inner membrane. Both effects (membrane potential and pH gradient) together are known as the *proton motive force* (Δp). Expressed as an equation, Δp is the sum of the pH gradient (the negative value comes from the -1.4 unit pH differential) and the membrane potential, or

$$\Delta p = \text{membrane potential} - \Delta\text{pH}.$$

The proton pumps, which are transmembrane proteins, are unidirectional in their action. Complexes I, III, and IV pump protons from the mitochondrial matrix to the IMS. On the other hand, Complex V (ATP synthase) which is also unidirectional for protons, facilitates the diffusion of H^+ from the IMS back into the matrix. The stoichiometry of ATP synthase requires the translocation of three protons per ATP synthesized.

Figure 10.7a–c summarizes the action of the various respiratory complexes with respect to proton and electron transfer.

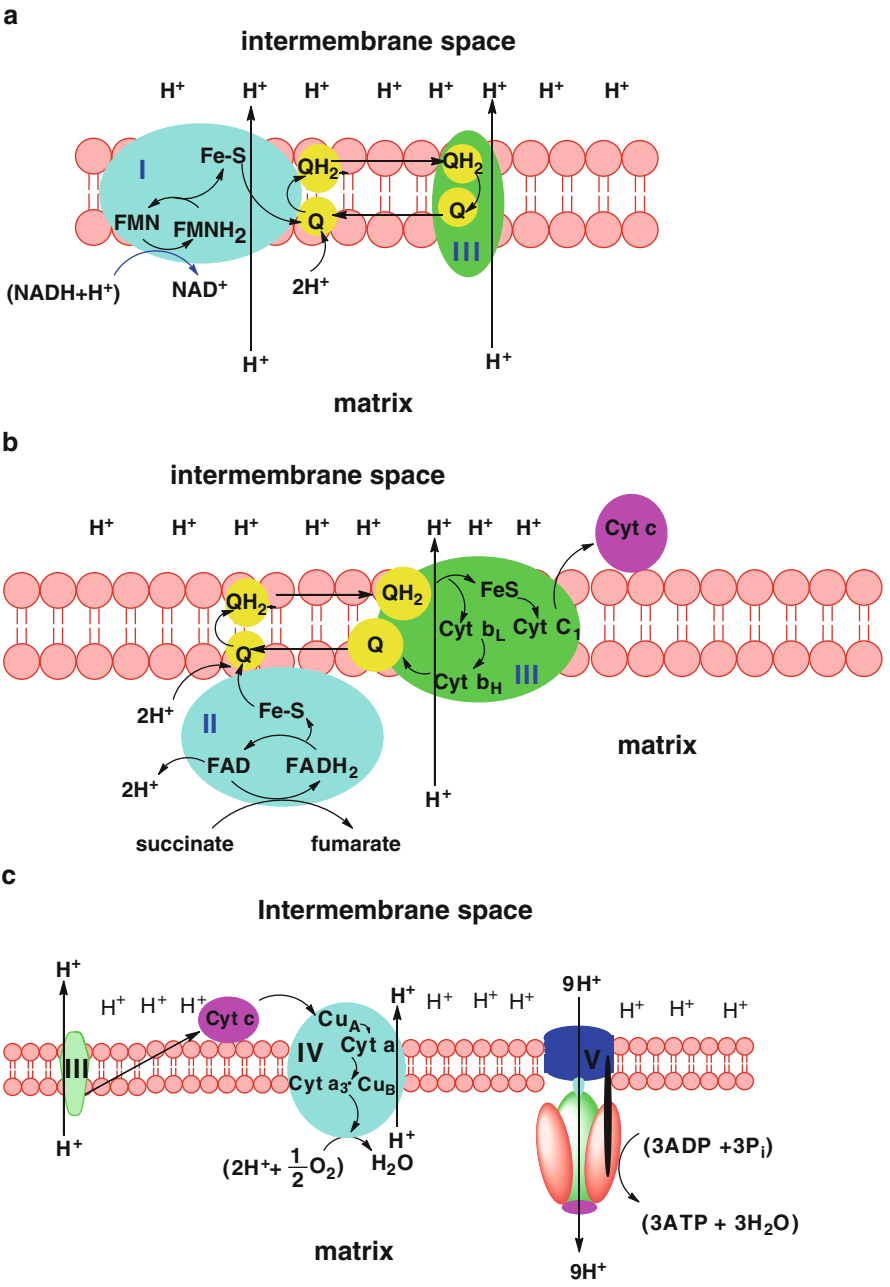

Fig. 10.7 (**a**) The relationship between the respiratory chain, chemiosmosis, and ATP synthesis. Electron flow down the electron transport chain from Complex I to Complex III in which CoQ is reduced to $CoQH_2$. Reoxidation of $CoQH_2$ occurs in complex III (**b**). The relationship between the respiratory chain, chemiosmosis, and ATP synthesis. Electron flow down the electron transport

10.5 ATP Synthase

ATP synthase, or F_0F_1-ATPase, is the site of ATP synthesis in oxidative phosphorylation. ATP synthesis activity requires that Complex V be intact. Before the mechanism of action of ATP synthase was understood it was found that disruption of the native complex gave rise to ATPase activity; hence the name F_0F_1-ATPase.

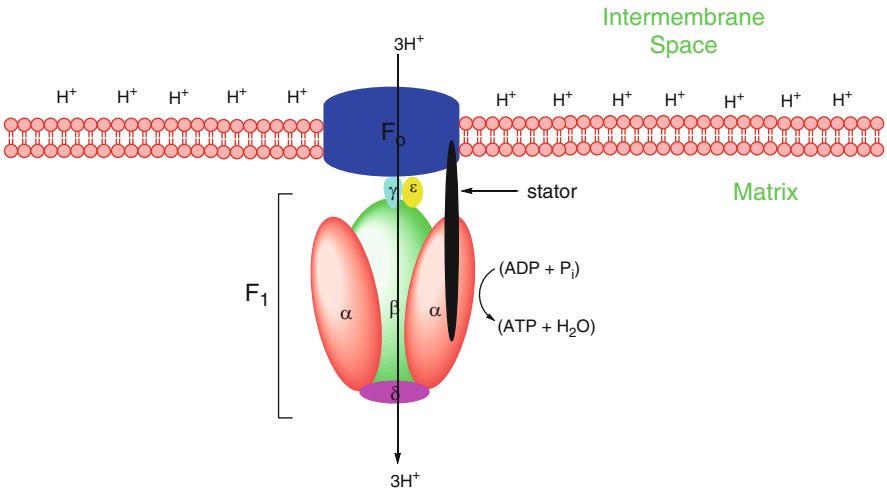

Fig. 10.8 Cartoon drawing of F_0F_1-ATPase. The F_0 portion of ATP synthase, which is a transmembrane protein, is embedded in the inner mitochondrial membrane, whereas F_1 extends into the mitochondrial matrix. When F_0 turns in a rotary fashion, powered by the electron transport chain, energy is transmitted to F_1 through the γ-subunit which is bound to F_0. The F_1 unit then undergoes a series of conformation changes (see Fig. 10.9) leading to the synthesis of ATP from ADP and P_i. The stator prevents the F_1 subunit from rotating on its own. The names of the various subunits are indicated in the figure

10.5.1 The Binding Change Mechanism

Shown in Fig. 10.8 is a cartoon representation of ATP synthase, which consists of two major components: F_0, which is embedded in the inner mitochondrial membrane; and F_1, which contains the catalytic site and extends into the matrix. F_0 is a rotary molecular motor, and F_0 and F_1 are connected by a shaft, the γ and ε subunits. The energy for the movement of F_0 is provided by the redox reactions

Fig. 10.7 (continued) chain from Complex II to Complex III in which CoQ is reduced to $CoQH_2$. No protons are pumped from the matrix to the intermembrane space at Complex II. Reoxidation of $CoQH_2$ occurs in complex III. (**c**). The relationship between the respiratory chain, chemiosmosis, and ATP synthesis. Electron flow down the electron transport chain from Complex III to Complex IV. Cytochrome *c* is the mobile carrier of electrons between Complex III and Complex IV

of the respiratory chain. On the other hand, the movement within F_1 is mechanical, i.e., it is powered by its force-driven connection to F_0. Overall, ATP synthase transforms electrical energy into chemical energy in the form of ATP.

Movement of F_1 components allows it to assume three different conformational states. This ingenious mechanism, known as the "Binding Change Mechanism" is a type of protein cooperativity that progressively modulates the synthase's affinity for its substrates ADP and Pi as well as its products ATP and H_2O. The Binding Change Mechanism was proposed by Paul Boyer [3] and is supported by a wealth of experimental chemical and physical data, including X-ray diffraction studies initiated by Walker [4]. Both scientists shared the Nobel Prize for their contributions to our understanding of oxidative phosphorylation. Excellent review articles on this subject are available [5, 6].

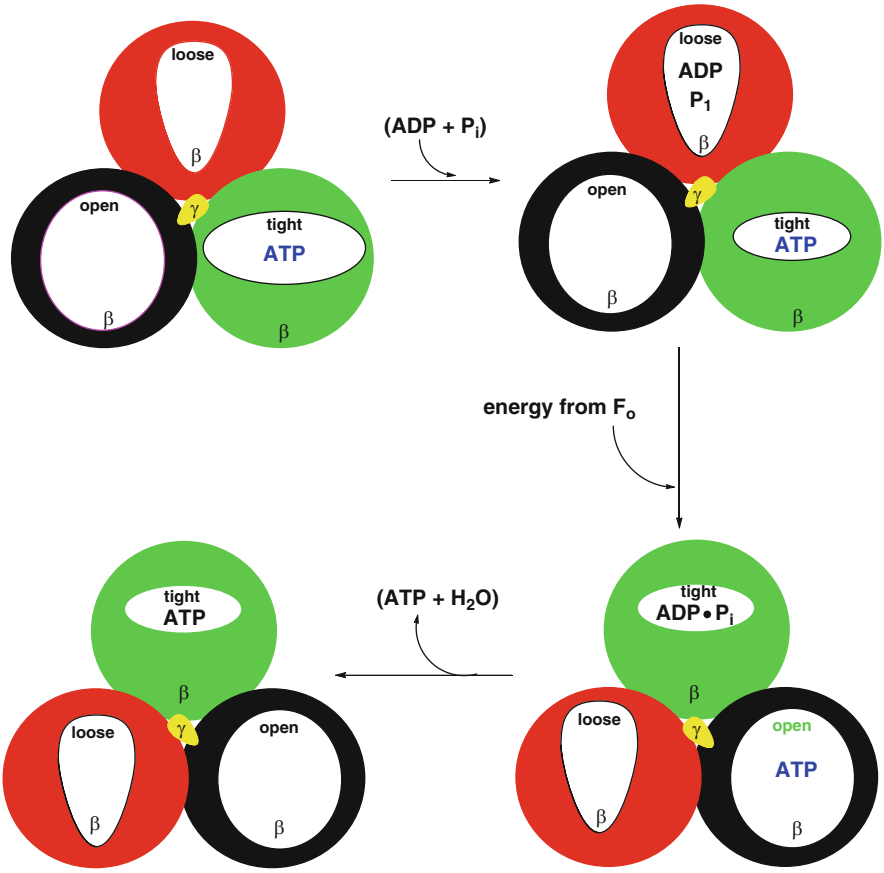

Fig. 10.9 The synthesis of ATP from ADP and P_i in the F_1 portion of ATP synthase as described by Boyer's binding change mechanism. Energy transduction from F_0 is responsible for formation of the phosphoanhydride bond in the "tight" subunit as well as conformational changes in the other subunits. The *Greek letters* indicate the subunit designations

In the Binding Change Mechanism, ADP and P_i bind to a so-called "*loose*" binding site. A conformational change in F_1, driven by the rotary movement of F_0, converts the loose substrate binding site into a "*tight*" binding site. It is at this site that a phosphoanhydride bond is formed between ADP and P_i with concomitant conversion of the tight site to an "*open*" site and the conversion of the open site back to a loose site. This cycle is then repeated and another molecule of ATP is formed. This sequence of events that occurs within the F_1 portion of the synthase is illustrated in Fig. 10.9.

10.5.2 Chemical Mechanism of the ATP Synthase Reaction

ATP synthase can function by two chemical mechanisms: a negatively charged oxygen atom from the β phosphoryl group of ADP can attack the inorganic orthophosphate, or a phosphate oxygen can make a nucleophilic attack on the β phosphorous atom of ADP. The mechanism shown in Fig. 10.10 was arrived at using [^{18}O] HPO_3^{2-} which shows the heavy isotope appearing in water and not in the β–γ bridge oxygen of ATP.

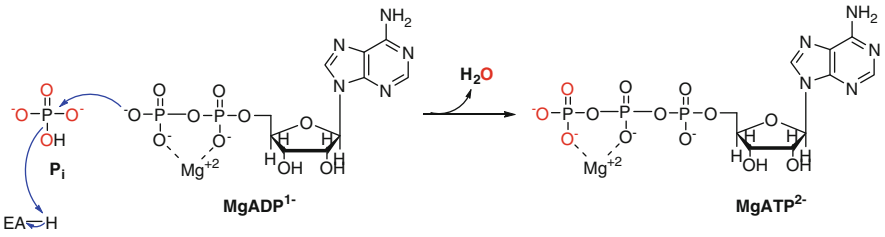

Fig. 10.10 The chemical mechanism of the ATP synthase reaction. [^{18}O] P_i is indicated in *red*. The β phosphoryl group of ADP attacks the phosphorous atom of P_i

10.6 Transport of Nucleotides and P_i Through Mitochondrial Membranes

Most of the ATP synthesized in eukaryotic cells is utilized for anabolic reactions either in other organelles or in the cytoplasm. The inner mitochondrial membrane is impermeable to ATP as well as ADP and P_i. When ATP leaves the mitochondrial matrix for passage through the inner membrane, an equivalent amount of ADP and P_i enters that compartment. ATP and ADP are transported in opposite directions, but they are transported by the same transport system, *adenine nucleotide translocase* (ANT). This type of system, which moves solutes in opposite directions is known as an *antiport* system. On the other hand, systems that move solutes,

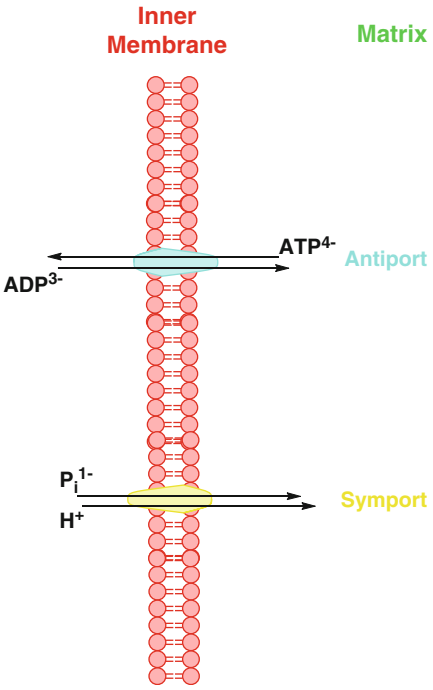

Fig. 10.11 Examples of an antiport transport system involving ADP and ATP and a symport transport system involving P_i and H^+ ions

such as P_i and H^+ in the same direction, are referred to as *symport* systems. The distinction between these two types of transport systems is illustrated in Fig. 10.11.

10.7 The Fate of NADH in Aerobic Tissue

When considering glycolysis (Chap. 8), it was pointed out that in "anerobic tissues," such as skeletal muscle, NADH produced in glycolysis is oxidized in the lactate dehydrogenase reaction. On the other hand, tissues that are aerobic (rich in mitochondria), such as brain, take advantage of *shuttle mechanisms* to oxidize NADH. By so doing, 1.5 ATP equivalents (i.e., 1.5 P–O–P phosphoanhydride bonds) are formed for every NADH molecule converted to NAD^+. Theoretically, each NADH molecule gives an ATP equivalent of 2.5; however, in the Glycerol-phosphate Shuttle (Fig. 10.12) the NADH electrons are passed on to a flavoprotein which when oxidized yields 1.5 ATP equivalents.

NADH within the cytosol is not capable of entering mitochondria; however, it can be oxidized in the presence of dihydroxyacetone phosphate by glycerol phosphate dehydrogenase. The product, glycerol-3-P, can enter the mitochondrion and in the presence of a membrane-bound flavoprotein dehydrogenase can yield $FADH_2$ and dihydroxyacetone phosphate. The $FADH_2$ is then utilized by the electron

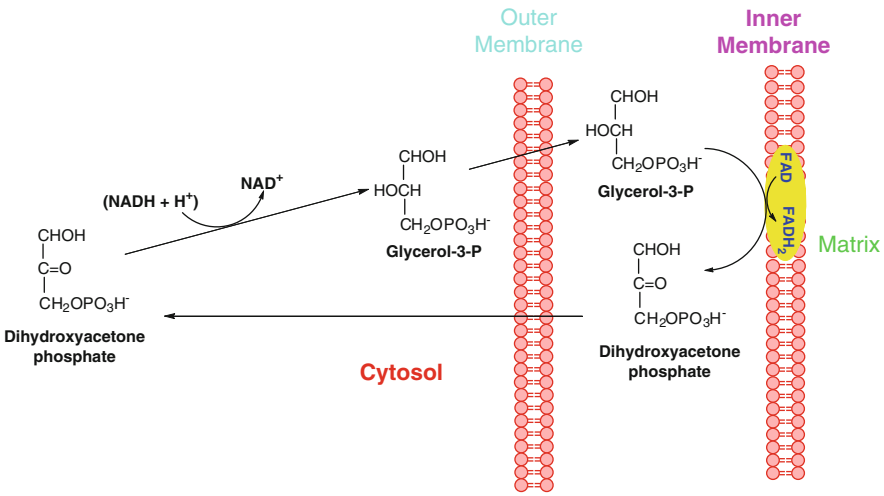

Fig. 10.12 The Glycerolphosphate Shuttle allows the reducing power of cytosolic NADH to be utilized in mitochondria. Glycerol-3-P is synthesized in the cytosol and passes into the mitochondria where it is oxidized to dihydroxyacetone phosphate which the reenters the cytosol

transport system of the inner mitochondrial membrane. The Glycerolphosphate Shuttle system is shown in Fig. 10.12.

10.8 The Regulation of Oxidative Phosphorylation

The role of oxidative phosphorylation is to produce ATP and reoxidize the coenzymes (NADH, $FADH_2$, and $FMNH_2$). There is no evidence for direct regulation of oxidative phosphorylation. Other pathways, such as glycolysis, and most importantly the TCA cycle, are the primary regulators of oxidative phosphorylation by providing the substrates (reduced coenzymes) for its activity.

10.9 Inhibitors of Oxidative Phosphorylation

A large number of compounds were used to study oxidative phosphorylation. Many of these compounds were "*uncouplers*" of oxidative phosphorylation (i.e., in their presence, electron transport occurs, but without ADP phosphorylation taking place). The best known uncoupler is *2,4-dinitrophenol* (DNP), a lipid-soluble molecule that is capable of passing from the cytosol face to the innermost mitochondrial membrane face. Because dinitrophenol can exist either as a phenol or as a phenolate anion, it serves as a proton shuttle. On the cytocylic side of the inner mitochondrial membrane, DNP takes up protons and exists as 2,4-dinitrophenol.

In so doing, DNP neutralize (or dissipates) the pH gradient so essential for ATP synthase activity. Thus, ATP synthesis will not occur, even though electron transport persists. The end-result of such uncoupling of electron transport and phosphorylation is the generation of heat. In the early twentieth century, redox uncouplers were used to promote weight loss, a practice no longer in use due to potentially deadly effects when oxidative phosphorylation is overly disrupted.

References

1. Keilin D (1926) On cytochromes, a respiratory pigment, common to animals, yeast, and higher plants. Proc R Soc London 98:312–339
2. Mitchell P (1961) Coupling of phosphorylation to electron and hydrogen transfer by a chemiosmotic type of mechanism. Nature 191:144–148
3. Boyer PD (1993) The binding change mechanism for ATP synthase. Biochim Biophys Acta 1140:215–250
4. Abrahams JP, Leslie AGW, Lutter R, Walker JE (1994) Structure at 2.8 Å resolution of F_1-ATPase from bovine heart mitochondria. Nature 370:621–628
5. Boyer PD (1997) The ATP synthase-a splendid molecular machine. Annu Rev Biochem 66:717–749
6. Walker JE (2000) (ed) The mechanism of F_oF_1-ATPase. Biochim Biophys Acta 1458:221–514

Further Readings

Hatefiy Y (1985) The mitochondrial electron transport chain and oxidative phosphorylation system. Annu Rev Biochem 54:1015–1069

Racker E (1980) From Pasteus to Mitchell: a hundred years of bioenergetics. Fed Proc 39:20–15

Schultz BE, Chan SJ (2001) Structures and proton-pumping strategies of mitochondrial respiratory enzymes. Annu Rev Biophys Biomol Struct 30:23–65

Chapter 11
Carbohydrate Metabolism B: Di-, Oligo-, and Polysaccharide Synthesis and Degradation

Sugars, other than monosaccharides, are among the most important classes of biomolecules in nature. Most of the carbon in living organisms exists in higher-order sugars. No other class of compounds fulfills more roles in living systems than carbohydrates. This chapter describes the better known higher-order carbohydrates; their structure, function, and metabolism.

11.1 Disaccharide Synthesis and Degradation

11.1.1 Sucrose (Table Sugar)

Sucrose is produced in plants and used to fulfill a number of important metabolic functions: It is a major product of photosynthesis and is the primary transport metabolite from leaves to other organs. In addition, it is a primary source of energy in plants. Sucrose is hydrolyzed in the intestine by the enzyme *sucrase (invertase)* to D-glucose and D-fructose. The disaccharide is synthesized by two enzymes, *sucrose phosphate synthase* and *sucrose-6-P phosphatase*. The sequence of reactions involving these two enzymes is:

(a) UDP-α-D-glucose + fructose-6-P → sucrose-6-P + UDP (sucrose phosphate synthase)
(b) Sucrose-6-P + H_2O → sucrose + P_i (sucrose-6-P phosphatase)

The structure of sucrose involves an α-1(glucose) → β-2(fructose) glycosidic linkage (Fig. 11.1).

Stereochemically, in the sucrose synthase reaction, there is a retention of configuration at the C-1 position of glucose, i.e., going from a C-1α in the donor substrate UDP-α-D-glucose to a C-1α in the product. Possible mechanisms for

H.J. Fromm and M.S. Hargrove, *Essentials of Biochemistry*,
DOI 10.1007/978-3-642-19624-9_11, © Springer-Verlag Berlin Heidelberg 2012

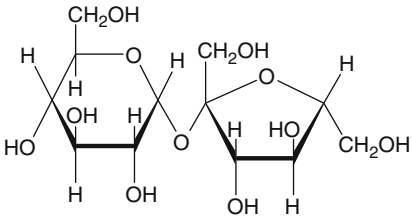

Fig. 11.1 The structure of the disaccharide sucrose

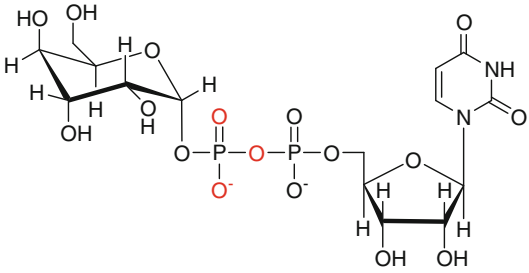

Fig. 11.2 UDP-α-D-glucose labeled with ^{18}O (*red*)

sucrose synthase are S_N1, two S_N2 reactions (covalent catalysis), and a single S_Ni reaction.

Singh et al. [1] used [β-$^{18}O_2$, αβ-^{18}O] UDP-glucose to study isotope scrambling, but found that no scrambling occurred with the enzyme and UDP-α-D-glucose. The open-circled oxygens are ^{16}O and the red-circled oxygens ^{18}O for the compound used in the scrambling studies (Fig. 11.2).

Thus, they were able to eliminate an oxocarbonium ion intermediate (S_N1), assuming that there is no impediment to free rotation of the β-phosphoryl group of UDP on the enzyme. This protocol also serves to eliminate mechanisms involving covalent catalysis. Therefore, the remaining possibilities consistent with the scrambling data are either an S_Ni reaction or an S_N1 reaction in which free rotation of the β-phosphoryl group of UDP does not occur. The S_Ni mechanism has been suggested, based on X-ray diffraction data, for a UDP-galactosyl transferase enzyme in which a retention of configuration was observed [2].

The mechanism of the invertase, or sucrase reaction, is better understood than that of sucrose phosphate synthase. The reaction consists of two steps: the first involves the formation of an oxonium ion intermediate and the second, nucleophilic attack by a OH^- generated from H_2O by the reaction of a basic group on the enzyme with a water proton (Fig. 11.3).

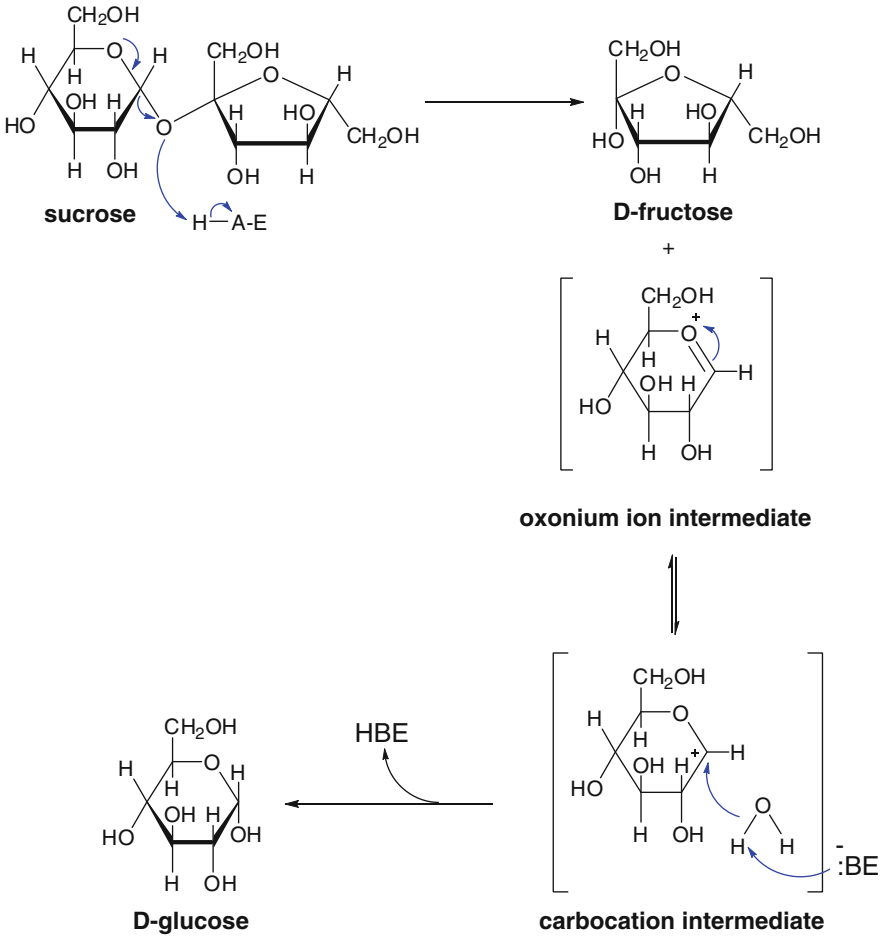

Fig. 11.3 The mechanism of the sucrase (invertase) reaction involves an oxonium ion intermediate

11.1.2 Lactose

Lactose is a disaccharide found exclusively in mother's milk and is known as "milk sugar." It is composed of D-galactose and D-glucose joined by a β-(1 → 4) glycosidic linkage (Fig. 11.4).

The enzyme *lactose synthase* is composed of two different subunits: a *galactosyl transferase* subunit which is present in the endoplasmic reticulum of the mammary

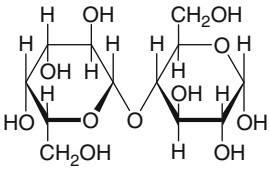

Fig. 11.4 The structure of lactose, a disaccharide composed of D-glucose and D-galactose

gland and α-*lactalbumin*, a protein that appears in mother's milk. The transferase subunit transfers galactosyl units to a variety of accepters. Accepter specificity for glucose is determined by α-lactalbumin. The reaction catalyzed by the synthase is:

$$\text{UDP-D-galactose} + \text{D-glucose} \rightarrow \text{lactose} + \text{UDP}.$$

A number of authors suggest that the substrate in other galactosyl transfer reactions is UDP-α-D-galactose [2]. If the substrate in the lactose synthase reaction is indeed UDP-α-D-galactose, as suggested from X-ray diffraction studies, than either an S_N1 or an S_N2 mechanism may be invoked to explain the stereochemistry of the reaction. The S_N1 case is less convincing based on kinetic studies which show the kinetics are sequential (rapid-equilibrium random) and not Ping Pong [3]; however, if the reaction does involve a galactosyl-enzyme intermediate and UDP does not dissociate before the addition of glucose, the kinetics will be sequential (see Appendix to Chap. 5). At present there is no experimental evidence to support an S_N1 type reaction, i.e., an oxocarbonium ion intermediate from isotope scrambling. X-ray diffraction crystallographic studies suggest that the substrates associate on the enzyme as indicated in Figs. 11.5 and and not as shown in 11.6 [4]. Thus, the most likely mechanism for the lactose synthase reaction is S_N2 as shown in Fig. 11.5.

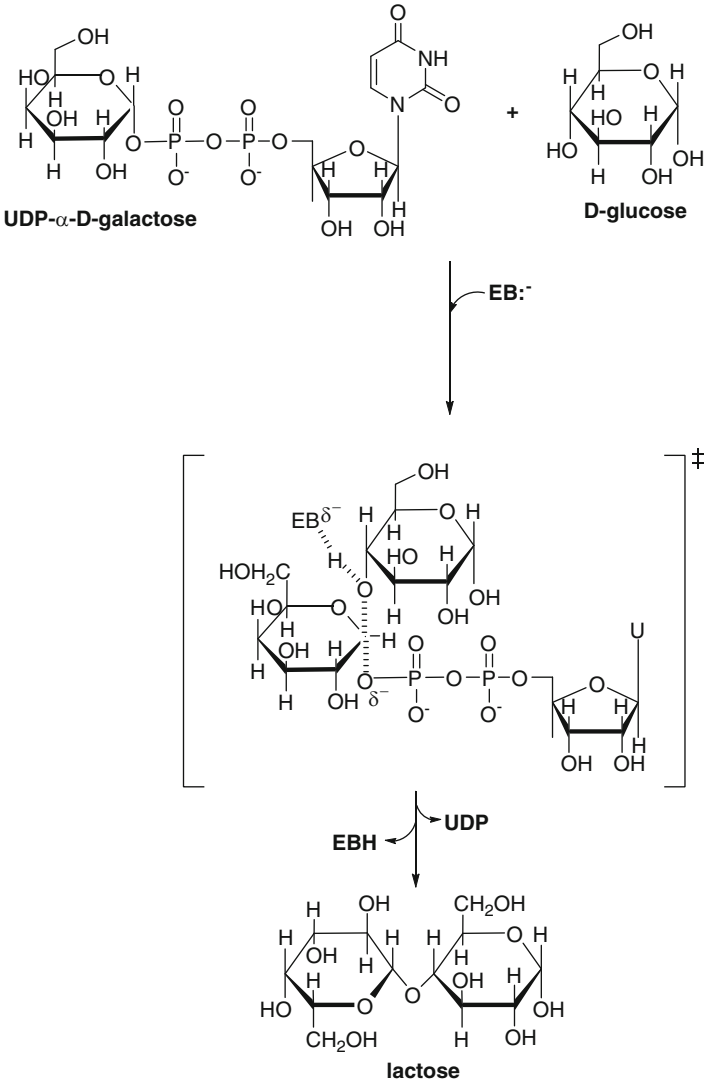

Fig. 11.5 Example of an S_N2 reaction mechanism for lactose synthase

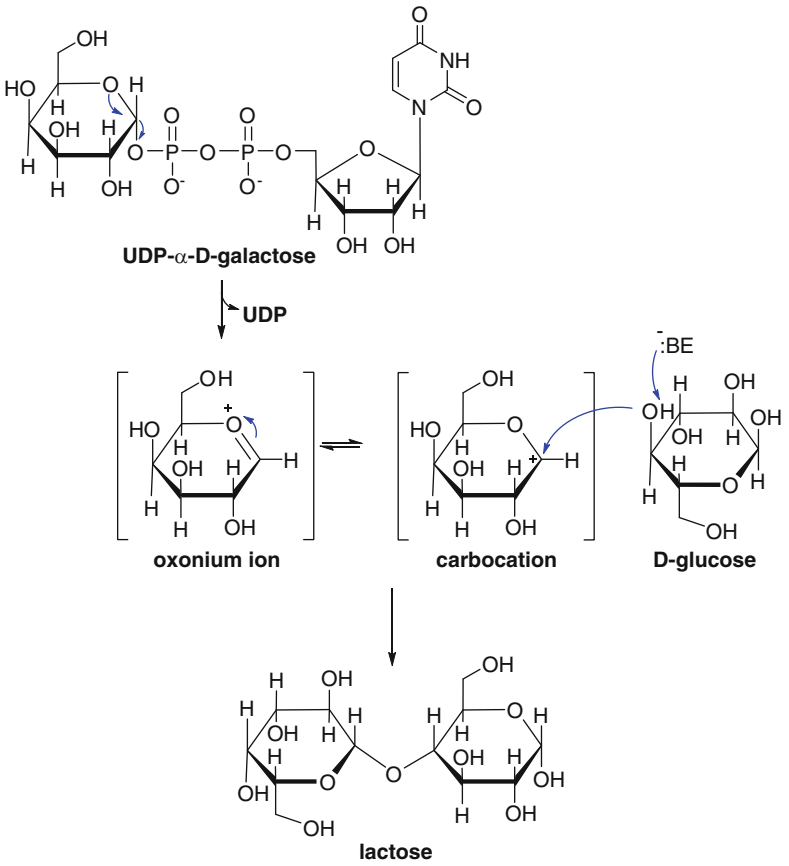

Fig. 11.6 The mechanism for lactose synthase assuming the reaction is S_N1

Lactose is hydrolyzed by the enzyme *lactase* in the small intestine; however, some individuals suffer from a condition known as *lactose intolerance* in which lactase activity is either low or absent, and where enteric bacteria ferment lactose to H_2, CO_2, and CH_4 which in turn causes gastric distress. Dietary supplements containing bacteria that hydrolyze lactose to its innocuous products are available commercially.

11.1.3 Maltose

The enzyme maltase is an α-glycosidase and catalyzes the last step in the hydrolysis of polysaccharides such as glycogen and starch to glucose. Maltase is a dimer of homologous subunits and is anchored to the brush-border cells of the intestine. It was found from X-ray diffraction studies of the N-terminal

catalytic subunit using *acarbose* as a competitive inhibitor of the substrate, that the active site accommodates two glucopyranosyl units; however, it is the side chains of the substrate and not the glycone rings that bind the enzyme [5]. Braun et al. [6] proposed an oxonium ion intermediate stabilized by an enzyme carboxylate. Thus the mechanism is similar to that for glucoamylase (Chap. 4) (Fig. 11.7).

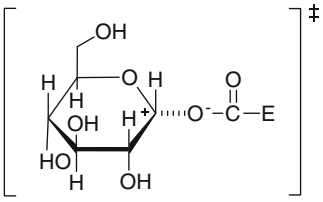

Fig. 11.7 An enzyme-carboxylate group is used to stabilize the oxonium ion intermediate in the maltase reaction

11.2 Glycogenolysis

Glycogen is the storage form of glucose in animals and is found in relatively high concentrations in skeletal muscle and liver. The polysaccharide is widely distributed in animal tissues and is even present in brain; however, brain is a heterogeneous organ and the glycogen is found in astrocytes (glia) and not in neuronal tissue. Tissue glycogen is present in the cytosol and is highly insoluble. It exists in the cell as *glycogen granules* rather than free glycogen. These granules also contain the enzymes involved in glycogen degradation (*glycogenolysis*) and glycogen synthesis (*glycogenesis*).

As pointed out in Chap. 2, glycogen is a polymer of glucose units covalently joined by $\alpha(1 \rightarrow 4)$ glycosidic linkages. There are branch points, $\alpha(1 \rightarrow 6$ linkages), every 12–18 glucan units along the linear $\alpha(1 \rightarrow 4)$ chain. The molecular weight of glycogen is in the 1–50 million range and thus there are large numbers of glucose units exposed at the nonreducing ends of the molecule. This fact is critical for an understanding of the biosynthesis and biodegradation of glycogen.

Three different enzymes: glycogen phosphorylase, glucan transferase, and $\alpha(1 \rightarrow 6)$ glycosidase (the debranching enzyme) are involved in glycogenolysis.

11.2.1 Glycogen Phosphorylase

Glycogen phosphorylase is a dimer that catalyzes the following reaction involving glycogen, $(CH_2O)_n$:

$$(CH_2O)_n + \text{Pi} \rightarrow (CH_2O)_{n-1} + \text{D-glucose-1-P}.$$

D-Glucose-1-P is then converted either by phosphoglucomutase to D-glucose-6-P or by UDP-glucose pyrophosphorylase to UDP-D-glucose:

$$\text{UTP} + \text{D-glucose-1-P} \rightleftharpoons \text{UDP-D-glucose} + \text{pyrophosphate}\ (\text{P}-\text{P}_\text{i}).$$

The equilibrium for this reaction lies far to the left; however, pyrophosphatases, which are ubiquitous in nature, hydrolyze pyrophosphate and in doing so shift the equilibrium to UDP-D-glucose formation.

As shown earlier (Chap. 8) in liver, but not muscle tissue, the D-glucose-6-P is hydrolyzed to D-glucose. An alternative fate for D-glucose-6-P is its conversion to pyruvate.

Glycogen phosphorylase is the rate-limiting step in glycogenolysis and its activity is rigidly controlled. The glycogen phosphorylase reaction occurs at the nonreducing end of glycogen chains. The mechanism is believed to involve an oxonium ion intermediate; a conclusion arrived at from X-ray diffraction crystallography and kinetic studies involving the transition state analog 1,5-glucolactone, a very potent inhibitor of the glycogen phosphorylase reaction. Recall that both the putative oxonium ion intermediate and 1,5-glucolactone share sp^2 geometry at the C-1 carbon atom.

It has been known for some time that glycogen phosphorylase requires pyridoxal phosphate (PLP) for activity and that the PLP is bound to a lysyl residue (Schiff base) at the enzyme's active site. The sequence of reactions, shown in Fig. 11.8, is thought to be the mechanism of glycogen phosphorylase.

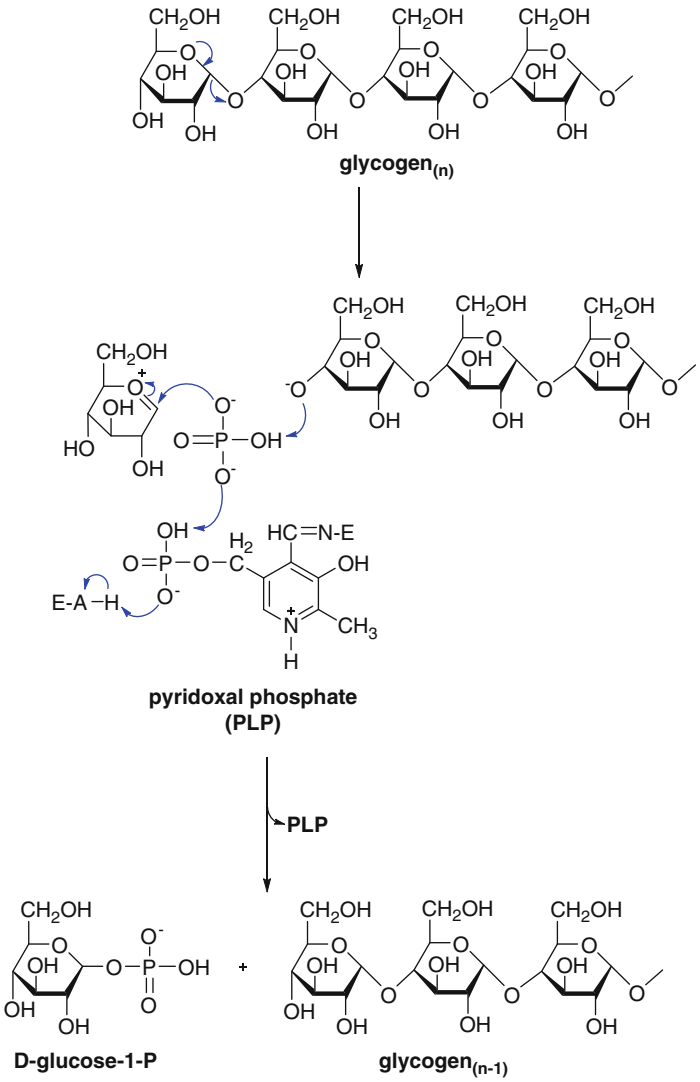

Fig. 11.8 The mechanism of the glycogen phosphorylase reaction uses the coenzyme PLP for activity

11.2.2 Glucan Transferase

Glycogen phosphorylase is incapable of degrading the linear α1 → 4 chain to its branch point. Instead, its action stops at the structure illustrated in Fig. 11.9. It is then acted upon by glucan transferase.

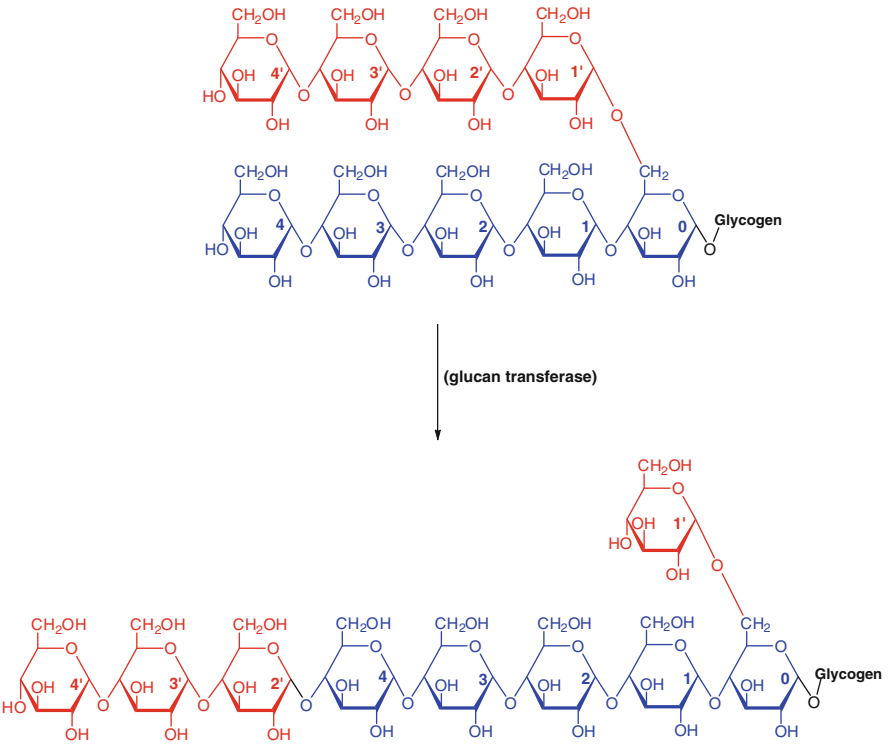

Fig. 11.9 The limit-structure (upper polysaccharide chain) beyond which glycogen phosphorylase will not act. Glucan transferase is required for phosphorolysis to continue

The glucan transferase reaction mechanism may be SN_1 as is the case for glycogen phosphorylase, or it may involve covalent catalysis in which two SN_2 reactions occur. Note that in the glucan transferase reaction there is a retention of configuration between glucan units 2′ and 4.

11.2.3 α(1 → 6) Glucosidase (Debranching Enzyme)

Subsequent to the action of glucan transferase, α(1 → 6) glucosidase catalyzes the hydrolysis of the α(1 → 6) glycosidic linkage. The reaction products are the linear chain of glycogen and D-glucose, which is then converted to D-glucose-6-P in the presence of hexokinase and ATP. After removal of the glycogen branch point (1′ in Fig. 11.9), glycogen phosphorylase resumes its action on the shortened glycogen chain and the sequence of reactions illustrated in Figs. 11.8 and 11.9 continues.

11.3 Glycogenesis

Glycogenesis, the synthesis of glycogen from glucose, is carried out by three different enzymes. One, UDP-glucose pyrophosphorylase, was already considered. The other two are glycogen synthase and the branching enzyme (amylo-[1,4 → 1,6] transglucanase). Recall that UDP-glucose can also be synthesized by UDP-glucose-4-epimerase from UDP-galactose.

When glucose enters a cell that synthesizes glycogen, enzymes such as hexokinase and phosphoglucoisomerase convert the sugar to D-glucose-1-P. It can then be acted upon by glycogen synthase and finally by the branching enzyme.

11.3.1 Glycogen Synthase

Glycogen synthase catalyzes the addition of the glucose unit from UDP-glucose to the nonreducing end of a *preexisting glycogen chain*. In a sense then glycogen is the "*primer*" for the glycogen synthase reaction.

$$\text{UDP-D-glucose} + (\text{glycogen})_n \rightarrow \text{UDP} + (\text{glycogen})_{n+1}.$$

The reaction mechanism is thought to involve an oxonium ion intermediate. This conclusion was arrived at from kinetic studies with the transition state inhibitor 1,5-gluconolactone and an observed secondary isotope effect with ^{2}H [7]. The putative reaction mechanism is shown in Fig. 11.10.

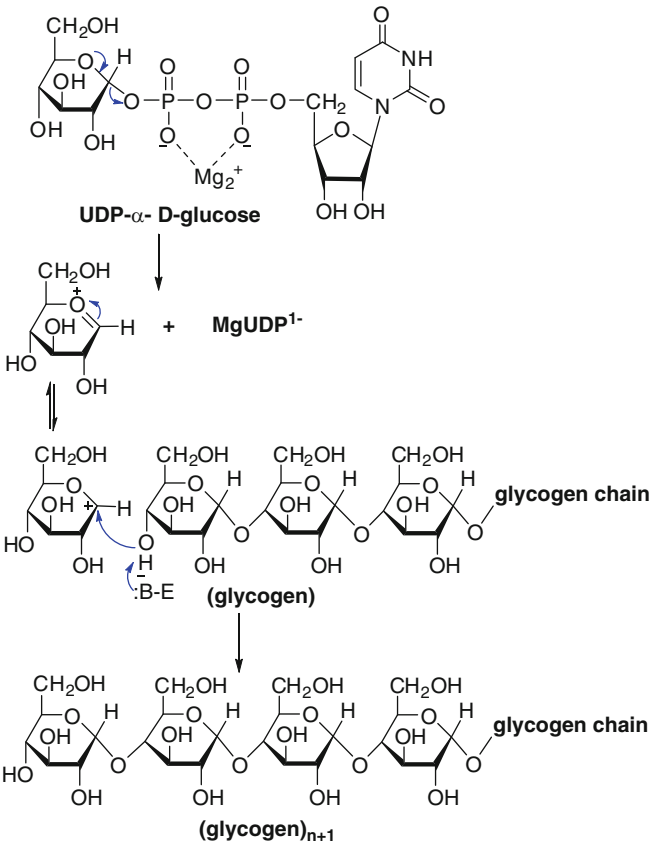

Fig. 11.10 The mechanism of action of glycogen synthase. A "primer," the glycogen chain, is required for enzyme activity

11.3.2 The Branching Enzyme *(Amylo-(1,4 → 1,6)-Transglucosylase)*

Animal glycogen contains (α1 → 6) branch points every 12–18 glucan units. Larner [8] was among the first to describe the specificity of the branching enzyme. In the branching reaction, illustrated in Fig. 11.11, the reaction sequence involves the cleavage of an (α1 → 6) glycosidic linkage involving a glucan chain containing seven glucose units. The cleavage residue then adds to a linear glucan chain at the six position of a glucose residue thus creating an (α1 → 6) branch point. Glycogen synthase can then add glucose residues to the nonreducing ends of both chains.

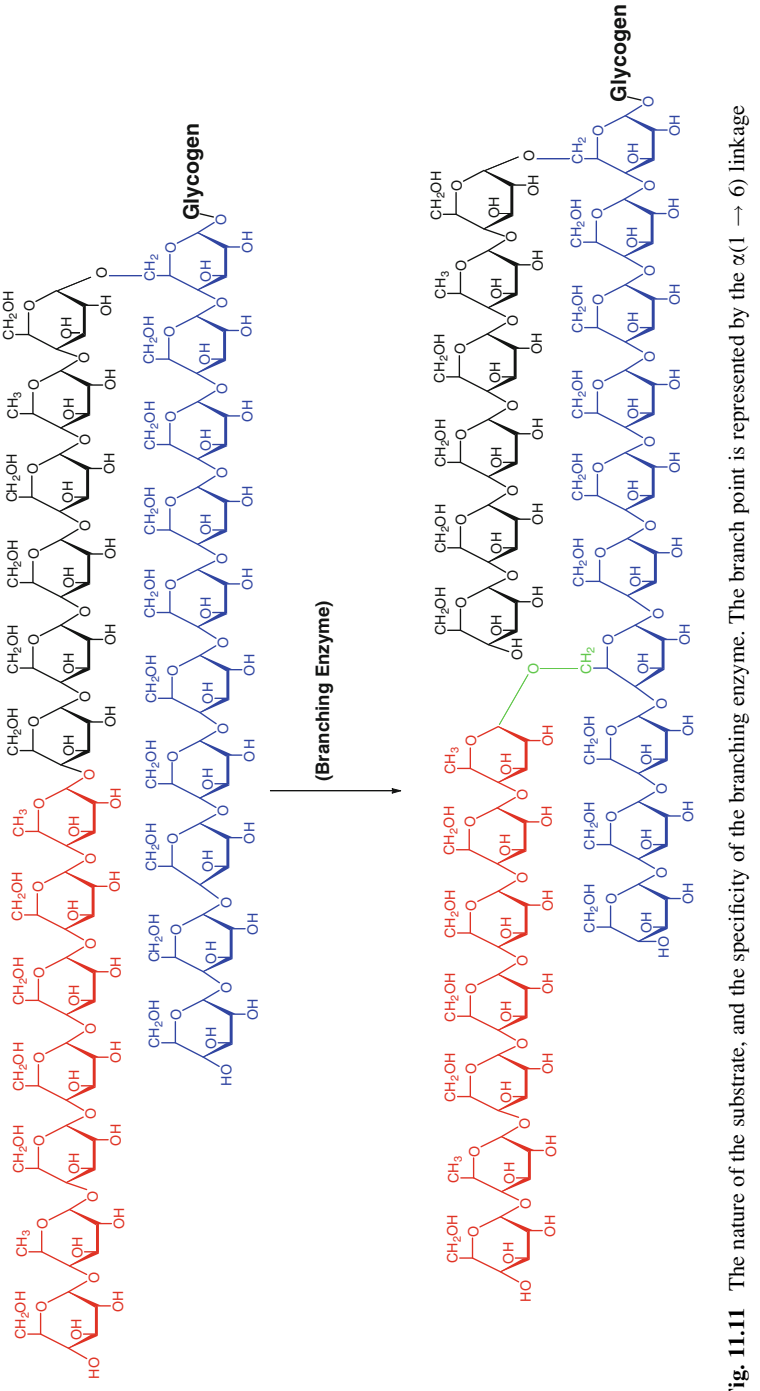

Fig. 11.11 The nature of the substrate, and the specificity of the branching enzyme. The branch point is represented by the $\alpha(1 \rightarrow 6)$ linkage

11.3.3 Glycogenin

It was long thought that a glycogen primer is required for the synthesis of larger glycogen molecules. It is now known that the self-glucosylating protein glycogenin catalyzes the attachment of a D-glucose unit from UDP-glucose to a tyrosine residue on the enzyme itself [9]. After the addition of up to seven additional glucose units, sequentially supplied by UDP-glucose, the activity of glycogen synthase is initiated. This finding infers that much of glycogen in the glycogen granule may be anchored to the protein glycogenin (Fig. 11.12).

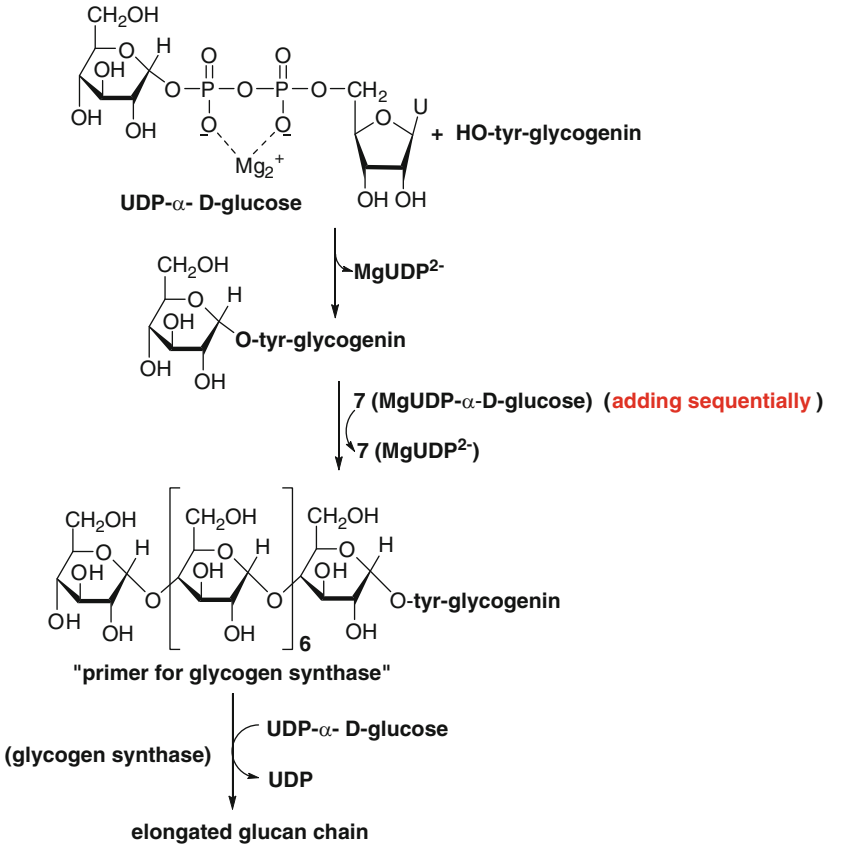

Fig. 11.12 The autocatalytic enzyme glycogenin adds glycosyl units to itself. This glycosylated protein acts as a "primer" for glycogen synthase

11.4 Regulation of Glycogen Metabolism

Glycogen biosynthesis (glycogenesis) and degradation (glycogenolysis) are highly regulated processes. Absent regulation, these two pathways would cause *futile cycling* and ultimately cell death. Consider the consequences of unregulated glycogen metabolism in terms of the enzymatic reactions involved in the synthesis and degradation of glycogen.

1. *Synthesis of glycogen (glycogenesis):*

$$\text{UTP} + \text{D-glucose} \rightleftharpoons \text{UDP-D-glucose} + \text{P-P}_\text{i}(\text{UDP-glucose pyrophosphorylase}),$$

$$\text{P-P}_\text{i} + \text{H}_2\text{O} \rightarrow 2\text{P}_\text{i}(\text{pyrophosphatase}),$$

$$\text{UDP-D-glucose} + (\text{glycogen})_{n-1} \rightarrow \text{UDP} + (\text{glycogen})_n(\text{glycogen synthase}).$$

Overall: $\text{UTP} + \text{D-glucose-1-P} + (\text{glycogen})_{n-1} + \text{H}_2\text{O} \rightarrow \text{UDP} + (\text{glycogen})_n + 2\text{P}_\text{i}$

2. *Degradation of glycogen (glycogenolysis)*:

$$(\text{glycogen})_n + \text{P}_\text{i} = (\text{glycogen})_{n-1} + \text{D-glucose-1-P}.$$

Subtracting degradation from synthesis: $\text{UTP} + \text{H}_2\text{O} \rightarrow \text{UDP} + \text{P}_\text{i}$

The two regulated enzymes in glycogen metabolism are glycogen phosphorylase and glycogen synthase. The activities of these enzymes are regulated by hormones (indirectly), small molecules that bind to allosteric sites, and covalent modification. The following discussion will be focused almost exclusively on the last point, covalent modification.

Edwin Krebs, not to be confused with Hans Krebs, and Edmond Fischer were the first to demonstrate that covalent modification of an enzyme could dramatically alter its catalytic properties [10, 11]. They showed that when inactive glycogen phosphorylase$_\text{b}$ was exposed to a protein kinase and ATP it was transformed into active enzyme phosphorylase$_\text{a}$. This finding led not only to an understanding of the regulation of glycogen metabolism, but laid the groundwork for other investigators to demonstrate how covalent modification of proteins influences gene transcription, protein synthesis, photosynthesis, muscular contraction, hormone action, and the regulation of protein and lipid metabolism. Both Krebs and Fischer were awarded the Nobel Prize for their pioneering research.

11.5 Regulation of Phosphorylase

A number of enzymes and small molecules are involved in the regulation of glycogen phosphorylase. These interactions are illustrated in Fig. 11.13

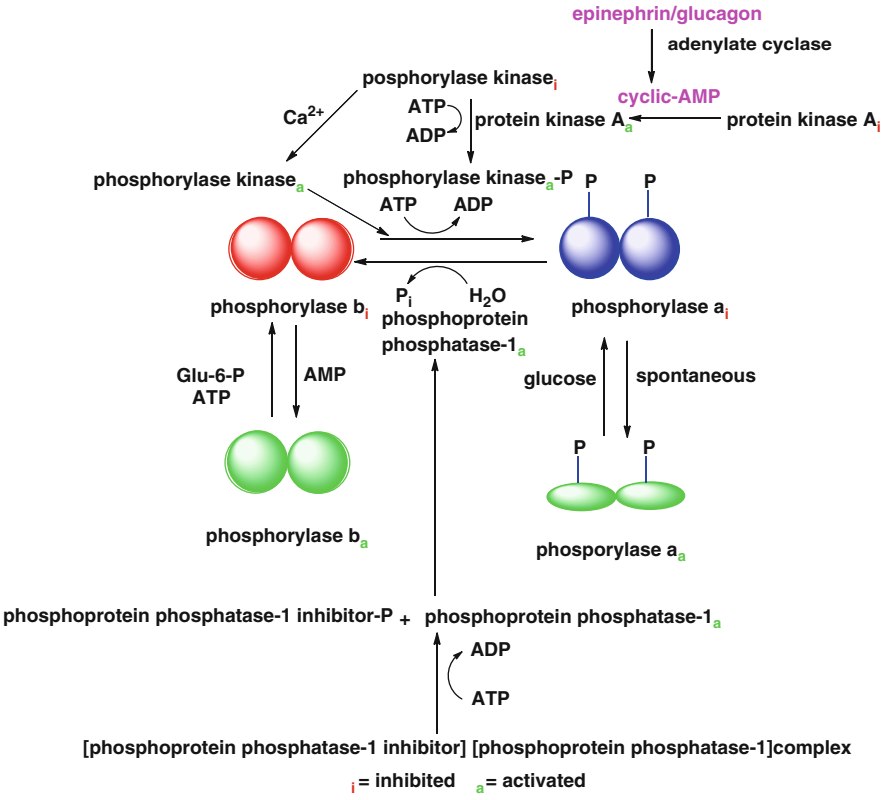

Fig. 11.13 The regulation of glycogenolysis by hormones, Ca^{2+}, allosteric effectors, protein kinases, and phosphoprotein phosphatases. The focal point of regulation is glycogen phosphorylase

11.6 Regulation of Glycogen Synthase

Illustrated in Fig. 11.14 is the outline of covalent modification of glycogen synthase which is central to its mode of regulation.

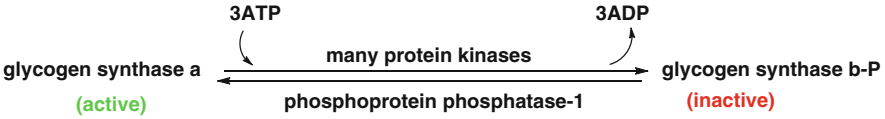

Fig. 11.14 The phosphorylation and dephosphorylation of glycogen synthase, the primary regulator of glycogenesis

Activators of glycogen synthase include: D-glucose-6-P which binds to an allosteric enzyme site and enhances dephosphorylation of glycogen synthase b, D-glucose, and the hormone insulin. One of the kinases, glycogen synthase kinase-3, is inhibited by insulin.

Inhibitors include: glucagon (which facilitates the production of 3′5′-cyclic AMP and activates protein kinase A), protein kinase A (which is involved in the phosphorylation of glycogen synthase), epinephrine (which acts like glucagon but targets skeletal muscle), ATP, ADP, and P_i.

11.7 Synthesis and Degradation of Starch

Recall that most starch is composed of two different polysaccharides, amylose and amylopectin. These compounds are synthesized in a manner analogous to glycogen. A major difference is that the glucosyl donor is ADP-D-glucose rather than UDP-D-glucose. The enzymes involved in plant starch biosynthesis are: ADP-D-glucose pyrophosphorylase, starch synthase, and branching enzyme. Obviously, the branching enzyme is not involved in amylose biosynthesis.

It is generally assumed that starch biosynthesis, or at least amylose biosynthesis, is analogous to glycogen biosynthesis in that chain growth occurs at the nonreducing end of the amylose chain. There is however some evidence that chain growth may occur from the reducing end of amylose [12].

Starch digestion in humans takes place initially in the mouth by the action of salivary α-amylase which converts starch to maltose, maltotriose (three glucose units), and maltotetrose (four glucose units). Mastication lasts a short period of time and only a small fraction of the starch in the mouth is digested. Upon entering the stomach, the α-amylase is inactivated by the low pH environment. The undigested starch then moves to the intestine where pancreatic amylase continues the hydrolytic action begun in the mouth. A number of so-called α-limit dextrans containing 4–6 glucose residues are formed around the branch point linkages of what had been amylopectin. Glucose is ultimately formed from the α-limit dextrans as well as the smaller nonbranched oligosaccharides through the action of an α-1,4-glucosidase and an α-1,6-glucosidase. The final breakdown product of starch, D-glucose, is ultimately converted to D-glucose-6-P by liver glucokinase.

11.8 Synthesis and Degradation of Cellulose

Cellulose is synthesized in plants and some bacteria by cellulose synthases which adds a single D-glucose unit to the nonreducing end of a cellulose chain. The D-glucose donor is UDP-D-glucose. The mechanism of cellulose synthesis is extremely complex and is not completely understood [13]. In addition to the enzymes and substrates, structures within the cell are required for cellulose biosynthesis. In terms of the enzymatic mechanism, here too, there is a lack of definitive information. Cellulose synthases add a glucose unit to the growing cellulose chain at the nonreducing end of the molecule from the donor, UDP-α-D-glucose, to form a $\beta(1 \rightarrow 4)$ glycosidic linkage. This inversion of configuration can be explained

either by the involvement of a single SN_2 reaction or an SN_1 mechanism, presumably involving an oxonium ion intermediate.

The structure of cellulose, particularly the intermolecular hydrogen-bonded network, render it both insoluble in water and difficult to hydrolyze either chemically (strong acids) or enzymatically. Certain fungi and bacteria secrete *cellulases* that initially attack the less ordered interior of the polysaccharide. This is followed by the removal of *cellobiose* (a disaccharide similar to maltose but with glucose units linked $\beta(1 \rightarrow 4)$ from the ends of the polysaccharide chains). The cellobiose is then hydrolyzed to D-glucose by a $\beta(1 \rightarrow 4)$ glucosidase.

References

1. Singh AN, Hester IS, Rauschel FM (1987) Examination of the mechanism of sucrose synthetase by positional isotope exchange. J Biol Chem 262:2554–2557
2. Bois E, Swaminathan GJ, Zhang Y, Natesh R, Brew K, Acharya KR (2001) Structure of UDP complex of UDP-galactose: -galactoside-a-1,3-galactosyltransferase at 1.53-resolution reveals a conformational change in the catalytically important C Terminus. J Biol Chem 276: 48608–48614
3. Bell JE, Beyer TA, Hill RL (1976) The kinetic mechanism of bovine milk galactosyltransferase. The role of alpha-lactalbumin. J Biol Chem 251:3003–3013
4. Ramakrishnan B, Qasba PK (2001) Crystal structure of lactose synthase reveals a large conformational change in its catalytic component, the β 1,4-galactosyltransferase-1. J Mol Biol 310:205–218
5. Sim L, Quezada-Calvillo R, Sterchi EE, Nichols BL, Rose DR (2008) Human intestinal maltase-glycoamylase: crystal structure of the N-terminal catalytic subunit and basis of inhibition and substrate specificity. J Mol Biol 375:782–792
6. Braun C, Brayer GD, Withers SG (1995) Mechanism-based inhibition of yeast glucosidase and human pancreatic-amylase by a new class of inhibitors: 2-deoxy-2, 2-difluoro-a-glycosides. J Biol Chem 270:26778–26781
7. Kim SC, Singh AN, Rauschel FM (1988) The mechanism of glycogen synthetase as - determined by deuterium isotope effects and positional isotope exchange experiments. J Biol Chem 263:10151–10154
8. Larner J (1953) The action of branching enzymes on outer chains of glycogen. J Biol Chem 202:491–503
9. Whelan WJ (1986) The initiation of glycogen synthesis. BioEssays 5:136–140
10. Fischer EH, Krebs EG (1955) Conversion of phosphorylase b to phosphorylase a in muscle extracts. J Biol Chem 216:121–132
11. Krebs EG, Kent AB, Fischer EH (1958) The muscle phosphorylase b kinase reaction. J Biol Chem 231:73–83
12. Mukerjea R, Robyt JF (2004) Starch biosynthesis: the primer nonreducing-end mechanism versus the nonprime reducing-end two-site insertion mechanism. Carbohydr Res 340:245–255
13. Saxena IM, Brown RM Jr (2005) Cellulose biosynthesis: current views and evolving concepts. Ann Bot 96:9–21

Chapter 12
Lipid Metabolism

Lipids play a central role in biology. As pointed out earlier (Chap. 2), one of the most important biological structures, biological membranes, is composed of lipids. In addition, lipids are important players in the storage of energy-rich compounds and many hormones and vitamins are lipids.

12.1 Lipid Digestion

Up to 90% of the lipids ingested by humans are triacyclglycerols, or storage lipids. These esters of long-chain fatty acids and glycerol are first emulsified (solubilized) in the intestine with the aid of bile salts from the liver. They are then hydrolyzed by pancreatic lipase primarily to 2-acylglycerols and two fatty acids. The catalytic activity of the lipase is enhanced by its association, in a 1:1 complex, with the binding protein, *colipase* (Fig. 12.1).

Pancreatic lipase is a serine protease [1] whose mechanism of action is very similar to that already described for chymotrypsin (Chap. 4). Note that the chemical mechanism outlined for chymotrypsin used *p*-nitrophenyl acetate as the substrate. In the case of pancreatic lipase, the substrate triacylglycerol is also an ester.

The fatty acids and other lipids along with the mono- and diacylglycerols plus emulsifying agents (bile salts and phospholipids) produce *micelles* from which the lipids are absorbed by the cells of the intestinal mucosa. The degraded triacylglycerols are then resynthesized in the intestinal mucosa to triacylglycerols of the type found in the species ingesting the dietary lipids. The lipid material (primarily phospholipids, triacylglycerols, cholesterol, cholesterol esters, and lipoproteins called *chylomicrons* – Table 12.1) is transported from the intestinal mucosa into the blood via the lymph. Transportation of the chylomicrons to muscle and adipose tissue results in degradation of the triacylglycerols to free fatty acids and glycerol by lipoprotein lipase.

H.J. Fromm and M.S. Hargrove, *Essentials of Biochemistry*,
DOI 10.1007/978-3-642-19624-9_12, © Springer-Verlag Berlin Heidelberg 2012

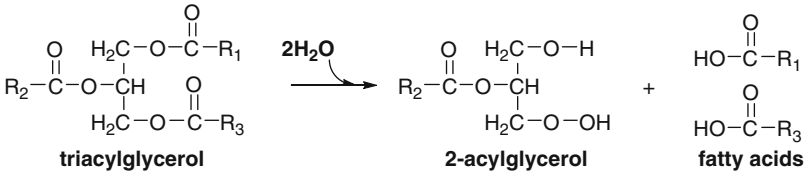

Fig. 12.1 The hydrolysis of triacylglycerol by pancreatic lipase occurs sequentially with the release of 2-acylglycerol

The synthesis of triacylglycerols also occurs in liver tissue from where they are transported via the blood with lipoproteins. This complex of lipid and protein is known as *very low-density lipoprotein* (VLDL). The degradation of triacylglycerols in adipose tissues results in the formation of free fatty acids which are transported in blood as a complex with serum albumin. The liberated glycerol may be converted to dihydroxyacetone phosphate for degradation in the glycolytic pathway as illustrated in Fig. 12.2 or converted to glucose in liver.

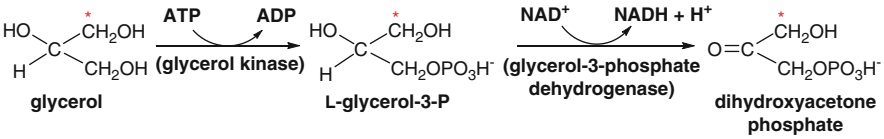

Fig. 12.2 The conversion of glycerol to dihydroxyacetone phosphate, an intermediate in glycolysis. Note that the glycerol kinase reaction is stereospecific. The *asterisk* (*) is taken to represent [^{13}C] in glycerol

12.2 Degradation of Fatty Acids

Fatty acids are an extremely important component of energy metabolism, e.g., the oxidation of lipid releases 37.6 kJ/gm of energy whereas protein and carbohydrate oxidation results in the production of 16.7 kJ/gm.

Important clues regarding how fatty acids are degraded came from the laboratories of the Dutch biochemist Knoop [2] and his American counterpart Dakin [3] in the early part of the twentieth century. They fed phenyl derivatives of fatty acids to animals and determined the nature of their urinary metabolic products. In short, that found that when odd numbered phenyl fatty acids, such as phenylpropionic acid were ingested, the end-product was hippuric acid, a condensation product of benzoic acid and glycine, whereas when even numbered fatty acids were fed, the product in the urine was a condensation product of phenylacetate and glycine, phenylacetylglycine. This led to the conclusion that in the metabolic

oxidation of fats, two carbon fragments, as a result of β-oxidation, followed by α,β-carbon–carbon bond cleavage, occurred. These were not only crucial experiments that led to an understanding of how fatty acids are oxidized, they also pointed the way to how substrates might be labeled in order to study their metabolism. Today these types of labeling studies are done with isotopes.

Lynen and Reichart [4] demonstrated that acetate was not a product of β-oxidation per se, but rather that a derivative of acetate, acetyl-CoA is.

Fatty acid degradation or oxidation occurs in mitochondria and specialized organelles called *peroxisomes*; however, they are first condensed with CoA in the cytosol. This reaction requires ATP as the energy source and the enzyme *acyl-CoA synthetase* (Fig. 12.3).

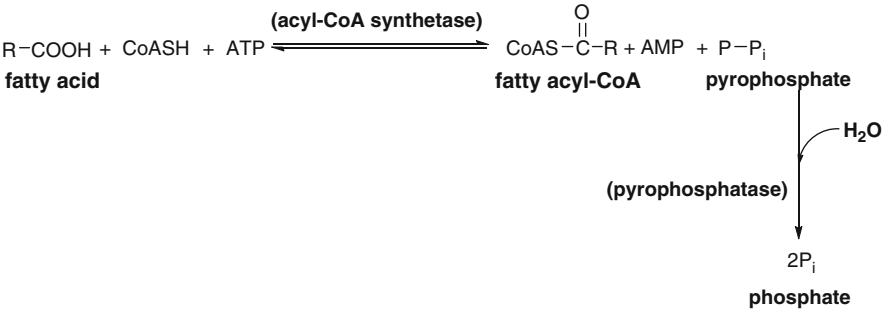

Fig. 12.3 Acyl-CoA synthetase activates the fatty acid to a "high energy" thioester. The hydrolysis of pyrophosphate is catalyzed by pyrophosphatases

The equilibrium of the acyl-CoA synthetase reaction lies far to the left; but, the presence of pyrophosphatases assures the adequate production of acyl-CoA; however, in the overall reaction, two ATP equivalents are used. The acyl-CoA synthetase reaction involves the formation of an acyl adenylate intermediate [5]. Fatty acid synthetases are ubiquitous in nature and fall into three categories depending upon the carbon chain length of the substrate: short, medium, and long. The mechanism of an acyl-CoA synthetase is illustrated in Fig. 12.4.

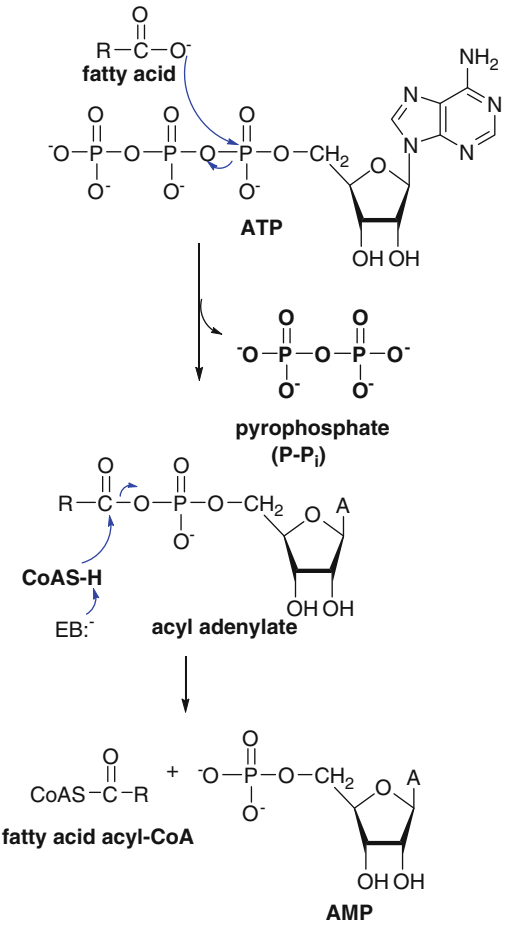

Fig. 12.4 The "activation" of a long-chain fatty acid to fatty acid acyl-CoA by the enzyme acyl-CoA synthetase

12.3 Transport of Fatty Acids into Mitochondria

Cytosolic fatty acyl-CoA is impermeable to mitochondria. To circumvent this problem, the acyl group is transferred to carnitine [6] by the enzyme *carnitine acyltransferase I* to form acylcarnitine which is then transported into mitochondria. Once present in mitochondria, the acyl group is transferred back to CoA by an isozyme of carnitine acyltransferase (*carnitine acyltransferase II*) (Fig. 12.5).

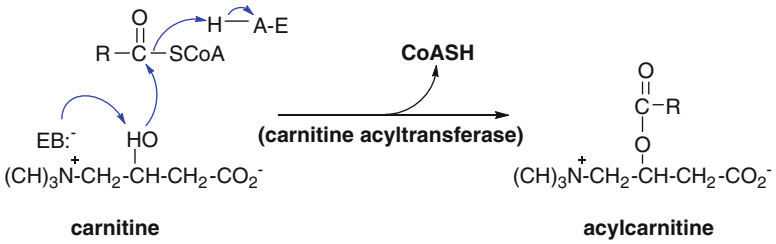

Fig. 12.5 The role of carnitine in the transportation of fatty acids into mitochondria

12.4 β-Oxidation of Fatty Acids

Oxidation of long-chain fatty acids involves a four-step sequence of reactions in which two carbon units at the CoA end of the acyl-CoA molecule are removed as acetyl-CoA. The purpose of these reactions is to produce very large amounts of ATP via oxidative phosphorylation. It should be noted that the long-chain fatty acids considered here are all even numbered.

Figure 12.6 describes the first sequence of events in β-oxidation of fatty acids leading to the formation of a single acetyl-CoA molecule. This process is then repeated until all the carbon atoms in the fatty acyl-CoA are converted to acetyl-CoA. There are four different acyl-CoA dehydrogenases in mitochondria. Their specificities are determined by the chain lengths of the fatty acyl-CoA.

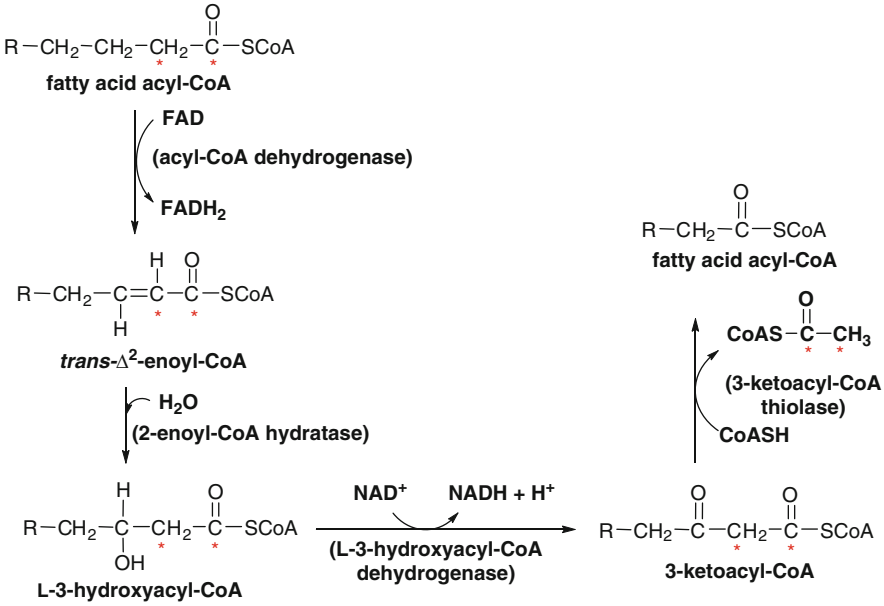

Fig. 12.6 The β-oxidation pathway for a long-chain fatty acid. The *asterisks* (*) trace fatty acid acyl-CoA's C-1 and C-2 atoms to acetyl-CoA

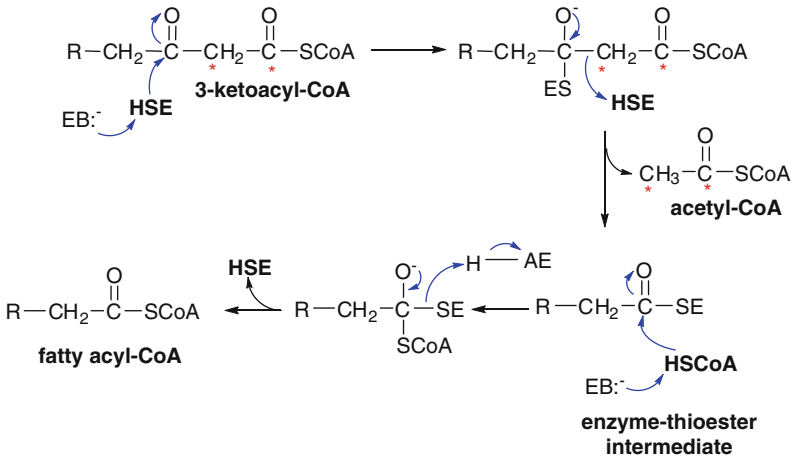

Fig. 12.7 The mechanism of the enzyme 3-ketoacyl-CoA thiolase. The *asterisks* (*) trace 3-ketoacyl-CoA's C-1 and C-2 atoms to acetyl-CoA

The enzyme *3-ketoaceyl-CoA thiolase* catalyzes a reverse Claisen-type reaction as shown in Fig. 12.7. The thioester shown in Fig. 12.7 is an "energy-rich" compound as is fatty acyl-CoA.

12.5 Energetics of the β-Oxidation Pathway

Each cycle of β-oxidation shown in Fig. 12.7 produces one acetyl-CoA, one NADH, and one $FADH_2$ molecule. Eight such cycles would occur in the case of stearoyl-CoA oxidation or,

$$\begin{aligned}&\text{Stearoyl-CoA} + 8\text{CoASH} + 8\text{NAD}^+ + 8\text{FAD} + 8\text{H}_2\text{O}\\&\rightarrow 9\text{Acetyl-CoA} + 8\text{NADH} + 8\text{FADH}_2 + 8\text{H}^+.\end{aligned}$$

Each molecule of acetyl-CoA when oxidized in the Krebs Cycle yields 10 ATP equivalents. The eight NADH and $FADH_2$ molecules when reoxidized produce 2.5 and 1.5 equivalents of ATP, respectively. Thus, the total amount of ATP produced from the β-oxidation of stearoyl-CoA is 122 ATP equivalents, minus the two ATP equivalent required to activate stearic acid to stearoyl-CoA. It is interesting to note that three glucose molecules, which like stearic acid contain 18 carbon atoms, when oxidized yield 90 ATP equivalents. This difference in energy potential is a result of the fact that glucose is more highly oxidized than the fatty acid.

12.6 β-Oxidation of Unsaturated Fatty Acids

Most unsaturated fatty acids have *cis* double bonds. When a fatty acid such as oleic acid (18:1 *cis* Δ^9) is degraded, it undergoes three cycles of β-oxidation as shown in Fig. 12.6. The C_{12} fatty acyl-CoA containing a *cis*-β,γ double bond cannot be utilized by 2-enoyl CoA hydratase. This problem is circumvented by the action of the enzyme enoyl-CoA isomerase which converts the *cis*-β,γ double bond to a *trans*-α,β double bond as shown in Fig.12.8. Once isomerization is accomplished, β-oxidation can proceed.

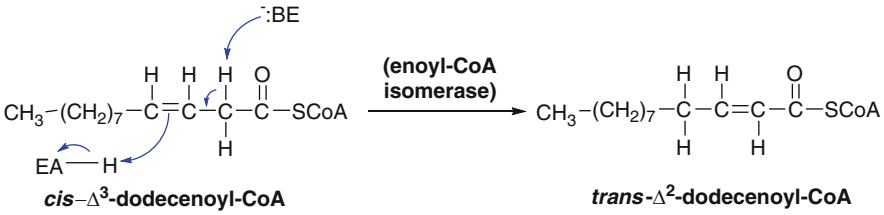

Fig. 12.8 Conversion of a β,γ-*cis* fatty acyl-CoA to an α,β *trans* fatty acyl-CoA by enoyl-CoA isomerase

12.7 Oxidation of Odd Numbered Fatty Acids

Odd numbered fatty acids are rare in nature but they do exist, being synthesized by certain plants and ruminants. They are degraded by β-oxidation to propionyl-CoA in addition to acetyl-CoA. Propionyl-CoA is then converted to (S)-methyl-malonyl-CoA by *propionyl-CoA carboxylase*, a *biotin-containing enzyme* whose mechanism of action is very similar to that of other biotin carboxylases (Chap. 6). A third enzyme, *methylmalonyl mutase*, then converts the (S)-methylmalonyl-CoA to succinyl-CoA which can undergo metabolism via the Krebs Cycle. This sequence of events in fatty acid oxidation is outlined in Fig. 12.9.

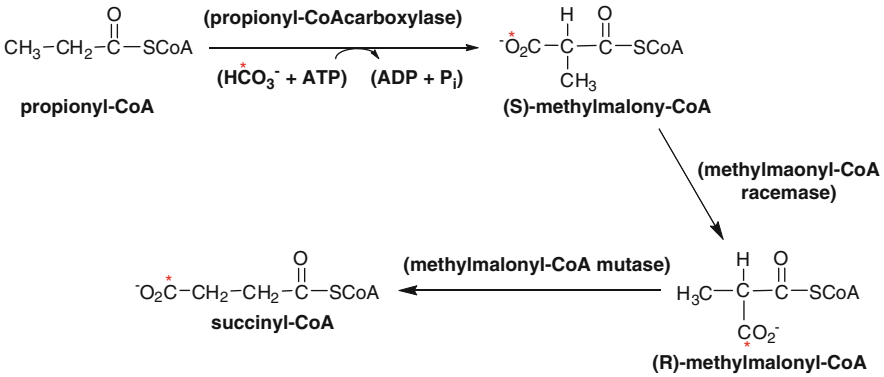

Fig. 12.9 Conversion of propionyl-CoA to succinyl-CoA, the end-product of odd numbered fatty acid oxidation. The *asterisks* (*) trace HCO_3^- to succinyl-CoA

12.8 Fatty Acid Biosynthesis

It was thought for some time that fatty acid synthesis (FAS) is simply the reversal of fatty acid degradation [7]; however, Langdon demonstrated in 1957 that FAS occurs in the cytosol of cells and its synthesis occurs by a pathway distinctly different from fatty acid oxidation [8]. The enzyme system, *fatty acid synthase* (FAS), is responsible for *de novo* fatty acid biosynthesis (see Fig. 12.11). The site of fatty acid biosynthesis is the *cytosol* of the cell, whereas fatty acid oxidation takes place in mitochondria. The synthesis itself occurs by the condensation of two-carbon units originating from acetyl-CoA and ends with the formation of palmitoyl-CoA (see Fig. 12.11). Other enzymes, known as *fatty acid elongases*, form the longer-chain fatty acids.

In *Escherichia coli*, FAS is made up of seven different enzymes and the protein, *acyl carrier protein* (ACP) [9], a 125-residue polypeptide, which serves as an anchor for the acyl and acetyl groups in the synthetic metabolic pathway. The FAS system in animals consists of two very long identical polypeptide chains which contain the seven different FAS activities as well as ACP.

The functional portion of ACP (see Fig. 12.10) is very similar structurally to that of CoA (Chap. 6).

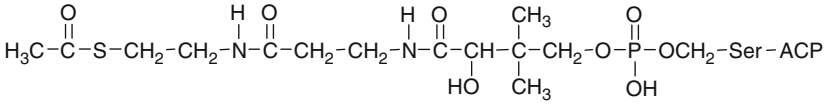

acetyl-ACP

Fig. 12.10 The structure of acetyl-ACP

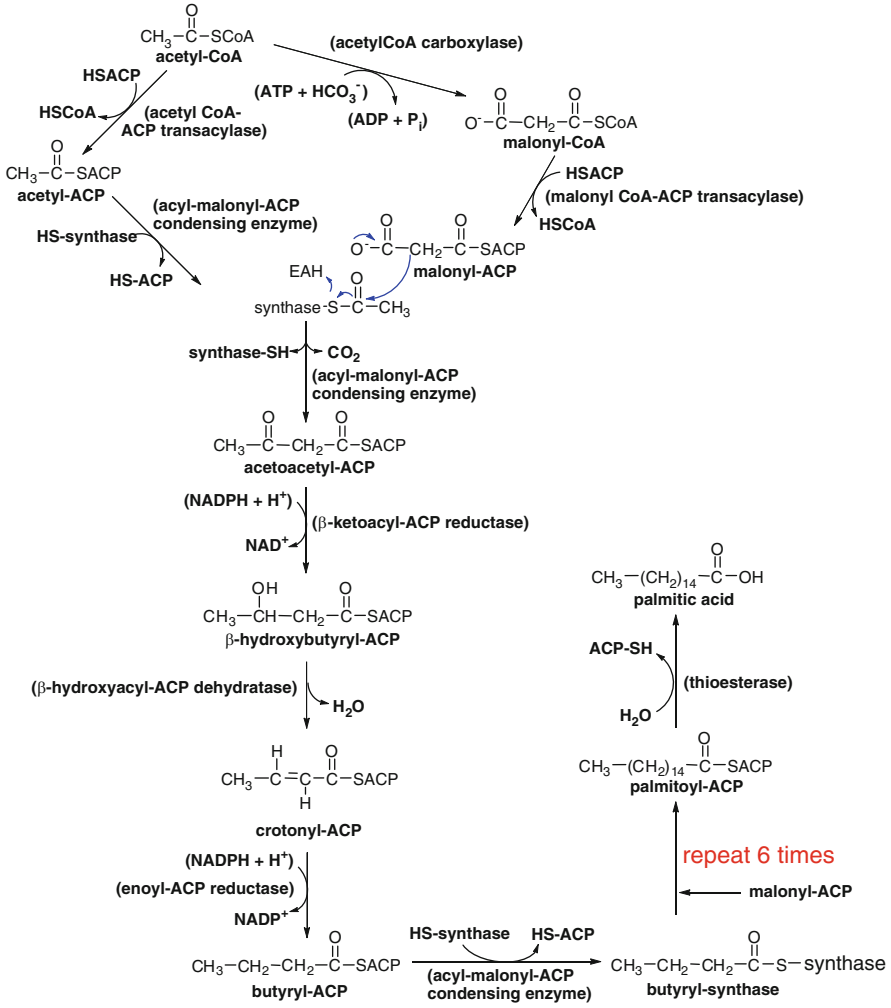

Fig. 12.11 *De novo* fatty acid biosynthesis starting with acetyl-CoA

12.9 Comments on the FAS system

1. Note that the acetyl group from acetyl-ACP is transferred to the synthase (acyl-malonyl-ACP condensing enzyme). The acetyl group moiety then reacts with malonyl-ACP to form acetoacetyl-ACP.
2. The reducing agent in the pathway is NADPH which arises from the Pentose Phosphate Pathway and via the "*malic enzyme*":

$$\text{malate} + \text{NADP}^+ \rightarrow \text{pyruvate} + \text{CO}_2 + \text{NADPH} + \text{H}^+.$$

3. The overall stoichiometry of the FAS pathway which starts with acetyl-CoA and ends with palmitic acid is:

$$\begin{aligned} 8\text{acetyl-CoA} + 7\text{ATP} + 14\text{NADPH} + \rightarrow \text{palmitic acid} \\ + 8\text{CoASH} + 14\text{NADP}^+ + 6\text{H}_2\text{O} + 7\text{ADP} + 7\text{P}_\text{i}. \end{aligned}$$

4. Palmitoyl-ACP may undergo a number of transformations:
   (a) It may be hydrolyzed to palmitic acid as in Fig. 12.11
   (b) It may undergo chain elongation
   (c) It may undergo desaturation to palmitoleic acid (*cis*-Δ^9-hexadecenoic acid) [10]
5. Three reactions in the FAS pathway are exergonic: the acyl-malonyl-ACP condensing enzyme, and the two reductase reactions.

Acetyl-CoA is synthesized from pyruvate in mitochondria by the pyruvate dehydrogenase complex; however, acetyl-CoA is a substrate for FAS which occurs in the cytosol. So how does acetyl-CoA get from the mitochondria to the cytosol? In mitochondria, acetyl-CoA is converted to citrate by *citrate synthase* in the presence of oxaloacetate. The citrate is then transported out of the mitochondrion to the cytosol where it is acted upon by *ATP-citrate lyase* [11] as shown in Fig. 12.12. The overall reaction is:

$$\text{citrate} + \text{ATP} + \text{CoASH} \rightarrow \text{acetyl-CoA} + \text{oxaloacetate} + \text{ADP} + \text{P}_\text{i}.$$

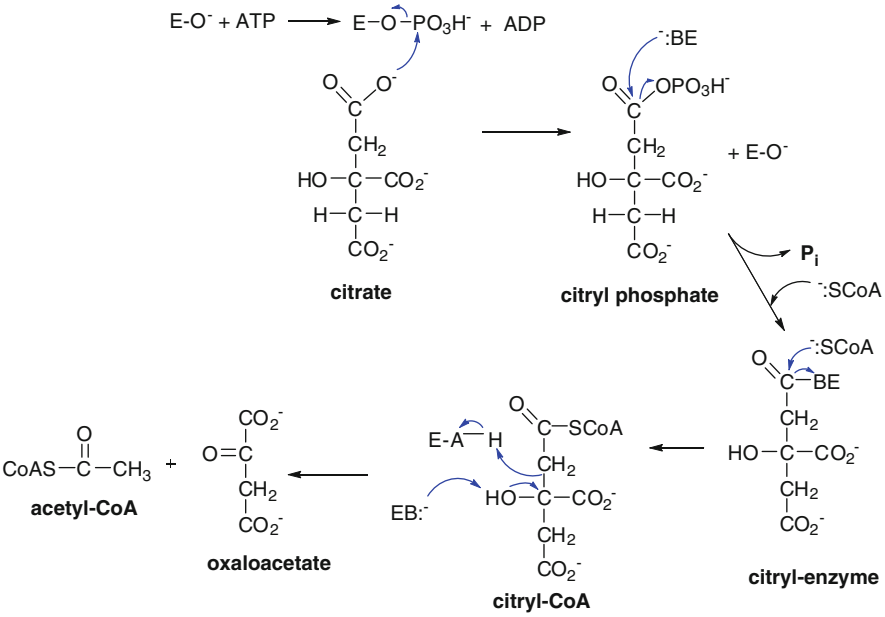

Fig. 12.12 The mechanism of action of ATP-citrate lyase

12.10 Regulation of Fatty Acid Metabolism

The enzymes of fatty acid metabolism are regulated by hormones, small molecules (allosteric control), and covalent modification. In the case of FAS, the first committed step is *acetyl-CoA carboxylase* which is activated by citrate and inhibited by the feedback regulator, palmitoyl-CoA. Elevated levels of citrate are a signal to the cell that it is being adequately supplied with nutrients and that storage of lipids, as triacylglycerols, is in order. Acetyl-CoA carboxylase activity is also inhibited by phosphorylation, a response to hormones such as glucagon and epinephrine, which causes the release of 3′,5′-cyclic AMP with the resulting activation of a c-AMP-dependent protein kinase (protein kinase A). In cell cultures, glucose activates the carboxylase by causing the release of insulin which serves to activate the carboxylase by facilitating its dephosphorylation [12, 13]. Scheme 12.1 summarizes the effects of allosteric and covalent modification on acetyl-CoA carboxylase.

Fatty acid oxidation is controlled at the enzyme level by the activity of triacylglycerol lipase and carnitine palmitoyltransferase. The transferase is allosterically inhibited by malonyl-CoA, whereas the lipase is activated by c-AMP-dependent protein kinase phosphorylation. Thus, 3′,5′-cyclic-AMP simultaneously stimulates fatty acid oxidation and inhibits its biosynthesis.

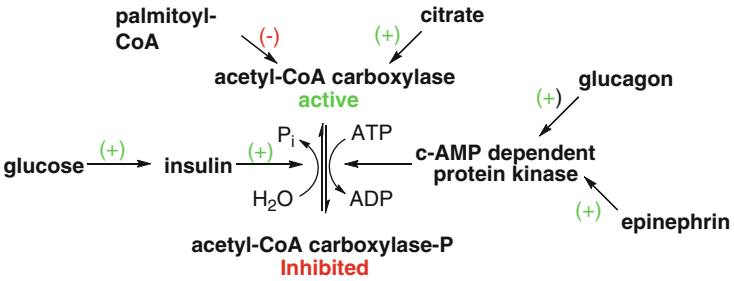

Scheme 12.1 Regulation of acetyl-CoA carboxylase by small molecules and hormones

In summary, the release of the hormones epinephrine and glucagon in response to elevated concentrations of blood glucose serves to inhibit FAS and activates triacylglycerol hydrolysis and ultimately, fatty acid oxidation.

12.11 Triacylglycerol Biosynthesis

The biosynthesis of triacylglycerols begins with the synthesis of glycerol-3-P. A second acyl group is then contributed by acyl-CoA. The 1,2-diacylglycerol-phosphate, known as *phosphatidic acid*, is next hydrolyzed to 1,2-diacylglycerol. Triacylglycerol is finally synthesized by the addition of a third acyl group supplied by the donor, acyl-CoA. This sequence of reactions is illustrated in Fig. 12.13.

Phosphatidic acid, in addition to being essential for triacylglycerol synthesis, is a precursor of a number of phosphoglycerides. These include phosphatidylserine, phosphatidylethanolamine, and phosphatidylinositol.

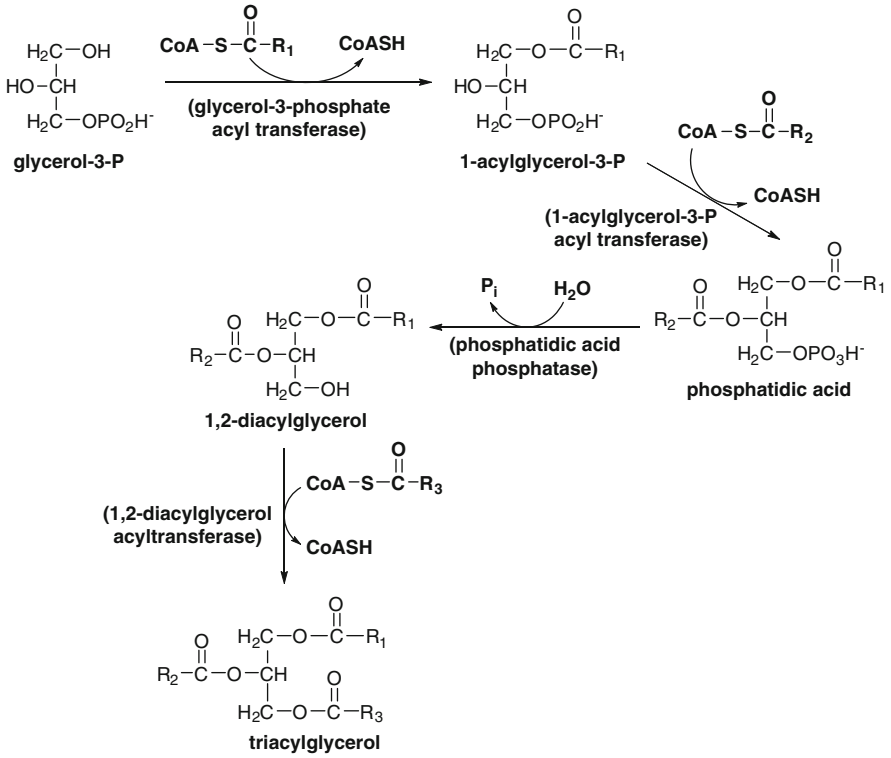

Fig. 12.13 The biosynthesis of triacylglycerol

12.12 Ketone Body Formation

Not all of the acetyl-CoA produced in the cell is used to synthesize fatty acids and produce ATP via the Krebs Cycle. In liver hepatocytes acetyl-CoA is also used to synthesize the three "ketone bodies": acetoacetic acid, β-hydroxybutyric acid, and acetone. Both acetoacetic acid and β-hydroxybutyric acid can be converted to acetyl-CoA in *extrahepatic tissues*.

Although these compounds are normal metabolites, they are produced in small amounts under normal physiological conditions. On the other hand, during starvation and untreated (lack of administered insulin) *diabetes mellitus* excessive amounts of ketone bodies are produced. Their excretion at neutral pH in urine along with the counter-ion, Na^+, leads to the potentially fatal condition known as *acidosis*.

A number of amino acids, known as *ketogenic amino acids*, are degraded to acetoacetic acid and acetyl-CoA. Phenylalanine, tyrosine, leucine, and lysine form acetoacetic acid. Others produce acetyl-CoA with the potential to form ketone bodies. These include threonine, tryptophan, leucine, and isoleucine.

In 1944, Weinhouse et al. [14] showed that ketone bodies are formed by condensation of two two-carbon intermediates, resulting from the β-oxidation of fatty acids. Indeed, ketone body synthesis begins with the condensation of two molecules of acetyl-CoA as shown in Fig. 12.14.

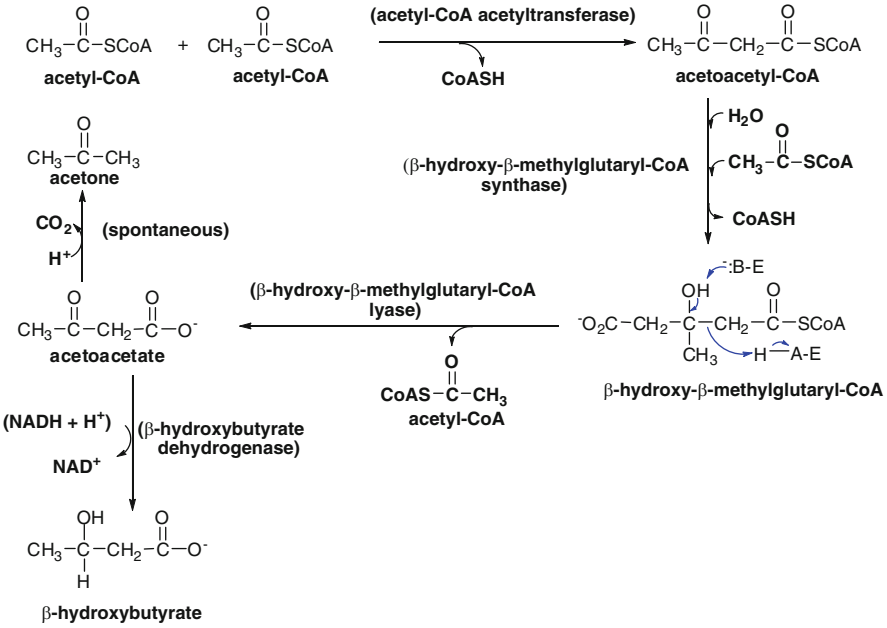

Fig. 12.14 The biosynthesis of ketone bodies in mammalian liver

Tissues other than liver (extrahepatic tissues) are capable of utilizing ketone bodies, other than acetone, for energy purposes by degrading these metabolites to acetyl-CoA as shown in Fig. 12.15.

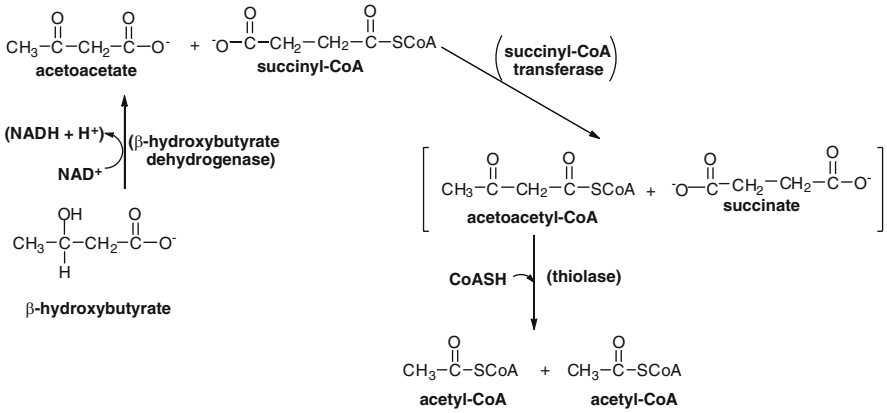

Fig. 12.15 Conversion of ketone bodies to acetyl-CoA in extrahepatic tissue mitochondria

12.13 Fatty Acid Elongation

The end-product of the FAS pathway is palmitic acid; however, 18 carbon and longer fatty acids are required by the cell. Both the *endoplasmic reticulum* (ER) and *mitochondria* contain enzyme systems, called *elongases* that synthesized very long-chain fatty acids. The ER enzymes use malonyl-CoA plus acyl-CoA for chain elongation, whereas in mitochondria, acetyl-CoA rather than malonyl-CoA is the acetyl group donor. In mitochondria, the reactions are analogous to those seen in the FAS pathway except that NADH rather than NADPH is used to reduce β-ketoacyl-CoA. Fatty acid chain elongation is illustrated in Fig. 12.16.

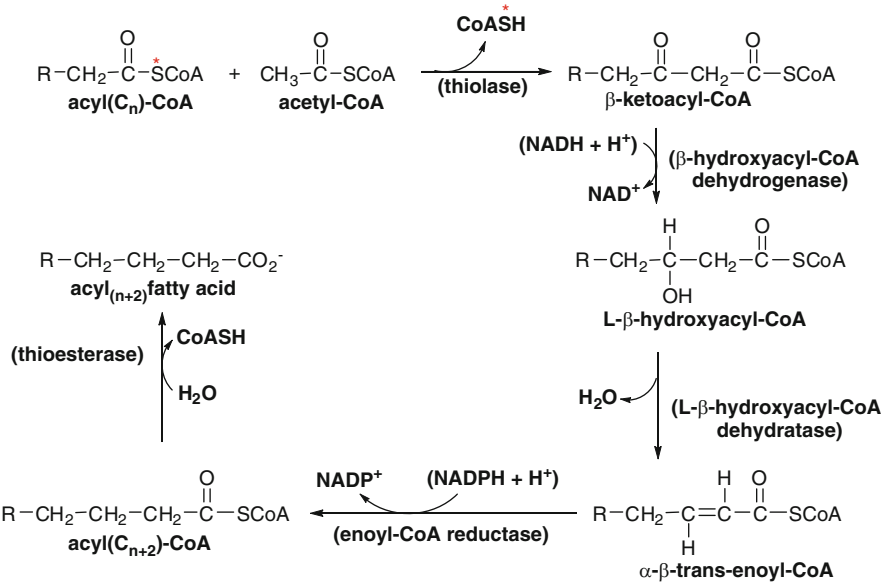

Fig. 12.16 The action of an elongase enzyme system that adds two carbon atoms to an existing fatty acid

12.14 Fatty Acid Desaturation

A number of unsaturated fatty acids exist in nature and are essential for cell survival. Most of these fatty acids are produced in vivo from saturated fatty acids, e.g., oleic acid is synthesized from stearic acid by the Δ^9-fatty acyl-CoA desaturase complex. Animals cannot introduce double bonds in fatty acids beyond C-9, thus fatty acids such as α-linolenic acid (all *cis*-$\Delta^{9,12,15}$-octadecatrienoic acid) are required for sustenance and must be ingested from the diet; they are therefore termed "essential fatty acids." Another essential fatty acid is linoleic acid (cis-$\Delta^{9,12}$-octadececadienoic acid) which is a substrate for the biosynthesis of

arachidonic acid (all *cis*-$\Delta^{5,8,11,14}$-eicosatetraenoic acid), a precursor of *eicosanoids*, which are hormone-like lipids involved in a variety of physiologically important processes.

The synthesis of arachidonic acid from linoleic acid involves five enzymes two of which are desaturases exhibiting different specificities. The synthesis as outlined in Fig. 12.17 begins with the activation of linoleic acid to linoleoyl-CoA by acyl-CoA synthase. Arachidonic acid is a precursor for a variety of lipid hormones known as *prostaglandins*. Prostaglandins are involved in a large number of

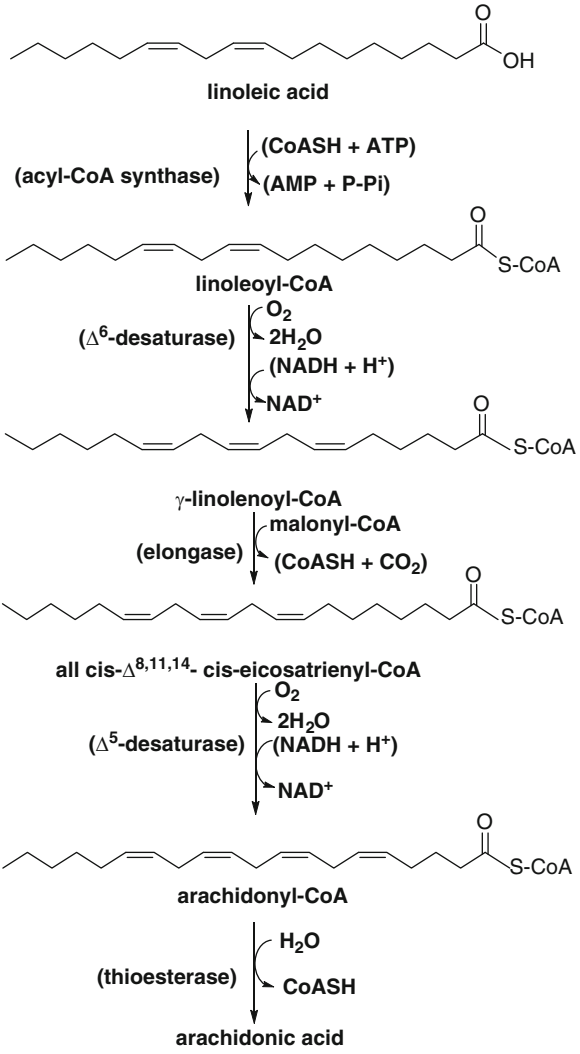

Fig. 12.17 The biosynthesis of arachidonic acid from linoleic acid

physiological functions in humans including the regulation of blood pressure, blood clotting, inflammatory response, and the sleep cycle (Fig. 12.18).

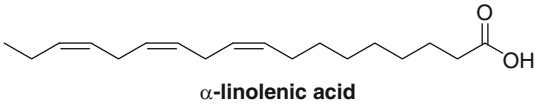

Fig. 12.18 The structure of the ω-fatty acid α-linolenic acid (all *cis*-$\Delta^{9,12,15}$octadectrienoic acid). In the designation ω there is a double bond at the three position relative to the methyl group

Another class of essential fatty acids, known as *omega (ω-3) fatty acids*, is involved in the normal development of tissues such as eyes, nerves, and brain. They are also important in reducing the incidence of coronary heart disease. A typical ω-3 fatty acid is α-linolenic acid.

12.15 Lipoproteins and Lipid Transport

Dietary lipids digested in the small intestine are emulsified and transported as miscelles (see Sect. 12.1). Triacylglycerols which are hydrolyzed primarily to 2-monoacylglycerols are transported to the cells lining the intestinal wall along with cholesterol and phospholipids. After the monoacylglycerol esters are converted to triacylglycerols in the intestinal mucosa they and the other lipids are incorporated into *chylomicrons*. Chylomicrons (Table 12.1) are huge amphipathic particles containing a hydrophobic core and a hydrophilic exterior. The core is made up of triacylglycerols and cholesterol esters, whereas the exterior is composed of cholesterol, phospholipids, and protein. Chylomicrons are transport vehicles that serve to solubilize the otherwise aqueous insoluble lipid material and deliver triacylglycerols to peripheral tissues and cholesterol to the liver. After release from the intestinal cells, the chylomicrons travel through the blood stream to the capillaries of adipose and muscle tissue where the triacylglycerols are either stored (adipose tissue) or acted upon by an extracellular lipoprotein lipase that converts

Table 12.1 Human plasma lipoprotein composition

			Composition (% by weight)				
Lipoprotein	Molecular mass (kDa)	Density (g/ml)	Protein	Cholesterol	Cholesterol esters	P-lipids	TAG[a]
Chylomicrons	40×10^4	0.92–0.96	2.0	2.5	3.3	7.3	86
VLDL	$1–8 \times 10^4$	0.95–1.01	9.0	6.8	13	17	54
IDL	$5–10 \times 10^3$	1.01–1.02	18	7.6	30	21	27
LDL	2.3×10^3	1.02–1.06	24	8.4	40	20	7.0
HDL	175–360	1.06–1.25	44	4.0	15	28	4.5

[a]*TAG* triacylglycerols

the triacylglycerols to glycerol and free fatty acids for metabolic utilization. The lipid-depleted chylomicrons, so-called *chylomicron remnants*, are transported through the blood to the liver where they are taken up by receptors and the cholesterol removed. This dietary cholesterol, along with *de novo* synthesized cholesterol, can reenter the intestine via the gall bladder and bile duct for excretion. In liver, cholesterol and triacylglycerols may be incorporated into "very low density lipoproteins", *VLDL*. The VLDL is exported to the capillaries of adipose tissue where triacylglycerols may again be removed for storage (adipose tissue) or muscle tissue where lipoprotein lipase hydrolyzes the triacylglycerols for metabolic utilization. The VLDL remnants, depleted of triacylglycerols, are then converted to *intermediate-density lipoproteins* (IDL) and then *low-density lipoproteins* (LDL). In the transformation of VLDL to LDL most of the protein is removed and much of the cholesterol is esterified by an acyltransferase using lecithin as the substrate. The cholesterol-containing LDLs are then transported to liver and extrahepatic tissue where they are taken up by LDL receptors by engulfment and brought into the cell (*endocytosis*). Cholesterol esters are hydrolyzed within cells by a lysosomal (small organelle) lipase which permits the cell to utilize the free fatty acids. The cholesterol can enter the cell membrane if required, or if present in excess, stored in the cell after re-esterification by acyl-CoA: cholesterol acyltransferase. Cholesterol is exported out of extrahepatic tissue by "high-density lipoprotein" (HDL), the so-called "good cholesterol."

Table 12.1 illustrates the various lipoproteins and their properties. The sequence of events describing cholesterol transport is summarized in Fig. 12.19 and in the 1985 Nobel Lecture by Brown and Goldstein [15].

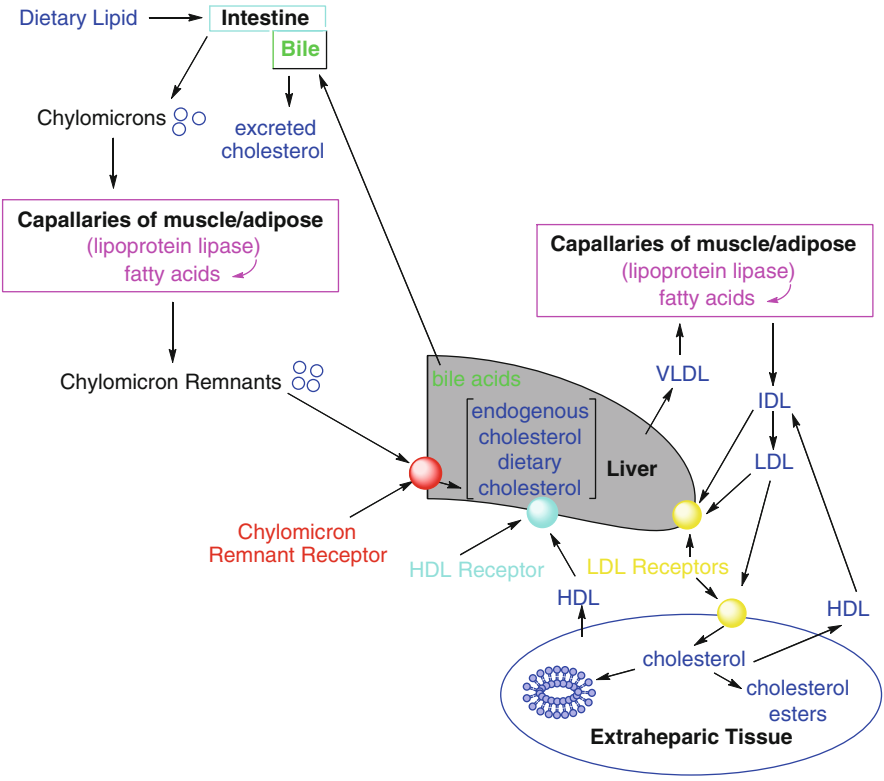

Fig. 12.19 Transport of cholesterol in animal tissues. Structures in *blue* indicate the presence of cholesterol

12.16 Cholesterol Biosynthesis

Cholesterol has two very important biological functions: it is an integral and essential part of biological membranes, and it is a precursor of sterol and steroid hormones as well as bile salts and acids.

Cholesterol biosynthesis takes place primarily in the liver. As with ketone body formation (Fig. 12.14), the synthesis of cholesterol starts with the condensation of two molecules of acetyl-CoA.

Before the discovery of acetyl-CoA by Lynen in 1951 [4], Little and Bloch [16] suggested that acetate was the basic building block of cholesterol. Other key elements in understanding cholesterol biosynthesis came with the discovery of the involvement of mevalonic acid [17], and the cyclization of squalene to lanosterol [18, 19]. The genesis of our knowledge of cholesterol biosynthesis is provided in the 1964 Nobel Lecture of Konrad Bloch [20].

The pathway for cholesterol synthesis is summarized in Fig. 12.20.

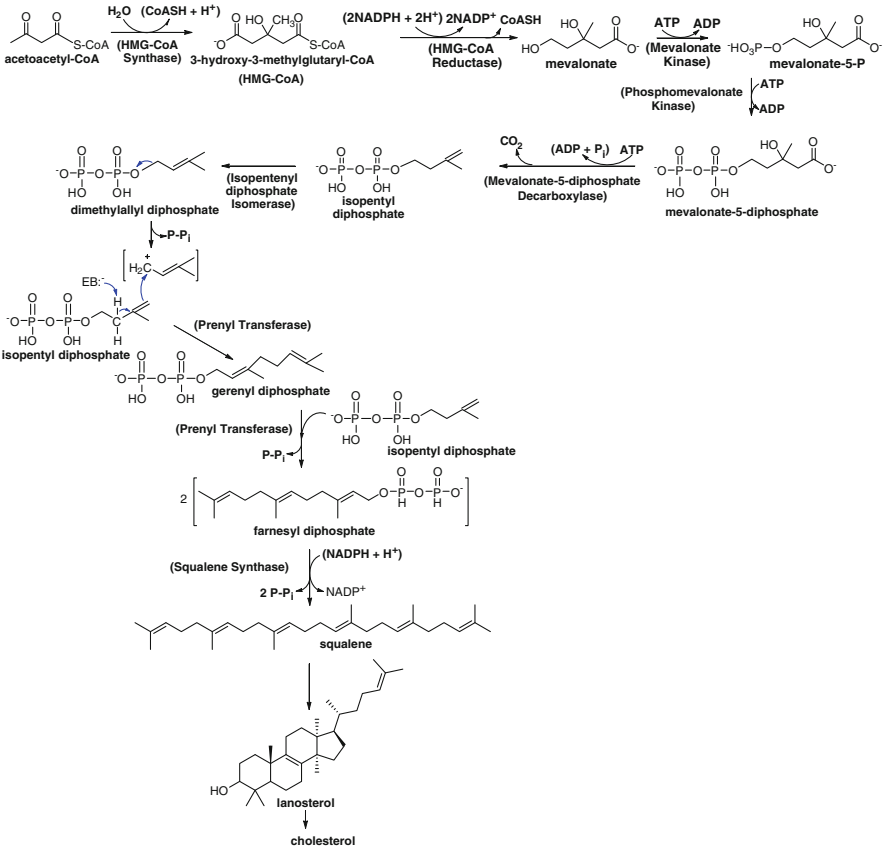

Fig. 12.20 *De novo* biosynthetic pathway for cholesterol biosynthesis

12.17 The Glyoxylate Cycle

Plants and certain bacteria, but not animals, have the ability to convert lipid, specifically acetyl-CoA, to carbohydrate. This capability is a result of two factors: first, there exists in plants an organelle, the *glyoxysome*, whose enzymes convert acetyl-CoA to succinate, and second, the succinate is utilized in mitochondria to synthesize malate and thus support gluconeogenesis through its conversion to cytosolic oxaloacetate. The oxaloacetate is ultimately converted to mono and disaccharides (Fig. 12.21).

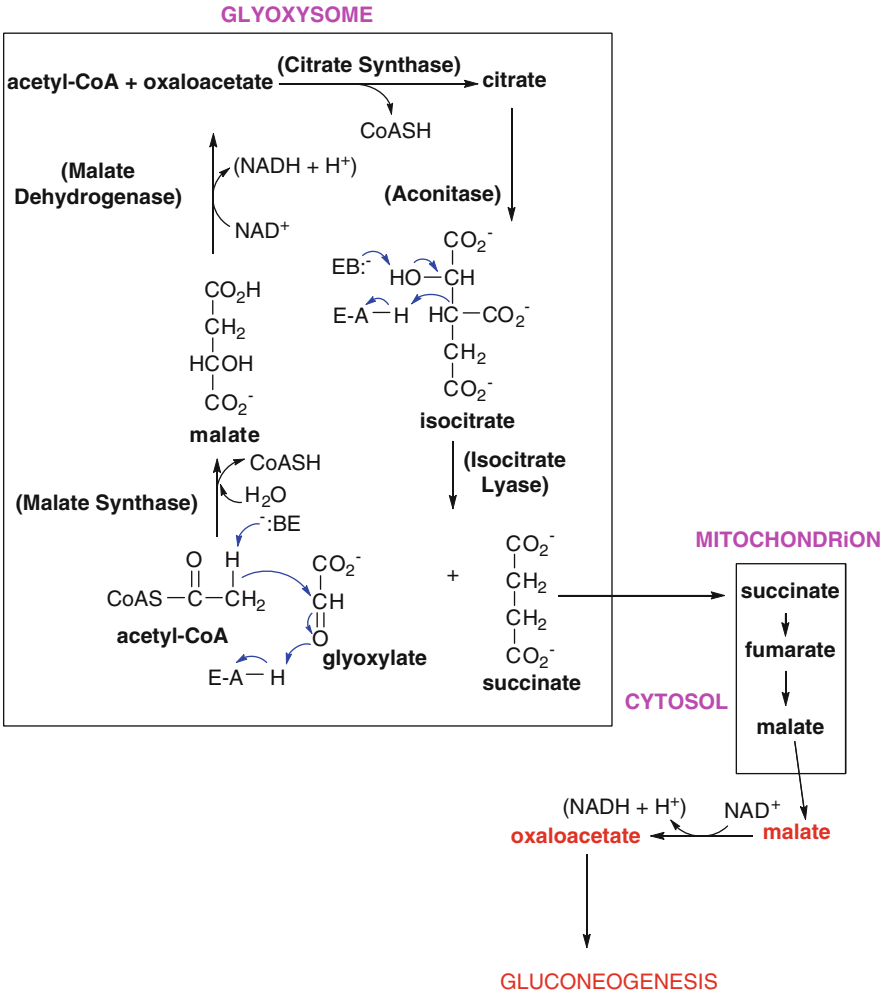

Fig. 12.21 The glyoxylate cycle (*left*) in coordination with Krebs Cycle enzymes produces oxaloacetate, a substrate for gluconeogenesis

References

1. Brady L, Brzozowski AM, Derewenda ZS, Dodson E, Dodson G, Tolley S, Turkenburg JP, ChristiansonL Huge-Jensen B, Norskov L, Thim L, Menge U (1990) A serine protease triad forms the catalytic centre of a triacylglycerol lipase. Nature 343:767–770
2. Knoop F (1904) Der Abbau Aromatischer Fettsauren im Tierkoper. Beitr Chem Physiol Pathol 6:150–162
3. Dakin HD (1909) The mode of oxidation in the animal organism of phenyl derivatives of fatty acids. IV Further studies on the fate of phenylpropionic acid and some of its derivatives. J Biol Chem 6:203–219

4. Lynen F, Reichert E (1951) The chemical structure of activated acetic acid. Angew Chem 63:47–48
5. Hisanaga Y, Ago H, Nakagania J, Hanada K, Ida K, Yamamoto M, Hori T, Arii Y, Sugahara M, Kuramitsu S, Yokoyama S, Miyano M (2004) Structural basis of the substrate-specific two-step catalysis of long chain fatty acyl-CoA synthetase dimer. J Biol Chem 279:31717–31726
6. Bieber LL (1988) Carnitine. Annu Rev Biochem 88:261–283
7. Lynen F, Ochoa S (1953) Enzymes of fatty acid metabolism. Biochim Biophys Acta 12:299–314
8. Langdon RG (1957) The biosynthesis of fatty acids in rat liver. J Biol Chem 226:615–629
9. Majerus PW, Alberts AW, Vagelos PR (1964) The acyl carrier protein of fatty acid synthesis: purification, physical properties, and substrate binding site. Proc Natl Acad Sci USA 51:1231–1238
10. Stetten DW Jr, Schoenheimer R (1940) The conversion of palmitic acid into stearic and palmitoleic acids in rats. J Biol Chem 133:329–345
11. Wells TN (1991) ATP-Citate lyase from rat liver. Characterization of the citryl-enzyme complexes. Eur J Biochem 199:163–168
12. Zhang S, Kim K-H (1995) Glucose activation of acetyl-CoA carboxylase in association with insulin sectrtion in a pancreatic β-cell line. J Endocrinol 147:33–41
13. Witters LA, Watts TD, Daniels DL, Evans JL (1988) Insulin stimulates the dephosphorylation and activation of acetyl-CoA carboxylase. Proc Natl Acad Sci USA 85:5473–5477
14. Weinhouse S, Medes G, Floyd NF (1944) Fatty acid metabolism. The mechanism of ketone body synthesis from fatty acids with isotopic carbon as tracer. J Biol Chem 155:143–151
15. Brown MS, and Goldstein JL (1985) A receptor mediated pathway for cholesterol homeostatis. Nobel Lecture, 9 December 1985, 284–324
16. Little HN, Bloch K (1950) Studies on the utilization of acetic acid for biological synthesis of cholesterol. J Biol Chem 183:33–46
17. Rudney H (1957) The biosynthesis of β-hydroxy-β-methylglutaric acid. J Biol Chem 227:363–377
18. Ruzicka L (1953) The isoprene rule and the biogenesis of terpenic compounds. Experientia 9:357–367
19. Maudgal RK, Tchen TT, Bloch K (1958) 1,2-methyl shifts in the cyclization of squalene to cholesterol. J Am Chem Soc 80:2589–2590
20. Bloch K (1964) The biological synthesis of cholesterol. Nobel Lecture, 11 December 1964, 78–100

Chapter 13
Amino Acid Metabolism

13.1 The Nitrogen Cycle

So far our discussions of metabolism have focused on molecules consisting predominately of carbon, oxygen, and hydrogen. We have also seen the importance of nitrogen in biological molecules, including proteins and nucleic acids. Thus, how nitrogen for the production of these molecules is assimilated and metabolized is a central concern in biochemistry. Inorganic nitrogen is found in many forms on earth, ranging in nitrogen oxidation number from nitrate ($NO_3^-, +5$) to ammonia (NH_3,-3), and including the most abundant form, gaseous nitrogen (N_2, 0). Compared to carbohydrate metabolism, the form of inorganic nitrogen utilized by different organisms is quite variable. Many organisms can metabolize oxidized or reduced forms of nitrogen, but few can work with N_2 directly, referred to as "nitrogen fixation."

$$N_2 + 3H_2 \rightarrow 2NH_3 \qquad \text{Nitrogen fixation.}$$

This reaction, which ultimately produces most biologically accessible nitrogen, is carried out by bacteria containing the nitrogenase enzyme complex [1, 2]. These bacteria can be free-living, or live in symbiosis with some plants. In both cases, however, oxygen must be excluded from nitrogenase as it is a potent inhibitor of nitrogen fixation. In free-living bacteria, N_2 fixation is carried out anerobically or under conditions where a collection of oxidase enzymes consume oxygen faster than it can react with nitrogenase. The symbiotic bacteria responsible for nitrogen fixation in plants have lost this capacity in a trade off for a plant-derived food supply. Instead, leguminous plants form specialized "nodules" on their roots containing a hemoglobin molecule called leghemoglobin (from the fact that many of these plants are legumes) that scavenges oxygen and transports it to the respiring bacteria encapsulated inside.

The ammonia resulting from nitrogen fixation can be utilized directly by the plant, but is often oxidized to nitrite and nitrate by other bacteria in the soil,

H.J. Fromm and M.S. Hargrove, *Essentials of Biochemistry*,
DOI 10.1007/978-3-642-19624-9_13, © Springer-Verlag Berlin Heidelberg 2012

a process called "nitrification." Thus, most plants obtain nitrogen in the form of nitrate from the soil. Two reactions are needed to reduce nitrate to ammonia. These are the conversion of NO_3^- to nitrite (NO_2^-) by nitrate reductase, and the reduction of nitrate to ammonium ion by nitrite reductase.

$$NO_3^- + NADPH + H^+ \overset{\text{Nitrate Reductase}}{\rightleftharpoons} NO_2^- + NADP^+ + H_2O,$$

$$NO_2^- + 3NADPH + 4H^+ \overset{\text{Nitrite Reductase}}{\rightleftharpoons} NH_4^+ + 3NADP^+ + H_2O + OH^-.$$

Plants incorporate ammonia into amino acids through synthetases that fix ammonia and transamination reactions.

13.2 Amino Acid Metabolism [3]

As pointed out in Chap. 2 there are ten "essential" and ten "nonessential" amino acids. These are strictly dietary terms; all 19 α-amino acids and the one α-imino acid (proline) are essential for human life. The pioneering research in this area of nutrition was carried out first on rats [4] and then on human subjects. Although most biochemistry textbooks cover the metabolism of all of these compounds in great detail, this chapter is limited to an outline of the biosynthesis of the amino acids. It should be noted that there are a multiplicity of pathways for amino acid metabolism depending upon the organism involved, i.e., whether it be plant, animal, or bacteria. In the case of bacteria especially, different genera may exhibit different pathways of biosynthesis or degradation for a particular amino acid.

The catabolism of the amino acids will focus on the catabolic end products and on some of their metabolic intermediates.

The human dietary nonessential amino acids are:

Alanine	Glutamine
Asparagine	Glycine
Aspartate	Proline
Cysteine	Serine
Glutamate	Tyrosine

13.3 Biosynthesis of the Nonessential Amino Acids

Amino acids that are synthesized directly from glycolytic and Citric Acid Cycle intermediates involving PLP-dependent transamination are alanine, aspartate, and glutamate. Pyruvate is not a member of the Citric Acid Cycle, but it is a precursor of

TCA intermediates. In the case of serine the glycolytic intermediate precursor is 3-phosphoglycerate (Fig. 13.1).

Amino acids that are synthesized directly from other amino acids are asparagine, glutamine, proline, tyrosine, and glycine (Fig. 13.2).

The biosynthesis of the sulfur containing amino acid L-cysteine occurs by a number of different pathways depending upon the organism. The simplest sequence of reactions involves plants and certain bacteria as illustrated in Fig. 13.3.

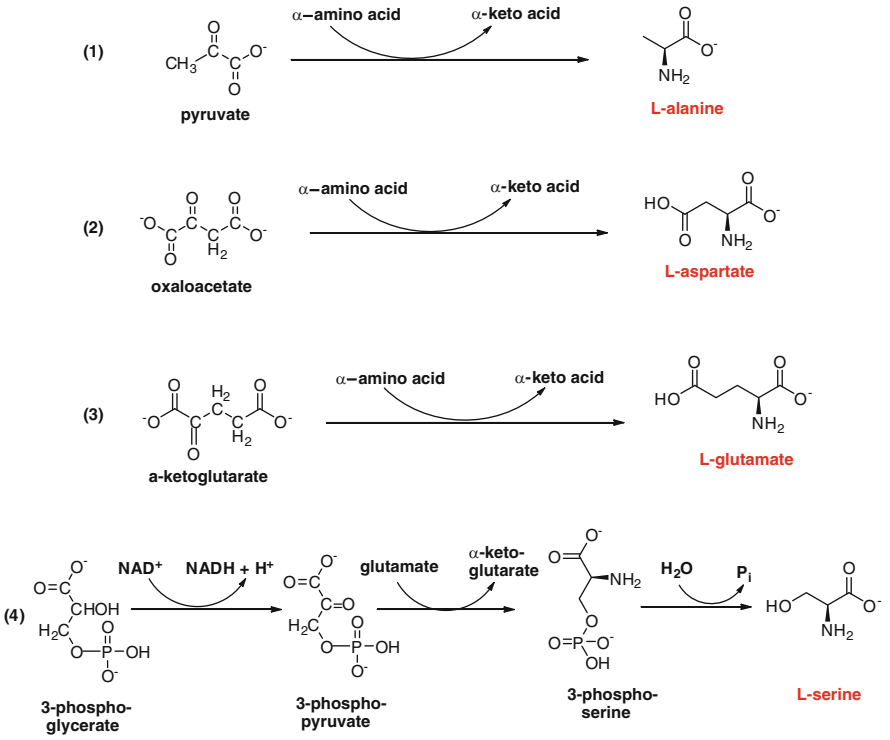

Fig. 13.1 The biosynthesis of L-alanine, L-aspartate, L-glutamate, and L-serine from glycolytic and Citric Acid Cycle precursors. Transamination is involved in all four reactions

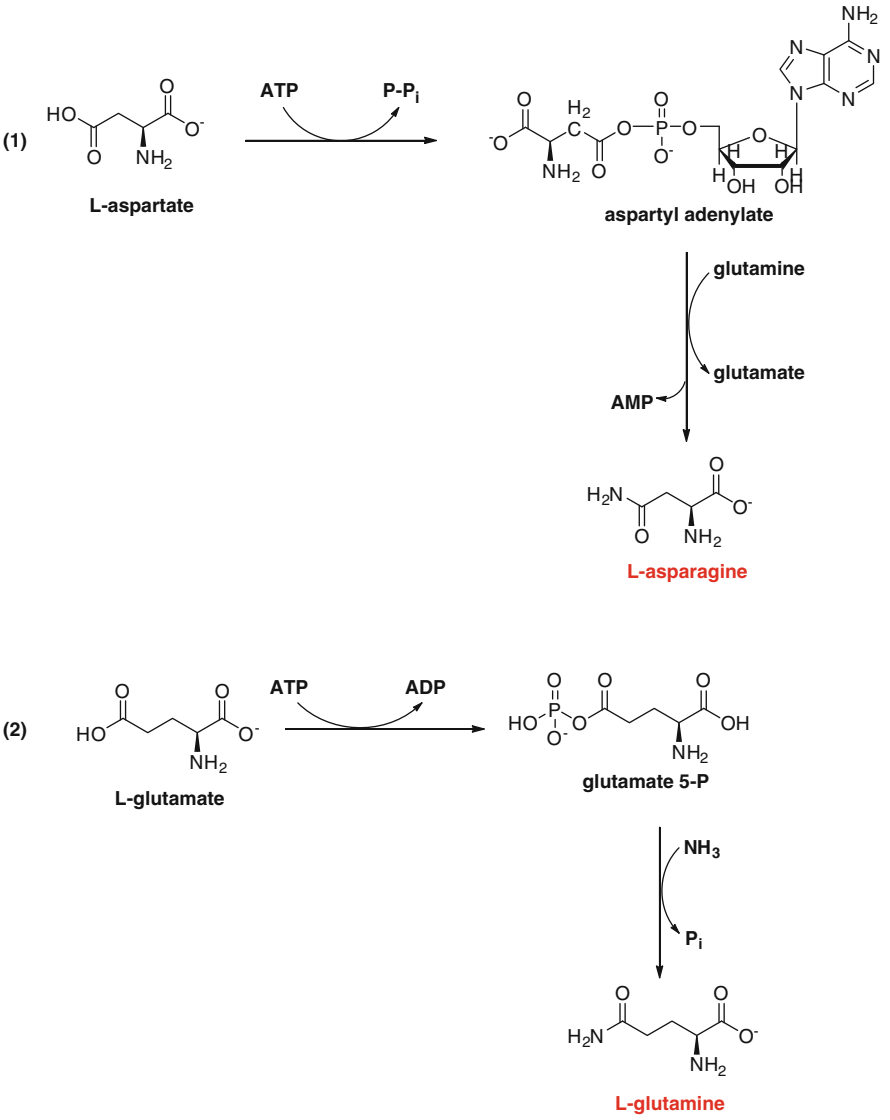

Fig. 13.2 (continued)

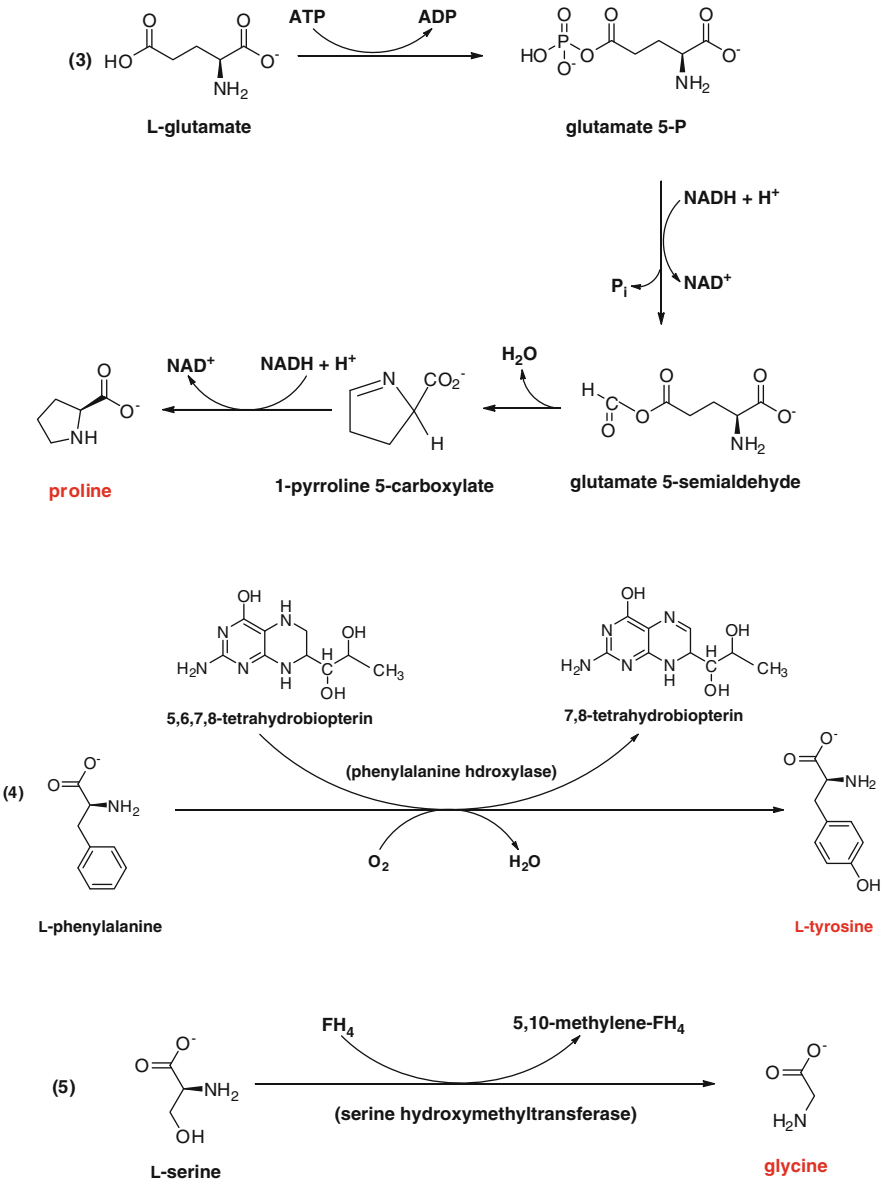

Fig. 13.2 The biosynthesis of asparagine, glutamine, proline, tyrosine, and glycine from amino acid precursors. Glycine can also be synthesized from threonine by the enzyme threonine aldolase (Chap. 6)

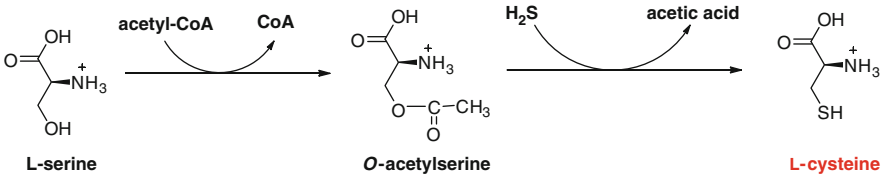

Fig. 13.3 A number of pathways are involved in the biosynthesis of cysteine. The pathway illustrated here demonstrates the utilization of H_2S which supplies the sulfur atom to the amino acid

13.4 Amino Acid Degradation

The carbon skeletons of amino acids are degraded in the TCA Cycle (Chap. 9). The fates of the various amino acids are outlined in Scheme 13.1.

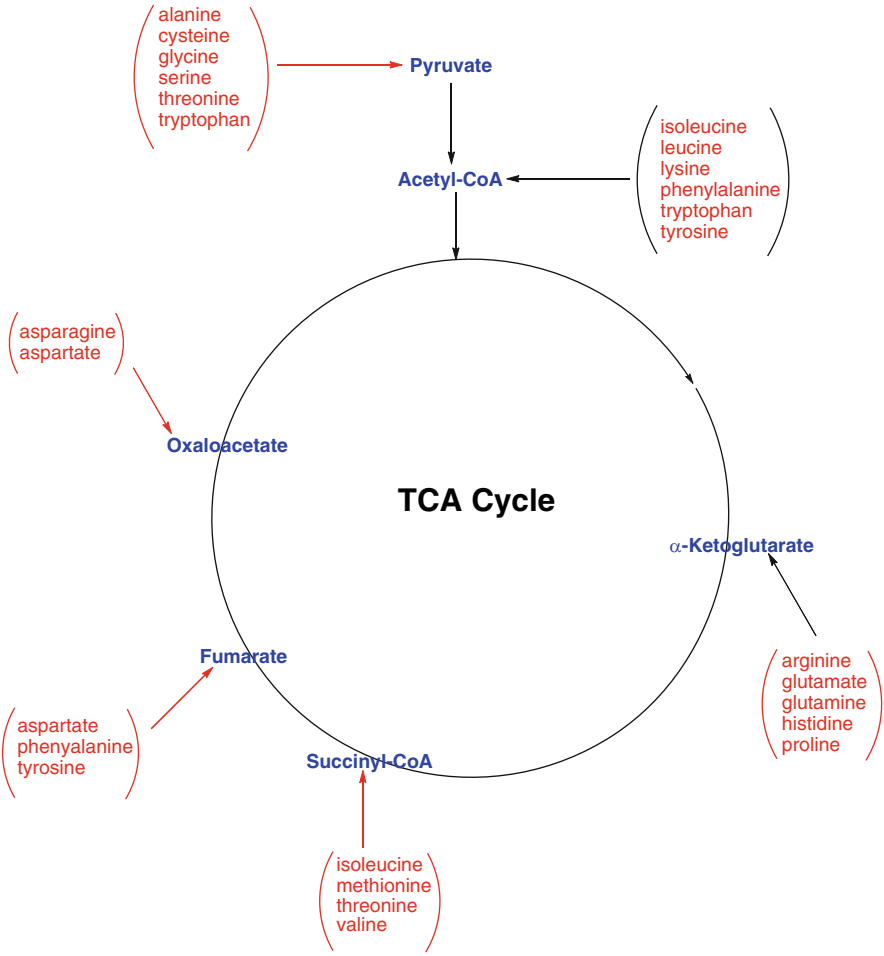

Scheme 13.1 The site of entry of amino acids into the TCA Cycle

13.5 Essential Amino Acids

The essential dietary amino acids required by humans are synthesized in plants and bacteria. The synthetic pathways involving common metabolic precursors and important intermediates are listed in Fig. 13.4.

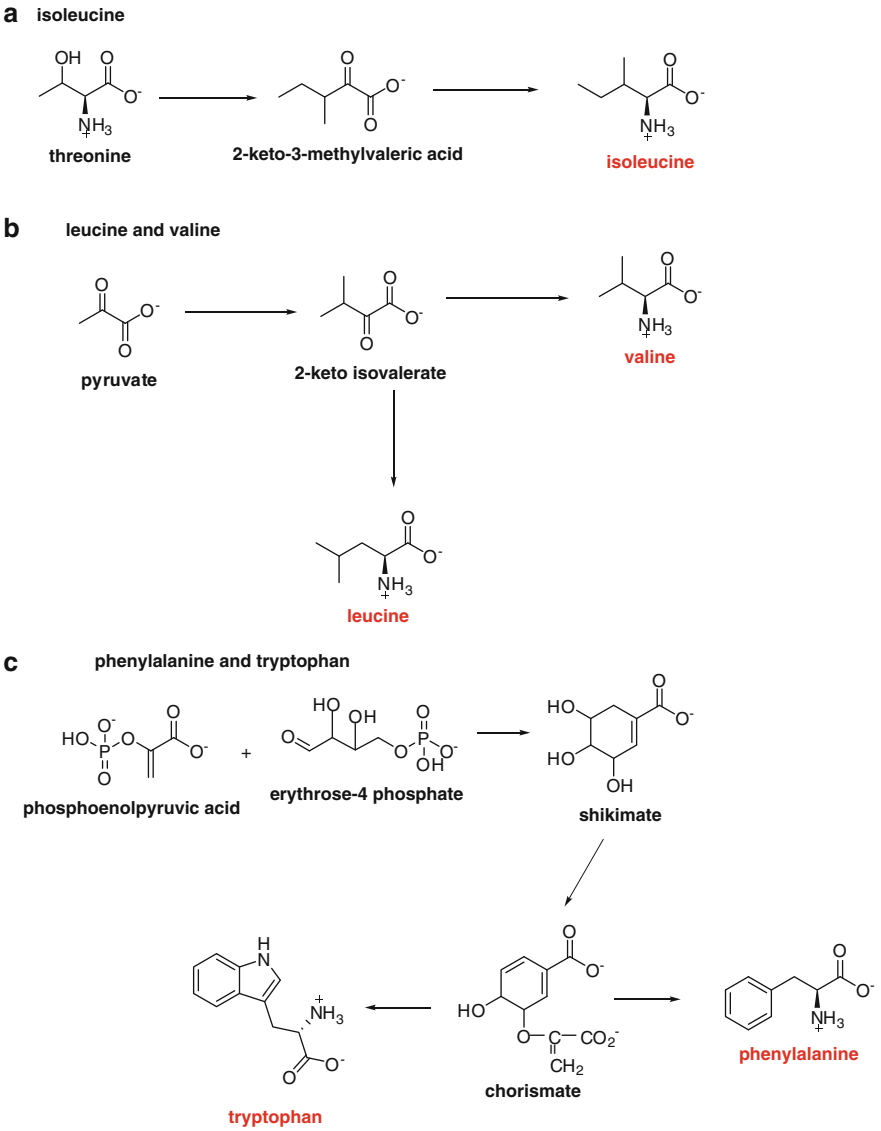

Fig. 13.4 (continued)

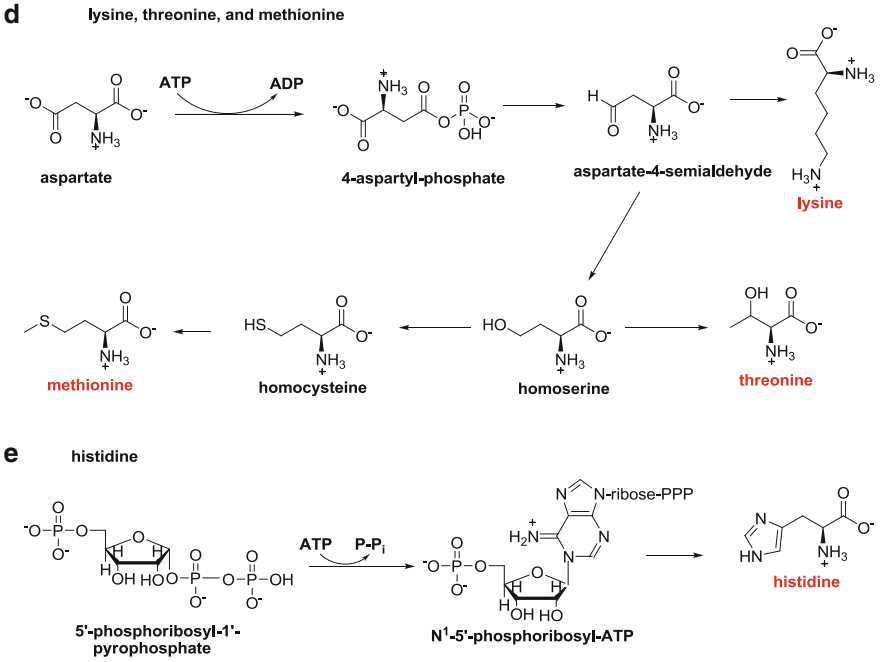

Fig. 13.4 Synthesis of the essential dietary amino acids

Arginine is synthesized in a pathway very similar to that described for proline (Fig. 13.2) [3] except that glutamate is acetylated to *N*-acetylglutamate and the acetyl group retained to prevent cyclization as is the case with proline. The *N*-acetylglutamate-5-semialdehyde is then aminated to *N*-acetylornithine. After deacylation, the resulting ornithine is converted to arginine as shown in Fig. 13.12.

13.6 Amino Acids are Precursors of Metabolic Regulators

Amino acids are precursors of metabolic regulators such as hormones and as intermediates for the synthesis of essential enzyme and cellular components. The following section illustrates a few of the compounds in this important class of biomolecules.

13.6.1 Glutathione

Glutathione is a tripeptide made up of glutamate, cysteine, and glycine. It can exist either in the oxidized or reduced forms and plays a major role in maintaining the cell's redox potential and the integrity of protein sulfhydryl groups (Fig. 13.5). In addition, it is involved in a number of detoxification and metabolic reactions.

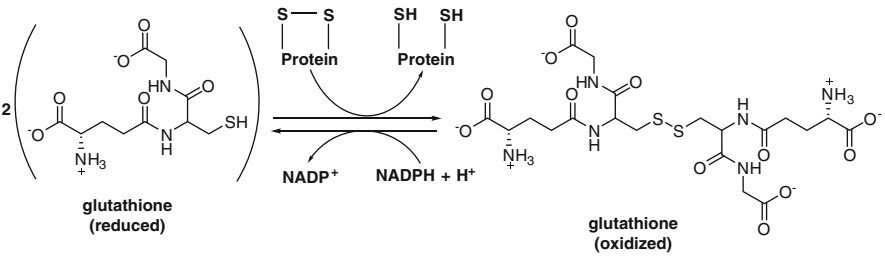

Fig. 13.5 Interconversion of the reduced and oxidized forms of the tripeptide glutathione. Note that the peptide bond between glutamate and cysteine does not involve the α-amino group of the dicarboxylic acid. Reduction of oxidized glutathione is catalyzed by the enzyme glutathione reductase

13.6.2 Epinephrine

Epinephrine or adrenalin is a hormone produced in the medulla of the kidney. It serves to increase blood pressure and the heart rate and also stimulates glycogenolysis. It is synthesized from tyrosine (Fig. 13.6).

Fig. 13.6 The structure of the hormone epinephrine

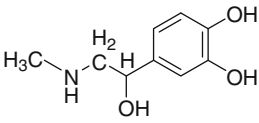

13.6.3 Histamine

Decarboxylation of L-histidine gives rise to histamine, a neurotransmitter. It is thought to trigger the inflammatory response. It also increases capillary permeability (Fig. 13.7).

Fig. 13.7 The structure of the neurotransmitter histamine

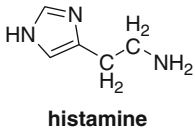

13.6.4 Serotonin

Serotonin is a neurotransmitter derived from the amino acid tryptophan; however, it is also involved in intestinal mobility. Serotonin is best known for its role in affecting one's sense of well-being (Fig. 13.8).

Fig. 13.8 Structure of the neurotransmitter serotonin

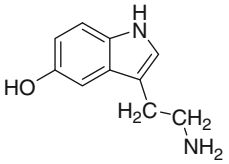

serotonin

13.6.5 Thyroxine

The hormone thyroxine is synthesized from tyrosine in the thyroid gland. Physiologically, it increases the rate of metabolism. It contains four atoms of iodine (Fig. 13.9), but it is not the only thyroid hormone produced in the gland, e.g., triiodothyronine contains three iodine atoms.

Fig. 13.9 Structure of the thyroid hormone thyroxine

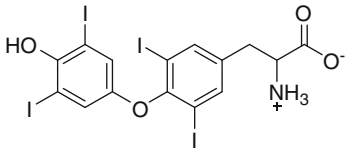

thyroxine

13.6.6 Nitric Oxide

Nitric oxide (NO), a neurotransmitter derived from arginine serves as a vasodilator and is also involved in the immune response.

13.6.7 S-*adenosylmethionine*

S-Adenosylmethionine (SAM), "active methionine," is a physiologically important methyl donor. It is involved in the methylation of DNA, guanidoacetate (to form creatine), norepinephrine, and RNA.

(a) Its biosynthesis from methionine is shown in Fig. 13.10.
(b) Figure 13.11 describes the methylation of norepinephrine by SAM.

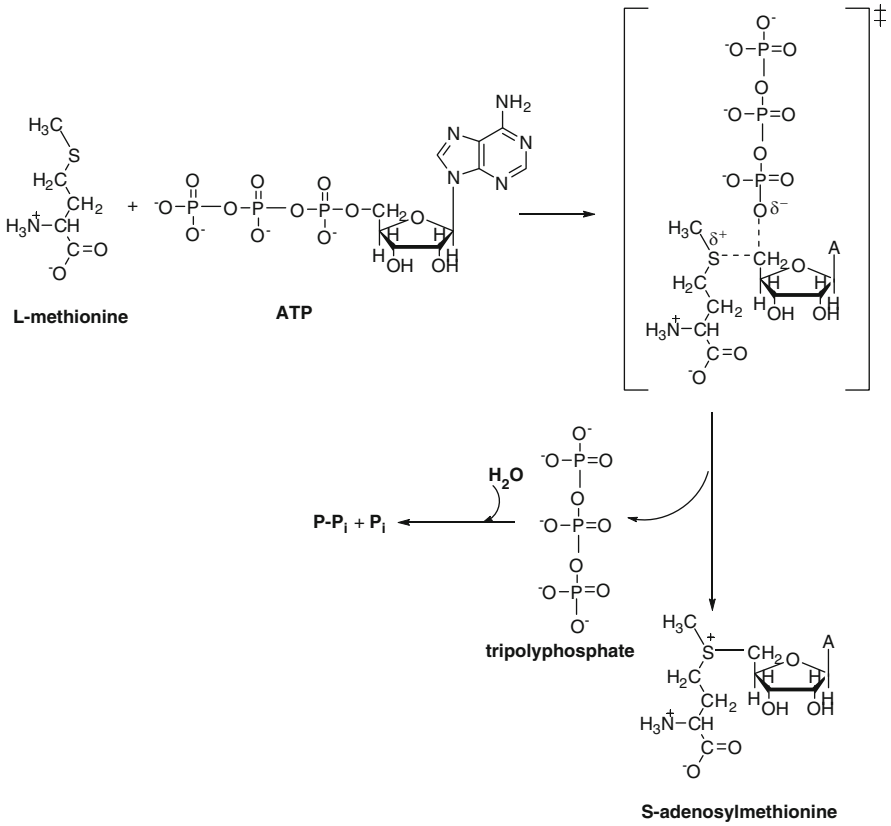

Fig. 13.10 The biosynthesis of *S*-adenosylmethionine (SAM) from methionine

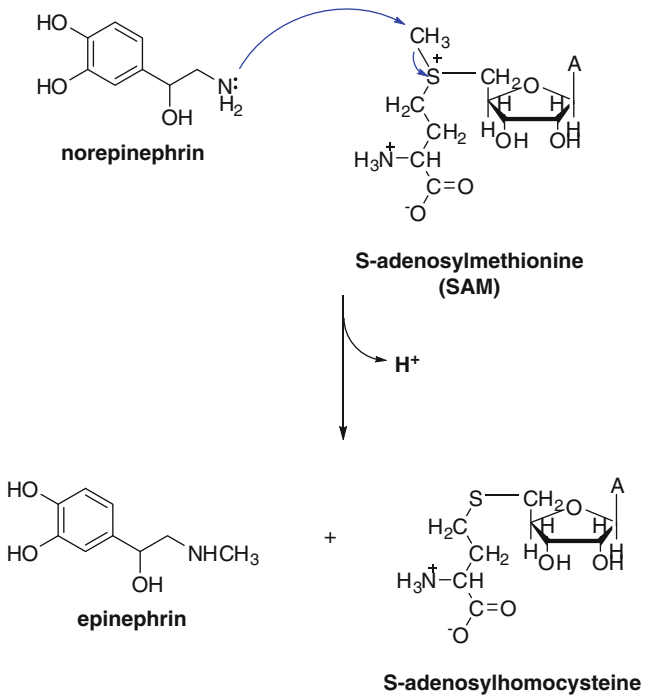

Fig. 13.11 Methylation of norepinephrine by *S*-adenosylmethionine to form epinephrine

13.7 The Krebs Urea Cycle

Ammonia (NH_3) is produced in the course of amino acid catabolism. Fish excrete NH_3 as such, whereas birds excrete their amino acid nitrogen as uric acid, and land animals eliminate their NH_3 as urea. Urea is synthesized in a process known as the Krebs Urea Cycle.

In the Krebs Urea Cycle, NH_3 is first incorporated into carbamoyl phosphate (Chap. 14) and ultimately into the amino acid L-arginine which is hydrolyzed to produce urea. Scheme 13.2 outlines the Krebs Urea Cycle [4].

The carbamoyl phosphate used in the first step of the Cycle is synthesized in the mitochondrial matrix and its reaction with ornithine to form citrulline also occurs in the matrix. The citrulline then leaves the mitochondrion for the cytosol where it reacts with L-aspartate to produce arginosuccinate. In Scheme 13.2 the reactions in *red* occur in mitochondria and those in *black* in the cytosol.

The individual reactions involved in the Krebs Urea Cycle are shown in Fig. 13.12 along with the enzymes and reaction mechanisms [5].

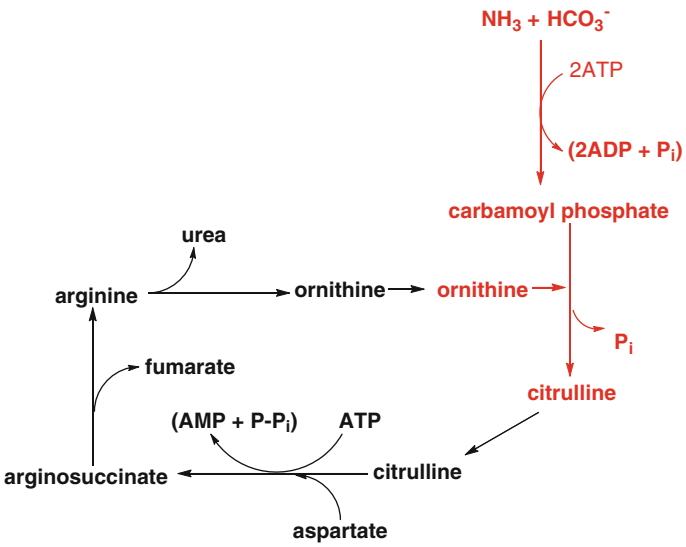

Scheme 13.2 The synthesis of urea from ammonia involves enzymes in the cytosol (black) and the mitochondria (red).

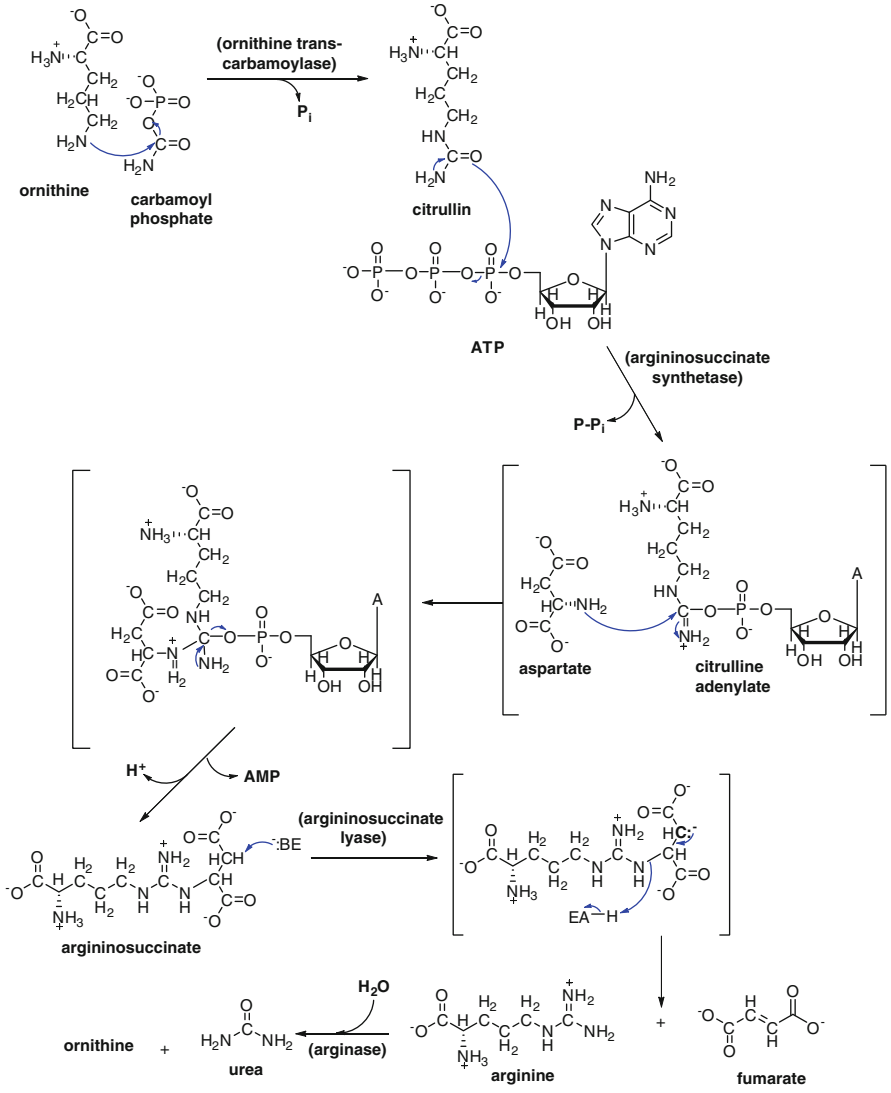

Fig. 13.12 The individual steps involved in the Krebs Urea Cycle

References

1. Campbell WH (1999) Nitrate reductase structure, function and reulation: bridging the gap between biochemistry and physiology. Annu Rev Plant Physiol Plant Mol Biol 50:277–303
2. Rees DC, Howard JB (2000) Nitrogenase: standing at the crossroads. Curr Opin Chem Biol 4:559–566
3. Bender DA (1985) Amino acid metabolism. Wiley, New York
4. Rose WC (1937) The nutritive significance of amino acids and certain related compounds. Science 86:298–300
5. Cohen PP (1981) The ornithine-urea cycle: biosynthesis and regulation of carbamoyl phosphate synthetase I and ornithine transcarbamylase. Curr Topic Cell Regul 18:1–19

Chapter 14
Nucleotide Metabolism

Nucleotide metabolism occurs in all living organisms. The most prominent biomolecule, in terms of the number of reactions that it participates in, is the nucleotide, ATP. Although nucleotide metabolism is universal, it does differ to some extent in different organisms, e.g., the enzymes of purine nucleotide biosynthesis are separate enzymes in *Escherichia coli*, whereas some of these same enzymes are part of dual-functional proteins in humans.

It would be beyond the scope of this text to cite all or even most of the early contributors to our knowledge of nucleotides and their metabolism; however, a few names do stand out: Emil Fischer, John Buchanan, Robert Greenberg, Arthur Kornberg, Arthur Pardee, and Peter Reichard.

Nucleotides are not only components of RNA and DNA but they also play a central role in energy metabolism: nucleoside di and triphosphates are substrates for ligases as well as components of coenzymes.

Nucleotides differ not only in their nitrogenous bases but also in their sugars. This chapter will consider both the biosynthesis and biodegradation of nucleotides.

14.1 *De Novo* Pyrimidine Nucleotide Biosynthesis

14.1.1 The Synthesis of Uridine-5′-Monophosphate

Using isotopes investigators were able to show that three elemental compounds, glutamine, L-aspartate, and bicarbonate are incorporated into the pyrimidine base in the course of *de novo* pyrimidine nucleotide biosynthesis. Furthermore, they were able to identify which of the six atoms in pyrimidines arose from these compounds (Fig. 14.1).

H.J. Fromm and M.S. Hargrove, *Essentials of Biochemistry*,
DOI 10.1007/978-3-642-19624-9_14, © Springer-Verlag Berlin Heidelberg 2012

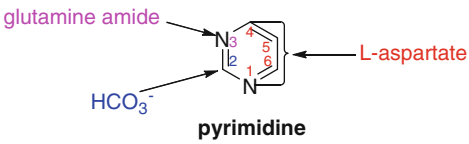

Fig. 14.1 The origin of atoms in the pyrimidine molecule and the numbering system of the pyrimidine ring

Aspartate, glutamine, and bicarbonate give rise to orotate which is the precursor of the three pyrimidine bases found in RNA and DNA–uracil, cytosine, thymine. Shown in Fig. 14.2 are the reactions that lead to the *de novo* synthesis of uridine-5′-monophosphate (UMP), the end-product of the pathway.

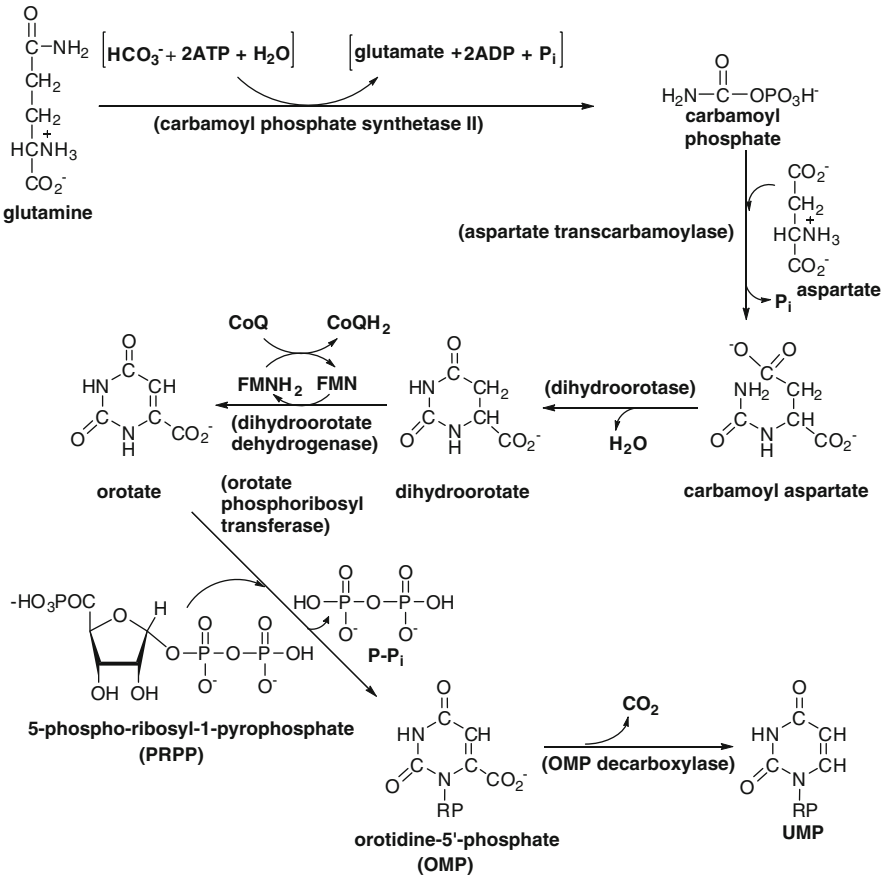

Fig. 14.2 The *de novo* biosynthesis of UMP from orotate and 5-phospho-ribosyl-1-pyrophosphate (PRPP)

The structures of Coenzyme Q (CoQ) and reduced CoQ, $CoQH_2$ are shown in Fig. 14.3.

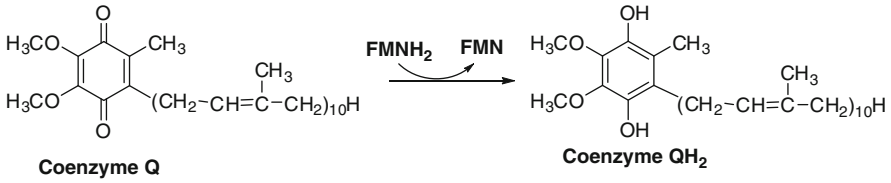

Fig. 14.3 Structures of oxidized and reduced forms of coenzyme Q

14.1.2 Enzymes of Pyridine Nucleotide Biosynthesis

In *E. coli*, the enzymes of pyrimidine biosynthesis are separate entities; however, in animals a single polypeptide chain may contain more than one enzyme activity, e.g., carbamoyl phosphate (CAP) synthetase II, dihydrooratase, and aspartate transcarbamoylase (ATCase) are on one polypeptide chain.

14.1.2.1 Carbamoyl Phosphate Synthetase II

CAP synthetase II uses NH_3 from the deamination of glutamine in the synthetase reaction. HCO_3^- rather than CO_2 is used to form carbamate, a probable intermediate, and thus does not require biotin as a coenzyme (Fig. 14.4).

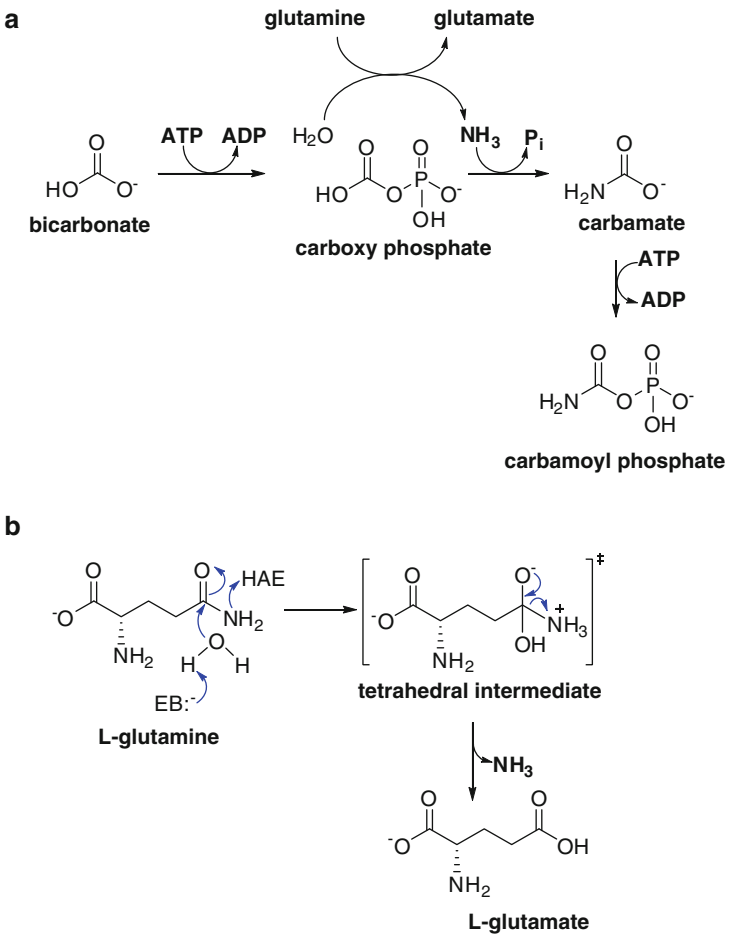

Fig. 14.4 CAP synthetase II uses HCO_3^- and two moles of ATP in the production of carbamoyl phosphate (**a**). Mechanism for the glutaminase activity inherent in CAP synthetase II is shown in (**b**)

14.1.2.2 Aspartate Transcarbamoylase (ATCase)

ATCase is the first committed step in pyrimidine nucleotide biosynthesis. The enzyme is a dodecamer consisting of six catalytic and six regulatory subunits. A plot of velocity versus L-aspartate is sigmoidal. The cooperativity has been explained based on the Monod two-state model [1].

Kinetic studies of the catalytic subunit have shown that the kinetic mechanism is Ordered Bi Bi with carbamoyl phosphate (CAP) adding first to the enzyme and P_i dissociating last [2]. Figure 14.5 presents the chemical mechanism based on studies of isotope effects on the kinetics of the system [3].

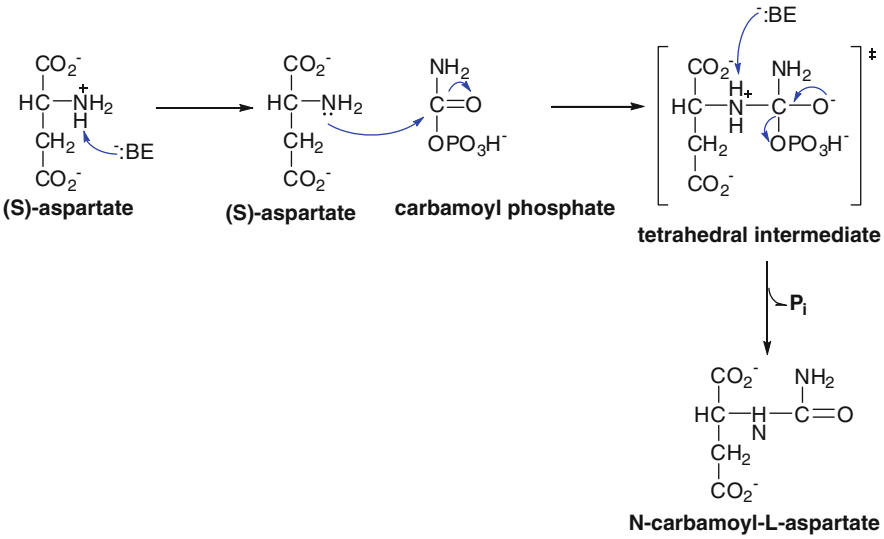

Fig. 14.5 ATCase produces carbamoyl-L-aspartate from L-aspartate and carbamoyl phosphate. A tetrahedral intermediate is thought to participate in the mechanism

14.1.2.3 Orotate Phosphoribosyl Transferase

Arthur Kornberg and his coworkers were the first to demonstrate the involvement of 5-phospho-ribosyl-1-pyrophosphate (PRPP) in the biosynthesis of pyrimidine nucleotides [4]. They also showed that orotidine-5′-phosphate (OMP) is a precursor of UMP and that the enzyme involved in OMP synthesis is a phosphoribosyltransferase.

There are two plausible mechanisms for orotate phosphoribosyltransferase. One involves an S_N1 and the other an S_N2 reaction. In both cases there is an inversion of configuration at the C-1′ of ribose in going from PRPP to OMP.

Goiten et al. [5] studied orotate phosphoribosyltransferase using the protocol of kinetic isotope effects and concluded that a carbocation is an intermediate in the transferase reaction. These investigations accord with mechanism *b* in Fig. 14.6.

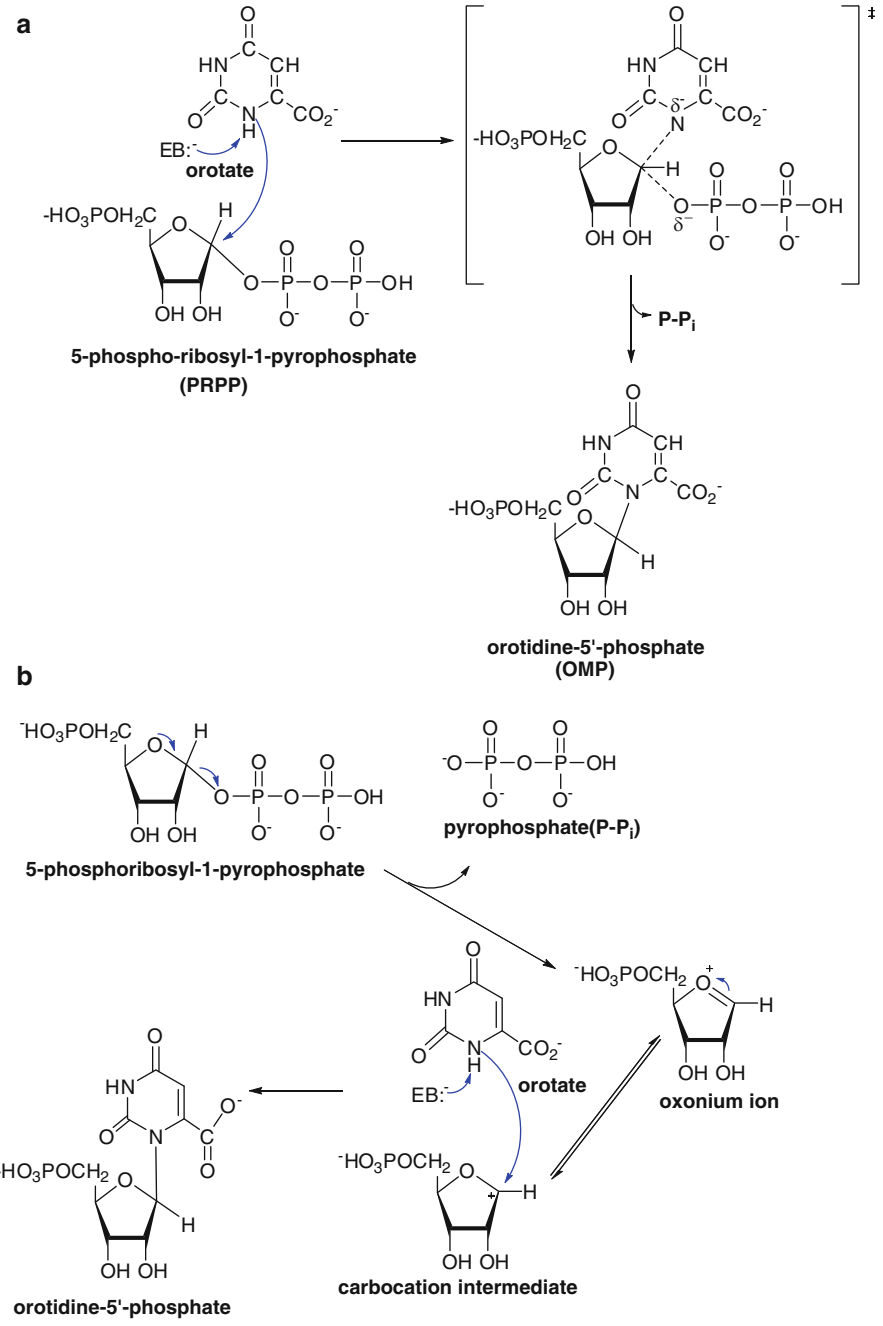

Fig. 14.6 Orotate phosphoribosyltransferase catalyzed synthesis of orotidine-5′-phosphate from orotate and PRPP. Mechanism **a** has a tetrahedral intermediate as part of the mechanism (S_N2). Mechanism **b** involves an oxonium ion intermediate (S_N1)

14.1.2.4 Dihydroorotase

The conversion of carbamoyl aspartate to dihydroorotate by dihydroorotase involves the participation of Zn^{2+} ions associated with the enzymes shown in Fig. 14.7.

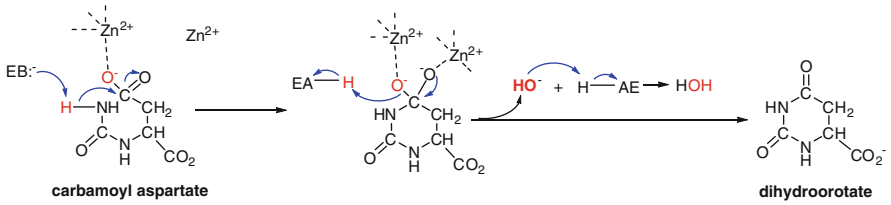

Fig. 14.7 Ring closure of carbamoyl aspartate catalyzed by dihydroorotase

14.1.2.5 Orotidine-5′-Phosphate Decarboxylase (OMP Decarboxylase)

The OMP decarboxylase reaction leads to the formation of the biologically important nucleotide UMP, the precursor of thymidine and cytidine nucleotides.

A number of mechanisms have been suggested for OMP decarboxylase. These include a zwitter ion mechanism, a carbene mechanism, a nucleophilic addition mechanism, and one in which the decarboxylation is facilitated by amino and carboxylate groups on the enzyme [6] (Fig. 14.8).

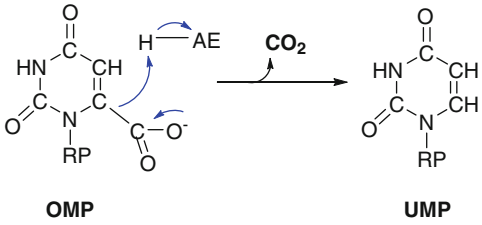

Fig. 14.8 The biosynthesis of UMP from OMP catalyzed by orotidine-5′-phosphate decarboxylase

14.1.3 Synthesis of Cytidine Nucleotides

Enzymes are not available in the cell for the amination of UMP to CMP. This synthesis requires UTP as a substrate. Nucleoside mono and diphosphate kinases exist which use different nucleoside triphosphates as phosphoryl group donors. Because the intracellular concentration of ATP exceeds the concentration of other nucleoside triphosphates, in most cases, it will contribute its γ-phosphoryl group to UMP and UDP.

$$\text{UMP} + \text{ATP} \xrightarrow{(\text{nucleoside monophosphate kinase})} \text{UDP} + \text{ADP}$$

$$\text{UDP} + \text{ATP} \xrightarrow{(\text{nucleoside diphosphate kinase})} \text{UTP} + \text{ADP}.$$

UTP is a substrate for the synthesis of CTP with the enzyme CTP synthetase. The system requires ammonia, either as free NH_3 or indirectly as NH_3 supplied by glutamine. In the latter case, the synthetase has inherent glutaminase activity. The glutaminase activity is enhanced by GTP.

The mechanism of the CTP synthetase reaction involves the intermediate 4-phosphoryl UTP (Fig. 14.9)

Thymidine nucleotide formation requires a deoxyuridine ribonucleotide substrate. Its biosynthesis will be considered in Sect. 14.3.

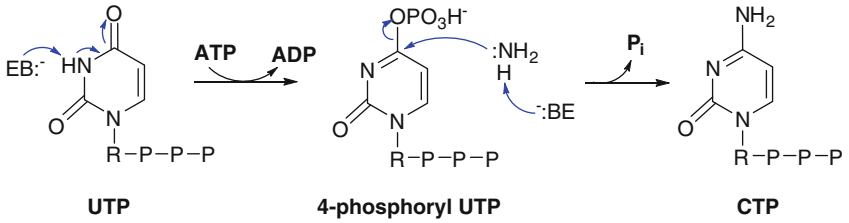

Fig. 14.9 The synthesis of CTP from UTP by CTP synthetase

14.1.4 Control of Pyrimidine Nucleotide Biosynthesis

Although CAP synthetase is the first step in pyrimidine nucleotide biosynthesis it is not necessarily the *first committed step* in the pathway. That distinction is reserved for aspartate carbamoylase in *E. coli*; however, the regulated step in animals is believed to be CAP Synthetase II.

14.1.4.1 Aspartate Transcarbamoylase

Grehart and Pardee [7] were the first to demonstrate feedback inhibition of *E. coli* ATCase and the characteristics of this regulatory phenomenon. *E. coli* ATCase is a dodecomer composed of six catalytic and six regulatory subunits. The enzyme exists in two states: an active R-state; and an inactive, or highly inhibited T-state, which are in equilibrium. This equilibrium can be shifted depending upon ligand binding, e.g., CTP shifts the equilibrium to the T-state, whereas ATP shifts it to the R-state. (These effects are referred to as *heterotrophic* or non-substrate or product effects). The effect of CTP on ATCase is also known as *feedback inhibition*. These findings with ATP and CTP are consistent with the notion that elevated levels of CTP are a signal that pyrimidine biosynthesis requires inhibition. On the other hand, when cellular levels of ATP are high, there is a need for pyrimidine nucleotides to keep pace with purine nucleotide levels for RNA and DNA synthesis. Inhibition by CTP alone is not complete; however, in the presence of UTP and CTP, ATCase activity is significantly inhibited. UTP in the absence of CTP is only slightly

inhibitory. The inhibition by CTP and UTP together is known as *synergistic inhibition*. Figure 14.10 shows the response of *E. coli* ATCase to ATP, UTP, and CTP.

A summary of feedback inhibition is presented in Scheme 14.1. UTP and CTP inhibit ATCase, whereas ATP activates ATCase and CTP synthetase.

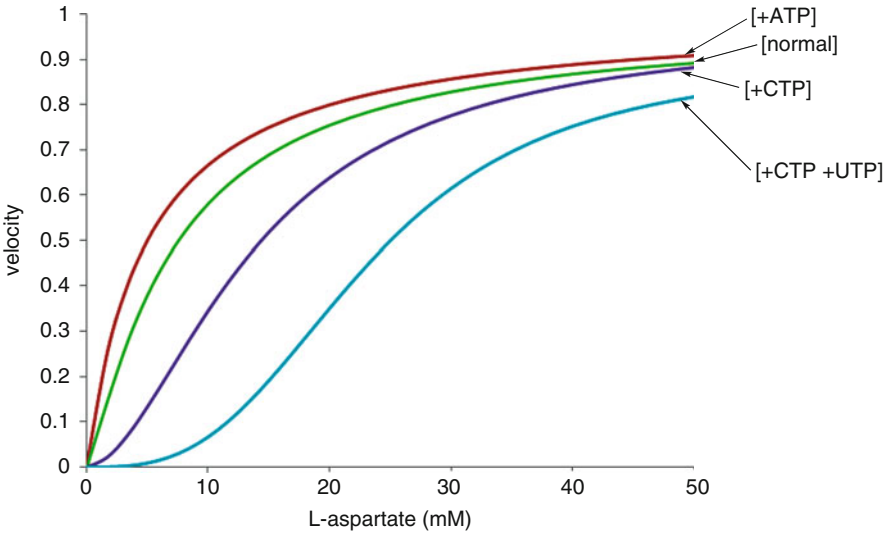

Fig. 14.10 Cooperative response of *E. coli* ATCase to nucleotide ligands

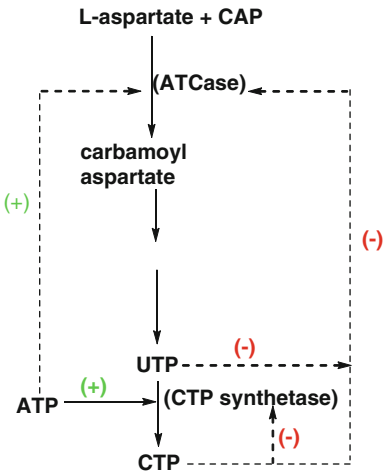

Scheme 14.1 Inhibition and activation of ATCase by nucleotides

14.1.4.2 CAP Synthetase II

CAP Synthetase II is inhibited by UDP and UTP and activated by ATP and 5-phosphoribosyl-1-pyrophosphate.

14.2 Pyrimidine Nucleotide Catabolism

Pyridine nucleotides undergo catabolism by first being attacked by nucleotidases that convert them to nucleosides. Ultimately, the nucleosides are degraded initially to pyrimidine bases and ultimately in the case of cytosine and uracil, to malonyl-CoA, a precursor of fatty acids. The end product of thymidine metabolism is methylmalonyl-CoA. An outline of pyrimidine nucleotide degradation is shown in Scheme 14.2.

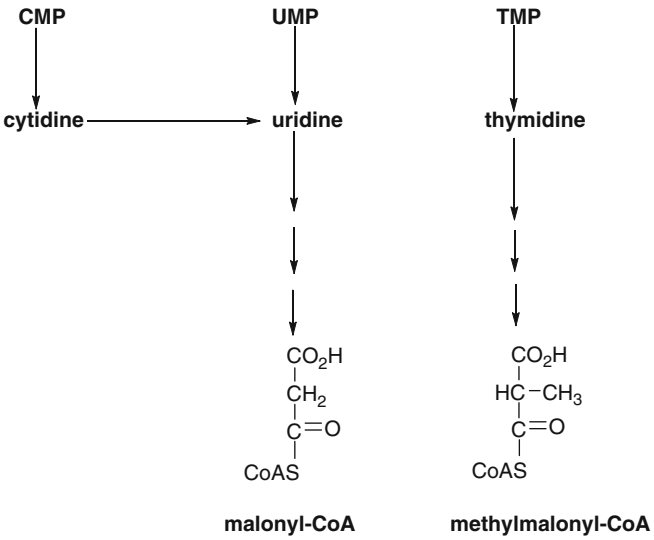

Scheme 14.2 Purine nucleotide catabolism

14.3 *De Novo* Purine Nucleotide Biosynthesis

Three pioneers, John M. Buchanan, G. Robert Greenberg, and Arthur Kornberg were largely responsible for establishing the science of *de novo* purine nucleotide biosynthesis [8]. Like pyrimidines, purine nucleotides are synthesized from common biomolecules. These include CO_2, aspartate, glycine, and one carbon units from N^{10}-formyltetrahydrofolic acid. Using isotopes which he fed to birds, Buchanan [9, 10] established their incorporation pattern into purines based upon isotope patterns in excreted uric acid. His findings are summarized in Fig. 14.11.

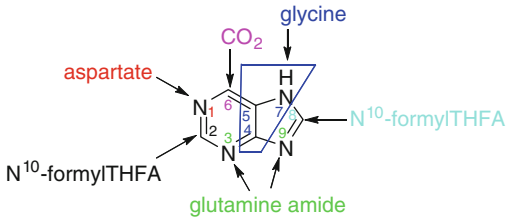

Fig. 14.11 The origin of atoms in *de novo* purine base synthesis

14.3.1 The Biosynthesis of Inosine-5′-Monophosphate

The first purine nucleotide synthesized *de novo* in the purine nucleotide biosynthetic pathway is inosine-5′-monophosphate (IMP). How this synthesis occurs starting with glutamine and PRPP is shown in Fig. 14.12. Like glycolysis, ten different enzymes are responsible for the synthesis of IMP.

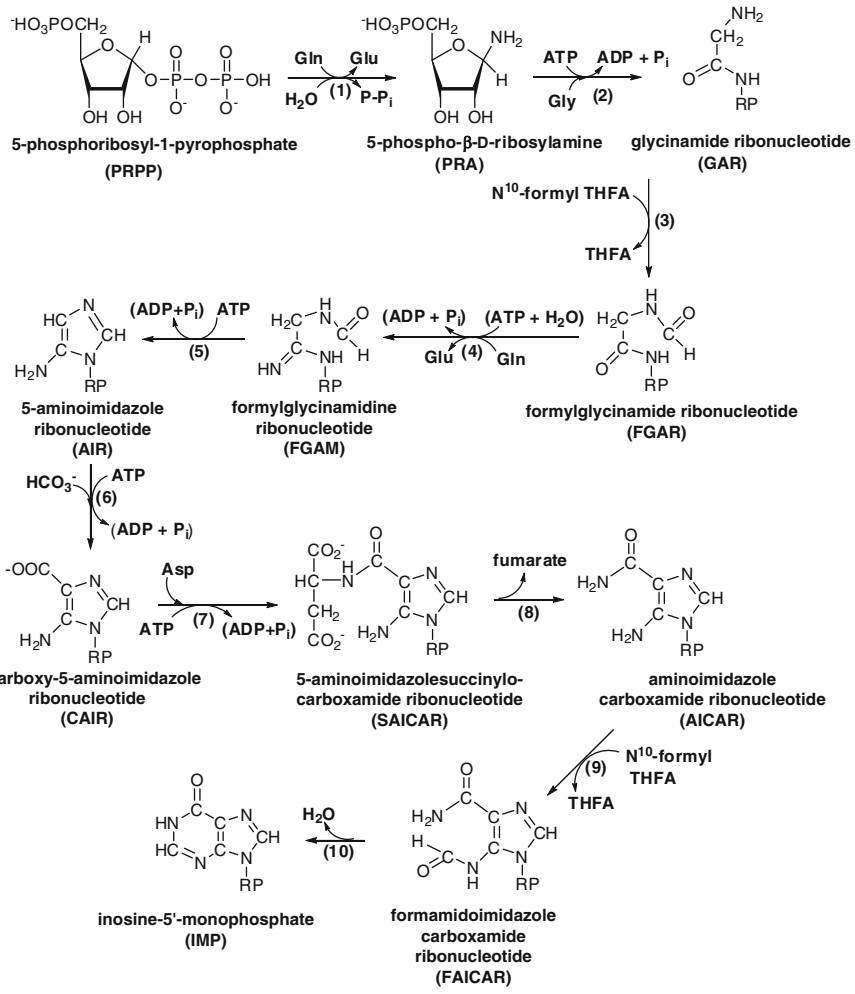

Fig. 14.12 The *de novo* synthesis of purine nucleotides begins with PRPP and glutamine and ends with IMP. The enzymes of purine biosynthesis are: (**1**) Glutamine PRPP amidotransferase, (**2**) GAR synthetase, (**3**) GAR transformylase, (**4**) FGAM synthetase (**5**), AIR synthetase, (**6**) AIR carboxylase, (**7**) SAICAR synthetase, (**8**) Adenylosuccinate lyase, (**9**) AICAR transformylase, (**10**) and IMP cyclohydrolase

14.3.2 AMP and GMP Biosynthesis

14.3.2.1 AMP

IMP is the branch point for the biosynthesis of adenosine and guanosine nucleotides. Each of these nucleotides is synthesized in separate two-step reactions (see Figs. 14.13 and 14.14).

Isotope scrambling was used to establish the probable participation of a 6-phosporyl intermediate in the adenylosuccinate synthetase reaction [11].

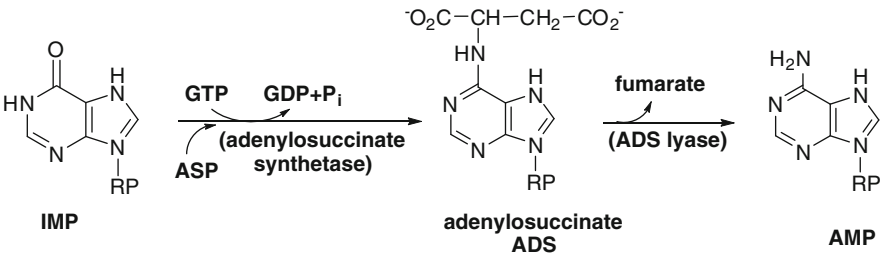

Fig. 14.13 The enzymes involved in the biosynthesis of AMP from IMP

14.3.2.2 GMP

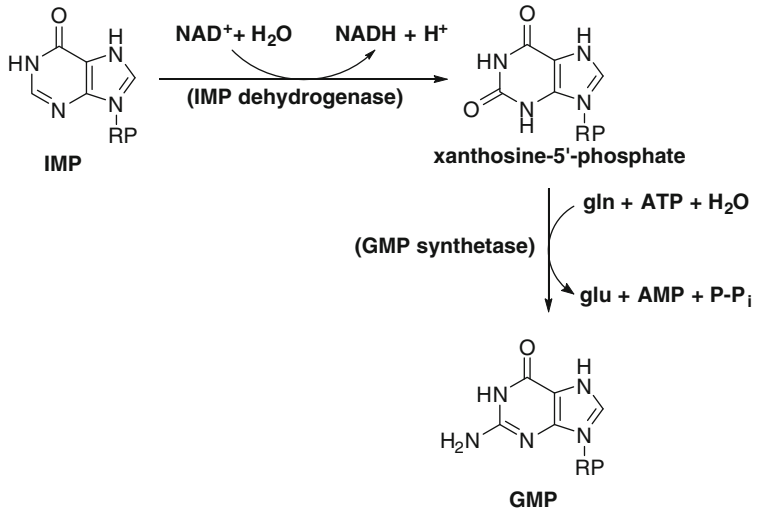

Fig. 14.14 The enzymes involved in the synthesis of GMP from IMP

14.3.3 Purine Nucleotide Biosynthesis: Enzyme Mechanisms

14.3.3.1 Glutamine PRPP Amidotransferase

In 1955 Kornberg et al. [12] implicated PRPP in the biosynthesis of purine nucleotides. PRPP is involved in the first step of *de novo* purine nucleotide biosynthesis and is a substrate along with glutamine for PRPP amidotransferase. The reaction mechanism for glutamine PRPP amidotransferase is similar to that described for CAP synthetase I except that in this case the ammonia is derived from the amide group of glutamine. The amide hydrolase activity is an intrinsic property of the enzyme.

14.3.3.2 GAR Synthetase

In the GAR synthetase reaction the substrate glycine is phosphorylated by ATP to form the carboxyl phosphate, glycine phosphate. This is followed by nucleophilic attack by the amino group at the β-C-1 position of PRA on the carbonyl group of glycine phosphate to form the product GAR (Fig. 14.15).

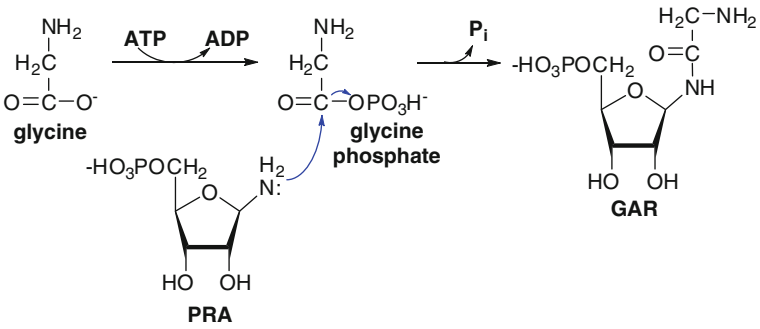

Fig. 14.15 The GAR synthetase reaction involves the condensation of PRA and glycine

14.3.3.3 GAR Transformylase

GAR transformylase transfers a formyl group from N^{10}-formyl THFA to the amino group of GAR in a nucleophilic substitution reaction. The reaction product is FGAR.

14.3.3.4 FGAM Synthetase

In the initial step in the synthesis of FGAM from FGAR, the amide of glutamine undergoes hydrolysis to provide ammonia for the synthesis of FGAM. Again, the glutaminase activity is an intrinsic property of the synthetase (Fig. 14.16).

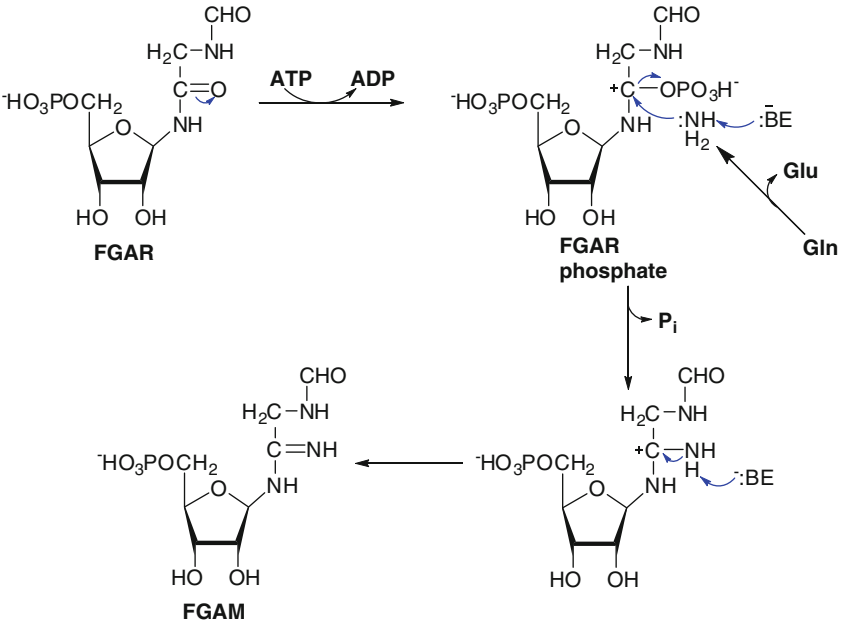

Fig. 14.16 FGAM synthetase is involved in the amination of FGAR to FGAM

14.3.3.5 AIR Synthetase

AIR synthetase catalyzes FGAM ring closure to form a substituted imidazole ribonucleotide. A cardinal feature of the mechanism is the phosphorylation of the carbonyl group of the substrate by ATP (Fig. 14.17).

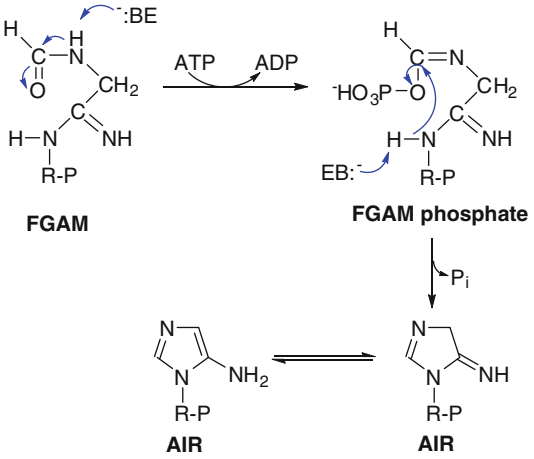

Fig. 14.17 Ring closure of FGAM to produce AIR involves the phosphorylated intermediate FGAM phosphate

14.3.3.6 AIR Carboxylase

Carboxylation of AIR requires HCO_3^- and ATP which form carboxyphosphate. The nitrogen of the amino group of AIR acts like biotin to accept the carboxyl group. Ultimately, CO_2 is formed which serves to carboxylate the C-4 of the imidazole moiety of AIR to produce CAIR. These reactions are shown in Fig. 14.18.

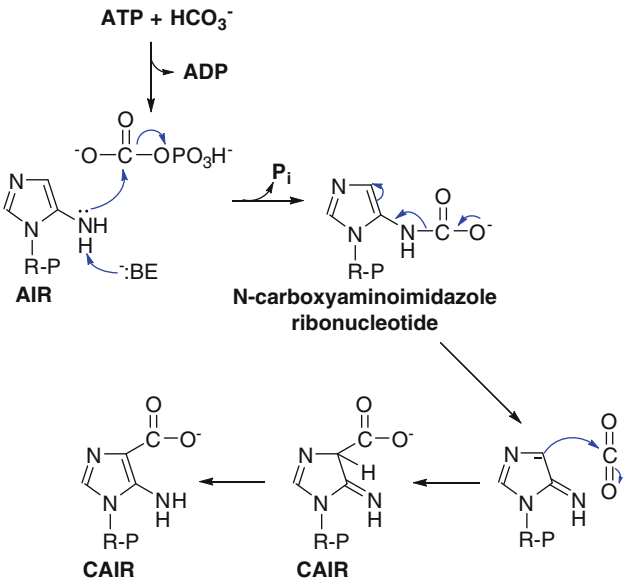

Fig. 14.18 Carboxyphosphate is the carboxylating agent for the biosynthesis of CAIR

14.3.3.7 SAICAR Synthetase

The SAICAR synthetase reaction is analogous to the GAR synthetase reaction; however, in this case the carboxyl group of CAIR is phosphorylated rather than that of glycine to yield a carbonyl phosphate intermediate [13]. In the last step of the reaction the amino group of aspartate makes a nucleophilic attack on the carbonyl of the carboxyl phosphate forming an amide linkage and in the process eliminating phosphate.

14.3.3.8 Adenylosuccinate Lyase

The adenylosuccinate (ADS) lyase reaction involves the loss of fumarate from SAICAR giving rise to AICAR (Fig. 14.19).

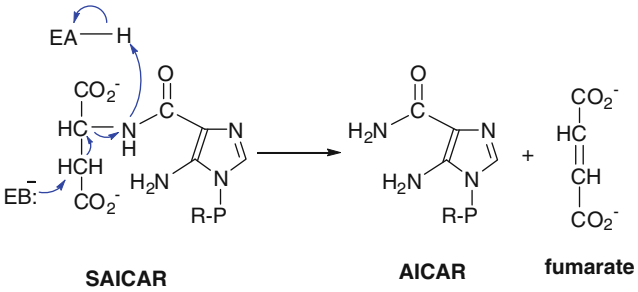

Fig. 14.19 The adenylosuccinate lyase reaction involves the removal of fumarate from SAICAR to form AICAR

14.3.3.9 AICAR Transformylase

The AICAR transformylase reaction is very similar to the reaction catalyzed by GAR transformylase. The reaction product is FAICAR. This is the penultimate step in IMP biosynthesis.

14.3.3.10 IMP Cyclohydrolase

The terminal step in the synthesis of IMP is a reaction in which H_2O is eliminated from FAICAR leading to ring closure. The reaction is analogous to Schiff base

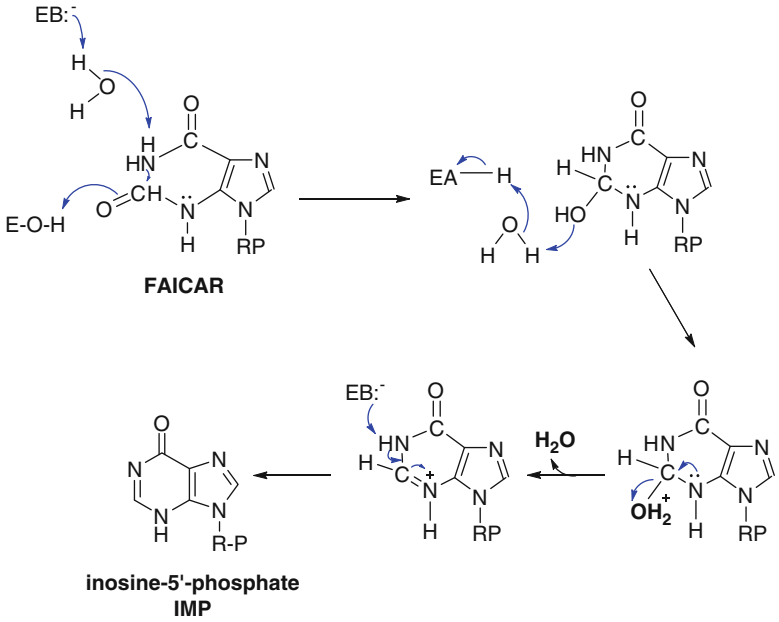

Fig. 14.20 Ring closure of FAICAR to yield the first nucleotide in purine nucleotide biosynthesis, IMP

formation and does not require ATP. X-ray diffraction studies of the enzyme led to the mechanism shown in Fig. 14.20. In humans, AIR transformylase and IMP cyclohydrolase activities are part of a single bifunctional enzyme [14].

An excellent review of the literature from an X-ray crystallographic perspective of the enzymes of purine nucleotide biosynthesis may be found in a review article by Ealick [15].

14.3.4 Regulation of Purine Nucleotide Biosynthesis

There are three primary control points in purine ribonucleotide biosynthesis. As might be expected the enzymes involved in regulation are glutamine PRPP amidotransferase, adenylosuccinate synthetase (ADS synthetase) and IMP dehydrogenase. There is some evidence to suggest that PRPP synthetase is a point of regulation in pyrimidine nucleotide biosynthesis.

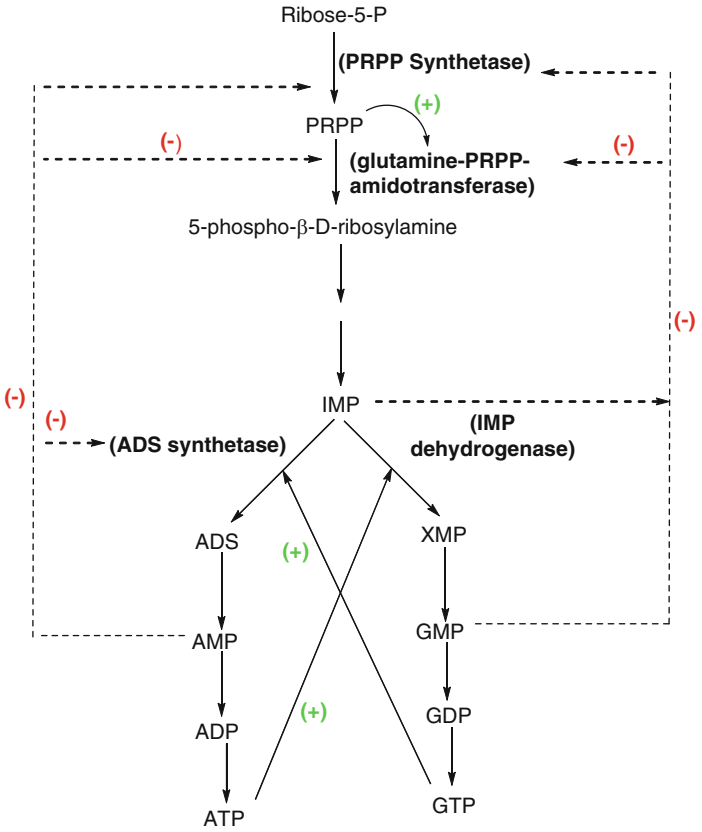

Fig. 14.21 Control points in *de novo* purine nucleotide biosynthesis by small molecules. (+) indicates activation, whereas (−) indicates inhibition

Feedback inhibition is a cardinal feature of the purine ribonucleotide biosynthetic pathway. Both AMP and GMP inhibit PRPP synthetase individually and in combination. There two allosteric sites on glutamine PRPP amidotransferase, one for adenine nucleotides and the other for guanine nucleotides. Purine ribonucleotide inhibition is synergistic with respect to glutamine PRPP amidotransferase. The branch point enzymes are also inhibited by small ligands. There is no evidence to suggest that ADS synthetase is allosterically inhibited; however, it is inhibited by AMP and by its product GDP. Elevated levels of ATP serve to enhance the activity of IMP dehydrogenase. ADS synthetase is a homodimer and normally exists as an inactive monomer. The enzyme dimerizes to the active state in the presence of IMP and GTP.

A summary of purine nucleotide biosynthesis regulation is shown in Fig. 14.21.

14.4 Deoxyribonucleotide Synthesis and Regulation

1. Unlike the ribonucleotides, the deoxyribonucleotides are not synthesized starting with 2-deoxy-D-ribose. They are instead produced by the reduction of ribonucleotides, e.g., 2′deoxyATP (dATP) and dGTP are synthesized from ADP and GDP respectively, by reduction and are then phosphorylated by nucleoside diphosphokinases to dATP and dGTP. In the case of the pyrimidine deoxyribonucleotides, UDP is converted first to dUDP and ultimately to dTMP and dCTP.

   The reduction of ribonucleotides to deoxyribonucleotides involves a free radical mechanism. The Swedish biochemist Peter Reichard [16] discovered the enzyme system ribonucleotide reductase which is responsible for the synthesis of deoxyribonucleotides. Three different ribonucleotide reductases have been found in nature thus far. Class I, found in prokaryotes and eukaryotes, uses ribonucleotide diphosphates as substrates whereas Class II ribonucleotide reductases present in some bacteria uses ribonucleotide triphosphates as substrates. Class III ribonucleotide reductanes are present in anerobic bacteria.

   These enzymes are all metalloproteins and all form the *thiyl* radical at their active sites. The mechanism of a generic ribonucleotide reductase is illustrated in Fig. 14.22.

   Note that at the completion of the reactions described in Fig. 14.22 two cysteine sulfhydryl residues on ribonucleoside reductase are oxidized to a disulfide linkage. In order for the enzyme to continue functioning, this disulfide linkage must be reduced. This is accomplished by the thioredoxin reductase enzyme system.

   Thioredoxin reductase is a redox enzyme which uses FAD as a prosthetic group. It function is to reduce the protein thioredoxin which in turn reduces the disulfide linkage that is produced in a single cycle of ribonucleoside reductase activity. The relationships between the various enzymes and coenzyme involved in the oxidation and reduction of ribonucleotide reductase is shown in Fig. 14.23.
2. Regulation of ribonucleotide reductase activity is essential for the maintenance of proper intracellular levels and ratios of the four deoxyribonucleotides and

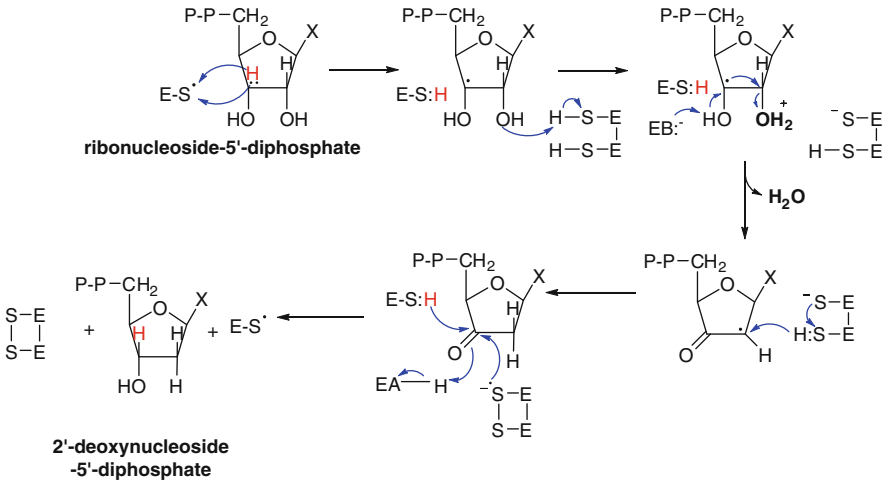

Fig. 14.22 The reduction of a nucleoside diphosphate to a deoxynucleoside diphosphate. X represents a nitrogenous base

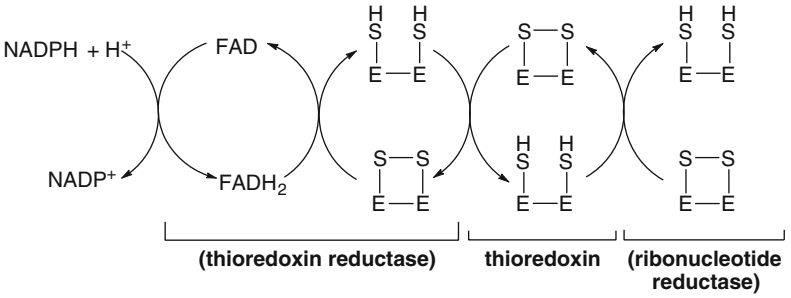

Fig. 14.23 The relationships between the various enzymes and coenzyme involved in the oxidation and reduction of ribonucleotide reductase (E)

ultimately for normal cell growth and division. The most studied ribonucleotide reductases are the Class I enzymes. They are heterotetramers made up of two α and two β subunits. The α_2 dimer, also called the R_1 protein, contains the active site, allosteric sites, and the redox active sulfhydryl groups. The β_2 dimer (R_2 protein) generates the thiyl radical.

The allosteric sites of the *Class I reductase* are of two types, *activity sites* and *specificity sites*. The activity site binds either ATP or dATP. The former nucleotide activates the enzyme, whereas the latter inhibits ribonucleotide reduction. The specificity site can be occupied by ATP, dATP, dGTP, and dTTP. These nucleotides when bound to the specificity site will determine the nature of the nucleoside diphosphate that will be acted upon, e.g., binding of GTP to the specificity site insures that the active site is specific for ADP [16].

14.5 Thymidylate Synthase

Thymine is one of four nitrogenous bases found in DNA and is thus essential for cell viability. Unlike other ribonucleotides, TDP, which does not exist in nature, is not converted to dTDP by ribonucleotide reductase. The enzyme thymidylate synthase [17] catalyzes the conversion of dUMP to dTMP (Fig. 14.24). dUMP is formed from UDP by the following reactions:

$$\text{UDP} \rightarrow \text{dUDP} \rightarrow \text{dUMP}.$$

The first reaction is catalyzed by ribonucleotide reductase and the second by a phosphatase. The other substrate for the thymidylate synthase reaction is N^5, N^{10}-methylene THFA.

The reaction itself is:

$$N^5, N^{10}\text{-methylene THFA} + \text{dUMP} \rightarrow \text{dihydro FA} + \text{dTMP}.$$

The initial step in the thymidylate synthase reaction is the addition of a thiolate anion from a cysteinyl residue on the enzyme to dUMP.

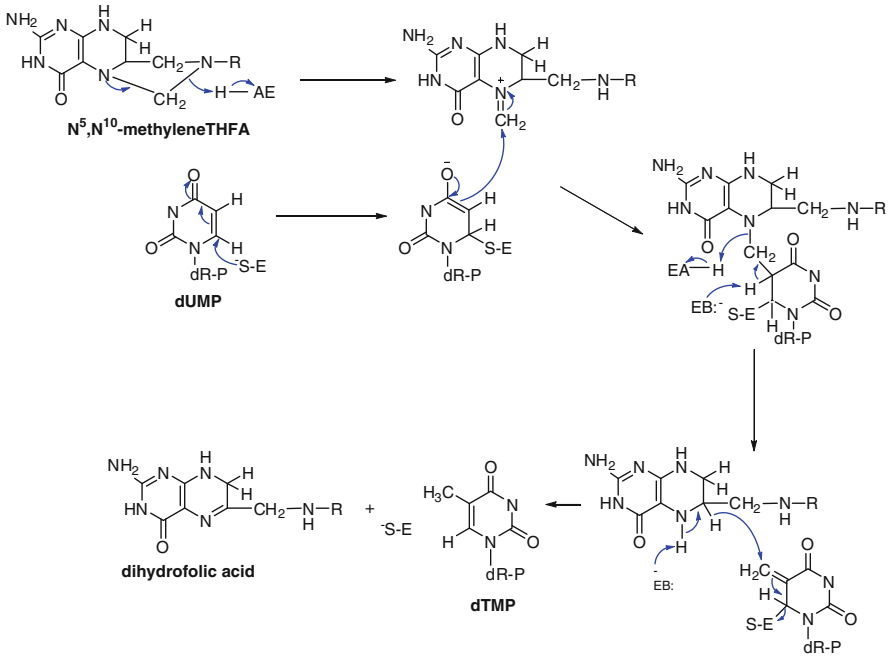

Fig. 14.24 The enzymatic conversion of dUMP to dTMP by the enzyme thymidylate synthase

14.6 Degradation of Purines

The end product of purine catabolism in humans and other primates is uric acid which is excreted in urine. An overproduction of uric acid leads to its deposition in joints, particularly in the large toe in humans, a condition known as *gout*. Most

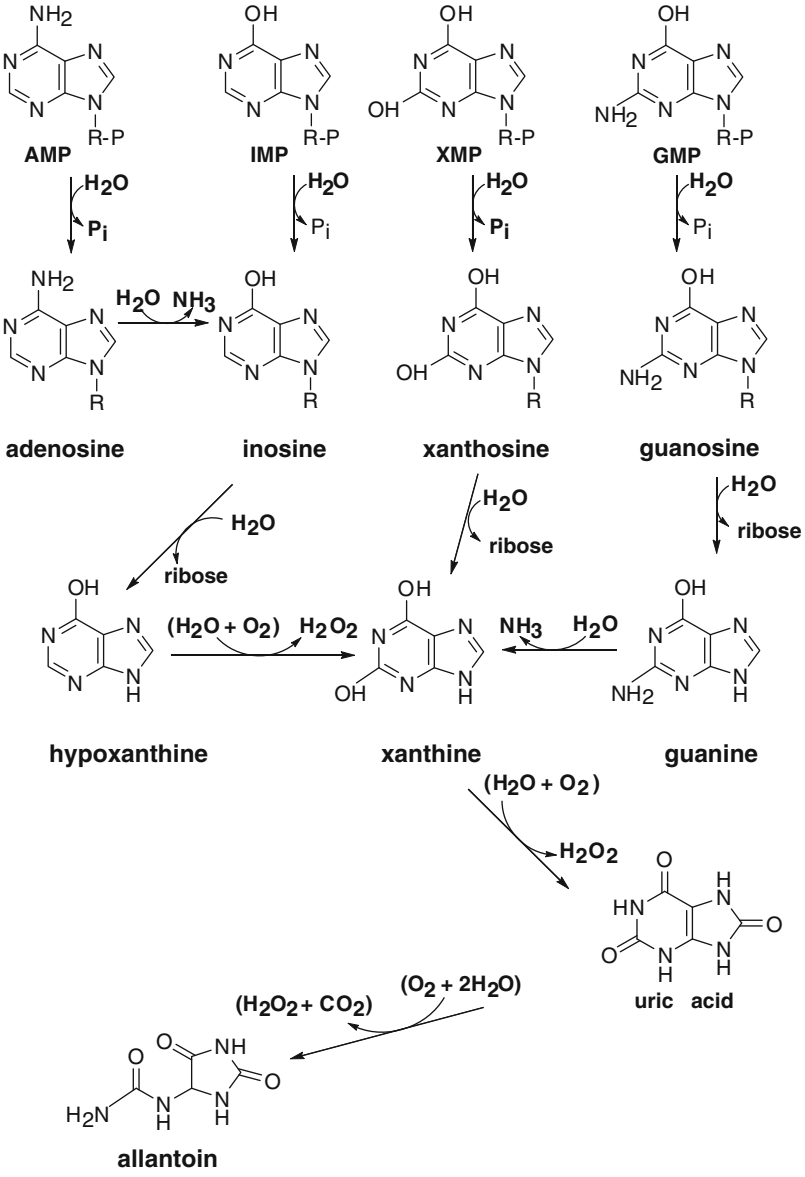

Fig. 14.25 Pathways for the degradation of purine bases to either uric acid or allantoin

animals are capable of degrading uric acid, e.g., dogs, with the exception of the Dalmatian, to *allantoin* which is then excreted in urine (Fig. 14.25).

14.7 Purine and Pyrimidine Nucleotide Salvage Pathways

Most purine and pyrimidine nucleotides are not synthesized *de novo* in the cell but are the result of reuse or salvage mechanisms. Cellular RNA and to some extent DNA are broken down by enzymes ultimately to purine and pyrimidine bases. The purines (adenine, guanine, and hypoxanthine) are converted to nucleotides through the action of enzymes that utilize PRPP. An example is the enzyme adenine phosphoribosyltransferase which converts adenine to AMP.

$$\text{adenine} + \text{PRPP} \rightarrow \text{AMP} + \text{P-P}_\text{i}.$$

Although the equilibrium of this reaction lies far to the left, ubiquitous pyrophosphatases hydrolyze the P-P_i to 2P_i molecules, and thus shift the equilibrium in favor of AMP synthesis.

Pyrimidine bases are salvaged by the enzyme orotate phosphoribosyltransferase, the same enzyme involved in *de novo* pyrimidine nucleotide biosynthesis:

$$\text{Pyrimidine base} + \text{PRPP} \rightarrow \text{pyrimidine nucleotide} + \text{P-P}_\text{i}.$$

References

1. Stevens RC, Lipscomb WN (1992) A molecular mechanism for pyrimidine nucleotide control of aspartate transcarbamoylase. Proc Natl Acad Sci USA 89:5281–5285
2. Portet RW, Modebe MO, Stark GR (1969) Kinetic studies of the catalytic subunit. J Biol Chem 244:1846–1859
3. Parmentier LE, Weiss PM, O'Leary MH, Schachman HK, Cleland WW (1992) ^{13}C and ^{15}N isotope effects as a probe of the chemical mechanism of *Escherichia coli* aspartate transcarbamoylase. Biochemistry 31:6577–6584
4. Kornberg A (1955) Enzymatic synthesis of pyrimidine nucleotides:orotidine-5′-phosphate and uridine-5′-phosphate. J Biol Chem 215:403–451
5. Goiten RK, Chelsky D, Parsons SM (1978) Primary ^{14}C and α secondary ^{3}H substrate kinetic isotope effects for some phosphoribosyltransferases. J Biol Chem 253:2963–2971
6. Appleby TC, Kinsland C, Begley TP, Ealick SE (2000) The crystal structure and mechanism of orotidine 5′-monophosphate decarboxylase. Proc Natl Acad Sci USA 97:2005–2010
7. Gerhart JC, Pardee AB (1962) The enzymology of control by feedback inhibition. J Biol Chem 237:891–896
8. Buchanan JM (1994) Aspects of nucleotide enzymology and biology. Protein Sci 3:2151–2157
9. Buchanan JM, Sonne JC, Delluva AM (1948) Biological precursors of uric acid: the role of lactate, glycine, and carbon dioxide as precursors of the carbon chain and nitrogen atom 7 of uric acid. J Biol Chem 173:81–98

10. Sonne JC, Buchanan JM, Delluva AM (1948) Biological precursors of uric acid: the role of lactate, acetate, and formate in the synthesis of the ureido groups uric acid. J Biol Chem 173: 69–79
11. Bass MB, Fromm HJ, Rudolph FB (1984) The mechanism of the adenylosuccinate synthetase reaction as studied by positional exchange. J Biol Chem 259:12330–12333
12. Kornberg A, Lieberman I, Simms ES (1955) Enzymatic synthesis of purine nucleotides. J Biol Chem 215:417–427
13. Ginder ND, Binkowski DJ, Fromm HJ, Honzatko RB (2006) Nucleotide complexes of *Escherichia coli* phosphoribosylaminoimidazolesuccino-carboxamide synthetase. J Biol Chem 281: 20680–20688
14. Vergis JM, Beardsley GP (2004) Catalytic mechanism of the cyclohydrolase activity of human aminoimidazole carboxamide ribonucleotide formy-transferase/inosine monophosphate cyclohydrolase. Biochemistry 43:1184–1192
15. Zhang Y, Morar M, Ealick SE (2008) Structural biology of the purine biosynthetic pathway. Cell Mol Life Sci 65:3699–3724
16. Jordan A, Reichard P (1998) Ribonucleotide reductases. Annu Rev Biochem 67:71–98
17. Carreras CW, Santi DV (1995) The catalytic mechanism and structure of thymidylate synthase. Annu Rev Biochem 64:721–762

Chapter 15
Photosynthesis

Nearly all energy on Earth is derived either directly or indirectly from the sun. Sunlight is responsible not only for the growth of plants and many bacterial species, but also for the existence of fossil fuels such as coal and oil. The sun provides the energy for the "fixing" of CO_2 as carbohydrate and the formation of O_2 from H_2O. This process, the capture of the sun's light energy to reduce CO_2 and oxidize H_2O, is known as *photosynthesis*. The overall reaction describing photosynthesis is:

$$CO_2 + H_2O \xrightarrow{\text{light}} [CH_2O] + O_2,$$

where $[CH_2O]$ represents carbohydrate.

All photosynthesizing organisms contain light-gathering pigments which when excited by light cause their electrons to move from their ground states to higher energy levels or excited states. When these excited electrons return to the ground state, energy that can do useful work is liberated. The excited electrons do not return to the ground state immediately but instead are passed through a number of acceptor molecules in a series of redox reactions ultimately resulting in the formation of NADPH. In the case of photosynthesizing organisms, this energy is also used to establish a proton gradient across a membrane very much like what occurs in oxidative phosphorylation (Chap. 10). The end result of this process is the biosynthesis of ATP by an ATP synthase system. Both NADPH and ATP are then used for the multitude of biosynthetic reactions one sees in these photosynthesizing organisms. In addition, photosynthesis produces O_2 which is obtained from the splitting of H_2O.

15.1 The Chloroplast

Photosynthesis in plants takes place in organelles roughly 5 μm in length called chloroplasts. Figure 15.1 illustrates the structure and components of a typical chloroplast.

H.J. Fromm and M.S. Hargrove, *Essentials of Biochemistry*,
DOI 10.1007/978-3-642-19624-9_15, © Springer-Verlag Berlin Heidelberg 2012

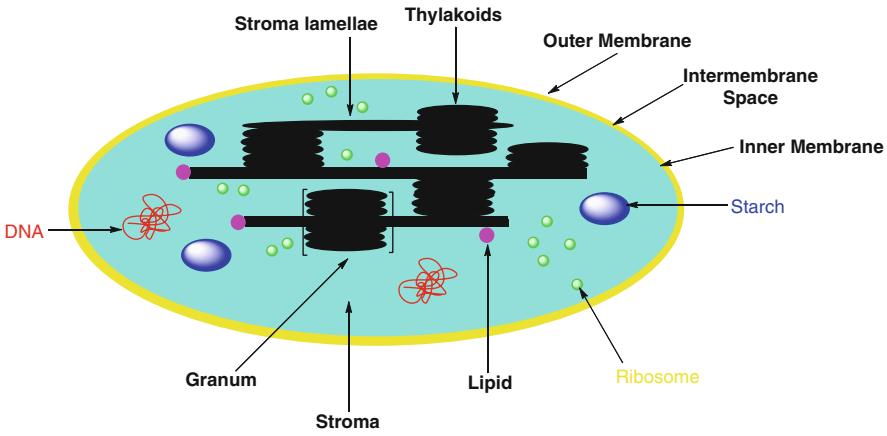

Fig. 15.1 Cartoon of a chloroplast. Like mitochondria, chloroplasts contain an inner and outer membrane and their own DNA and ribosomes for the synthesis of proteins. The photosynthetic machinery is contained within a structure, the thylakoid membrane. These membranes are involved in redox reactions analogous to those found in mitochondria. The granum represents a stack of thylakoids. The "dark reactions" are carried out in the stroma

In photosynthesizing bacteria, which lack chloroplasts, photosynthesis is carried out in membrane-like structures.

15.2 Light and Its Properties

According to quantum mechanics theory, light can be considered both as a wave and as a particle. As the latter, it can be taken to be a beam of particles or photons. Photons of energy are expressed as quanta and according to Plank's law:

$$E = h \times v,$$

where E is energy, h, Plank's constant, and v, frequency. Thus, light energy is a function of its frequency or wave length.

When an electron is excited by light energy it can do four things:

1. It can fall back to its ground state and give up heat
2. It can decay back to its ground state and emit fluorescent energy
3. It can pass its energy on to another molecule
4. It can pass its excited electron on to another molecule

The sun's light energy, in the visible and near infrared regions of the spectrum, is gathered by photosynthesizing pigments in plants and other photosynthesizing organisms. The energy inherent in this light, according to Plank's law, is sufficient to break and make chemical bonds.

15.3 Photosynthesis Pigments

Shown in Fig. 15.2 are the absorption spectra of two of the plant pigments involved in photosynthesis, chlorophylls *a* and *b*.

It is clear that these photoreceptors are well suited to absorb the sun's radiation. The structures of two very prominent pigments, chlorophylls *a* and *b*, are presented in Fig. 15.3. Like heme and the cytochromes, chlorophylls have four pyrrole rings bound to a metal; however, they contain another five-membered ring which is fully reduced. Additionally, in the case of chlorophyll, the metal is Mg^{2+} and like the iron in hemoglobin, it does not participate in redox reactions.

In plants the light-sensitive pigments, or photoreceptors, are contained within thylakoid membranes in chloroplasts. Most of the chlorophyll and other light-gathering molecules within this structure act as *antenna molecules*, i.e., they

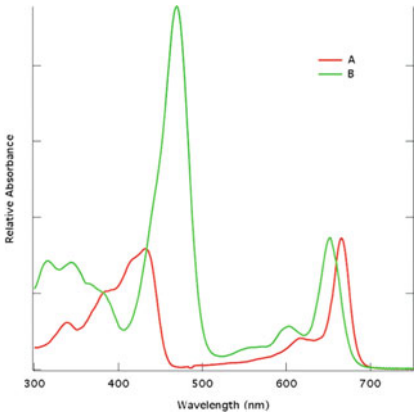

Fig. 15.2 Absorption spectra of chlorophyll *a* (*red*) and *b* (*green*). The spectra of other light-gathering pigments, although not illustrated, but found in the chloroplast, absorb in regions of the visible spectrum where the chlorophylls exhibit weak absorbance

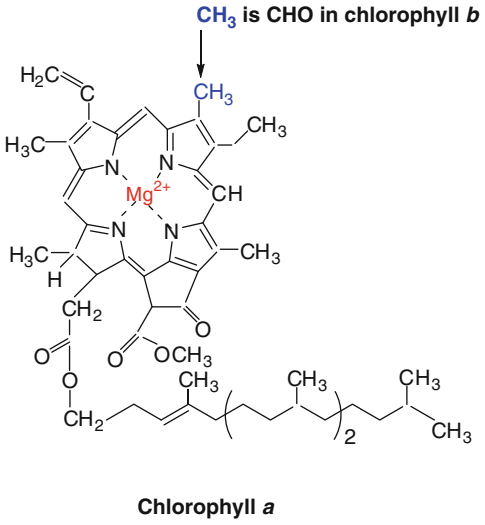

Fig. 15.3 The structure of chlorophyll *a* and chlorophyll *b*

absorb light energy which excites their electrons; however, they pass this energy on by *resonance energy transfer* to two chlorophyll molecules located in a *reaction center*. An example of a light-gathering pigment other than chlorophyll found in chloroplasts is β-carotene (Fig. 15.4).

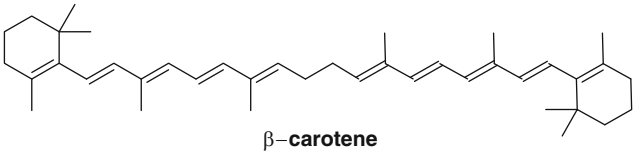

Fig. 15.4 β-Carotene is an example of one light-gathering pigment found in chloroplasts other than chlorophyll *a* or *b*

The chlorophyll molecules found in the reaction centers are called *special pairs* to distinguish them from the antenna chlorophylls. The environment around the chlorophyll molecules in the reaction center differs from that of the antenna molecules. This environmental difference insures that the reaction center chlorophyll molecules' excited state energy level is lower than that of the antenna chlorophyll molecules. After achieving the excited state, chlorophyll in the reaction center (the special pair) can lose *one* electron (oxidation) and assume a positive charge (Chlorophyll$^+$). Chlorophyll$^+$ is a very strong oxidant and strips an electron from a very weak reductant after which it returns to the ground state. This sequence of events is illustrated in Fig. 15.5.

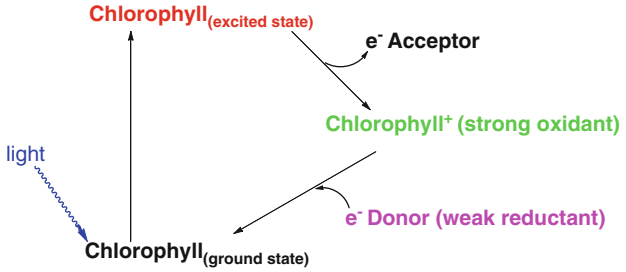

Fig. 15.5 Chlorophyll in the ground state can be activated to the excited state by absorbing a photon of light. After loss of an electron it will assume a net-positive charge relative to its status in the ground state. Upon reduction it will return to the ground state

15.4 The Photosystems

Chloroplasts contain two photosystems. One of these, *Photosystem II (PSII)*, is responsible for the generation of O_2, protons, and electrons from H_2O. The other, *Photosystem I (PSI)*, produces NADPH from electron transport. PSII contributes

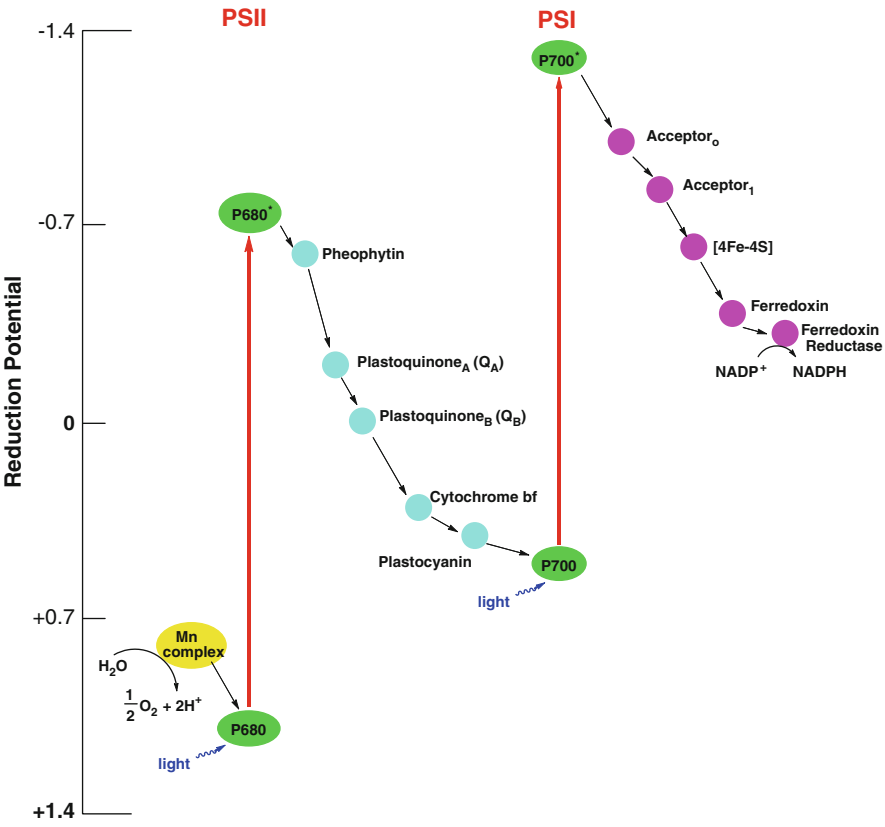

Fig. 15.6 Z-scheme of photosynthesis. The two photosystems, PSI and PSII and their components which are involved in plant photosynthesis. The *stars* (*) associated with the photosystems indicate activation of the special pair chlorophyll electrons. The *arrows* indicate electron movement

directly to the proton gradient responsible for the energy used to drive ATP synthesis from ADP and P_i. The two systems are interrelated by a pathway involving *cytochrome b_6f (cytochrome bf)* as shown in Fig. 15.6 in the so-called *Z-Scheme*. The genesis of the term Z is a result of the "zig-zag" character of the scheme shown in Fig. 15.6.

15.4.1 PSII

PSII, a transmembrane complex that absorbs light below 680 nm, is extremely large and is embedded in the thylakoid membrane. It consists of more than 20 protein subunits and more than 30 chlorophyll antenna molecules. The PSII system is involved in the splitting of H_2O to $2H^+$ and $\frac{1}{2}O_2$ at a manganese center within

the complex. The PSII special pair, after losing an electron, is positively charged. This positive charge is neutralized by the oxygen electrons from water at the manganese center.

The Q/QH_2 redox pair has a lower reduction potential than the $(2H^+ + \frac{1}{2}O_2)/H_2O$ pair, and one would expect electron flow from QH_2 to O_2 ($QH_2 + \frac{1}{2}O_2 \rightarrow Q + H_2O$); however, this unfavorable thermodynamic effect is overridden by absorption of light energy by the PSII system.

After light excitation of a chlorophyll molecule at the reaction center, the activated electron is passed first to *pheophytin*, a chlorophyll-like molecule but one lacking Mg^{2+}, and then to tightly polypeptide-bound *plastoquinone* (Q_A) and finally to a mobile electron carrier, *plastoquinone* (Q_B). A second electron from the reaction center allows for the reduction of Q to plastoquinol (QH_2) as shown in Fig. 15.7.

From QH_2, the electrons are passed to the cytochrome bf complex. The cytochrome bf complex catalyzes the transfer of electrons from QH_2 to *plastocyanin*, a copper-containing protein, as follows:

$$QH_2 + 2\ \text{Plastocyanin}(Cu^{2+}) \rightarrow Q + 2\ \text{plastocyanin}(Cu^{1+}) + 2H^+.$$

The two protons generated in the reaction enter the lumen and contribute to the proton gradient between the lumen and stroma. The two electrons from plastocyanine are then passed on to PSI and the plastocyanine is reoxidized.

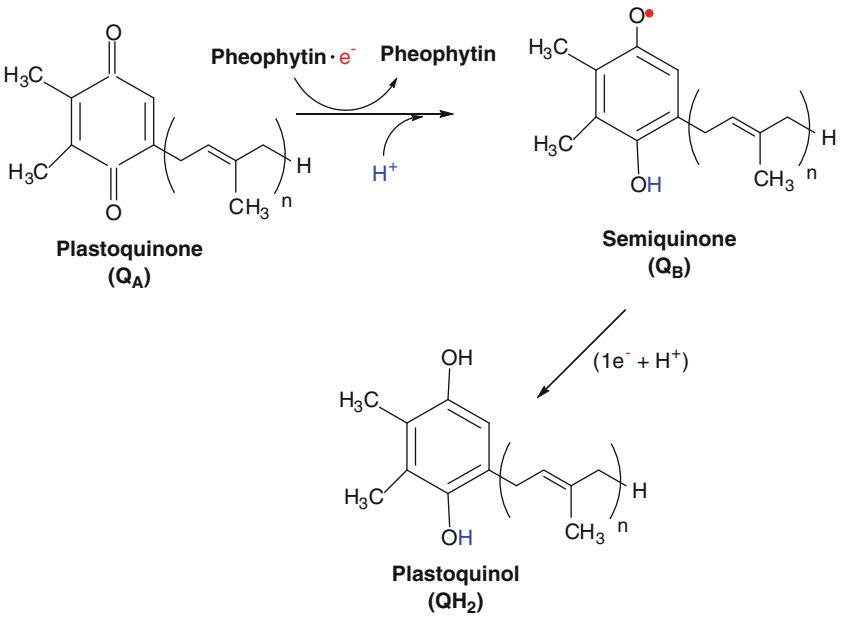

Fig. 15.7 Plastoquinone (Q_A) is reduced to plastoquinol (QH_2). *n* ranges in value from 6 to 10 for different species

In summary, the overall reaction of PSII is:

$$H_2O \xrightarrow{(\text{light energy})} 2H^+ + 2e^- + \frac{1}{2}O_2.$$

The electrons and protons generated by the PSII system are used by PSI to generate both NADPH and ATP.

15.4.2 PSI

The primary roles of PSI and PSII in photosynthesis are to produce NADPH and ATP for the synthesis of sugars and other metabolites required by the plant for maintenance and growth.

After activation of the special pair of chlorophyll molecules at the PSI reaction center, an electron is passed on to another chlorophyll at site A_0 and then to a quinone at site A_1. From the quinol, produced by reduction, the electrons move to ferredoxin. Ferredoxin is a small iron–sulfur (2Fe–2S) protein in which the iron–sulfur cluster is covalently bound to the protein through a cysteinyl residue on the protein (see Chap. 10). The terminal electron accepter is $NADP^+$. This last reaction of PSI is catalyzed by the enzyme *ferredoxin–NADP$^+$ reductase*.

The ferredoxin–$NADP^+$ reductase reaction uses FAD and the mechanism involves two one-electron transfers. An outline of the ferredoxin–$NADP^+$ reaction is shown in Fig. 15.8.

Figures 15.6 and 15.9 summarize the sequence of events involving PSI and PSII after their activation by light.

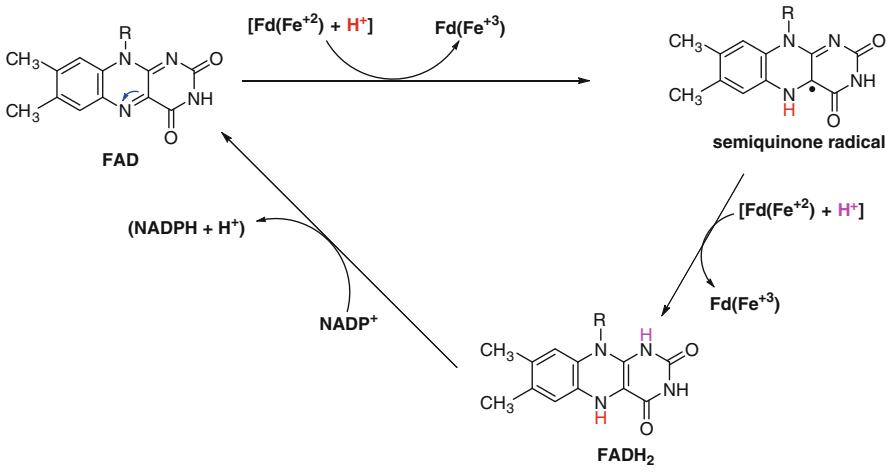

Fig. 15.8 The mechanism of the ferredoxin–$NADP^+$ reductase reaction involves a radical intermediate. Fd is taken to be ferredoxin

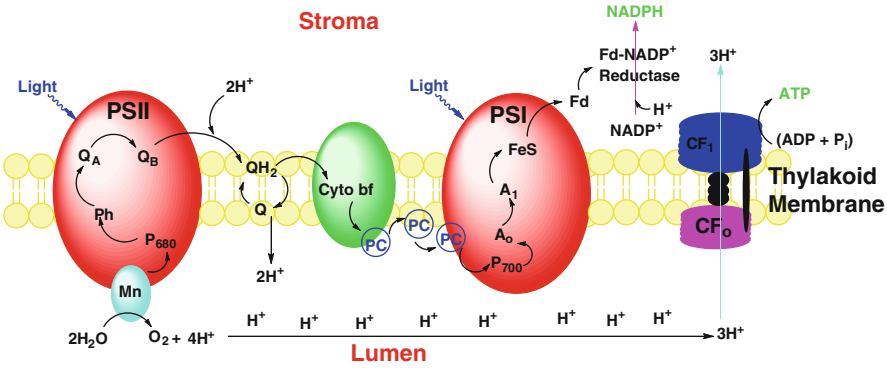

Fig. 15.9 The figure summarizes the reactions involved in PSI and PSII after absorption of light. PSII is directly involved in the production of O_2 from H_2O and the proton gradient responsible for ATP biosynthesis. Electrons that originate at PSII are ultimately used to synthesize NADPH. *Abbreviations*: *Mn*: Mn oxygen evolving complex, *Ph*: pheophytin, *Q*: plastoquinol, *PC*: plastocyanin, *Fd*: ferredoxin, A_0: chlorophyll a, A_1: phylloquinone and *FeS* iron–sulfur cluster. *Arrows* indicate electron and proton flow

15.5 ATP Synthesis

The mechanism of ATP synthesis from ADP and P_i in chloroplasts is similar to that already described for oxidative phosphorylation involving mitochondrial ATP synthase (Chap. 10). Recall that a proton gradient was set up by the flow of electrons through the respiratory chain which establishes a proton gradient across the inner mitochondrial membrane.

In 1966 Andre Jagendorf [1] demonstrated that when he established an artificial pH gradient in chloroplasts, ATP synthesis from ADP and P_i occurred. In his experiments, he first added chloroplasts to a beaker containing a solution at pH 4.0 and allowed it to incubate. He then exposed the chloroplasts to a solution at pH 8.0 containing ADP and P_i. This protocol led to the synthesis of ATP. These studies allowed him to reach two conclusions: (1) a pH gradient is responsible for ATP synthesis from ADP and P_i, and (2) the observations were supportive of the Mitchell hypothesis of a proton motive force driving ATP synthesis. These experiments ultimately led to the discovery of ATP synthase in plants. In plants, the ATP synthase is sometimes referred to as CF_1CF_0-ATPase.

15.6 The Light Independent Reactions

Photosynthesis consists of two phases: the "Light" and "Light Independent" reactions. The former can proceed only in the light whereas the later uses ATP and NADPH produced in the light reactions to fix CO_2. We have seen how photosynthesis provides ATP and NADPH both of which are required for the biosynthesis of sugars in plants. There are two basic pathways for carbohydrate

synthesis in plant stroma, the Calvin Cycle and the Pentose Phosphate Pathway (Chap. 8).

15.7 The Calvin Cycle

The Calvin Cycle was named after Melvin Calvin who was the major contributor to our understanding of how plants "fix" or incorporate CO_2 into carbohydrates. He was awarded with the Nobel Prize in 1961 for his research [2].

The cycle consists of three phases: (1) CO_2 fixation, (2) reduction using NADPH, and (3) regeneration of D-ribulose 1,5-bisphosphate.

An outline of the Calvin Cycle is shown in Fig. 15.10.

The complete Calvin Cycle is shown in Fig. 15.11.

Enzymes of the Calvin Cycle (Fig. 15.11) are:

1. Ribulose-1,5-bisphosphate carboxylase (Rubisco)
2. 3-Phosphoglycerate kinase
3. Glyceraldehyde-3-phosphate dehydrogenase
4. Triose phosphate isomerase
5. Aldolase
6. Sedoheptulose-1,7-bisphosphatase
7. Transketolase
8. Aldolase
9. Fructose-1,6-bisphosphatase
10. Phosphopentose isomerase
11. Phosphopentose epimerase

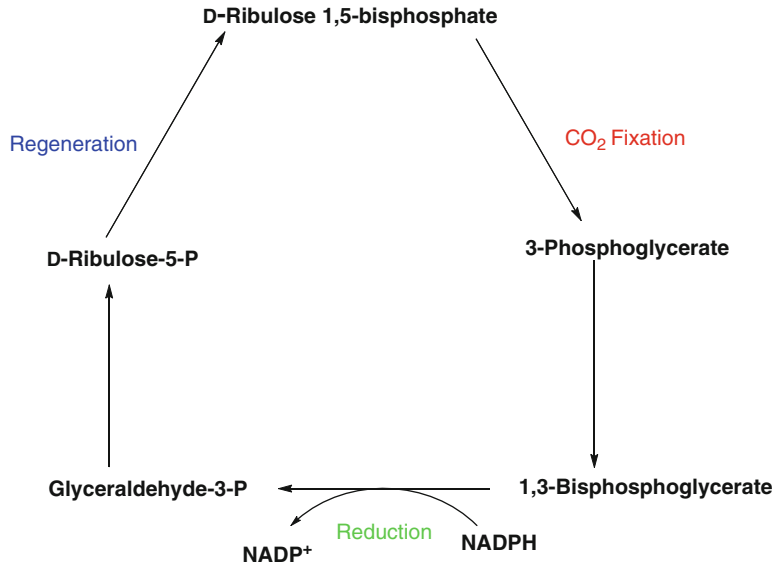

Fig. 15.10 Outline of the Calvin Cycle illustrating in color the three phases of the cycle

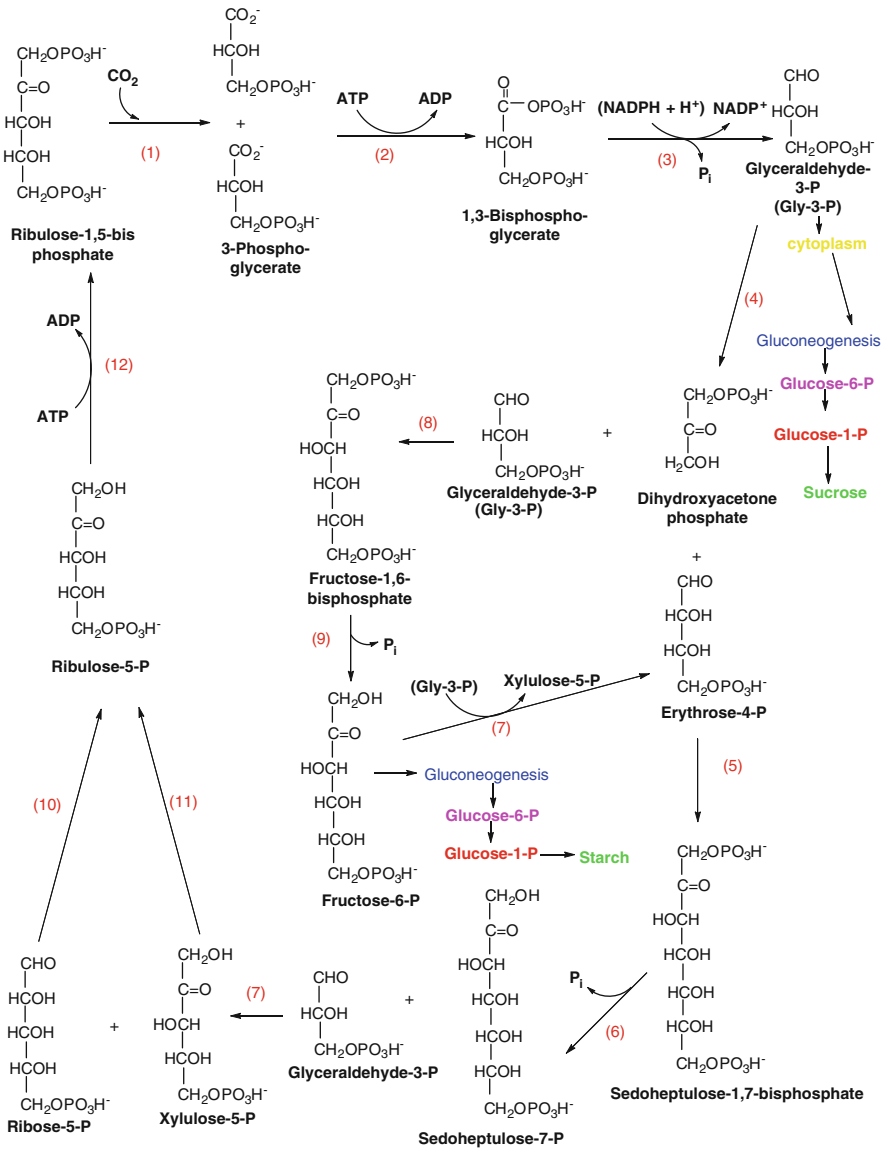

Fig. 15.11 The Calvin Cycle starts with the carboxylation of D-ribulose-1,5-bisphosphate by Rubisco (1) and ends with the regeneration of ribulose-1,5-phosphate from D-ribulose-5-P

The mechanism of action of these enzymes, with the exception of Rubisco, has been considered in detail in Chap. 8. Rubisco is the most plentiful enzyme on Earth. One of its more interesting characteristics is its extremely low turnover number (3 s^{-1}) which is one of the lowest ever recorded for an enzyme: however, its slow catalytic rate is more than made up for by its high concentration. Its mechanism of action is illustrated in Fig. 15.12.

15.7.1 The Mechanism of the Rubisco Reaction

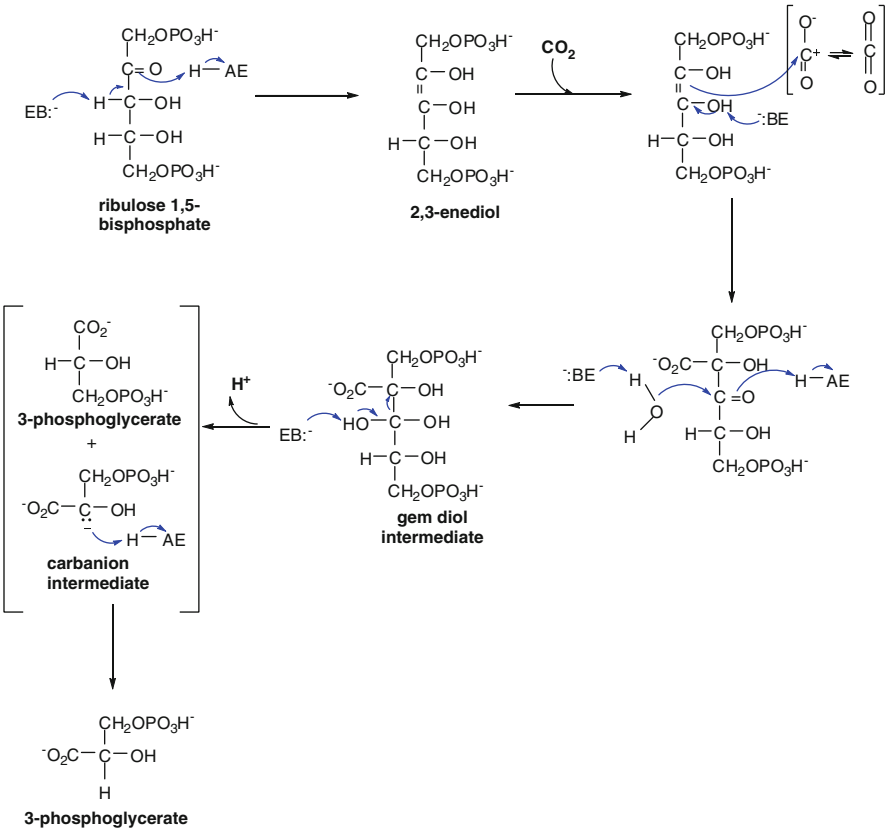

Fig. 15.12 The mechanism of the Rubisco reaction

15.7.2 Starch and Sucrose Can Be Used to Synthesize D-Glucose

D-Glucose synthesis does not take place in plants via gluconeogenesis the same way that it occurs in animals. Instead, the D-glucose-6-P which can be synthesized from D-fructose-6-P can be converted to D-glucose-1-P and then to ADP-D-glucose. Starch can then be synthesized in the chloroplast from ADP-D-glucose and hydrolyzed to glucose (see Chap. 11).

Both glyceraldehyde-3-P and dihydroxyacetone phosphate can be exported to the cytosol for sucrose synthesis by converting D-glucose-1-P to UDP-D-glucose. D-Glucose can be obtained by the plant from sucrose through the action of invertase (sucrase) (see Chap. 11).

15.7.3 Regulation of the Calvin Cycle

Probably, the most important factor regulating the Calvin Cycle is the availability of light. In isolation this may not seem plausible, however, absent light, ATP and NADPH, which are generated in photosynthesis, would not be available as Calvin Cycle substrates.

The rate-limiting step in the Calvin Cycle is the Rubisco reaction. CO_2 and Mg^{2+} are activators of the enzyme. Another factor controlling the flux through the cycle is the redox state of ferredoxin, i.e., it must be in the reduced state, $Fd(Fe^{+2})$; however, reduced ferredoxin can be oxidized by a low-molecular-weight protein, *thioredoxin*. Thioredoxin, which contains a reactive disulfide bond is reduced by ferredoxin (Fe^{+2}) in the presence of the enzyme *ferredoxin–thioredoxin reductase*. Reduced thioredoxin serves to activate a number of plant cell enzymes by reducing their disulfide bonds. These include glyceraldehyde-3-phosphate dehydrogenase, sedoheptulose-1,7-bisphosphatase, and ribulose-5-phosphate kinase.

The redox reaction involving thioredoxin and ferredoxin is illustrated in Fig. 15.13.

In order for ferredoxin–$NADP^+$ reductase to function in photosynthesis, ferredoxin must be present in the reduced or Fe^{+2} state, i.e.,

$$2\ \mathrm{Fd(Fe^{+2})} + \mathrm{NADP^+} + \mathrm{H^+} \rightarrow \mathrm{NADPH} + 2\mathrm{Fd(Fe^{+3})}.$$

Thus, the status of the reductase will depend upon light for the passage of electrons to its substrate, oxidized ferredoxin to form reduced ferredoxin.

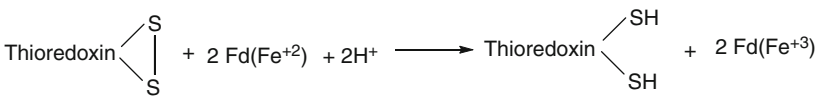

Fig. 15.13 The reduction of thioredoxin by ferredoxin catalyzed by ferredoxin–thioredoxin reductase

15.7.4 Comments on the Calvin Cycle

The purpose of the Calvin Cycle is to produce carbohydrate for the plant. Carbon leaves the Calvin Cycle at two points: (a) at glyceraldehyde-3-P, which can isomerize to dihydroxyacetone phosphate (triose phosphate isomerase). These two compounds are exported to the cytosol and can then condense (aldolase) and give rise to fructose-1,6-bisphosphate which will yield glucose-6-P via gluconeogenesis and ultimately sucrose. (b) At fructose-6-P which can be converted to ADP-glucose and then to starch.

The purpose of photosynthesis is to produce ATP and NADPH for carbohydrate biosynthesis. A cursory examination of the Calvin Cycle (Fig. 15.11) shows why ATP and NADPH are so essential for carbohydrate synthesis. Starting with CO_2,

three ATP and two NADPH molecules are required for each turn of the cycle. Thus, for every molecule of hexose synthesized, 18 ATP and 12 NADPH molecules are required. Most of this material ends up in either starch or sucrose. The overall reaction for the Calvin Cycle leading to the synthesis of one triose molecule is:

$$3CO_2 + 9ATP + 6NADPH \rightarrow \text{Glyceraldehyde-3-P} + 9ADP + 8P_i + 6NADP^+ .$$

This process obviously requires a great deal of energy, but fortunately the energy which is supplied to the plant by the sun is limitless.

References

1. Jagendorf AT, Uribe E (1966) Photophosphorylation and the chemi-osmotic hypothesis. Brookhaven Symposium 19:215–245
2. Calvin M (1961) The path of carbon in photosynthesis. Nobel Lecture, Stockholm, Sweden

Further Readings: Photosystems

Allen JF (2004) Cytochrome b_6 f: Structure for signaling and vectorial metabolism. Trends Plant Sci 9:130–137

Barber J (2002) Photosystem II: A multisubunit protein that oxidizes water. Curr Opin Struct Biol 12:523–530

Chitnis PR (2001) Photosystem I: function and physiology. Annu Rev Plant Physiol Plant Biol 52:593–626

Fromme P, Melkozernov A, Jordan P, Krauss J (2003) Structure and function of photosystem I: Interaction with its soluble electron carriers and external antenna systems. FEBS Lett 555:40–44

Heathcote P, Fyfe PK, Jones MR (2002) Reaction centers: the structure and evolution of biological solar power. Trends Biochem Sci 27:79–87

The Light Independent Reactions

Cleland WW, Andrews TJ, Gutteridge S, Hartman FC, Lorimer GH (1998) Mechanism of rubisco: the carbonate as general base. Chem Rev 98:549–561

Schnarrenberger C, Martin W (1997) The Calvin cycle – a historical perspective. Photosynthetica 33:331–345

Chapter 16
DNA, RNA, and Protein Metabolism

16.1 DNA

16.1.1 Structure

DNA has long been recognized to be involved in heredity. Metaphorically, it is the instruction manual for cell duplication, construction, and the operation of its components. Because of the efforts of Rosalind Franklin [1] and Watson and Crick [2], and many other scientists, we have an understanding of how genetic information is transferred from one generation to the next with extraordinarily high fidelity.

DNA is a polymer of deoxyribonucleotides that exist as a double-stranded helix (Fig. 16.1) with the strands running in opposite or antiparallel directions, i.e., from $5' \rightarrow 3'$ on one strand and $3' \rightarrow 5'$ on the other. Each base in one strand is hydrogen-bonded to a base on the other, or *complementary*, DNA strand. The bases found in the deoxyribonucleotides are adenine, guanine, cytosine, and thymine. The two strands are thus stabilized by hydrogen-bonding or *base-pairing*. Figure 16.2 illustrates the types of base-pairing found in DNA and Fig. 16.3 depicts the polarity of the two strands.

Although each strand of DNA is a polymer of deoxyribonucleic acids, it contains segments that code for numerous cellular components. Each segment, called a *gene*, consists of sequences of deoxyribonucleotides that signal the start and termination of genes. In eurokaryotic cells, the DNA makes up part of the chromosomes which are enclosed by a membrane. This structure is termed the *nucleus*, and the sum total of all of the genetic material is referred to the *genome*. DNA exists in places other than the nucleus in eurokaryotes, e.g., mitochondria. The genetic material, commonly referred to as DNA, consists primarily of one type of DNA, B-DNA, but other types of DNA such as A-DNA and Z-DNA do exist.

H.J. Fromm and M.S. Hargrove, *Essentials of Biochemistry*,
DOI 10.1007/978-3-642-19624-9_16,

Fig. 16.1 Space-filling representation of a segment of the double-stranded helical structure of DNA. The two complementary helical strands of the 2′-deoxyribonucleic acids run in opposite directions and are stabilized by hydrogen bonding between the nitrogenous bases in the two chains

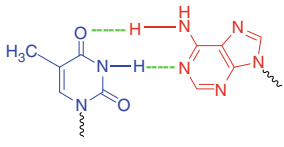

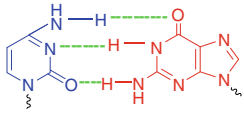

Fig. 16.2 Base-pairing between complementary strands of DNA. Hydrogen bonding between the bases is in *green*

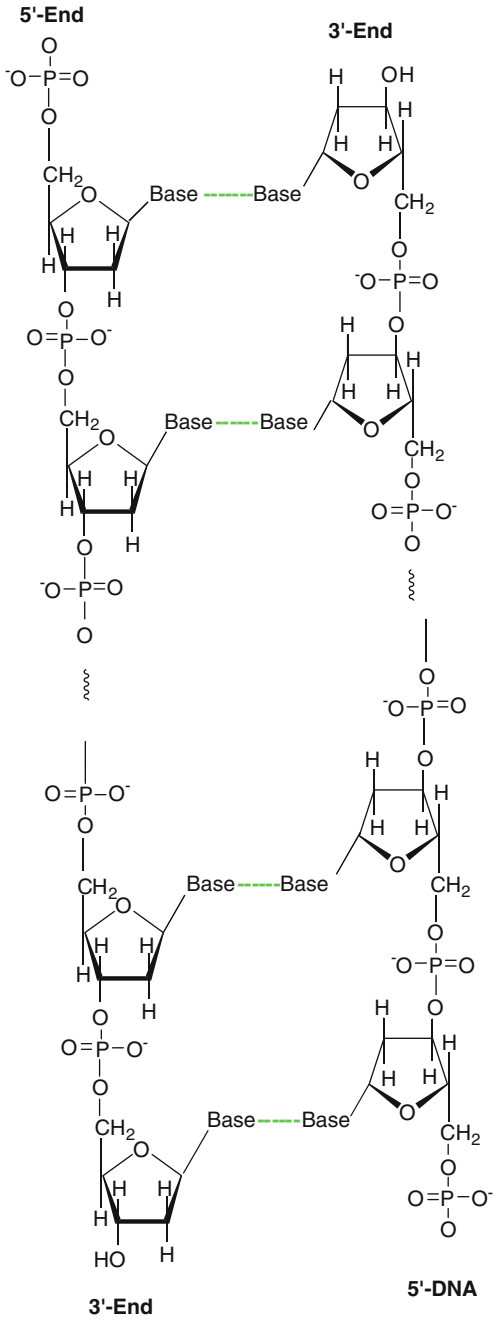

Fig. 16.3 Illustration of base-pairing of complementary strands of DNA indicating polarity of the two chains. Note that at the ends of the DNA the 5′-hydroxyl is phosphorylated, which is usually the case, whereas the 3′-hydroxyl is free. Hydrogen bonding between the chains is in *green*

16.1.2 DNA Replication

In the process of DNA replication, a number of factors including enzymes associate at the *replication initiation site*. The two DNA strands unwind, catalyzed by the enzyme *helicase*, and a complementary strand is formed using each original DNA strand as a template. DNA replication is catalyzed by a number of enzymes, among them, DNA polymerases. The discovery of the first DNA polymerase was made by Arthur Kornberg [3], who was able to synthesize DNA in the test tube and was awarded the Nobel Prize in 1959 for his research on DNA replication.

DNA polymerases act by adding a single deoxyribonucleotide, supplied by a deoxynucleoside-5′-triphosphate (dNTP) to the 3′ end of the growing DNA chain. The reaction is

$$(\mathrm{dNMP})_n + \mathrm{dNTP} \xrightarrow[\text{DNA template}]{(\text{DNA polymerase})} (\mathrm{dNMP})_{n+1} + \text{P-P}_i,$$

where $(\mathrm{dNMP})_n$ represents the growing deoxypolyribonucleotide chain and dNTP the deoxyribonucleoside-5′-triphosphate.

The template, or original DNA strand, provides the *specificity* for the growing DNA chain by virtue of *hydrogen-bonding* between the bases on adjacent chains and the complementarity between the parent and daughter chains. How this is accomplished is illustrated in Fig. 16.4.

Newly formed DNA is synthesized in the 5′ → 3′ direction. This point is also illustrated in Fig. 16.4 and shows hydrogen bonding between the bases in adjacent chains giving rise to the complementarity of the newly formed DNA.

The synthesis of newly formed DNA proceeds simultaneously on both parent DNA strands in the 5′ → 3′ direction as shown in Fig. 16.5.

Due to the opposite polarities of the leading and lagging strand templates, the DNA polymerases must copy their DNA templates in opposite directions. However, leading and lagging strand synthesis is highly coupled and both polymerases move in the same overall direction. To allow this to occur, the lagging strand template forms a large loop, which expands and contracts with each cycle of lagging strand synthesis (Fig. 16.6). This arrangement of the replication fork was first envisioned by Bruce Alberts and has been termed the "*trombone model*" of DNA synthesis. The leading strand is synthesized in a continuous fashion, whereas the lagging strand is discontinuous. Each cycle of lagging strand synthesis forms what is known as an *Okazaki fragment*. The size range of a eukaryotic Okazaki fragment is 100–200 bases, whereas in prokaryotes the size range is 1,000–2,000 bases long. Because DNA polymerases cannot initiate DNA synthesis, each Okazaki fragment is initiated using an RNA primer that is synthesized by the enzyme *primase* using unwound DNA at the *replication fork* as its template. Okazaki fragment maturation involves the removal of the RNA primer, filling of the gap by a DNA polymerase, and the synthesis of a phosphodiester bond between two adjacent Okazaki fragments by the enzyme *DNA ligase*. The chemical mechanism of how the Okazaki fragments are joined is shown in Fig. 16.7.

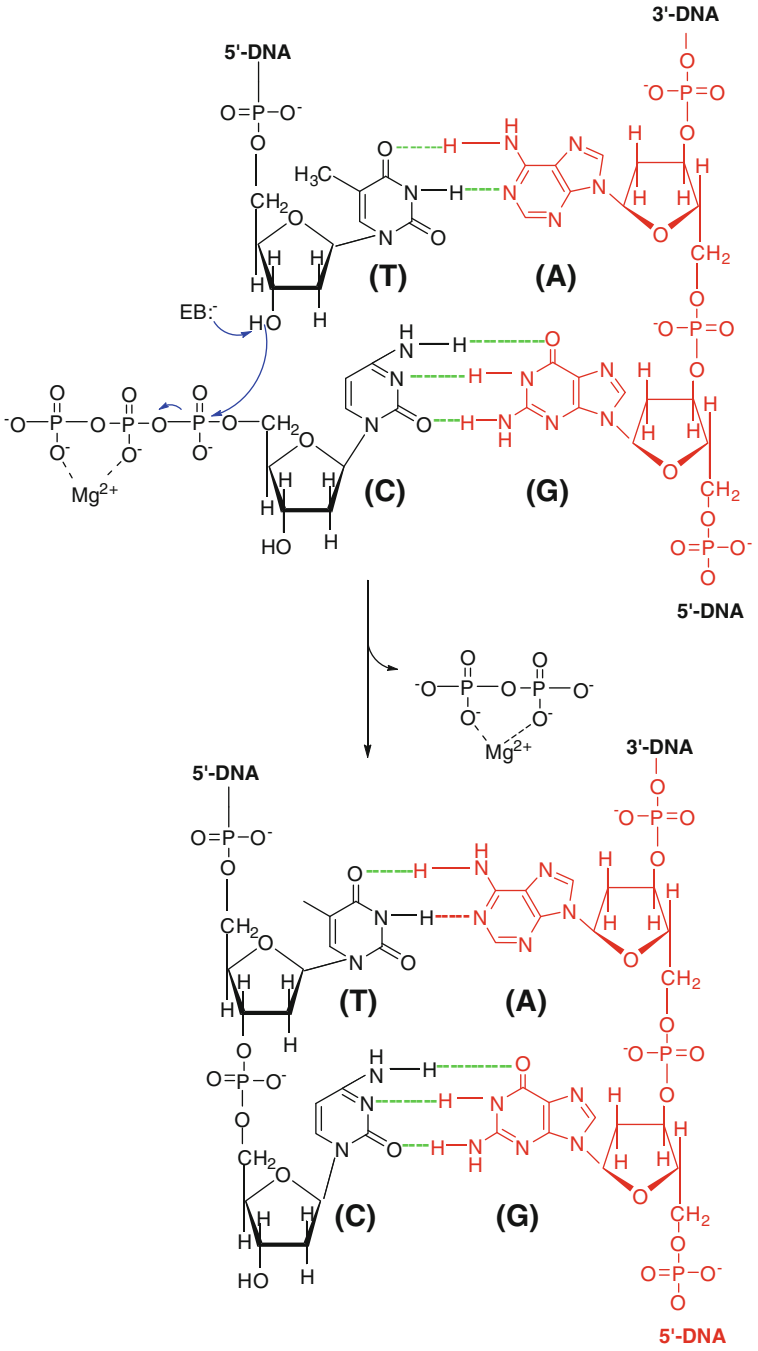

Fig. 16.4 The elongation reaction as part of DNA replication catalyzed by DNA polymerase. The parent DNA strand shown in *red* determines the specificity of the added deoxyribonucleotide by hydrogen-bonding to the deoxyribonucleotide substrate, in this case deoxycytosine-5′-triphosphate. Base-pairing is illustrated by the *dashed green lines*. Note that a phosphodiester linkage is produced in the course of the polymerase reaction

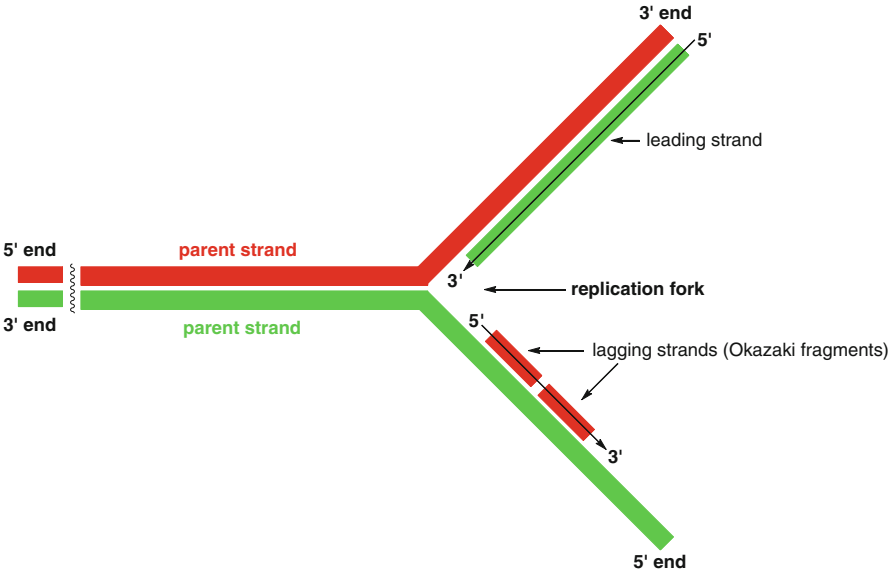

Fig. 16.5 Separation of the parent strands of the double-stranded helix catalyzed by helicase at the replication fork. The daughter DNA strands are synthesized in the 5′ → 3′ direction and the short or lagging strands in *red* are taken to be Okazaki fragments. Leading and lagging strand synthesis is catalyzed by DNA polymerase III and DNA polymerase I, respectively

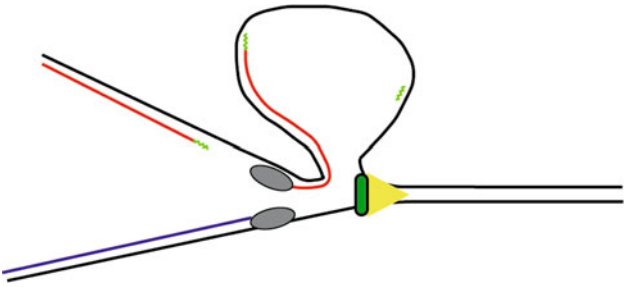

Fig. 16.6 The trombone model for the replication fork. The leading and lagging strand polymerases are represented by the *gray ovals* and the primase and helicase are represented by the *green ellipse* and *yellow triangle*, respectively. The nascent continuous leading strand is *blue* and the nascent discontinuous lagging strand is *red* and the RNA primers that are used to initiate Okazaki fragment synthesis are *red*. The leading and lagging strand polymerases are traveling in opposite directions (5′ to 3′ relative to their templates) but because the lagging strand template forms a loop, the replication fork remains coupled and moving in the same overall direction

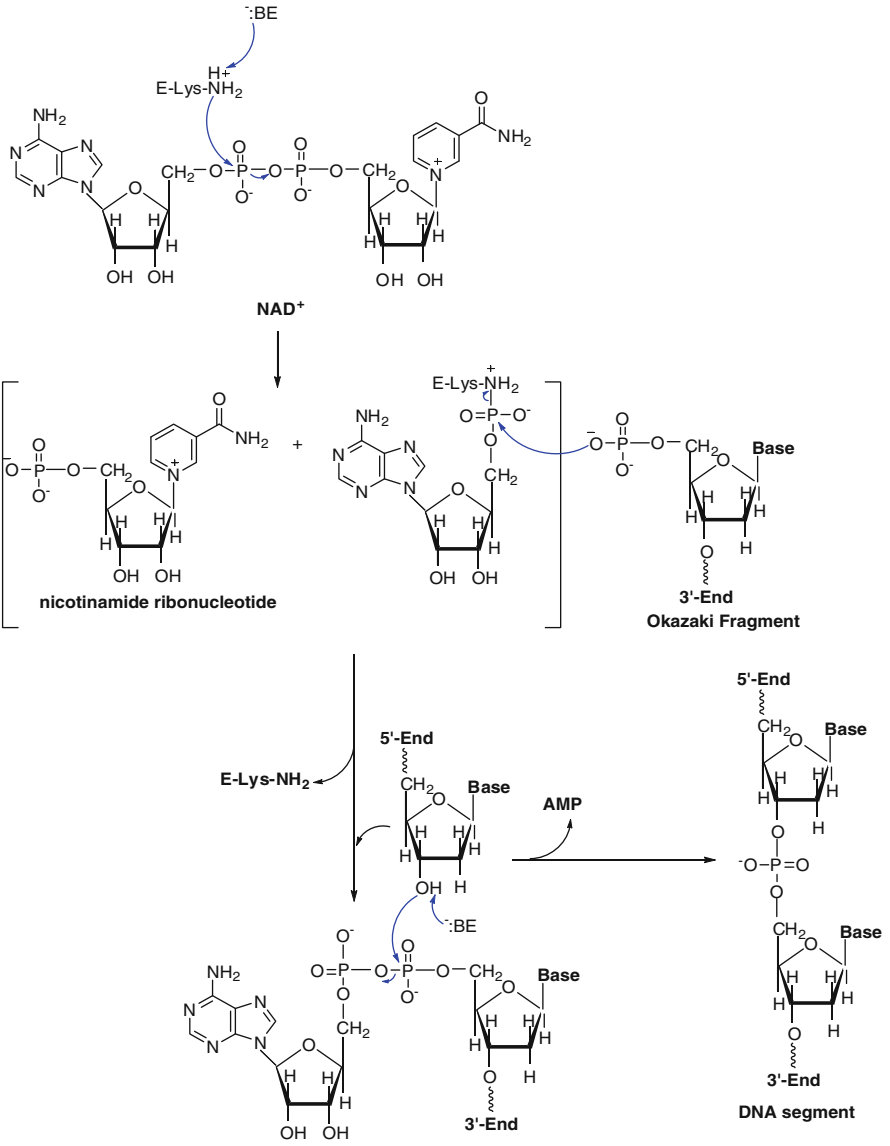

Fig. 16.7 The mechanism of action of *E. coli* DNA ligase involves the coenzyme NAD^+. A phosphodiester linkage is formed in the course of the reaction between two short Okazaki fragments

16.1.3 Repair of DNA

DNA can be damaged by endogenous agents such as reactive oxygen species or by exogenous agents such as UV light or chemical mutagens. The cell has a variety of

mechanisms for repairing damaged DNA. Mechanisms for repairing damaged bases include the direct chemical reversal of the damaged base, base excision, nucleotide excision, or mismatch repair. In addition to chemical modifications of the DNA base, the backbone of the DNA can be interrupted and form what is known as a double-strand break (DSB). DSBs are among the most deleterious forms of DNA damage and can lead to gross chromosomal rearrangements and cellular dysfunction. DSBs are repaired through two possible pathways, nonhomologous end-joining (NHEJ) and homologous recombination (HR). NHEJ is generally thought of as error-prone since minor base deletions at the end of the DSB are not repaired prior to the joining of the DNA ends. On the other hand, HR uses an undamaged homologous DNA template to direct the repair of the DSB, and it is considered to be an error-free pathway.

16.1.4 Degradation of Cellular DNA

DNA can be degraded in cells by enzymes known as *nucleases* that hydrolyze the terminal deoxyribonucleotides (*exonucleases*) or within the deoxypolynucleotide chain (*endonucleases*). The latter class of enzymes may exhibit specificity after cutting the DNA chain by degrading the DNA in either the $5' \rightarrow 3'$ or the $3' \rightarrow 5'$ direction.

16.2 RNA

RNA, or ribonucleic acid, unlike DNA, is a single chain polymer of ribonucleic acids. From a chemical perspective, there are two major differences between RNA and DNA. One is the fact that the substituents differ at the $2'$ position of the sugar and the other involves the composition of the nitrogenous bases. RNA contains four bases: adenine, guanine, cytosine, and uracil; however, in DNA thymine is substituted for uracil.

Most single-stranded RNA molecules fold back on themselves and assume secondary and tertiary structures that form helixes which are stabilized by base-pairing. Some RNA molecules exist as double-stranded helixes. Unlike DNA whose primary role is to store and transmit genetic information, RNA is involved in a number of dynamic biological functions. These include as follows:

1. Messenger RNA (mRNA).
   mRNA carries information on the primary structure of proteins from DNA to the ribosome where protein biosynthesis takes place. Its nucleotide sequence is complementary to a short portion of DNA which codes for a particular gene. mRNA that comprises approximately 3% of the cell's RNA is the least stable member of the RNA family.

2. Ribosomal RNA (rRNA).
   Approximately three-fourths of the cell's RNA is rRNA. It is contained in huge structures, the ribosomes, which are second in size only to the pyruvate dehydrogenase complex (Chap. 9). The *Escherichia coli* ribosome is 70 Svedberg units (S). It contains two subunits, one of 50 S (150 × 200 × 200 Å) and the other of 30 S (55 × 220 × 225 Å). (The S values are not additive and are terms used to describe sedimenting particles in the ultracentrifuge). The 50 S subunit contains two rRNA molecules: 23 and 5 S rRNA plus 31 proteins. The smaller 30 S subunit contains 21 proteins and a single 16 S rRNA. Eukaryotic ribosomes, although functionally similar to prokaryotic ribosomes are larger (80 S) and consist of a 60 S and a 40 S subunit.

   The ribosome is the site of protein biosynthesis. The structure of the ribosome was recently elucidated [4].
3. Transfer RNA (tRNA).
   tRNAs contain very short polyribonucleotide sequences – less than 100 bases. Their biological role is to transport amino acids to the ribosome for peptide bond (protein) synthesis and to ensure proper decoding of mRNA.
4. Miscellaneous RNA.
   Miscellaneous RNAs are biomolecules that represent a small fraction of the total cellular RNA. These include:

   (a) *ribozymes* which are catalytic in nature.
   (b) $_{mi}$*RNA* (micro RNA) which binds to mRNA and inhibits its translation.
   (c) $_{si}$*RNA* (small-interfering RNA) which binds to mRNA and aids in its degradation.
   (d) $_{sn}$*RNA* (small nuclear RNA) which participates in RNA processing as part of the spliceosomes.
   (e) $_{\mathbf{sno}}$RNA (small nucleolar RNA) which participate in nucleolar RNA processing.

16.2.1 The Central Dogma Hypothesis

Francis Crick in 1958 proposed the hypothesis, known as the Central Dogma Theory, which states that information flows in a single direction from DNA to RNA for protein biosynthesis [5]. This notion involves two processes: "*transcription*" and "*translation*":

$$\text{DNA} \xrightarrow{\text{transcription}} \text{RNA} \xrightarrow{\text{translation}} \text{Protein.}$$

Most generalizations, as appealing as they may be, may not be absolutely correct. This is indeed the case with the Central Dogma Theory, e.g., information can flow from RNA to DNA with *reverse transcriptase*, an enzyme found in retrovirus infected cells such as HIV.

16.2.1.1 Transcription

Transcription, or DNA-directed RNA synthesis, is carried out by the enzyme *RNA polymerase*. The purpose of this reaction is to pass information contained within DNA to RNA. The enzyme requires a DNA template in addition to its nucleotide substrates, ATP, GTP, CTP, and UTP. The action of RNA polymerase involves first the unwinding of a segment of DNA and its subsequent rewinding. A number of other factors, in addition to RNA polymerase and its substrates, are required for transcription to proceed, e.g., protein transcription factors bind promoters, a region of DNA that facilitates a gene's transcription, and either turns genes on or off. In prokaryotes, the promoter can be found near the transcription start site.

The RNA polymerase reaction is analogous to its counterpart in DNA biosynthesis, DNA polymerase:

$$\text{mRNA}_{(n)} + \text{NTP} \xrightarrow{\text{DNA template}} \text{mRNA}_{(n+1)} + \text{P-P}_i,$$

where NTP is a ribonucleoside-5′-triphosphate.

The equilibrium of the reaction lies to the left; however, when pyrophosphate is hydrolyzed by pyrophosphatase, the overall reaction becomes thermodynamically favorable:

$$\text{mRNA}_{(n)} + \text{NTP} \rightarrow \text{mRNA}_{(n+1)} + 2\text{P}_i.$$

16.2.1.2 The Role of DNA and Base-Pairing in mRNA Biosynthesis

mRNA biosynthesis is catalyzed by the enzyme RNA polymerase and occurs in three distinct phases: *initiation*, *chain elongation*, and *termination*. Initiation takes place at a site on DNA known as the *promoter site*. As is the case with DNA polymerase, mRNA synthesis proceeds in the $5' \rightarrow 3'$ direction. Chain elongation catalyzed by RNA polymerase occurs with a high degree of fidelity because of base-pairing between the DNA template and the newly synthesized mRNA. mRNA synthesis ceases when a termination site on DNA is reached. At this point, the entire DNA sequence or gene has been transcribed into the mRNA.

The reaction catalyzed by RNA polymerase is very similar to that shown in Fig. 16.4 for DNA polymerase. There are, however, differences between the two polymerase enzymes. First, the RNA polymerase reaction is much slower than its DNA polymerase counterpart. Second, the product, mRNA, is single stranded, and third, the association or complementarity occurs over approximately an eight base segment of DNA and not the entire molecule. Finally, mRNA synthesis does not require an RNA primer; it can be synthesized directly from a DNA template.

In order for RNA polymerase to function using DNA as a template, the DNA must unwind so that one strand of DNA hydrogen bonds to the ribonucleotide-5′-triposphate substrates. The unwound DNA forms a double-stranded *hybrid helix* with the newly formed mRNA approximately 8 bp in length. After dissociation

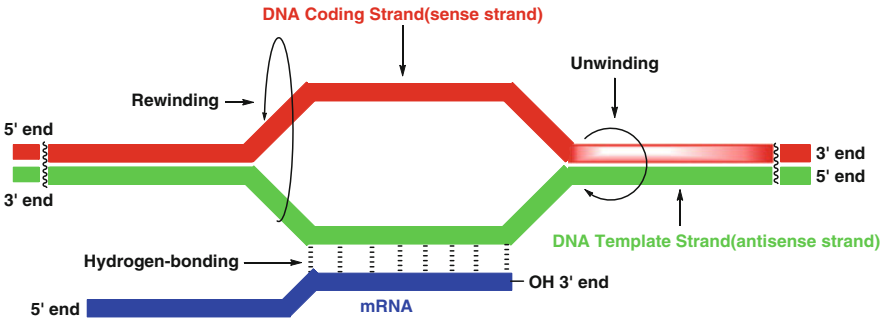

Fig. 16.8 The relationship between DNA and newly synthesized mRNA on RNA polymerase. Complementarity occurs between one strand of DNA, the template strand, and the newly formed mRNA. The base sequence in the mRNA will be identical to that of the DNA coding strand except that uracil will be substituted for thymine. After a segment of the mRNA has been synthesized, rewinding of the two DNA stands occurs and a new segment of DNA unwinds before forming an RNA–DNA hybrid

of the newly formed mRNA from the DNA, the DNA rewinds to form a double-stranded helix, and another piece of DNA unwinds to form a new hybrid helix. The unwinding and rewinding of the DNA occur as the RNA polymerase moves along the DNA chain.

Figure 16.8 illustrates the relationship between DNA and the biosynthesis of mRNA as catalyzed by RNA polymerase. Note that the newly synthesized mRNA hydrogen bonds to the DNA template strand and assumes the base sequence of the DNA *coding or sense strand*.

The newly synthesized mRNA will incorporate UMP in place of dTMP, and hydrogen-bonding will take place between adenine in the DNA template strand and the substrate UTP. Hydrogen-bonding as might be expected will also take place between guanine and cytosine.

mRNA elongation ceases when a termination site on the DNA template strand is reached. The mRNA then dissociates from the DNA and rewinding of the DNA is completed.

16.2.2 Posttranslational Modification of tRNA, rRNA, and mRNA

Most of the newly synthesized RNA transcripts in eukaryotic cells are *spliced* prior to their use in the cell as "mature" or functional RNA. After being spliced or cut, a portion of the RNA is excised and discarded. The newly formed ends of the RNA are then joined or ligated to form functional RNA. This series of reactions takes place in a complex of enzymes and small RNA molecules called the *splicesome*.

Bacterial DNA is made up of genes in which there is a continuous sequence of bases that make up the triplet codons. In eukaryotic DNA, the continuous series

of bases coding for a protein, or more specifically for portions of a protein, are interrupted by base sequences that are not translated. The translated sequences are referred to as *exons* (expressed sequences) and the nontranslated sequences as *introns* (intervening sequences). Newly transcribed mRNA, called pre-mRNA, contains both exons and introns; however, the introns are excised and the newly formed mRNA used for translation. Figure 16.9 illustrates splicing and ligation of RNA.

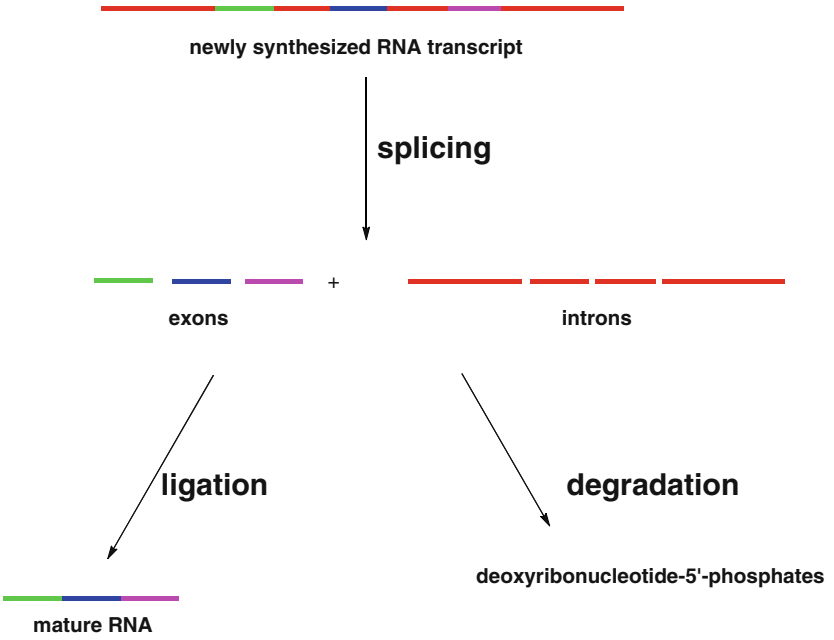

Fig. 16.9 The removal of introns from an RNA transcript by splicing. The RNA is spliced and the introns are excised from the RNA. The exon fragments are then ligated to form the mature RNA molecule

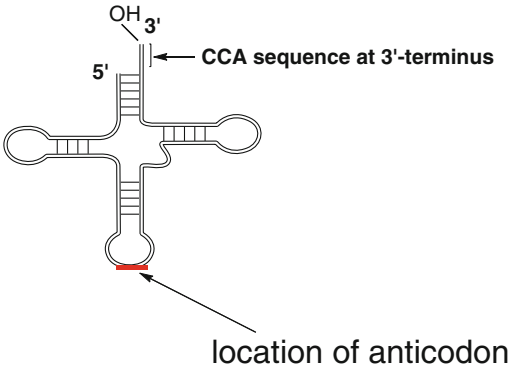

Fig. 16.10 Cartoon of tRNA. The 3′ end of the molecule contains the triplet sequence CCA and the location of the anticodon (in *red*) that base pairs with mRNA. The 3′ hydroxyl group of adenine in the CCA sequence reacts with the aminoacyl adenylate (see Fig. 16.13)

The newly synthesized transcripts of tRNA also undergo posttranslational modification. As shown in Fig. 16.10, the active tRNA contains a hydroxyl group with the sequence *CCA* at the 3′ end. In addition, a number of bases in tRNA are enzymatically altered by posttranslational modification, e.g., some adenine residues are converted to inosine, while others are methylated.

All subunits of rRNA are processed from a single transcript that is cleaved by a series of endo- and exonucleases to produce 5, 16, and 23 S rRNA. rRNA also undergoes additional posttranslational modification before it associates with protein to form the active ribosome. One such modification involves methylation of rRNA by *S*-adenosylmethionine (SAM) (Chap. 13), which methylates adenine residues at the $O^{2'}$ of ribose. These posttranslational modifications are thought to enhance the stability of the rRNA.

16.2.3 Ribozymes

As pointed out in Chap. 4 not all biological catalysts are proteins. Certain RNA molecules, not associated with proteins, exhibit catalytic activity. These catalysts are referred to as ribozymes.

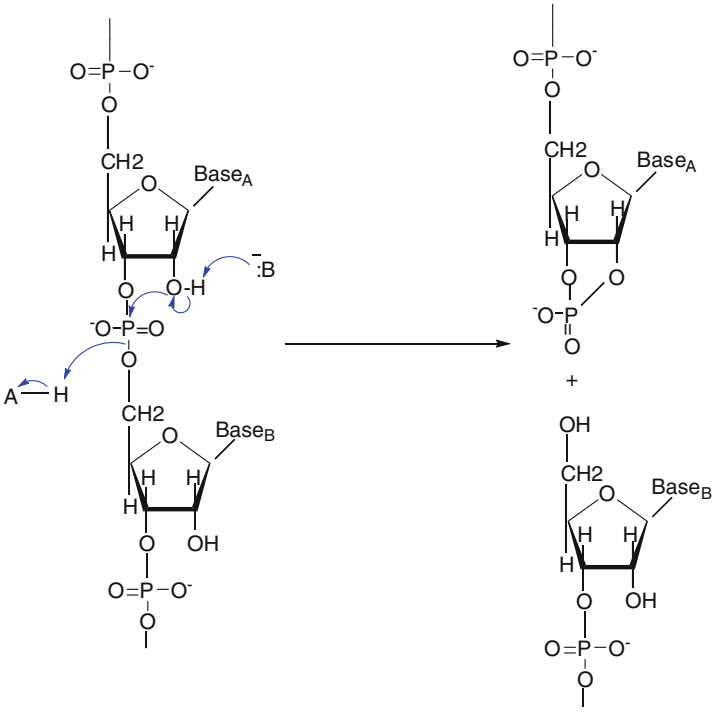

Fig. 16.11 Cleavage of a segment of RNA by the hammerhead ribozyme

Probably the best known ribozyme is the hammerhead which is a 3′,5′-phosphodiesterase (Fig. 16.11); however, ribozymes are known to facilitate a number of other biologically important reactions [6]. These include self-splicing introns and ribonuclease P which catalyzes the site-specific hydrolysis of precursor RNA substrates such as tRNA and 55 rRNA, and peptidyl transferase.

16.2.4 Degradation of RNA

A number of nucleases are present in cells that catalyze the hydrolysis of RNA. Many of these fall into the endo- and exonuclease classes.

16.3 Protein Metabolism

16.3.1 Protein Synthesis

Proteins are synthesized from "*activated amino acids*" on the ribosome. Coding information on the primary sequence of proteins comes from DNA. This information is transmitted in the form of specific base sequences of tRNA and mRNA.

16.3.1.1 Amino Acid Activation

The first step in the biosynthesis of proteins involves the formation of an *amino acid adenylate* (*aminoacyl adenylate*) or "activated amino acid". This reaction is followed by the transfer of the amino acid to tRNA. This sequence of events is accomplished by highly specific aminoacyl-tRNAs. These two reactions, carried out by the ribozyme *aminoacyl-tRNA synthetase*, can be cast in chemical form as follows:

$$\text{amino acid} + \text{ATP} \rightarrow \text{aminoacyl adenylate} + \text{P-P}_\text{i}, \tag{16.1}$$

$$\text{aminoacyl adenylate} + \text{tRNA} \rightarrow \text{aminoacyl-tRNA} + \text{AMP}, \tag{16.2}$$

The overall aminoacyl-tRNA synthetase reaction is:

$$\text{amino acid} + \text{ATP} + \text{tRNA} \rightarrow \text{aminoacyl-tRNA} + \text{P-P}_\text{i} + \text{AMP}. \tag{16.3}$$

The tRNA which is the receptor of the aminoacyl group is specific for one of the 20 amino acids found in proteins. Figure 16.12 depicts the formation of an aminoacyl adenylate.

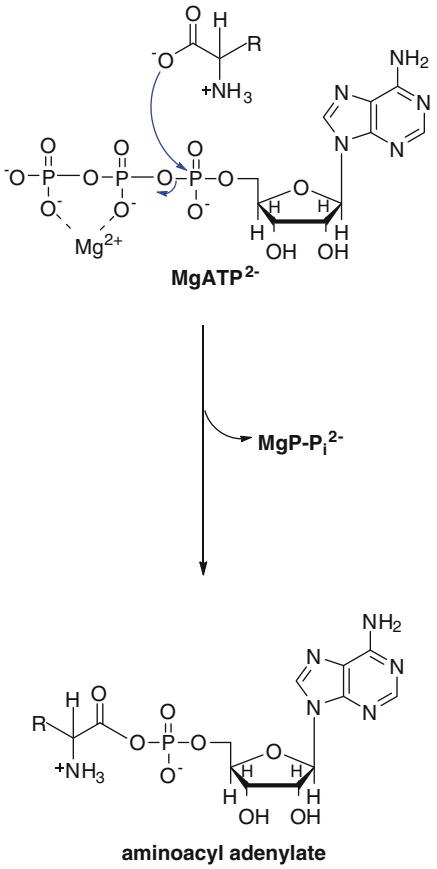

Fig. 16.12 The activation of an amino acid in the aminoacyl-tRNA synthetase reaction

The second step of the aminoacyl-tRNA synthetase reaction involves the transfer of the aminoacyl group to the 3′-hydroxyl group of the adenine ribonucleotide at the 3′-terminus of the tRNA (see Fig. 16.13).

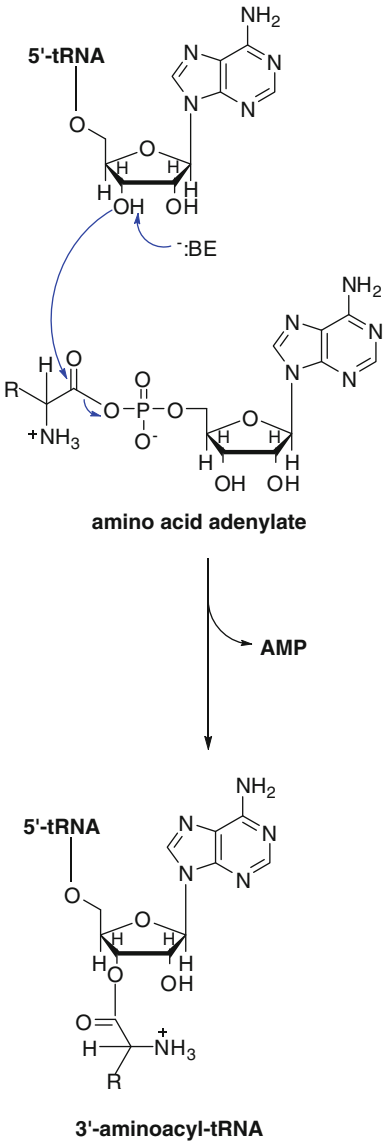

Fig. 16.13 The transfer of the amino acid to tRNA in the aminoacyl- tRNA synthetase reaction

16.3.1.2 Specificity of Aminoacyl-tRNA for mRNA

Shown in Fig. 16.10 is a cartoon of tRNA. At the bottom of the structure is the three base sequence known as the *anticodon*. It is this anticodon that binds, through base-pairing, to a three base codon on mRNA when the tRNA is loaded with the amino acid. It is this interaction between the mRNA and the aminoacyl-tRNA that provides the high degree of fidelity observed in the transfer of genetic information from DNA to proteins.

The Triplet Code (Genetic Code)

A sequence of three bases in DNA identifies each of the 20 amino acids that are to be incorporated into the newly synthesized protein. This information is incorporated into mRNA which is synthesized using DNA as the template. If, the four bases that appear in mRNA were used as a doublet (4^2) there would be 16 different two base sequences to direct 20 amino acids; clearly not enough to eliminate amino acid substitutions. Because three bases are required at a minimum (4^3) 64 code words are possible, more than enough to uniquely accommodate the 20 amino acids. In fact, many triplets that are used to define a single amino acid are redundant, and many of these become "low use codons". In addition, some "extra" triplet sequences are used as *stop* codons to terminate protein synthesis. AUG is used as the start codon for the N-terminal amino acid in eukaryotes and Archaea as well as for internal methionine residues.

Table 16.1 illustrates the triplet code that directs the synthesis of proteins. Research over many years from the laboratories of Nirenberg [7] and Khorana [8] led to the discovery of the triplet code.

Table 16.1 The genetic code

	Position#2				
Position#1	**U**	**C**	**A**	**G**	Position#3
	UUU F	UCU S	UAU Y	UGU C	**U**
	UUC F	UCC S	UAC Y	UGC C	**C**
	UUA L	UCA S	UAA Stop	UGA Stop	**A**
U	UUG L	UCG S	UAG Stop	UGG W	**G**
	CUU L	CCU P	CAU H	CGU R	**U**
	CUC L	CCC P	CAC H	CGC R	**C**
	CUA L	CCA P	CAA Q	CGA R	**A**
C	CUG L	CCG P	CAG Q	CGG R	**G**
	AUU I	ACU T	AAU N	AGU S	**U**
	AUC I	ACC T	AAC N	AGC S	**C**
	AUA I	ACA T	AAA K	AGA R	**A**
A	AUG M	ACG T	AAG K	AGG R	**G**
	GUU V	GCU A	GAU D	GGU G	**U**
	GUC V	GCC A	GAC D	GGC G	**C**
	GUA V	GCA A	GAA E	GGA G	**A**
G	GUG V	GCG A	GAG E	GGG G	**G**

The three letter genetic code defines the amino acids (*underline*) in the polypeptide

Protein Synthesis

(a) A number of compounds, in proper alignment, are required for the biosynthesis of proteins. In *E. coli*, protein synthesis occurs within a cavity between the small (30 S) and large (50 S) subunits of the ribosome, and as mRNA

biosynthesis, can be conveniently divided into three phases: initiation, elongation, and termination.

1. Initiation of protein synthesis begins when the protein initiator factor IF-3 binds to the 30 S subunit of the ribosome and causes its dissociation into its 30 and 50 S components. The small ribosomal subunit then binds to the 5' side of mRNA which carries information in a triplet code (three consecutive ribonucleotides) from DNA. The 30 S subunit is then translocated in the $5' \rightarrow 3'$ direction along the mRNA where it meets the large ribosomal subunit, other protein *initiator factors*, and *initiator tRNA*. The tRNA is bound to either *N*-formyl methionine (*E. coli*) or methionine (eukaryotes and Achaea) at a site in the ribosome known as the *P site*.
2. In the elongation phase of protein synthesis, a specific aminoacyl-tRNA, directed by hydrogen bonding interactions between the anticodon region of the aminoacyl-tRNA and the codon region of mRNA, adds to a site distinct from the P site, the *A site*. The A and P sites are, however, in close proximity. After correct positioning of the two aminoacyl-tRNA molecules, the ribozyme *peptidyl transferase* catalyzes peptide bond formation between the substrates [9].
3. The newly formed dipeptide is first shared by both the A and P sites before appearing exclusively in the A site.
4. The aminoacyl-free tRNA in the P site moves to an exit tunnel in the ribosome, the *E site*, and is deposited in the cytosol.
5. The newly synthesized tRNA bound dipeptide then moves from the A site to the P site.
6. After translocation of the ribosome in the 5' → 3' direction along the mRNA to expose a new codon, an aminoacyl-tRNA molecule of proper identity binds to the mRNA at the A site and the peptidyl transferase reaction is again initiated.

Shown in Fig. 16.14 is a summary of these events in protein synthesis involving a dipeptidyl-tRNA bound to the P site.

The mechanism of the peptidyl transferase reaction involving chain elongation is illustrated in Fig. 16.15. The reaction mechanism is believed to involve a tetrahedral intermediate [10].

As the polypeptide chain grows through subsequent cycles of amino acid residue incorporation, it emerges from the ribosome and undergoes folding into its native secondary and tertiary conformations both spontaneously and with the aid of *chaperones* (ATP-requiring proteins that facilitate the proper folding of the polyperpide chain). Peptide bond synthesis ceases when a stop codon on the mRNA is reached. This termination site will not bind aminoacyl-tRNA and peptide synthesis stops. *Release factors* allow the newly synthesized protein to dissociate from the ribosome.

(b) Protein synthesis is regulated at the level of transcription.

(c) *Posttranslational modification of proteins.*

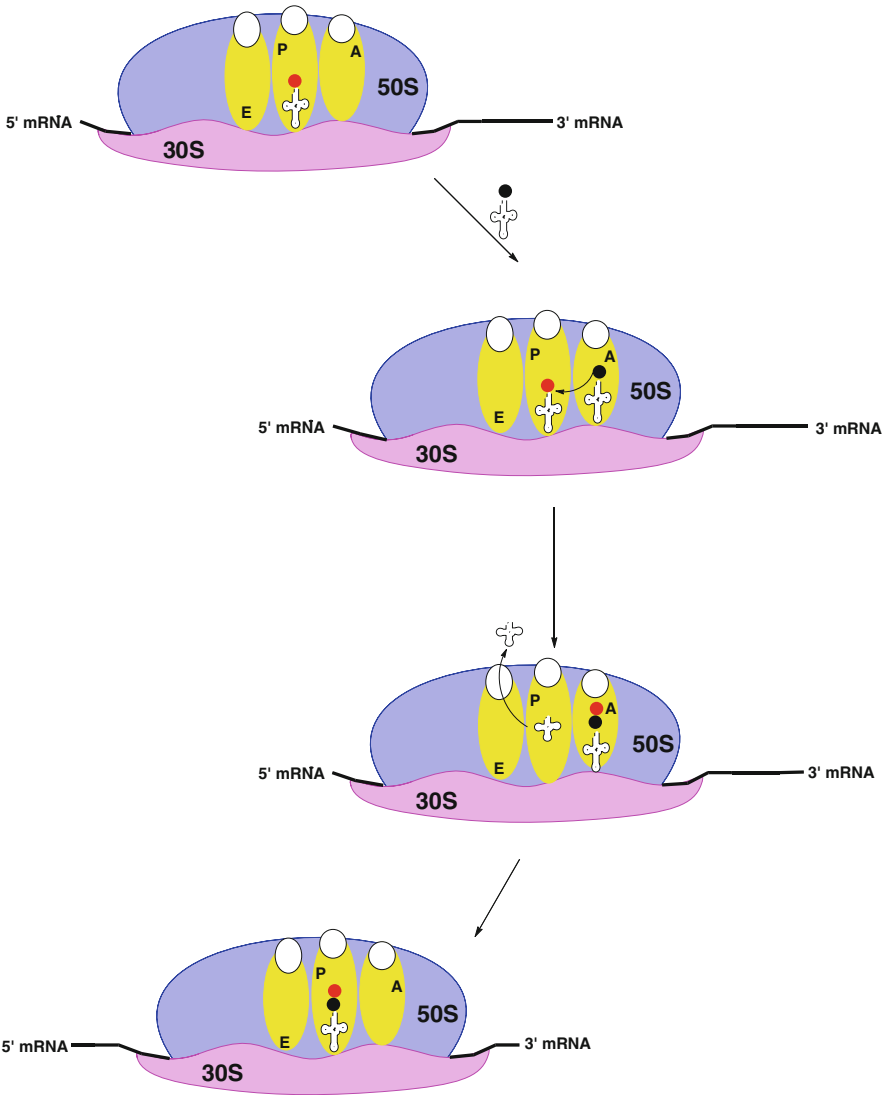

Fig. 16.14 Cartoon of protein synthesis. The sequence of events as outlined involves biosynthesis of a dipeptidyl-tRNA molecule from two aminoacyl-tRNA molecules using the machinery of the 70 S *E. coli* ribosome and translation provided by mRNA. The roles of ribosome sites A, P, and E in protein biosynthesis are indicated in the figure. The N-terminal residue (*red*) is *N*-formylmethionine. Note that the ribosome has translocated along the mRNA in the $5' \rightarrow 3'$ direction in order to receive the next aminoacyl-tRNA molecule at site A

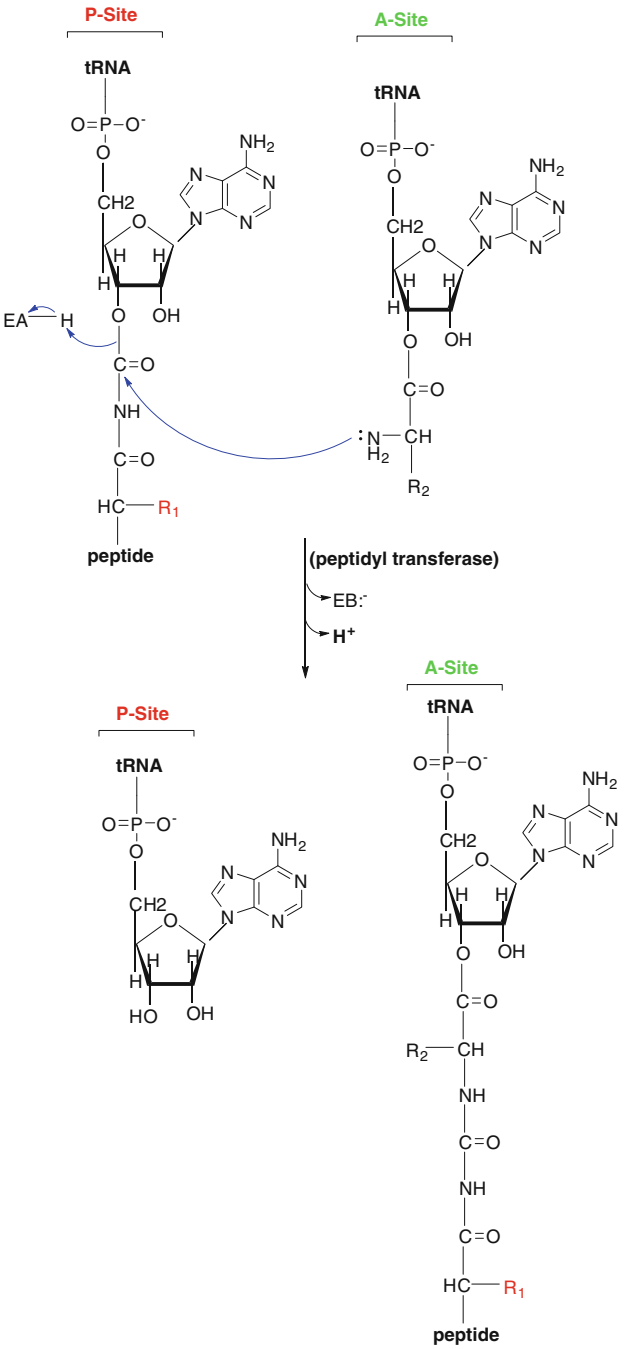

Fig. 16.15 The mechanism of action of the ribozyme peptidyl transferase. The addition of an amino acid residue to the growing polypeptide chain requires aminoacyl group transfer from aminoacyl-tRNA

Cytosolic, Golgi Complex and rough endoplasmic reticulum enzymes catalyze modification of many newly synthesized proteins.These include:

1. Deformylation of *N*-formylmethionine at the N-terminus of prokaryotic proteins.
2. Removal of the N-terminal methionine.
3. Acetylation of the N-terminal amino group.
4. Glycosylation; addition of a polysaccharide to form a glycoprotein.
5. Phosphorylation.
6. Oxidation of cysteine residues to form disulfide bonds.
7. Conversion of zymogens to active enzymes.

(d) Signal peptides.

In some proteins, the initial portion of the N-terminus acts as a signal peptide sequence. This sequence of amino acid residues allows the protein to associate with certain specific cellular structures. An example of such a protein is the enzyme brain hexokinase which associates with the outer mitochondrial membrane (Chap. 8). Other signal sequences allow proteins to enter specific organelles within eukaryotic cells.

16.3.2 Intracellular Protein Catabolism

Intracellular proteins are constantly being synthesized and degraded, a process known as *protein turnover*. Most protein turnover results in a steady state; however, in the case of certain proteins, e.g., regulatory proteins, there may be a need for their degradation after their regulatory functions cease. A variety of mechanisms for protein degradation are available. In eukaryotic cells, some proteins may be engulfed by a complex of proteolytic enzymes in *lysosomes*. Others may covalently bind to the protein *ubiquitin* which is targeted for degradation by a complex of proteases (*proteosomes*).

References

1. Franklin R, Gosling RG (1953) Molecular configuration in sodium thymonucleate. Nature 171:740–741
2. Watson JB, Crick FHC (1953) A structure for deoxyribose nucleic acid. Nature 171:737–738
3. Kornberg A (1957–1959) Enzymatic synthesis of deoxyribonucleic acid. Harvey Lect 53:83–112
4. Ban N, Nissen P, Hansen J, Moore PB, Steitz TA (2000) The complete atomic structure of the large ribosomal subunit at 2.4 Å resolution. Science 289:905–920
5. Crick FHC (1970) Central dogma of molecular biology. Nature 227:561–563
6. Doudna JA, and Cech TR (2002) The chemical repertoire of natural ribozymes. Nature 418:222–8

7. Nirenberg M (1977) The genetic code, Nobel Lectures in Molecular Biology, 1933–1975, Elsevier, pp. 335–360
8. Khorana HG (1977) Nucleic acids synthesis in the study of the genetic code. Nobel Lectures in Molecular Biology, 1933–1975, Elsevier, pp. 303–331
9. Zhang B, Cech TR (1998) Peptidyl-transferase ribozymes: trans reactions, structural characterizations, and ribosomal RNA-like features. Chem Biol 5:539–553
10. Seila AC, Okuda K, Nunez S, Seila AF, Strobel SA (2005) Kinetic isotope effect analysis of the ribosomal peptidyl transferase reaction. Biochemistry 44:4018–4027

Index

H.J. Fromm and M.S. Hargrove, *Essentials of Biochemistry*,
DOI 10.1007/978-3-642-19624-9,

H